CHEMICAL REVIEWS

Review

pubs.acs.org/CR

Artificial Molecular Machines

Sundus Erbas-Cakmak, David A. Leigh,* Charlie T. McTernan, and Alina L. Nussbaumer

School of Chemistry, University of Manchester, Oxford Road, Manchester M13 9PL, United Kingdom

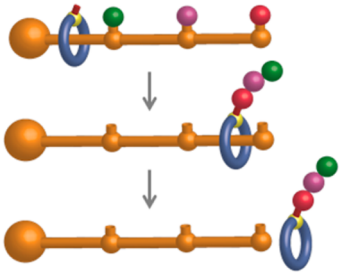

CONTENTS

Received: March 29, 2015
Published: September 8, 2015

DOI: 10.1021/acs.chemrev.5b00146
Chem. Rev. 2015, 115, 10081−10206

1. INTRODUCTION

The widespread use of molecular machines in biology has long suggested that great rewards could come from bridging the gap between synthetic molecular systems and the machines of the macroscopic world. In the last two decades, it has proved possible to design synthetic molecular systems with architectures where triggered large amplitude positional changes of submolecular components occur. Perhaps the best way to appreciate the technological potential of controlled molecular-level motion is to recognize that nanomotors and molecular-level machines lie at the heart of every significant biological process. Over billions of years of evolution, nature has not repeatedly chosen this solution for performing complex tasks without good reason. When mankind learns how to build artificial structures that can control and exploit molecular level motion and interface their effects directly with other molecular-level substructures and the outside world, it will potentially impact on every aspect of functional molecule and materials design. An improved understanding of physics and biology will surely follow.

The first steps on the long path to the invention of artificial molecular machines were arguably taken in 1827 when the Scottish botanist Robert Brown observed the haphazard motion of tiny particles under his microscope.[1,2] The explanation for Brownian motion, that it is caused by bombardment of the particles by molecules as a consequence of the kinetic theory of matter, was later provided by Einstein, followed by experimental verification by Perrin.[3,4] The random thermal motion of molecules and its implications for the laws of thermodynamics in turn inspired Gedankenexperiments ("thought experiments") that explored the interplay (and apparent paradoxes) of Brownian motion and the Second Law of Thermodynamics. Richard Feynman's famous 1959 lecture "*There's plenty of room at the bottom*" outlined some of the promise that manmade molecular machines might hold.[5,6] However, Feynman's talk came at a time before chemists had the necessary synthetic and analytical tools to make molecular machines. While interest among synthetic chemists began to grow in the 1970s and 1980s, progress accelerated in the 1990s, particularly with the invention of methods to make mechanically interlocked molecular systems (catenanes and rotaxanes) and control and switch the relative positions of their components.[7−24]

Here, we review triggered large-amplitude motions in molecular structures and the changes in properties these can produce. We concentrate on conformational and configurational changes in wholly covalently bonded molecules and on catenanes and rotaxanes in which switching is brought about by various stimuli (light, electrochemistry, pH, heat, solvent polarity, cation or anion binding, allosteric effects, temperature, reversible covalent bond formation, etc.). Finally, we discuss the latest generations of sophisticated synthetic molecular machine systems in which the controlled motion of subcomponents is used to perform complex tasks, paving the way to applications and the realization of a new era of "molecular nanotechnology".

1.1. The Language Used To Describe Molecular Machines

Terminology needs to be properly and appropriately defined and these meanings used consistently to effectively convey scientific concepts. Nowhere is the need for accurate scientific language more apparent than in the field of molecular machines. Much of the terminology used to describe molecular-level machines has its origins in observations made by biologists and physicists, and their findings and descriptions have often been misinterpreted and misunderstood by chemists. In 2007 we formalized definitions of some common terms used in the field (e.g., "machine", "switch", "motor", "ratchet", etc.) so that chemists could use them in a manner consistent with the meanings understood by biologists and physicists who study molecular-level machines.[14]

The word "machine" implies a mechanical movement that accomplishes a useful task. This Review concentrates on systems where a stimulus triggers the controlled, relatively large amplitude (or directional) motion of one molecular or submolecular component relative to another that can potentially result in a net task being performed. Molecular machines can be further categorized into various classes such as "motors" and "switches" whose behavior differs significantly.[14] For example, in a rotaxane-based "switch", the change in position of a macrocycle on the thread of the rotaxane influences the system only as a function of state. Returning the components of a molecular switch to their original position undoes any work done, and so a switch cannot be used repetitively and progressively to do work. A "motor", on the other hand, influences a system as a function of trajectory, meaning that when the components of a molecular motor return to their original positions, for example, after a 360° directional rotation, any work that has been done is not undone unless the motor is subsequently rotated by 360° in the reverse direction. This difference in behavior is significant; no "switch-based" molecular machine can be used to progressively perform work in the way that biological motors can, such as those from the kinesin, myosin, and dynein superfamilies, unless the switch is part of a larger ratchet mechanism.[14]

1.2. The Effects of Scale

Machines need to be designed according to the environment in which they are intended to operate. The significance and consequences of random thermal motion, heat dissipation, solvation, momentum, inertia, gravity, etc., differ significantly at the molecular and macroscopic levels, meaning that nanoscale machines cannot simply mimic the mechanisms of their macroscopic brethren.

The forces with the greatest influence on dynamics in the nanoworld are not those we commonly rely on in the macroscopic world. For large objects, inertial terms, which depend on the mass of the particle, dominate motion. As particle size decreases to or below the micrometre scale, viscous forces and Brownian motion become dominant while momentum and gravity become increasingly irrelevant. This effect can be quantified by the Reynolds number (R) for a particle of radius a, velocity v in a medium of density ρ and viscosity μ:[25,26]

DOI: 10.1021/acs.chemrev.5b00146
Chem. Rev. 2015, 115, 10081−10206

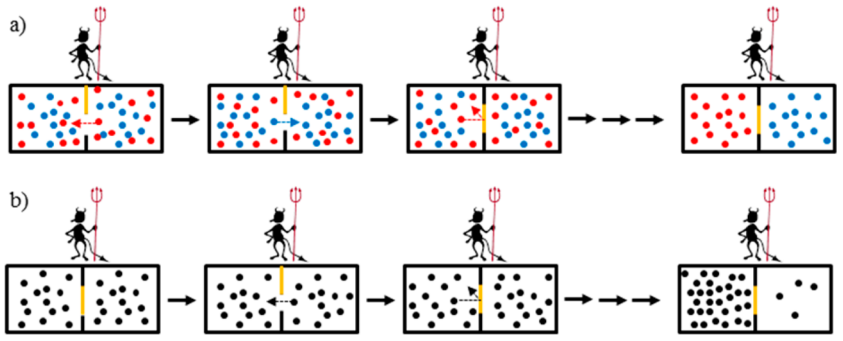

Figure 1. Maxwell's demons. (a) A "temperature demon" sorts particles according to velocity, generating a temperature gradient. (b) A "pressure demon" sorts particles according to their direction of movement, generating a pressure gradient.[37]

$$R = \frac{av\rho}{\mu} \quad (1)$$

Because the Reynolds number decreases with radius, molecular-sized machines typically operate under low Reynolds number conditions. Furthermore, the larger surface:volume ratio of small particles makes them increasingly adhesive, decreasing mobility. These effects must be carefully considered in the design of molecular machines.[14]

1.3. Thought Machines Exploring Brownian Motion

Molecular motors rely on exploiting random thermal fluctuations for directional motion by employing ratchet mechanisms. Thought experiments such as Maxwell's demon,[27,28] Smoluchowski's trapdoor,[29] and Feynman's ratchet-and-pawl[30] have investigated potential ways to cause the directional motion of Brownian particles.[31]

The Second Law of Thermodynamics states that the entropy of an isolated system tends to increase, leading to an equilibrium distribution with maximum entropy. To achieve any distribution other than the thermodynamic equilibrium, work must be done on the system. Various thought experiments have been proposed that attempt to violate this premise and drive a system away from equilibrium without expending work. In the Maxwell's Demon thought experiment, particles in a container are sorted by an "intelligent gatekeeper", the "demon" (Figure 1).[32] Gas particles are distributed in a container partitioned into two sections in an isolated system. The spontaneous formation of a heat or pressure gradient would lead to a decrease in entropy and thus violate the Second Law. The gatekeeper is able to detect the velocity of each particle and can control the gate accordingly. The demon allows particles with higher than average speeds (shown in red in Figure 1a) to pass from the right section to the left, but not from the left to the right. The opposite holds for slower particles (shown in blue in Figure 1a). The gatekeeper thus causes a nonuniform distribution of particles between the two sections, creating a temperature gradient. Similarly, a demon capable of detecting the direction of the particle and opening the gate accordingly can concentrate particles in one section and thus generate a pressure gradient (Figure 1b). If the gate is frictionless, then in both cases a nonequilibrium distribution has been achieved seemingly without doing work, which would violate The Second Law. The solution to the apparent paradox lies in considering the information required by the demon to know when to open the door. As the demon must measure the velocity or direction of each particle approaching the door[33] and cannot have infinite memory,[34] at some point the demon must "forget" this information. The destruction of information has a minimum enthalpic cost associated with it[35] as has been experimentally verified,[36] which always exceeds the decrease in entropy in the container. Thus, a local decrease in entropy is paid for by a generalized increase upon information deletion.

Smoluchowski proposed a system that did not rely on an intelligent observer based on a spring-loaded one-way gate, opened by thermal fluctuations (Figure 2a).[29,38,39] However,

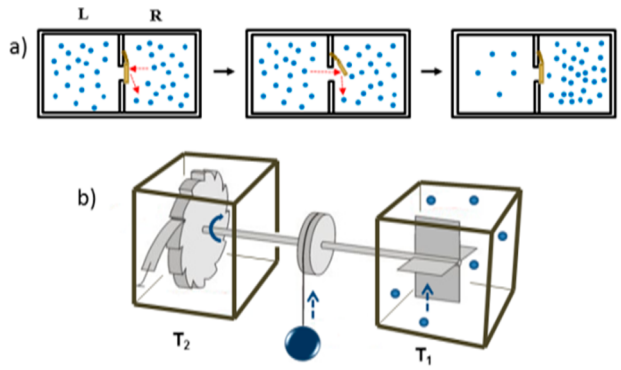

Figure 2. (a) In Smoluchowski's Trapdoor, a spring-loaded gate separates the two sections of a container. The lack of energy dissipation leads to a longer duration of opening and thus a uniform particle distribution between the sections.[29] (b) Feynman's ratchet-and-pawl device. The asymmetry of the teeth of the ratchet cog was intended to drive directional movement. However, when $T_1 = T_2$, the rotation is nondirectional.[30]

directional transport was proven to be impossible in this system as the gate is unable to dissipate energy from collisions with gas particles. This leads to ever longer open periods for the gate and so to equilibration of the particles across the container.

In Feynman's ratchet-and-pawl, the asymmetric cog teeth could have allowed directional rotation powered by Brownian motion (Figure 2b).[30,40−44] Although in line with the second law, no work could be extracted when $T_1 = T_2$ (the pawl is at the same temperature as the rest of the device and thus fluctuates between open and closed states and so fails to act as a ratchet), but work can be done when $T_1 > T_2$. This is an important point for the design of nanoscale machines. As the system moves from a nonequilibrium state toward equilibrium ($T_1 = T_2$), directional work can be done. Hence, if a nonequilibrium situation can be created, its relaxation can drive directional motion. In other words, an energy input is required to do work and to break detailed balance (see section 4.4).

1.4. Inspiration from Nature

Perhaps the most important lesson to learn from biological systems is that molecular machines are viable and can perform

DOI: 10.1021/acs.chemrev.5b00146
Chem. Rev. 2015, 115, 10081−10206

extremely complex tasks. In nature, molecular machines play a vital role, being involved in almost every major biological process and allowing a vast array of chemical and mechanical tasks to be accomplished.[45−47] The ways in which nature has overcome the problems of scale, Brownian motion, viscosity, nonequilibrium distribution and environment provide some general directions for the design of molecular machines.

Cellular processes are compartmentalized by lipid barriers, which allow nonequilibrium distributions to be built up and maintained. A range of molecular machines control the transport of various charged and polar species across these membranes using relay channels or mobile carrier entities.[48−50] This transfer can be driven by passive diffusion down a concentration gradient or by the generation of an electrochemical gradient (where a species is moved against its concentration gradient but down another gradient, such as electrical potential). If the motion is driven by the coupled transport of another system, the two species can migrate in either the same (symport) or opposite (antiport) directions across the membrane. Highly selective transport across lipid bilayers is made possible by the large number of specific channels and carriers in biological systems driven by the relaxation of transmembrane electrochemical gradients toward thermodynamic equilibrium.

These electrochemical gradients are maintained by only a few ion pumps, most commonly ATPases that hydrolyze ATP and generate directional transport using the resulting release of energy. Although the mechanism of directional motion in these motor proteins is not yet fully understood, conformational changes leading to altered binding affinities seem to be particularly important.[51−60] Access to the binding sites of these pumps is often "closed" by conformational changes after ion binding to increase the directionality of the process.[58,61]

Proton pumping across membranes is a particularly important process as it creates the proton motive force that drives ATP synthases' production of ATP, which in turn powers a large variety of active transport processes. This proton generated transmembrane potential is most commonly created by electron transport chains where redox reactions are used to separate charges across a membrane.[60] Proton pumping powered directly by light, as in bacteriorhodopisin (where *cis*/*trans* isomerization leads to directionality), is less common.[62−67] Interlocked structures are often exploited in biology to help ensure high sequentiality, for example, in the ribosome,[68−70] and various DNA polymerases.[71]

Biological molecular machines are used to transport cargo about a cell (e.g., kinesin), to power the movement of organisms (e.g., bacterial flagellar motors), to synthesize proteins (e.g., the ribosome), and to separate strands of DNA (e.g., helicases). There are many crucial differences between these machines and those familiar to us in the macroscopic world, in terms of both the tasks they accomplish and the manner in which they do so. Several concepts pertinent to the synthesis of artificial molecular machines can be extrapolated from these natural machines.

(1) Biological machines cannot use thermal gradients due to the rapid dissipation of heat at the scale on which they operate.

(2) Biological motors often use chemical energy from favorable bond forming/breaking events (e.g., ATP hydrolysis), or concentration gradients to drive their operation.

(3) Biomachines operate in solution and on surfaces under high viscosity conditions.

(4) Biological machines exploit Brownian motion rather than fight against it. They "ratchet" the random thermal motion of their components and substrates. Brownian motion also ensures the rapid mixing of machines, fuel, and substrates.

(5) Friction is irrelevant in such a viscous medium, where constant Brownian motion ensures the mobility of individual parts.

(6) Mobile biomachines, such as kinesin, often operate along tracks to reduce the available degrees of freedom of the machine. Kinetic association of the machine on track for the duration of operation is vital to achieve directed transport.

(7) Noncovalent interactions are often significant features of the structure and operation of biological systems.

(8) Biomachines are often made by self-assembly processes from a limited range of basic motifs such as amino acids, lipids, nucleic acids, and saccharides.

(9) Compartmentalization is often required to allow systems to be maintained and operate away from equilibrium.

(10) Small binding events can often cause large conformational changes.

Although biological molecular machines are of a level of complexity unattainable by the current generation of molecular machines, they are constricted by the evolutionary processes that gave rise to them and the environment in which they operate. Natural selection ensures that the first successful solution to a problem tends to be retained, and improved gradually over many iterations. These restrictions, in terms of chemistry, and solutions, do not apply to manmade systems. Biomachines also operate in a highly cluttered environment and thus must exhibit an extremely high tolerance to collisions with unrelated/unreactive species. Additionally, the study of less elaborate artificial systems may well give rise to a greater understanding of the sophisticated biological systems that inspired them. Nonequilibrium statistical mechanics can provide a more precise understanding of the basic mechanisms and processes used by the current crop of molecular machines and will be explored in the next section.

1.5. Directional Transport and Work under Brownian Motion

The Principle of the Detailed Balance provides important constraints on the relationship between equilibrium and rate constants. An understanding of this concept is important in the field of synthetic molecular machines and for the design of potential mechanisms for directional motion.[72−74] The Principle of the Detailed Balance states that, at equilibrium, each transition has an equal probability (and thus rate) of occurring in a forward or reverse direction (e.g., $k_1 = k_{-1}$). This means that at equilibrium no net flux is generated across any barrier and no task can be performed. This rules out the maintenance of an equilibrium by a cyclic process such as A → B → C → A; rather each substrate must be in equilibrium with every other that it is in exchange with, that is, A⇆ B + B ⇆ C + C ⇆ A instead. It follows that Smoluchowski's trapdoor could not operate as it would break the Principle of Microscopic Reversibility. Breaking detailed balance is a requirement of doing work at the length scales on which Brownian motion occurs.[75] Stochastic pumping breaks detailed balance using an oscillating parameter to generate net flux and maintain a nonequilibrium steady state, and is seen in nature, for example, in the ATPases.[76,77] Several theoretical

DOI: 10.1021/acs.chemrev.5b00146
Chem. Rev. 2015, 115, 10081−10206

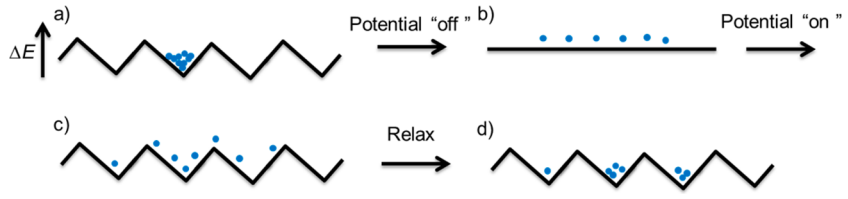

Figure 3. An on−off ratchet: (a) the particles are located in an energy minima, (b) the potential is turned off so that diffusion can occur for a short time, and (c) the potential is turned on again. As the potential is asymmetric, particles have a greater probability of being trapped in an adjacent well to the right of the original one than to the left. (d) Relaxation into the local energy minima leads to the average position of the particles moving to the right.[128]

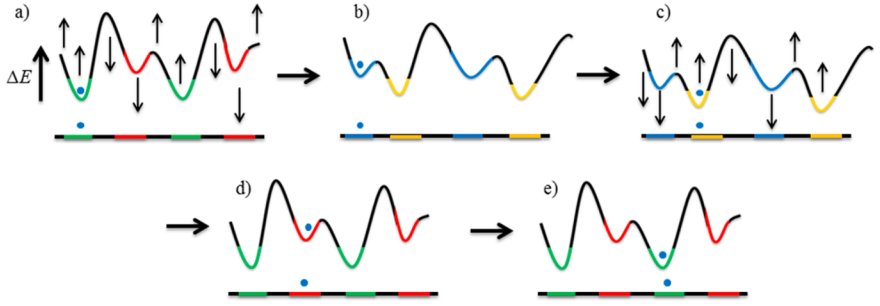

Figure 4. A flashing ratchet. In (a) and (c), the particle starts in a green or orange well, respectively. Raising this energy minima while lowering the adjacent maxima and minima triggers movement by Brownian motion (b) to (c) or (d) to (e). By continuously varying the relative heights of the energy barriers and minima of the energy wells, the particle can be directionally transported.[128]

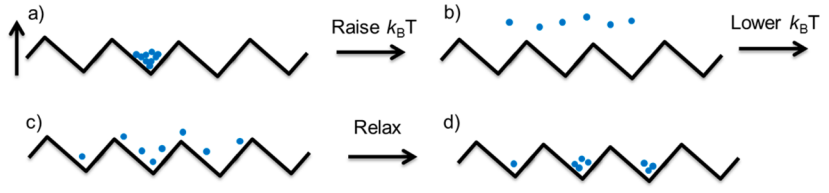

Figure 5. A temperature or diffusion ratchet. (a) The particles are located in an energy minima on the potential-energy surface, with energy barriers $\gg k_BT_1$. (b) The temperature is increased so that the height of the barriers is $\ll k_BT_2$, and free diffusion is allowed to occur for a short time. (c) As the temperature is lowered again, the asymmetric potential energy surface means that the particles have a greater probability of being trapped to the right of their initial position. (d) Relaxation to the local energy minima.[128]

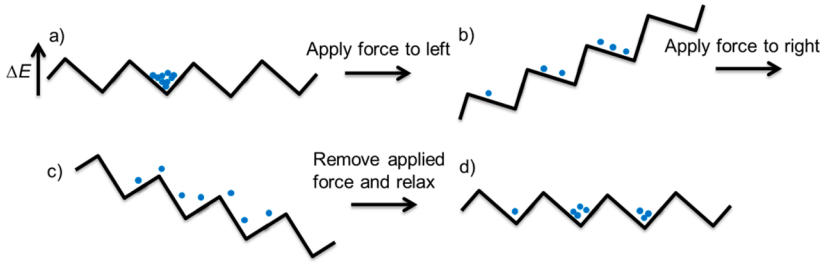

Figure 6. A rocking ratchet. (a) Particles are located in an energy minima on the potential energy surface. (b) A directional force is applied to the left. (c) An equal and opposite directional force is applied to the right. (d) Removal of the force and relaxation to an energy minima leads to the average position of the particles moving to the right.[128]

frameworks have been developed to explain various fluctuation driven transport modes such as stochastic pumping, which govern transport in Brownian motors and ratchets.[78−126] Some particularly relevant examples are discussed below.

1.6. Ratchet Mechanisms

Brownian ratchet mechanisms fall into two general classes: energy ratchets (pulsating and tilting ratchets are subcategories of energy ratchets) and information ratchets.[127−129]

1.6.1. Pulsating Ratchets. In pulsating ratchets, potential-energy minima and maxima are varied in a periodic or stochastic manner with no reference to the position of the particle on the potential-energy surface.[128] The simplest form is an on−off ratchet where the potential is repeatedly turned on and off more rapidly than the diffusion of the Brownian particles over their potential energy surface. This results in the net directional transport of particles across the surface (Figure 3).

A flashing ratchet is a subtype of the pulsating ratchet, consisting of a repeating series of maxima and minima. The sequential lowering and raising of parts of this potential energy surface leads to directional transport (Figure 4).

An asymmetric potential energy surface is not strictly necessary to generate a pulsating ratchet.[128] A periodic array of local minima traveling at a constant velocity (i.e., a traveling

DOI: 10.1021/acs.chemrev.5b00146
Chem. Rev. 2015, 115, 10081−10206

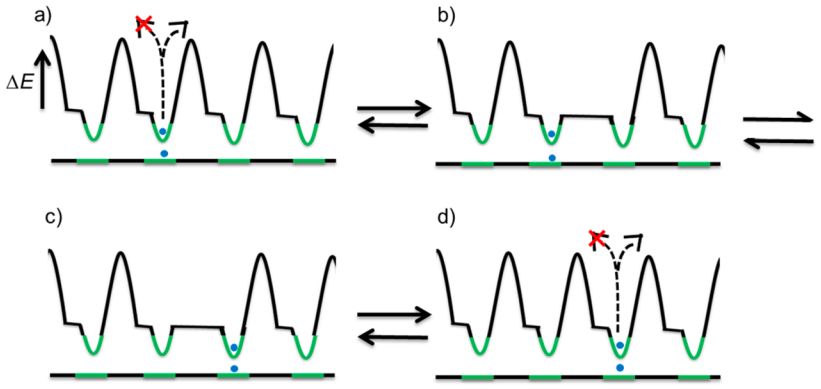

Figure 7. An information ratchet. In (a) and (d) the dotted lines represent the transfer of information about the position of the particle. (b) The position of the particle lowers the energy barrier to movement to the right-hand well but not the left. (c) The particle moves by Brownian motion.[128]

wave) can be used to form a traveling potential ratchet. In terms of realistic systems, the traveling potential ratchet mechanism has most relevance for the field-driven processes discussed in section 5 and the self-propulsion mechanisms of section 6.

1.6.2. Tilting Ratchets. In a tilting ratchet, the underlying potential energy surface remains unchanged, and detailed balance is broken by the application of an unbiased driving force to the particles, such as heat.[128] When the applied force is heat, the ratchets are also referred to as temperature or diffusion ratchets (Figure 5). In its simplest form, the mechanism is very similar to that of the on−off ratchet. Here, particles cannot cross the energy maxima at low temperature, but a brief increase in temperature allows the diffusion of particles across the surface. A lowering of temperature traps this movement in a manner similar to the on−off pulsating ratchet leading to directional transport. The period of raised temperature must be brief to prevent general diffusion, which would destroy any directionality initially gained.

Directional motion can also be achieved by the application of a periodic directional force to an asymmetric potential energy surface in a rocking ratchet. Although the net driving force averages to zero, directional motion is driven by exploiting the asymmetry of the potential energy surface (Figure 6).

Similarly, in a fluctuating force ratchet, the applied driving force is randomly generated and varies stochastically. Finally, in an asymmetric tilting ratchet, the particles lie on a symmetric potential energy surface, but the applied potential provides the required asymmetry. For example, in a rocking ratchet, the tilt in one direction would be longer than in the other.

1.6.3. Information Ratchets. Energy ratchets operate by the application of an external force or the modulation of a potential energy surface irrespective of the particle's position.[128] Information ratchets, on the other hand, rely on raising or lowering an energy barrier according to the position of the particle on the potential energy surface (Figure 7). This results in the distribution of particles being driven away from equilibrium. This process requires information transfer from the particle to the potential-energy surface, in a manner reminiscent of Maxwell's demon.

1.6.4. Language Necessary To Describe the Operation of Molecular Machines. Four terms are useful for describing the relationship of the components/substrates of molecular machines in terms of dynamics: balance, linkage, ratcheting, and escapement.[75] Having the components/substrates in a state of "balanced/unbalanced" or "linked/unlinked" plays a crucial role in determining whether or not a machine can perform a task. "Balance" is the thermodynamically preferred distribution of a particle (or submolecular component) in a molecular system. The trigger for net transportation comes from the balance being broken (i.e., the system being in a nonequilibrium state) (section 4.4). "Linkage" is the communication necessary for the transport of a particle between parts of the machine. However, the ability to exchange a particle between two parts of a machine does not necessarily allow a task to be performed, as a driving force is also required. Linking and unlinking operations are not limited to the addition or removal of steric bulk. They refer to any action that has an influence on the rate of a reaction. The movement of a particle up an energy gradient is described as ratcheting. It involves capturing the transitory positional displacement of a particle through the imposition of a kinetic energy barrier. Escapement is the counterpart to ratcheting in which the lowering of a kinetic energy barrier allows a ratcheted substrate to relax from a statistically unbalanced system toward a thermodynamic sink.

2. CONTROLLING MOTION IN COVALENTLY BONDED MOLECULAR SYSTEMS

2.1. Controlling Conformational Changes

2.1.1. Correlated Motion through Nonbonded Interactions. At room temperature, organic compounds typically fluctuate between rapidly equilibrating stereoisomeric structures through the perturbation (rotation, lengthening, and shortening) of covalent bonds. The relative stability and energy barrier to interconversion of configurational and conformational isomers depend on intramolecular and intermolecular interactions. The rotational and vibrational freedom of a single substituent of a molecule is not only determined by its connectivity, shape, and size, but also its interactions with neighboring substituents.[130−133] For example, Mislow et al. demonstrated the steric influence of neighboring groups on rotation as part of their work on molecular propellers such as compound **1** where two or more aryl rings are attached to a single atomic center (Z) (Figure 8). The rotation of one aryl ring about a C−Z axis is sensed by the other rings. Mislow suggested that the motion of the rings is coupled in the sense that none of the rings move independently of the others and described such correlated motion as "sympathic".[130,134−138]

Öki's group conducted pioneering investigations into restricted rotation about sterically hindered single bonds in molecules such as 9-arylfluorenes and triptycenes.[140−149] These molecules showed very high rotational barriers, and, in some

DOI: 10.1021/acs.chemrev.5b00146
Chem. Rev. 2015, 115, 10081−10206

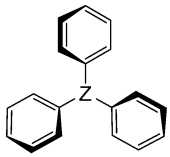

1

Figure 8. Chemical structure of a triaryl molecule as an example of a molecular propeller.[130,139]

cases, it was possible to isolate the rotational isomers (rotamers). Inspired by this work, Mislow and Iwamura simultaneously introduced the concept of dynamic gearing of proximate substituents in crowded molecules in molecular analogues of propellers and bevel gears.[150−167] The first molecular bevel gear consisted of two 9-triptycyl groups joined through their bridge head carbons to a central atom (Figure 9). Experimental and theoretical studies confirmed that the triptycyl groups are tightly intermeshed and undergo correlated disrotatory motion.[150,156]

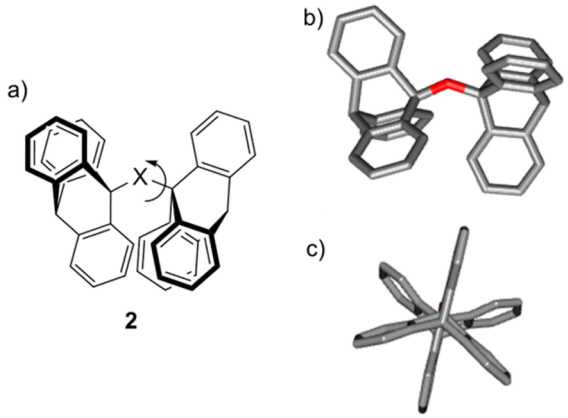

2

Figure 9. (a) Molecular bevel gear **2**, consisting of two 9-triptycyl groups joined through a bridge head carbon to a central atom.[150] (b) X-ray structure of the molecular bevel gear (side view). (c) X-ray structure of the molecular bevel gear (top view). Adapted with permission from ref 156. Copyright 1984 American Chemical Society.

Many other examples of dynamic gearing have since been published including a range of triptycene derivatives,[168−174] metallocene-based gears,[175,176] conformationally restricted amides,[177−181] and a series of propeller molecules and other molecules with selective rotation,[132,133,139,182−194] such as 1,2-di-*o*-tolylnaphthalene moieties.[195,196]

The sandwich-shaped trinuclear silver(I) complex $[Ag_3(\mathbf{3})_2]$ (Figure 10) developed by Shionoya and co-workers[197−199] is an example of a different type of a rotational device. The complex consists of two disk-shaped ligands, **3**, consisting of three thiazolyl or 2-pyridyl ligands and three *p*-tolyl groups attached to a central benzene ring. The three *p*-tolyl groups force the neighboring ligands to adopt a nonplanar arrangement with respect to the central aromatic ring, and make the coordination sites more accessible for silver(I) cations. The exterior rings tilt at 30° in the same sense and thus form helical structures with *P* and *M* geometries. A change from *P* to *M* helicity, and vice versa, was induced by 120° relative rotation of the ligand in these complexes (Figure 10). These observations were further studied using a heterotopic system $[Ag_3(\mathbf{3})(\mathbf{4})]$ consisting of a hexa-monodentate ligand **4** and a tris-monodentate thiazolyl ligand **3**, which complex three silver(I) cations.[200] In the case of the hexa-monodentate thiazolyl ligand **4**, only every second ring is coordinated to a silver cation. Correlated flipping motion of the coordinating rings (and ligand exchange) results in the conversion from *M* to *P* and a 60° rotation of the two disks (Figure 10d).

Related heterotopic complexes were later used to transform the rotational motion of the sandwich-shaped trinuclear silver(I) complex into translational motion using a molecular crank mechanism. In molecular crank **5**, a [2]rotaxane was attached as a translational segment (Figure 11).[201]

Recently, Anderson et al. reported a zinc-porphyrin macrocycle coordinated by two templates containing multiple pyridines (wheels) forming a caterpillar track complex.[202] NMR exchange spectroscopy (EXSY) experiments showed that the ring underwent correlated motion with correlated motion of the templating "wheels".

The examples shown in this section clearly show the influence that steric interactions can have on submolecular motion. However, at equilibrium, these motions are nondirectional, even during a partial rotation.

2.1.2. Stimuli-Induced Control of Conformation about a Single Bond. An early example of controlled random rotary motion about a single bond was provided by Kelly et al.,[203−205] who utilized a cation binding event to halt the free rotation of a triptycene moiety in "molecular brake" **6** (Scheme 1). The two pyridine groups must be coplanar to maximize binding with Hg^{2+}, thus raising the energy barrier to rotation by "putting a stick in the spokes". Sulfur oxidation has similarly been used to inhibit free rotation in **7** with mono- or dioxidation significantly slowing the rotation.[206] Rotation about a single bond has also been promoted by substrate protonation by Shimizu and co-workers in **8**.[207] Protonation of the quinoline nitrogen led to an increase in the rate of rotation by 7 orders of magnitude, through a proposed hydrogen-bonding stabilization of the rotation transition state (Scheme 1). The same group observed that utilizing an acetate guest's hydrogen-bonding interactions to "turn on" rotation provided a more modest accelerating effect.[208] Again, this was suggested to be via a lowering of the energy of the rotational transition state. Other examples have also been reported.[209,210]

Singlet oxygen has been used to promote rotation in combination with thermal relaxation in a system based on rotation between the *cis* and *trans* isomers of **9** (Scheme 2). Reaction with singlet oxygen forms the *cis*-substituted 9,10-endoperoxide selectively. Thermal reversion generates the *cis*-anthracene, which upon extensive heating furnishes the more thermodynamically stable *trans*-anthracene **9**, completing the cycle.[211]

Kelly and co-workers reported an attempt to create a Feynman adiabatic ratchet-and-pawl.[212−214] The design utilized a helicene pawl whose inherent helical chirality was intended to bias the rotation of the triptycene cog. Although this design realizes an asymmetric potential energy surface, ^{1}H NMR showed no directional bias with equal rates of rotation in both directions. This is in line with Feynman's thought experiment[215] and illustrates that the rate of rotation depends solely on transition state energy and temperature, and not on the shape of the barrier to rotation. State functions, for example, free energy, do not depend on the system's history (Figure 12).

The key factor required to break detailed balance and allow directional motion of the triptycene cog is an energy input to drive the system away from equilibrium. Although a rapid periodic variation in temperature could in theory cause the system to act as a temperature ratchet, it would be very difficult to

DOI: 10.1021/acs.chemrev.5b00146
Chem. Rev. 2015, 115, 10081−10206

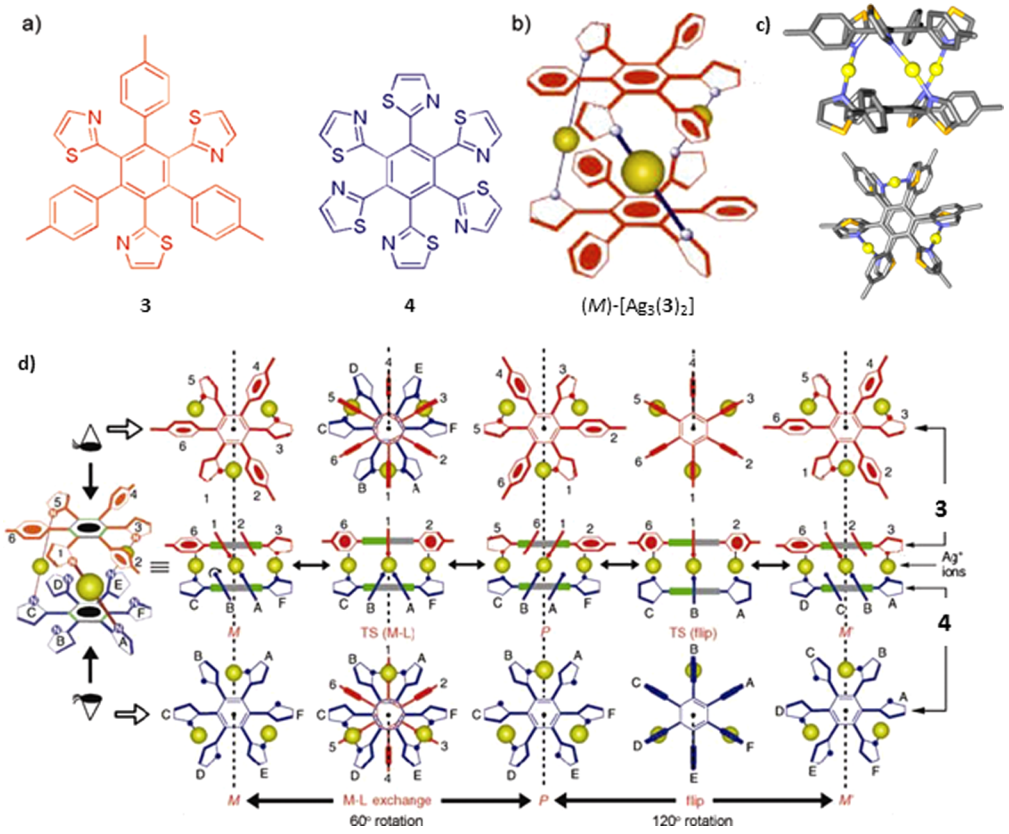

Figure 10. (a) Chemical structure of tris-monodentate disk shaped ligand **3** and hexakis-monodentate ligand **4**. (b) Schematic representation of complex $[Ag_3(\mathbf{3})_2]$ shown as its *M*-helical enantiomer. (c) X-ray structure of complex $[Ag_3(\mathbf{3})_2]$.[197] (d) Schematic representation of the flipping motion of the rings attached to the disks and subsequent ligand exchange from 1-A, 3-E, and 5-C in *M* to 1-B, 3-F, and 5-D in *P*. The direction of rotation in the *M* to *P* transition is opposite to that of a subsequent *P* to *M*′ transition.[200] Reprinted with permission from refs 197 and 200. Copyright 2003 and 2004 Wiley-VCH Verlag GmbH & Co. KGaA, Weinheim.

verify this experimentally. As such, Kelly et al. instead proposed the modified structure **11**,[216,217] where a chemical reaction drives the system from equilibrium (Scheme 3). The helicene pawl oscillates in the energy minima between blades, and, ignoring the amine group, all three minima are identical. Formation of the isocyanate from reaction with phosgene activates the system. In the course of random fluctuations, sometimes the helicene is close enough to the isocyanate to react. After reaction, the helicene is trapped part way up the energy barrier; that is, the helicene is "ratcheted" part way to rotation. Random thermal fluctuations may then overcome the smaller barrier to rotation, and the urethane can be cleaved to give overall 120° rotation. This machine is a landmark achievement in the realization of chemically fueled directed rotation in molecular machines and demonstrates most of the basic tenants of a directional motor. However, attempts to modify the rotor to allow 360° rotation have thus far failed.[218]

Mock and Ochwat have proposed a minimal molecular motor in which epimerization of a stereogenic center, that is, a formal 180° rotation, is driven by the hydration of a ketenimine fuel.[219] A biaryl lactone motif reported by Branchaud has been used to control motion about a single bond in a nondirectional rotor based on the facially selective ring opening of a chiral lactone.[220] They later improved on this system to report 180° directional rotation.[221] Feringa et al. achieved full 360° directional motion about a single bond in a related biaryl system (Scheme 4).[222,223] Rotation was driven by four sequential chemical "power strokes" with felicity of rotation for each step being between 90% and 100%. The cycle involved four conformationally restricted intermediates, **12**−**15**, with **12** and **14** locked by covalent bonds, and **13** and **15** locked by their steric bulk. Although **13** and **15** are free to dynamically equilibrate between helical forms, the chiral information in the reducing agent is used to discriminate between them and thus drive directional motion. The first step involved asymmetric ring opening with the (*S*)-CBS reagent, and regioselective protection of the resulting phenol with an allyl group. After oxidation and PMB deprotection with spontaneous lactonization, 180° rotation was achieved. Another stereoselective ring opening and regioselective phenol protection as the PMB ether followed, before oxidation and ring closure furnished the product of 360° rotation in high fidelity. Additionally, rotation in the opposite sense can be achieved by utilizing the (*R*)-CBS reagent and reversing the order of PMB/allyl protection.

2.1.3. Stimuli-Induced Conformational Control in Organometallic Systems. Control of the rotary motion of ligands in metal sandwich or double-decker complexes is somewhat conceptually similar to controlling rotation around covalent single bonds. Aida and co-workers demonstrated that porphyrin ligands in double decker complexes such as **16** can rotate with respect to each other depending on the central metal atom and their steric bulk (Figure 13a).[224,225] Studies on a variety of metal complexes found that the central metal had an influence on the speed of rotation.[226] Complexes synthesized from two D_{2h} symmetry porphyrin free-bases are chiral, and therefore their rotary motion corresponds to enantiomerization and can thus be

DOI: 10.1021/acs.chemrev.5b00146
Chem. Rev. 2015, 115, 10081−10206

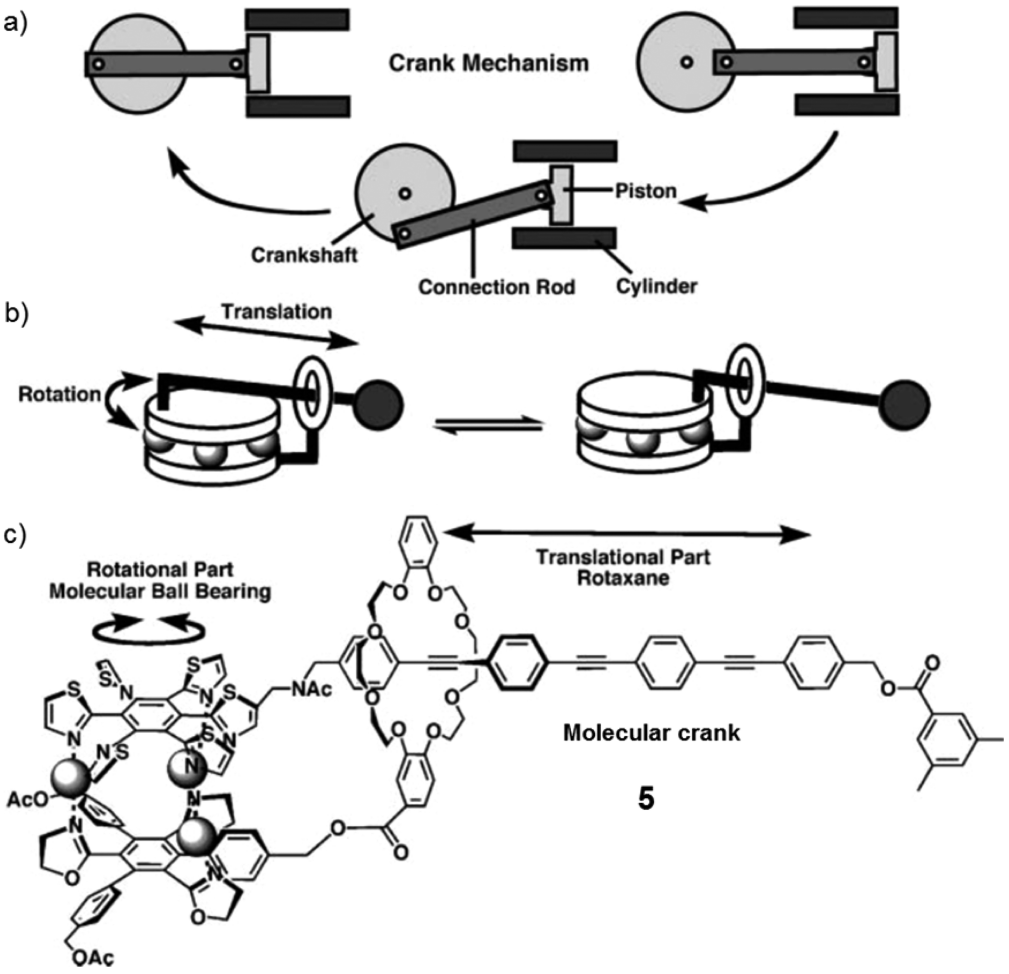

Figure 11. (a) Schematic illustration of a crank mechanism that translates linear motion into rotary motion in cylinder engines. (b) Schematic representation of a molecular crank mechanism. (c) Chemical structure of a synthetic molecular crank **5**.[201] Reprinted with permission from ref 201. Copyright 2010 Royal Society of Chemistry.

Scheme 1. Molecular Brakes Operated by (a) Hg^{2+} Binding and (b) Sulfur Oxidation; and (c) Proposed Transition State Stabilization in Shimizu's System[203,206,207]

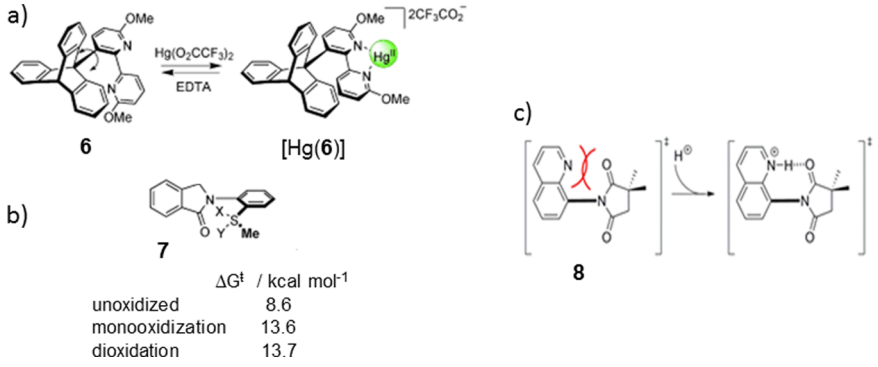

studied by CD spectroscopy. Racemization can be induced by protonation or reduction of the metal center. The second reduces $\pi-\pi$ interactions between the two ligands as a consequence of the larger ionic radius of the metal center.[227]

It was shown that the rotation of the cerium(IV) bis[tetrakis-(4-pyridyl)porphyrinate] **17** could be suppressed by successive cooperative guest binding of dicarboxylic acids (Figure 13b).[229,230] The double decker complex shows a large allosteric effect in this molecular recognition event (once rotation has been suppressed by the first guest molecule, guest binding becomes increasingly favorable). Further guest molecules have been tested such as β-dicarboxylate anions,[231] potassium ions,[232] mono- and oligosaccharides,[233−235] and silver cations.[236] In the case of silver ions, it was shown that their cooperative binding leads to a progressive and nonlinear increase in the rate of rotation.[237−244] The rotation of a similar cerium double decker complex has been monitored on a single molecule level, by the attachment of a bead visible under optical microscopy.[245]

Ever more complicated systems such as multidecker pophyrin complexes[246] and mechanically interlocked porphyrin systems

DOI: 10.1021/acs.chemrev.5b00146
Chem. Rev. 2015, 115, 10081−10206

Scheme 2. A Molecular Switch Flipped by Singlet Oxygen[211]

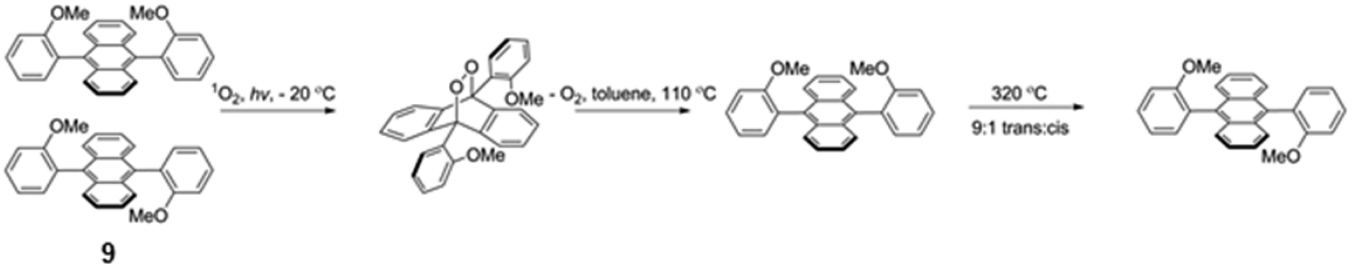

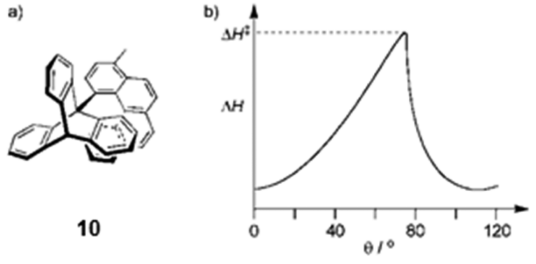

Figure 12. (a) Kelly's ratchet-and-pawl **10**. (b) Enthalpy change on rotation of helicene. Reprinted with permission from ref 212. Copyright 1997 Wiley-VCH Verlag GmbH & Co. KGaA, Weinheim.

like **18** have been synthesized (Figure 14).[247−249] The latter consist of cerium(IV) or lanthanum(III) bis(porphyrinate) double decker complexes and one or two orthogonal porphyrin molecules. In these "molecular gears", the rotation of the top and side units could be partially coupled through mechanical interactions between the different units. A folding ruler based on similar principles has been reported.[250] A dodecanuclear four level complex that mimics a double ball bearing has also been synthesized.[251]

Ferrocene is a prototypical sandwich complex with an iron atom symmetrically aligned between two C_5H_5 (cyclopentadienyl) rings.[252,253] The barrier to rotation of the two rings about the C_5 axis is very small in the gas phase. Using electrospray ionization and theoretical studies, it was shown that ferrocene derivative $\mathbf{19}^{2-}$ can serve as a two-state rotary switch, which works through proton transfer (Scheme 5). Differing electrostatic interactions lock $\mathbf{19}^{2-}$ and $[\mathbf{19}\cdot H]^-$ in two different conformations. The *trans* conformation of $\mathbf{19}^{2-}$ is more stable because of Coulombic repulsion between the negative charges, while the *cis* conformation of $[\mathbf{19}\cdot H]^-$ is stabilized through hydrogen bonding (Scheme 5).

This finding was followed by studies of many more ferrocene derivatives, and the control of their rotary motion through different stimuli such as electron transfer and photochemistry.[254,255] Ferrocene-based rotors have recently been used to form self-assembled nanostructures.[256]

Metallocarboranes tend to have rather high barriers to rotation around the metal−ligand axis, but some complexes, for example, nickel complex $[Ni(\mathbf{20})_2]$, can be used as electrochemically controlled rotary switches (Figure 15).[257−261]

2.1.4. Stimuli-Induced Conformational Control over Several Covalent Bonds. In biological systems, host−guest binding is often used to induce conformational and functional changes. These changes can vary from small, localized, bond deformations to long-range rearrangements across multiple covalent bonds. These deformations are frequently used to alter binding at distal sites, that is, allosteric regulation. There are several synthetic examples where host−guest binding causes a sufficiently large amplitude change to merit discussion in this Review. Some of the earliest examples of allosteric receptors came from Rebek and co-workers.[262] For example, the binding of tungsten by negative allosteric receptor **21** reduces the receptor's affinity for potassium ions, as in this more rigid conformation binding to potassium would induce a degree of strain (Scheme 6).[263,264] The positive allosteric receptor **22** developed by the same group depends on the initial mercury binding event preorganizing the linked receptor for a second, more favorable binding event.[265] These early examples have sired an extraordinary and diverse array of synthetic allosteric receptors.[262,264,266−279]

Scheme 3. Chemically Driven Directional 120° Rotation of Kelly's Triptycene Rotor 11[216]

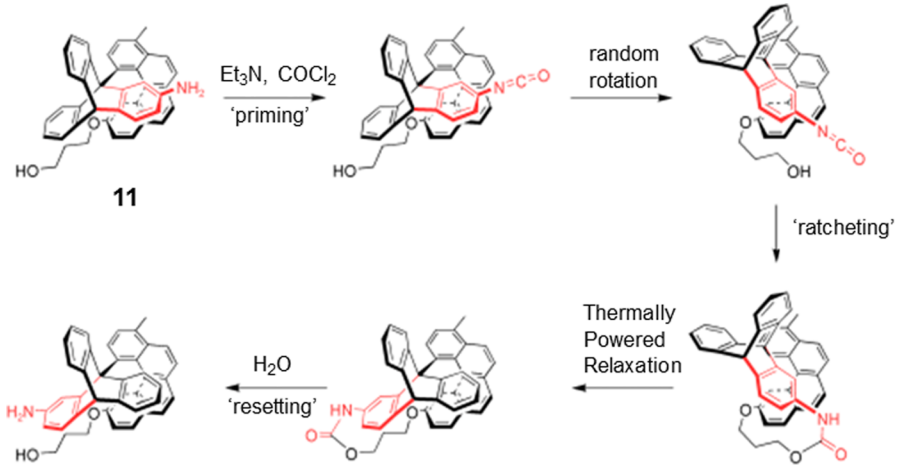

DOI: 10.1021/acs.chemrev.5b00146
Chem. Rev. 2015, 115, 10081−10206

Scheme 4. Directional 360° Rotation about a Single Bond via Four States A–D[a]

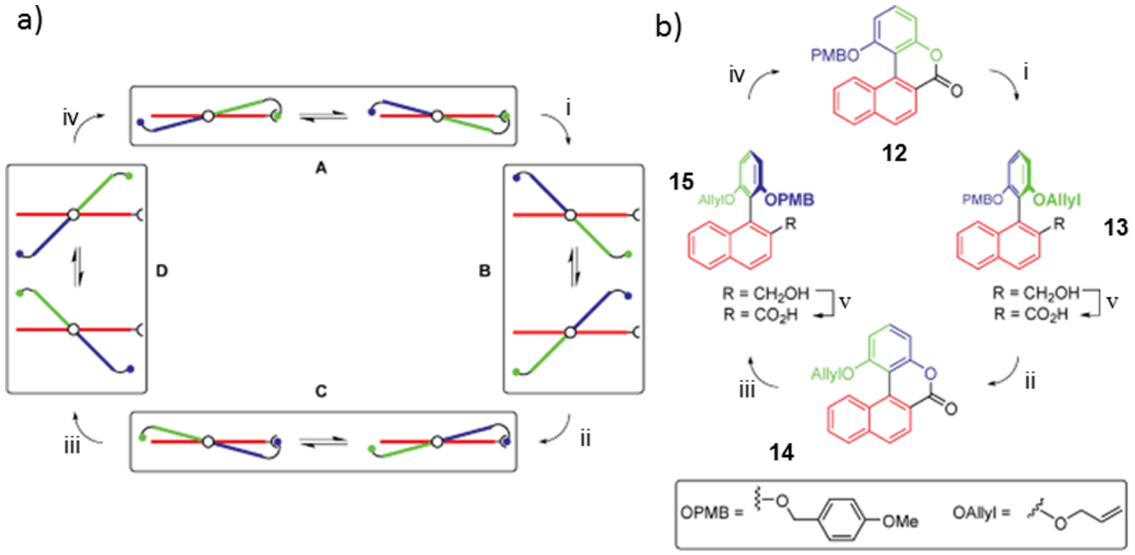

[a]Rotation is restricted in **A** and **C** by covalent bonds, although helical inversion is allowed, and in **B** and **D** by nonbonded interactions, with directional control of rotation being provided by stereospecific covalent bond cleavage.[222]

Organic guests can also cause large-scale changes to host molecules, as they maximize favorable interactions such as in molecular tweezer **23** (Figure 16) where the distance between sidewalls halves on binding certain guests.[280,281] A large amplitude change was observed in the flexible system **24** with an extended conformation being exchanged for a more rigid "sandwich" form to maximize guest binding.[282] Guest-induced change is also observed in clip **25** where the **sa** form predominates in solution in the absence of a guest, but the **aa** form dominates in the presence of a suitable guest (Figure 16).[283−285] This system has been further modified in **26** where the binding of a potassium ion to each crown ether preorganizes the system for organic guest binding with increased affinity.[286]

Metal coordination has been used by Lehn et al. to switch from an arrangement where parallel anthracene units can bind electron-poor 2,4,7-trinitro-9-fluorenone (TNF) in a tweezer-like manner, to an open form **27** (Scheme 7). Here, coordination of copper in a bidentate manner by the aromatic nitrogens causes a rotation about the heterocyclic axis and opens the guest binding cavity, preventing TNF coordination. In related **28**, zinc coordination is a prerequisite of TNF binding.[288]

A notable example of chelation control of conformation was provided by trisaccharide **29** (Scheme 8). Although the tetra-equatorial isomer is the dominant form in solution,[289] the addition of Pt(II) led to coordination, and a preference for the tetra-axial form, the better to bind the metal ion. This process could be reversed by removal of the Pt(II) with excess NaCN.[290,291] This process has been replicated with a variety of cyclic substrates using both metal ion binding[292−294] and pH variation.[295−297] Sauvage reported the collapse of a porphyrin containing [4] rotaxane on copper removal.[298] Haberhauer's molecular hinge, **30**, based on a 2,2′-bipyridine motif, is another example of large amplitude motion controlled by coordination of a metal ion. In this case, the open system was free to rotate over 180° with its rotation being constrained by an inflexible backbone. Upon coordination of Cu(II), the hinge shut. Upon copper removal, the hinge was again able to open, but only in one direction due to the constraints of the backbone.[299] A light-driven switch and a chirality pendulum based on a similar system have been reported by the same group.[300,301]

Cavitands derived from resorcin[4]arenes have been shown to undergo large conformational changes between open "kite" and closed "vase" forms of **31** (Scheme 9).[302] Because of solvation effects, the kite form is normally favored at lower temperatures and the vase at higher.[302−304] However, this change has also been achieved using protonation of or metal coordination to the quinoxaline nitrogens,[305−308] or by altering the design to incorporate redox-active centers.[309,310] Substitution of the cavitand with amide groups can lead to stabilization of the vase form by dimerization or guest complexation.[311−320] As an alternative to coordination of a guest causing a change in conformation, complexation can be intramolecular as in macrocycle **32** reported by Stoddart et al. The system rests in the self-complexed form until reduction of the cyclophane decreases subcomponent interactions, followed by release of the system to an unrestrained, unencapsulated form.[321−326] A similar system, **33**, was realized by Feringa and Qu[327] with directional rotation inhibited in the complexed state, but allowed when uncomplexed (Scheme 9).

Hamilton and co-workers introduced conformational switch **34** (Scheme 10) where in the initial state the equilibrium is mildly biased toward the benzamide station (1.3:1). Upon protonation of the dimethylamine with TFA, a dramatic reversal of this bias is observed (1:99).[328] The oxidation of a copper center has been used to trigger coupled rotation and copper exchange between two independent switches (based on the structure shown in Scheme 45).[329]

Oligomeric systems have been used to great effect in generating large-scale conformational changes, often exploiting the helical secondary structures that can be formed by many species.[330−367] Polyamide **35** resides in a helical arrangement, but protonation of four diaminopyridine units causes a dramatic extension to the linear form of **35** (Scheme 11). Further protonation leads to another helical form, and the system can be returned to its initial form by deprotonation.[330] An extension of this system was shown to expand from 12.5 to 57 Å upon protonation.[368] An alternating pyridine and pyrimidine oligomer

DOI: 10.1021/acs.chemrev.5b00146
Chem. Rev. 2015, 115, 10081−10206

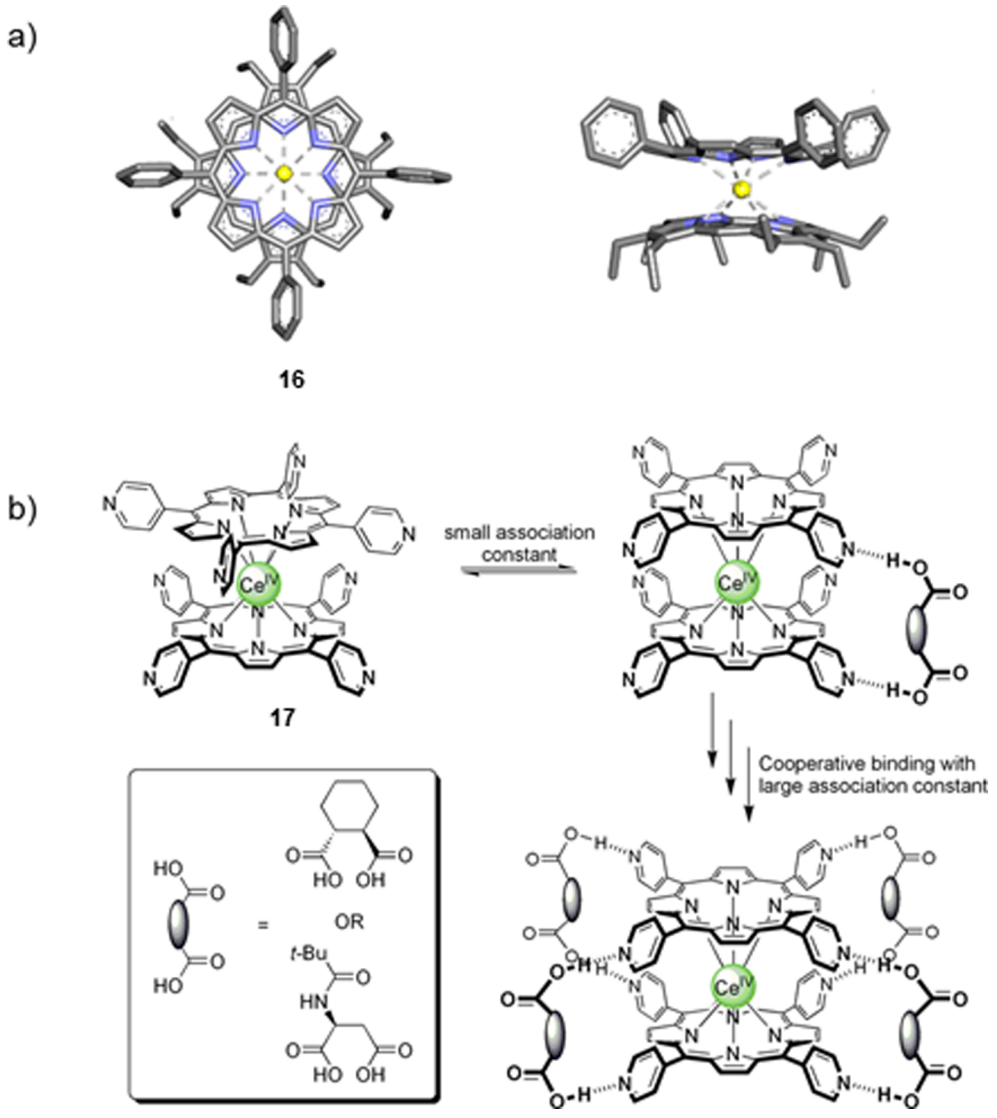

Figure 13. (a) X-ray crystal structure of porphyrin double decker complex **16** with cerium(IV). Reprinted with permission from ref 228. Copyright 1989 Wiley-VCH Verlag GmbH & Co. KGaA, Weinheim. (b) Representation of the cooperative binding of guest molecules to porphyrin double decker complex **17**.[229]

formed helices (due to the favored disposition of neighboring rings being transoid), but upon addition of Pb(II) to **36**, coordination led to a linear form with a concurrent increase in length from 7.5 to 38 Å (Scheme 12). This process could be made switchable by sequestering the Pb(II) until needed in pH responsive cryptand **37**.[369] A similar process has been achieved using Ag(I) to modulate expansion.[370]

An interesting recent example was provided by Stadler and Lehn[371] where a linear and a helical domain were synthesized in the same molecule. In this two-domain system, coordination of Pb(II) led to the unfurling of the helical domain with concurrent curling of the linear portion of the molecule. Upon removal of Pb(II), the system reverted to its original state, thus representing a reversible device where an extension process is coupled to a furling one, on both complexation and decomplexation of a metal ion.

2.2. Controlling Configurational Changes

Changes in configuration, especially *cis*/*trans* isomerization, have been used in many molecular systems to control motion.[372] Although the sometimes small amplitude motion is not always useful for the design of molecular machines, it represents an interesting tool for inducing directional motion in synthetic and supramolecular systems. The most prominent examples of this type of system are the photoisomerization of stilbenes and azobenzenes,[373−377] the reversible electrocyclization of diarylethenes,[378−382] the photochromic reactions of fulgides,[383,384] the interconversion of spiropyrans with merocyanin,[385] as well as chiroptical switching of overcrowded alkenes.[386−388] In recent years, this topic has become an extensive area of research, and a wide range of applications exploiting switchable systems have been proposed and realized.[389−395] Most of these applications rely on intrinsic electronic and spectroscopic changes on interconversion between the two species, but some use small configurational changes in a more mechanical fashion, and the resulting devices can be seen as molecular machines.

Configurational changes, especially the photoisomerization of azobenzenes, have been used to induce changes in the structures of biologically relevant molecules such as antibiotics, peptides, and DNA,[374,396−406] but also as part of small-molecule systems such as molecular scissors, tweezers, and other molecular

DOI: 10.1021/acs.chemrev.5b00146
Chem. Rev. 2015, 115, 10081−10206

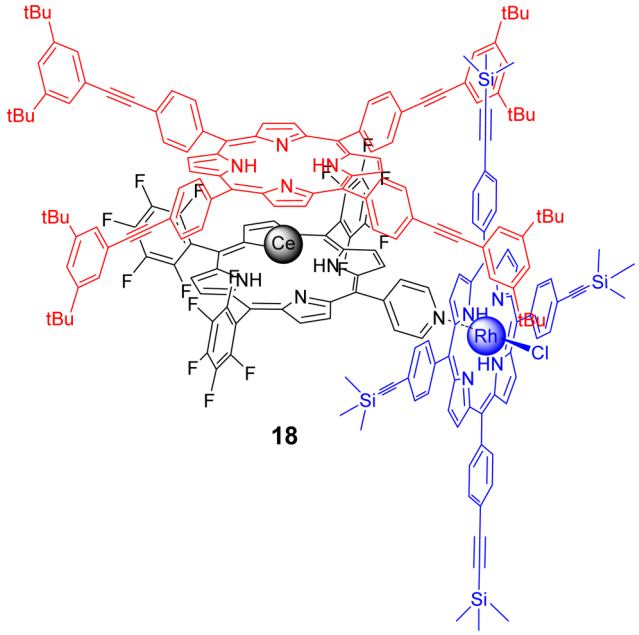

Figure 14. Cerium(IV) bis(porphyrinate) double decker (top unit) and a rhodium(III) porphyrin-based side cog. The two units are connected through a coordination bond between rhodium(III) and a pyridyl group.[249]

Scheme 5. Control of Rotation in Ferrocene Complex 19 through Protonation[253]

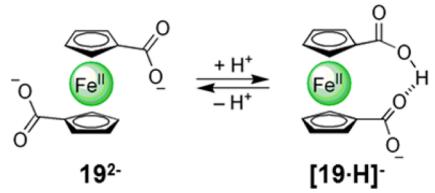

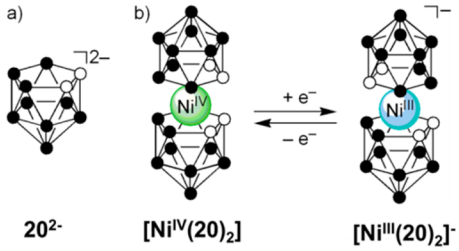

Figure 15. (a) Dicarbollide ligand $\mathbf{20}^{2-}$. (b) Metallocarborane [Ni(**20**)$_2$], an electrochemically controlled rotary switch.[261]

machines.[407−412] Some of them will be introduced in the following section.

Molecular scissors **38**, described by Aida and co-workers, consist of an azobenzene unit and a ferrocene unit (Scheme 13a).[413,415] The open and closed forms were interconverted by photoisomerization of the double bond of the azobenzene unit, which led to an angular change of 49° around the cyclopentadienyl rings of the ferrocene. Another example was the synthesis of the molecular hinge **39** where two xanthene rings were connected by −N═N− linkers (Scheme 13b).[414] Photoisomerization at 366 nm from the *trans*/*trans*, which is almost planar, to the *cis*/*cis* state resulted in a change of approximately 90° in the angle between the two aromatic rings. Reisomerization could be achieved by irradiation at 436 nm. Azobenzenes have been used for the construction of photoswitchable azomacrocycles.[389,416] Azo-macrocycles have found applications in host−guest chemistry as they can selectively and reversibly bind ions. Cyclic azobenzenes have been used to switch on or off the rotation of subunits.[417,418] A recent example showed that the rotation of a 2,5-dimethylbenzene rotor in the cyclic azobenzene **40** could be switched off in the *E*-isomer of the azobenzene, while rotation was allowed in the *Z*-isomer (Figure 17).

Azobenzenes have also been used to control motion in molecular shuttles (see also section 4.3) and to control the threading and dethreading rate of a macrocycle when attached to the ends of a thread. In a recently published example, $E \rightarrow Z$ photoisomerization of azo-end groups slowed the threading−dethreading of a ring and turned the pseudorotaxane into a kinetically inert rotaxane.[419]

The substitution of an alkene can lead to steric overcrowding around a double bond. When the substituents are large enough, the planarity of the double bond can be disrupted and a variety of twisted and folded conformations can be adopted, including helices. The area where the substituents come into close proximity is often referred to as the fjord region. These types of compounds still undergo photoisomerization and can be used as chiroptical molecular switches.[386,420,421] Feringa et al. have developed several molecular motors exploiting overcrowded alkenes as chiroptical molecular switches.[422−428] The first generation of this molecular motor (Scheme 14, compound **41**) featured two identical halves connected by a central double bond.[429−436] Each of the halves had a stereocenter, which was crucial to controlling the rotational process. Rotation of 360° around the double bond was repetitive and directional. Two light induced *cis*−*trans* isomerizations led to a 180° rotation and were each followed by thermally controlled helicity inversion, which effectively blocked reverse rotation. The *cis*−*trans* photoisomerization was evident from ^{1}H NMR, and the simultaneous exchange of *P* to *M* was detected by circular dichroism (CD). A number of different structures have been synthesized to optimize the rotation process and to explore the limits of the system.[437−444]

In the second generation of Feringa's molecular motor **42**, two halves that are not identical were connected by a central double bond.[445−447] One half was replaced by a tricyclic aromatic group and there was only one stereogenic center present, but the rotation operated according to the same principles as the first generation motor **41** (Figure 18). Some dramatic enhancements of rotary speed were achieved in the second generation of motors.[428,448−453]

Feringa and co-workers have shown that transmission of molecular rotation from one part of a molecule to another is possible. In motor **43**, a xylyl unit was attached to the lower half of an overcrowded alkene-based switch. By switching between the *cis*- and *trans*-forms, the rotation of the xylyl group could be controlled (Figure 19).[454,455] Imines have recently been used as directional light-driven rotors by Lehn and Greb.[456]

It has long been known that irradiation of hydrazones can induce $E \rightarrow Z$ isomerization around the imine bond (C═N). However, the *Z*-isomer is usually thermodynamically unstable and thus short-lived.[457,458] Intramolecular hydrogen bonding in various hydrazone derivatives can kinetically stabilize the *Z*-isomer, which is formed by irradiation.[459−461] The Aprahamian group has studied the *E*/*Z* isomerization of hydrazones using chemical switching inputs such as protons and zinc ions.[462−467]

In their original system, $E \rightarrow Z$ isomerization was induced by protonation of a pyridyl ring that initially acts as an intra-

DOI: 10.1021/acs.chemrev.5b00146
Chem. Rev. 2015, 115, 10081−10206

Scheme 6. (a) Negative Allosteric Receptor 21, Where Binding of Tungsten Forces Ring Contraction and Steric Clash of the 3- and 3′-Substituents of the Bipyridyl Unit; and (b) Positive Allosteric Receptor 22[263,264]

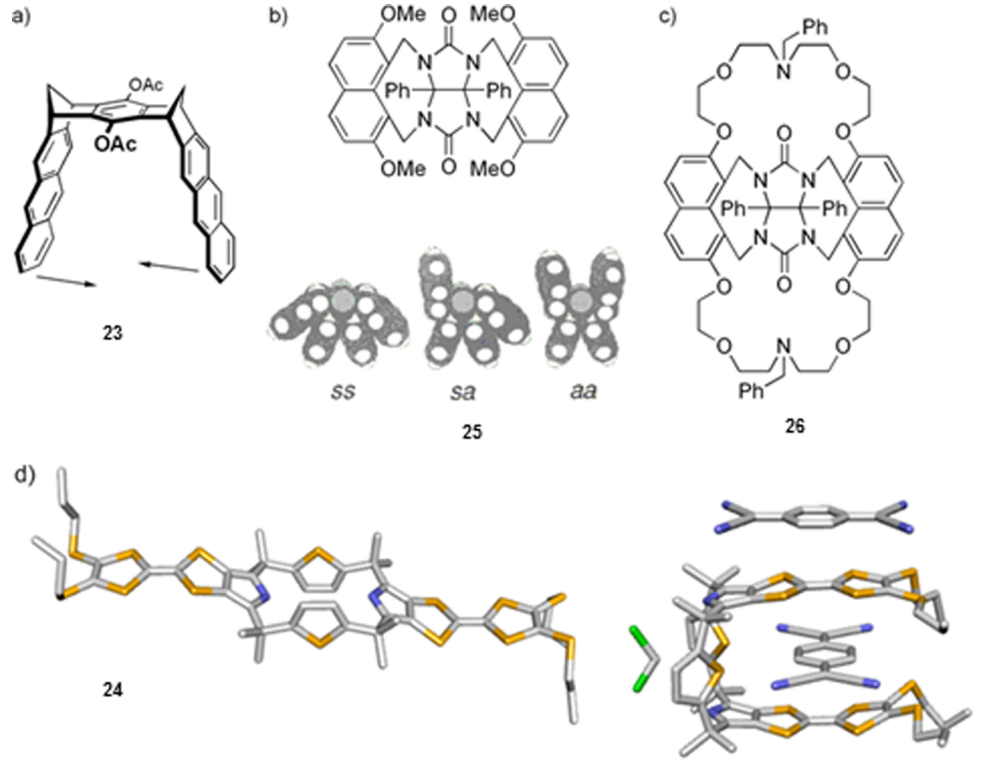

Figure 16. (a) Molecular tweezer **23**, arrows indicate direction of contraction. (b) Clip **25**, where the **aa** form is favored in the presence of a guest. (c) Clip **26**, where ion binding enhances guest affinity. (d) Crystal structure of uncomplexed and complexed **24**.[282,283,286,287] X-ray crystal structure reprinted with permission from ref 282. Copyright 2007 American Chemical Society.

molecular hydrogen-bond acceptor in the *E*-isomer (Scheme 15, compound (*E*)-**44**).[468,470] In the *Z*-isomer, the carbonyl oxygen stabilizes the *Z*-H$^+$ form of the molecule because the pyridyl unit is no longer available as a hydrogen-bond acceptor. Upon deprotonation, the process is reversed. However, the *Z*-isomer is metastable, and as a consequence the removal of the proton does not lead to an immediate change. The thermodynamically more stable *E*-isomer reappears with time. The Aprahamian group has also replaced the naphthalene unit with a quinoline unit (see (*E*)-**45**), thus introducing an additional hydrogen-bond acceptor and an additional metal ion binding pocket next to the hydrazone.[469] In this system, a Zn^{2+} ion now triggers $E \rightarrow Z$ isomerization. The most recent system showed that on addition of Zn^{2+} to (*E*)-**46** and (*E*)-**47**, a switching cascade could be initiated.[471] Coordination of Zn^{2+} to (*E*)-**46** lowers the pK_a of the imidazole N−H by 3 units and allows the protonation of (*E*)-**47**, which in turn allows switching of this moiety. Without metal coordination, the imidazole is not acidic enough to catalyze switching in (*E*)-**47**, making this sequence an elegant example of one switching event acting as the input for another, in one pot. Because the stator and rotor are held in fixed relative positions, the switches developed by Aprahamian and co-workers represent very promising tools for the control of directional motions in molecular machines (Scheme 16). A hydrazone switch has been used to dope a liquid crystal with the color of the liquid changing upon switching.[472]

DOI: 10.1021/acs.chemrev.5b00146
Chem. Rev. 2015, 115, 10081−10206

Scheme 7. (a) Prevention of Organic Guest Binding on Complexation of Copper to 27; and (b) Organic Guest Is Only Bound in the Zinc-Complexed Form of 28[288]

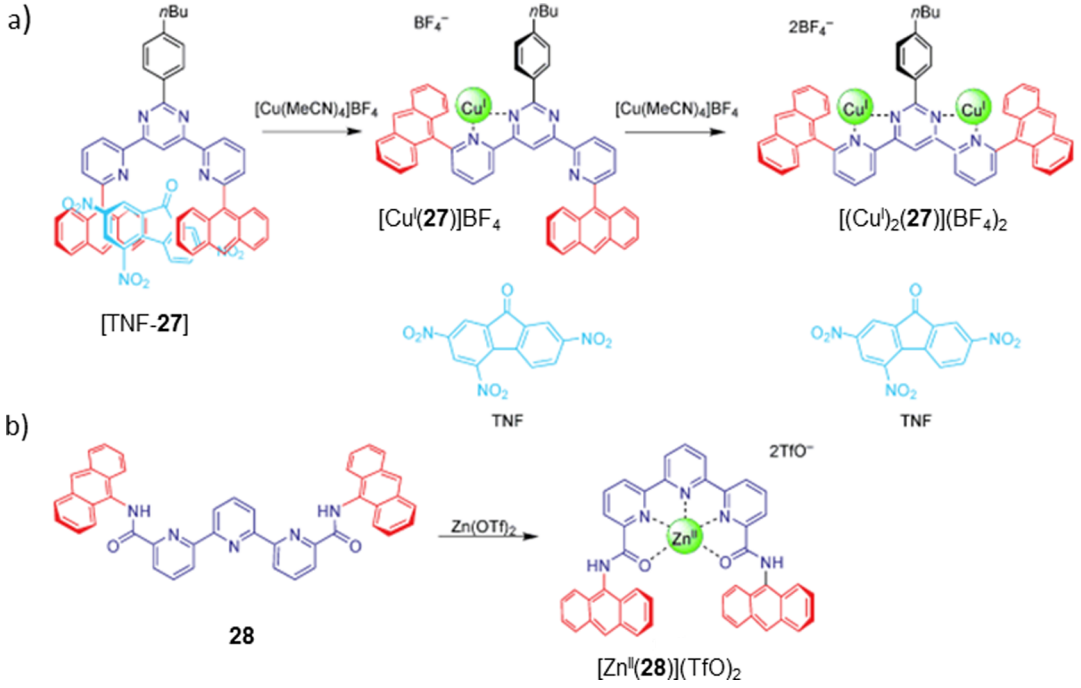

Scheme 8. Chelation Control of Equatorial/Axial Conformers and Haberhauer's Molecular Hinge[290,299,a]

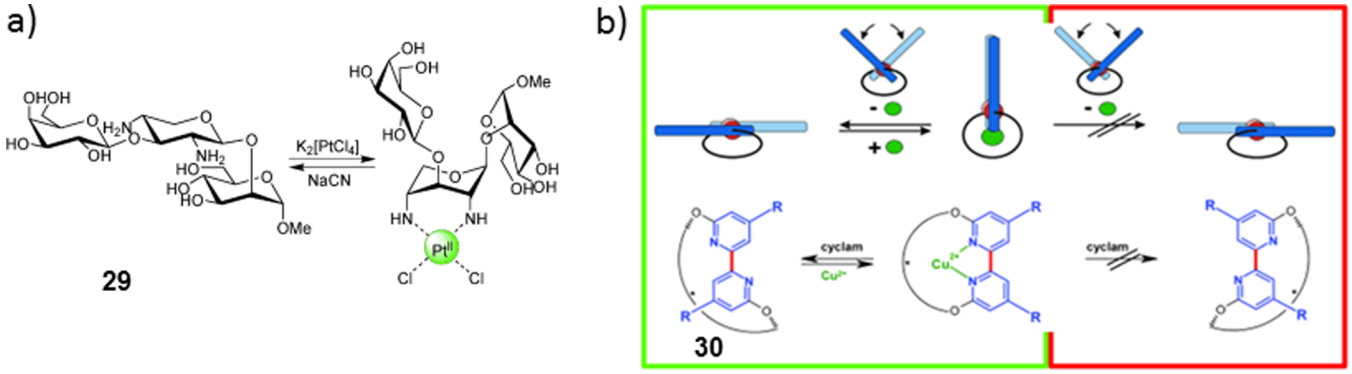

[a]Reprinted with permission from ref 299. Copyright 2008 Wiley-VCH Verlag GmbH & Co. KGaA, Weinheim.

3. CONTROLLING MOTION IN SUPRAMOLECULAR SYSTEMS

The use of supramolecular systems in molecular machines is challenging as competing processes such as the association and dissociation of subcomponents from and to the bulk must be controlled.[473,474] These processes can interfere with the integrity and/or processivity of the machine unless the binding is part of the motion generation process itself or the effect of unbound elements is restricted. If host−guest interactions are used to assemble a machine, then exchange with free hosts or guests in solution should be avoided to maintain the integrity and kinetic stability of the machine. Disassembly or exchange can, in certain cases, be intentionally exploited for functional purposes and to provide communication with external species. Controlled motion in supramolecular systems must be built on cooperative interactions of individually weak but collectively strong noncovalent interactions.

In biology, large-scale molecular motion generated upon guest binding is a common process. Acetylcholine neurotransmitters are among such guests and bind to a transmembrane channel receptor, inducing a large conformational change, resulting in the controlled flux of ions through the membrane.[475] In this case, any guests in the bulk can act as an inducer of molecular motion and at the same time as a messenger of the microenvironment enabling dynamic communication with the surroundings. The stabilities of most biological functional assemblies are well maintained by restriction of bulk exchange. If this was not so, rapid exchange of the ribosome complex or individual subunits of the ribosome during protein synthesis would detach the enzyme from the substrate mRNA and release a partially synthesized peptide, unlikely to be of any use. However, mRNA and the ribosome form a kinetically stable complex, subunit exchange with the bulk is restricted, and the enzyme processively produces large proteins.[476]

3.1. Guest Binding Generating, or Assisted by, Large-Scale Intramolecular Motion

Considering the above discussion, molecular machines and devices based on noncovalent assemblies require careful design.

DOI: 10.1021/acs.chemrev.5b00146
Chem. Rev. 2015, 115, 10081−10206

Scheme 9. Resorcin[4]arene 31, Vase and Kite Conformers, Stoddart's Self-Complexing Lock 32, and Feringa's Self-Complexing Rotor 33[98,321,322,327,a]

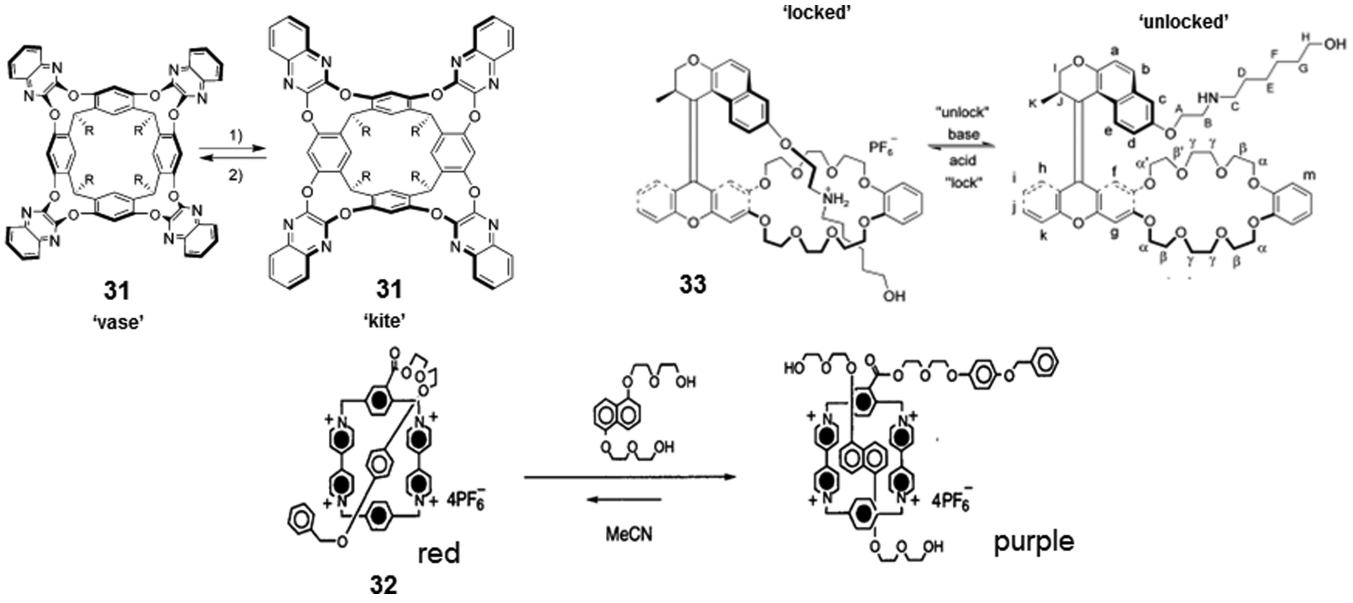

[a]Reprinted with permission from refs 321 and 327. Copyright 1997 and 2010 Wiley-VCH Verlag GmbH & Co. KGaA, Weinheim.

Scheme 10. Hamilton's Acid Sensitive Switch[328]

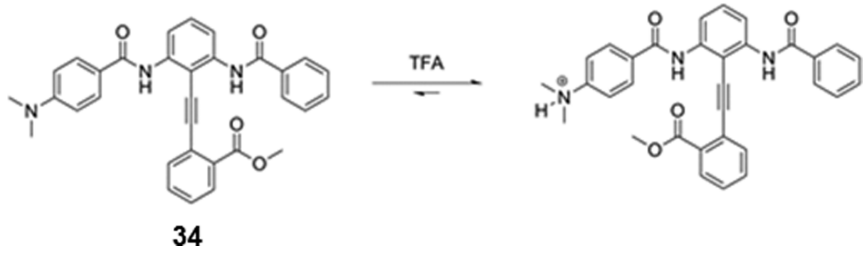

The relatively large molecular level motions generated upon guest binding are of great importance in the design of practical molecular machines. Guest-induced molecular motion has been widely studied in the literature with organic compound,[477] anion,[478] cation,[479−481] metal,[464,471,482,483] or proton guests.[484,485] Switches based on pseudorotaxanes have also been reported.[486−518] These supramolecular complexes display interesting operational properties that are useful for device development.[495,519−564] These switches can be used to build relatively sophisticated devices such as the molecular tweezers **23**−**26**.[280,281,287,288,565−575] This concept conventionally refers to receptors having a cavity with two binding motifs. The binding pocket can either readily encapsulate the guest (lock and key type) or evolve to a more suitable conformation upon guest binding (induced fit type). Molecular machines can be regulated by responsive tweezers, with motion induced and regulated through an external stimulus such as the binding of guest molecules.

One of the earliest examples of a molecular machine was a "molecular tweezer" based on the photoisomerization-dependent binding of cations in a crown ether-bearing azobenzene, developed by Shinkai et al. (Scheme 17).[575,576] The open *trans* form can bind smaller cations such as Na^+ selectively, whereas the *cis* form prefers to bind larger Rb^+ ions by forming a sandwich complex with the cation. Moreover, the *cis* isomer can be stabilized by the sandwich complex in the presence of Rb^+, and the photostationary state biased toward the *cis* isomer, causing the molecule to relax to the *trans* isomer much more slowly. Hence, in addition to photoisomerization-dependent changes in the affinity of the receptor, guest binding can alter the kinetics of the photoisomerization process.

Intercalation of electron-poor aromatic guests by molecular tweezers having two π-systems has also been explored by several groups.[577−581] The binding and release of the guest is modulated by the motion of the receptor components. Intramolecular motion has been induced allosterically by means of various stimuli including metals,[582−584] anions,[585,586] electrochemical reduction,[587] and pH change.[573] 2,6-Substituted pyridine **49** has been shown to change conformation upon protonation of the pyridine, such that the methoxy groups form hydrogen bonds with the pyridinium proton (Scheme 18).[573] This hydrogen bonding results in a rotation around the single bond moving the naphthyl moieties away from each other. Intramolecular motion results in the release of the hydrophobic drug mitoxanthron, which had been bound by $\pi-\pi$ interactions between two naphthyl receptors.

Extracting work from machines depending solely on supramolecular interactions would be difficult due to the rapid exchange of bound and unbound guests. However, some supramolecular host−guest systems are moderately stable and might be suitable for use in the assembly of molecular devices. A methylviologen (compound **50**, MV^{2+}) and a *trans*-azobenzene

DOI: 10.1021/acs.chemrev.5b00146
Chem. Rev. 2015, 115, 10081−10206

Scheme 11. pH-Driven Conformational Change in Oligomeric System 35[330]

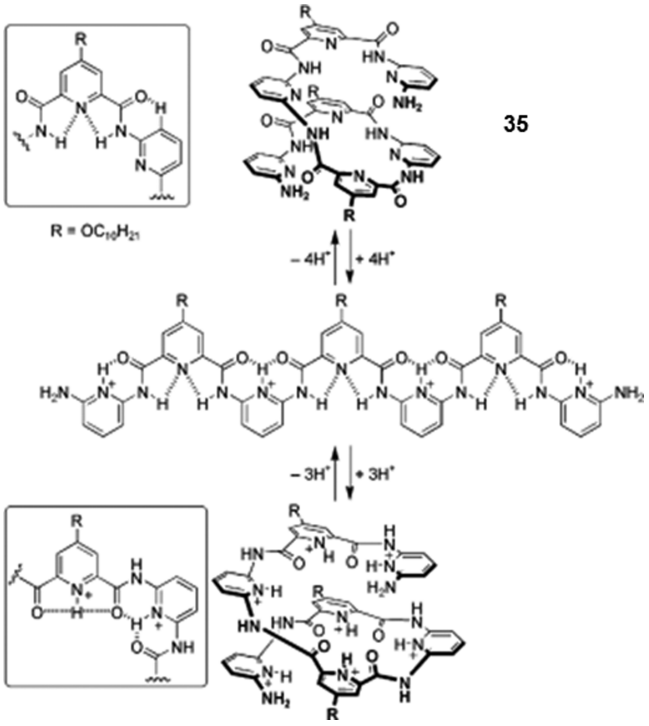

derivative (compound **51**, *trans*-AB) were encapsulated by a cucurbit[8]uril (CB[8]) host (Figure 20). Each guest has distinct properties: MV^{2+} is redox active, and the azobenzene can be isomerized to its *cis*-form (*cis*-AB) on irradiation.[588] One electron reduction of methylviologen ($MV^{+\bullet}$) results in a binary encapsulation of the reduced species in the host and *trans*-AB is kicked out. Photoisomerization of azobenzene to its *cis*-isomer results in its ejection due to steric repulsion. Therefore, the initial heteroternary complex of MV^{2+}, *trans*-AB, and CB[8] can be orthogonally switched to give two distinct complexes. In one complex, one-electron reduction of MV^{2+} forces out the azobenzene to form a homoternary complex $(MV^{+\bullet})_2CB[8]$, while in the other photoisomerization of the azobenzene ejects *cis*-AB, while MV^{2+} stays encapsulated to form $(MV^{2+})CB[8]$.

These three distinct, stimuli-dependent, modes of complexation allow greater control over molecular behavior. To transfer this to the macroscopic world, thiol-functionalized *trans*-azobenzenes were attached to a gold surface. Upon complexation by CB[8], together with the fluorescently labeled MV^{2+}, the surface became fluorescent, and due to the charged nature of viologen, a substantial increase in wettability was observed. Upon irradiation, the azobenzene was kicked out as its *cis* isomer, returning the surface to a nonfluorescent, hydrophobic state, after the unbound fluorescent viologen–CB[8] complex was washed away from the surface. The orthogonal control of switching processes is a vital tool for the creation of even more complex molecular devices, especially in memory device construction.[588]

One of the interesting emerging properties of supramolecular host–guest systems is the stimuli-dependent expansion and contraction of molecular constructs. This behavior will be revisited in rotaxane systems in section 8. In double-stranded helicate **52** (bridged by spiroborates at each end), sodium ion-induced reversible extension and contraction was observed with an accompanying directional twisting (Figure 21).[589] In the presence of Na^+, the molecule was forced to twist its central tetraphenol moiety to better coordinate the cation. The handedness of the helicate was preserved during this process. This process could be reversed by the sequestration of Na^+ by [2.2.1]cryptand.

The tetraphenolic central compartment could be replaced by two porphyrins to create a hydrophobic cavity for aromatic guests to stack inside.[590] Upon intercalation of electron-deficient

Scheme 12. Large-Scale Extension of a Ligand Strand upon Pb(II) Complexation[369,370]

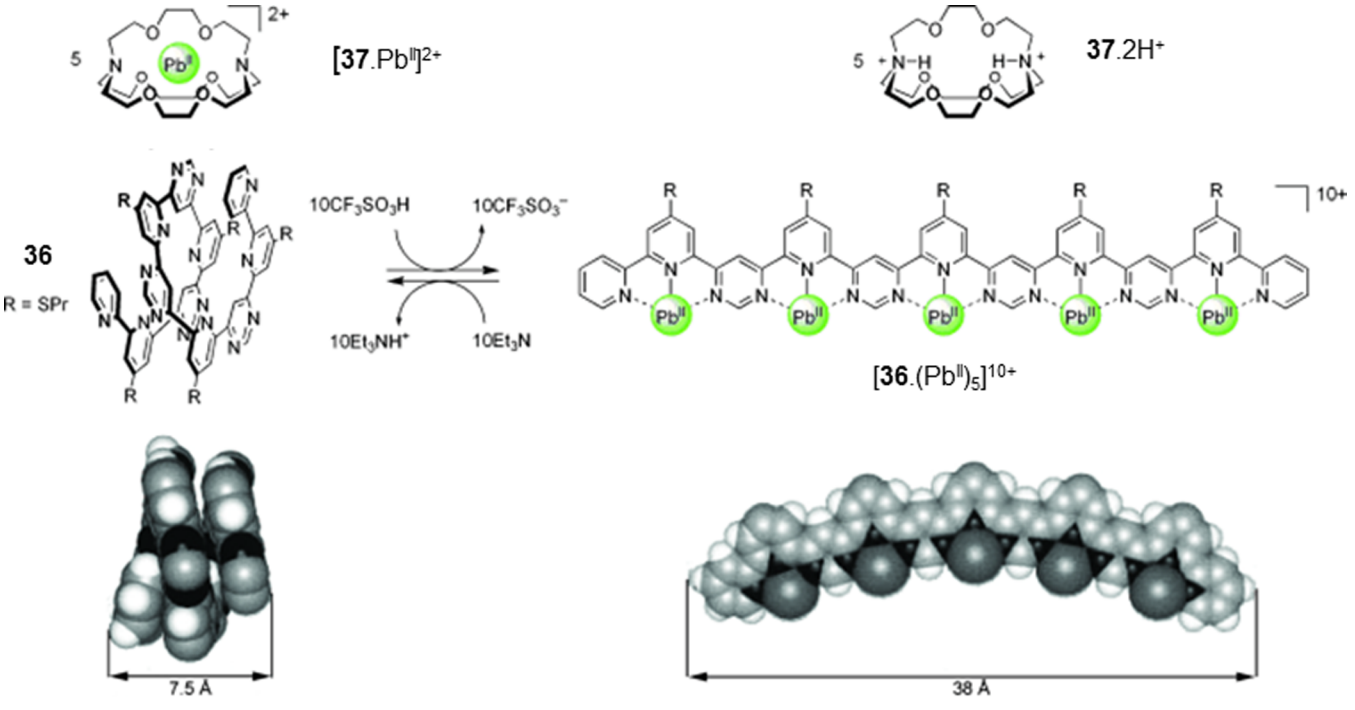

DOI: 10.1021/acs.chemrev.5b00146
Chem. Rev. 2015, 115, 10081–10206

Scheme 13. (a) Molecular Scissors 38;[a] and (b) Structure of Molecular Hinge 39[414]

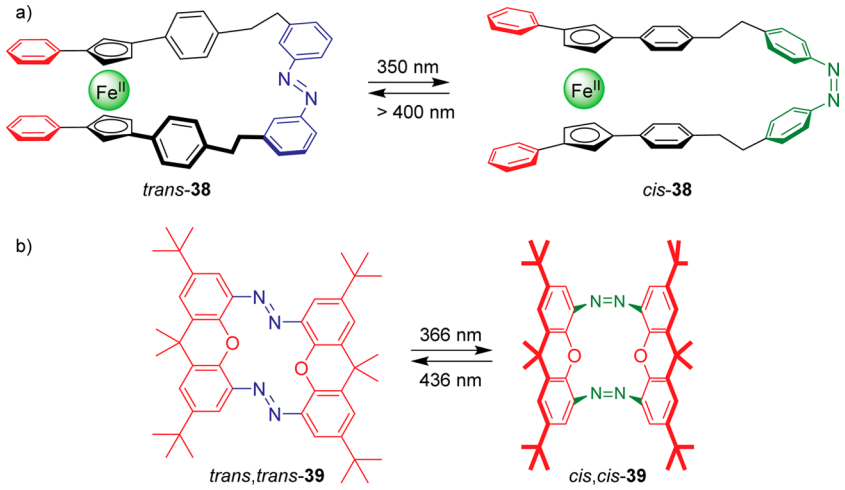

[a]Irradiation at 350 nm initiates photoisomerization from the *trans* to *cis* isomer of the azobenzene moiety (closed to open molecular scissor); irradiation at >400 nm induces the reverse.[413]

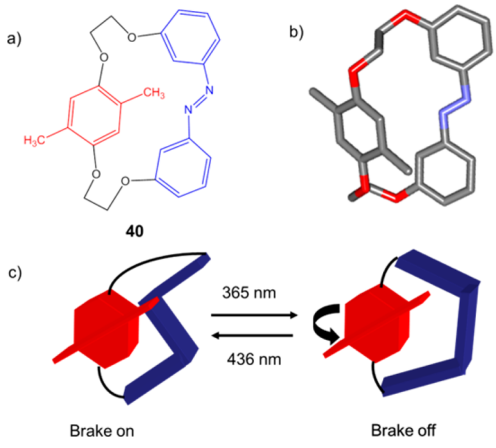

Figure 17. (a) Chemical structure of a molecular brake **40** with a 2,5-dimethylbenzene unit as the rotor. (b) X-ray crystal structure. (c) Schematic representation of this photoinduced molecular brake. X-ray crystal structure reprinted with permission from ref 418. Copyright 2011 Wiley-VCH Verlag GmbH & Co. KGaA, Weinheim.

Scheme 14. Minimization of Steric Interactions between Aromatic Groups and Substituent Results in (*P,P*)-(*trans*)-41-Stable Ground-State Conformation, with Axial Substituents[a]

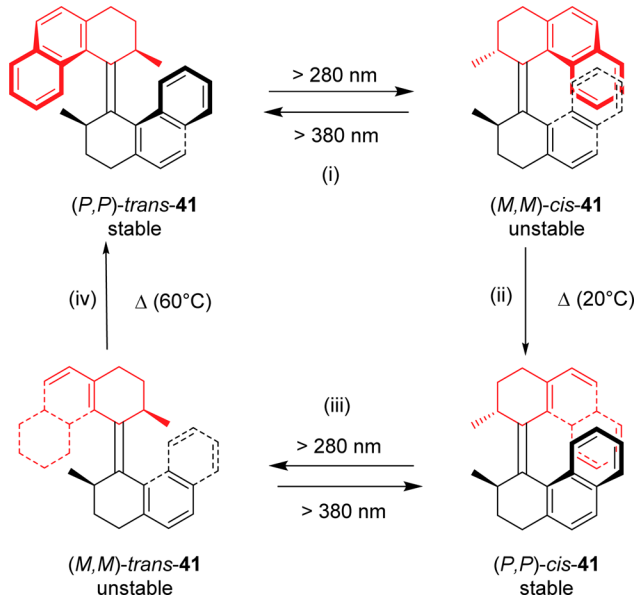

[a](i) Photochemical isomerization leaves substituents in the unstable equatorial conformation (*M,M*)-(*cis*)-**41**-unstable. (ii) Steric strain is released by a thermally activated helicity inversion leading to (*P,P*)-(*cis*)-**41**-stable. (iii) Photoisomerization from *cis* to *trans*. (iv) Helical inversion completes a full rotation.[429]

aromatic guests between the porphyrin rings, the distance between the two porphyrin units increased from 4.1 to 6.8 Å. This expansion in the central region induced a rotation, which reduced the torsion angle, and, due to steric constraints, the capping spiroborates unwound in a directional manner, demonstrating the first guest-induced rotary motion with accompanying corkscrewing motion. Guest control of screw motion, involving simultaneous linear translation and rotation, has been reported.[591] In this case, the guest acted as a template for the formation of helicates based on hydrogen bonding and biased the formation of one of the two equilibrium structures.

Stimulus-driven molecular level conformational change and subsequent control over the binding affinity of guest molecules have been used to regulate anion concentration in solution.[592−594] Flood et al. developed a triazole-based foldamer bearing an azobenzene moiety in the structure (Figure 22).[595] Hydrogen bonding between the triazole units and a chloride anion together with π-stacking within the foldamer backbone kept the anion buried in the interior.[592,596−602] Photoisomerization of the azobenzene moieties disrupted the stacking, inducing unfolding and releasing the anions. This photoinduced release and capture of anions is completely reversible. Calculated K values in acetonitrile decrease significantly from 3000 to 380 M^{-1} upon irradiation with UV-light. In addition, the conductivity of the irradiated sample increased due to release of anions into solution. Helical inversion caused by ion binding has also been observed.[603] Stimuli responsive switches have great potential in drug release and ion-cargo transport applications. Nitschke et al. have reported a complex system, where the addition of various signal molecules to a helical complex led to a cascade of changes

DOI: 10.1021/acs.chemrev.5b00146
Chem. Rev. 2015, 115, 10081−10206

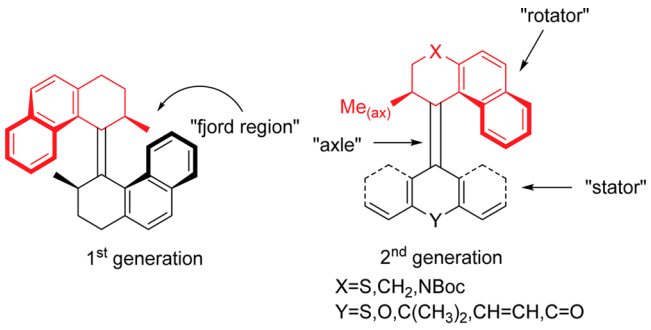

Figure 18. Comparison of the general structures for the first (**41**) and second (**42**) generations of Feringa's molecular motors.[425]

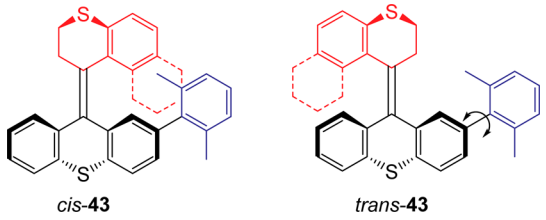

Figure 19. Structure of molecular brake **43**.[454]

Scheme 15. Hydrazone-Based Switches[a]

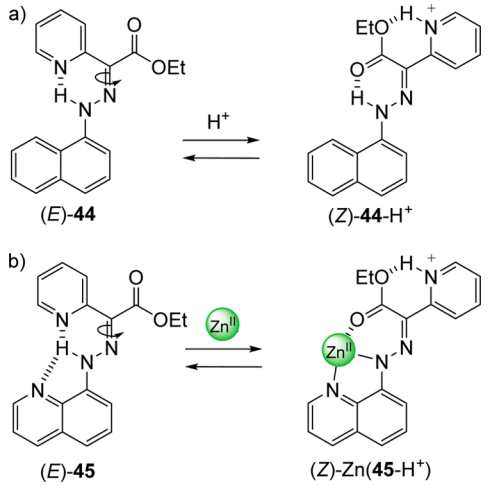

[a](a) Protonation of the pyridyl nitrogen of compound (*E*)-**44** induces *E* → *Z* isomerization.[468] (b) The quinoline unit in (*E*)-**45** provides a binding site for a Zn^{2+} ion, which is now the trigger for *E* → *Z* isomerization.[469]

in the self-assembled system and various product distributions could be formed.[604]

In the above examples, binding properties are regulated by an external stimulus or by allosteric control. Large-scale molecular motions regulated by guest binding are of particular interest in molecular machine design, because the presence of the regulator acts as a chemical communication between the environment and the machine. This dynamic interaction would allow the development of smart molecular machinery that performs advanced operations dependent on the chemical environment, or perhaps allows communication between machines.

3.2. Intramolecular Ion Translocation

The molecular basis for the conversion (in archea) of photon energy into more useful potential energy relies on proton translocation between a photoisomerized retinal molecule and the amino acid residues on the protein scaffold in which it is buried. This process occurs with a well-defined directionality, leading to light-mediated directional proton pumping across a membrane.[384,605] In supramolecular systems, for accurate translocation to take place, the ion to be translocated should be more kinetically available for intramolecular motion than the bulk ion. An electrochemical gradient cannot be achieved if each ion acceptor takes ions from the bulk. Ion translocation can be controlled by changing the affinity of organic receptors or metal centers for the ion of interest, through external stimuli such as light or reduction/oxidation.[606] In the case of proton transfer, some molecules have distinct photophysical properties such as a change in the pK_a of the molecule in the excited state, which enables rapid dissociation of the proton from one part of the molecule and reassociation with another, intramolecular acceptor, in an "excited-state intramolecular proton transfer" (ESIPT).[607] This process has been extensively studied using 2-(2-hydroxyphenyl)-benzothiazole (HBT, Scheme 19).[608] Fast proton transfer from the hydroxyl group to the nearby thiazole nitrogen takes place upon excitation of the molecule to generate a *cis*-keto form with a distinct, solvent-dependent, spectroscopic character. In this molecule, intramolecular hydrogen bonding mediates this fast proton transfer between different regions of the molecule.

Metals having more than one stable oxidation state can be translocated by oxidation or reduction or incorporated into a scaffold along with other ions that can be translocated. For either process, the molecule should bear more than one binding site, with different affinities, to drive the motion of the ion. Flexible receptors are most often used for ion translocation, but rigid aromatic systems can be suitable as well. These processes are usually accompanied by a visible color change due to changes in absorption after a change in the oxidation state of the metal, or due to ligand exchange. The reversible translocation of a chloride anion from a Cu(II) center to a Ni(III) center was an early example of a flexible system (Scheme 20a).[609] The concentration-independent nature of the process indicated that anions translocate from the Cu(II) center in an intramolecular fashion rather than via exchange with the bulk.

Work by Mirkin et al. showed reversible intramolecular shuttling of a chloride anion from a bisurea binding site to Rh(I) in the presence of carbon monoxide (Scheme 20b).[610] The hydrogen-bonding ability of the urea was further enhanced by attaching electron-withdrawing 3,5-bis(trifluoromethyl)benzyl groups. Rh(I) adopts a distorted square-planar geometry with these phosphine and thioether ligands, as shown by the crystal structure. Initially, chloride was encapsulated between the urea tweezers. With the aid of polar solvents (dimethyl sulfoxide or dimethylformamide) and in the presence of CO, chloride was translocated to Rh(I) with accompanying CO coordination. The Rh−S bonds were cleaved concurrently. Translocation was driven by both the weakening of hydrogen-bonding interactions in the urea and the more favored and less distorted geometry adopted at the Rh center with the new ligands. This is an important example of ion translocation in view of the fact that it involves two different types of interaction (hydrogen bonding and metal−ligand coordination) to enable shuttling and may open a path to the development of further molecular devices by the orthogonal control of these two interactions.

The first intramolecular cation translocation driven by auxiliary redox reactions was reported by Shanzer et al.[611] A triple-stranded helical scaffold was used with ditopic hydrox-

DOI: 10.1021/acs.chemrev.5b00146
Chem. Rev. 2015, 115, 10081−10206

Scheme 16. Switching Cascade of Hydrazone Rotary Switches[471]

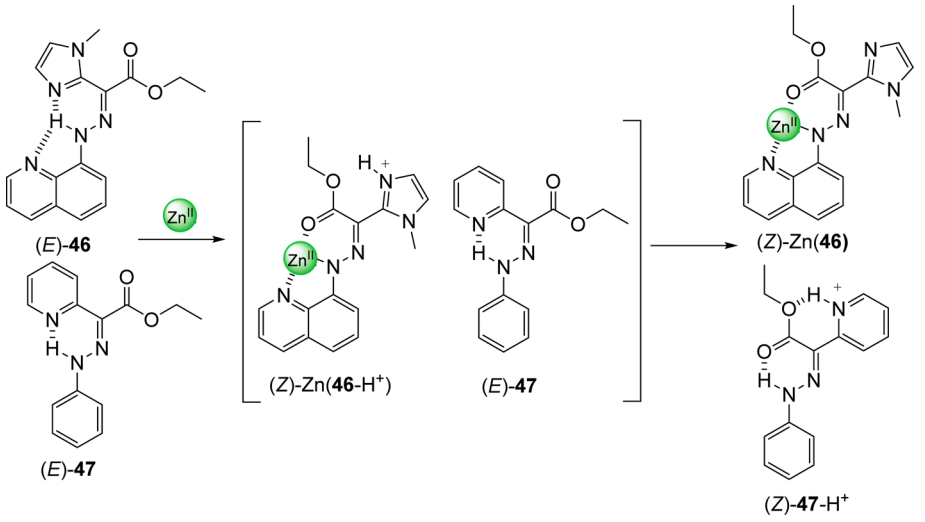

Scheme 17. Light-Operated Molecular Tweezers[575]

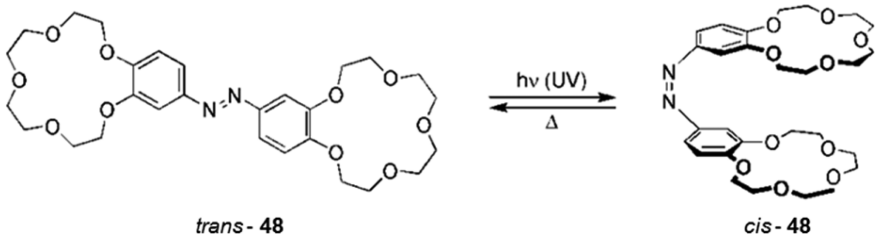

Scheme 18. Decreased Drug Binding Affinity by a pH-Induced Conformational Change[573]

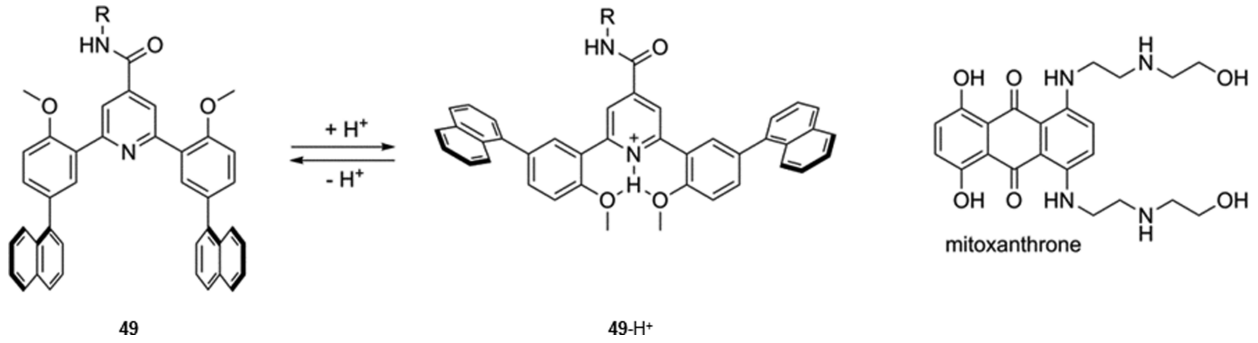

amate and bpy ligands, which bind preferentially to Fe(III) and Fe(II), respectively (Scheme 21). Chemical reduction of Fe(III) with ascorbic acid relocated the cation to the bpy ligand with a visually observable color change from pale brown to violet-red. Reversibility was obtained by oxidation with $(NH_4)_2S_2O_8$. Even though the process takes place slowly (minutes to hours), the overall movement of the cation is intramolecular.

Several other examples of anion and cation translocation between ligands separated by flexible linkers have been investigated.[480,612−614] Metals are also known to translocate over rigid sp^2 hybridized carbon surfaces.[615] Sandwich complexes of two dipalladium units (four palladium nucleii arranged in two separate regions) clustered between π-conjugated ligands showed redox-driven reversible translocation, resulting in a tetrapalladium complex (Scheme 22).[616] In a complex with further extended conjugation, redox reaction conditions resulted in reversible carbon−carbon formation between the dipalladium clusters. This barrier (the new C−C bond) built by the mobility driving force used in the first complex (redox reaction) prevented translocation in the second complex and hence confined the metals to their original positions.

Supramolecular host−guest systems with distinct stimuli responsive switching behavior, guest sorting character, and emergent photophysical properties have been developed with implications for the design of molecular machines. To enable controlled mechanical motion, these systems should be kinetically stable enough to avoid exchange of components with the bulk on the time scale of the operation. Mechanically bonded molecular assemblies are viable candidates for machine architectures, considering their stable interlocked structure, and the relative ease of controlling their mobility.

4. SHUTTLING IN ROTAXANES: INHERENT DYNAMICS

Motion in rotaxanes is constrained by the nature of the mechanical bond. Very limited motion is permitted orthogonal to the axle, while a "shuttling" motion "powered" by random

DOI: 10.1021/acs.chemrev.5b00146
Chem. Rev. 2015, 115, 10081−10206

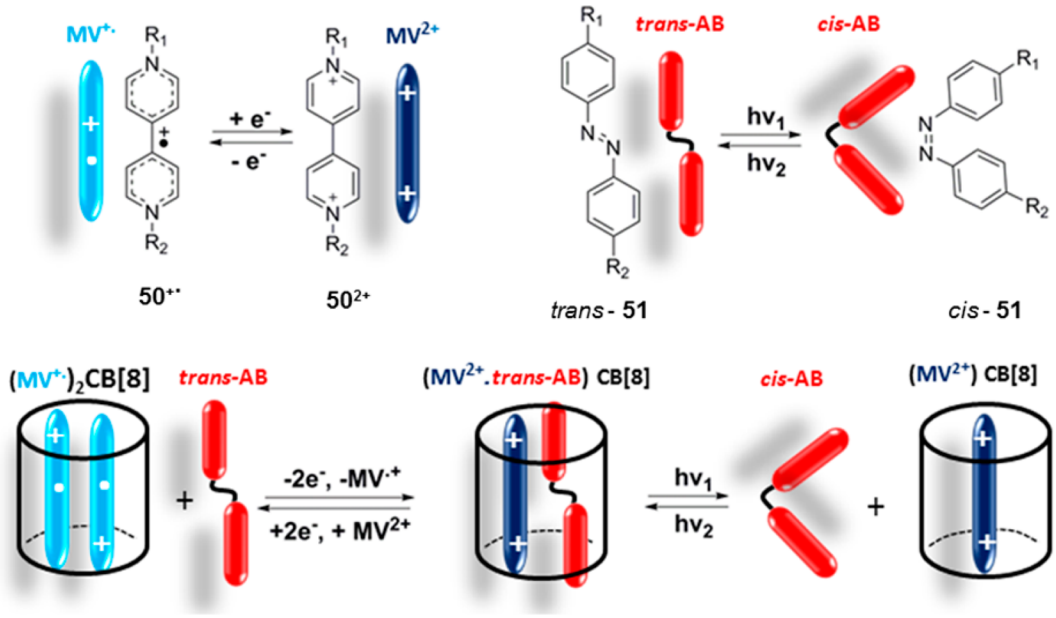

Figure 20. Orthogonal exclusion of an azobenzene and a viologen encapsulated by CB[8].[588]

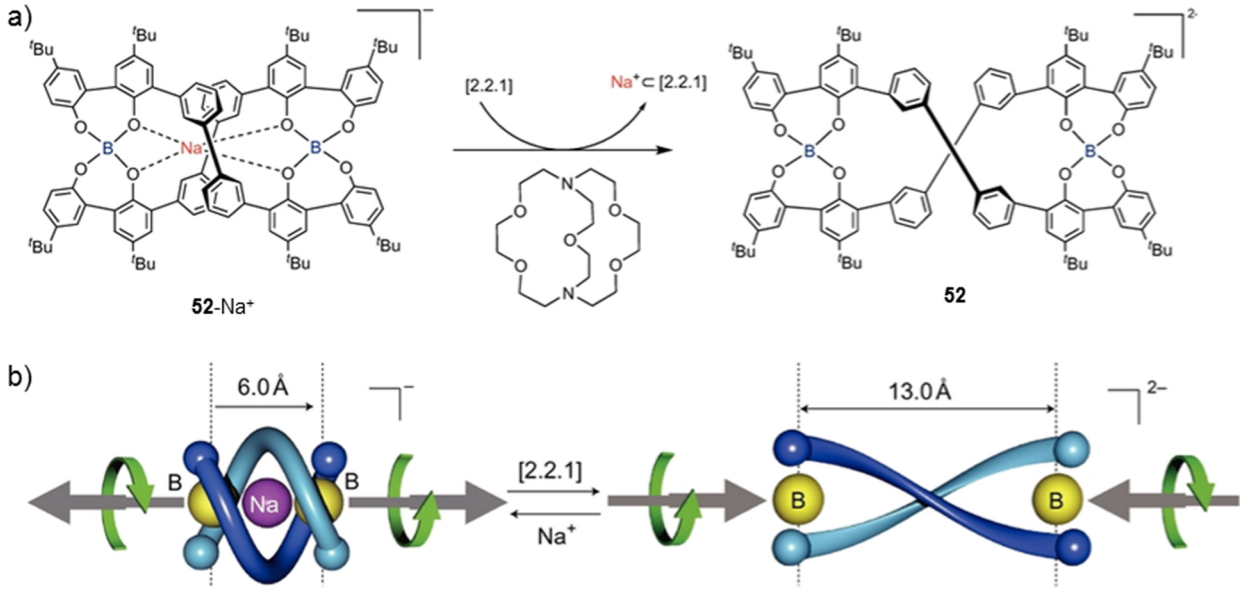

Figure 21. Na^+-induced twisting in helicate **52**. Reprinted with permission from ref 589. Copyright 2010 Nature Publishing Group.

Brownian motion can be observed along the axle (as bounded by large stoppers). As the templating methods typically used to form interlocked structures normally leave recognition motifs,[23,617−676] it is rare, although not unknown, to form a rotaxane without residual interactions between thread and macrocycle.[504,672,677−689] These residual interactions are typically viewed as "stations" on the rotaxane, and the shuttling of the macrocycle between these stations grants a useful handle in these molecules. The rates of shuttling between stations and their occupancy can be controlled by the strength of station−macrocycle interactions.

4.1. Shuttling in Degenerate, Two-Station, Molecular Shuttles

The first two-station degenerate [2]rotaxane **61** was reported by Stoddart et al. and exhibited temperature-dependent shuttling between the two equivalent hydroquinol groups, as shown by ^1H NMR.[690] Many rotaxanes based on similar macrocycles and stations have since been reported.[691,692] Similar processes are observed in the amide rotaxanes **62**−**64** where two diglycine units are separated by various linkers. In **62**−**64**, rapid shuttling of the macrocycle between the degenerate stations was observed at 298 K. Only when the linker was replaced with a bulky *N*-tosyl group was shuttling inhibited (removal of the tosyl group restored rapid shuttling) (Scheme 23).[693]

As movement between the binding sites must involve at least partial rupture of the hydrogen-bonding network, the migration can be represented by the simplified energy diagram in Figure 23. Hydrogen-bonding solvents have been shown to disrupt macrocycle−thread interactions in single station rotaxanes,[694] and here addition of 5% [D_4]methanol increased the rate of shuttling 100-fold, consistent with lowering the energy barrier to migration by disrupting station−macrocycle interactions and

DOI: 10.1021/acs.chemrev.5b00146
Chem. Rev. 2015, 115, 10081−10206

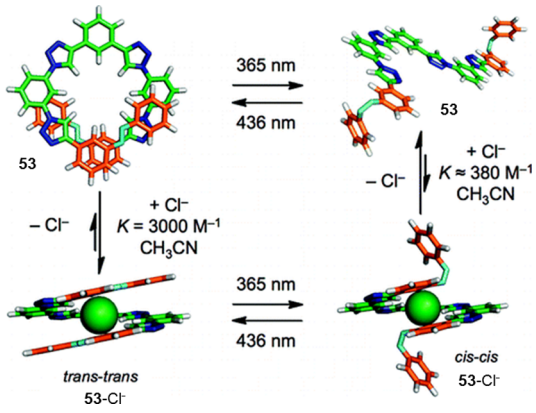

Figure 22. Control of anion concentration in solution by a photoresponsive foldamer. Reprinted with permission from ref 595. Copyright 2010 American Chemical Society.

Scheme 19. Excited-State Intramolecular Proton Transfer in HBT[607,608]

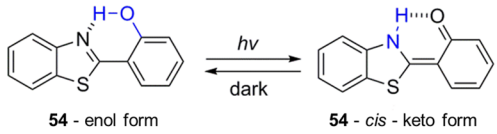

thus raising ground-state energies.[693,695−697] The effect of water on the rate of shuttling has been investigated and was found to be greatly superior to that of other protic solvents.[698] This effect was attributed to the ability of water to form three-dimensional hydrogen-bonding networks.

The use of a phenol/phenolate central group where the formation of a phenolate/cation pair significantly slowed shuttling[699] has also been explored. Cleavage of a nitrogen protecting group has been used to induce degenerate shuttling.[700] A large barrier to shuttling could be introduced in **65** where the dimerization of the rotaxane, as templated by Cu(I) addition, prevented shuttling (Scheme 24). This could be reversed by copper removal with an ion-exchange resin.[701,702]

Scheme 21. Redox-Mediated Intramolecular Ion Translocation[611]

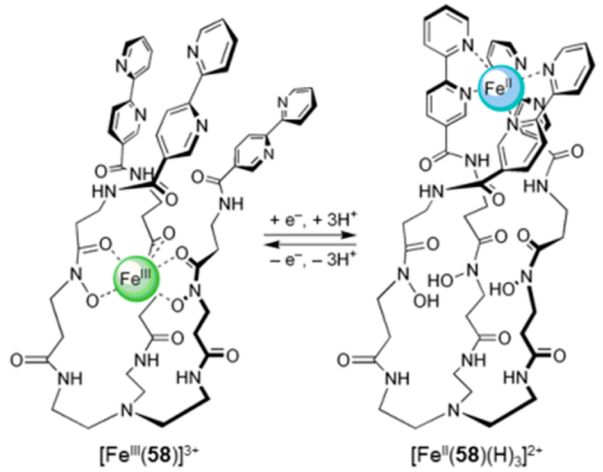

Berna and co-workers have recently reported a system in which the binding of a guest hydrogen-bond acceptor−donor−acceptor molecule to the thread led to the trapping of the macrocycle to the linker region between the two stations.[703] Upon removal, by external complexation, of the guest, interstation shuttling was restored. Control of shuttling rate has also been achieved by the oxidation/reduction of hydrogen-bonding stations[704] and by photochemical ring contraction of a macrocycle.[705]

4.2. Physical Models of Degenerate, Two-Station Rotaxanes

A decrease in the rate of shuttling was observed upon lengthening the alkyl chain of **63** as compared to **62**, the magnitude of which corresponds to an increase in activation barrier of ca. 5 kJ mol^{-1}. This effect was attributed to the increased distance the macrocycle must travel between binding stations.[693] This process can be modeled by considering the macrocycle as a particle confined to a one-dimensional potential energy surface (the mechanically interlocked nature of the rotaxane preventing significant motion of the macrocycle

Scheme 20. Intramolecular Anion Translocation Mediated by (a) Redox[609] **and (b) Ligand Exchange**[610]

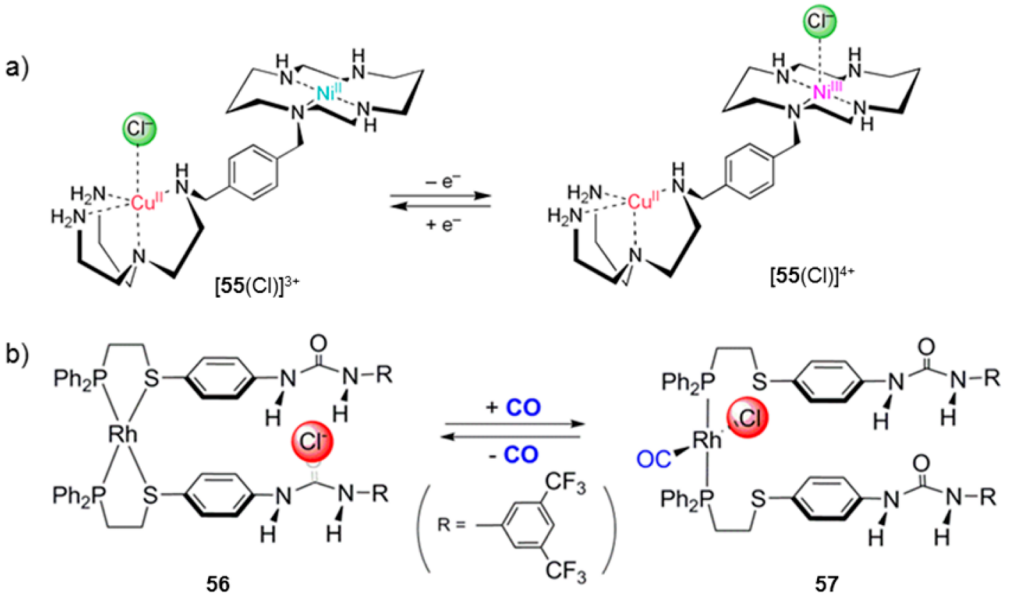

DOI: 10.1021/acs.chemrev.5b00146
Chem. Rev. 2015, 115, 10081−10206

Scheme 22. Redox-Mediated Pd Translocation in an Aromatic Sandwich Complex[616]

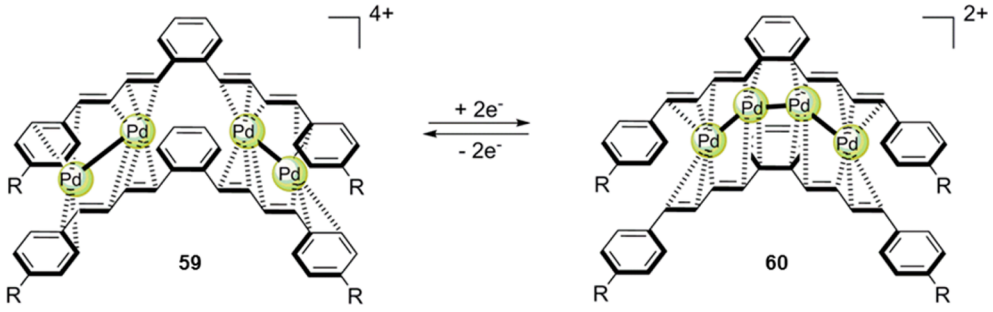

Scheme 23. (a) The First "Molecular Shuttle", 61;[690] and (b) Degenerate Peptide-Based Molecular Shuttles 62−64 of Varying Linker Length[693]

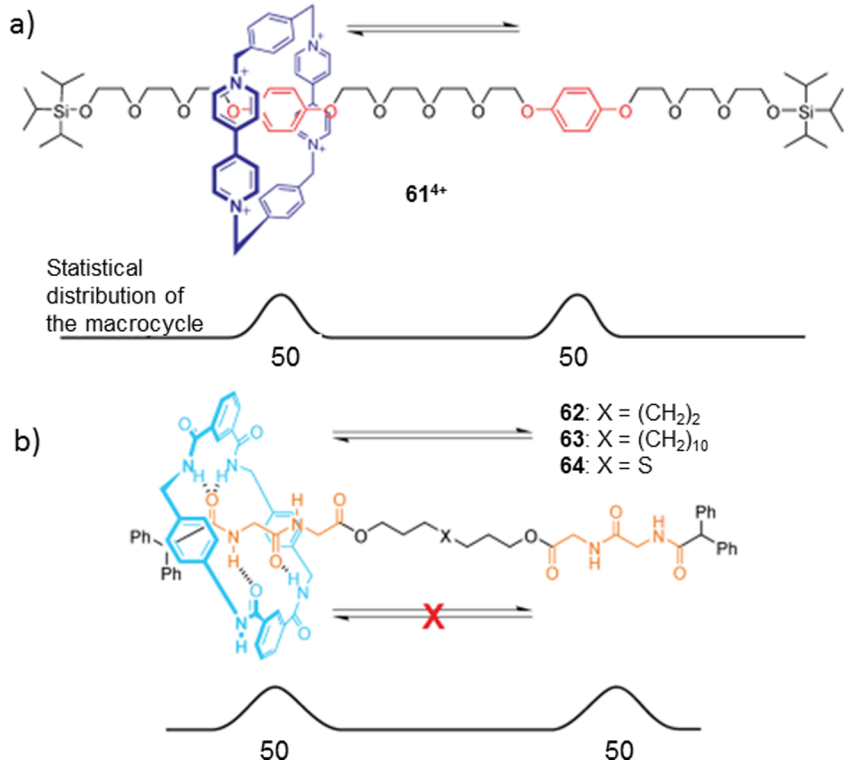

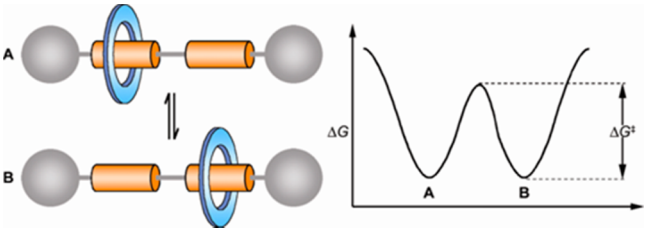

Figure 23. Idealized model of binding in degenerate molecular shuttles. Barrier height is dependent on the energy required to break interactions between macrocycle and station and a distance-dependent diffusional component.[14]

orthogonal to the thread). Assuming that thread−macrocycle interactions between stations are negligible leads to the energy profile shown in Figure 24. The rate of escape from the station energy well can then be modeled by an Arrhenius equation with a contribution from a distance-dependent diffusion factor to the overall rate of shuttling. A quantum mechanical treatment of this system has found that, as the lengthening of the spacer has no effect on the activation for breaking the hydrogen bonds, the effect on the rate of shuttling is due to the widening of the overall potential energy well. This leads to a greater density of states per unit energy, thermal population of a greater number of energy levels, and thus a larger partition function and activation energy.[706] An alternate explanation of the dependence of shuttling rate on linker length was proposed by Brouwer and Günbaş who proposed that shuttling in a similar system was facilitated by hydrogen bonding between the macrocycle and the station to which it is not currently bound.[707] As the linker length increases, this bridging conformation becomes increasingly entropically unfavorable. Some support for this proposal comes from recent examples from Hirose et al. and Sissel and co-workers,[708,709] and Stoddart and co-workers,[710] who in different systems with rigid spacing units found no correlation between spacer length and shuttling rate.

4.3. Stimuli Responsive Molecular Shuttles

Molecular motion in mechanically interlocked and thus kinetically stable rotaxanes can be controlled using multiple binding sites with affinities for the macrocycle that vary under

DOI: 10.1021/acs.chemrev.5b00146
Chem. Rev. 2015, 115, 10081−10206

Scheme 24. Complexation of Copper Leads to the Introduction of a Large Kinetic Barrier to Shuttling[701]

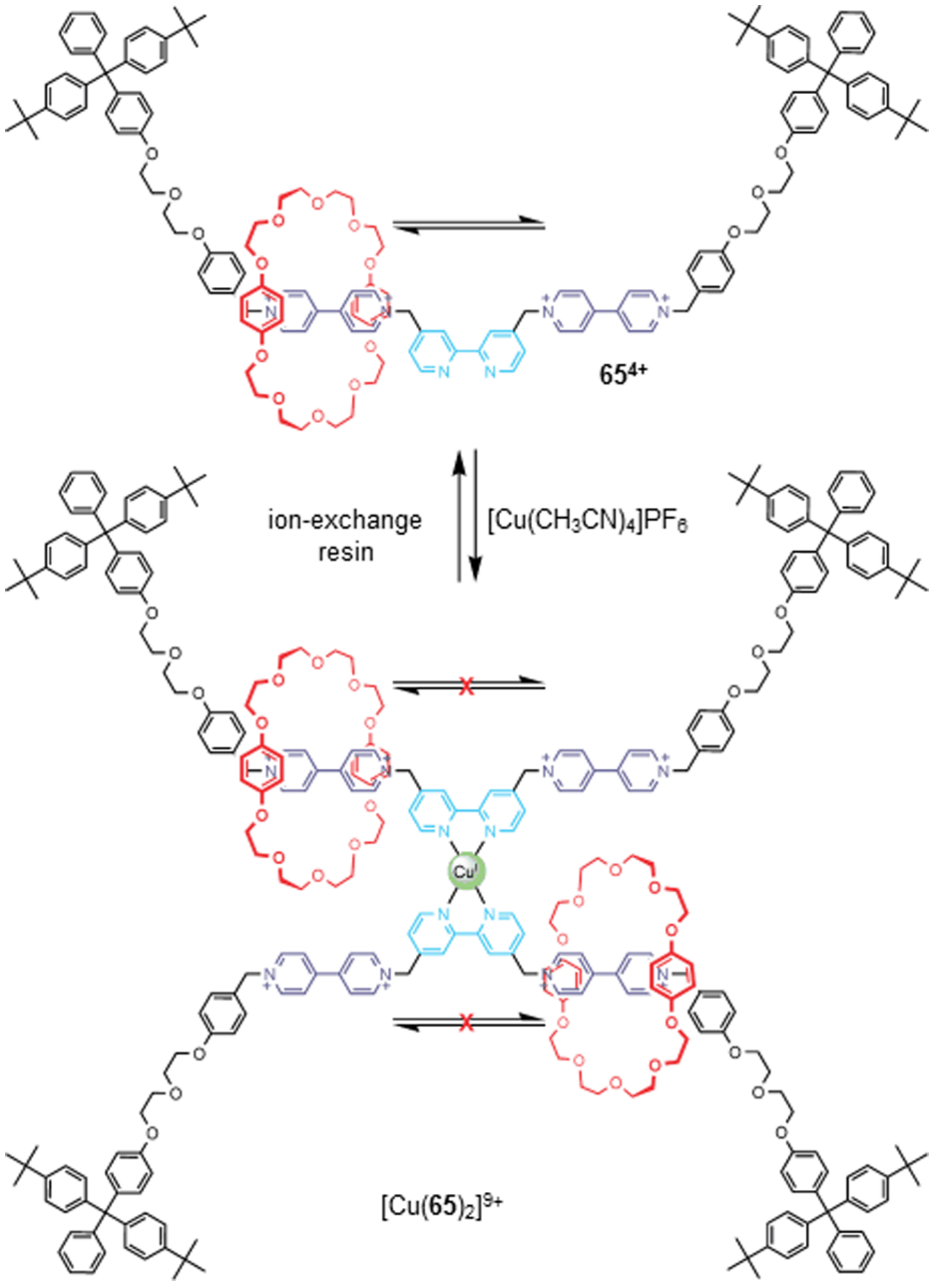

different conditions. The conditions can be modified by electrochemical redox processes, light, pH, and environmental changes. Once detailed balance is broken by the applied stimulus, as with temperature difference in Feynmann's ratchet-and-pawl, useful mechanical work can be done, provided there is an additional operation to prevent it being undone. By weakening the existing interaction or increasing the affinity of a competing binding site, the macrocycle can be driven to shuttle to a new equilibrium position. For a reverse or further translational motion to take place, a new stimulus is required to perturb the new equilibrium.

4.3.1. Stimuli Responsive Molecular Shuttles with Single Binding Site. Shuttling in a single binding site system can be obtained by reducing the affinity of either the macrocycle for the station or the station to the macrocycle, by the application of an external stimuli. Light controlled switching was observed in a rotaxane made from a "bluebox" macrocycle, an electron-rich dioxyerene station, and redox-active ferrocenyl stoppers.[711] Light-induced electron transfer from the station to the macrocycle was accompanied by electron hole transfer to one of the ferrocenyl stoppers, thereby inducing unfolding of the rotaxane and shuttling of the macrocycle away from the station. Photodriven shuttling in single station rotaxanes was also observed with the increase of steric bulk generated upon photoisomerization of an azobenzene or stilbene station.[712,713] Among these examples, directional shuttling of cyclodextrin (CD) on a symmetrical thread is of particular importance due to the fact that it serves as a ratchet for a directional bias maintained purely by the asymmetric nature of the CD rims.[713] Shuttling was biased to the direction that locates the 6-rim of the CD in a position facing the central stilbene unit (Scheme 25).

DOI: 10.1021/acs.chemrev.5b00146
Chem. Rev. 2015, 115, 10081−10206

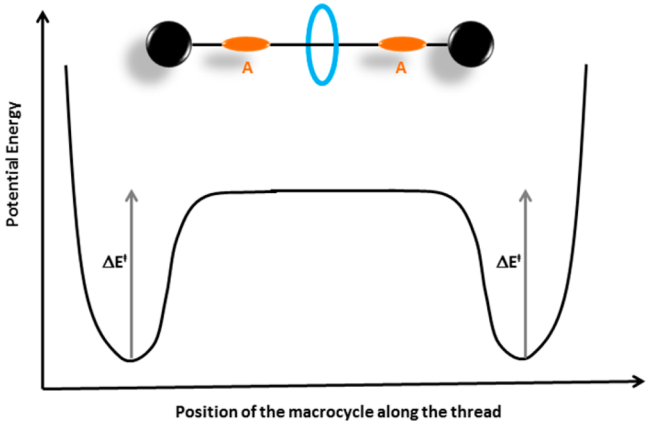

Figure 24. Idealized potential energy surface for macrocycle shuttling in a degenerate, two-station molecular shuttle.

Solvent-dependent shuttling is generally achieved by switching between hydrogen-bonding and non-hydrogen-bonding solvents.[714] Hydrogen bonding between macrocycle and thread is weakened in the presence of a competing solvent. In a peptide-based rotaxane with a benzyl amide macrocycle, hydrogen-bonding interactions were weakened by addition of MeOH (Scheme 26).[715] Because of a solvent-induced relocation of the macrocycle, the chiral center located on the thread now had an influence on the macrocycle. The original system could be restored in $CHCl_3$. More recently, a rotaxane based on a pillar[5]arene macrocycle was shown to shuttle upon either solvent exchange or heating.[716] This system was found to form supramolecular gels in pure DMSO, and in a similar system this shuttling was exploited to form a solvent-driven molecular spring.[717]

4.3.2. Stimuli Responsive Molecular Shuttles with Two or More Binding Sites. At a given temperature, the macrocycle of a rotaxane distributes itself among the existing stations according to the binding affinity of each. Perturbation of the binding energies of any of the stations results in the redistribution of the macrocycle toward a new equilibrium state, as driven by thermal motion. Changing the position of the macrocycle in a well-determined way is possible, by making the binding affinity of the less occupied station more favorable (Figure 25, transformation of station B to B′),[14] or by destabilizing the interaction between the most occupied station and the macrocycle (Figure 25, transformation of station A to A′). Stimuli responsive modification of the macrocycle can also drive such shuttling processes. Redox, pH, light, and microenvironment (temperature, solvent, etc.) switches are commonly used to control translational movement in rotaxane architectures, and will be discussed in the following sections.

Scheme 26. Solvent-Dependent Shuttling and Induced CD Response in a [2]Rotaxane[715]

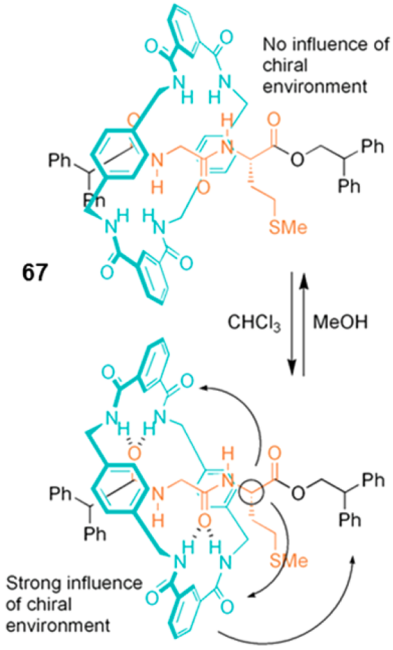

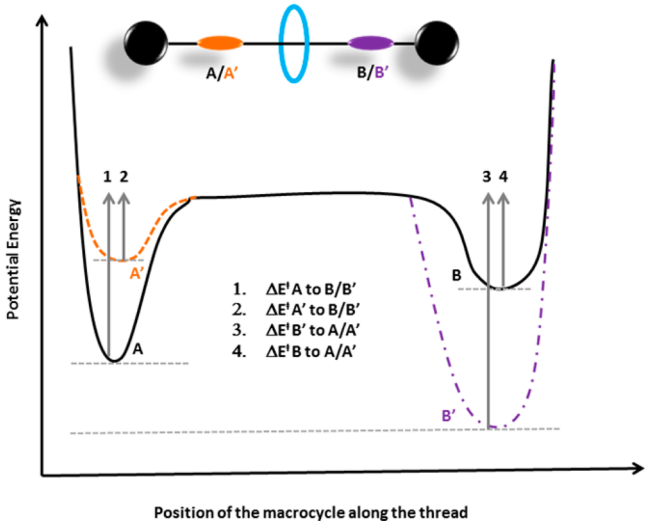

Figure 25. Potential energy diagram of a rotaxane-based bistable molecular shuttle.[14]

4.3.2.1. pH-Driven Molecular Shuttles. Variation in pH is one of the most useful stimuli used to drive translational motion in rotaxanes because hydrogen bonding, electrostatic, and ion–

Scheme 25. Light-Driven Directional CD Shuttling in a [2]Rotaxane[712]

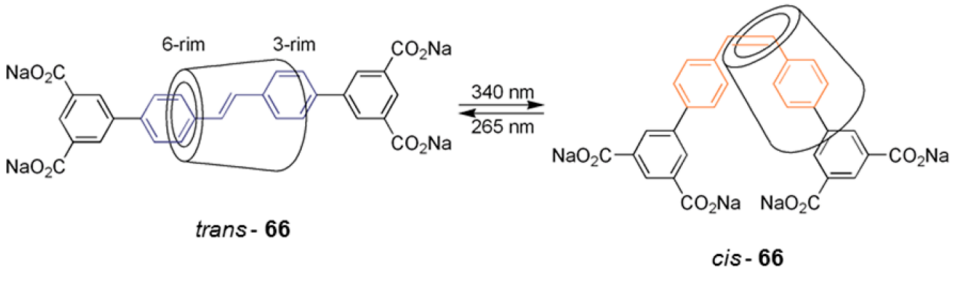

DOI: 10.1021/acs.chemrev.5b00146
Chem. Rev. 2015, 115, 10081–10206

Scheme 27. A pH-Driven Molecular Shuttle[718]

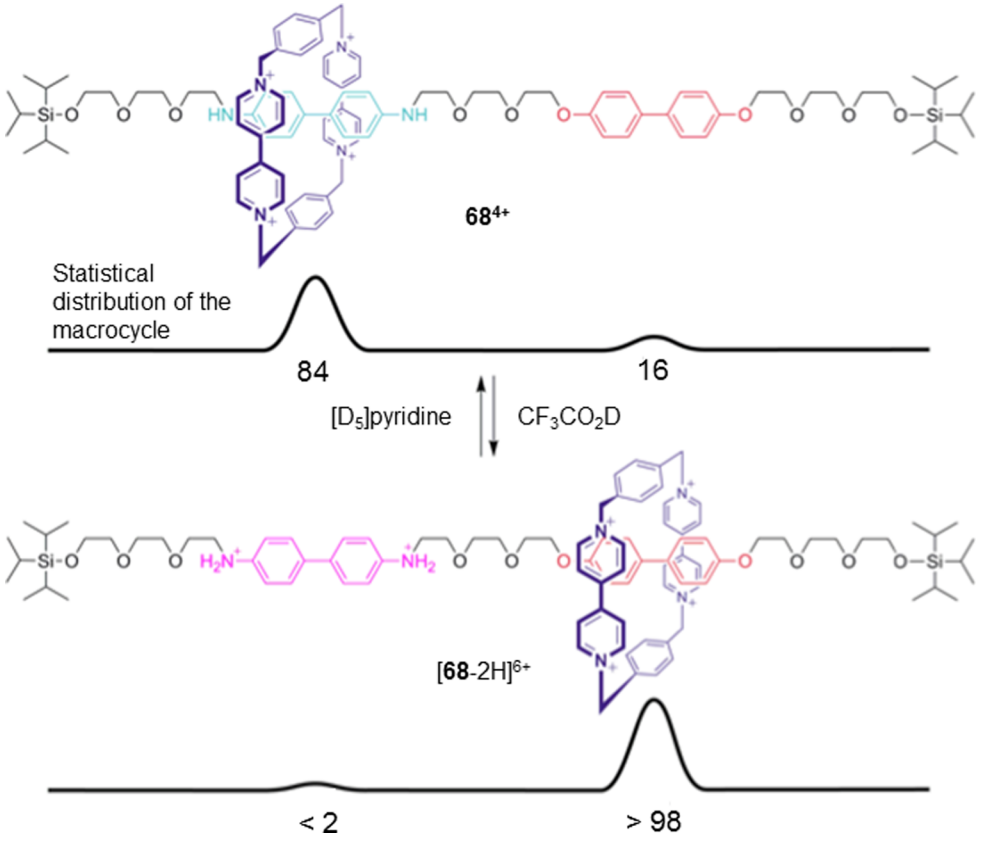

dipole interactions can be effectively controlled by protonation or deprotonation. Indeed, the first molecular shuttle developed by Stoddart et al. depended on acid-driven relocation of the electron poor, positively charged, cyclophane macrocycle from a protonated benzidine station to a biphenol station (Scheme 27).[718] Initially, under neutral pH and at 229 K, the macrocycle preferentially rested on the benzidine station (with 84:16 distribution), stabilized by donor−acceptor interactions. Upon protonation of this station, a decrease in the strength of the interaction and an increased electrostatic repulsion caused the macrocycle to relocate to the other station with a new equilibrium distribution of more than 98:2 in favor of the biphenol station. Complexation of the cyclophane macrocycle in similar systems has inspired a variety of computational research.[719−728]

A relatively low temperature was required to obtain an acceptable distribution bias in favor of the benzidine station under neutral conditions. This necessitated the development of a system, which exclusively resided on one station under standard conditions. Positional discrimination with a ratio of more than 98:2 was obtained in a rotaxane composed of a dibenzocrown ether macrocycle and ammonium-bipyridinium and ammonium-triazole stations. This interaction has been exploited in many systems.[729−743] In a structurally similar rotaxane dimer, pH-induced contraction and expansion was made to function as a "molecular muscle".[744−746] The pH-dependent relocation of an amide-based macrocycle from a succinamide to an hydroxyl-cinnamate station was observed, with enhanced hydrogen bonding between the deprotonated cinnamate derivative and the macrocycle.[747] Rotaxanes in which repositioning to another station was driven by macrocycle protonation have been reported.[748,749] Shuttling of a metal−macrocycle complex from one ligand to another on a rotaxane as a result of protonation of one of the ligands has been investigated.[750] The pH-driven shuttling of cucurbit[7]uril between bipyridinium and carboxylate stations has recently been reported.[751] Attempts were made to couple this motion to an oscillating pH background reaction, but the pH oscillation was rapidly damped in this case. Autonomous translocation is an important concept in molecular machine design, but requires further research.

4.3.2.2. Redox-Driven Molecular Shuttles. Rotaxanes with electron donor−acceptor units or transition metal complexes can be controlled by redox chemistry, provided that redox potentials of the interacting units are carefully chosen.[752−756] After the redox process, the products should be stable on the shuttling time scale, and rapid charge recombination must be prevented. Redox control processes can be chemical, electrochemical, or photochemical.

An early example of redox-mediated shuttling was reported by Leigh et al. and took advantage of a redox-active naphthalimide, which was introduced at one end of the thread. The amide-based macrocycle migrated from a succinimide station to the napthalamide station upon one-electron reduction of the naphthalamide (Scheme 28).[757−759] Increased electron density on the imide carbonyl of the naphthalamide station outcompeted the succinimide station, and the macrocycle rested almost exclusively at the naphthalamide station. The shuttling was reversible and could be performed through photochemical excitation accompanied by reduction with an external electron donor.

Benzidine, tetrathiafulvalene, viologen, naphthalimide, and dioxynaphthalene derivatives have been widely used as redox-active stations.[760−777] Redox-induced changes in the coordination preference of transition metal complexes bound to the

DOI: 10.1021/acs.chemrev.5b00146
Chem. Rev. 2015, 115, 10081−10206

Scheme 28. A Redox-Driven Molecular Shuttle[757,758]

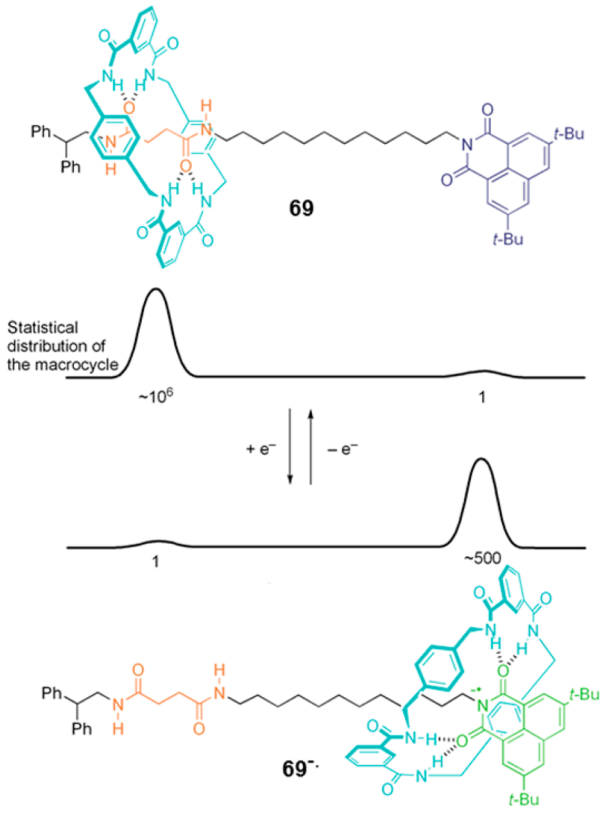

macrocycle have also been used to drive biased Brownian motion toward different stations.[778] A tristable rotaxane has been reported where the position of the macrocycle over each of the three stations could be controlled solely using electrochemistry.[779]

4.3.2.3. Ion-Driven Molecular Shuttles. The presence of ions usually affects the conformation and stability of the macrocycle on a station by either interfering with the existing hydrogen bonding, ion−dipole, and dipole−dipole interactions or by sterically disfavoring the binding. This effect can be strong enough to drive translocation of the macrocycle to another station on the thread. In crown ether-based macrocycles, metal ions can be chelated by the macrocycle and thus alter the affinity of the macrocycle for their binding sites, and in some cases induce shuttling. Lithium was reported to mediate the shuttling of crown ether-based macrocycles from a naphthalimide station to a pyromellitic diimide, presumably due to stronger ion−dipole interactions with this station in the presence of a cation.[780] Shuttling could be reversed by the addition of an excess of [18]crown-6, which sequestered the lithium cation, returning the macrocycle to its original equilibrium distribution. Rather than interacting directly with the macrocycle or a station, ions can bind to another position on the rotaxane and affect the affinity of the macrocycle with either station. Shuttling under similar allosteric control was observed using a bis(2-picolyl)amine stopper that chelates cadmium ions.[781,782] Binding to the nearby station was disrupted in the presence of cadmium, and the macrocycle repositioned itself to the distal station. Cadmium could be removed by cyanide complexation to reverse the process.

Chloride coordination to a palladium complex was reported to drive shuttling from a triazole station to a pyridinium station (Scheme 29).[783] In the absence of chloride anions, the palladium metal was chelated by the macrocycle with the fourth coordinate site being occupied by the triazole unit on the thread. Addition of chloride to the solution as its tetrabutylammonium salt resulted in displacement of the triazole ligand and the macrocycle detached from the station. When this occurred, the crown-ether moiety of the macrocycle was free to interact with the pyridinium station, which promoted translocation. The process could be

Scheme 29. Chloride-Induced Molecular Shuttling in a [2]Rotaxane[783]

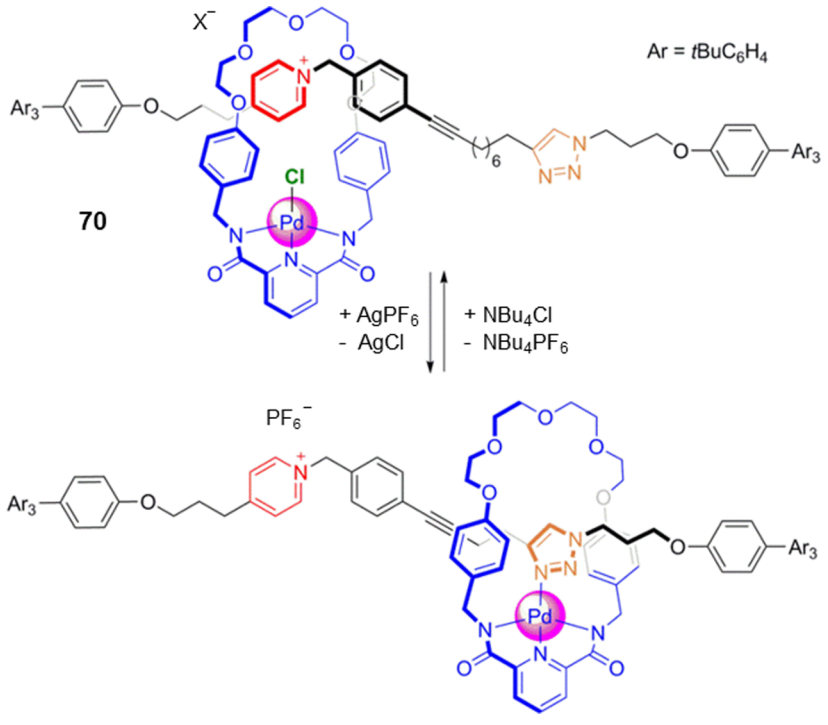

DOI: 10.1021/acs.chemrev.5b00146
Chem. Rev. 2015, 115, 10081−10206

Scheme 30. Hydrolytic or Entropically Driven Restriction of Shuttling in a [2]Rotaxane[792]

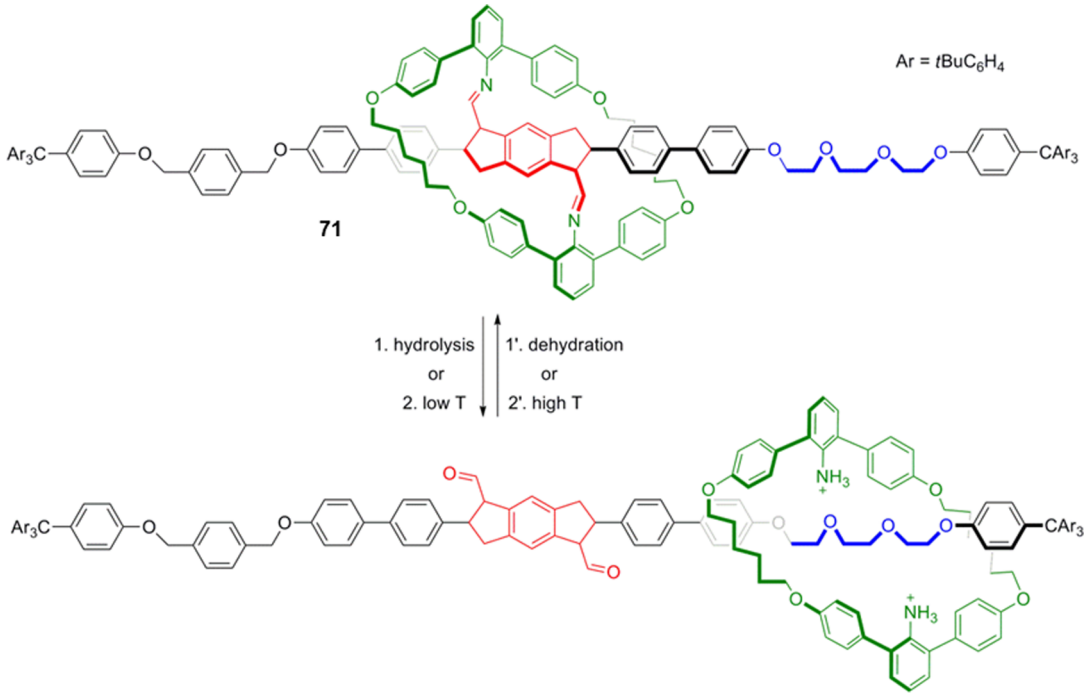

Scheme 31. Chemically Driven Shuttling in a [2]Rotaxane[793]

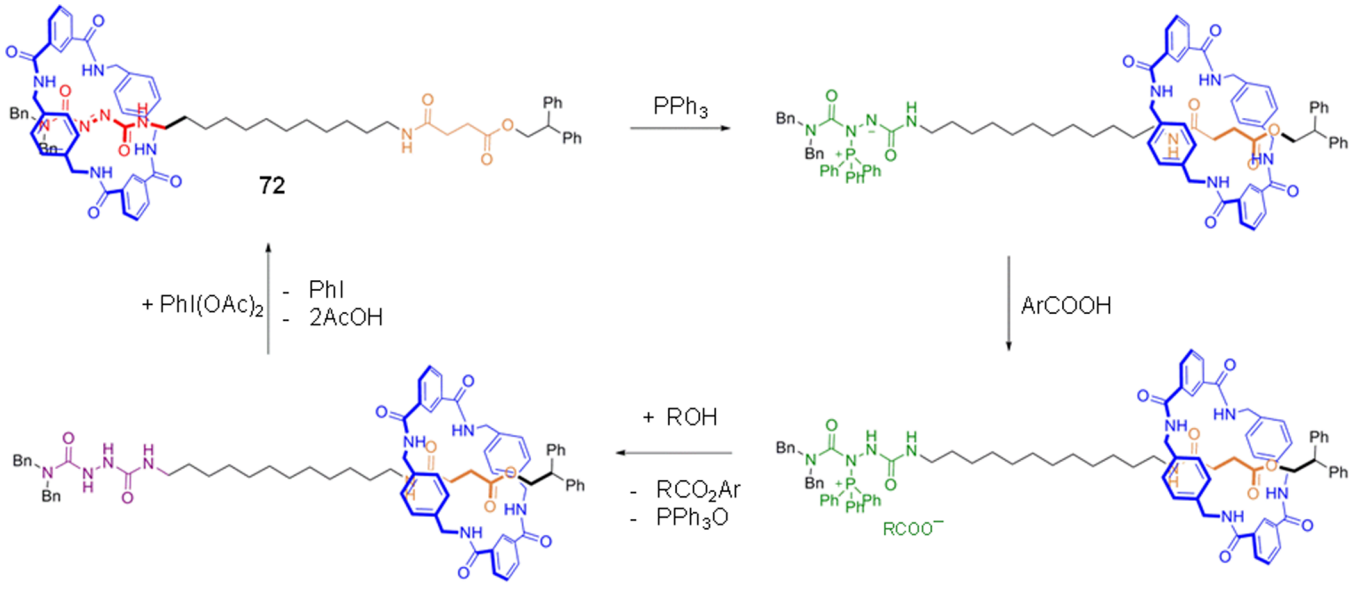

reversed by addition of $AgPF_6$. Metal-free, anion-induced shuttling between naphthalimide and triazolium stations was also reported in which shuttling could be monitored by UV−vis spectroscopy.[784] Iodide addition has been used to induce shuttling in a halogen/hydrogen-bonding rotaxane.[785]

In separate work, a shift in fluorescence was obtained by chloride-induced displacement of a macrocycle from a central squaraine station to either of two weakly binding degenerate stations.[786] In a tristable rotaxane bearing urea, ammonium, and phosphine oxide (listed in descending binding ability) stations on the thread, macrocycle shuttling could be induced by the binding of an acetate anion to the urea and subsequently to the ammonium site, which sequentially blocked these higher affinity stations and forced the macrocycle to bind to the weakly coordinating phosphine oxide station.[669] Similarly, the binding of a macrocycle to a guanidinium station was found to be inhibited by PO_4^{3-} addition.[787] In the presence of Zn^{2+}, the macrocycle preferentially bound the central 2,2′-bipyridyl station. In the presence of PO_4^{3-}, but not Zn^{2+}, the macrocycle moved to the weakly coordinating carbamate station. Copper removal followed by guest complexation between porphyrins in the two macrocycles has been used to drive shuttling of a [3]rotaxane.[788]

4.3.2.4. Shuttling Induced by Reversible Covalent Modification. Dynamic covalent bond formation and reversible reactions are important tools in the synthesis of supramolecular devices and machines. This is due to the ability to control their stability and lability by varying external conditions. These chemical tools enable shuttles to do work by "compartmentaliz-

DOI: 10.1021/acs.chemrev.5b00146
Chem. Rev. 2015, 115, 10081−10206

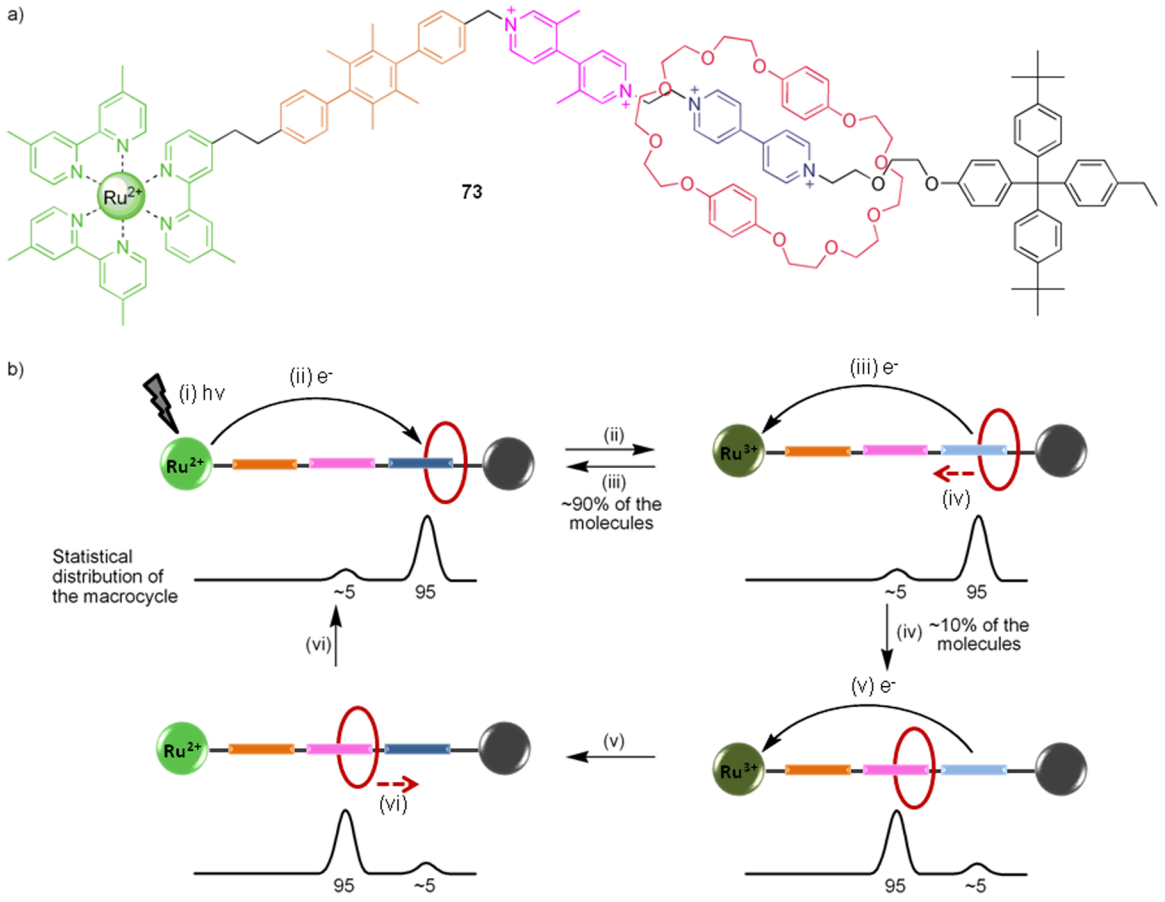

Figure 26. Photoinitiated redox-driven shuttling in a [2]-rotaxane initiated by (i) irradiation and (ii) subsequent reduction of viologen station. (iii) Competing back electron transfer from one-electron reduced viologen to Ru^{3+}. (iv, v) With continuous irradiation the macrocycle shuttles to the dimethylviologen station. (vi) Ceasing illumination restores the macrocycle to its original position.[794]

ing" the macrocycle on a station and acting as a physical barrier to prevent random Brownian motion reversing the desired translational motion during re-equilibration steps. This phenomenon will be discussed in detail in the following sections.

Reaction-based shuttling can be achieved in several ways. A station can be blocked by introducing a new chemical group, or destabilizing the binding of a macrocycle for steric or electronic reasons. The macrocycle can be chemically trapped on one station. Shuttling between hydrogen-bonding stations has been controlled by Diels–Alder and retro-Diels–Alder reactions, which block and unblock the better-binding fumaramide station.[789] In another example, photoinduced heterolytic cleavage of a C–O bond in a diaryl cycloheptatriene generated a positively charged tropylium station, and thus repelled the cationic cyclophane macrocycle, displacing it to a different station.[790,791] Oxidation or reduction of sulfoxide-based stations and subsequent changes in the hydrogen bonding to a benzylic amide macrocycle have also been used to control shuttling.[627]

Kawai et al. reported intrarotaxane imine formation between a diamino macrocycle and two formyl groups at one of the stations. This reaction locked the macrocycle at the station and maintained a positional discrimination (Scheme 30).[792] Hydrolysis of the imine in wet $CDCl_3$ in the presence of acid released the macrocycle from the station and also protonated the amino moieties, making the polyether station more favorable due to hydrogen bonding and ion–dipole interactions. Shuttling of the macrocycle could also be promoted by heating and cooling. This entropy-driven shuttling was possible because of the release of two water molecules on formation of the imine bonds. The entropic favorability of the imine state could be more easily overcome at lower temperatures by enthalpic contributions.

As with fumaramides, *trans*-azodicarboxamide modules have chemical structures preorganized for strong hydrogen bonding with benzylic amide-based macrocycles. The interaction of the macrocycle with the *trans*-azodicarboxamide station is stronger than that with the succinamide station. Induced shuttling of a macrocycle to the less favored succinamide station could be achieved chemically by blocking the favored station by reaction with triphenylphosphine (Scheme 31).[793] This bulky substituent drove the macrocycle away from the station. Under subsequent Mitsunobu reaction conditions, in the presence of a carboxylic acid and an alcohol, the triphenylphosphonium was cleaved from the station as triphenylphosphine oxide. After oxidation, the macrocycle returned to its initial position.

4.3.2.5. Photodriven Molecular Shuttles. Photoinduced shuttling is an attractive mode of control over translational motion due to the ease of stimuli introduction and removal. Moreover, if the back reaction or operation is spontaneous and does not require an additional input, then the overall process becomes autonomous; shuttling will occur as long as energy is supplied in the form of light. However, instead of a continuous light source, flashes of light must be used to prevent the system reaching and staying at a steady-state distribution. Although photodriven shuttling can be an efficient approach, the kinetics of translation and photochemical processes have to be carefully considered. If the photoinduced process involves a redox

DOI: 10.1021/acs.chemrev.5b00146
Chem. Rev. 2015, 115, 10081–10206

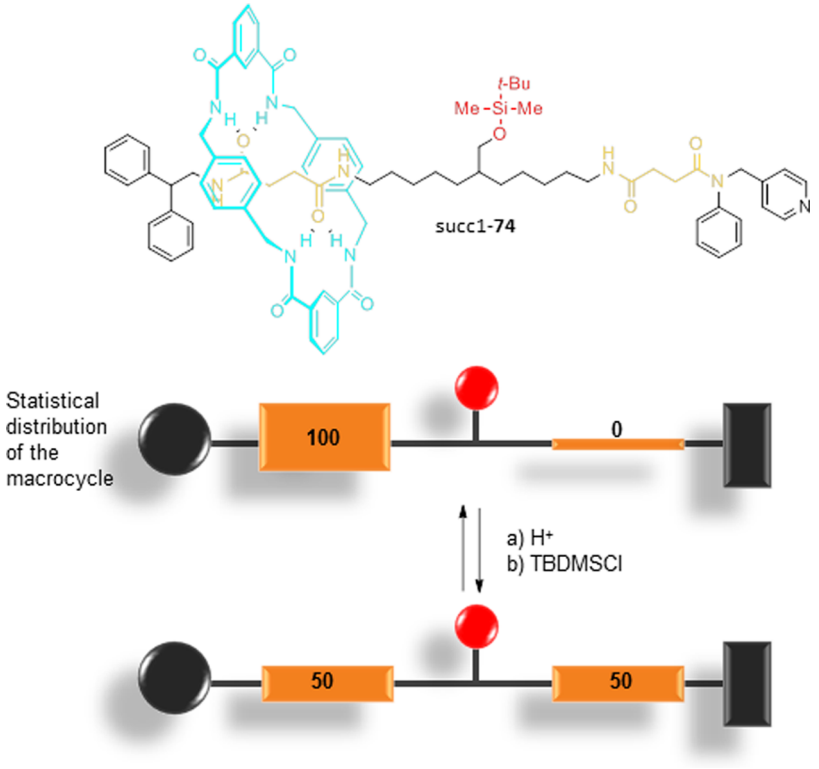

Figure 27. [2]Rotaxane **74** acts as an irreversible mechanical switch. The silyl ether is too bulky to allow macrocycle shuttling between the two succinamide stations.[75]

reaction, then rapid charge recombination can take place before positional displacement of the macrocycle. To avoid this, either excited states with a long lifetime are required or external reagents must be used to reduce or oxidize the species.

In a carefully designed shuttle reported by Stoddart et al., translational switching was obtained by one-electron reduction of a viologen station by a ruthenium trisbipyridine stopper (Figure 26).[794] Relatively slow back electron transfer permitted ca. 10% of the macrocycle to reposition to the dimethyl viologen station on each electron transfer. Continuous irradiation maintained a 95:5 distribution of the macrocycle in favor of the dimethyl viologen station. The system equilibrated back to the original viologen position once irradiation ceased with spontaneous back electron transfer allowing reversion.

Alongside the photoinduced redox reactions discussed above, improved excited-state hydrogen-bonding interactions[795] and the photoisomerization of stilbene,[796] azobenzene,[797] and other olefinic moieties leading to altered hydrogen bonding or steric bulk creation have also been used to drive shuttling processes.[798] Absorbance and fluorescence has been used to monitor the progress of shuttling along the rotaxane in some of these systems.[16,799−801] Likewise, other photochromic compounds such as spiropyrans have been exploited to control molecular shuttles, by switching between photoisomers that form hydrogen bonds of different strengths.[802]

4.3.2.6. Molecular Shuttles Driven by Changes in the Microenvironment. The term "microenvironment" usually refers to the temperature and solvent system. The easiest way to control shuttling via solvent choice is through the disruption of hydrogen-bonding interactions between the macrocycle and the station. Several examples of macrocycle relocation induced by a change in solvent polarity or rotaxane solvation have been reported.[803] In some cases, solvent molecules facilitate a shuttling process already driven by other stimuli.[698,797,804] For entropy-driven shuttles, the rearrangement of solvent molecules in or around the macrocycle is an important parameter controlling the shuttling process.

Rotaxanes bearing more than two stations and even polymeric rotaxanes driven by these stimuli have been reported.[797,805,806] In these shuttles, work is undone in each reverse shuttling. Directional shuttling via a ratchet mechanism has been achieved and will be discussed in the next section.

4.4. Compartmentalized Molecular Machines

Stimuli-responsive molecular shuttles are rotaxanes in which the net position of the macrocycle on the thread is controlled by external triggers (light, heat, electrons, chemical, pH, binding events, etc.). In general, these triggers change the properties of the binding sites and subsequently have an influence on macrocycle/thread interactions. In this section, various stimuli-induced mechanisms to create and control nonequilibrium conformations will be presented. Rotaxane succ1-**74** has two identical stations, which are distinguishable due to the differing stoppers. The thread is divided into two compartments by a bulky silyl ether barrier, preventing the macrocycle from shuttling between the two stations.[75] By removing the silyl ether group, dynamic exchange of the macrocycle was enabled and the system moved toward equilibrium. This resulted in a 50:50 distribution of the macrocycle between the two stations. The operation is irreversible, because the attachment of the bulky silyl group again does not change the average position of the macrocycle, and will not restore the initial distribution of the macrocycle; the position of the macrocycle is not determined by the state of the machine. The machine starts in a statistically unbalanced state (the bulky silyl group prevented the macrocycle restoring balance by moving toward an equilibrium distribution). By "linking" the system, removing the bulky group, the machine

DOI: 10.1021/acs.chemrev.5b00146
Chem. Rev. 2015, 115, 10081−10206

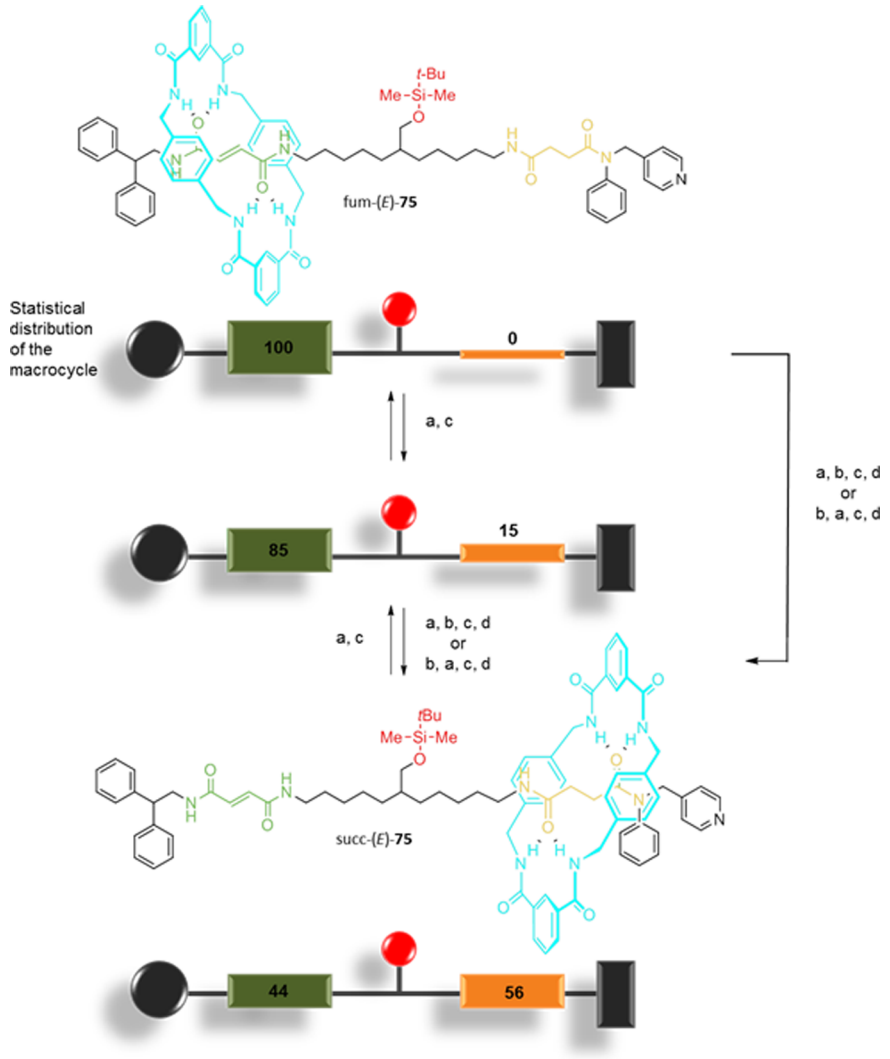

Figure 28. Operation of a compartmentalized molecular machine, which corresponds to a two-state Brownian flip-flop. Operation steps: (a) Desilylation (80% aqueous acetic acid); (b) $E \rightarrow Z$ photoisomerization ($h\nu$ at 312 nm); (c) resilylation (TBDMSCl); and (d) $Z \rightarrow E$ thermal isomerization (catalytic piperidine).[75]

could reach its equilibrium state, because free movement of the macrocycle was no longer prevented by the barrier. Therefore, the macrocycle had "escaped" to a lower energy distribution (Figure 27).

Recently, Coutrot and co-workers synthesized a two-compartment molecular machine consisting of a dibenzo-24-crown-8 macrocycle and a thread with anilinium and monosubstituted pyridinium amide stations.[807] The rotaxane was synthesized via CuAAC chemistry. Subsequent *N*-benzylation of the triazole moiety, which is located in the middle of the thread, was found to serve as a barrier as well as a third station for the macrocycle. Depending on which station the macrocycle was located, the *N*-benzylation of the triazole allowed trapping of the macrocycle in either the left or the right compartment.

The Leigh group has extended their initial system using the same design described above, but with two different stations **75** (a fumaramide station and succinamide station) (Figure 28).[75]

In this system, the exchange of the macrocycle between stations could be controlled by the introduction of a barrier in the middle of the thread (kinetic control) as well as by altering the binding affinity of the macrocycle to the two different stations (thermodynamic control). Initially, 85% of the macrocycle bound the fumaramide station and 15% the succinamide station. The system was still unlinked because of the kinetic barrier and therefore not in equilibrium. A balance-breaking stimulus (photoisomerization at 312 nm) generated a 49:51 *E*:*Z* photostationary state. Removal of the barrier, the linking stimulus, allowed the balance to be restored by the macrocycle equilibration. Restoring the barrier unlinked the system. The last step was $Z \rightarrow E$ olefin isomerization, which made the system statistically unbalanced, unlinked, and not in equilibrium. After one operational cycle of the machine, 56% of the macrocycles were located on the succinamide station. The thread had therefore changed the net position of the macrocycle. Because the succinamide station binds the macrocycle less strongly than the fumaramide station, this process has moved the macrocycle energetically uphill; that is, it has performed a ratcheting operation, transporting a particle away from equilibrium. This system and its function is an experimental realization of the transportation task required in Smoluchowski's trapdoor and Maxwell's pressure demon, which are discussed in the introduction (section 1) and are powered by chemical and light energy. Figure 29 shows a schematic representation of the four sequential steps performed by rotaxane **75** to transport the

DOI: 10.1021/acs.chemrev.5b00146
Chem. Rev. 2015, 115, 10081−10206

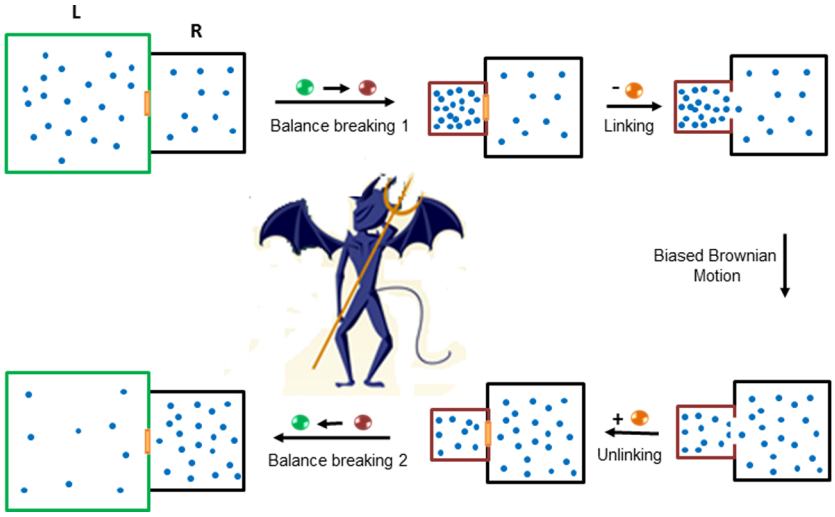

Figure 29. Initially the system is balanced (in proportion to the sizes of the two compartments), with an equal density of particles in the left and the right compartments. By changing the volume of the left-hand compartment, the system becomes statistically unbalanced. Opening the door allows the particle to redistribute according to the new size of the compartments. Closing the door ratchets the new distribution of the particles. Restoring the left compartment to its original size results in a concentration gradient of the Brownian particles across the two compartments. Here, the size of the compartment represents the energy level of the macrocycle-station system.[75]

system energetically uphill: balance-breaking 1, linking, unlinking, balance breaking 2 (resetting the machine but not the substrate).

There are many different types of compartmentalized molecular machines, some of which have been described in this section. Three main machine types exist. First is the two-state (or multistate) Brownian switch, which is a machine that can reversibly change the distribution of a Brownian substrate between two distinguishable sites as a function of state of the machine. It does this by biasing the Brownian motion of the substrate (section 4.3). Second is a two-state (or multistate) Brownian flip-flop, a machine that can reversibly change the distribution of a Brownian substrate between two (or more) distinguishable sites and that can be reset without restoring the original distribution of the substrate. The distribution of the substrate cannot be determined from the state of the flip-flop, but rather it is determined by the history of the operation of the machine. Rotaxane **75** is an example of a two-state Brownian flip-flop. Third, a Brownian motor is a machine that can repetitively and progressively change the distribution of a substrate while the machine can be reset without restoring the original distribution of the substrate. The rotary motors designed by Feringa and co-workers are examples of this category of device. Additional examples will follow in section 4.5.

Brownian ratchet mechanisms fall into two general classes: energy ratchets and information ratchets (section 1). The above rotaxane is an energy ratchet in which the energy minima and maxima of the potential energy surface are varied without regard to the particle's location. In the next section, examples of the second class of Brownian ratchets, information ratchets, will be explored where a barrier is raised or lowered according to the position of a Brownian particle on a potential energy surface, resulting in the particle distribution being directionally driven away from equilibrium.

4.4.1. Molecular Information Ratchets. An information ratchet, such as Maxwell's pressure demon, requires knowledge of the position of each particle and is able to open the door if the particle is approaching from a certain direction. This positional sorting allows the accumulation of particles in one side of the container and thus results in a pressure gradient. The first example of a molecular information ratchet was described by Leigh and co-workers (Scheme 32).[808] Molecular machine **76** consisted of a dibenzo-24-crown-8-based macrocycle, which was mechanically locked on a linear thread by bulky 3,5-di-*t*-butylphenyl stoppers. An α-methyl stilbene unit divided the thread into two compartments, both with ammonium binding stations. The rotaxane used photosensitized energy transfer from the macrocycle to the stilbene unit as the key step in changing the macrocycle distribution. When the stilbene unit adopted the *E* form, the macrocycle could move randomly along the full length of the thread by Brownian motion, while when the *Z* form is adopted, the macrocycle was trapped in one or the other of the two compartments. To keep the machine as the *Z*-isomer, it was operated in the presence of the photosensitizer PhCOCOPh. The sensitized photostationary state of α-methyl stilbene is 82:18 *Z:E*. Selective "gate opening" was achieved by photosensitized energy transfer from the macrocycle (which has a benzophenone (PhCOPh) moeity attached) to the stilbene unit. This led to a 55:45 *Z:E* ratio of the α-methyl stilbene. As energy transfer was distance dependent, this photosensitized transfer was more likely to happen when the macrocycle was in the blue compartment (Scheme 32). When the macrocycle was on the green station, intramolecular energy transfer from the macrocycle was not efficient and the gate stayed closed, biasing macrocyclic distribution. This is an example of using the positional information on a Brownian particle to break detailed balance, driving macrocycle distribution away from equilibrium.

An alternate approach to a molecular information ratchet using chemical fuel to directionally transport a macrocycle was later published by Leigh and co-workers (Scheme 33).[809] In this example, a phenyl ester attached to a chiral carbon center separated two degenerate fumaramide binding sites. The close proximity of the stations to the hydroxyl bearing carbon enabled the chiral center to influence the position of the macrocycle. At equilibrium, the macrocycle rested equally at either degenerate station. When a barrier was introduced by benzoylation with an achiral dimethylamino pyridine (DMAP) catalyst, an equal distribution of products was obtained. However, when the chiral

DOI: 10.1021/acs.chemrev.5b00146
Chem. Rev. 2015, 115, 10081−10206

Scheme 32. Structure and Mechanism of the Information Ratchet[a]

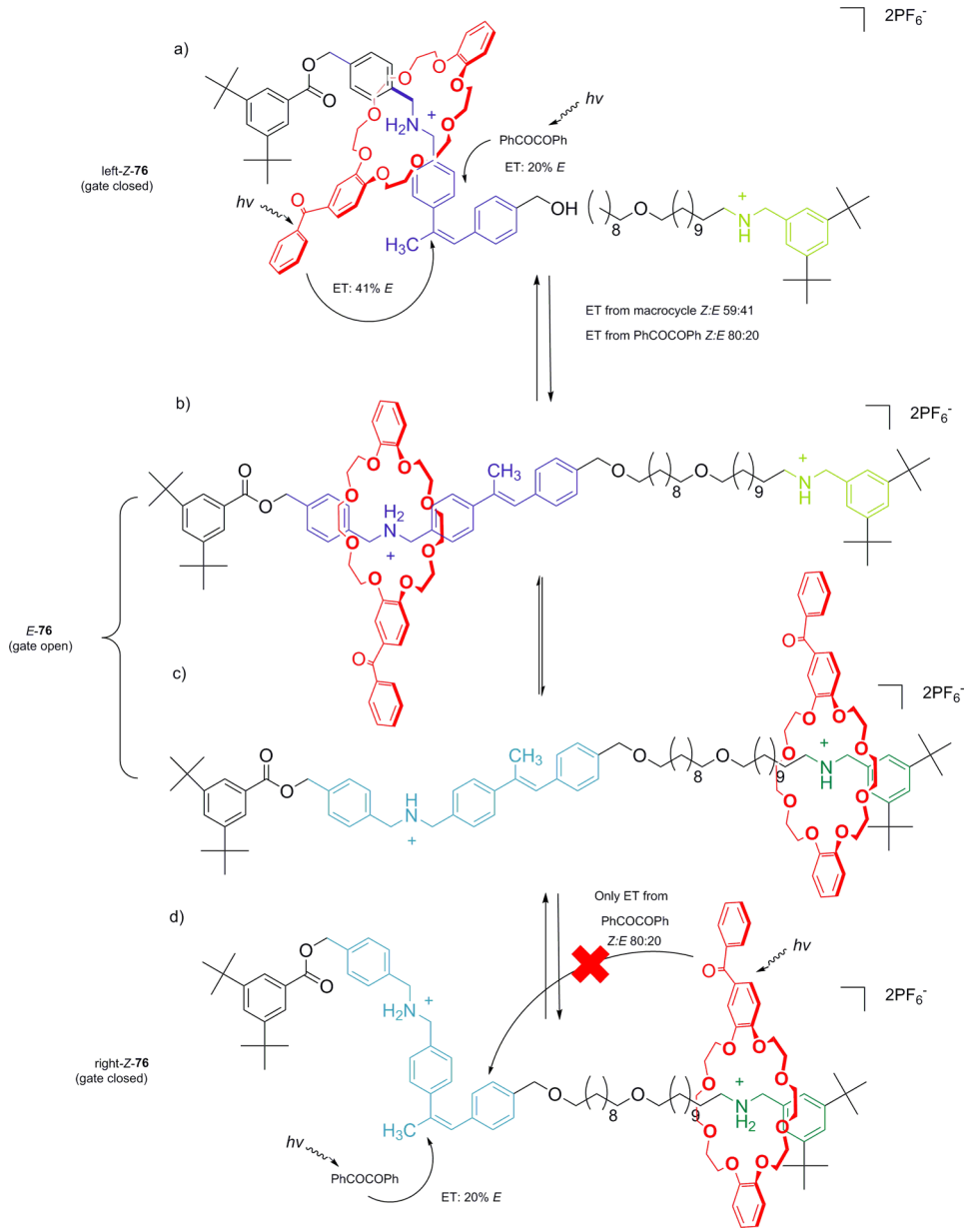

[a](a) Gate closed, but energy transfer from the macrocycle is efficient. (b and c) Gate is open, allowing free shuttling of the macrocycle. (d) The macrocycle is on the green station, intramolecular energy transfer (ET) from the macrocycle is inefficient; intermolecular energy transfer from PhCOCOPh dominates (closing the gate).[808]

DMAP-based catalyst (*S*)-**79** was used, a 33:67 distribution in favor of the pro-(*S*)-fumaramide (*S*)-**80** station was obtained. Using catalyst (*R*)-**79** resulted in a reverse bias in the position of the macrocycle. Because the stations were identical, macrocycle relocation resulted in a decrease in entropy, with identical enthalpic interactions, and thus a ratcheting operation was achieved. Motion away from an enthalpically favored location was achieved in a similar rotaxane, but with fumaramide and succinamide stations of different binding strengths. Using the same chiral catalyst, 15% of the molecules were relocated to the enthalpically unfavored succinamide station.

This concept was further developed in the three-compartment, chemically driven, molecular information ratchet **82**.[810] Here, the compartments contained fumaramide groups and were separated by hydroxyl groups (Scheme 34). The macrocycle could be efficiently trapped at either end of the track by sequential benzoylation of the hydroxyl groups in the presence of the chiral catalyst **83** resulting in a 1:21:79 distribution of the macrocycle. The steric barriers formed prevented the macrocycle from passing, and trapped the ring in a certain compartment. It was shown that the macrocycle had an influence on the rate of benzoylation of the hydroxyl groups on the thread resulting in acylation taking place preferentially far from the macrocycle. The distributional bias could be reversed with the enantiomeric catalyst **83**, and when both chiral catalysts were used the macrocycle preferentially resided in the central station with a 10:77:13 distribution.

Directional translational motion along the axis of pseudorotaxane has also been reported (Figure 30).[553,811,812] Threading and dethreading of the macrocycle could be controlled by

DOI: 10.1021/acs.chemrev.5b00146
Chem. Rev. 2015, 115, 10081−10206

Scheme 33. Chemically Driven Molecular Information Ratchet[809]

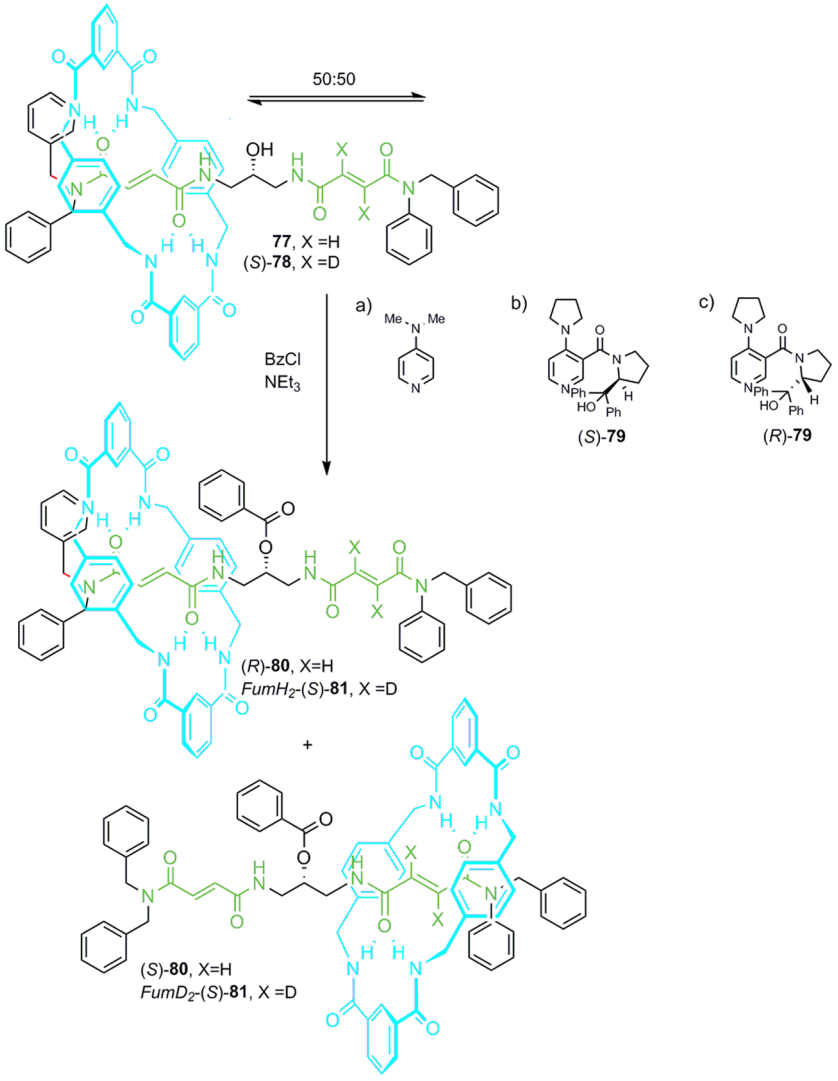

Substrate	Conditions	Product
77	(a)	(*R*)-**80**:(*S*)-**80** 50:50
77	(b)	(*R*)-**80**:(*S*)-**80** 33:67
(*S*)-**78**	(a)	*FumH*$_2$-(*S*)-**81**:*FumD*$_2$-(*S*)-**81** 50:50
(*S*)-**78**	(b)	*FumH*$_2$-(*S*)-**81**: *FumD*$_2$-(*S*)-**81** 33:67
(*S*)-**78**	(c)	*FumH*$_2$-(*S*)-**81**: *FumD*$_2$-(*S*)-**81** 67:33

photochemical, chemical, or electrochemical redox reactions. The pseudorotaxane axis has three different chemical motifs responsible for directional translocation. The first is a 2-isopropylphenyl group, a neutral energy barrier at one side of the axle. An electron-rich 1,5-dioxynaphthaline occupied the center, and at the other end was a positively charged 3,5-dimethylpyridinium station. A tetracationic electron-poor cyclobis(paraquat-*p*-phenylene) macrocycle formed a π-complex with the electron-rich 1,5-dioxynaphthaline group. To form the complex, the macrocycle had to pass one of the energy barriers, and the neutral 2-isopropylphenyl moiety presented a lower energy barrier. Hence, threading took place selectively from this side of the axis. Upon one-electron reduction of the macrocycle, interaction with the 1,5-dioxynaphthaline station was weakened. Additionally, as a result of the reduced positive charge on the macrocycle, electrostatic repulsion from the pyridinium site became less potent, allowing the macrocycle to pass over this barrier with greatly reduced activation energy. Hence, once reduced, the macrocycle dethreaded over the pyridinium group. The macrocycle threaded and dethreaded in a directional manner via a ratcheting mechanism (flashing ratchet) acting on the potential energy surface of the pseudorotaxane axle. The same group later reported a flashing ratchet based on similar principles, in a pseudorotaxane with one stopper, where threading was driven by reduction, and dethreading slowly occurred after rapid shuttling away from a reoxidized bipyridinium station.[813] Recently, Credi et al. also reported the photodriven directional threading/dethreading of a crown ether macrocycle on an axle using a flashing ratchet mechanism.[814,815]

4.5. Controlling Rotational Motion in Mechanically Bonded Structures

An alternative way to extract work from mechanically interlocked structures would be to control the relative rotation of their components. The rate of macrocycle pirouetting can easily be controlled through temperature, electric field strength, light,

DOI: 10.1021/acs.chemrev.5b00146
Chem. Rev. 2015, 115, 10081−10206

Scheme 34. Directional Transport of a Macrocycle in a [2]Rotaxane Three-Compartment Chemical Information Ratchet

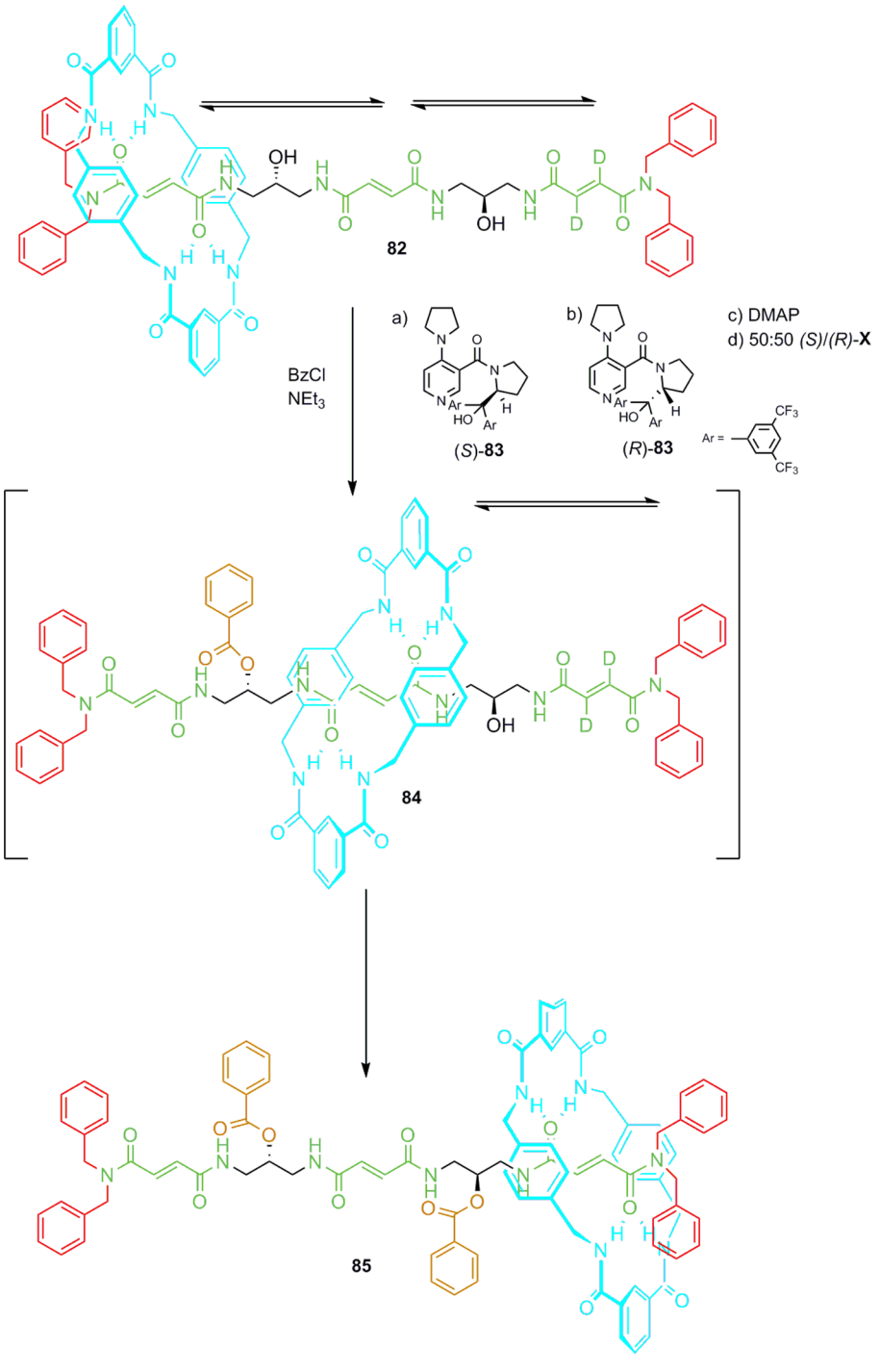

Conditions	Catalyst	Product Distribution(± 3%)
(a)	*(S)*-**83**	*left*-**85**:*center*-**85**:*right*-**85** <1:21:79
(b)	*(R)*-**83**	*left*-**85**:*center*-**85**:*right*-**85** 75:25:<1
(c)	DMAP	*left*-**85**:*center*-**85**:*right*-**85** 39:18:43
(d)	50:50(S)/(R)-**83**	*left*-**85**:*center*-**85**:*right*-**85** 10:77:13

structural freedom, or by altering its interaction using other chemical moieties or solvents.[564,698,816−819] Nevertheless, controlling the directionality of this movement requires careful design.

4.5.1. Controlling Rotational Motion in Rotaxanes. The pirouetting frequency of a macrocycle around a thread depends strongly on the strength of the interactions between the macrocycle and the thread (and environment), which must be broken and reorganized during the movement of the macrocycle. The rate of macrocyclic pirouetting in some hydrogen-bonding rotaxanes can be controlled by changing the strength of an electric field, which alters the strength of the hydrogen

DOI: 10.1021/acs.chemrev.5b00146
Chem. Rev. 2015, 115, 10081−10206

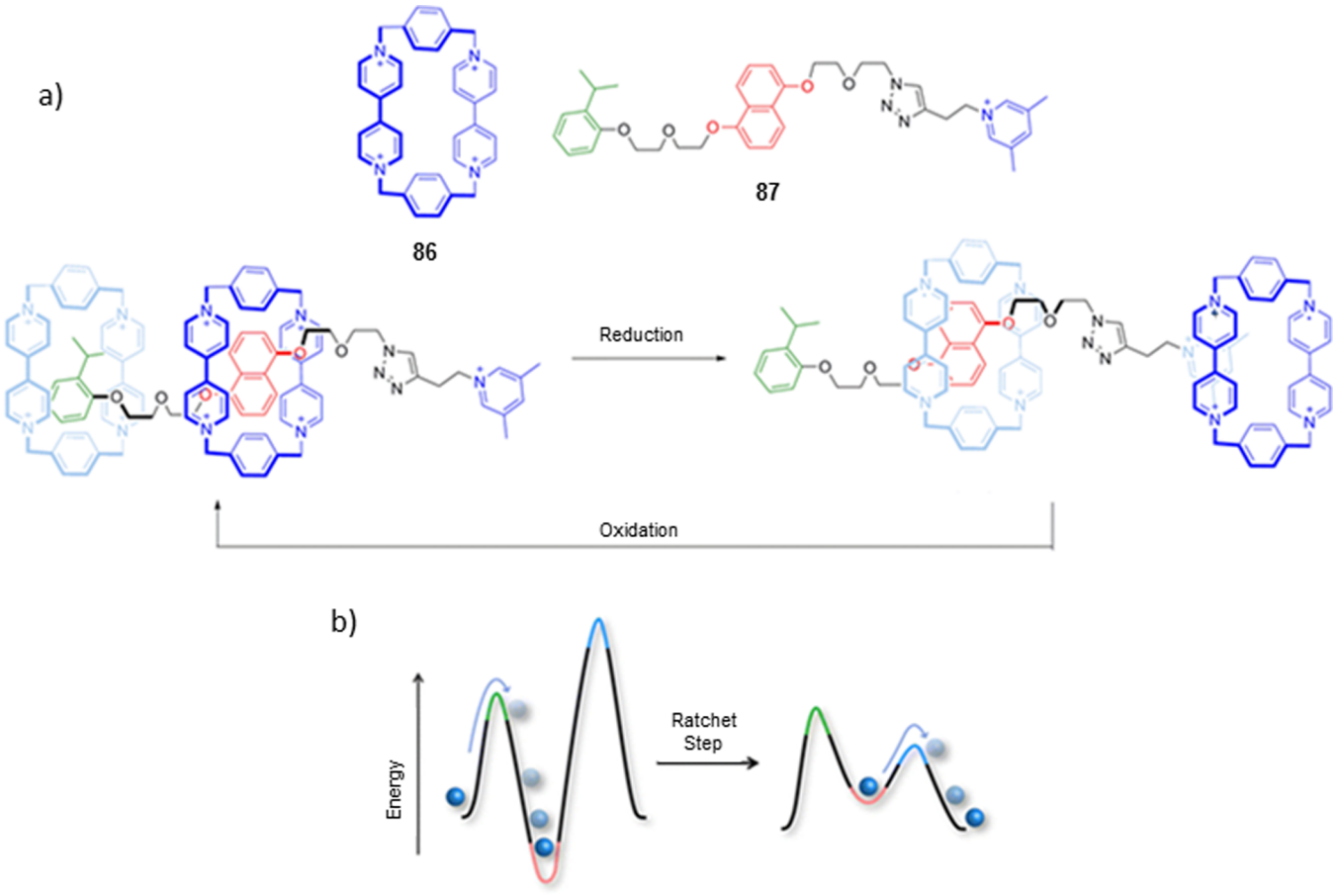

Figure 30. Photodriven directional translational motion in pseudorotaxanes **86**−**87**. Reprinted with permission from ref 811. Copyright 2013 American Chemical Society.

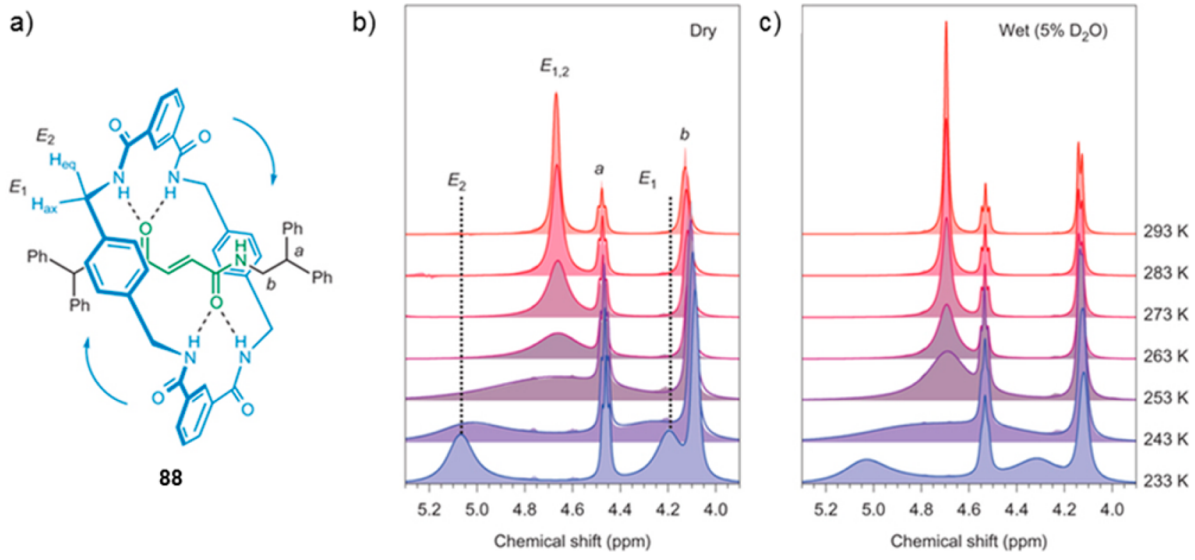

Figure 31. Effect of water on the rate of pirouetting of a macrocycle about an axle. Reprinted with permission from ref 698. Copyright 2013 Nature Publishing Group.

bonds.[820−824] In some cases, direct manipulation of macrocycle/axle interactions can either restrict rotation or increase its frequency by weakening intracomplex interactions. The formation of weaker hydrogen bonds with maleamide units as compared to fumaramide units has been discussed in previous sections. Fumaramide preorganizes two hydrogen-bonding motifs to bind the macrocycle, leading to an increase in binding strength. On the other hand, the *cis*-form of this olefinic structure can only form hydrogen bonds with one site of the macrocycle. As a consequence, the station−macrocycle interactions are weaker, and thus rotation was observed to increase in frequency by 6 orders of magnitude on photoisomerization.[825]

DOI: 10.1021/acs.chemrev.5b00146
Chem. Rev. 2015, 115, 10081−10206

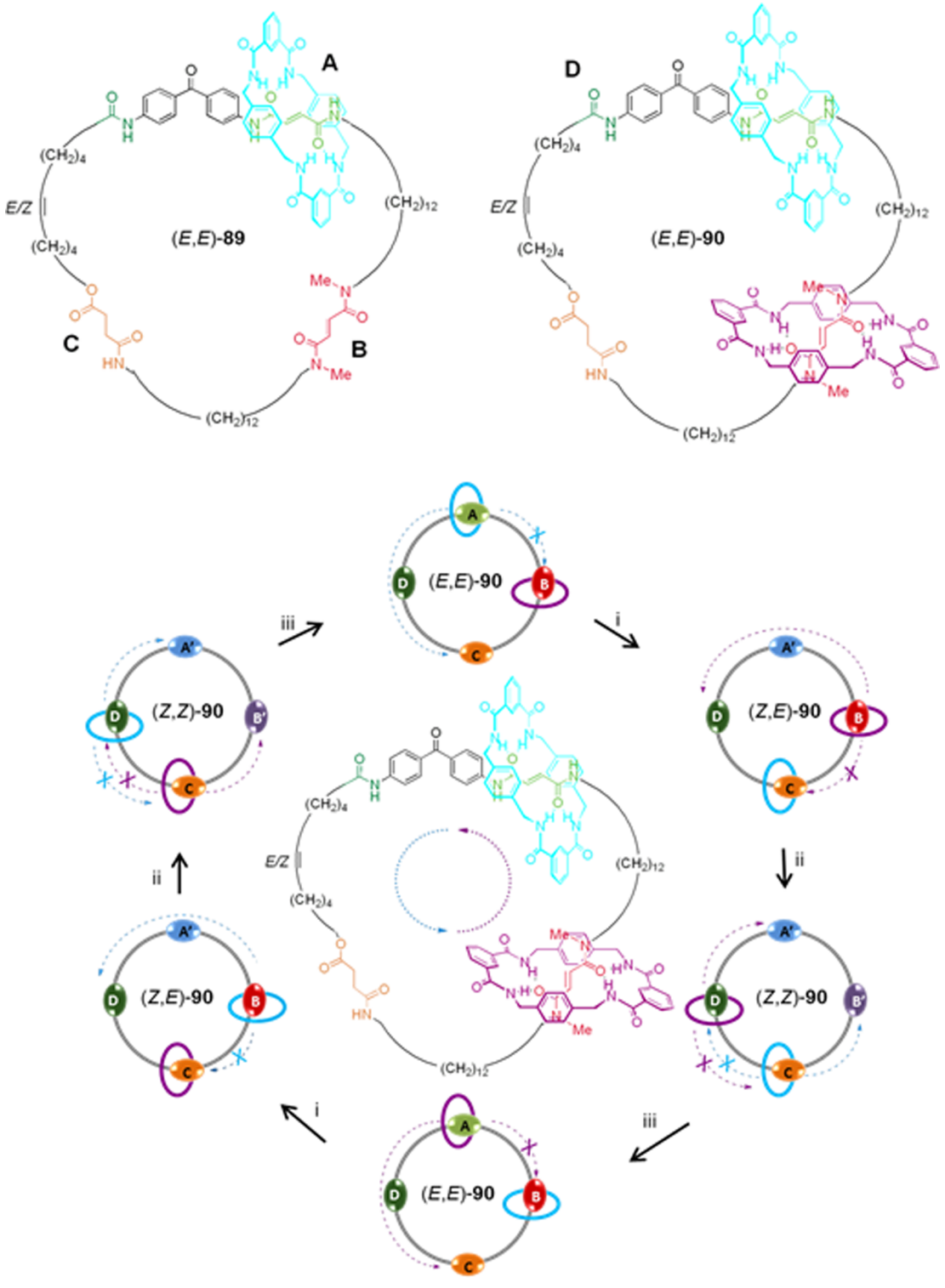

Figure 32. Directional circumrotation in a [3]catenane. (i) $h\nu$ (350 nm), (ii) $h\nu$ (254 nm), (iii) heating; or heating with catalytic ethylenediamine; or catalytic Br_2, $h\nu$ (400−670 nm). Adapted with permission from ref 883. Copyright 2003 Nature Publishing Group.

Like photoisomerization-dependent disruption of hydrogen bonding,[825] solvent choice can also play a role in controlling these noncovalent interactions and hence influence the rate of pirouetting in a rotaxane system.[826] Comparison of the rate of exchange between axial (E_1) and equatorial (E_2) protons, which was determined by the pirouetting rate, showed that, as compared to heating in dry pyridine, the exchange was greatly accelerated when the pyridine contained 5% D_2O (Figure 31).[698,827] Addition of water sped up redox-driven shuttling in a different rotaxane system by hydrogen-bonding dependent "lubrication" of the mobile elements. Interestingly, other protic solvents (alcohols, nitromethane) had less effect on the pirouetting rate. This was attributed to the ability of water to form 3-D hydrogen-bonding networks. The effect on macrocycle−thread interactions of the sequential addition of single

DOI: 10.1021/acs.chemrev.5b00146
Chem. Rev. 2015, 115, 10081−10206

Scheme 35. Directional Circumrotation in [2]Catenane 91[885]

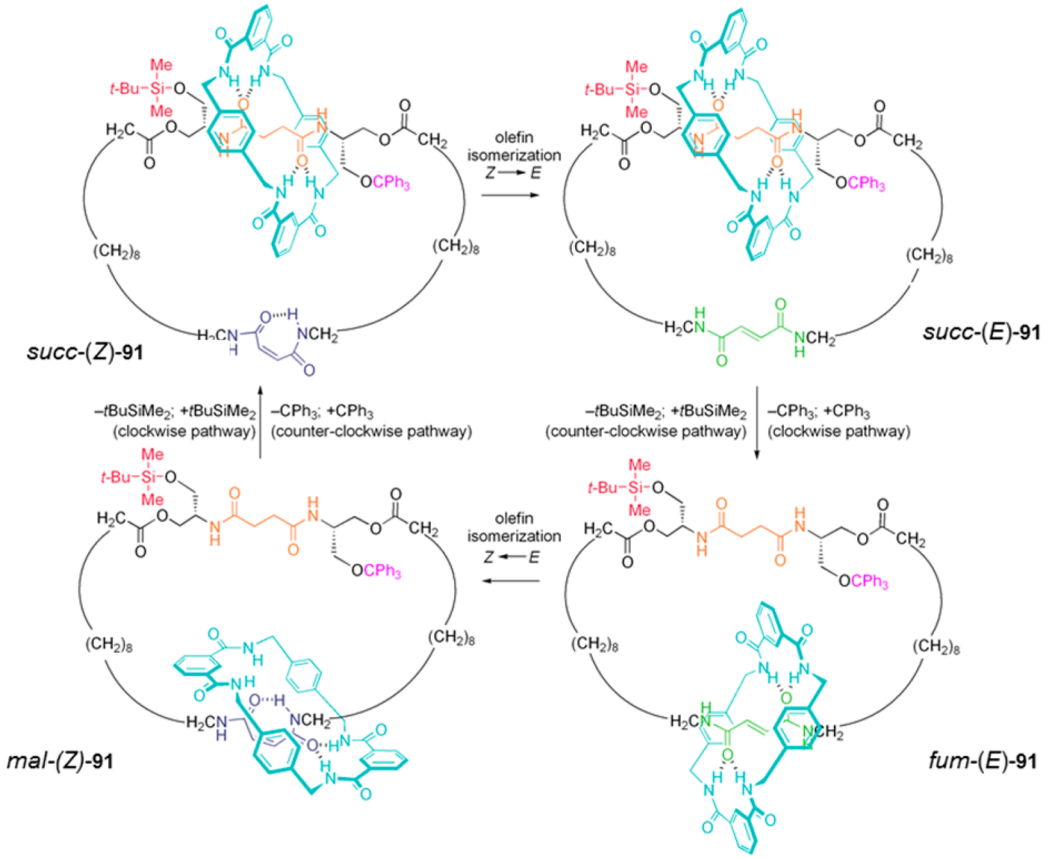

methanol molecules has been probed by IR spectroscopy of rotaxane-solvent clusters.[828,829]

Besides hydrogen-bonding, cation-induced restraint of motion in a crown ether-based macrocycle has been reported with a corresponding increase in pirouetting rate upon demetalation.[817,818,830−834] Redox-dependent switching between coordinating ligands on a macrocycle has been used to control rotational orientation of a macrocycle about a rotaxane axle.[818] In a hybrid organic−inorganic rotaxane, hydrogen bonding between fluorines on the macrocycle and ammonium stations resulted in slow shuttling but fast rotation.[835,836] This rapid rotation was attributed to the array of hydrogen-bonding interactions formed in which a new bond had already started to form before the original was completely broken.

4.5.2. Controlling Rotational Motion in Catenanes. The points discussed above for rotaxanes also apply to rotational motion in catenanes. In a catenane, the rate of rotation of one macrocycle with respect to the other depends on the strength of interactions between the two. Therefore, any stimuli altering this interaction should result in a change in rotational rate. The solvent dependence of the rate of macrocycle rotation in catenanes containing benzylic amides has been measured by NMR analysis and also by AFM-based single molecule measurement techniques.[837] In the second method, catenanes with different intercomponent hydrogen-bonding ability were attached to poly(ethylene oxide) polymers and analyzed in dimethylformamide (DMF) and tetrachloroethane ($C_2H_2Cl_4$). As a measure of equilibrium conformational entropy, the persistence length of the polymer was analyzed for two different compounds in two different solvents to estimate the restriction of motion of the macrocycle in the catenane. In agreement with the NMR analysis, in a single molecule experiment using the AFM method, the mobility of the macrocycle was shown to be accelerated by polar solvents or by disrupting the hydrogen-bonding ability by chemical modification.

Ion exchange,[838−840] pH,[841−844] redox,[845−856] demetalation,[842,857−869] light or redox-mediated ligand exchange of metals,[853,855,870] photochemical switching,[870−878] photoisomerization-dependent sequestering of macrocycle[879] and solvent,[826,880−882] photoisomerization-dependent change in hydrogen-bonding potency,[883] and the self-assembly of liquid crystal phases[884] have also been reported to control the rotation of the macrocycle in catenanes. However, directional rotation of one macrocycle with respect to another in a catenane structure has rarely been investigated. Directional rotation was achieved with a [3]catenane in which the presence of a third macrocyclic component helps to restrict the rotational freedom of the molecule (Figure 32).[883] The large macrocycle on which the two small macrocycles rotate bears four different interaction sites: two fumaramide motifs with different binding affinities (light green and red, the methylated station has a lower affinity for steric reasons), one succinic amide ester (orange), and finally an amide group (dark green). A benzophenone unit is attached close to the first fumaramide station to enable selective photosensitized isomerization of this olefinic group through energy transfer using a higher wavelength than required for nonsensitized isomerization.

Initially, in the absence of any stimuli, one of the macrocycles (blue) rests on the most favored fumaramide station, while the second macrocycle (purple) resides on the second most favored, the methyl-fumaramide station (Figure 32). Upon photosensitized isomerization of station A, hydrogen-bonding

DOI: 10.1021/acs.chemrev.5b00146
Chem. Rev. 2015, 115, 10081−10206

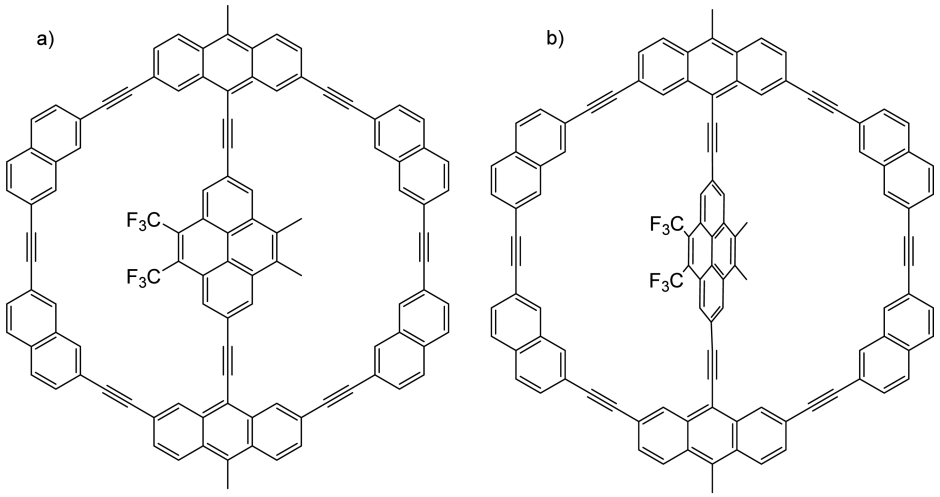

Figure 33. Schematic representation of an electric revolving door. (a) Door closed-switch on leading to high conductance. (b) Door open-switch off leading to low conductance.[932]

Scheme 36. A Molecular Rectifier[a]

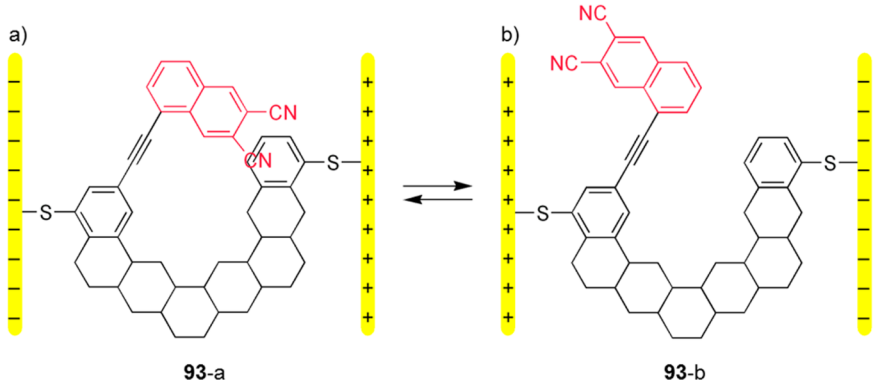

[a](a) High conductance predicted. (b) Low conductance predicted.[934]

interactions between the blue macrocycle and the station weaken, and because the second most favored site is already occupied by the purple macrocycle, the blue macrocycle moves to the third most favored, succinimide amide ester station C. Further photoisomerization of the methyl-fumaramide station triggers the shuttling of the purple macrocycle to the final binding site, station D. The fumaramide stations are converted to the *cis*-isomers either by heating in the presence of a catalytic amount of ethylenediamine or via irradiation at 400−670 nm in the presence of a catalytic amount of Br_2. This time, however, the relative orientations of the macrocycles force repositioning to the newly formed fumaramide stations in the opposite, with respect to the initial, distribution. A second round of stimuli is necessary to fully reset the system and to bring the macrocycles back to their initial positions. The combination of control of station binding affinity and macrocycle position allowed directional rotation in this catenane.

A directional [2]catenane rotary motor has also been reported with a simpler chemical/photoinduced mode of operation and well-defined ratcheting mechanism.[885] In this example, the balance breaking operation (to create a new equilibrium distribution) was photoisomerization of the fumaramide station. However, the macrocycle's rotation to the new energy minima was blocked by two orthogonal protecting groups: an acid labile trityl and base labile *tert*-butyl-dimethylsilyl. Selective deprotection of one of these protecting groups allowed the movement of the macrocycle to the succinamide station in only one direction. For clockwise rotation, trityl deprotection was required. Under equilibrium conditions, the alcohol had to be protected once more to avoid the work being undone. Full rotation was attained by deprotection and reprotection of the *tert*-butyldimethylsilyl moiety with reisomerization of the fumaramide station. The sequence of deprotection−reprotection reactions could be reversed to achieve counter clockwise circumrotation. The repositioning of the macrocycle to its new equilibrium position was via only one of two degenerate pathways, and thus the system acts as a directional molecular rotor (Scheme 35).

5. MOLECULAR LEVEL MOTION DRIVEN BY EXTERNAL FIELDS

In most synthetic molecular machines described to date, control over motion arises from the selective restriction of Brownian fluctuations through control of steric and noncovalent bonding interactions (via manipulation of chemical structure). The application of external fields can cause the bulk movement or orientation of a molecular species with electric field-directed alignment of liquid crystals being the most important

DOI: 10.1021/acs.chemrev.5b00146
Chem. Rev. 2015, 115, 10081−10206

technological application. Several research groups aim to use electromagnetic fields to control submolecular motion, with most examples concentrating on generating submolecular rotary motion. Molecular rotation involves passage over the minima and maxima of a torsional potential energy surface. An external field can either induce an excited state, where the torsional potential energy surface is altered, or interact with a permanent or induced molecular dipole and so orient the molecule in a particular direction. The interaction between the field and the rotor provides the energy necessary to surmount kinetic barriers and overcome energy dissipation and thermal randomization. To date, molecular dynamics simulations of molecular rotatory systems have dominated the field.[886−930] Only a few examples exist where theoretical studies have led to the synthesis of rotors and their examination under the influence of an electric field.

A recent example is the simulation of a single-molecule electric revolving door based on a phenyl-acetylene macrocycle published by Hsu, Li, and Rabitz.[931,932] The authors found, based on simulations, that the opened and closed-door states of **92**, whose exchange was accompanied by significant conductance variation, could be operated by an external field. Furthermore, they proposed that due to the large on−off conductance ratio, the molecular machine could also serve as an effective switching device (Figure 33).

An earlier example of a computational investigation was published by Ratner and Troisi.[933,934] Compound **93** bound between two electrodes exhibited motion under the influence of an electric field (Scheme 36). The authors suggested that the system could find applications in molecular electronics and could be used to create switchable molecular junctions. Theoretical studies revealed that the conformers of **93** (which could be interchanged by an external field) also showed differences in conductance across the junction and could thus be used as a conformational molecular rectifier.[935−937]

Fujimura and co-workers undertook a series of theoretical studies into the mechanism of rotation in gas-phase directional chiral motors driven by picosecond pulses of a linearly polarized laser.[938−950] In one study, aldehyde **94** was examined as a chiral molecular motor with the formyl group as the rotor (Figure 34).

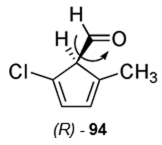

(R) - **94**

Figure 34. One enantiomer of chiral molecule **94**, in which directional rotational motion was driven by linearly polarized laser pulses and studied by quantum and classical mechanical simulations.[940]

They considered both enantiomers in their studies and came to the conclusion that directional motion originated from the asymmetric potential-energy surface of the chiral molecules and time-correlated forces created by laser-permanent dipole interactions.[940] The process is reminiscent of a rocking Brownian ratchet (section 1.6.2), but here thermal energy is not required to surmount kinetic barriers.[951]

Several examples of surface-mounted molecular rotors have been reported where motion could be driven by alternating electric fields or the absorption of pulses of light.[952−962] Michl and co-workers synthesized, on the basis of computational studies, a series of surface-mounted rotors.[963−965] Figure 35 shows the structure of polar and nonpolar versions of their altitudinal rotor. Polar rotor **96** consisted of a 9,10-dihydrophenanthrene substituted by four fluorine atoms on the central ring and had a calculated dipole moment of 3.7 D. The nonpolar rotor was a 4,5,9,10-tetrahydropyrene whose D_2 symmetry precluded a dipole moment. X-ray photoelectron spectroscopy (XPS), scanning tunneling microscopy (STM), and IR spectroscopy showed that for a fraction of the molecules, the static electric field from an STM tip induced a change in the orientation of the polar rotor, but not in the nonpolar analogue.[966] Several molecular dynamics simulations studying the influence of an electric field or a fluid flow on the rotation of a molecule fixed on a surface have been published by the same group.[967,968] One recent example simulated carborane-based molecular propellers and showed that they could be successfully driven at GHz rates by an oscillating electric field or by a flow of gas.[969]

Molecular machines in the solid state and condensed phase will be discussed in more detail in section 8.6.1. A number of research groups have been working in the field of crystalline molecular machines with the goal of creating new materials with interesting properties and that are responsive to external stimuli such as external electric fields.[970−975] Amphidynamic crystals are a form of condensed-phase matter with anisotropic molecular order and controlled dynamics, and they offer a good platform for the design of these new materials.[976] Molecular rotors are one of the most promising molecular structures for the synthesis of amphidynamic crystals. Structural designs analogous to macroscopic gyroscopes and compasses are one possibility in the design of such molecular rotors. Several examples have been published consisting of a rotating unit linked to a shielding box or stator by an axle.[977−980] The shielding box generates the local free volume required for unhindered rotation in an otherwise densely packed environment. The study of the orientation of and dipole−dipole interactions in dipolar rotor arrays are important in understanding the dielectric properties of these materials and

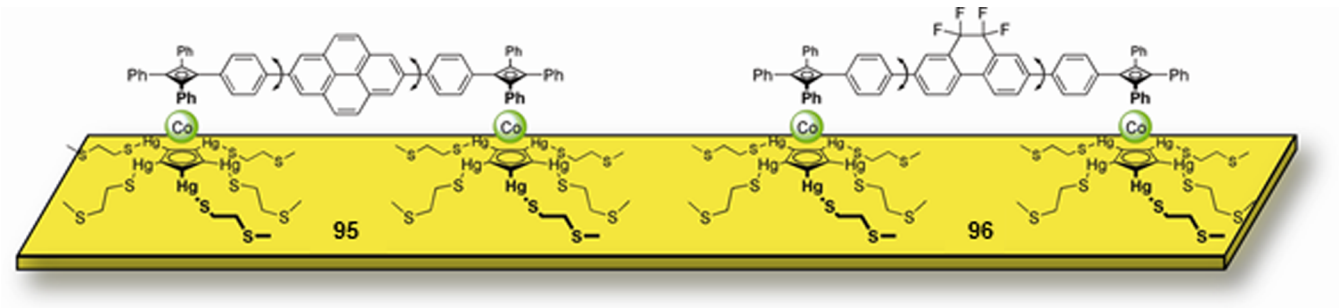

Figure 35. Nonpolar **95** and dipolar **96** altitudinal rotors mounted on an Au(111) surface. Note that rotor and flanking aryl rings are arbitrarily shown perpendicular to the surface for clarity.[966]

DOI: 10.1021/acs.chemrev.5b00146
Chem. Rev. 2015, 115, 10081−10206

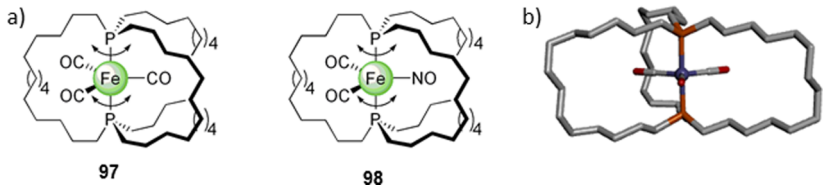

Figure 36. (a) Molecular structure of transition-metal-based gyroscopes **97** and **98**. (b) X-ray structure of compound **97**. X-ray crystal structure reprinted with permission from ref 983. Copyright 2004 Wiley-VCH Verlag GmbH & Co. KGaA, Weinheim.

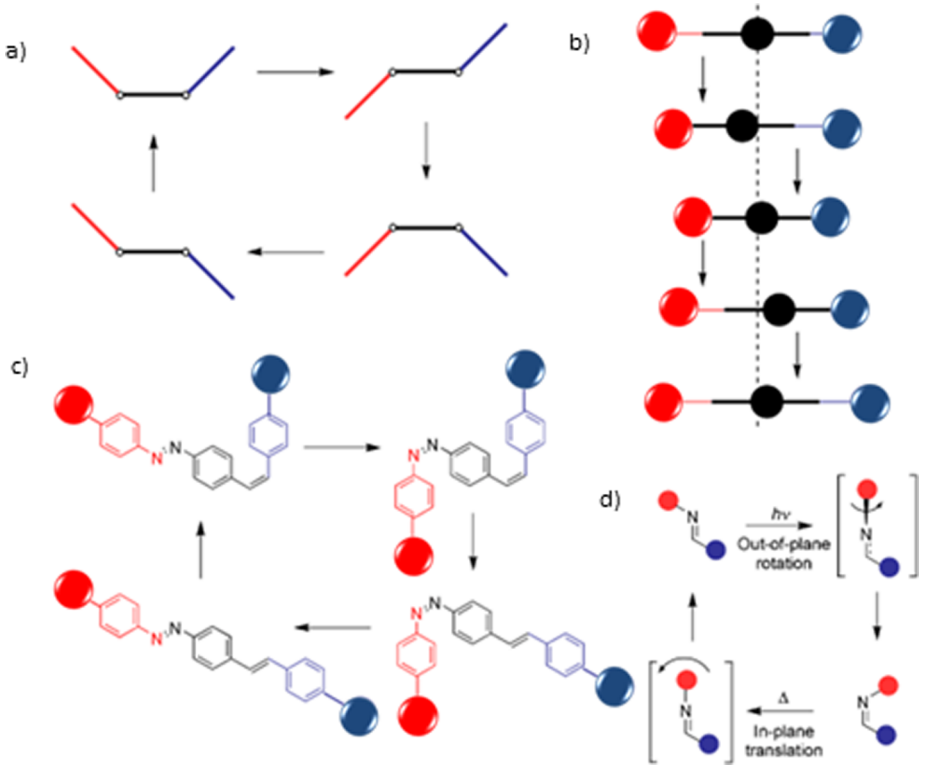

Figure 37. (a,b) Proposed designs for swimmers viable at the nanoscale. (c,d) Potential molecular solutions.[14]

the dynamics of the dipolar rotors. Furthermore, materials containing dipolar rotors can be controlled and reoriented by external electromagnetic fields or optical stimuli.[981,982] Examples of molecular gyroscopes have been reported by Gladysz et al., who developed transition metal-based systems in which *trans* phosphorus donor atoms are bridged by three methylene chains or related linkers. For example, the system shown in Figure 36 contains either a $Fe(CO)_3$ or a $Fe(CO)_2(NO)^+$ rotor. The latter possesses a dipole moment, which could be a possible handle for external control.[983] A series of studies have been carried out by the same group using gyroscope-like platinum and palladium complexes with *trans*-spanning bis(pyridine) ligands.[984]

Molecular gyroscopes with two bulky stators such as triarylmethyl or triptycyl groups, creating space for a 1,4-phenylene, have been reported.[985−1002] Some of these wheel and axle motifs (see also section 8.6.4) showed a dielectric response as a function of external alternating electric fields.[981,1003]

6. SELF-PROPELLED NANOSTRUCTURES

The mechanical self-propelled motion of microscopic objects such as bacteria and the motion of camphor or soap "boats" driven by interfacial forces have long fascinated scientists. More recently, focus has shifted to the control of nanoscale motion in synthetic systems.[1004,1005] These systems are driven not by thermal energy, but by other mechanisms more relevant on the nanoscale. Motion may be generated either autonomously when the energy required for movement is continuously supplied or nonautonomously.

6.1. Propulsion by Manipulation of Surface Tension

If surface tension is not balanced between two sides of a droplet of liquid or a bubble of gas, directional transport may occur. This is known as the Marangoni effect and is observed in several natural systems exhibiting spontaneous flow.[1006,1007] Temperature gradients have typically been used in artificial systems to generate Marangoni flows.[1008−1014] A droplet containing a species that absorbs to the surface, irreversibly modifying the surface energy thereof, has also been used to illustrate this effect in a "chemical Marangoni effect".[1015−1018]

The autonomous motion of millimeter scale objects on a liquid surface driven by the catalytic decomposition of hydrogen peroxide was reported by Whitesides et al.[1019] A small area of platinum near the edge of each disc catalyzes this decomposition and releases oxygen bubbles, which drive the movement by a recoil force. Others, however, observed the motion of platinum−gold rods toward the oxygen producing platinum end.[1020−1025] The contributions of driven and Brownian motion could be distinguished at aqueous/organic interfaces,[1022] and a rotor based on the same principles has also been synthesized.[1026] A

DOI: 10.1021/acs.chemrev.5b00146
Chem. Rev. 2015, 115, 10081−10206

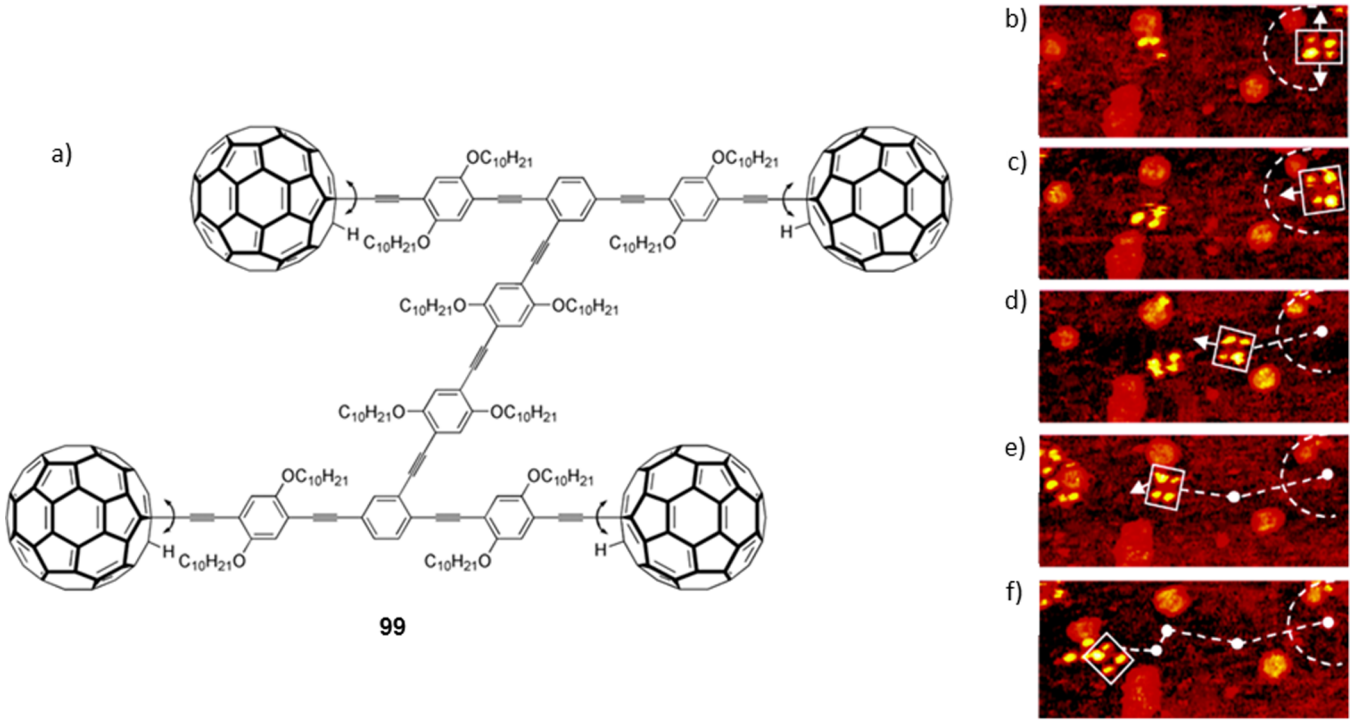

Figure 38. (a) Chemical structure and (b–f) STM micrographs of translational motion of a four-wheeled "nanocar" on an Au(111) surface at 200 °C. Wheels are shown by yellow spots, and the path is highlighted with a white arrow. Reprinted with permission from ref 1129. Copyright 2005 American Chemical Society.

similar system was reported by Manners and co-workers.[1027] Ozin et al. reported platinum–silica sphere dimers, which showed quasi-linear motion in bulk solution and rotational motion at the solution–glass interface.[1028] Rotors of decreased size and increased rotational rate have since been reported,[1029] both once more based on hydrogen peroxide decomposition.[1030] The catalytic domain has been scaled down to a molecular level by Feringa et al.,[1031] who utilized a surface bound dinuclear manganese catalase analogue.

Recently, Fischer et al. reported a self-propelling nanoparticle of only 30 nm diameter, a size comparable to certain enzymes, based on a Pt–Au system.[1032] Feringa and co-workers reported the use of carbon nanotube bound enzymes in autonomous propulsion.[1033] As an alternative to the ubiquitous use of hydrogen peroxide to propel nanoparticles, hydrogen evolution by a magnesium domain has been exploited to drive autonomous motion.[1034] Finally, Sen et al. reported the use of ring-opening metathesis polymerization using a modified Grubbs' catalyst to propel a nanoparticle. Motion was generated by the consumption of monomer only on one side of the nanoparticle, that where the catalyst is bound. This creates a concentration gradient across the nanoparticle and thus movement.[1035]

6.2. Mechanical Self-Propulsion

In contrast to most synthetic, surface tension driven, self-propelled systems, microorganisms almost exclusively utilize mechanical self-propulsion, akin to a swimming motion or the corkscrew motion of a boat's motor. The low Reynolds number at the nanoscale limits the number of swimming mechanisms that are viable,[1036] as any useful motion must involve a nonreciprocal motion to break the time reversal symmetry.[26,1037−1044] Various solutions have been proposed (Figure 37).[1041,1045−1050] The key point in each is that they must possess at least two hinge points; no system with a sole hinge point can be nonreciprocal. The sequential use of each hinge point allows motion at low Reynolds number.

No molecular solutions have yet been reported. However, a microscopic artificial swimmer has been reported.[1051] A major difficulty in realizing any molecular design would be carrying out the driven motion rapidly and frequently enough to be observable against random Brownian motion. The repetitive, directional, rotation of a chiral molecule is also a nonreciprocal motion. The field-driven directional motion of an unconfined chiral molecular rotor would result in its propulsion via a screw-propeller type mechanism, such as the bacterial flagella system. Such a system has been theoretically studied as a means to spatially resolve a racemic mixture of propeller-like molecules.[1052,1053]

7. MOLECULAR-LEVEL MOTION DRIVEN BY ATOMICALLY SHARP TOOLS

The development of single molecule imaging techniques such as atomic force microscopy (AFM), scanning tunneling microscopy (STM), and optical and magnetic tweezers has significantly enhanced our understanding of the mechanical properties and working mechanisms of molecular motor proteins.[1054−1068]

Instead of average statistical information obtained from an ensemble of species, these techniques allow direct measurement of molecular level forces, mechanical properties and motions such as rotation, gliding, and translation, pivoting of an individual molecule, supramolecular host–guest exchange, and coconformational changes within interlocked molecular assemblies.[1061,1069−1089] Beside their imaging abilities, the use of such tools to drive molecular level motion has also been explored.

Molecular scale motion is driven by different forces than in the macroscopic world. Gravity is essentially irrelevant at low Reynolds number, and frictional forces differ greatly.[606,1090−1101] The driving forces/interactions must be sufficient to overcome

DOI: 10.1021/acs.chemrev.5b00146
Chem. Rev. 2015, 115, 10081−10206

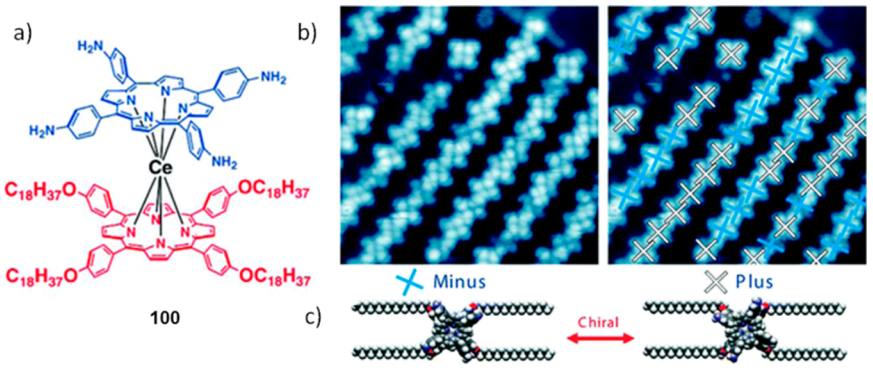

Figure 39. (a) Structure of a cerium-centered double-decker molecule. (b) STM micrographs of the molecules assembled on Au(111) surface. The two distinct isomers, due rotational chirality, are shown in white and blue crosses. (c) Space-filling model of the two chiral species. Reprinted with permission from ref 1134. Copyright 2011 American Chemical Society.

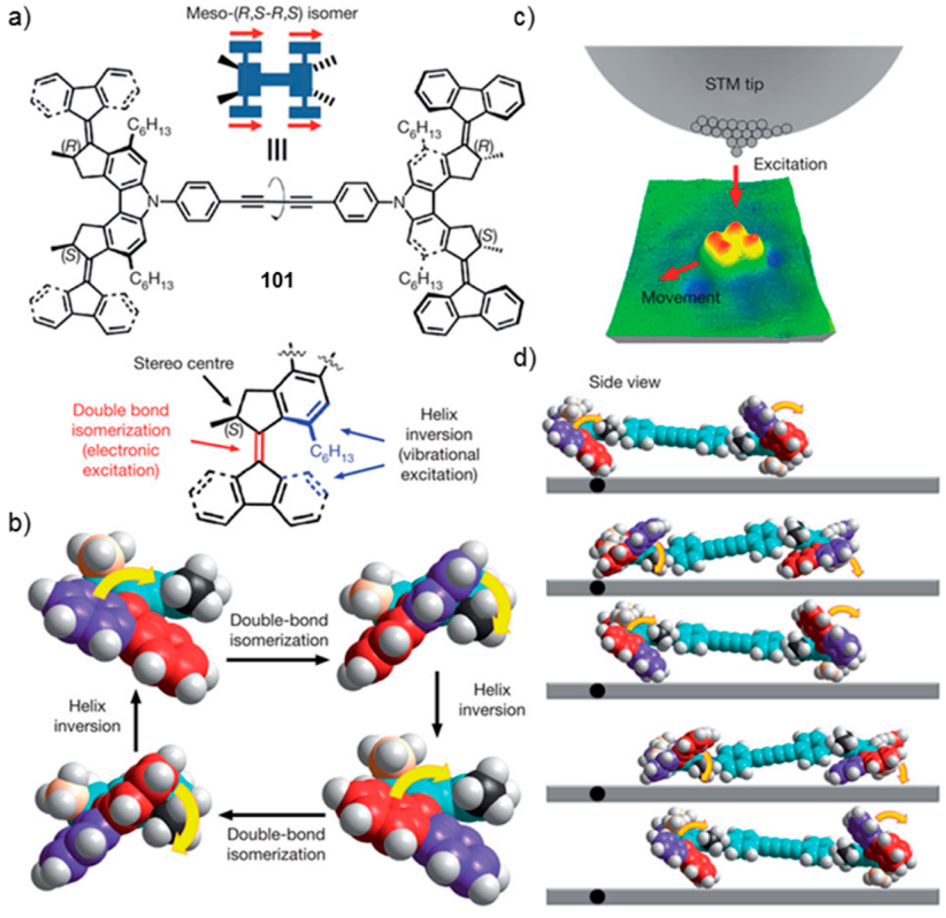

Figure 40. (a) Chemical structure of a rotary motor with the groups responsible for double-bond isomerization (red) and helix inversion (blue) highlighted. (b) Schematic representation of a full 360° rotation with sequential double-bond isomerization and helix inversion (hexyl substituents are omitted for clarity). (c) Schematic representation of electron tunneling exciting the molecule and inducing translational motion on the surface. (d) Cartoon representation of the motion. Reprinted with permission from ref 1135. Copyright 2011 Nature Publishing Group.

significant thermal fluctuations. For the desired motion to be obtained (i.e., translational motion via rotation of the wheels of a "nanocar" instead of gliding), surface−molecule interactions should be neither too strong nor too weak to balance dissociation and immobility.

STM-driven positional displacement of xenon atoms at low temperature was reported by Eigler et al.[1102] The rotation of oxygen and acetylene molecules adsorbed on Pt(111) and Cu(111) surfaces, respectively, was shown to be induced by the tunneling of electrons from an STM tip at low temperatures.[1103,1104] STM- or AFM-driven motions of aromatic molecules on surfaces have been investigated extensively.[1105−1116] The STM-driven directional diffusion of 9,10-dithioanthracene over a Cu(111) surface has been reported.[1117] STM-induced translational motion of porphyrins along the voids of a porphyrin monolayer on a Cu(100) surface was attributed to the rotation of a *t*-butyl substituent.[1113] Displacement to a region with less structural restriction led to more frequent rotation, and thus the STM probe mediated a switch between a rotating and a

DOI: 10.1021/acs.chemrev.5b00146
Chem. Rev. 2015, 115, 10081−10206

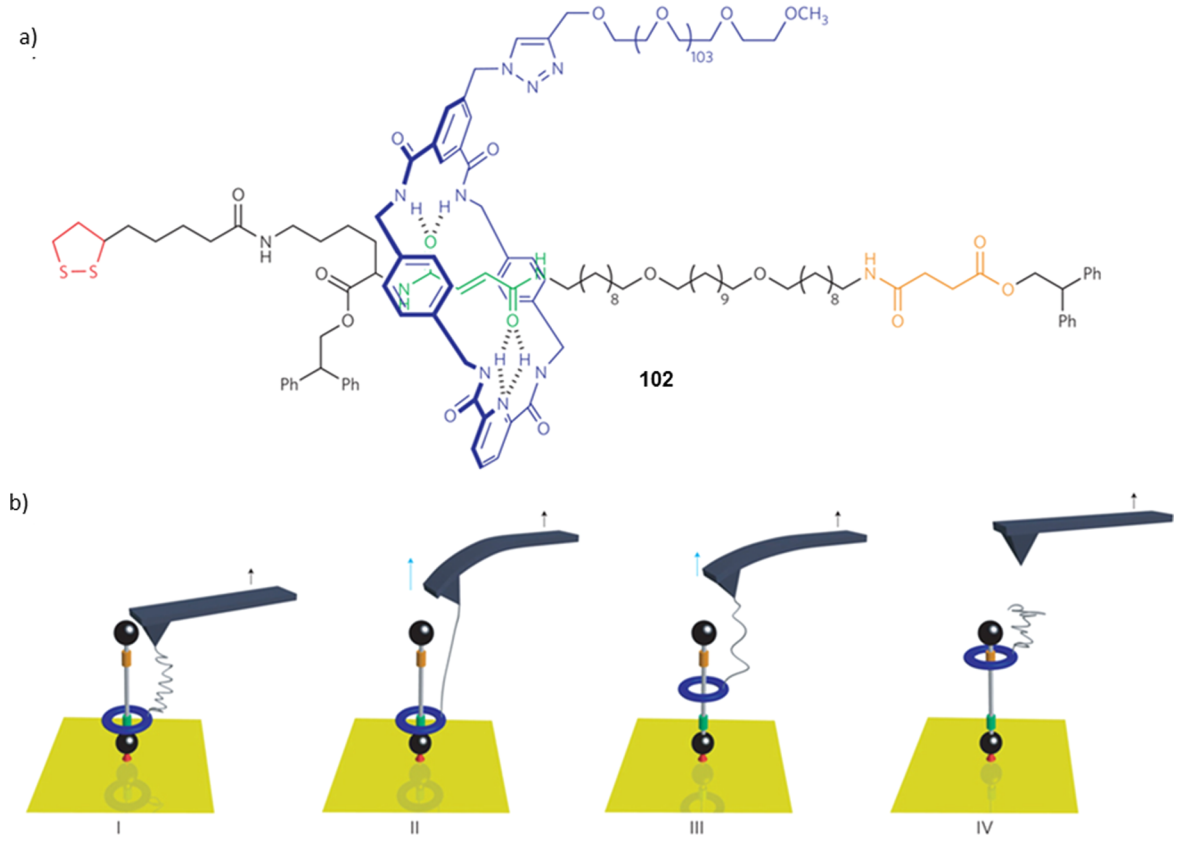

Figure 41. (a) Chemical structure of a rotaxane with fumaramide and succinamide stations depicted in green and orange, respectively. (b) Schematic representation of macrocycle movement on a thread attached to a gold surface as a result of the force exerted by an AFM probe. Application of force by cantilever movement (I,II) was followed by repositioning of the macrocycle (III) or detachment of the PEO tether (IV) depending on the strength of the force. Reprinted with permission from ref 1143. Copyright 2011 Nature Publishing Group.

nonrotating porphyrin. Cyclic molecules and fluorinated C_{60} derivatives were also shown to roll across surfaces.[1118−1120]

Translational motion mediated through rolling structural units (wheels) has been reported in a number of independent publications. Initial attempts to develop a "molecular wheelbarrow" resulted in overly strong surface−-molecule interactions, and the STM tip caused fragmentation.[1121−1124] STM-driven rolling of a single molecule deposited on a Cu(111) surface was first achieved by Grill et al.[1125] A chemically switchable metalloporphyrin pinwheel was reported by Lambert et al.[1126] The reversible attachment of two CO_2 molecules to a diffusing anthraquinone on a Cu(111) surface was an important example of the potential of artificial molecular cargo transporters.[1127] Chiaravalloti et al. designed the first molecular system acting as a rack and pinion device, using self-assembled hexa-*tert*-butyl-pyrimido-pentaphenylbenzene on Cu(111).[1128] Interlocked arrays formed by self-assembly allowed the rotation and translocation of a single molecule along the array by manipulation with an STM tip.

In a four-wheeled "nanocar" with fullerene wheels, thermally induced translational motion on a Au(111) surface was observed (Figure 38).[1129] Directional motion perpendicular to the axles of the molecule suggested that the observed movement was generated by rolling of the fullerene wheels rather than sliding of the entire molecule on the surface. In addition to thermal activation, an STM tip could be used to drive the motion. Pivoting also took place, clearly visible as small-angle perturbations to the path of translation in the STM images (Figure 38e,f). In a structurally related three-wheeled molecule, pivoting was observed to be the dominant motion on the surface, suggesting that the four-wheeled molecular structure was important for a rolling translational motion. Similar examples of four- and three-wheeled fluorescent molecules with different wheel sizes (adamantane and *p*-carboranes as wheels) have been reported, and their diffusion constants on glass surfaces were determined by fluorescence measurement.[1130,1131] The photoisomerization kinetics of a similar four-wheeled molecule functionalized with a rotary motor have also been investigated.[1132] When fullerene wheels were used no photoisomerization took place, whereas with carborane wheels, efficient isomerization was observed in solution.

The rotation of dialkylthioethers adsorbed on Cu(111) surfaces has been extensively studied and electrons from an STM tip found to drive a 5% bias in rotational direction.[1133] Electrical excitation of C−H stretching modes in the molecule contributed to ratcheting in the rotation. The direction and rate of rotation depended on the chiralities of both the molecule and the STM tip. In a cerium-centered double-decker molecule self-assembled on a Au(111) surface, an interesting phenomenon was detected (Figure 39).[1134] The rotational chirality of individual molecules generated two different orientations on the gold surface, which could clearly be distinguished by STM. Upon scanning the surface with the STM tip, an irreversible, abrupt change in the chirality of some of the molecules was observed. The switch resulted from the rotation of the upper porphyrins, and the irreversibility was attributed to damage caused to the molecules by the high applied voltage.

DOI: 10.1021/acs.chemrev.5b00146
Chem. Rev. 2015, 115, 10081−10206

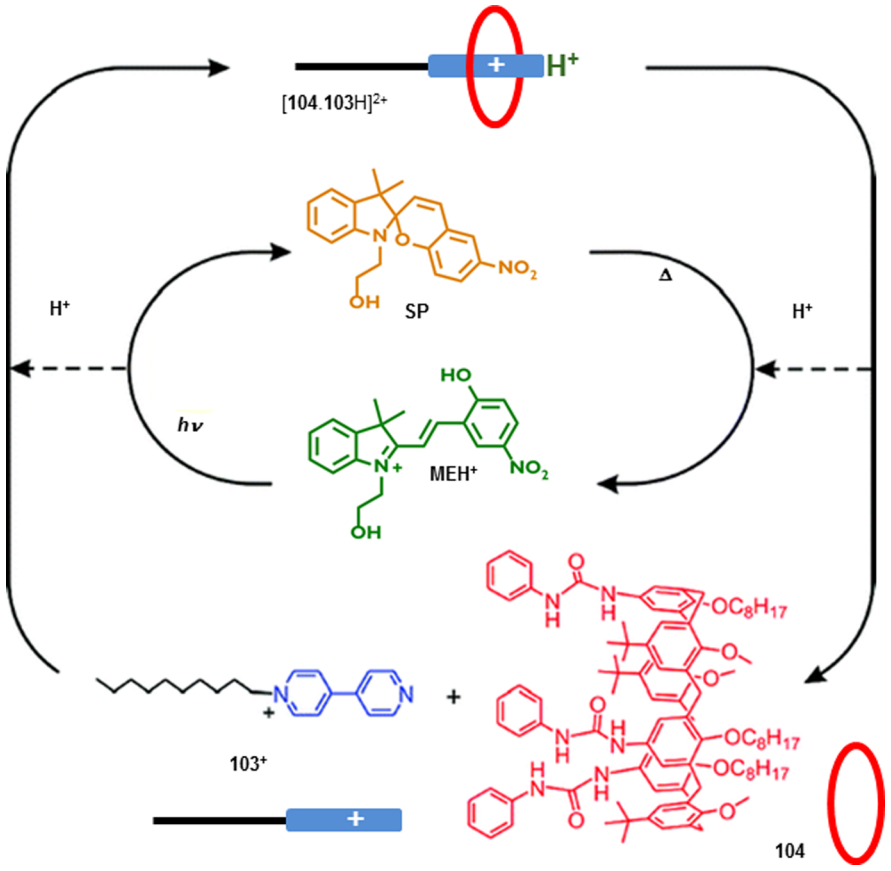

Figure 42. Communication between molecular devices. Acid generated upon conversion of merocyanine (MEH^+) to spiropyran (SP) protonates a pyridine, and leads to subsequent complexation of the pyridinium ion ($\mathbf{103}^+$) by a calix[6]arene (**104**).[1246]

Directional rotary motors undergoing well-defined structural and/or chemical changes on the application of an external stimuli were discussed in section 5. Feringa et al. developed a system utilizing paddle-wheel type directional motion over a Cu(111) surface upon sequential electronic and vibrational excitation (Figure 40).[1135] Electron tunneling induced by a STM tip stimulated double bond isomerization, which was followed by helicity inversion. These sequential configurational and conformational changes in the molecule propelled it across the surface. For the molecule to move on the surface linearly, the four rotary wheels had to rotate in the same direction upon application of the voltage. This is only possible when the molecule was attached to the surface as the *meso*-(*R*,*S*–*R*,*S*) isomer. In other isomers, a lack of coherent rotation prevented translational motion or induced spinning.

Hao et al. monitored the strength of metal–ligand complexation with an AFM tip.[1136] One terpyridine ligand was attached to a gold surface while another was tethered to a gold-coated AFM tip, and the bonding forces between osmium and the ligands were analyzed. The use of atomic tools to induce relative motion in an interlocked molecular system is of particular interest in the development of molecular machines, because each component can be designed to function like the mechanical components of a macroscopic machine.[1137,1138] In a polyrotaxane architecture adsorbed on MoS_2, cyclodextrin ring was translocated by a STM tip along a polyethylene glycol thread.[1139] Such shuttling was thought to be responsible for the conductance switch observed upon the application of a voltage via a STM tip in a bistable [2]rotaxane.[1140] The potential use of interlocked molecular constructs in information storage was highlighted by Leigh et al., who showed that regular patterns of deformations could be successfully generated on a rotaxane monolayer with the aid of a STM tip.[1141] These arrays formed due to the relative ease of intercomponent mobility in these molecular constructs. The effect of electrostatic and steric forces on the shuttling of a bistable [2]rotaxane tethered to an AFM tip has been investigated both experimentally and theoretically.[1142] A molecular shuttle made up of fumaramide and succinamide stations has been attached to a gold surface by thiol linkers (Figure 41).[1143] The macrocycle was tethered to an AFM probe using poly(ethylene oxide) (PEO). Strong hydrogen-bonding interactions with the fumaramide station resulted in a 95:5 distribution of macrocycle in favor of this station. As the stretching of the PEO tether continued, and the force exerted by the PEO linker exceeded the hydrogen-bonding forces between the macrocycle and the fumaramide station, the ring moved away from the fumaramide station. Tension in the tether decreased as a result of the shuttling. Further movement of the cantilever resulted in the detachment of the PEO linker from the probe.

In addition to molecular level motion generated by atomic tools, modulation of conductivity by molecular switches attached to nanojunctions is of great interest.[1144−1152] A STM tip could cause the rotation of selected moieties in the structure of a polyaromatic scaffold, in the hope of developing switchable nanowires.[1110,1153−1160] Although most examples are still far from practical application, significant progress has been made in this area.[1161−1182]

DOI: 10.1021/acs.chemrev.5b00146
Chem. Rev. 2015, 115, 10081−10206

Scheme 37. Expansion and Contraction Allosterically Controlled by Ligand Coordination[a]

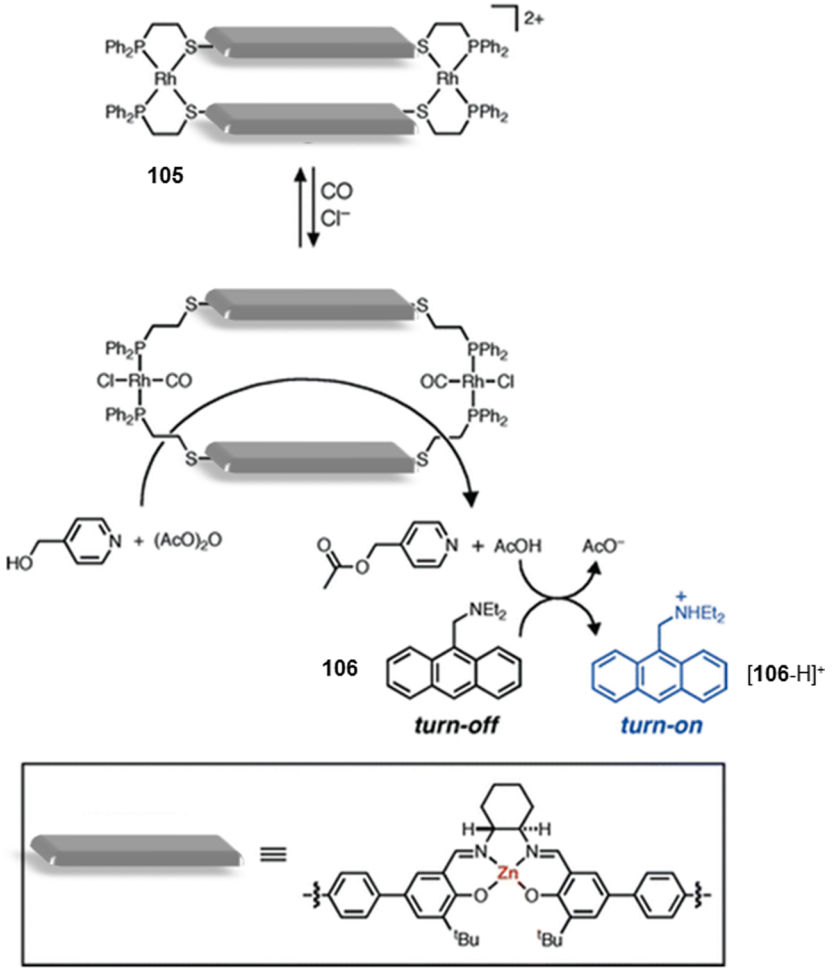

[a]The Zn(II) center acts as a catalytic unit, and diethylaminomethylanthracene is used as the reporter.[1267]

8. TOWARD APPLICATIONS OF MOLECULAR MACHINES

8.1. Current Challenges: Constraining, Communicating, Correlating

Extracting useful work at the molecular scale requires the restriction of the thermal movement of submolecular components or the exploitation of thermal motion with additional ratcheting. Shuttling, switching, and rotation processes in solution can be modulated externally, and the directionality of each motion can be controlled in single molecules. Considering an ensemble of such molecules in solution, however, the biased motions average to give no net directionality. For various applications, the integrity of the molecular system must be conveyed to the macroscopic world. Although there are possible applications of molecular machines/devices in solution, such as their use in molecular logic gate construction or molecular sensing, they are not compatible with typical solid-state technology. For this reason, molecular machines on solid supports are needed. This challenge is being addressed with molecular devices and machines being built on surfaces, interfaces, and polymer matrixes with a variety of electronic, mechanical, or biological applications.[1183−1209] Controlled drug release through nanovalves,[1210−1226] molecular electronics,[1227−1234] artificial molecular muscles,[18,1224,1235−1242] information storage,[1141,1243,1244] and modulation of surface properties[1245] are topics of active research in this area.

Communication between molecular machines is another pertinent challenge in this area. In biological systems, the work done by one machine can be harvested by another and the second can then operate. Raymo and Credi have developed a system that addresses this challenge.[1246,1247] They used a merocyanine-type photoacid to release protons as the molecule transforms from its open form to the closed form. The acid protonated a terpyridine osmium complex and decreased the efficiency of singlet oxygen generation.[1247] These photogenerated protons were also used to reversibly complex and decomplex a 1-alkyl-4,4′-bipyridin-1-ium (**103**$^+$) in a calix[6]arene wheel (**104**) (Figure 42).[1246] Thus, the control of one moiety caused a change in another via the transfer of a proton. Recently, Aprahamian and co-workers successfully coupled a hydrazone switch (section 2.2) with a merocyanine unit and used the photogeneration of acid to drive the switch reversibly with high efficiency.[1248]

8.2. Reporting Controlled Motion in Solution

Submolecular movement can be designed to give a detectable output. The output can be used as a measure of stimulant concentration (sensing) or it can be used for information storage. In theory, any detectable nondestructive output that provides a reliable distinction between states of the system is acceptable

DOI: 10.1021/acs.chemrev.5b00146
Chem. Rev. 2015, 115, 10081−10206

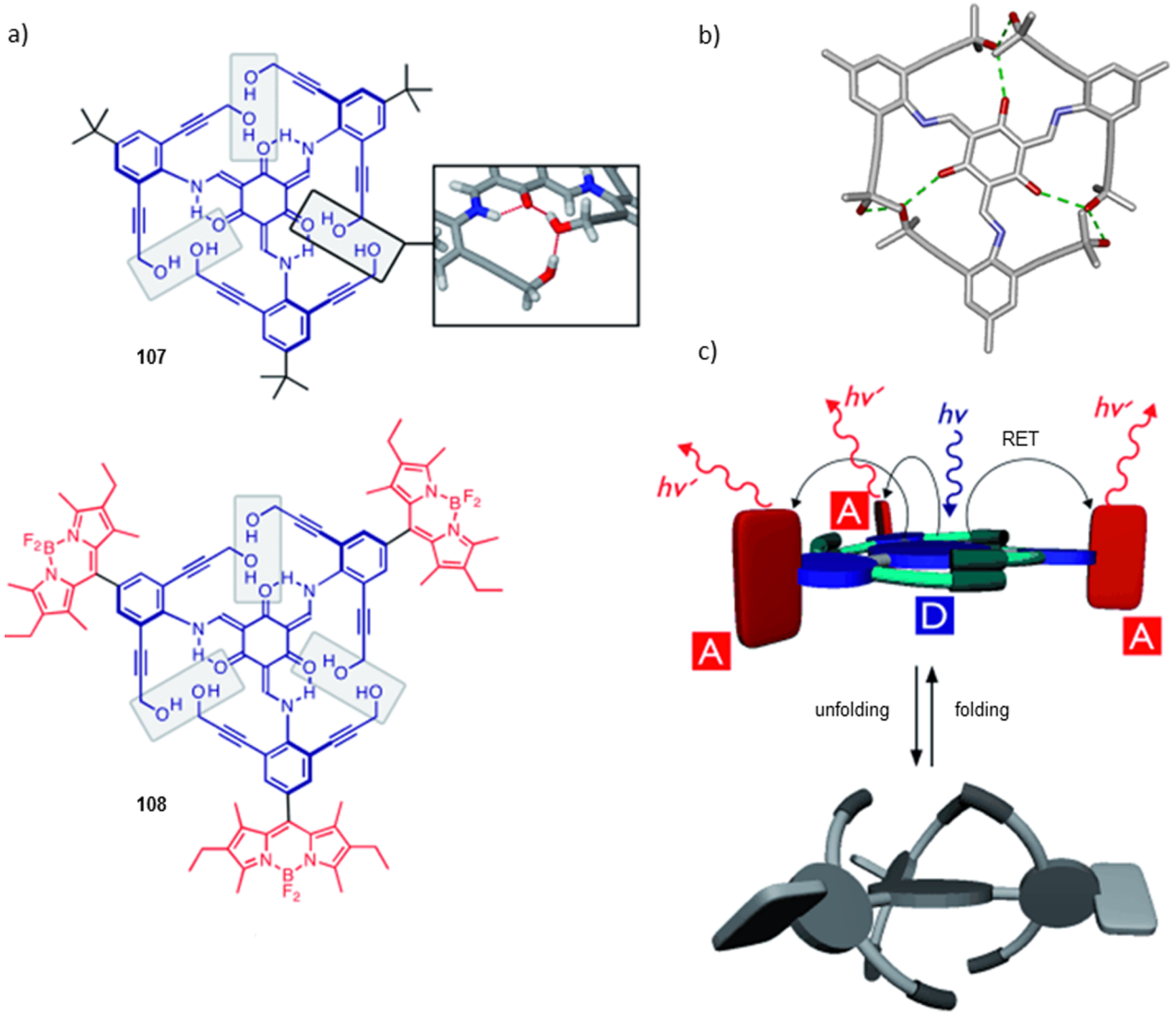

Figure 43. (a) Chemical structure of the *t*-butylphenyl and BODIPY-substituted foldamers, and (b) X-ray structure of the *t*-butylphenyl functionalized foldamer. Carbon atoms of the *t*-butyl groups and all hydrogen atoms except OH and NH have been omitted for clarity. (c) Schematic representation of conformational switching. D and A represent energy donor and acceptor modules, respectively.[1268−1270] Parts (a) and (c) are adapted with permission from ref 1268. Copyright 2007 Wiley-VCH Verlag GmbH & Co. KGaA, Weinheim. Part (b) is reprinted with permission from ref 1269. Copyright 2006 American Chemical Society.

(NMR, CD response, etc.). However, for most useful applications, more practical and easily readable optical, electronic, or mechanical outputs are preferred. The response rate can be crucial in certain applications such as memory devices and molecular sensors. In these systems, fast-responding reporters are preferred. For a molecular system to be used repeatedly, stability and fatigue resistance are important.

8.2.1. Conformational Switches in Solution. The restriction of molecular motion or switching between bistable conformations can be achieved by external stimuli such as ion or organic molecule binding, pH change, or by photoisomerization of the molecule. Conformational perturbations in polymers or carbon chains with interesting properties have been reported.[1249−1261] Fluorescence readouts have been widely used to detect such submolecular motions in part due to their high signal-to-noise ratios.[16,1262−1266] One way to obtain a fluorescence response is by changing the electron transfer efficiency between a fluorescent component and other moieties in the system by inducing an electronic change in the acceptor or donor units. Ligand binding or protonation can effectively change the HOMO and/or LUMO levels of molecules, which in turn affects electron transfer to or from the fluorescent moiety. The change in relative energy levels upon reduction or oxidization determines the ease of detection of the fluorescence response. A greater response can be obtained by decreasing rotational degrees of freedom or by energy transfer. Because energy transfer processes are highly distance dependent, variations in distance between the donor and acceptor units in different conformational isomers can determine the efficiency of energy transfer. Emission from dimers of certain chromophores is also widely used as a reporter of molecular processes. This emission requires the close proximity of similar (excimer) or different (exciplex) chromophores.

Mirkin et al. developed an allosterically regulated supramolecular catalyst based on ligand-dependent contraction or expansion to reveal or conceal a catalytic unit (Scheme 37). They were able to measure the conformational change indirectly using the reaction byproduct, acetic acid.[1267] The tetrametallic species

DOI: 10.1021/acs.chemrev.5b00146
Chem. Rev. 2015, 115, 10081−10206

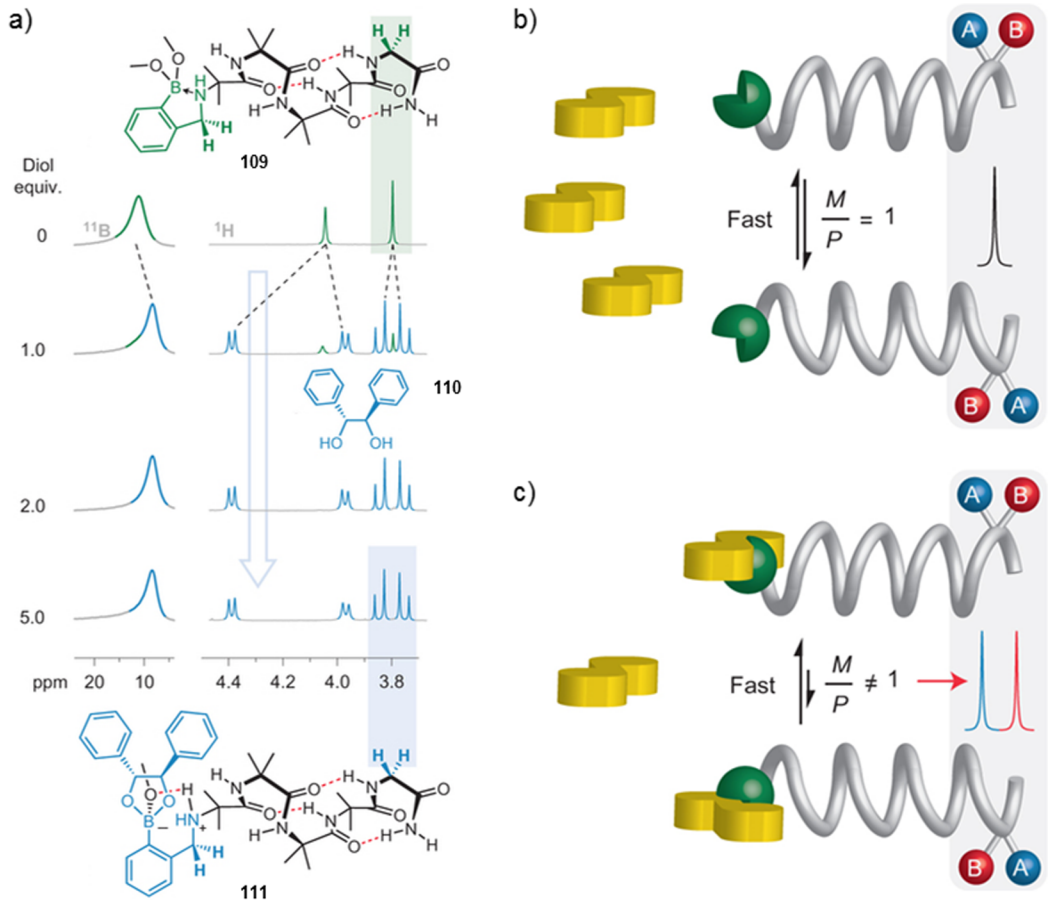

Figure 44. (a) Ligand-induced variation of the chemical shifts (^{11}B (160 MHz) and ^{1}H NMR (500 MHz)) of the helix in CD_3OD at 298 K. (b) Schematic representation of fast exchange between two degenerate helical conformers with a single NMR signal and (c) induced bias of helicity upon ligand binding (yellow), and the anisochronous NMR signal generated. Adapted with permission from ref 1298. Copyright 2013 Nature Publishing Group.

was made of two catalytic cofacially aligned Zn(II) centers attached via two Rh(I) centers. The rate of catalysis of the acyl transfer reaction by the core Zn(II) ions was enhanced when the cavity between the two units was larger. Exchange of Rh(I) ligands from labile thioethers to chloride and carbon monoxide led to an expansion and thus an enhancement of catalytic activity. As the acetic acid byproduct protonated the amine of diethylaminomethylanthracene, an increase in fluorescence was observed caused by blocking photoinduced electron transfer from the amine moiety.

Lee et al. developed a conformational switch based on a cyclic hydrogen-bonding network in a tris(*N*-salicylideneaniline) derivative (Figure 43).[1268−1271] Structural distortion induced by folding and unfolding processes resulted in a significant change in the electronic properties of the system. BODIPY chromophores were tethered to the molecule as fluorescent energy acceptors. In the folded form, the molecule adopted a highly ordered hydrogen-bonding array, and energy transfer took place from the core tris(*N*-salicylideneaniline)moiety to the BODIPYs. When a hydrogen-bond acceptor such as fluoride was added, the molecule unfolded, and a substantial decrease in the fluorescence of the BODIPY dyes was detected. Because each mobile element cooperated in the folding process via hydrogen bonding, conformational change was highly cooperative. The initial fluorescence intensity could be recovered when the fluoride anions were captured by trimethylsilyl chloride.

A number of different fluorescent sensors reporting conformational changes have been synthesized on the basis of energy transfer,[1272−1274] excimer formation,[1275−1282] or charge transfer mechanisms.[1283−1286] Optical responses have been obtained by simple stimuli-dependent conformational change,[796,1262,1273,1275,1287−1289] folding processes,[1276−1278,1290] shuttling,[799,1272,1283−1285,1291−1294] switching,[1273] and transitions between coiled and helical structures.[1295] Optical outputs have been used to develop molecular logic gates.[1291,1292,1296] Recently, Tian et al. used both phosphorescence and an induced circular dichroism output to develop an INHIBIT molecular logic gate by taking advantage of the photoisomerization-dependent inclusion of an azobenzene and a bromonaphthalene in the β-CD cavity.[1297]

Techniques other than optical responses have been used to measure conformational change. Flood et al. used a change in conductance to directly measure a folding process because unfolding released a bound chloride anion and changed the conductance (Figure 22 in section 3.1).[595] A change in CD response can be a useful indicator of molecular motion and helicity inversion.[1298−1308] Many shape changes can be easily analyzed by NMR spectroscopy. Recently, Clayden et al. showed, by ^{11}B, ^{1}H, and ^{13}C NMR, that the equal distribution of left-handed (*M*) and right-handed (*P*) conformers of a helical foldamer could be perturbed by the addition of a chiral ligand (Figure 44).[1298] Upon ligand complexation to the boronic ester, chiral information was transferred along the helix, and the

DOI: 10.1021/acs.chemrev.5b00146
Chem. Rev. 2015, 115, 10081−10206

Scheme 38. Photoisomerization-Dependent Shuttling of an α-Cyclodextrin on an Azobenzene and Stilbene Bearing Thread with Two Naphthalimide Derivatives as Fluorescent Stoppers[a]

I1 (380 nm)	I2 (313 nm)	O1 (ΔF) XOR gate	O2 (ΔA) AND gate
0	0	0	0
1	0	1	0
0	1	1	0
1	1	0	1

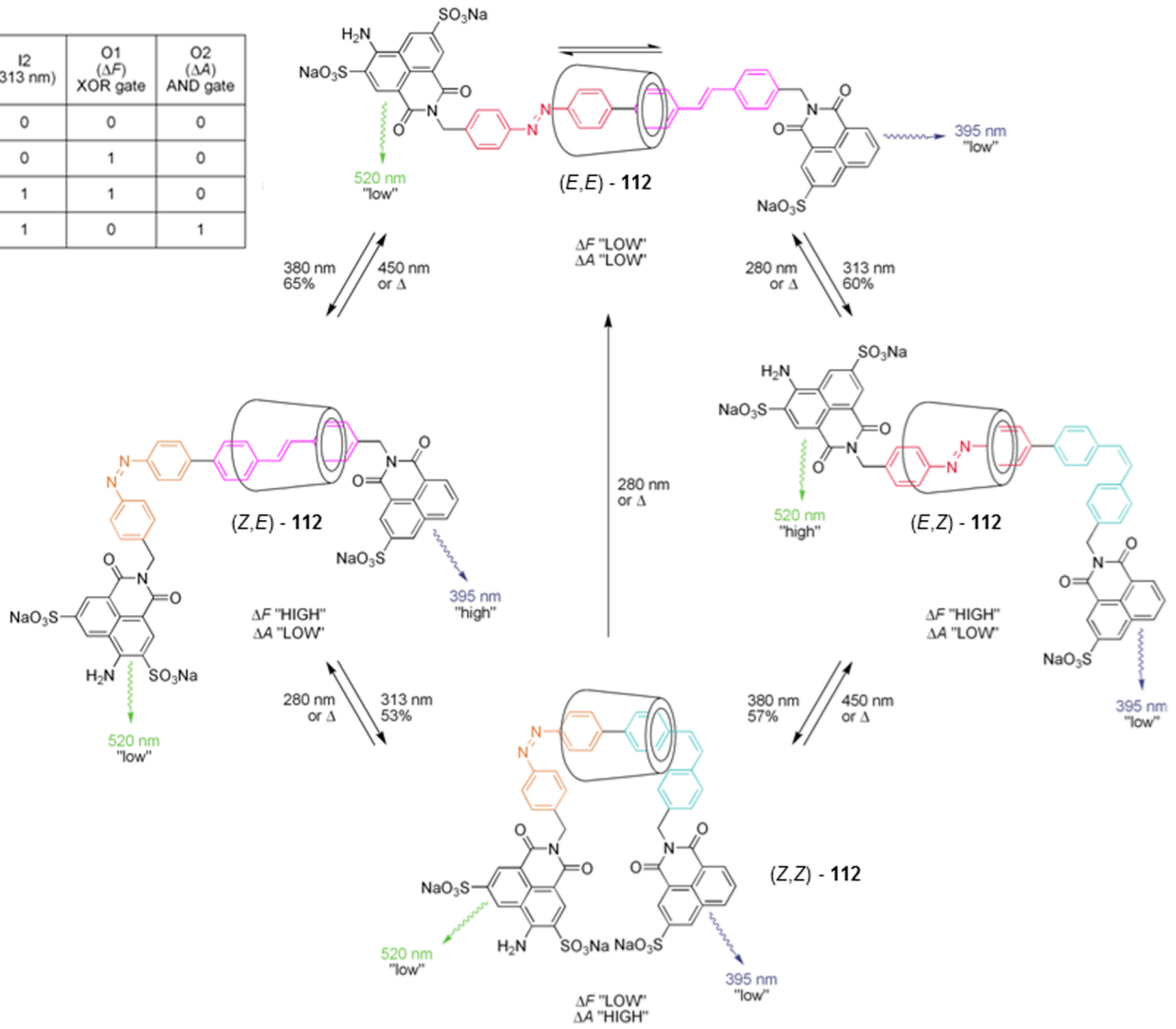

[a]The percentage of the major isomer in the photostationary state is shown over the reaction arrows. The truth table for a half-adder logic gate is shown, with the inputs being 380 nm (I1) and 313 nm (I2) irradiation, and outputs being the change in absorbance (O2) and fluorescence (O1) values.[1291]

isochronous NMR signals of the diastereotopic nuclei were transformed into anisochronous signals, indicating a bias in the distribution of helical conformers. When the *meso* diastereoisomer of the diol was used to complex the boronic ester, no splitting of the ^{1}H NMR signals was observed due to the symmetry of the ligand.

8.2.2. Rotaxane Switches in Solution. Fluorescence spectroscopy has been widely used to detect shuttling processes in interlocked systems, particularly in rotaxanes. The strong distance dependence of fluorescence quenching by electron transfer has frequently been exploited to measure the relative position of molecular subcomponents. Photoisomerization-dependent shuttling of a pyridinium bearing macrocycle along a two station thread was monitored by changes in the fluorescence of an anthracene group tethered near one station.[1285] When the distribution of macrocycle was biased to this station, charge transfer from the anthracene to the pyridinium moiety quenched the fluorescence, thus providing a detectable fluorescence response due to macrocyclic position. The location of a macrocycle along an alkyl chain in a rotaxane structure has also been probed using similar techniques.[1272]

Greater rotational and vibrational freedom leads to a greater probability of nonradiative processes and hence a lower fluorescence quantum yield. Any interaction affecting rotation or vibration can influence emission intensity. Tian et al. used this effect with a 4-aminonaphthalimide fluorophore in a stilbene bearing rotaxane where the steric hindrance generated by photoisomerization of the stilbene unit resulted in the relocation of the α-cyclodextrin macrocycle along the thread.[796] As a result of this movement, fluorescence increased by 46%, which was attributed to the restriction of molecular motion of the nearby linker moieties. The same group utilized an azobenzene as an additional photoisomerizable moiety to develop a molecular half adder logic gate (Scheme 38).[1291] This logic gate performs binary addition using two inputs and two outputs to provide both XOR and AND gates. When either the azobenzene or the stilbene moiety was isomerized, fluorescence emission of the naphthalimide close to photoisomerized species increased ((*Z*,*E*)-**112**

DOI: 10.1021/acs.chemrev.5b00146
Chem. Rev. 2015, 115, 10081−10206

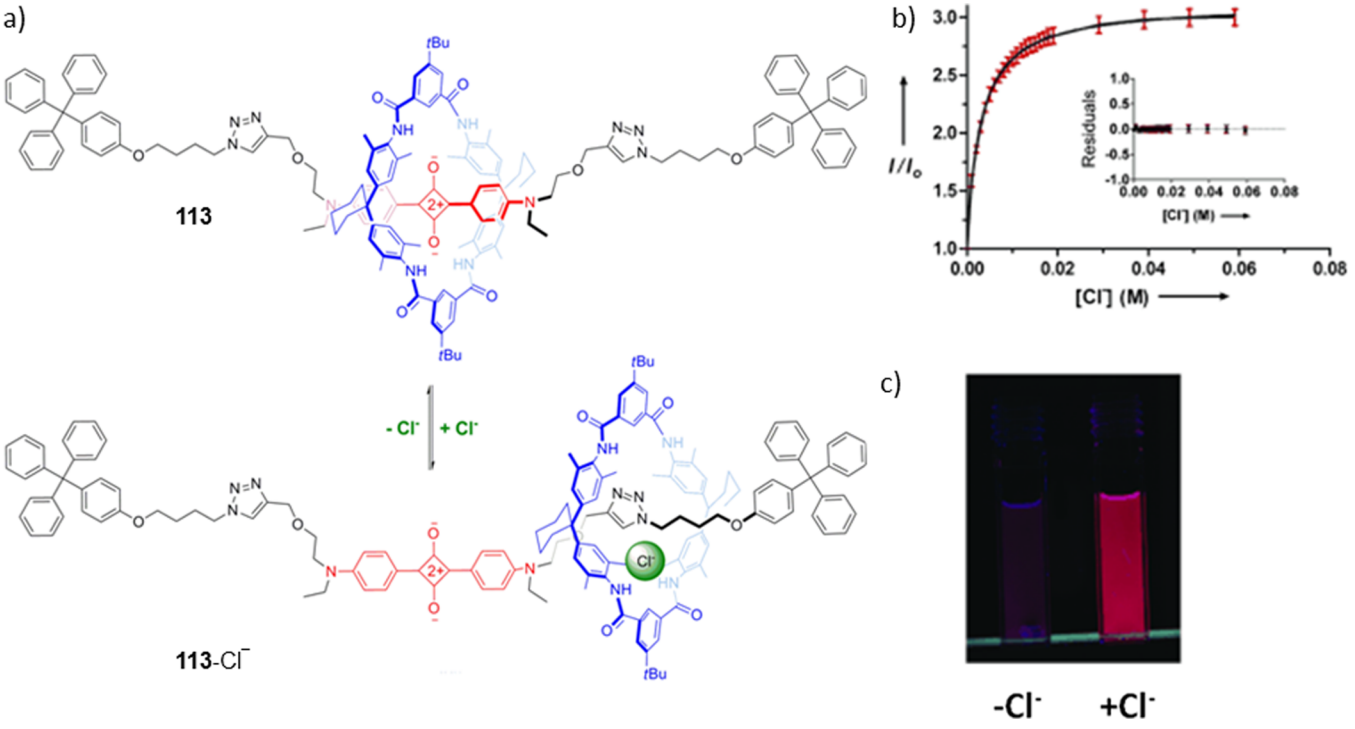

Figure 45. (a) Chloride-dependent shuttling of tetralactam macrocycle, and (b) subsequent fluorescence enhancement in $CHCl_3$ upon titration with tetrabutylammonium chloride. (c) Rotaxane solution in the absence (left) or presence (right) of chloride. Adapted with permission from ref 1310. Copyright 2010 Wiley-VCH Verlag GmbH & Co. KGaA, Weinheim.

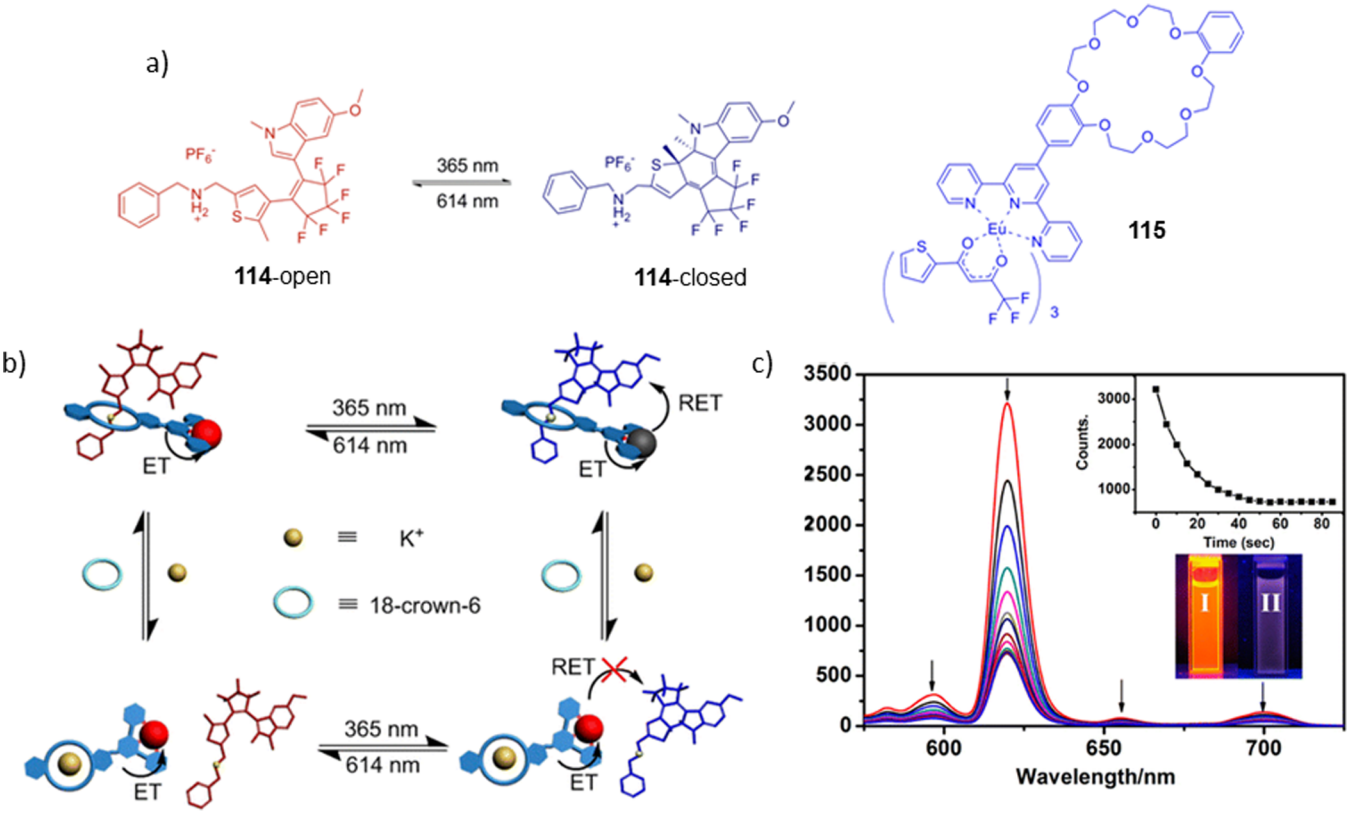

Figure 46. (a) Chemical structures of **115**, and the open and closed forms of **114**. (b) Schematic representation of light modulated switch and K^+/18-crown-6-mediated complexation. (c) Fluorescence quenching of the Eu^{3+} complex upon UV irradiation in 1:1 $CH_3CN/CHCl_3$. Fluorescence before (I) and after (II) excitation at 390 nm (c inset). Reprinted with permission from ref 1314. Copyright 2013 American Chemical Society.

or (*E*,*Z*)-**112**). However, if none or both of them were isomerized ((*E*,*E*)-**112** or (*Z*,*Z*)-**112**), fluorescence intensity decreased due to rapid shuttling of the ring between the stations in the nonisomerized form or because the ring was trapped in the

DOI: 10.1021/acs.chemrev.5b00146
Chem. Rev. 2015, 115, 10081−10206

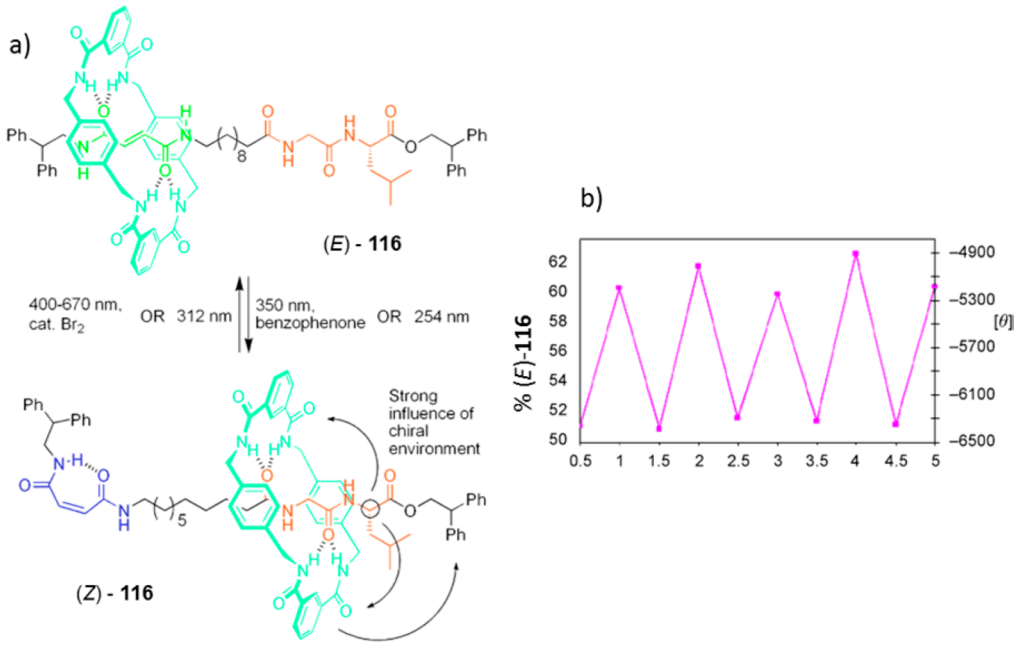

Figure 47. (a) Chiraloptical switching upon photoinduced shuttling of the macrocycle between fumaramide (green) and peptide (orange) stations; the chiral center of the peptide station is highlighted by a black circle. (b) Percentage of *E* isomer calculated using ^{1}H NMR (left *y* axis) and induced CD absorption at 246 nm after alternating irradiation between 254 nm (half integer) and 312 nm (integers) (right *y* axis). Reprinted with permission from ref 1326. Copyright 2003 American Chemical Society.

center of the thread when both functional moieties were isomerized. These fluorescence outputs collectively result in a XOR gate (output 1 in the truth table). The photoisomerization-dependent decrease in absorbance at 350 nm and increase at 270 nm were used as an additional output for the construction of the AND gate of the half adder. The change in absorbance at the isosbestic point (301 nm) was followed and only breached a predetermined threshold when both units were isomerized. As such, an interlocked molecular system was successfully used as an all-photonic logic gate in solution where the inputs induce submolecular motion and outputs are reporters of their motion. Acid−base and redox switchable bistable rotaxanes with crown ether macrocycles have been used to create an INHIBIT logic gate.[1292] Room-temperature phosphorescence and CD responses have been used in a pseudo[1]rotaxane to create a primitive logic gate.[1297]

Indicator displacement assays involving supramolecular complexes and interlocked molecules are widely used for molecular sensing applications.[1309] In these systems, a fluorescent molecule with complexation-dependent fluorescence properties is usually used as a guest. The optical change generated upon exchange of the fluorescent guest with the analyte is used as the reporting function. Smith et al. used a similar idea to develop a chloride anion sensor based on a rotaxane (Figure 45).[1310,1311] A [2]rotaxane (**113**) was synthesized using a tetralactam macrocycle and a squaraine dye as building blocks. Tetralactam macrocycles are known to bind to and quench the emission of red light from squaraines.[1312] The exposure of this dye, upon chloride-induced displacement of the macrocycle, restored fluorescence. The process could be reversed by chloride precipitation as the NaCl salt. When the same rotaxane was adsorbed on a C-18 coated reverse-phase silica gel plate and dipped into different concentrations of aqueous solutions of chloride, the change in fluorescence was large enough to be visually observable. Later, a ratiometric chloride sensor based on the same squaraine rotaxane was reported.[786] Interlocked systems are useful in such dye-displacement assays, as the displaced dye typically diffuses away preventing reversibility, whereas the stable rotaxane structure allows reversibility and reusability. In a similar example, the sodium ion-dependent shuttling of a [2.2.2]cryptand away from a squaraine station enhanced squaraine emission.[1312] Interlocked architectures have been mounted on metal nanoparticles and shown to keep their switching ability.[1313]

Liu et al. have developed a [2]pseudorotaxane with a dual stimulus luminescent lanthanide switch using a diarylperfluorocyclopentene as the photochromic component (Figure 46).[1314] The diarylperfluorocyclopentene (**114**) bears a benzyl ammonium recognition unit and reacts reversibly to generate its closed form upon absorption of UV irradiation (365 nm). The open form can be obtained via irradiation at 614 nm. The Eu^{3+} complex of terpyridinyldibenzo-24-crown-8 (**115**) was used to reversibly complex the ammonium moiety of **114**. This Eu^{3+} center fluoresces at 619 nm through intramolecular energy transfer from an excited terpyridine ligand. Upon complexation of the two compounds through crown ether−ammonium interactions, a small amount of quenching of the lanthanide fluorescence at 619 nm was observed (ca. 10%) due to the poor spectral overlap between the donor emission and acceptor absorbance (which is required for resonant energy transfer (RET)). Upon UV irradiation to form the closed form of compound **114**, spectral overlap increased and fluorescence was quenched by 80%, with an accompanying 3-fold decrease in excited-state lifetime. The pseudorotaxane could be reversibly disassembled by the addition of potassium cations and regenerated by the addition of 18-crown-6.

The responsive nature of induced circular dichroism makes it an interesting phenomenon to study with the CD response of one species changing upon its interaction with another.[387,1315−1319] The transformation of an achiral carbon center to a chiral one upon hydrogen-bonding-dependent symmetry breaking provided an early example of the influence of

DOI: 10.1021/acs.chemrev.5b00146
Chem. Rev. 2015, 115, 10081−10206

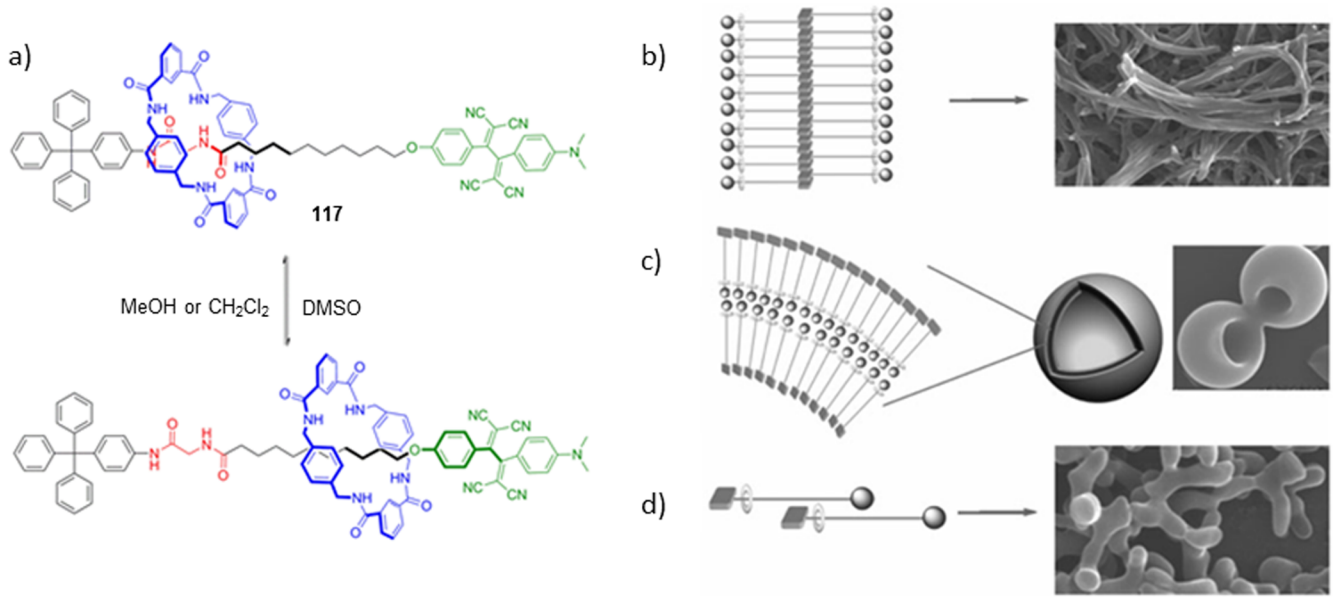

Figure 48. (a) Solvent-induced shuttling on a tetracyanobutadiene bearing rotaxane **117**. (b) Proposed assembly of rotaxane and SEM images in $CHCl_3$/*n*-C_6H_{14} (1/1, v/v), (c) in $CHCl_3$/MeOH (1/1, v/v), and (d) in DMSO. Reprinted with permission from ref 1327. Copyright 2009 Wiley-VCH Verlag GmbH & Co. KGaA, Weinheim.

supramolecular interactions on chirality.[1320] A number of chiral supramolecular assemblies,[1315,1316,1321] chiral spaces (dissymmetric cavities),[1322] and helices[1323−1325] have been reported. The solvent-dependent rearrangement of a macrocycle along a thread has been shown to alter the CD response of a rotaxane (section 4.3.1).[715] The position of a macrocycle has been used to control the reactivity of a secondary alcohol toward esterification in the presence of a chiral catalyst in a chemical information ratchet (section 4.4.1).[809,810] Similarly, a chiraloptic switch has been reported based on a benzylic amide macrocycle and fumaramide/peptide stations (Figure 47).[1285,1326] Photoisomerization-dependent relocation of the macrocycle to the peptide station altered the CD response due to proximity-dependent macrocycle−leucine residue interactions. A large reversible difference in elliptical polarization response (>1500 deg cm^2 $dmol^{-1}$) was obtained upon isomerization of the fumaramide station from *E* to *Z*.

Li et al. synthesized rotaxane **117** bearing a tetracyanobutadiene (TCBD) stopper, which tends to form aggregates via intermolecular dipole−dipole interactions, to attempt to control this clustering behavior (Figure 48).[1327] The position of macrocycle relative to the TCBD group determined the strength of intermolecular interactions and hence the structure of the assemblies formed. In a hexane:chloroform mixture (1/1, v/v), the macrocycle rested on the peptidic station, and the TCBD units were free to interact to generate nanofibers (Figure 48b). In methanol:chloroform (1/1, v/v), the amphiphilic nature of the molecules generated perforated nanocapsules (Figure 48c). Finally, when DMSO was used as the solvent, the macrocycle relocated closer to the TCBD group, interfering with aggregation and generating a worm-like nanostructure (Figure 48d). A similar phenomenon was reported in which a fumaramide bearing rotaxane displayed different nanostructures when the macrocycle bound Zn^{2+} metal in the presence or absence of irradiation.[1328] Anion and acid/base-dependent control over the formation of an organogel has been achieved using a [2]rotaxane architecture.[1329] In this system, stimuli-induced shuttling of the macrocycle between urea and ammonium stations led to sol−gel phase transitions. Polyrotaxane structures have been formed in a concentration-dependent manner in solution using the interaction of an electron-deficient macrocycle with a monoanionic species.[1330] Recently, light and acid/base-dependent threading and dethreading of pseudorotaxane structures embedded in nanofibers was reported to induce a macroscopic change (more than 1.5-fold enhancement of Young's modulus upon dethreading).[1331]

The concept of a "molecular muscle", created from doubly threaded rotaxanes or interlocked daisy chain molecular structures, was developed by Sauvage et al.[1332] In these systems, submolecular movement drives a relative motion that either contracts or expands the entire molecule upon metal exchange,[1332] solvent exchange,[1333,1334] redox reaction,[1236,1238,1335] or acid/base exchange.[18,1336−1339] Photoinduced contraction/expansion has also been reported.[1340] The concept has been used to cause the macroscopic bending of a microcantilever by means of redox-driven shuttling of the surface-adsorbed macrocycle along a thread (section 8.6.4).[1238,1341]

The design of enzyme-responsive molecular machines is an emerging area and could find applications in biotechnology. Biodegradable polyrotaxanes have been studied as selective drug and gene delivery systems.[1342−1349] Leigh and co-workers published two generations of [2]rotaxane-based propeptides (**118**, **119**) where the peptide axle is protected from degradation from general peptidases by the macrocycle.[1350,1351] The introduced glycosidase-cleavable stopper allows the release of the free peptide in a controlled fashion through treatment with a specific glycosidase. The sequence of reactions triggered by the *β*-galactosidase leading to the decomposition of the stopper is shown in Scheme 39. This approach offers a promising alternative delivery system for peptide-based therapies, because many bioactive peptides suffer from in vivo instability and poor bioavailability. Similar principles have been used to deliver a deactivated cancer drug (acting as a stoppering moiety in a rotaxane) via the blood before the macrocycle immolates inside a cell. This releases the thread, and enzyme-mediated hydrolysis

DOI: 10.1021/acs.chemrev.5b00146
Chem. Rev. 2015, 115, 10081−10206

Scheme 39. β-Galactosidase-Triggered Release of Triglycyl Peptide 120 from the [2]Rotaxane Propeptide 118 and 119[1351]

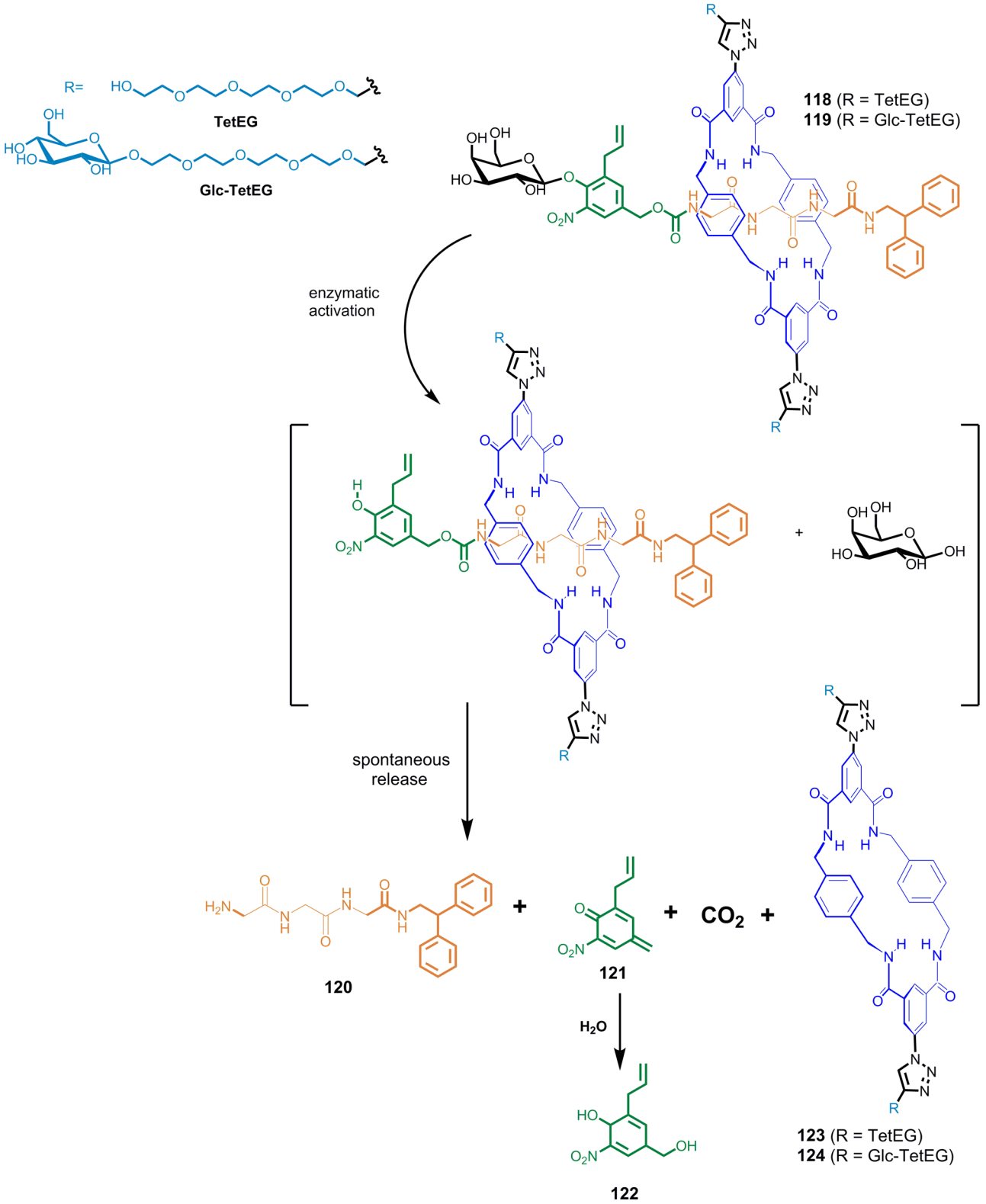

furnishes the active drug molecule. The rate of hydrolysis in cancerous cells versus benign cells was somewhat enhanced due to their overexpression of the hydrolyzing enzyme.[1352]

8.3. Synthetic Molecular Walkers

8.3.1. Introduction. Biological motor proteins have evolved a plethora of functionalities. DNA, RNA, and protein synthesis machineries (DNA polymerases, RNA polymerases, the ribosome) work cooperatively with helper proteins to "unzip" molecules (helicases,[1353] poly(ADP-ribose) polymerases),[1354] release strain in a substrate (gyrase,[1355,1356] topoisomerase),[1357,1358] slide over the substrate, and processively synthesize a product (DNA polymerases, RNA polymerases, the ribosome).[68−70] The ATPase rotary motor is the energy factory

DOI: 10.1021/acs.chemrev.5b00146
Chem. Rev. 2015, 115, 10081−10206

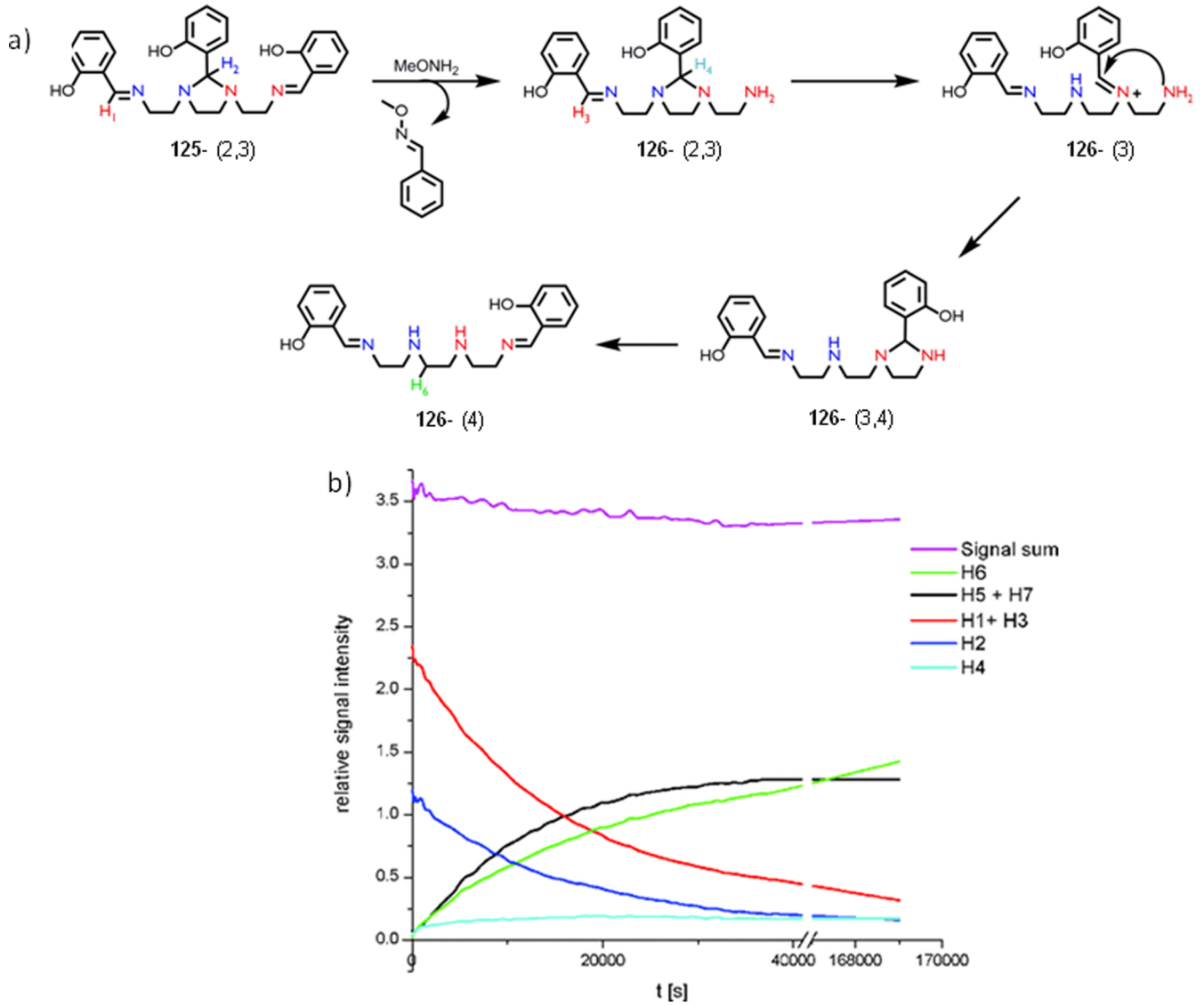

Figure 49. (a) The structure and operation of walker **125**, which uses dynamic imine exchange chemistry. Amine footholds are highlighted in blue and red. Each molecule is labeled with one or two numbers in parentheses indicating the amine footholds to which the walker is attached (foothold amines are assigned with numbers starting from the left). (b) ^{1}H NMR spectra of indicated protons in $CDCl_3$. H_7 corresponds to a side product in which the walker is detached from the track. Reprinted with permission from ref 1395. Copyright 2012 American Chemical Society.

of the cell producing ATP via complex mechanical processes.[1359] Pumps[1360] and pores[1361] are essential to maintain communication and transportation across the membranes of different compartments (functioning at organelle, cell−environment, or cell−cell boundaries). Among these machines, molecular walkers are attracting increasing attention as their mechanism of action has been revealed. Dynein, myosin, and kinesin are walker proteins of the ATPase family and differ in their structure, function, and use of energy.[1362−1365] Proteins such as collagenase and exonucleases, which are not traditionally viewed as walker proteins, migrate along their substrate tracks by destroying the track via a "burnt-bridges" mechanism.[1366−1368]

Biological walkers have some important characteristics.[1369] First, they must be supplied with energy to do work against random Brownian fluctuations. ATP hydrolysis normally provides this energy. Second, attachment to a track results in a restriction of their degrees of freedom facilitating directional 1-D or 2-D walking in solution. Inertia and momentum under conditions of low Reynold's number are irrelevant, and work is performed under the influence of viscous and thermal motions. Third, to drive the walker away from equilibrium, that is, to generate directional motion, a ratcheting process (either an energy or an information ratchet) must take place. In addition to the requirements of a Brownian motor, certain additional characteristics are necessary for a motor to be defined as a walker.

(i) Processivity is a measure of the integrity of walker−track interactions during its operation. A walker should remain attached over multiple operations to extract useful work.

(ii) Directionality is the exclusive or preferential movement of the walker in one direction along the track.

(iii) Repetitive operation means the motor should be able to carry out similar mechanical cycles repetitively.

(iv) Progressive operation is the ability of the motor to culmulatively perform work with each operating cycle.

(v) Autonomous operation allows the motor to function continuously without external intervention, as long as an energy source (fuel) is available.

DOI: 10.1021/acs.chemrev.5b00146
Chem. Rev. 2015, 115, 10081−10206

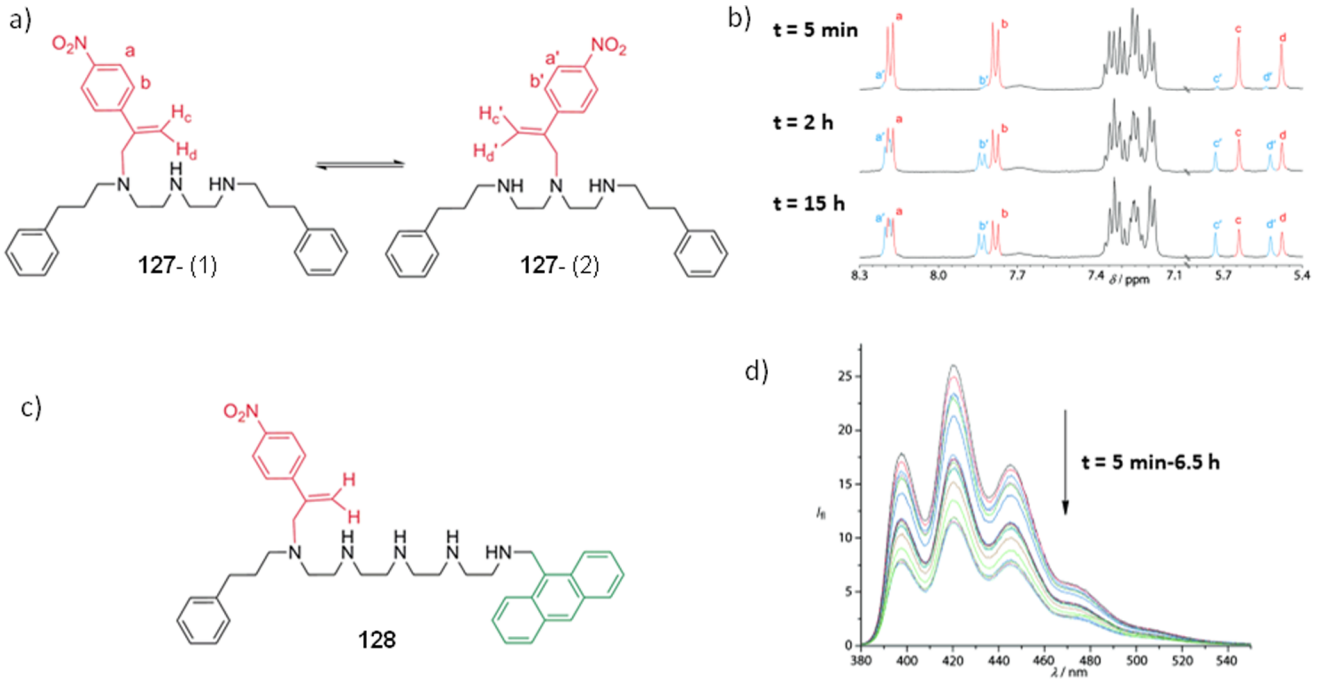

Figure 50. (a) The chemical structure of the model walker **127**, and (b) gradual change in ^{1}H NMR of the model walker in d_6-DMSO upon formation of new positional isomer on the track. Ratio of (1):(2) isomers reaches 1:0.9 after 15 h of operation. (c) Chemical structure of the walker on a larger track bearing an anthracene moiety, **128**. (d) Fluorescence quenching of anthracene after 6.5 h of walking. Reprinted with permission from ref 1397. Copyright 2012 Wiley-VCH Verlag GmbH & Co. KGaA, Weinheim.

Conventional kinesin (kinesin I) meets all of these criteria and was first isolated by Vale et al. in 1985.[1370] It is a homodimeric protein with two identical heads that interact with a microtubule track. Through cyclical binding, hydrolysis, and then release of ATP, it can walk along the track by an asymmetric hand-over-hand mechanism.[1371−1373] Because at any time one of the heads remains attached to the track during the walking process, processivity is high. On average, this walker takes 100 steps before detaching from the track.[1374−1377] Although walkers with two attachment points or more are common, this is not a requirement for processivity. The KIF1A kinesin protein processively walks along microtubules using a single leg.[1378] In contrast, some 2-legged biological walkers such as myosin-II are nonprocessive.[1365] Even without being processive, myosin-II can still move directionally, and in a large ensemble it can generate macroscopic motions such as muscle contraction.

DNA has the notable ability to form predictable hydrogen bonds with a complementary strand and can be synthesized using machine-assisted technologies. Strand displacement provides a versatile design for walking processes, and the ability to make complex 3-D structures can be exploited to perform complex physical tasks. The first artificial walkers were made of DNA. Directional walkers,[1379] autonomous walkers,[1380] walkers using the burnt-bridges mechanism,[1380] cargo-carrying walkers,[1381] and a light-driven walker[1382,1383] based on DNA have been reported, and will be examined in section 9.4. Aside from DNA-based walkers, the preferential diffusion of molecules along the higher symmetry axis of a metal surface has also been observed.[1117,1127] Huskens et al. reported the gradient-driven diffusion of molecules bearing two adamantane legs across α-cyclodextrin-functionalized surfaces.[1384] Processive crown ether migration on an oligoglycine chain[1385] and migration of metal atoms on aromatic scaffolds[615,1386,1387] have also been explored. Rearrangement reactions enable the migration of a fragment along a molecule (such as the Claisen[1388,1389] and Cope[1390−1393] rearrangements). However, progressive and repetitive operation using sigmatropic rearrangement reactions is generally challenging.

For the design of processive small molecule synthetic molecular walkers, mechanically interlocked architectures are good candidates, because the walker (macrocycle) is mechanically bonded to the track (thread). However, their interlocked-structure prevents resetting because each resetting process undoes the walking process, by relocating the walker to its original position.[1369] Moreover, the macrocycle cannot choose a new path without bond breaking, which would result in detachment from the thread. A two-leg system operating under orthogonal conditions could provide a viable synthetic molecular walker. Orthogonal dynamic covalent exchange reactions can provide a suitable balance of reversibility and kinetic stability. A rigid track can decrease the possibility of overstepping.

8.3.2. Spontaneous Walking of Small Synthetic Molecular Walkers. Reversible and processive migration of a Michael acceptor along a protein was reported in 1979 by Lawton et al.[1394] More recently, Lehn et al. used dynamic imine exchange to transport a salicylidene walker **125** along an amine bearing track (Figure 49).[1395] Deprotection of the amine at one side of the track using methoxyamine initiated the dynamic exchange reactions. The speed of exchange was shown to be modulated when substitution, composition of the solvent, or temperature was altered. ^{1}H NMR analysis in $CDCl_3$ proved that the relative intensity of a characteristic signal corresponding to the transported walker (H_6) increased gradually and in 2 days the transported walker was the dominant product in solution. Recently, the same group reported a modified version of their walker with thermodynamic sinks at each end of the track. These trap the stochastic walker at one end in acid as an imine, or as a lactone at the other end under basic conditions.[1396]

DOI: 10.1021/acs.chemrev.5b00146
Chem. Rev. 2015, 115, 10081−10206

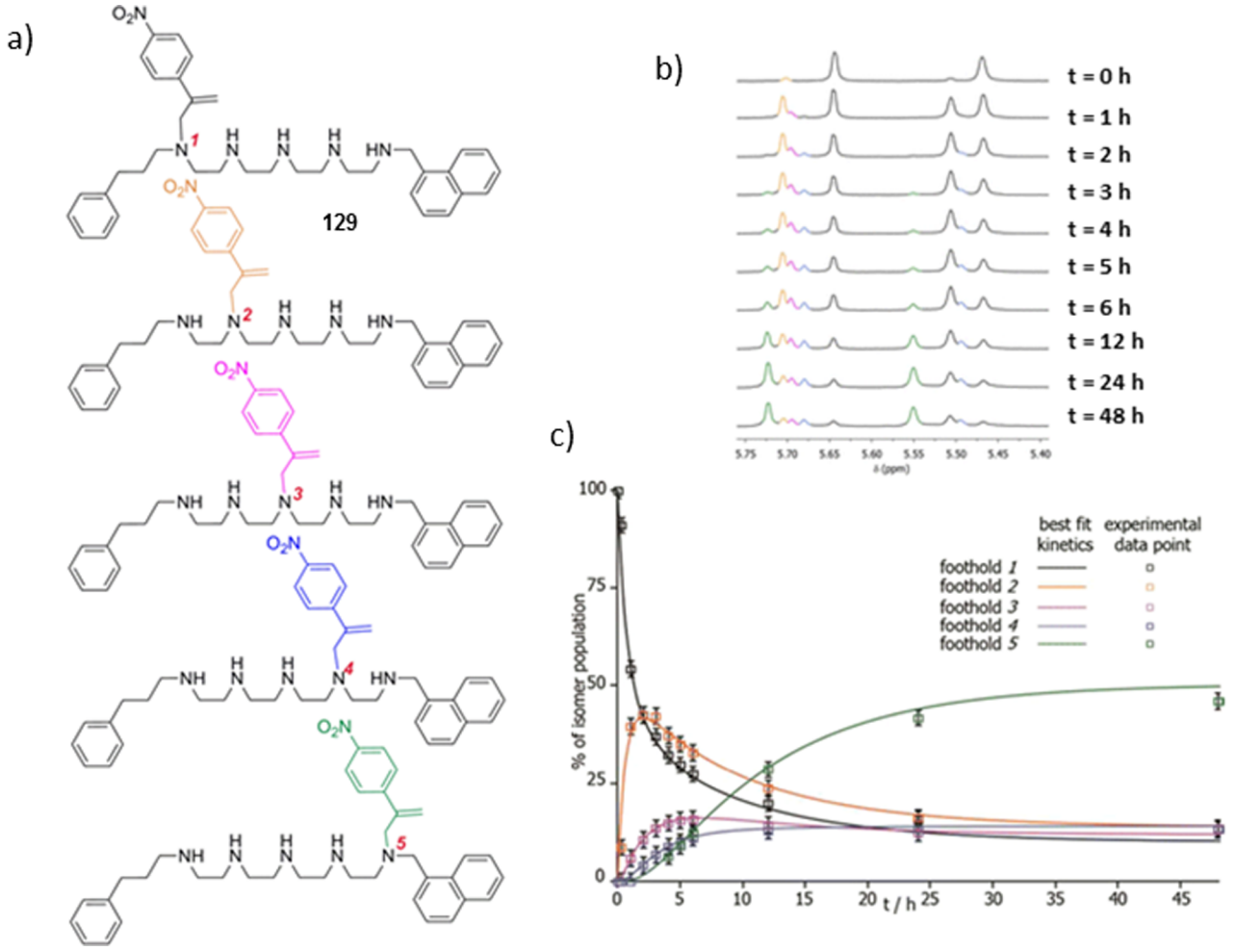

Figure 51. (a) Chemical structure of walker **129**, with each positional isomer labeled in a different color, and amines numbered. (b) Change in the partial ^{1}H NMR spectra over 48 h of operation. (c) Occupancy of each foothold over time. Reprinted with permission from ref 1398. Copyright 2013 American Chemical Society.

Scheme 40. Structure and Operation of a Small Molecule Walker, Walking along a Molecular Track[a]

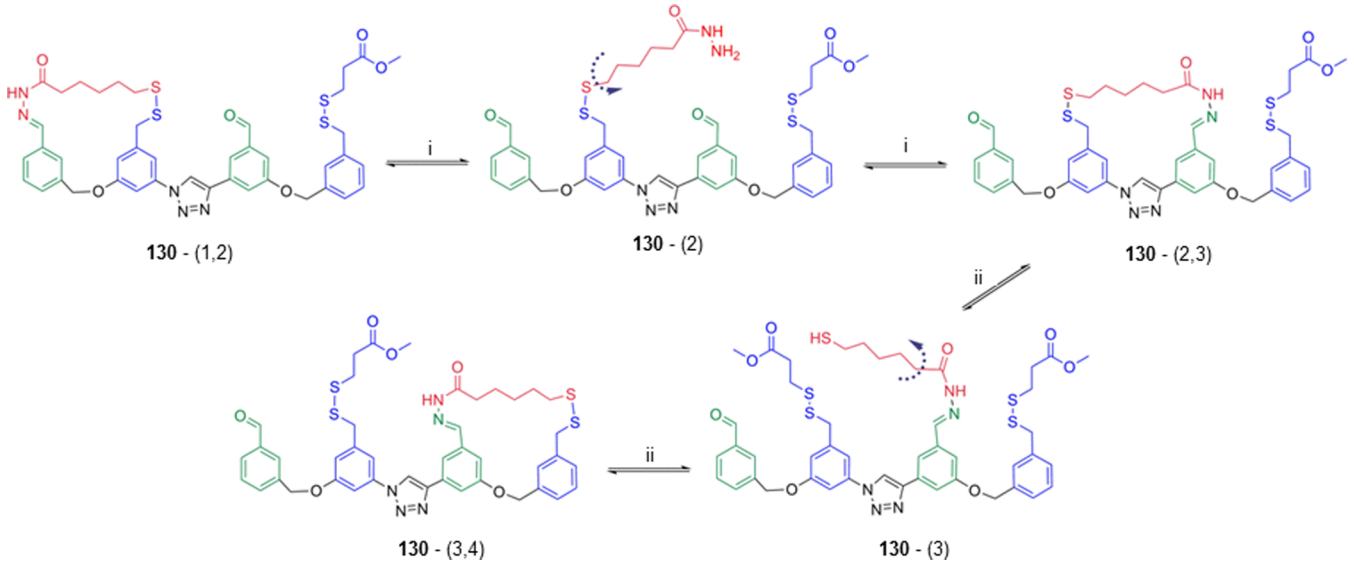

[a]Footholds are shown in blue and green; the walker unit is depicted in red. Numbering shows the footholds to which the walker is attached.[1399]

Leigh et al. reported a spontaneous walking process using a Michael addition reaction between an α-methylene-4-nitrostyrene walker and a polyamine track (Figure 50).[1397] It was shown that the walker translocated preferentially through

DOI: 10.1021/acs.chemrev.5b00146
Chem. Rev. 2015, 115, 10081−10206

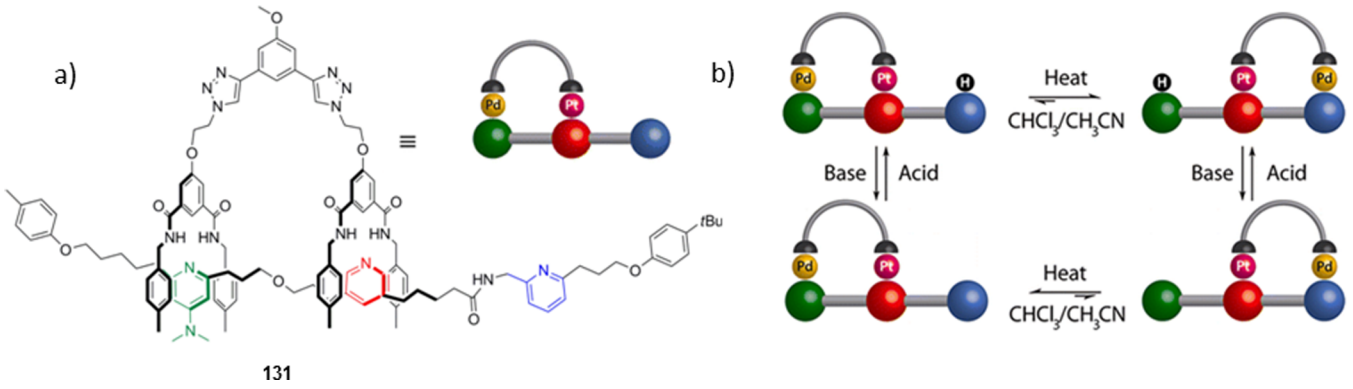

Figure 52. Toward directional molecular walkers. (a) Chemical structure and schematic representation of the walker attached to the track, and (b) operation of walking through successive acid–base addition and heating cycles. Reprinted with permission from ref 1403. Copyright 2014 American Chemical Society.

Scheme 41. Light-Driven Transport of a Molecular Walker along a Molecular Track[a]

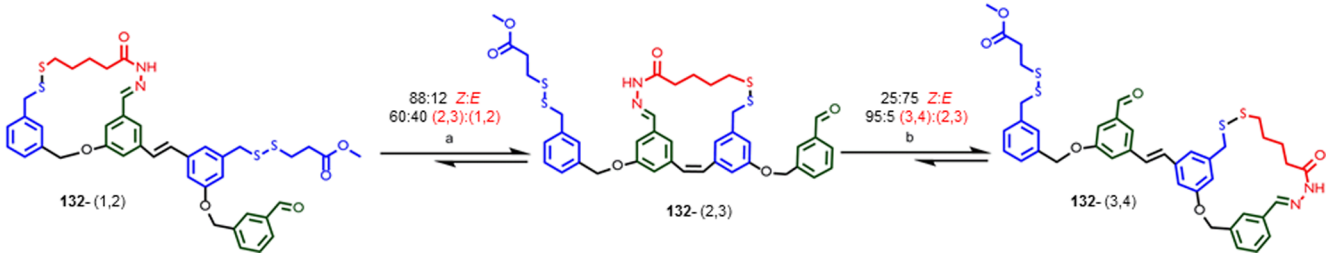

[a]Footholds are shown in blue and green; the walker unit is depicted in red. Each molecule is labeled with two numbers in parentheses indicating the two footholds to which the walker is attached. (a) (i) $h\nu$ (365 nm), CD_2Cl_2, (ii) DBU, DTT, $CHCl_3$; (b) (i) I_2, $h\nu$ (500 nm), CD_2Cl_2, (ii) TFA, $CHCl_3$.[1404]

successive 1,4-*N*,*N*-migration rather than by overstepping. After 48 h, no out of sequence *N*,*N*-migration was observed with a model walker (Figure 50a,b). ^{1}H NMR analysis showed that the walking was highly solvent dependent and accelerated in polar solvents such as dimethylformamide and dimethyl sulfoxide. In d_6-DMSO, the walker reached an equilibrium distribution in 15 h. A ratio of 1:0.9 between the occupancy of initial position and the central amine of the track was achieved over this time period. Intermolecular exchange of less than 6% took place when the model walker was mixed with a longer free track for 3 days. This indicates a high processivity (on average 530 steps taken before detachment). Using a longer track modified with an anthracene at the far end, it was possible to monitor walking via an observed decrease in fluorescence as the walker approached the anthracene. As the nitrostyrene walker approached the edge of the track, it quenched the fluorophore (Figure 50d). Leigh et al. have since reported an extended system with a naphthalene moiety at one end of the track (Figure 51 a).[1398] In the presence of excess base (iPr$_2$NEt), the walker was "trapped" by the naphthylmethylamine, which was the thermodynamic sink. ^{1}H NMR analysis showed that the steady-state distribution of the walker was biased and 46% of walker molecules had reached the final benzylic foothold in 48 h (Figure 51b,c). When a longer track (with 9 footholds) was used, the percentage at the final station dropped to 19%.

A walker with two chemically different legs that labilize under orthogonal conditions has been reported by Leigh et al. (**130**, Scheme 40).[1399] The walker unit was attached to the thread by hydrazone and disulfide linkages. Hydrazone exchange took place under acidic conditions, while under these conditions the disulfide bond was stable. Disulfide exchange required basic conditions, which did not affect the hydrazone bond. Successive acid–base cycles led to a 39:36:19 (1,2:2,3:3,4) distribution of walker, with only 6% forming the overstepped (1,4) isomer. Changing the length of the walker alkyl chain from 6 carbons to 5 and using oxidation instead of base exchange at the final step, the distribution could be biased in favor of the (3,4) isomer, which was attributed to strain in the (2,3) isomer.[1400]

Recently, Bayley et al. monitored an organoarsenic molecule walking along a cysteine bearing track in a protein pore, by measuring changes in ionic current. The walker "stepped" by thiol exchange reactions and displayed a limited degree of processivity and directionality (the latter due to the thermodynamic sink at the track terminus).[1401] An inchworm walker able to walk on a copper surface has been reported. It could be constrained to one dimension of motion by the use of oligomeric "fences".[1402]

8.3.3. Directional Synthetic Small Molecule Walkers. The biased migration of molecules along a track requires either a preference for one isomer over others under the operating conditions or that strain should be released upon stepping. An efficient ratcheting step is needed. Recently, the use of metal complexes in a molecular biped was explored by Leigh et al. (Figure 52).[1403] The track contained three different pyridine derivatives: 2,6-dialkyl-4-*N*,*N*-dimethylaminopyridine (foothold 1, green), 3,5-dialkylpyridine (foothold 2, red), and 2,6-dialkylpyridine (foothold 3, blue). The walker consisted of pincer ligands able to complex the pyridine foothold via Pd(II) or Pt(II) centers. Initially, the walker was attached to the track by complexation of Pd(II) with foothold 1, and Pt(II) with foothold 2. Upon protonation of the free 2,6-dialkylpyridine foothold (foothold 3) and heating, exchange of the Pd(II) complex

DOI: 10.1021/acs.chemrev.5b00146
Chem. Rev. 2015, 115, 10081–10206

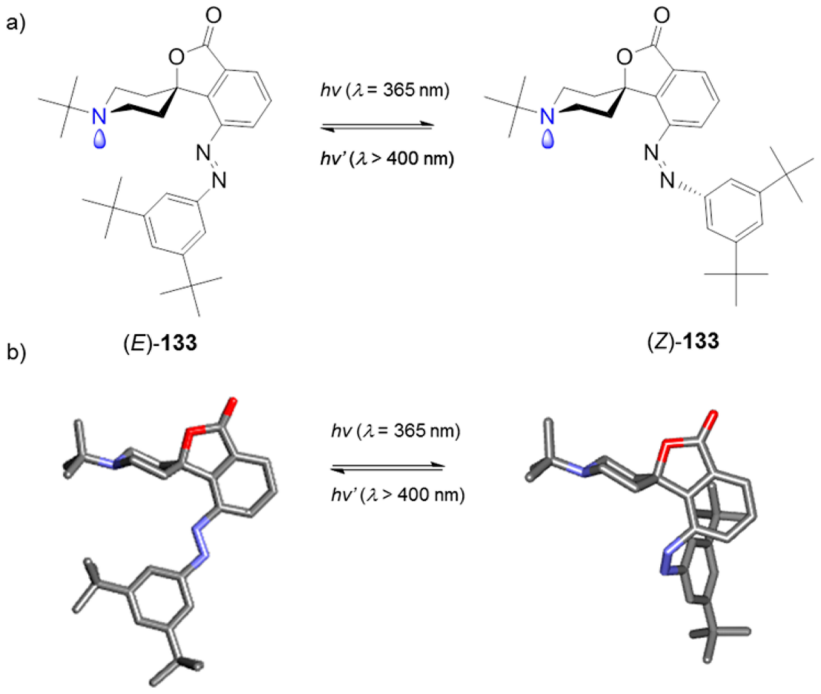

Figure 53. (a) Molecular structure of the photoswitchable piperidine base **133**, and (b) X-ray structure of the photoswitchable piperidine base **133**. X-ray crystal structure reprinted with permission from ref 1418. Copyright 2008 Wiley-VCH Verlag GmbH & Co. KGaA, Weinheim.

between foothold 1 and foothold 3 took place. A distribution of 15:85 in favor of foothold 3 was observed. The proton on foothold 3 was captured by the more strongly basic foothold 1 in this process. Migration could be reversed when the first foothold was deprotonated and the solution was heated. A ratio of 95:5 in favor of the initial position was obtained. Even though this example is not truly a walker, the significant directional bias in the stepping process of the metal-based biped could be used to inform more advanced designs.

Finally, a small molecule walker displaying all of the desired properties of an artificial walker, save autonomy, has been reported by Leigh et al. (Scheme 41).[1404] The walker was based on the previously published **130** (Scheme 40), but a stilbene moiety now linked footholds 2 and 3 (Scheme 41). The walker operated by the same hydrazone and disulfide exchange reactions, but with photoisomerization of the stilbene moiety driving directionality. Isomerization led to greater proximity between footholds 2 and 3 (over 1 and 2) in the *cis* form of the stilbene, resulted in a steady-state distribution of 40:60 in favor of the (2,3) positional isomer. During the second hydrazone exchange step, reisomerization to *trans* stilbene moved footholds 2 and 3 apart, which led to almost exclusive (5:95) formation of the (3,4) isomer.

8.3.4. Challenges Yet To Be Overcome. Significant progress has been achieved in the synthesis of synthetic molecular walkers with highly processive, progressive, and in some cases directional walkers being reported. The exploration of additional, reversible, walker−track interactions may lead to greater control over the directionality of motion. Autonomous walking remains a challenge to be addressed. Polymeric tracks could be designed for cargo transport over large distances. The ability to immobilize walkers on surfaces could lead to future technological applications.

8.4. Switchable Catalysts

In the living cell, many processes and reactions occur in parallel. To make sure that these reactions and their products do not interfere with each other, these operations must be rigorously controlled and switched on or off when necessary. In nature, enzymes control the outcome and rate of the large majority of reactions taking place in a cell. Recently, a number of biologically inspired systems have been published using molecular machines to control the outcome of reactions by switching on and off catalytic units or by controlling the enantioselectivity of the process.[1405−1412] In this section, switchable catalysts controlled by stimuli such as light, pH change, ion influx, and redox chemistry will be explored.

8.4.1. Photoswitchable Catalysts. Several examples of photoswitchable catalytic systems have been reported.[1407,1413−1415] The reactivity of the catalytic unit is typically controlled through alteration of the steric shielding of the active site or by bringing the catalytic units into closer proximity. In these examples, switching between the *cis* and *trans* forms of a photochromic group such as an azobenzene or a stilbene, or the electrocyclization of a diarylethene, provides the requisite control. An early example of a photoswitchable catalyst was published by Rebek Jr. and co-workers.[1416] Two adenine receptors capable of forming complexes with purine bases were linked through a *trans* azobenzene moiety. When the system was isomerized to its *cis* conformation, the rate of reaction between an amine and *p*-nitrophenyl ester was markedly increased due to greater proximity between the reactive groups, which increased the effective molarity of these groups and thus increased the rate of reaction. A switchable catalyst based on a light-responsive cavitand was published by the same group. The cavitand was functionalized with an azobenzene switch and the cavity of the *trans* state accessible to a guest molecule, while the *cis* conformation could not bind guests. Piperidinium acetate was used as the guest, and it could be shown that the host−guest complex significantly accelerated a Knoevenagel condensation

DOI: 10.1021/acs.chemrev.5b00146
Chem. Rev. 2015, 115, 10081−10206

between malononitrile and an aromatic aldehyde.[1417] Hecht and co-workers described the photoswitchable tertiary piperidine derivative **133**, which could function as a general base catalyst in a Henry reaction between *p*-nitrobenzaldehyde and nitroethane (Figure 53). Catalysis was regulated through the shielding/deshielding of the catalytic site upon irradiation of an azobenzene unit.[1418] The reversible shielding and deshielding of a catalytic site by photoisomerization has also been used to control the organocatalytic activity of a thiourea and a guanidine catalyst.[1419,1420]

The photoswitchable organocatalyst **134** consisting of a photochromic diarylethene (DAE) unit and an imidazolium salt was reported by Bielawski and co-workers.[1421,1422] Under ambient light and in the presence of base, the imidazolium species catalyzed transesterification and amidation. These reactions were considerably slowed upon photoinduced formation of the ring-closed isomer (Scheme 42).[1421]

Scheme 42. Ring-Opened and Ring-Closed Isomers of the DAE-Modulated Photoswitchable Organocatalyst 134[1421]

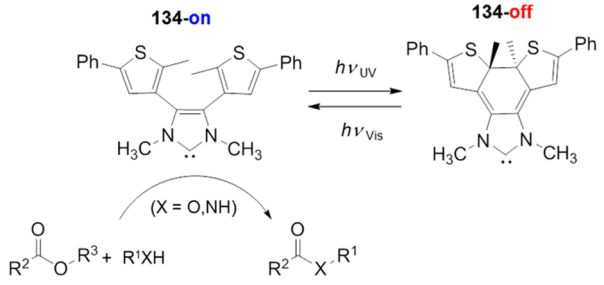

Exploiting the ability of dithienylethene to switch between ring-closed and ring-opened isomers upon irradiation, Branda et al. designed a photo responsive system mimicking enzyme cofactor pyridoxal 5′-phosphate **135** (PLP) (Scheme 43). PLP is responsible for amino acid metabolism and participates in a diverse range of enzymatic reactions such as transamination, racemization, decarboxylation, and various elimination processes. The structural features responsible for the action of PLP are the conjugated aldehyde and pyridinium functional groups. Branda and co-workers replaced the core ring of PLP with a dithienylethene where, in the ring-open form, the pyridinium and aldehyde units were electronically isolated from each other preventing catalytic activity (**138**-inactive). However, photoirradiation to form the ring-closed (**138**-active) isomer resulted in a fully conjugated structure, which restored the connectivity between the pyridinium and the aldehyde groups and therefore led to catalytic activity.[1423]

Feringa et al. used one of their rotary molecular motors based on a chiral overcrowded alkene, which can perform a directional 360° rotary cycle fueled by light and heat to create a photoswitchable catalyst. During this rotation, the helicity of the motor changes, which changes the overall chirality of the system. A DMAP (dimethylaminopyridine) Brønsted base (Figure 54) and a thiourea hydrogen-bonding donor group, which together comprise a bifunctional organocatalyst, perform Michael additions when in close proximity. As a consequence, the catalytic activity as well the stereoselectivity can be controlled. Michael addition of 2-methoxy thiophenol to cyclohexanone was used as a test system. The (*P*,*P*)-*trans*-**140** isomer resulted in a racemic (*R*,*S*)-thiol adduct in low yield (7%) after a lengthy reaction. When the (*M*,*M*)-*cis*-**140** isomer was used, the Michael addition proceeded significantly faster furnishing a 50% yield of product, with an er of 75/25 (*S*/*R*). Finally, the (*P*,*P*)-*cis*-**140** isomer led an 83% yield with an inversion in enantioselectivity providing an er of 23/77 (*S*/*R*).[1424] Recently, the same group reported a bisphosphine derivative of the same photoswitchable rotary motor. Both product enantiomers of a palladium-catalyzed desymmetrization reaction could be formed, although in situ switching experiments were complicated by the photosensitivity of the active palladium complex.[1425]

8.4.2. pH-Dependent Switchable Catalysts. Several rotaxanes containing a catalytic unit have been reported. However, these cannot typically be switched on/off.[1318,1426−1430] Leigh et al. described the rotaxane-based switchable organocatalyst **141**, in which catalytic activity could be controlled by pH-dependent macrocycle shuttling (Scheme

Scheme 43. (a) Reaction of an Amino Acid with PLP Showing the Aldimine 136 Initially Produced, and the Molecular Structure of the Quinonoid 137 Formed after Removal of the Amino Acid's α-Hydrogen, Which Leads to Racemization; and (b) Photoresponsive PLP Mimic 138[1423]

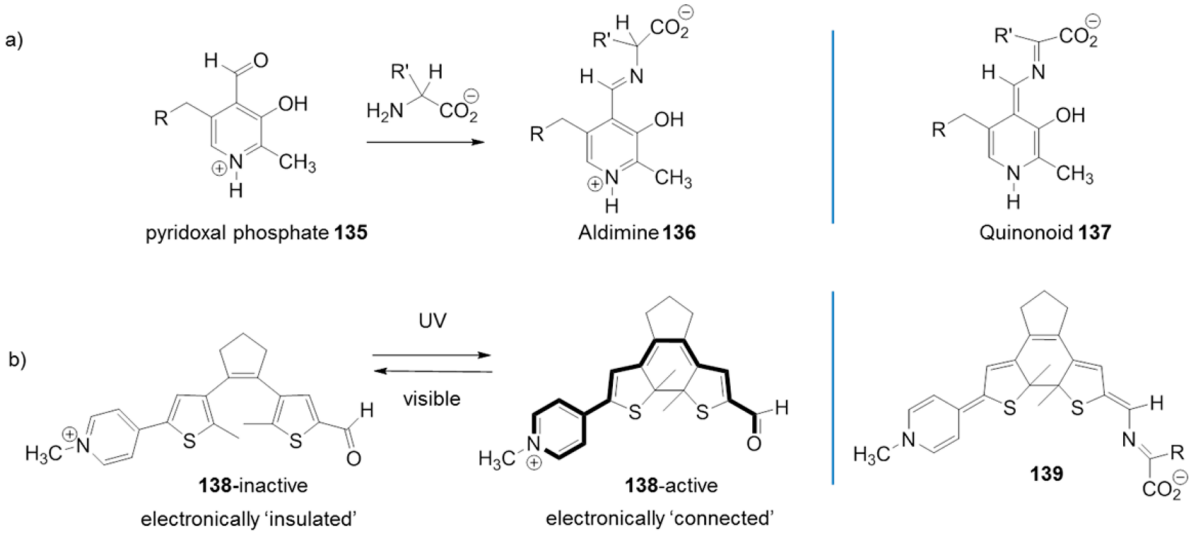

DOI: 10.1021/acs.chemrev.5b00146
Chem. Rev. 2015, 115, 10081−10206

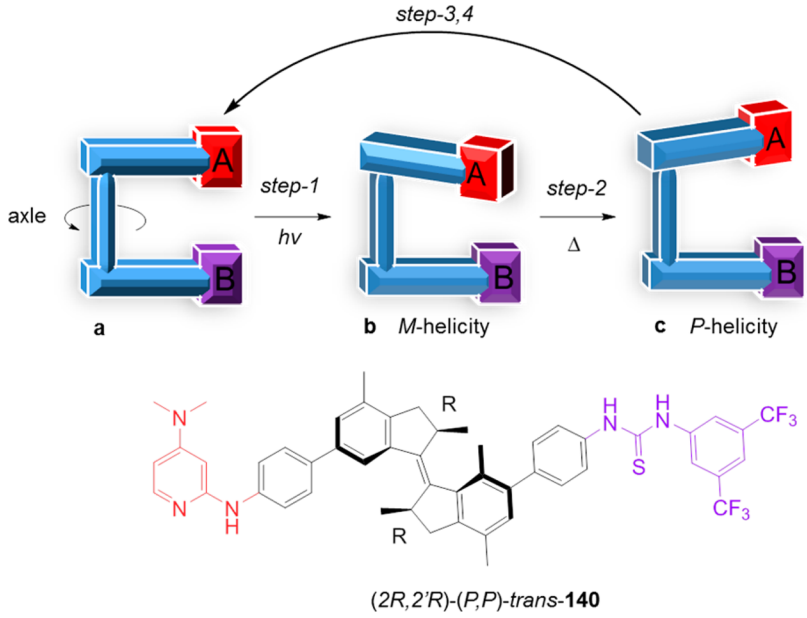

Figure 54. Schematic representation and molecular structure of a bifunctional organocatalyst integrated in a directional light-driven molecular motor. A, DMAP; B, thiourea hydrogen-bonding donor group. (a) A and B are remote. (b) A and B are in close proximity with *M* helicity in the (*M*,*M*)-*cis*-**140** isomer, preferentially providing the (*S*) enantiomer of the reaction product. (c) A and B are in close proximity with *P* helicity in the (*P*,*P*)-*cis*-**140** isomer, generating (*R*) enriched product. Step 1: irradiation at 312 nm at 20 °C. Step 2: heating at 70 °C. Step 3: irradiation at 312 nm at −60 °C. Step 4: temperature −10 °C.[1424]

Scheme 44. Acid−Base Switching of the Position of the Macrocycle, Which Conceals or Exposes the Catalytic Site on the Rotaxane[1431]

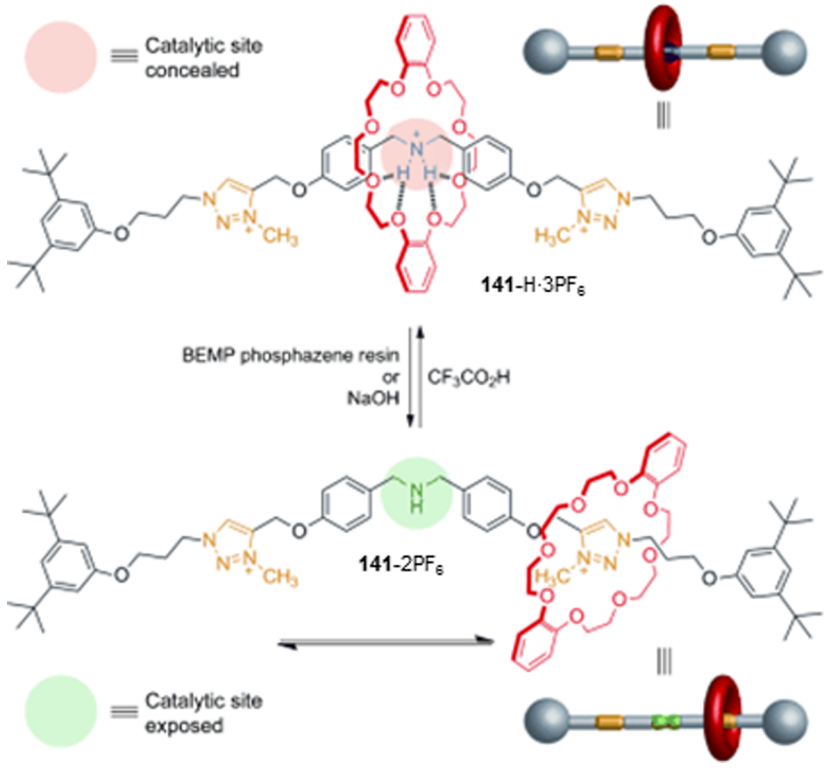

44). The design consisted of a dibenzo[24]crown-8 macrocycle and an axle containing both triazolium rings and a dibenzylamine/ammonium moiety. The secondary amine/ammonium group was able to carry out iminium catalysis. However, when the rotaxane was protonated, the ammonium group was a better binding site for the macrocycle than the triazolium ring, and so the macrocycle blocked the catalytic center, preventing the reaction. When the secondary amine of the rotaxane was not protonated, the triazolium ring provided a better binding site for the macrocycle and the dibenzylamine group was exposed, and could therefore participate in catalysis. As a model reaction, the Michael addition of an aliphatic thiol to *trans*-cinnamaldehyde

DOI: 10.1021/acs.chemrev.5b00146
Chem. Rev. 2015, 115, 10081−10206

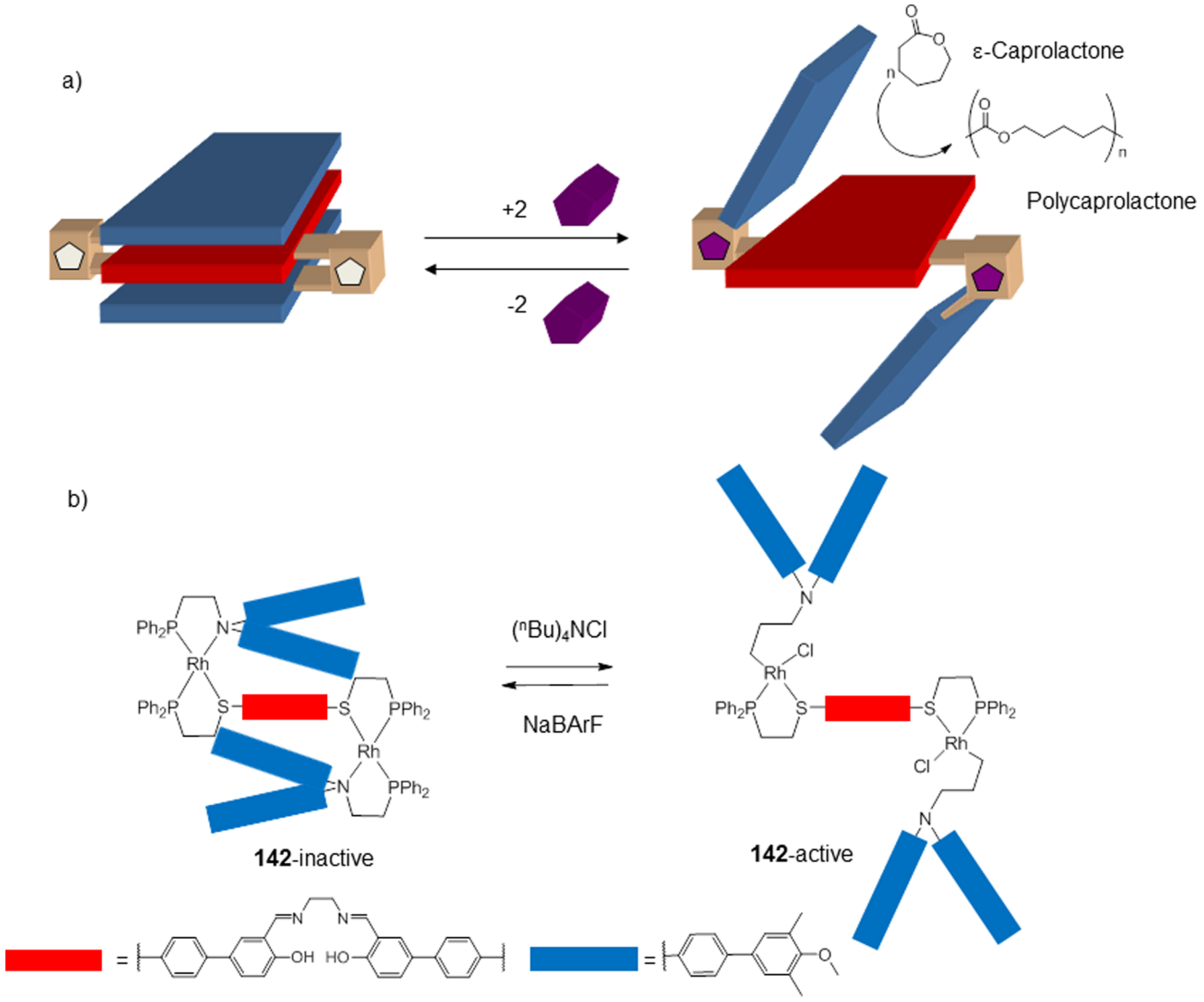

Figure 55. (a) Allosteric supramolecular triple-layer complex **142**, which regulates the catalytic living polymerization of ε-caprolactone. (b) Molecular structures of the components.[1435]

Scheme 45. Schematic Representation of the Reversible Locking and Unlocking of Switchable Catalyst 143[1439]

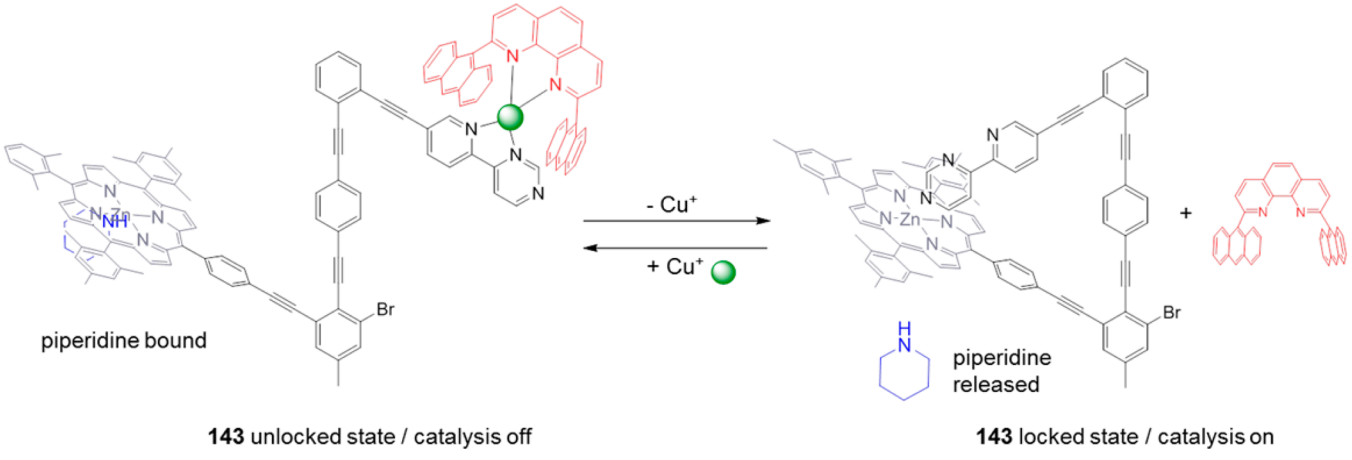

was performed. The free thread was found to efficiently catalyze the reaction in both its protonated and its deprotonated states.[1431] Recently, Leigh and co-workers explored the activation modes of rotaxane catalyst **141** and published a chiral version of this design, with a chiral center next to the secondary amine.[1432,1433] This chiral organocatalyst was able to perform an asymmetric Michael addition with good stereoselectivity.[1433] The pH-driven shuttling of a pyridyl-2,6-dicarboxyamide

DOI: 10.1021/acs.chemrev.5b00146
Chem. Rev. 2015, 115, 10081−10206

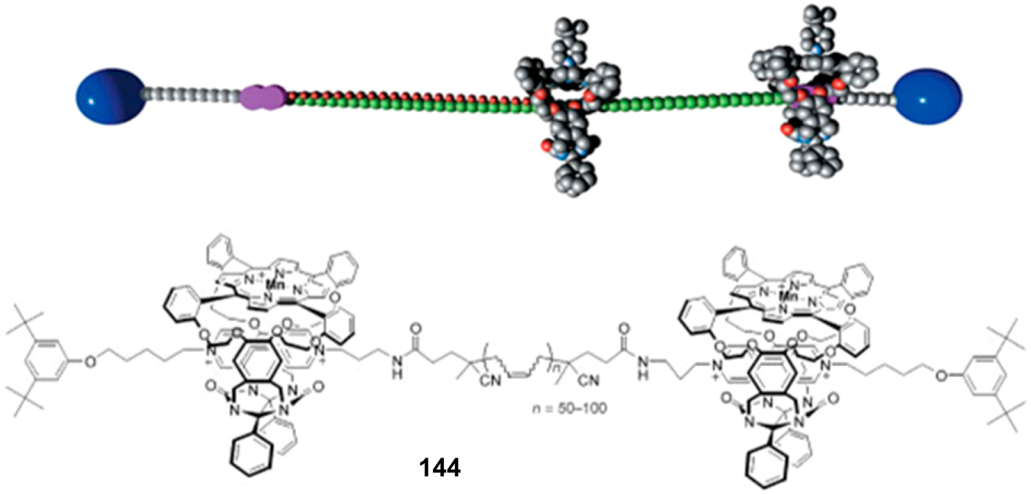

144

Figure 56. Porphyrin-catalyzed epoxidation of a butadiene polymer by **144**, utilizing a rotaxane architecture. Reprinted with permission from ref 1456. Copyright 2003 Nature Publishing Group.

macrocycle between squaramide (hydrogen bond catalyst) and ammonium (iminium catalyst) stations has been reported.[1434] The macrocycle blocks the site it is bound to, allowing the selective exposure of catalytic sites and the generation of different products.

8.4.3. Allosteric Regulation of Switchable Catalysts through Ion Addition. A different approach to the regulation of catalytic activity is via the addition of small molecules such as ions, which can change the supramolecular structure of the catalyst, as is observed in many enzymatic processes. Mirkin and co-workers reported the synthesis of triple-layer complex **142** composed of two transition metal hinges, two chemically inert blocking exterior layers, and a single catalytically active interior Al(III)-salen complex, which can act as a ring-opening polymerization catalyst for ε-caprolactone (Figure 55). Polymer growth and molecular weight could be controlled by the addition of Cl^- (catalytic layer exposed) or of the Cl^- abstracting agent $NaB(ArF)_4$, which results in the fully closed complex **142**.[1435−1437] Recently, the same research group reported an allosterically regulated photoredox catalyst based on a similar switching mechanism.[1438]

Another ion triggered switch was the self-locking system published by Schmittel and co-workers (Scheme 45).[1439−1441] Their design consisted of a zinc porphyrin and a 4-aza-2,2′-bipyridine tether, which either coordinated to the zinc porphyrin or formed a complex with copper and a shielded phenanthroline. In the presence of copper, the tether was removed from the zinc porphyrin center, and piperidine was bound at the coordination site. When copper was removed, piperidine was liberated and able to catalyze Knoevenagel reactions.[1439]

8.4.4. Redox-Driven Switchable Catalysts. Canary and co-workers have reported a redox-switchable chiral catalyst capable of delivering either enantiomer of a nitro-Michael addition product depending on the oxidation state of a single copper atom. The design, inspired by previous work carried out in their group and by others,[1442−1444] is based on complexes derived from methionine, which were shown to undergo inner sphere ligand rearrangement upon one-electron oxidation or reduction of copper. The rearrangement is coupled to the orientation of quinolone rings to afford enantiomeric configurations. Urea catalysis produced the (*S*) enantiomer in 72% ee and 55% yield, and the in situ reduced complex produced the (*R*) enantiomer in 71% ee and 43% yield.[1445]

8.5. Synthesis Using Artificial Molecular Machines

Nature provides us with many examples of biological molecular machines that engage in sequence-specific chemical synthesis. For example, the ribosome utilizes sequence information stored in mRNA to synthesize proteins with excellent fidelity.[68−70] The various DNA polymerases provide further examples of sequence-specific polymer synthesis by biological molecular machines.[71] The inherently programmable nature of DNA has been used by synthetic chemists to accomplish sequential oligomer synthesis. A common strategy is exemplified by the seminal work of Liu et al.,[1446] where complementary sequences of DNA capped with different, mutually reactive end groups are annealed to create an extremely high local concentration of the two reactive species ensuring intracomplex bond formation predominates. After the first reaction is complete, a biotin tag on one strand allows its selective removal, after which a new reactive partner can be annealed to the existing strand and a second reaction conducted. Peptide,[1446−1448] carbon−carbon,[1449−1452] carbon−heteroatom bond forming reactions,[1453] and even cycloaddition reactions have all been reported on the basis of this type of methodology.[1454] More elaborate DNA systems have been used by Seeman and co-workers to create a "molecular assembly line" where three gold nanoparticles could be combined to form eight differently composed products, illustrating the complexity that can be achieved with DNA-based molecular machines.[1455]

In a seminal example of a synthetic system mimicking some of the properties of an enzyme, Nolte, Rowan et al. reported a rotaxane-based catalytic system.[1456] A glycoluril clip-based macrocycle containing a manganese porphyrin catalyst catalyzed the epoxidation of a butadiene polymer, which formed the thread of the rotaxane. A greatly enhanced proportion of *cis*-epoxide was observed in the product, consistent with previous work showing that when the reaction occurred in the macrocyclic cavity steric constraints favored the *cis* product.[1457] This system has been further optimized by substitution of the porphyrin macrocycle with protective ligand groups, which increase turnover number (TON) and provide even greater *cis* selectivity by preventing reaction on the exterior face of the macrocycle (Figure 56).[1458] The rate of threading of their macrocycle onto polymeric materials was also studied and found to be highly dependent on

DOI: 10.1021/acs.chemrev.5b00146
Chem. Rev. 2015, 115, 10081−10206

Scheme 46. Cyclodextrin Dimer 145 Polymerization Catalyst[1460,a]

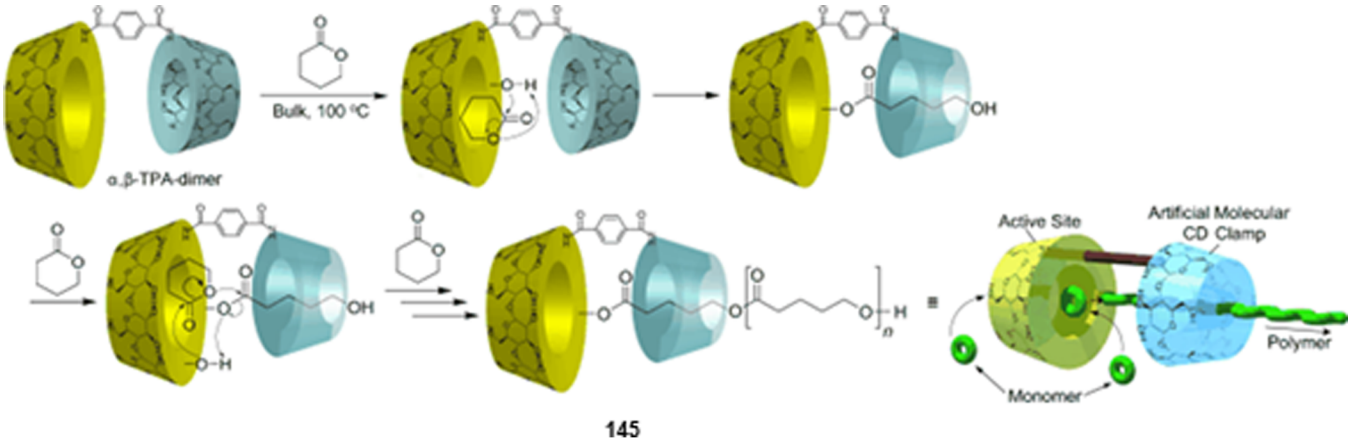

[a]Reprinted with permission from ref 1460. Copyright 2011 Wiley-VCH Verlag GmbH & Co. KGaA, Weinheim.

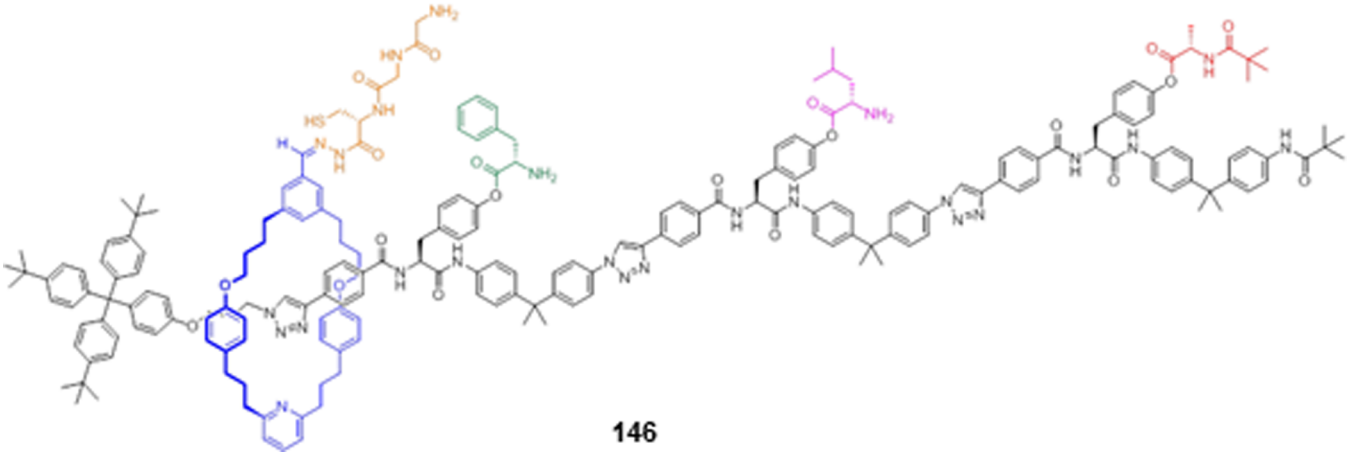

Figure 57. Leigh's small molecule peptide synthesizer, **146**.[666]

interactions between the thread and the outside of the macrocycle preassociating the two moieties.[1459]

A cyclodextrin dimer has been used as both a catalyst (for the polymerization of δ-valerolactone) and a molecular "clamp", which guides the output of the polymer.[1460] In this system, an α-cyclodextrin acts as the active site while a β-cyclodextrin acts as the clamp guiding the growing chain away from the active site (Scheme 46). An additional example was provided by Takata et al.,[1430] where the cyclization of propargyl or allyl urethane groups in the rotaxane backbone to oxazolidinones was catalyzed by a palladium center, bound to the macrocycle.

Recently, Leigh et al. reported the first small molecule artificial molecular machine (**146**) capable of sequence-specific peptide synthesis.[666] The machine is based on a rotaxane architecture, which is used to ensure processivity in a manner reminiscent of both the ribosome-mRNA structure and the DNA clamp of DNA polymerases.[68−71] Sequence information contained in the track is directly converted into the sequence of the peptide synthesized, and thus the track plays some aspects of the role of mRNA in the ribosomal system. Reactive phenolic ester groups take the place of tRNA-bound amino acids and are sequentially "picked up" by the catalytic arm of the macrocycle. The catalytic arm bears a cysteine group and operates by native chemical ligation (NCL) chemistry where the thiolate of the cysteine unit reacts first with the ester group before transferring the activated amino acid to the end of the growing chain.[1461] The steric bulk of the loaded amino acid prevents the macrocycle passing over the barrier unit before this reaction has taken place but allows free passage of the macrocycle after being cleaved. This prevents the peptide sequence from being scrambled and allows sequential reaction. Rigid spacing units between each loaded amino acid minimize the likelihood of the catalytic arm encountering an out of sequence amino acid. The catalytic unit consists of a cysteine-glycine-glycine motif with the second two amino acids present to prevent an unfavorable 1,8-*S*,*N*-acyl shift transition state during the second ligation (Figure 57).

After the third and final amino acid has been cleaved from the thread, the macrocycle can dethread and be isolated. The fidelity of sequence transfer in this process was demonstrated by tandem mass spectrometry of the macrocyclic product, identical to an authentic sample synthesized by conventional methods. No out of sequence or abbreviated products were observed by HPLC−MS underlining the extremely high level of control afforded by this system. This molecular machine showed processivity, sequence specificity, and autonomy and an exceptional level of control at the molecular level. However, several problems remain with this design. The rate of reaction is vastly slower than that of the ribosome; one peptide bond takes an average of 12 h to form, whereas the ribosome makes approximately 20 amide bonds every second.[68] Additionally, information is read in a destructive manner; once the macrocycle has cleaved the ester bonds, there is no way to reload the machine for a second run. Finally, the

DOI: 10.1021/acs.chemrev.5b00146
Chem. Rev. 2015, 115, 10081−10206

Scheme 47. Operation of Leigh's Peptide Synthesizer[666,a]

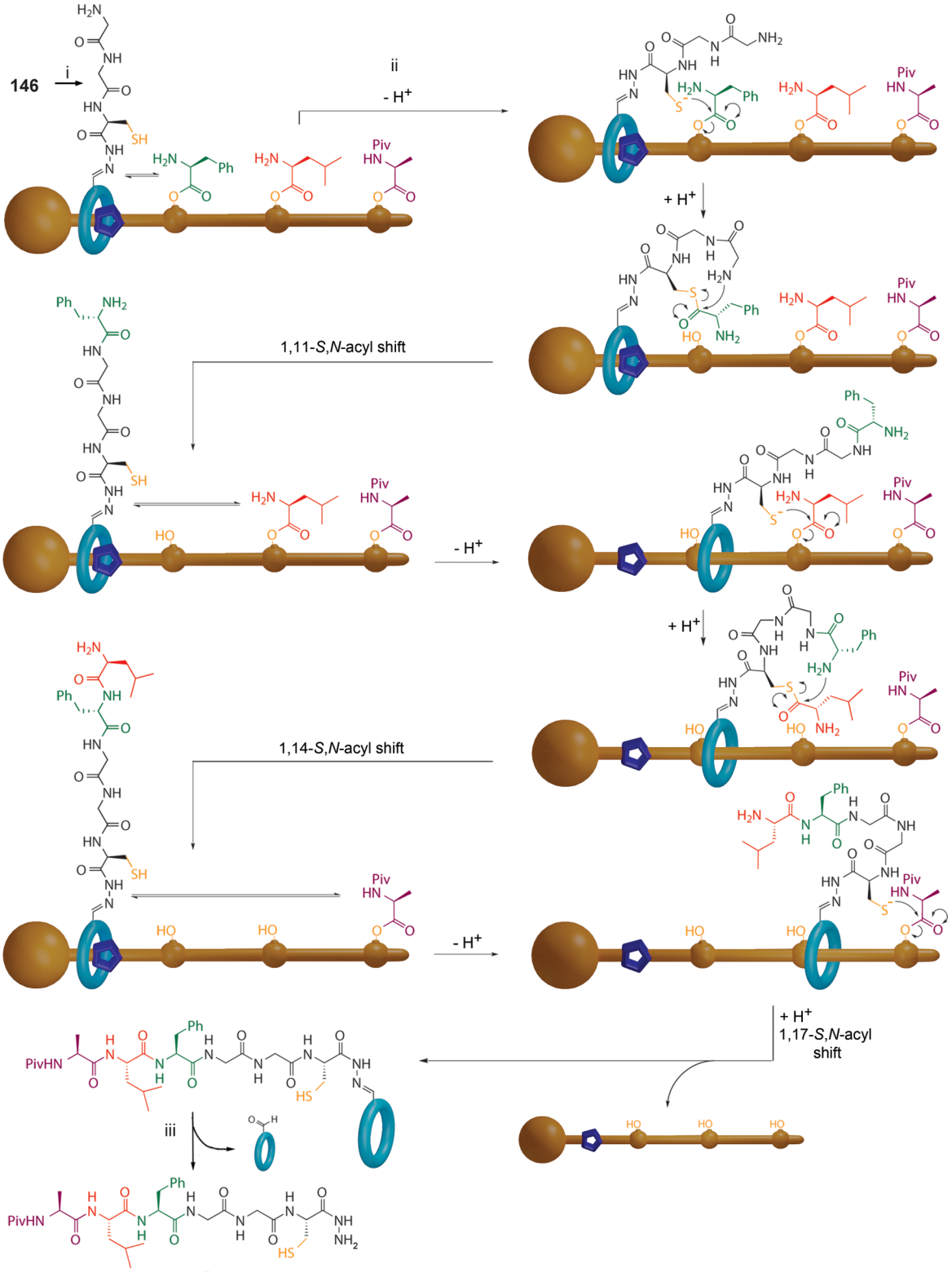

[a]Reprinted with permission from ref 666. Copyright 2013 American Association for the Advancement of Science (AAAS).

NCL reaction used to catalyze peptide formation limits the scope of amino acids that can be incorporated into the growing peptide chain.

Recently, Leigh et al. reported an extension to this system, creating a four barrier machine whose final product is a macrocycle-bound heptapeptide.[661] The sequence specificity of the product was again confirmed by tandem mass spectrometry and compared to an authentic sample. Although no problems were encountered in this system, whose final bond formation involves a 20-membered ring *S,N*-acyl transfer, the ever-expanding size of the required cyclic transition state will at

DOI: 10.1021/acs.chemrev.5b00146
Chem. Rev. 2015, 115, 10081−10206

some point limit the length of potential peptide products formed by the current design (Scheme 47).

8.6. Controlled Motion on Surfaces, in Solids, and Other Condensed Phases

8.6.1. Controlled Motion in Solids and Condensed Phases. A major challenge is to use molecular machines for practical applications by utilizing molecular scale changes to create macroscopic effects. Using molecular machines in the solid state or other condensed-phase matter could lead to new materials with a higher level of complexity with controlled cooperative molecular motion leading to changes in the properties and function of the material on a macroscopic scale. In recent years, several examples of molecular motion in condensed-phase matter have been described, some of which show promise for applications in the fields of electronics and optoelectronics.

Garcia-Garibay and co-workers have investigated the rotational dynamics and photophysical properties of the crystalline, linearly conjugated, phenyleneethynylene molecular dirotor **147** (Figure 58). A pentiptycene unit was incorporated as a central

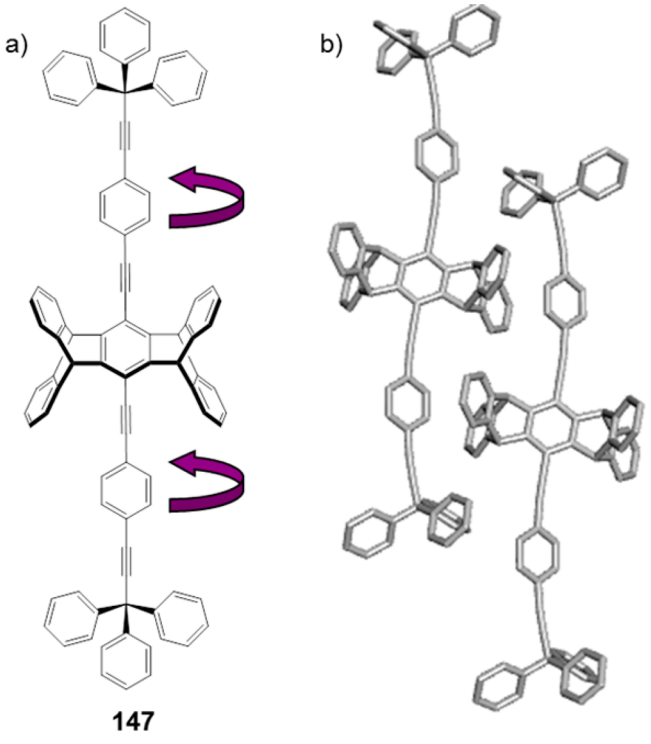

Figure 58. (a) Molecular structure of linear conjugated phenylethynylene molecular dirotor **147**. Rotation of the phenylene rotor (shown with an arrow) creates rotamers with varying degrees of π-conjugation and so wavelengths of emission. (b) X-ray structure of the dirotor **147**. X-ray crystal structure reprinted with permission from ref 1462. Copyright 2013 American Chemical Society.

stator about which the two flanking ethynylphenylene rotators could adopt various torsion angles. X-ray diffraction studies showed that in the solid-state structure of molecular dirotor **147** all of the phenyleneethynylene chromophors are arranged parallel to one another and therefore shared the same rotation axis. The chromophore displayed significant fluorescence changes as a function of interphenylene torsion angles. The authors suggest that with this system external control of the rotation could be achieved by the application of an electric field, which would allow a rapid shift of solid-state fluorescence emission and optical properties upon the application of appropriate stimuli.[1462−1470]

Sozzani and co-workers have published several examples of molecular rotors in crystals with open porosity, as well as molecular rotors embedded in porous frameworks such as aromatic or organosilica frameworks. In some of these systems, the rotational motion can be actively regulated in response to guest molecules such as CO_2, I_2, tetraethylammonium chloride, and water. These responsive materials may find applications spanning from sensors to actuators, which could capture and release chemicals on command.[1471−1474] Recently, Schurko and Loeb published a metal−organic framework (MOF) material containing dynamically interlocked components.[1475] They used [2]rotaxane **148** as the organic linker and binuclear Cu(II) units as the nodes (Figure 59). Void spaces inside the rigid framework allowed the macrocyclic ring of the rotaxane to rotate rapidly. Initially the macrocycle is locked in place through hydrogen bonding from an ether oxygen atom of the macrocycle to a copper-bound H_2O. Dynamic motion occurs upon removal of the water molecules by heating to 150 °C under vacuum, destroying hydrogen-bond interactions and allowing rapid circumrotation about the rotaxane axle. Rotation can be quenched by the addition of water. This type of material could be useful for the creation of solid-state molecular switches and machines.[1475] A rotaxane-based molecular shuttle incorporated into the structure of a MOF has recently been reported.[1476]

8.6.2. Solid-State Molecular Electronic Devices. In a series of ground-breaking but controversial experiments interfacing switchable rotaxanes and catenanes with silicon-based electronics, molecular shuttles have been employed in solid-state molecular electronic devices.[1146,1477−1485] Bistable [2]rotaxanes and [2]catenanes have been the subject of numerous experimental investigations in the course of the development of such molecular electronic devices.[1233,1478,1486−1495] Here, the bistable [2]catenanes and [2]rotaxanes feature a cyclobis(paraquat-*p*-phenylene) ($CBPQT^{4+}$) macrocycle and two stations, often a tetrathiafulvalene (TTF) site and a dioxynaphtalene site (DNP). Initially the macrocycle preferentially resides over the TTF site due to strong aromatic charge-transfer interactions between the components; this is referred to as the ground-state coconformation (GSCC). Electrochemical oxidation of the TTF station to form TTF^{2+} generates Coulombic repulsion between $CBPQT^{4+}$ and TTF^{2+}, and drives the translation of the macrocycle to the DNP station, to give the metastable state coconformation (MSCC). The process can be reversed on reduction of TTF^{2+} to TTF followed by either thermal relaxation of the macrocycle to the TTF station, or reduction of the bipyridinium units in the cyclophane ring to the corresponding radical cations, which reduces the activation barrier to shuttling, restoring the system to the GSCC. These two mechanically distinguishable states exhibit different characteristic tunneling currents. On the basis of quantum mechanical computational studies, the MSCC state is predicted to be the more highly conducting state. The switching cycle can be detected by a number of experimental techniques including time- and temperature-dependent electrochemistry and spectroscopy. Studies have shown that current levels on switching are influenced by temperature, the structure of the rotaxane/catenane, and the environment in which the molecular machines are embedded.[1496−1498] Different environments, including Langmuir−Blodgett (LB) films,[1499−1501] self-assembled monolayers (SAMs),[1502−1506] and solid-state molecular-switch tunnel

DOI: 10.1021/acs.chemrev.5b00146
Chem. Rev. 2015, 115, 10081−10206

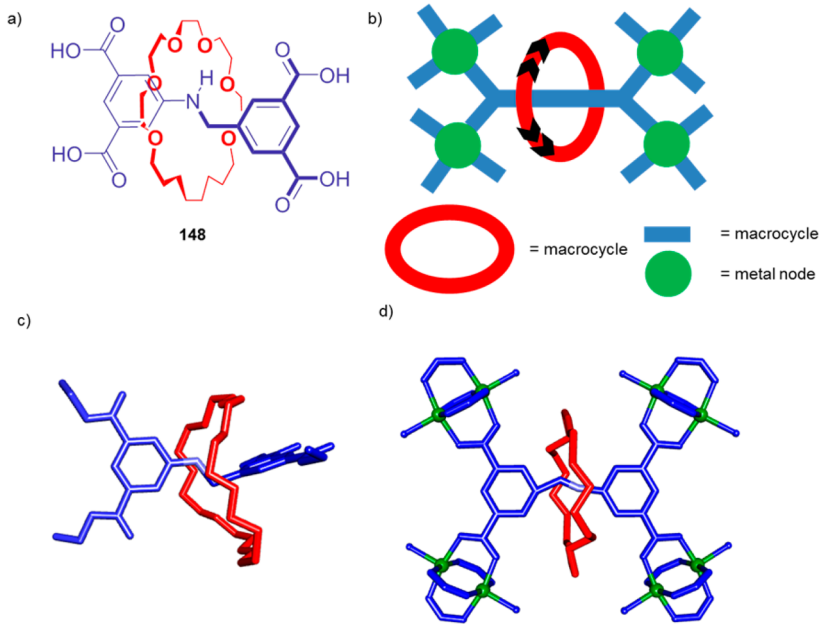

Figure 59. (a) Structure of [2]rotaxane **148**. (b) Schematic representation of the structural design components used to create the metal−organic framework. (c) X-ray structure of the tetra-ester precursor to [2]rotaxane **148**. (d) X-ray structure of a single unit of the mechanically interlocked molecule, coordinated to four Cu(II) paddlewheel clusters. X-ray crystal structure reprinted with permission from ref 1475. Copyright 2012 Nature Publishing Group.

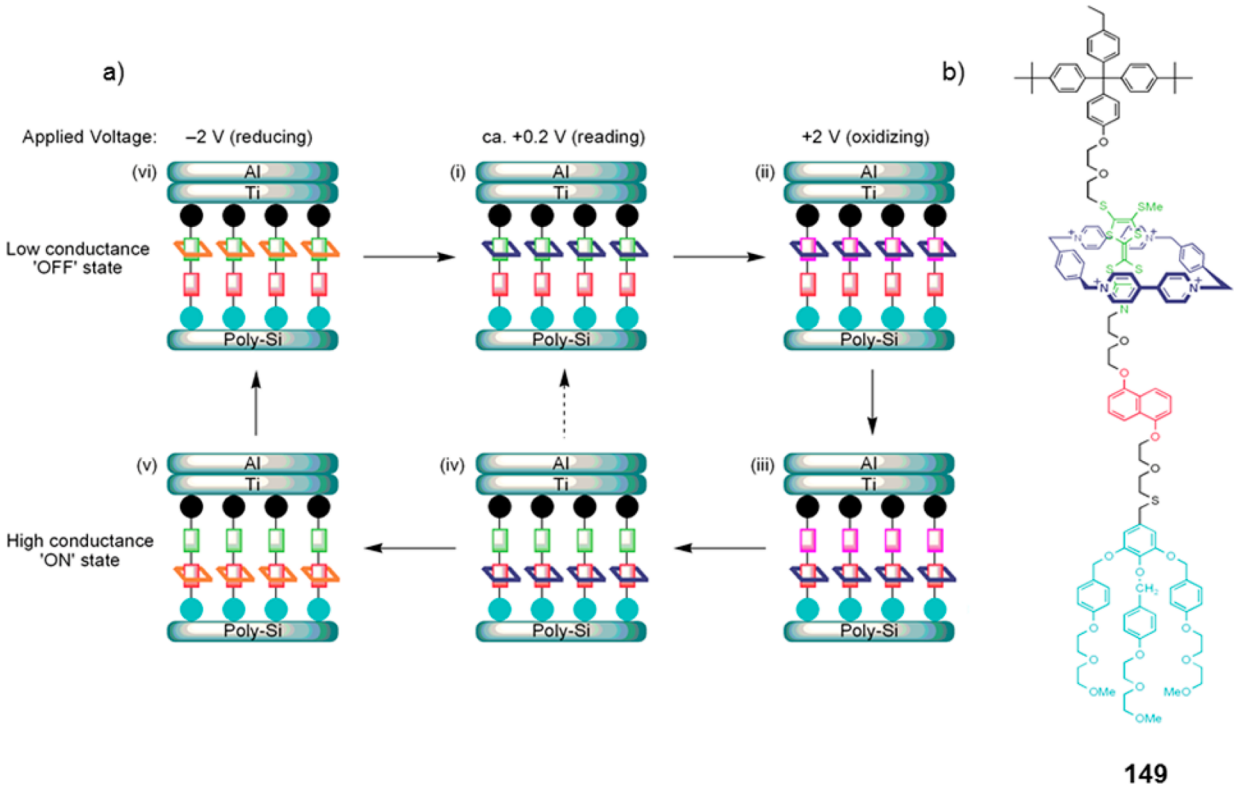

Figure 60. (a) Rotaxane **149**-based molecular switch tunnel junctions and proposed mechanism for the operation. (i) In the ground state, the tetracationic cyclophane (dark blue) mainly encircles the TTF station (green) and the junction exhibits low conductance. (ii) Application of a positive bias results in one- or two-electron oxidation of the TTF units (green → pink), and increases electrostatic repulsion causing (iii) shuttling of the macrocycle to the DNP station (red). (iv) Returning the bias to near −0 V provides a high conductance state, in which the TTF units have been regenerated, but translocation of the cyclophane has not yet occurred due to a significant activation barrier to movement. Thermally activated decay of this metastable state may occur slowly ((iv) → (i), in a temperature-dependent manner) or can be triggered by the application of a negative voltage (v), which temporarily reduces the cyclophane to its diradical dication form (dark blue → orange), allowing facile recovery of the thermodynamically favored coconformation (vi). (b) Example of one design of a molecular switch. The coloring of the functional units corresponds to that used for the structural diagrams.[1479,1482,1483] Reprinted with permission from ref 14. Copyright 2007 Wiley-VCH Verlag GmbH & Co. KGaA, Weinheim.

DOI: 10.1021/acs.chemrev.5b00146
Chem. Rev. 2015, 115, 10081−10206

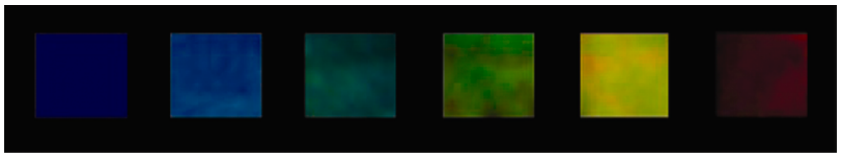

Figure 61. Color changes in a liquid-crystal film doped with a light-driven rotor. Reprinted with permission from ref 1528. Copyright 2002 American National Academy of Sciences.

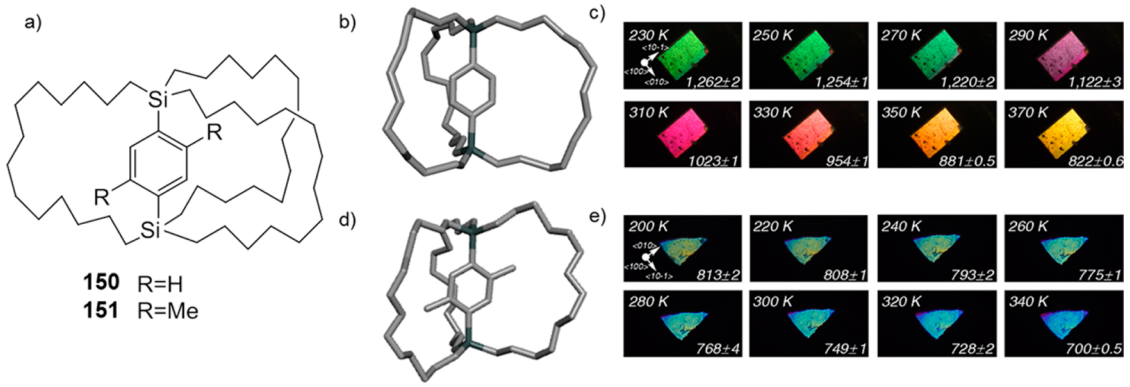

Figure 62. (a) Molecular structure of gyrotops **150** and **151**. The bulkier **151** does not exhibit rotation. (b) X-ray structure of **150**. (c) Single crystal of **150** irradiated with polarized white light. (d) X-ray structure of **151**. (e) Single crystal irradiated with polarized white light. For **150**, a continuous change in color was observed, due to thermal expansion. Reprinted with permission from ref 1530. Copyright 2012 American National Academy of Sciences.

junctions (MSTJs), have been extensively studied.[1150,1151,1488,1489,1507−1512] In one particular MSTJ, a monolayer of switchable rotaxane **149** was embedded between two conducting electrodes (Figure 60). This MSTJ acts as a gate, which can be opened or closed in response to an applied voltage by changes in conductivity and resistance and could be used in molecular logic gate designs. The reported design showed stable switching voltages of −2 and +2 V, with reasonable on/off ratios and low switch-closed currents. Nanometer-scale devices have been built using this approach and connected to form 2-D crossbar circuit architectures.[1144] As a next step, the authors published the design of a 160-kilobit molecular electronic memory circuit consisting of 400 silicon-nanowire electrodes (16 nm wide) and crossed by 400 Ti electrodes sandwiching a monolayer of bistable [2]rotaxanes.[1513] Despite the interesting findings, many remain skeptical about the utility of rotaxanes in electronics, and an array of scientific and engineering challenges remain to be addressed such as device robustness, improved etching tools, and improved switching speed.[1514−1516]

8.6.3. Using Mechanical Switches To Affect the Optical Properties of Materials. Molecular machines can influence the optical properties of materials in the solid state as well as in solution (section 8.2.2). Numerous molecular-machine-functionalized materials where changes can be visually monitored have been reported. Some pertinent examples are discussed below.

Liquid crystals have become widespread in numerous technological applications.[1517−1520] The photoalignment of liquid crystals has considerable potential for display and other optoelectronic applications. The reorienting effect of light on nematic liquid crystals is well-known.[1521−1525] However, the effect can be greatly enhanced by the presence of a dopant dichroic dye. Studies have suggested that the mechanism of this effect involves the photoexcited dye molecules acting as Brownian rotors in the nematic liquid crystal.[1526,1527] The change in orientation was attributed to a ratchet mechanism operating via the generation of torque. Feringa and co-workers reported a chiral nematic liquid crystal film doped with a previously reported chiral light-driven molecular motor. Irradiation of the film resulted in directional motion of the molecular motor, which induced a rotation of the rod-like liquid crystal molecules. This rotation led to the alteration of the color of the film over a large part of the visible spectrum (Figure 61).[1528,1529]

Yamaguchi et al. reported crystalline molecular gyrotop, which showed temperature-dependent changes in optical properties as a result of structural expansion upon rotor acceleration (Figure 62).[1530−1532] Utilizing a phenylene moiety as the rotor, they observed that the orientation of the rotor in the crystal was ordered below 270 K, but became disordered above this temperature generating a slight deformation of the crystal lattice. Using the temperature-dependent features of the crystal, the birefringence (Δn) of the crystal could be controlled. At 280 K, the phenylene moiety undergoes a 180° flipping between two equilibrium states, which provides an almost constant Δn. Above this temperature, Δn decreases as the phenylene moiety rapidly rotates, and the cage expands. The dynamic and optical properties are reversible.[1530]

A pseudorotaxane that acts as a thermally driven molecular switch in a crystalline state was recently published by Horie and co-workers.[1533−1535] Crystals of the pseudorotaxane underwent phase transitions upon heating with accompanying changes in optical properties.

Leigh et al. used [2]rotaxanes to control fluorescence by distance-dependent intercomponent electron transfer both in solution and on a polymer film. The thread of these rotaxanes included an anthracene fluorophore as a stopper attached to a glycylglycine hydrogen-bonding station and a C_{11} alkyl chain that could act as a second station. The macrocycles in **152** and **153**·$\mathbf{2H}^{2+}$ contained nitrophenyl and pyridinium moieties, respectively, which are known to quench the fluorescence by distance-dependent electron transfer. Macrocyclic shuttling could be induced by changes in solvent with strongly hydrogen-bonding solvents displacing the macrocycle from the glycylglycine station

DOI: 10.1021/acs.chemrev.5b00146
Chem. Rev. 2015, 115, 10081−10206

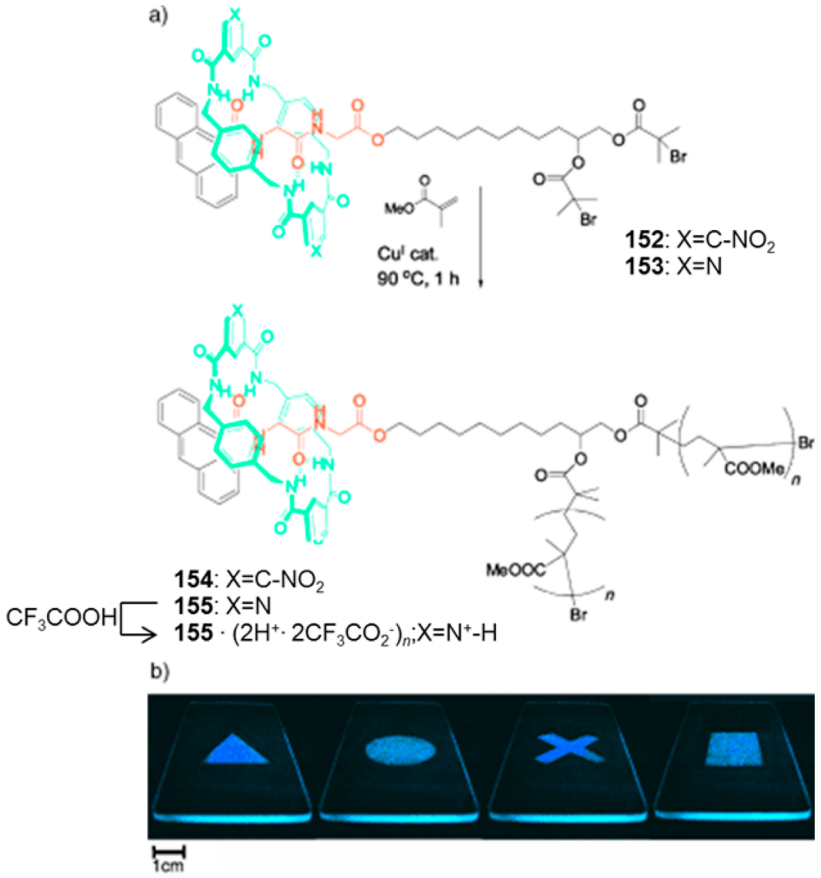

Figure 63. (a) Chemical structures of rotaxane initiators **152** and **153** and the corresponding PMMA-based polymers **154**, **155**, and **155**·$2H^{2+}$. (b) Images obtained by casting films of polymer **154** on quartz slides, then covering the films with aluminum masks and exposing the unmasked area to DMSO vapor for 5 min. The photographs were taken while illuminating the slides with an 8-W UV lamp (254−350 nm). Reprinted with permission from ref 1536. Copyright 2005 Wiley-VCH Verlag GmbH & Co. KGaA, Weinheim.

to the alkyl thread. In non-hydrogen-bonding solvents (e.g., benzene, CH_2Cl_2, CH_3CN), the macrocycle was located on the glycylglycine station and fluorescence was completely quenched. In strongly hydrogen-bonding solvents (e.g., DMSO and NH_2CHO), the macrocycle encapsulated the alkyl chain and fluorescence was restored. Polymer/rotaxane hybrids were used to prepare transparent films on quartz slides. Initially, no fluorescence was detected when the slides coated with a **154** containing film were illuminated with UV light (254−350 nm). However, after the slides were exposed to DMSO vapor, prior to illumination, a characteristic blue fluorescence was observed showing that similar shuttling processes were occurring on the polymer film as were observed in solution. Masking regions of the film from the DMSO vapor allowed the transitory etching of patterns on the polymeric films (Figure 63).[1536]

Polymeric **155**·$2H^{2+}$ films responded to two different stimuli. Protonation of the macrocycle by CF_3CO_2H vapor caused quenching of fluorescence, while DMSO vapor induced shuttling of the macrocycle and subsequently restored fluorescence emission. The response of **155**·$2H^{2+}$ to the different combinations of two stimuli (DMSO and protons) corresponds to an INHIBIT Boolean logic gate (Figure 64).[1536]

Hydrosol−gel systems represent another example of a nonsolution media. The effect of doping these systems with rotaxanes has been studied by various groups.[1208,1537−1541] Light-driven rotaxanes based on α-cyclodextrin and cucurbit[7]uril have been dispersed in thermoreversible hydrogel systems by Tian and co-workers. They observed that when the rotaxanes were embedded in the hydrogel, their optical performance (fluorescence and induced circular dichroism) improved. They attributed this observation to the restriction of movement in the hydrogel system.[1539,1542]

8.6.4. Using Mechanical Switches To Affect the Mechanical Properties of Materials. Piezoelectric materials provide the most common example of an external stimulus being converted into a mechanical change in the material. Materials incorporating molecular machines could provide a far greater level of control over macroscopic properties than is currently possible, and their development has been the focus of great interest.[1543,1544] Conformational changes in polymers leading to macroscopic mechanical changes have been extensively studied. Hydrogels, consisting of water-swollen cross-linked networks of neutral or ionic amphiphilic polymers, have been shown to undergo reversible phase transitions in response to changes in temperature, solvent, pH, electric field, or irradiation with an up to 100-fold expansion on phase change.[1545−1558] Katchalsky et al. first exploited these properties to develop devices that converted chemical potential energy into macroscopic mechanical work.[1559,1560] A large variety of devices based on the characteristics of these materials have been proposed[1561−1581] including guest binding and release,[1582] control of enzyme activity,[1583] and the macroscopic motion of a polymer gel by selective contraction of alternate sides of a gel.[1571] Finally, guest binding by built-in recognition sites can lead to large-scale changes in the volume of the host gel.[1584−1598]

DOI: 10.1021/acs.chemrev.5b00146
Chem. Rev. 2015, 115, 10081−10206

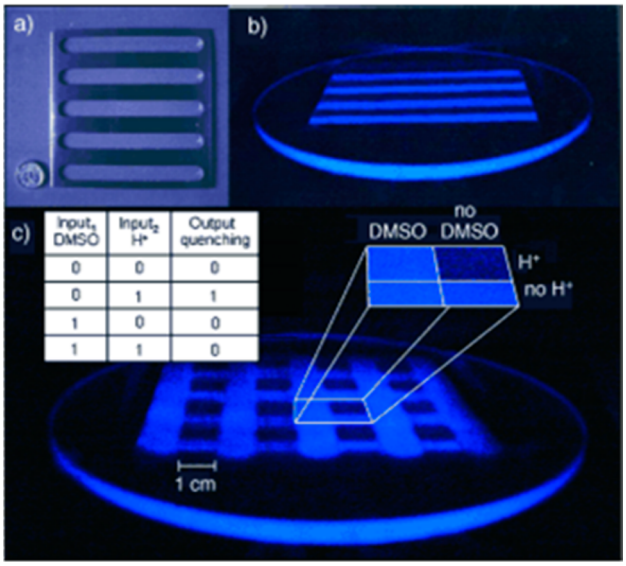

Figure 64. (a) Aluminum grid used in the experiment. (b) Pattern generated when films of **155** were exposed to trifluoroacetic acid vapor for 5 min through the aluminum-grid mask. (c) Mesh pattern obtained by rotation of the aluminum grid by 90° and exposure of the film shown in (b) to DMSO vapor for a further 5 min; only regions exposed to trifluoroacetic acid but not to DMSO were quenched as shown in the magnified view. Inset: Truth table for an INHIBIT logic gate. The photographs were taken while illuminating the slides with an 8-W UV lamp (254−350 nm). Reprinted with permission from ref 1536. Copyright 2005 Wiley-VCH Verlag GmbH & Co. KGaA, Weinheim.

Shape memory materials have also been designed that utilize control at a molecular level.[1599,1600] While most of these systems rely on a temperature variation-induced shape change, a system utilizing a photoinitiated radical reaction to rearrange covalent cross-links and recover the "memorized" shape has been reported.[1601] A reversible cross-linking [2 + 2] cycloaddition has also been used to achieve this control.[1602]

Conducting polymers have been used to create stimuli responsive mechanical changes.[1603−1605] Electrochemical oxidation can induce counterion expulsion or inclusion and thus volume change, although these changes tend to be slow in aqueous solution.[1606−1609] Solid state,[1610] gel,[1611] and ionic liquid electrolytes have been shown to accelerate this process.[1612] Conformationally flexible calix[4]arenes have been used as "hinges" to form conducting oligothiophenes where the cone (but not the kite) form of the calix[4]arene maximizes the desired $\pi-\pi$ interactions and switching could be utilized to provide macroscopic mechanical motion.[1613,1614]

In the previous examples, a macroscopic change was induced by the sum of multiple, relatively uncontrolled conformational changes in a polymeric network; that is, the observed change is not an inbuilt feature of the molecular components. The use of particular submolecular conformational/configurational switches to directly trigger macroscopic changes has numerous benefits such as overcoming problems caused by slow diffusion of guests or solvents and ensuring a uniform response in the material. The use of configurational switches to control long-range order in liquid crystalline phases has been discussed elsewhere (section 8.6.3), but a similar application in synthetic polymers often furnishes a useful result.

Azobenzenes are often used to control reversible contraction in polymers, a process that has been observed at a molecular level using AFM,[1615] as well as properties such as viscosity and solubility.[1616,1617] In the aforementioned AFM experiment, the application of a "load" to the AFM tip and subsequent isomerization toward the *cis* isomer provided the first direct measurement of the conversion of light to mechanical energy. Chiral azobenzene side chains can allow control over the screw sense of artificial helical polymers with isomerization leading to interconversion of the *P* and *M* forms.[1618−1620] Several liquid crystal polymeric systems have been reported.[209,1621−1635] Macroscopic motion was induced in liquid crystal polymer springs devised by Fletcher, Katsonis et al.[1636] Here, a chiral dopant, a polymerizable liquid crystal, and a polymerizable azobenzene switch were used to generate a liquid crystal polymeric spring. Irradiation with UV light caused *cis*−*trans* isomerization of the azobenzene switch, which in turn led to coiling/uncoiling or helical inversion of the spring. More complex behavior such as side to side bending could be induced by careful manipulation of the initial helical state and directed illumination.[1636]

Light-driven directional rotor **156** has been used to drive the macroscopic motion of a glass rod.[1637,1638] When doped at 1 wt % into a liquid crystal, the helicity of the rotor induced a helical arrangement in the liquid crystal, giving rise to a characteristic "fingerprint" texture in the liquid crystal's surface. Irradiation altered the distribution of isomers of the rotor and thus caused the liquid crystal's helical nature to rearrange. This process could be observed by the clockwise rotation it caused of a glass rod laid on the surface and of the "fingerprint" pattern. Eventually, however, rotation stopped as the system reached a photostationary state with the distribution of molecules between isomers reaching equilibrium. When the light source was removed, the isomer distribution decayed back to its initial state, with concomitant reverse rotation. The use of the opposite isomer of the rotor led to inversion of the direction of rotation (Figure 65).

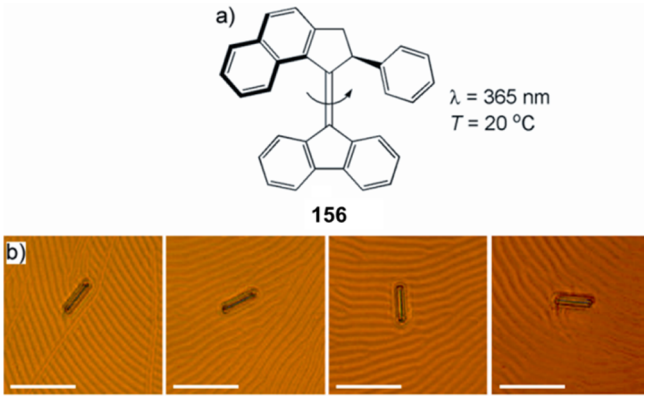

Figure 65. (a) Rotor **156**. (b) Rotation of micrometer scale glass rod on doped liquid crystal film. Photos taken at 15 s intervals. Reprinted with permission from ref 1637. Copyright 2001 Wiley-VCH Verlag GmbH & Co. KGaA, Weinheim.

Shuttling in [3]rotaxane **157** has been used to generate a macroscopic mechanical response, deformation of a microcantilever beam, which had been coated with a monolayer of ca. 6 billion rotaxanes.[1238,1341] Oxidation of the tetrathiafulvalene (TTF, green) station decreased the affinity of the macrocycle for this station, and induced shuttling to the naphthalene (red) station. A deformation of 550 nm was recorded, and the process could be reversed and repeated (with diminishing amplitude) over several cycles (Scheme 48).[1238,1341] Microcantilever

DOI: 10.1021/acs.chemrev.5b00146
Chem. Rev. 2015, 115, 10081−10206

Scheme 48. Molecular Motion Generating a Macroscopic Mechanical Response[1238,1341,1647,a]

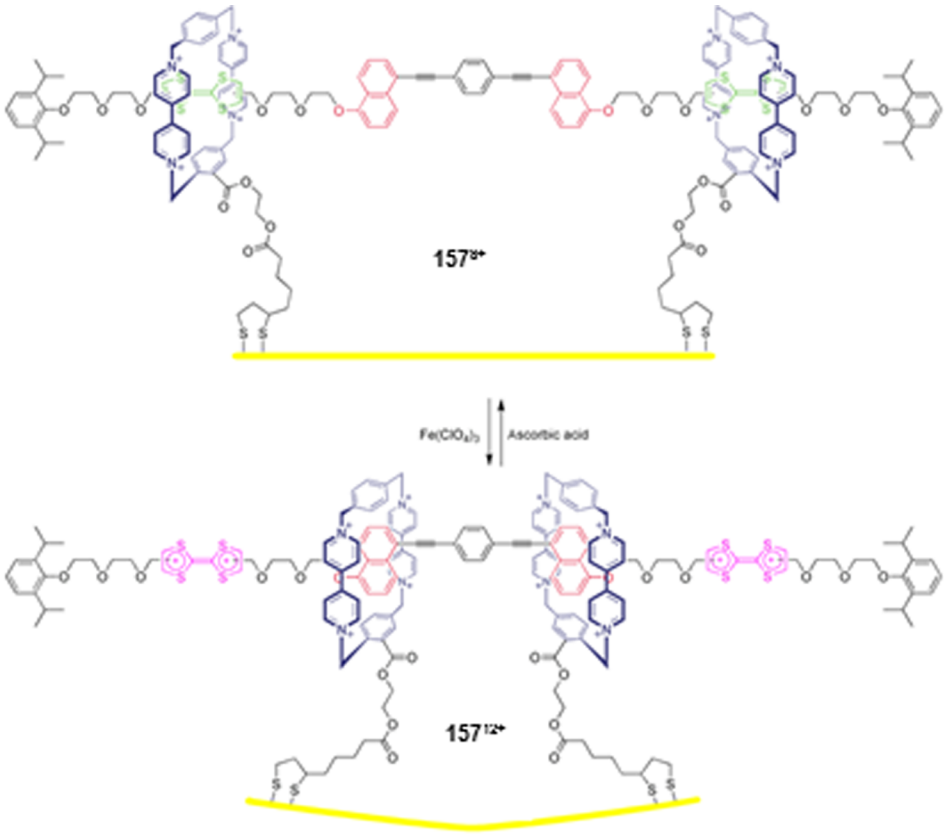

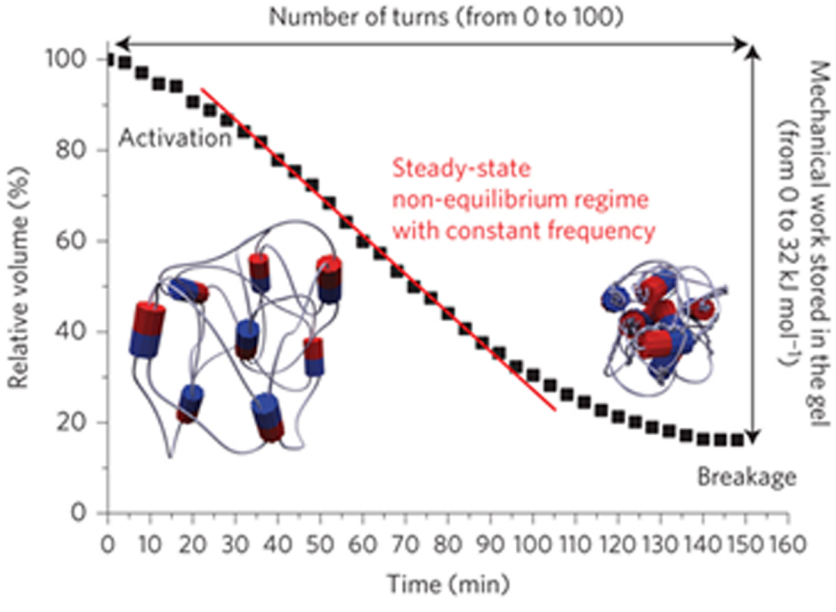

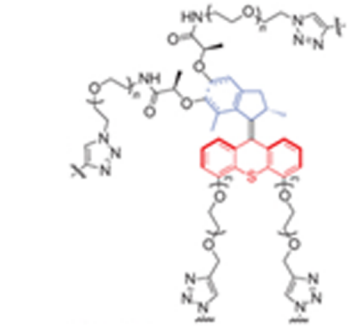

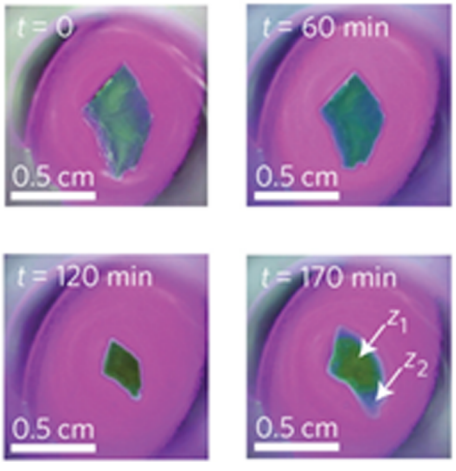

[a]Reprinted with permission from ref 1647. Copyright 2015 Nature Publishing Group.

DOI: 10.1021/acs.chemrev.5b00146
Chem. Rev. 2015, 115, 10081−10206

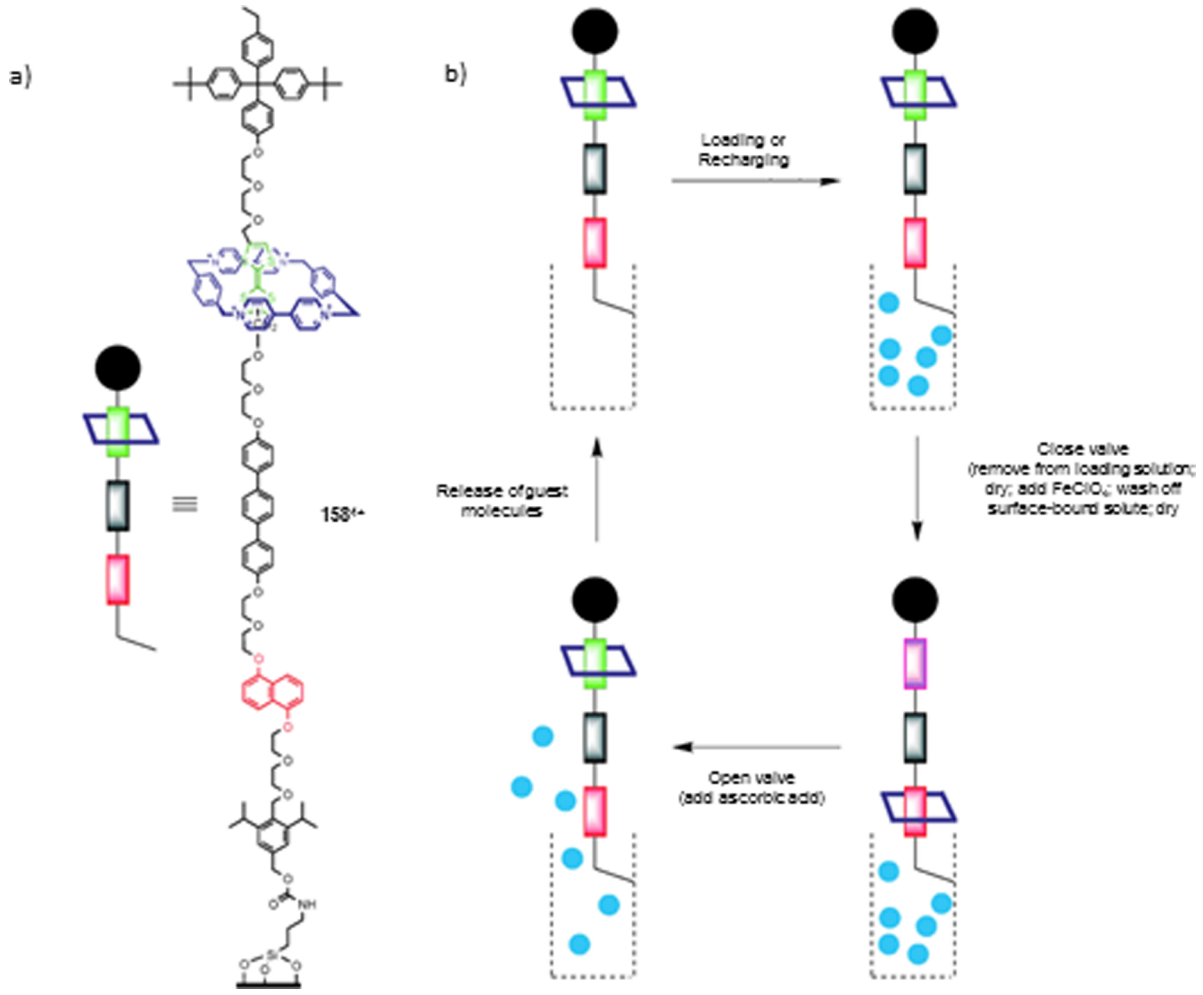

Figure 66. (a) Structure of nanopore gate, and (b) controlled release of guest from nanopores.[1664] Reprinted with permission from ref 14. Copyright 2007 Wiley-VCH Verlag GmbH & Co. KGaA, Weinheim.

Scheme 49. Electrode Controlled Macrocycle Shuttling, Leading to Control of the Hydrophilicity of the Surface[1672]

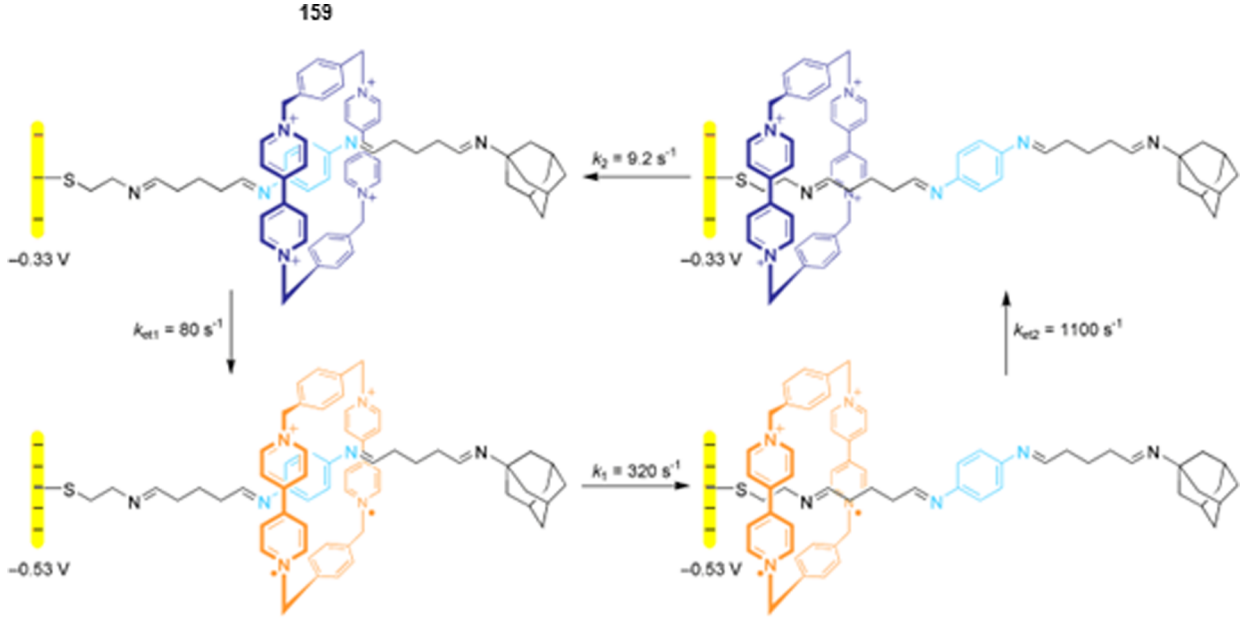

deformation by guest recognition at the surface has been used by several groups as a "read-out" from molecular detectors.[1639−1646]

A polymer has been reported that contracts upon illumination based on a directional light-driven rotor (Scheme 48).[1647] A

DOI: 10.1021/acs.chemrev.5b00146
Chem. Rev. 2015, 115, 10081−10206

photodriven rotary motor has also been used to induce the disassembly of self-assembled nanotubes.[1648]

8.6.5. Using Mechanical Switches To Affect Interfacial Properties. The ability to easily modify the properties of surfaces in a reversible manner would be extremely valuable in the design and synthesis of technologically useful devices. Stimuli-responsive polymer modification of surfaces can lead to control over wettability, adhesive ability, porosity, patterning, and interfacial interactions; this topic has been reviewed elsewhere.[1649−1663]

Interlocked architectures such as bistable rotaxane **158** have been used to restrict or allow access to the pores in materials such as mesoporous silica particles.[1664] The positively charged macrocyclic ring initially prefers the TTF station, and in this conformation, diffusion into and out of the nanopores of the silica is allowed. Oxidation of the TTF moiety causes shuttling of the ring to the dioxynaphthalene station, and closure of the nanopores, trapping a portion of the solvent/solute mixture. Solvent exchange and reduction of the oxidized TTF station leads to guest release (Figure 66). The aggregation and deaggregation of a polymeric material has been caused by the formation of pseudorotaxanes between strands. This has been used to transiently trap nanoparticles in the pores formed upon aggregation.[1665]

The translation of the macrocyclic ring of **159** has been converted into an electric signal.[1666−1668] A gold electrode was used in place of one stopper of the rotaxane, and a cyclodextrin ring with an attached ferrocene was used as the macrocycle. On photoactivated shuttling, the change in rate of distance-dependent oxidation of the ferrocene moiety allowed detection of the shuttling motion.[1669] When a glucose oxidase enzyme was attached via a rotaxane architecture to a gold electrode, the $CBPQT^{4+}$ macrocycle of the rotaxane acted as a two-electron shuttle and allowed enzyme operation, which was prevented when the enzyme was attached solely by the thread.[1670] A similar effect was seen in a system involving a CdS nanoparticle in place of the enzyme in which the observed photocurrent was amplified 8-fold in the rotaxane over the thread.[1671] In a simpler analogue of these systems involving a $CBPQT^{4+}$ macrocycle and a diiminobenzene station (**159**), electrode-induced shuttling could be directly observed.[1672] The reduction in macrocycle charge on shuttling was shown to decrease the hydrophilicity of the surface, and thus increased the contact angle of a drop of water on the surface (Scheme 49).

This control of wettability has been exploited by many groups to form a wide range of interesting systems, especially in the development of "self-cleaning" surfaces.[1673−1679] Surface wettability has been controlled by surface mounted photochromic switches.[1680] Self-assembled monolayers of carboxylate-terminated alkanethiols on gold have been switched between hydrophilic (carboxylate exposed, gold electrode at a negative potential) and hydrophobic (carboxylate surface bound, gold electrode at a positive potential) states by varying the electric potential.[1681] Bipyridinium groups have been used in place of carboxylates to similar effect.[1682]

Several methods for the photoswitchable change of surface wettability have been developed. Systems based on the reversible exposure of hydrophobic groups upon shuttling of a cyclodextrin ring,[1683] or the release of a hydrophilic guest,[1684] have been successfully exploited. Feringa and co-workers exploited a tripodal stator to fix a molecular directional rotor to a surface, which upon irradiation exposed or hid a hydrophobic fluorinated chain providing control over surface wettability (Figure 67).[1685]

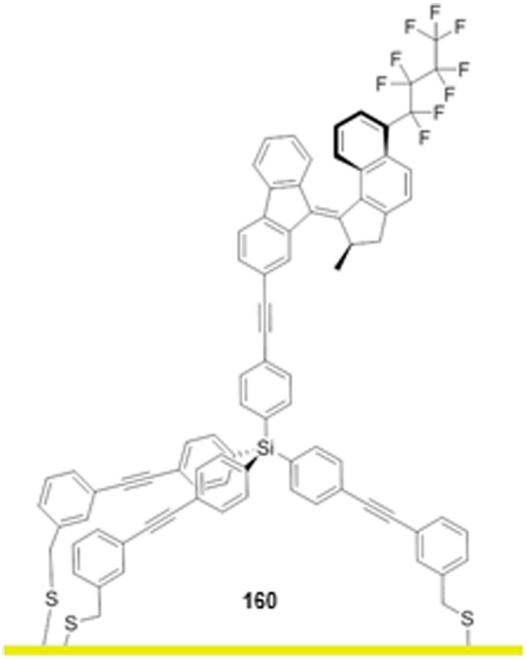

Figure 67. Feringa's tripodal wettability switch **160**.[1685]

Perhaps the most powerful demonstration of the usefulness of control over wettability is in the macroscopic transport of a liquid across a surface. The earliest example came from Whitesides and Chaudhury who created a hydrophilicity gradient on a silica wafer by reaction with a trichloroalkylsilane vapor and observed the motion of a droplet of water up a 15° incline.[1677] Numerous examples of droplet motion driven by surface energy gradients/steps have since been reported.[1686−1690] However, remotely controlling wettability to generate droplet motion has remained challenging.[1691] This remote control would be particularly useful in "lab-on-a-chip" type applications where it could provide a gentle and cheap alternative to expensive microscopic pumps and strong electric fields.[1692]

Azobenzene containing calix[4]resorcinarene **161**, when deposited as a monolayer, provided the first example of remote control of surface energy and therefore droplet motion by irradiation.[1693] The monolayer initially consisted of all *cis* isomers. However, a droplet of olive oil has more favorable interactions with the extended *trans* form, where interactions with the alkyl chain of the calix[4]arene can be maximized. As such, when an asymmetric light source irradiated the droplet, forming more *trans*-calix[4]arene on one side of the droplet than the other, a surface energy gradient was created and the droplet moved away from the *trans* enriched area. This movement could be continued if the light source followed the rear edge of the droplet (Figure 68).

Photoresponsive control of droplet motion has also been achieved using a system based on bistable rotaxane **162**, adsorbed onto a gold surface using a thiol linker.[1245] Diiodomethane drops could be transported on a millimeter scale across a surface using the macrocycle of **162** to either hide or expose the fluoroalkane region of the rotaxane and thus modify surface energy. Using this strategy, a microliter droplet could be moved up a 12° incline. Roughly 50% of the absorbed photon energy was converted into gravitational potential energy of the drop (Figure 69).

The above examples of macroscopic control utilizing molecular motion underscore the potential importance of this concept for technological applications. Similar control of motion

DOI: 10.1021/acs.chemrev.5b00146
Chem. Rev. 2015, 115, 10081−10206

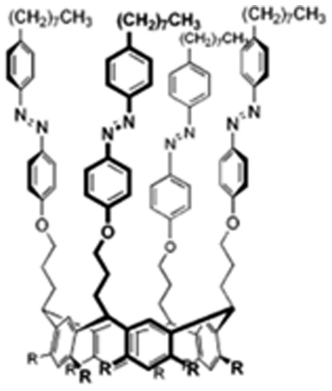

Figure 68. Calix[4]arene **161**, used to control surface wettability.[1693]

has been achieved with surfaces microscopically patterned with thermoresponsive polymers[1694−1696] and by amplifying the effect of the photochemical switching of a spiropyran-functionalized surface.[1697]

9. ARTIFICIAL BIOMOLECULAR MACHINES

9.1. Hybrid Biomolecular Systems

Biological systems make extensive use of motor proteins such as ATPase, kinesin, myosin, and dynein. These biological motors provide both examples of machines viable at the nanoscale and useful building blocks for the creation of hybrid systems. The availability of preformed nanoscale machines has greatly expedited the creation of complex nanotechnological systems. Although a thorough exploration of this topic is beyond the purview of this Review and has been covered elsewhere,[15,47,1364,1698−1702] a brief overview is useful. The initial purpose of these biohybrid experiments was to further probe the complex mechanisms by which biological machines operate. An early example was provided by Kinosita et al., who reported a series of experiments exploring the F_1-ATPase rotary motor.[1703−1707] They were able to observe the 360° rotation of the motor, powered by the hydrolysis of ATP, directly, via microscopy, for individual motors mounted on glass. Mechanical rotation has also been observed in an F_0F_1-ATPase, where the rotor domain is coupled to a proton transporting domain.[1708] Even more remarkably, ATP synthesis has been driven by rotating a magnetic bead attached to an F_1-ATPase with electromagnets.[1709] This is a stunning example of chemical synthesis driven by an external mechanical force. ATPase systems have been less exploited in recent years due to the difficulties in using them in synthetic systems.[1710] However, a recent example showed the insertion of ATP synthases into an artificial lipid microcapsule and their subsequent use to generate ATP inside the capsule.[1711]

Kinesin, myosin, and dynein systems have been much more extensively utilized.[1712−1722] They have been shown to transport cargos in artificial systems, although cargos must typically be large to outcompete diffusive forces.[1375,1723−1727] These biological walkers have been controlled by the design of appropriate tracks,[1728−1730] or by the application of external forces. Kinesin has been used to stretch a length of DNA,[1715] and to enable the detection of nanomolar concentrations of a targeted protein.[1731] Cross-linked actin and myosin gels were found to move over each other in the presence of ATP.[1732] Microtubule containing gels combined with kinesin and ATP have been shown to spontaneously generate autonomous motility.[1733,1734] As a further benefit to using biological motors, ATPase motors have been shown to operate at a near 100% efficiency,[1707,1735−1737] and kinesin at >50%,[1738] whereas in a typically used polymeric system where phase transitions are used to generate molecular level forces, an efficiency of 0.0001% was observed. The field of biomolecular electronics often uses molecular motion as a

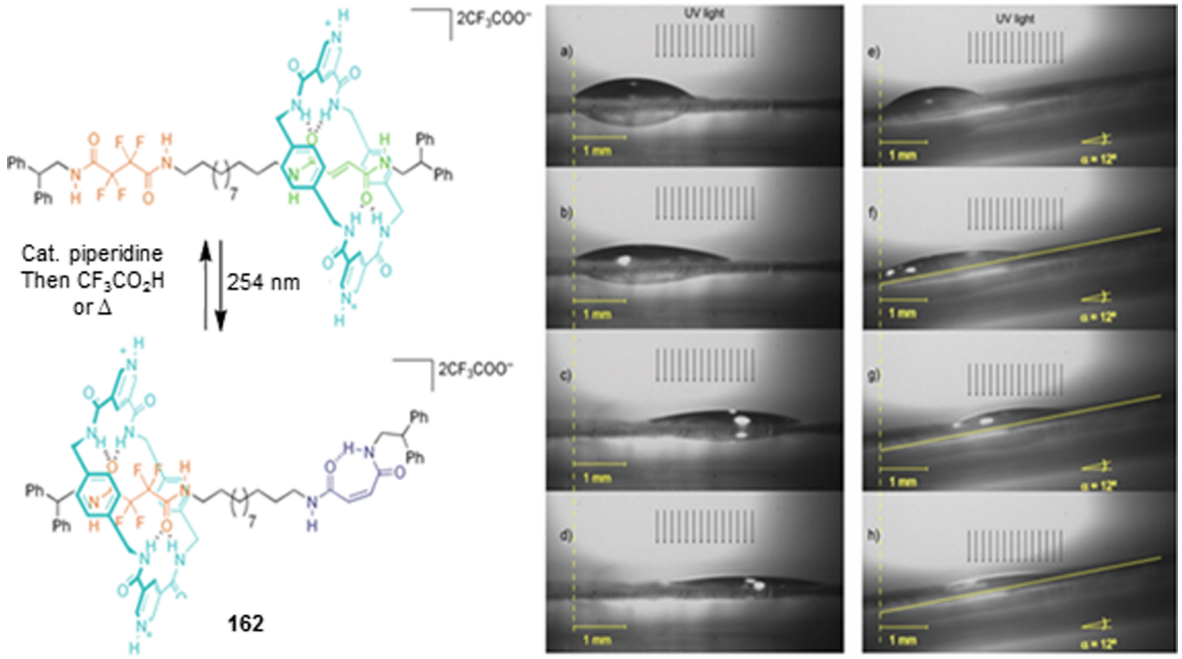

Figure 69. Light switchable rotaxane **162**, and transport of a microliter drop of CH_2I_2 across a flat surface (a−d) and up a 12° incline (e−h). Reprinted with permission from ref 1245. Copyright 2005 Nature Publishing Group.

DOI: 10.1021/acs.chemrev.5b00146
Chem. Rev. 2015, 115, 10081−10206

switching mechanism, particularly in systems utilizing photoactive proteins (be they native or engineered).[1739−1750]

9.2. Hybrid Membrane-Bound Machines

Ionophores and ion channels, both synthetic[1751−1755] and biological,[1756−1766] have been extensively explored and exploited. Biological ion channels have been inserted into artificial membranes and used to sequence single strands of DNA,[1756] to open the pore of a nonselective efflux channel,[406,1767,1768] and to effect the light-driven production of ATP by F_0F_1-ATPase.[1769] Feringa et al. reported the switching of the "mechanosensitive channel of large conductance' (MscL) of *E. coli*, which can be opened in response to the introduction of charged entities at a certain location in the protein channel.[406] Initially, a light-cleavable group was used to release acetate anions and thus open the channel, with a reversible version, utilizing a spiropyran switch, also reported (Scheme 50). Ion channel proteins

Scheme 50. (a) Irreversible Photocleavage of 163 Leading to Pore Opening; and (b) Reversible Photoswitching of 164, Leading to Pore Opening[a]

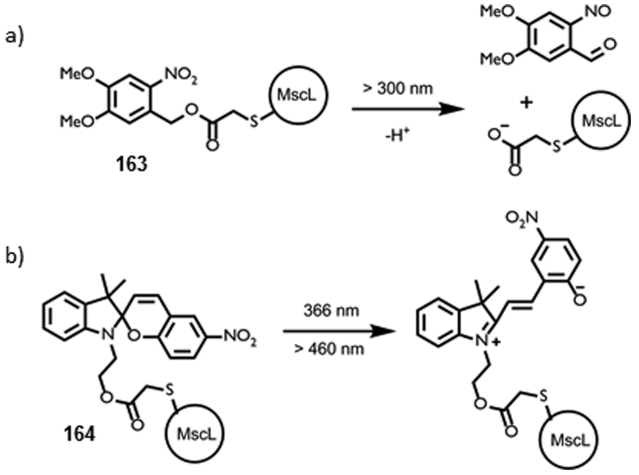

[a]MscL = mechanosensitive channel.[406]

modified postsynthetically to be light switchable have been inserted into living cells, and successfully opened and closed.[1770−1777] Unnatural, light switchable amino acids have also been incorporated into ion channel proteins.[400,1778−1780]

Active transport between aqueous phases across an organic phase,[1781−1783] and lipid bilayers,[1784] has been observed, driven by differing redox potentials in each aqueous phase. An electron donor−acceptor molecule has been directionally inserted into a lipid bilayer, which on irradiation created a redox potential gradient and ferried protons across the bilayer establishing a pH gradient. However, the quantum yield for the process was only 0.004.[1785] Calcium ions have been transported across a membrane in a similar system.[1786] Work to establish longer lived photoinduced charge separated states, which might lead to greater quantum yields and further applications, has continued.[627,1787−1807] Alternating currents have been induced in a protein-based photoelectrochemical cell by irradiation with intermittent light.[1808] An interesting recent example utilized the light-induced ring-opening of spiropyrans under ultraviolet light and their ring closure under visible light illumination. When a membrane doped with spiropyran **165** was illuminated with ultraviolet light on one side and visible light on the other, the differing proton affinities of ring-opened and ring-closed spiropyran led to proton shuttling across the membrane and the generation of an electric potential of ca. 210 mV and pH gradient of ca. 3.6 pH units (Figure 70).[1809]

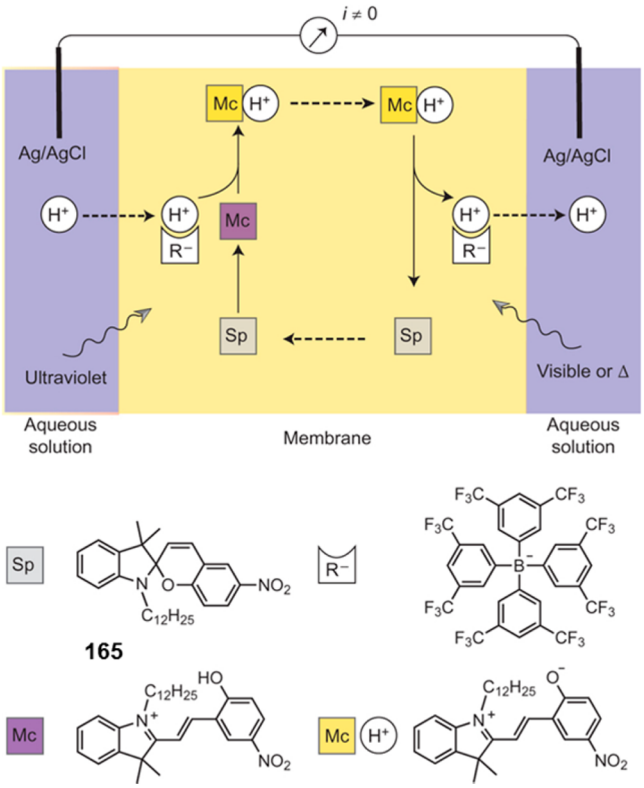

Figure 70. Proton gradient established by spiropyran (**165**) shuttling upon differential illumination of the two sides of a membrane. Reprinted with permission from ref 1809. Copyright 2014 Nature Publishing Group.

9.3. DNA-Based Motors and Switches

Biological building blocks have been used to design and create molecular machines by many research groups.[1810−1828] A large number of DNA-based molecular motors,[1829−1832] walkers,[1382,1833−1838] tweezers,[1839] gears,[1840] springs,[1841] robots,[1842,1843] transporters,[1844] and interlocked structures such as DNA rotaxanes and catenanes can be found in the literature.[1845−1850] All are built by self-assembly, exploiting the sequence-specific interactions that bind complementary oligonucleotides together to form double helix or triplex structures.[1851−1870] Beside base-pairing, other structural motifs can be formed and used in the design of molecular machines such as the pH-induced self-assembly of C-rich sequences into *i*-motif configurations,[1871,1872] the ion-induced self-organization of G-rich sequences into G-quadruplexes,[1873−1876] and the metal−ion bridging of duplex DNA by T−Hg^{2+}−T or C−Ag^{+}−C complexes.[1877,1878] Various fuels such as single-stranded oligonucleotide fragments, pH variation, metal ions, and light have been used to trigger these DNA devices.[1879−1884] These systems have been used in molecular sensing, drug delivery and other medical applications, the construction of logic gates, the control of chemical transformations, and for many other purposes.[1874,1885−1911]

DNA tweezers represent a simple class of DNA machines.[1884,1912] They are two-armed constructs bridged by a DNA linker that can undergo transitions between open and

DOI: 10.1021/acs.chemrev.5b00146
Chem. Rev. 2015, 115, 10081−10206

closed states in response to external triggers such as the addition of single-stranded DNA or metal ions, or a change in pH. Willner et al. reported a biomolecular logic gate based on three different DNA tweezers **A**, **B**, and **C**. These were activated by different inputs: protons, Hg^{2+} ions, and nucleic acid strands (Figure 71).

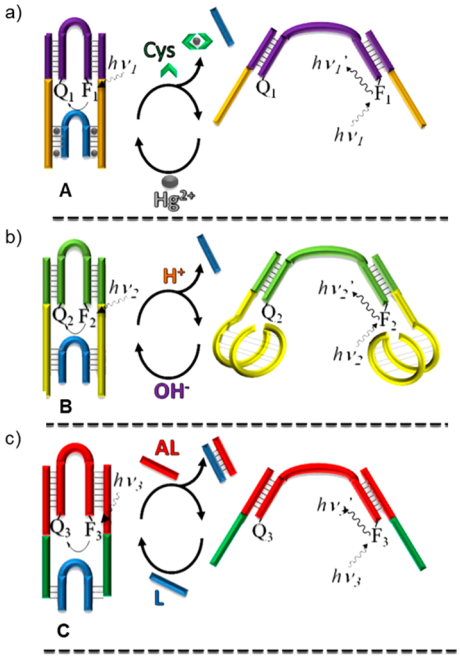

Figure 71. (a) Tweezer **A**: in the closed form the arms are bound to the linker unit (blue) by Hg^{2+} ions through T−Hg^{2+}−T bonds. To open the molecular tweezer, Hg^{2+} is sequestered by the addition of cysteine. (b) Tweezer **B**: in acid the arms form an *i*-motif, thus releasing the linker unit, whereas at pH = 7.2, the *i*-motif is destroyed resulting in the stabilization of the closed structure. (c) Tweezer **C**: the linker unit can be released by a complementary strand, the antilinker that opens the tweezers. Reprinted with permission from ref 1914. Copyright 2010 American National Academy of Sciences.

The output delivered by this machine depends both on the inputs provided and its initial internal state. Depending on the input, there are eight possible configurations of the three tweezers (open or closed for each). The output could be studied by measuring the Förster resonance energy transfer (FRET) between different pairs of fluorophore and quenching molecules attached to the arms of each of the three tweezers. The linker unit is common to all three tweezers, meaning that tweezers **A** and **B** can also be opened by the complementary antilinker. Thus, for any pair of tweezers, there are two different inputs that cause a change in the state of the device. In total, the device can adopt 16 different states and can furthermore be used as a memory storage system because each state and output is dependent not only on the most recent input but also on past states and inputs.[1913,1914]

DNA machines have been used to regulate enzyme cascade reactions.[1890,1891] Liu and co-workers reported a machine containing DNA double crossover (DX) motifs, which formed two rigid arms, joined by an immobile four-way junction (Figure 72).[1915] A DNA motor that could switch between stem-loop and double-helix structures, driven by a strand displacement reaction, was incorporated at the center of the machine to cycle between open and closed states. This design amplifies the small motion generated by the DNA motor into a much greater change in separation between the ends of the two arms where glucose oxidase (GOx) and horseradish peroxidase (HRP) were attached. In this biochemical cascade system, GOx first catalyzed the oxidation of glucose to generate gluconic acid and hydrogen peroxide. Hydrogen peroxide is catalytically reduced by HRP into H_2O. At the same time, HRP turns $ABTS^{2-}$ into $ABTS^{-}$, which allowed the kinetics of the peroxidase to be monitored. HRP has a much higher turnover rate then GOx, so the distance hydrogen peroxide must diffuse has a crucial influence on the rate of reaction. Therefore, when the two enzymes are attached to the two arms, the diffusion distance of hydrogen peroxide can be changed from 6 to 18 nm by operation of the DNA motor, regulating the rate of enzymatic reaction. Sequential addition of fuel and antifuel strands showed that this regulation was reversible.

Willner and co-workers have used catenated DNA machines as carriers of Au nanoparticles.[1916] Ordered assemblies of nanoparticles with defined geometries have recently attracted a great deal of interest as these engineered nanoparticle systems are anticipated to show unique plasmonic properties.[1917,1918] The synthesis and structural characterization of DNA catenanes has

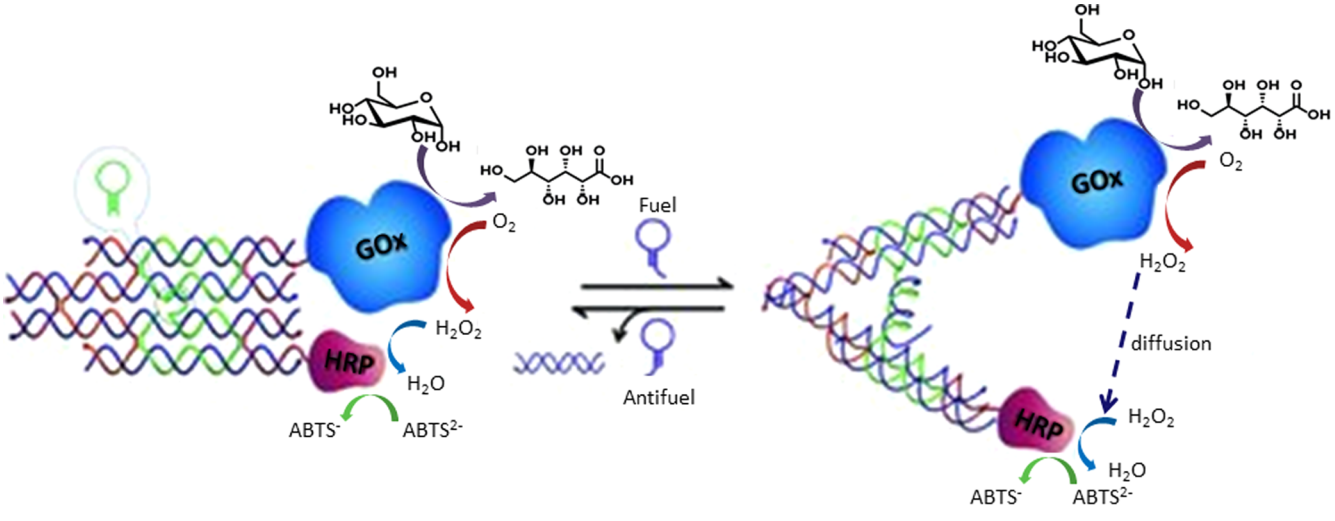

Figure 72. DNA machine reported by Liu and co-workers, which could be used to regulate an enzyme cascade reaction. Reprinted with permission from ref 1915. Copyright 2013 Wiley-VCH Verlag GmbH & Co. KGaA, Weinheim.

DOI: 10.1021/acs.chemrev.5b00146
Chem. Rev. 2015, 115, 10081−10206

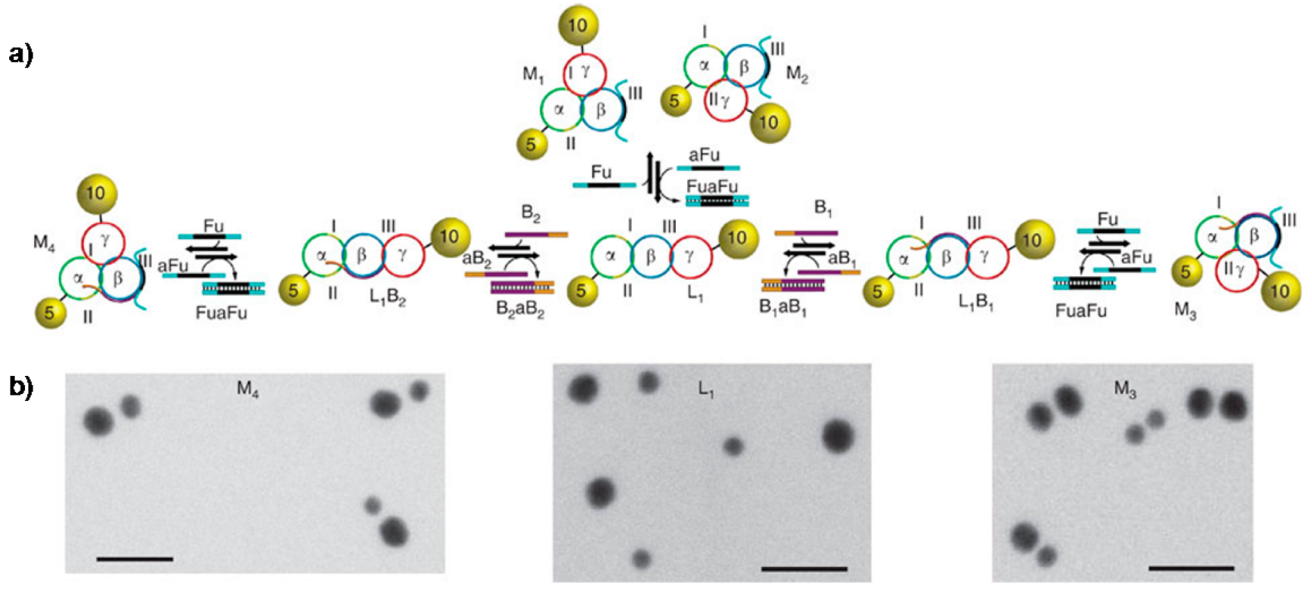

Figure 73. (a) Programmed migration of two Au nanoparticles. (b) STEM images corresponding to the different structures; the bar corresponds to 20 nm. Reprinted with permission from ref 1916. Copyright 2013 Nature Publishing Group.

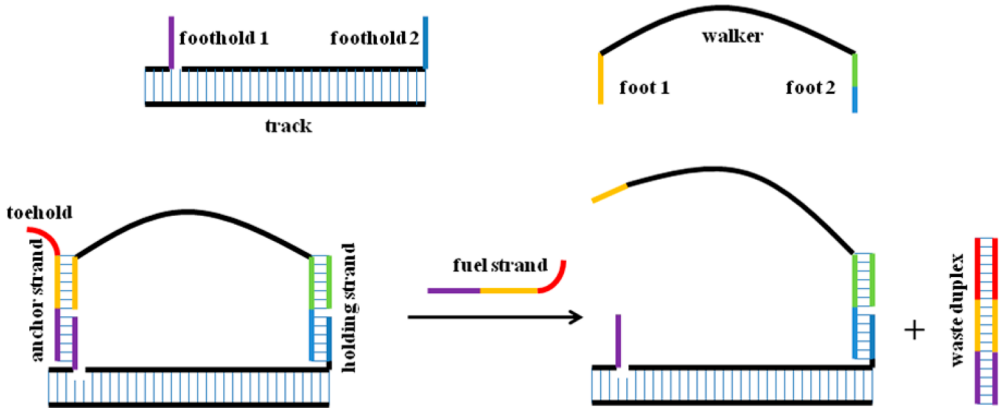

Figure 74. Schematic representation of a DNA-based walker and track system. Footholds protrude from the track as single-stranded DNA fragments. Anchor and holding strands enable the walker unit to bind to the footholds by hybridization. Areas with functional importance are labeled, and complementary strands are depicted in the same color for clarity.

been reported previously,[1847,1849,1919,1920] as has a three-station directional DNA catenane rotary motor.[1921] A three-ring catenated nanostructure has been used to program the assembly of two Au nanoparticles (of 5 and 10 nm diameter, Figure 73). One of the nanoparticles was attached to ring α and the other to ring γ (L_1). Ring α included two equivalent domains, I and II, which are complementary to domain III on ring γ. While the initial duplex between rings β and γ in region III is energetically favored, treatment of the linear catenated system L_1 with a fuel strand (Fu) displaces ring γ, which then translocates through hybridization to either site I or II of ring α (structures M_1 or M_2). In the presence of the appropriate blocker units (B), the directional translocation of ring γ proceeds below or above the central ring β to yield the configurations M_3 or M_4, respectively. The changes in proximity of the nanoparticles led to changes in plasmonic coupling, which was theoretically modeled. Such systems could have uses in nanomedicine and intracellular diagnostics.[1916]

9.4. DNA Walkers

The controlled and predictable strand displacement of DNA and RNA has been used to construct complex devices.[1369,1869,1922−1932] Among them, walkers represent a major subclass. The basic principle behind 1-D walking is illustrated in Figure 74. A relatively rigid and stable DNA track functionalized with protruding single-stranded anchorage points (footholds) is typically used.[1369,1933] Unlike the direct interactions of biological walker proteins with polymeric tracks, the footholds are attached to the track and bind the walker unit by base paring. The walker unit consists of regions with different nucleotide sequences (feet), which are attached to the track via another DNA fragment (the anchor strand), that can hybridize with both the walker and one of the footholds leaving a "toehold region" unpaired. Addition of the fuel strand results in base-pairing with an anchor strand, starting from the protruding toehold, and forms a more thermodynamically favored waste duplex. The removal of the anchor strand liberates the foothold and one foot of the walker. Walking is processive because the other foot is still attached to the track by a holding strand, which provides additional

DOI: 10.1021/acs.chemrev.5b00146
Chem. Rev. 2015, 115, 10081−10206

stabilization. The walker can be reattached to the track via the addition of another anchor strand.

Stimuli-dependent positional DNA switches[1934,1935] and DNA-based devices performing multistep organic synthesis while migrating along a track have been reported.[1447] An in silico "tumbleweed" walker design has also been proposed.[1936] The first DNA-based walker was nonautonomous and bipedal and was reported by Sherman and Seeman.[1834] High dilution conditions were used to prevent the walker from scrambling betwen different tracks. Sequential addition of two different anchor and fuel strands in an aqueous buffer at 16 °C led to the desired walking motion being obtained. The products were characterized by polyacrylamide gel electrophoresis (PAGE). The energy required for directional walking was provided by the additional base-pairing in the waste duplex (red toehold region, Figure 74). Mechanistically, this walker is an inchworm walker because the leading foot remains the same throughout the operation. A hand-over-hand DNA walker (the mechanism of operation of kinesin) has been published by Shin and Pierce who used a similar design.[1833] Transport of a cargo over a DNA origami tile and the synthesis of nanoparticle sequences have been reported. It used a DNA origami walker unit with four "feet" for controlled movement, and three "arms" for picking up cargo, each consisting of single strands of DNA (Figures 75 and 76).[1455,1937,1938] Fuel strands (F_i) were used to drive the motion and to remove the anchor strands (A_i). Each station was loaded with a distinct gold nanoparticle cargo and could be switched between states where cargo delivery was possible and where it was not. By manipulating the selective release of each foot from complementary strands of DNA on the DNA tile, the movement of the walker could be controlled. When coupled to the ability of the stations to be switched "on" or "off", this allowed the formation of eight, differently composed, noncovalently bound products from the full operational sequence. This remarkable level of control on the nanoscale shows that the forces of Brownian motion can be exploited to great effect in the synthesis of complex supramolecular products. Transportation of a DNA cargo on a DNA origami tile over 16 consecutive steps has also been reported.[1939]

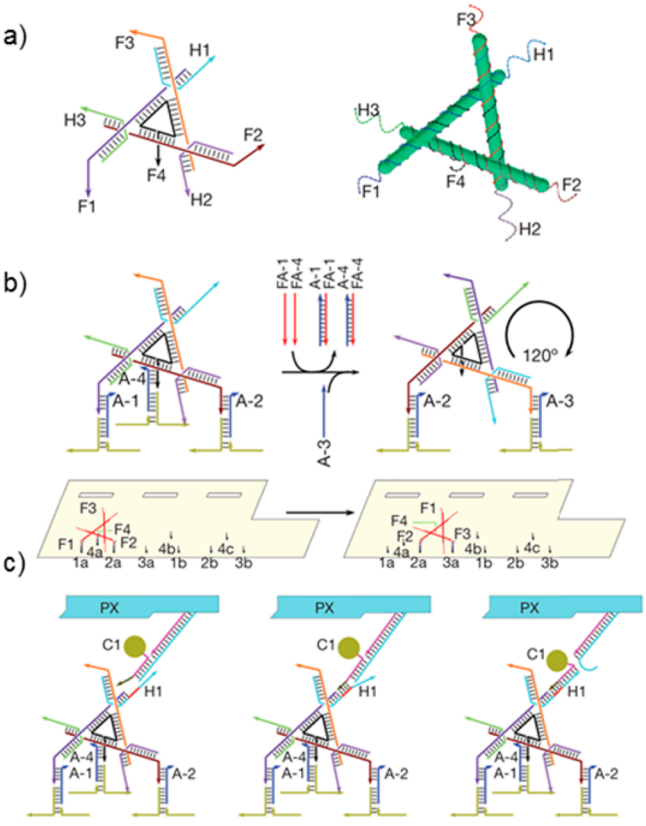

Figure 75. (a) Structure of the DNA walker with four "feet" (F1−4) and three "hands" (H1−3). (b) Movement of walker across the DNA origami tile driven by sequentially added DNA "fuel" strands labeled FA. (c) Loading of cargo onto DNA walker. Reprinted with permission from ref 1455. Copyright 2010 Nature Publishing Group.

Turberfield, Reif, and Yan have reported autonomous walking in a DNA-based system.[1379] Three enzymes, the PfIM I and BstAP I restriction enzymes, and T4 ligase, were required for autonomous operation. Successive cleavage and ligation of the walker-foothold duplex resulted in directional walking along the track. Two autonomous burnt-bridges walkers have been reported using either a restriction endonuclease as an additive[1940] or a walker unit with intrinsic DNAzyme activity.[1380,1941,1942] An autonomous DNA motor whose propulsion was driven by random polymerization has been synthesized.[1829] DNA strands were propeled at the growing end of the polymer by the energy gained from hybridization. A number of enzyme-free autonomous DNA walkers have since been published.[1836,1943−1945] Autonomous multipedal walkers[1842,1946] and walkers performing autonomous and progressive acylation reactions have been disclosed.[1447] Autonomous DNA walkers that are driven by pyrene-mediated photocleavage of disulfide bonds,[1947] or photoisomerization-dependent hindrance/exposure of a complementary strand,[1383] have been designed.

A vital requirement for useful cargo transport is the ability to choose the correct path at a junction point. The walker should be capable of crossing the junction, and the path choice should be programmable. Turberfield et al. were able to autonomously regulate the transport of a DNA cargo on a branched track (Figure 77).[1843] Successive Holliday junctions formed between the selected fuel, foothold, and the cargo as the walker migrated. These led to strand exchange (equivalent to junction migration), followed by loop opening, which allowed the controlled migration of the cargo from one foothold to another. The same group have since used a single nucleoside, adenosine, to control the route taken at the track junction.[1381]

10. CONCLUSION AND OUTLOOK

Perhaps the best way to appreciate the technological potential of controlled molecular-level motion is to recognize that molecular machines lie at the heart of every significant biological process. Over billions of years of evolution, nature has not repeatedly chosen this solution for achieving complex task performance without good reason. In stark contrast to biology, none of mankind's fantastic myriad of present-day technologies exploit controlled molecular-level motion in any way at all: every catalyst, every material, every polymer, every pharmaceutical, and every reagent all function through their static or equilibrium dynamic properties. When we learn how to build artificial structures that can control and exploit molecular-level motion, and interface their effects directly with other molecular-level substructures and the outside world, it will potentially impact on every aspect of functional molecule and materials design. An improved understanding of physics and biology will surely follow.

DOI: 10.1021/acs.chemrev.5b00146
Chem. Rev. 2015, 115, 10081−10206

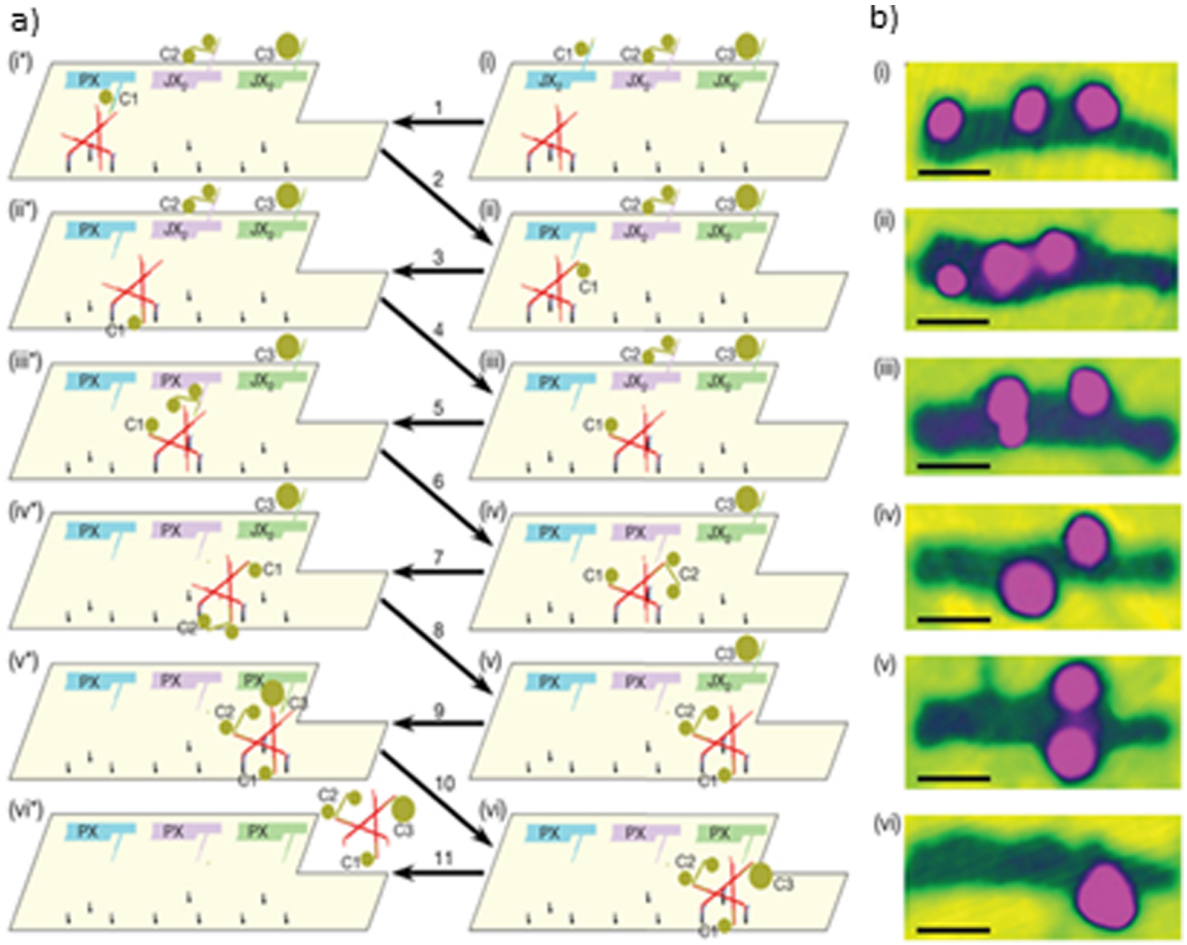

Figure 76. (a) Operation of DNA-based walker. (b) AFM images of walker. Reprinted with permission from ref 1455. Copyright 2010 Nature Publishing Group.

As indicated by the many examples that appear in this Review, the future for the field of artificial molecular machines is very bright.[1948] After a somewhat difficult period in the 1990s, when chemists struggled to understand the basic differences between machines at the macroscopic and nanometer length scales, scientists now have the know-how and synthetic tools available to enable them to make suitable machine architectures (e.g., catenanes, rotaxanes, overcrowded alkenes, molecules that walk upon tracks, etc.). They can switch the position of components (often by clever manipulation of noncovalent interactions between the various parts), they understand how to use ratchet mechanisms to create motor-mechanisms, and they are learning how to introduce them into more complex molecular machine systems.

Yet there are still several basic challenges to overcome for molecular machines to be able to fulfill their potential:

(i) In contrast to motor proteins, powered by ATP hydrolysis or proton gradients, there are as yet no chemically driven synthetic small-molecule motors that can operate autonomously (i.e., move or rotate directionally as long as a chemical fuel is present), the closest counter-examples being the Feringa overcrowded alkene motors that rotate continuously under irradiation with light.[429−453]

(ii) Most of the synthetic molecular machines reported to date are based on only a single functioning part that moves, stops, fluoresces, catalyzes a reaction, etc. To perform tasks that cannot be accomplished by conventional chemical means, it will be necessary to design systems with multiple integrated parts, each component performing a dedicated role within the machine ensemble. This will not be straightforward because unlike a watch where the second hand, say, does not interfere with the components in the escapement mechanism, the components of a chemical machine are not easily isolated from each other (or the environment) and interference from one reactive part of a machine with another will be a significant issue as complexity increases beyond the current rather trivial systems.

(iii) The machines we are familiar with in the macroscopic world are generally stable, operating unchanged through many cycles, and by and large they do not make "mistakes". This contrasts with those in the biological world where the stochastic nature of molecular dynamics mean that motors stall, or step backward, or detach from tracks, or make errors in synthesis that are spotted or corrected by other machines. These are intrinsic differences that require fundamentally different philosophies in terms of the way machines carry out tasks that chemists have not yet started to tackle.

(iv) The "reading" of a sequence of functional groups on a polymer stand (mRNA or DNA) is how biological molecular machines are programmed to carry out synthesis operations in the correct sequence. Although it is possible to use biological polymers to do this, molecular machines made from DNA are obviously far more limited in terms of operating conditions, chemical stability, and functionality than wholly synthetic systems. As yet there is no small-molecule "Turing machine",[1949]

DOI: 10.1021/acs.chemrev.5b00146
Chem. Rev. 2015, 115, 10081−10206

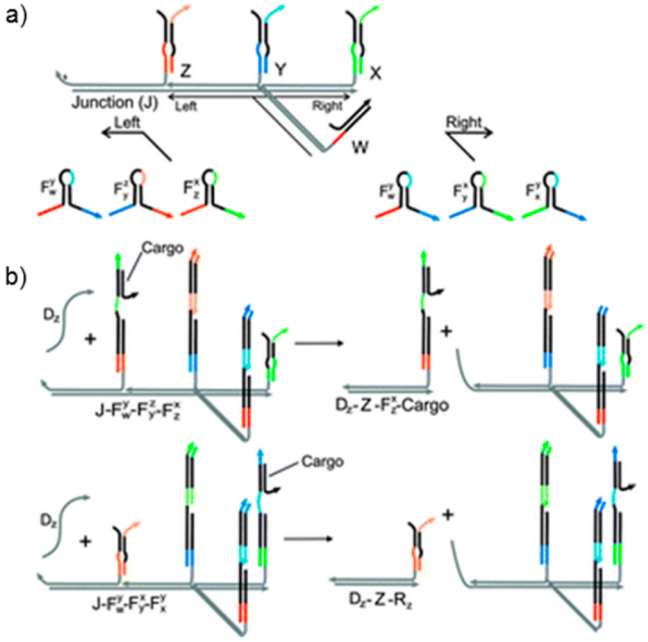

Figure 77. Walker with a choice of path at a junction. (a) Initially cargo resides on position W, and (b) the use of different set of fuels (F) leads to transport of cargo to either position. A displacing strand (Dz) was used for the fragmentation of the molecular ensemble and subsequent analysis of the cargo position. Reprinted with permission from ref 1843. Copyright 2011 American Chemical Society.

that is, a molecular machine that can read information from a symbol-encoded molecular strand. Programming of small-molecule machines with an information-rich non-DNA strand (rather than the sequential addition of chemical stimuli, say) would be a game-changing development.

There are also issues on which protagonists in the field have differing points-of-view. The debate continues over whether it will ultimately prove more productive to build molecular machines based on macroscopic objects (e.g., Stoddart's "molecular elevator"[730] and "molecular pistons"[527] and Tour's "nanocars",[1129−1132] etc.) or based on biological machines (e.g., artificial systems that seek to reproduce aspects of the behavior of kinesin[1398−1400] or the ribosome[666]). Certainly mimicking biology is not the only way to achieve complex functionality: computer chips are manufactured from silicon wafers rather than being wet and carbon-based like our brains. Yet equally machines have to be designed according to the environment they are intended to operate in, and there may be reasons why biology uses motors and not switches, and tracks and not wheels, to transport molecular cargoes. Or it may be that evolution just did not discover these solutions to such problems and that mankind, with the whole of the periodic table and known synthetic chemistry to work with, can. Perhaps the most productive approach will ultimately be found by following neither of these lines of investigation too closely, for example, by using chemical principles for "molecular robotics" in which ratcheted motions of molecular components (i.e., biologically inspired mechanisms) are used to perform tasks that have their origins in innovations introduced to advance developments in macroscopic technology (e.g., factory assembly lines).

The environments that molecular machines can most productively operate in also remain an open question. Efforts to incorporate molecular machines into regular arrays within crystalline solids (e.g., MOFs) are progressing apace and should allow tethered molecular machines to interact effectively with solution- or gas-phase substrates. It will be interesting to see what applications such systems are being tailored for. Molecular machines mounted on surfaces should allow for surface properties to be changed in a facile and effective manner using a minimal amount of the high-cost molecular structures. However, whether monolayers of molecular machines can be sufficiently robust will no doubt be an issue for practical applications. Most biological molecular machines operate while dissolved in solution, a situation that has no equivalent for macroscopic mechanical machines, and so chemists will have to consider carefully how to effectively address and utilize such machines in that environment. Molecular machines have the potential to act productively under each of these conditions; what is important is that the application is appropriate for which to use synthetic molecular machines. In most cases, the cost of synthesis will mean that this will only be the case if there is no way to carry out the task without using a molecular machine. So rotaxane-based "molecular muscles" have to compete with shape-memory polymers (or even stilbene-containing polymers) to be effective, and rotaxane-based switches, which work through the physical displacement of submolecular components, will have to compete with electron movements in silicon for applications. Chemical synthesis is one area where artificial molecular machines may one day be able to perform tasks that are not possible to achieve using conventional chemical methods, a potential "killer app"!

A quarter-of-a-century after chemists made the first fledging molecular protomachines, the tantalizing prospect of artificial molecular machines that can perform useful tasks is moving ever closer to becoming a reality. Molecular machines with multiple integrated parts are in design terms a fusion of the familiar with the strange. Examples of mechanical engineering from the world around us provide a conceptual framework for what we want tiny machines to achieve. Biology shows us how machines cope with the nature of the environment in performing tasks at nanometer length scales, and physics explains the often counterintuitive ways that such small objects must behave. Yet ultimately, while drawing on all of these disciplines for ideas, guidance, and inspiration, such machines have to be designed, built, and operated through chemistry, the central science.

ASSOCIATED CONTENT

Special Issue Paper

This paper is an additional review for *Chem. Rev.* **2015**, *115*, 15, "Supramolecular Chemistry".

AUTHOR INFORMATION

Corresponding Author

*E-mail: david.leigh@manchester.ac.uk.

Notes

The authors declare no competing financial interest.

DOI: 10.1021/acs.chemrev.5b00146
Chem. Rev. 2015, 115, 10081−10206

Biographies

Sündüs Erbaş Çakmak obtained her B.Sc. degree in Molecular Biology and Genetics in 2007 from Boğaziçi University in Istanbul, Turkey. She carried out her Ph.D. degree (2013) in Materials Science and Nanotechnology at the National Nanotechnology Institute, Bilkent University, under the supervision of Prof. Engin U. Akkaya, investigating concatenation and the use of molecular logic gates for the activity modulation of photodynamic therapy agents. She worked under the supervision of Amar H. Flood in Indiana University for 6 months during her Ph.D. working on the development of fluorescent anion sensors. In 2013 she joined Prof. David A. Leigh's group as a Marie-Curie Intra-European Post-Doctoral Fellow. Her research interests include artificial molecular machines, supramolecular catalysis, and molecular computing.

David Leigh was born in Birmingham (UK) and obtained his B.Sc. and Ph.D. degrees from the University of Sheffield. After postdoctoral research in Ottawa (1987−1989), he was appointed to a Lectureship at the University of Manchester Institute of Science and Technology (UK). After spells at the Universities of Warwick and Edinburgh, he returned to Manchester in 2012, where he currently holds the Sir Samuel Hall Chair of Chemistry. Prizes and awards for his group's research contributions include the 2007 International Izatt-Christensen Award for Macrocyclic Chemistry, 2007 Feynman Prize for Nanotechnology, 2007 EU Descartes Prize for Research, 2009 RSC Merck Award, 2010 RSC Tilden Prize, 2013 Royal Society Bakerian Lecture and Prize, and the 2014 RSC Pedler Prize. In 2009 he was elected to the Fellowship of the Royal Society (London). His research interests include the design, synthesis, and operation of artificial molecular-level motors and machines.

Charlie Thomas McTernan was born in London and obtained his M.Chem. from the University of Oxford. His Part II project was conducted under the supervison of Prof. Tim Donohoe, investigating the synthesis of isoquinoline motifs using palladium-catalyzed α-arylation. He joined David Leigh's group in 2013, funded by a University of Manchester Dean's Faculty Award. His research interests include the synthesis of artificial molecular machines, switchable catalysts, and rotaxanes.

Alina Laura Nussbaumer was born in Bern (Switzerland) and obtained her B.Sc. and M.Sc. degrees from the University of Bern. She completed her Ph.D. under the supervision of Prof. Robert Häner at the same University, investigating DNA as a scaffold for chromophore assembly toward the development of novel DNA-based materials and the production of supramolecular polymers based on DNA-conjugates that show strong amplification of chirality. In 2012, she joined David Leigh's group as a Swiss National Science Foundation Post-Doctoral Fellow. Her research interests include controlled molecular motion and the development of new synthetic tactics toward topologically complex molecules.

ACKNOWLEDGMENTS

We thank the ERC and EPSRC for financial support and the European Union Seventh Framework Marie Curie Intra-European Fellowship Program and the Swiss National Science Foundation for Postdoctoral Fellowships (to S.E.-C. and A.L.N., respectively).

ABBREVIATIONS

AB	azobenzene
ABTS	2,2′-azino-bis(3-ethylbenzothiazoline-6-sulfonic acid)
AFM	atomic force microscope
ATP	adenosine triphosphate

DOI: 10.1021/acs.chemrev.5b00146
Chem. Rev. 2015, 115, 10081−10206

BODIPY	boron-dipyrromethene
Bpy	bipyridine
CB	cucurbituril
CBPQT	cyclobis(paraquat-*p*-phenylene)
CBS	Corey−Bakshi−Shibata
CD	circular dichroism or cyclodextrin
CuAAC	copper-catalyzed azide−alkyne cycloaddition
Cys	cysteine
D	displacing strand
DAE	diarylethene
DBU	1,8-diazabicycloundec-7-ene
DMAP	4-dimethylaminopyridine
DMF	dimethylformamide
DMSO	dimethyl sulfoxide
DNA	DNA
DNP	dioxynaphtalene
DTT	dithiothreitol
ee	enantiomeric excess
ESIPT	excited-state intramolecular proton transfer
EXSY	exchange spectroscopy
F	fuel strand
FRET	Förster resonance energy transfer
GOx	glucose oxidase
GSCC	ground-state coconformation
HBT	2-(2-hydroxyphenyl)-benzothiazole
HOMO	highest occupied molecular orbital
HPLC	high-performance liquid chromatography
HRP	horseradish peroxidase
iPr$_2$NEt	*N*,*N*-diisopropylethylamine
IR	infrared
LB	Langmuir−Blodgett
LUMO	lowest unoccupied molecular orbital
MOF	metal organic framework
Mc	merocyanine
MS	mass spectrometry
MSCC	metastable state coconformation
MscL	large-conductance mechanosensitive channel
MSTJ	molecular switch tunnel junction
MV	methyl viologen
NCL	native chemical ligation
NMR	nuclear magnetic resonance
XPS	X-ray photoelectron spectroscopy
PAGE	polyacrylamide gel electrophoresis
PEO	poly(ethylene oxide)
PLP	pyridoxal 5′-phosphate
PMB	*p*-methoxybenzyl
PMMA	poly(methyl methacrylate)
R	Reynolds number
RET	resonance energy transfer
RNA	ribonucleic acid
SAM	self-assembled monolayer
SEM	scanning electron microscope
Sp	spiropyran
STM	scanning tunneling microscope
T	temperature
TBDMSCl	*tert*-butyldimethylsilyl chloride
TCBD	tetracyanobutadiene
TFA	trifluoroacetic acid
TNF	2,4,7-trinitro-9-fluorenone
TON	turnover number
TTF	tetrathiafulvalene
UV	ultraviolet

REFERENCES

(1) Brown, R. A Brief Account of Microscopical Observations Made on the Particles Contained in the Pollen of Plants. *Philos. Mag.* **1828**, *4*, 171−173.
(2) Brown, R. On the Particles Contained in the Pollen of Plants; and on the General Existence of Active Molecules in Organic and Inorganic Bodies. *Edinb. New Philos. J.* **1828**, *5*, 358−371.
(3) Perrin, J. In *Atoms* (English Translation), 2nd ed.; Hammick, D. L., Ed.; Constable and Co.: London, 1923.
(4) Einstein, A. Über die von der Molekularkinetischen Theorie der Wärme Geforderte Bewegung von in Ruhenden Flüssigkeiten Suspendierten Teilchen. *Ann. Phys.* **1905**, *17*, 549−560.
(5) Feynman, R. P.; Leighton, R. B.; Sands, M. *The Feynman Lectures on Physics*; Addison-Wesley: Reading, MA, 1963; Vol. *1*, Chapter 46.
(6) Smalley, R. E.; Drexler, K. E. Nanotechnology. *Chem. Eng. News* **2003**, *81*, 37−42.
(7) Balzani, V.; Credi, A.; Raymo, F. M.; Stoddart, J. F. Artificial Molecular Machines. *Angew. Chem., Int. Ed.* **2000**, *39*, 3348−3391.
(8) Credi, A. Artificial Molecular Motors Powered by Light. *Aust. J. Chem.* **2006**, *59*, 157−169.
(9) Paxton, W. F.; Sundararajan, S.; Mallouk, T. E.; Sen, A. Chemical Locomotion. *Angew. Chem., Int. Ed.* **2006**, *45*, 5420−5429.
(10) Tian, H.; Wang, Q.-C. Recent Progress on Switchable Rotaxanes. *Chem. Soc. Rev.* **2006**, *35*, 361−374.
(11) Leigh, D.; Pérez, E. Dynamic Chirality: Molecular Shuttles and Motors. In *Supramolecular Chirality*; Crego-Calama, M., Reinhoudt, D., Eds.; Springer: Berlin, Heidelberg, 2006; Vol. *265*, pp 185−208.
(12) Hess, H. Self-assembly Driven by Molecular Motors. *Soft Matter* **2006**, *2*, 669−677.
(13) Browne, W. R.; Feringa, B. L. Making Molecular Machines Work. *Nat. Nanotechnol.* **2006**, *1*, 25−35.
(14) Kay, E. R.; Leigh, D. A.; Zerbetto, F. Synthetic Molecular Motors and Mechanical Machines. *Angew. Chem., Int. Ed.* **2007**, *46*, 72−191.
(15) Balzani, V.; Credi, A.; Venturi, M. Molecular Machines Working on Surfaces and at Interfaces. *ChemPhysChem* **2008**, *9*, 202−220.
(16) Ma, X.; Tian, H. Bright Functional Rotaxanes. *Chem. Soc. Rev.* **2010**, *39*, 70−80.
(17) Wang, J.; Manesh, K. M. Motion Control at the Nanoscale. *Small* **2010**, *6*, 338−345.
(18) Coskun, A.; Banaszak, M.; Astumian, R. D.; Stoddart, J. F.; Grzybowski, B. A. Great Expectations: Can Artificial Molecular Machines Deliver on Their Promise? *Chem. Soc. Rev.* **2012**, *41*, 19−30.
(19) Yang, W.; Li, Y.; Liu, H.; Chi, L.; Li, Y. Design and Assembly of Rotaxane-Based Molecular Switches and Machines. *Small* **2012**, *8*, 504−516.
(20) Neal, E. A.; Goldup, S. M. Chemical Consequences of Mechanical Bonding in Catenanes and Rotaxanes: Isomerism, Modification, Catalysis and Molecular Machines for Synthesis. *Chem. Commun.* **2014**, *50*, 5128−5142.
(21) van Dongen, S. F. M.; Cantekin, S.; Elemans, J. A. A. W.; Rowan, A. E.; Nolte, R. J. M. Functional Interlocked Systems. *Chem. Soc. Rev.* **2014**, *43*, 99−122.
(22) Zhang, M. M.; Yan, X. Z.; Huang, F. H.; Niu, Z. B.; Gibson, H. W. Stimuli-Responsive Host-Guest Systems Based on the Recognition of Cryptands by Organic Guests. *Acc. Chem. Res.* **2014**, *47*, 1995−2005.
(23) Xue, M.; Yang, Y.; Chi, X. D.; Zhang, Z. B.; Huang, F. H. New Class of Macrocycles for Supramolecular Chemistry. *Acc. Chem. Res.* **2012**, *45*, 1294−1308.
(24) Gil-Ramirez, G.; Leigh, D. A.; Stephens, A. J. Catenanes Fifty Years of Molecular Links. *Angew. Chem., Int. Ed.* **2015**, *54*, 6110−6150.
(25) Colinvaux, P. Life at Low Reynolds-Number. *Nature* **1979**, *277*, 353−354.
(26) Purcell, E. M. Life at Low Reynolds-Number. *Am. J. Phys.* **1977**, *45*, 3−11.
(27) Shenker, O. R. Maxwell's Demon 2: Entropy, Classical and Quantum Information, Computing. *Stud. Hist. Philos. M. P.* **2004**, *35B*, 537−540.
(28) Maxwell, J. C. *Theory of Heat*; Longmans, Green and Co.: London, 1871; Chapter 22.

DOI: 10.1021/acs.chemrev.5b00146
Chem. Rev. 2015, 115, 10081−10206

(29) Smoluchowski, M. S. On Opalescence of Gases in the Critical State. *Philos. Mag.* **1912**, *23*, 165−173.
(30) Feynman, R. P.; Vernon, F. L. The Theory of a General Quantum System Interacting with a Linear Dissipative System. *Ann. Phys.* **1963**, *24*, 118−173.
(31) Ehrenberg, W. Maxwell's Demon. *Sci. Am.* **1967**, *217*, 103−110.
(32) For the first private written discussion of the "temperature demon", see: Maxwell, J. C. *Letter to P. G. Tait, 11 December 1867; quoted in C. G. Knott, Life and Scientific Work of Peter Guthrie Tait*; Cambridge University Press: London, 1911; p 213; and reproduced in: *The Scientific Letters and Papers of James Clerk Maxwell 1862*; Harman, P. M., Ed.; Cambridge University Press: Cambridge, 1995; Vol. *II*, p 331.
(33) Szilard, L. On the Minimization of Entropy in a Thermodynamic System with Interferences of Intelligent Beings. *Eur. Phys. J. A* **1929**, *53*, 840−856.
(34) Bennett, C. The Thermodynamics of Computation—A Review. *Int. J. Theor. Phys.* **1982**, *21*, 905−940.
(35) Landauer, R. Irreversibility and Heat Generation in the Computing Process. *IBM J. Res. Dev.* **1961**, *5*, 183−191.
(36) Berut, A.; Arakelyan, A.; Petrosyan, A.; Ciliberto, S.; Dillenschneider, R.; Lutz, E. Experimental Verification of Landauer's Principle Linking Information and Thermodynamics. *Nature* **2012**, *483*, 187−189.
(37) The idea of a "pressure demon" was introduced by Maxwell in a later letter to Tait (believed to date from early 1875); quoted in: Knott, C. G. *Life and Scientific Work of Peter Guthrie Tait*; Cambridge University Press: London, Cambridge, 1911; p 214; and reproduced in: *The Scientific Letters and Papers of James Clerk Maxwell 1874*; Harman, P. M., Ed.; Cambridge University Press: London, Cambridge, 2002; Vol. *III*, p 185.
(38) Zheng, J. Z.; Zheng, X.; Zhao, Y.; Xie, Y.; Yam, C. Y.; Chen, G. H.; Jiang, Q.; Chwang, A. T. Maxwell's Demon and Smoluchowski's Trap Door (vol 75, art no 041109, 2007). *Phys. Rev. E* **2007**, *75*, 041109.
(39) Skordos, P. A.; Zurek, W. H. Maxwell's Demon, Rectifiers, and the Second Law: Computer Simulation of Smoluchowski's Trapdoor. *Am. J. Phys.* **1992**, *60*, 876−882.
(40) Parrondo, J. M. R.; Espanol, P. Criticism of Feynman's Analysis of the Ratchet as an Engine. *Am. J. Phys.* **1996**, *64*, 1125−1130.
(41) Sakaguchi, H. A Langevin Simulation for the Feynman Ratchet Model. *J. Phys. Soc. Jpn.* **1998**, *67*, 709−712.
(42) Hondou, T.; Takagi, F. Irreversible Operation in a Stalled State of Feynman's Ratchet. *J. Phys. Soc. Jpn.* **1998**, *67*, 2974−2976.
(43) Magnasco, M. O.; Stolovitzky, G. Feynman's Ratchet and Pawl. *J. Stat. Phys.* **1998**, *93*, 615−632.
(44) Jarzynski, C.; Mazonka, O. Feynman's Ratchet and Pawl: An Exactly Solvable Model. *Phys. Rev. E: Stat. Phys., Plasmas, Fluids, Relat. Interdiscip. Top.* **1999**, *59*, 6448−6459.
(45) Jahn, R.; Fasshauer, D. Molecular Machines Governing Exocytosis of Synaptic Vesicles. *Nature* **2012**, *490*, 201−207.
(46) Piccolino, M. Biological Machines: From Mills to Molecules. *Nat. Rev. Mol. Cell Biol.* **2000**, *1*, 149−153.
(47) Kinbara, K.; Aida, T. Toward Intelligent Molecular Machines: Directed Motions of Biological and Artificial Molecules and Assemblies. *Chem. Rev.* **2005**, *105*, 1377−1400.
(48) Pomorski, T.; Hrafnsdóttir, S.; Devaux, P. F.; Meer, G. V. Lipid Distribution and Transport Across Cellular Membranes. *Semin. Cell Dev. Biol.* **2001**, *12*, 139−148.
(49) Haydon, D. A.; Hladky, S. B. Ion Transport Across Thin Lipid Membranes: A Critical Discussion of Mechanisms in Selected Systems. *Q. Rev. Biophys.* **1972**, *5*, 187−282.
(50) Whittam, R.; Wheeler, K. P. Transport Across Cell Membranes. *Annu. Rev. Physiol.* **1970**, *32*, 21−60.
(51) Gouaux, E.; MacKinnon, R. Principles of Selective Ion Transport in Channels and Pumps. *Science* **2005**, *310*, 1461−1465.
(52) Jorgensen, P. L.; Hakansson, K. O.; Karlish, S. J. D. Structure and Mechanism of Na,K-ATPase: Functional Sites and Their Interactions. *Annu. Rev. Physiol.* **2003**, *65*, 817−849.
(53) Hayashi, S.; Ueno, H.; Shaikh, A. R.; Umemura, M.; Kamiya, M.; Ito, Y.; Ikeguchi, M.; Komoriya, Y.; Iino, R.; Noji, H. Molecular Mechanism of ATP Hydrolysis in F_1-ATPase Revealed by Molecular Simulations and Single-Molecule Observations. *J. Am. Chem. Soc.* **2012**, *134*, 8447−8454.
(54) Nakanishi-Matsui, M.; Sekiya, M.; Nakamoto, R. K.; Futai, M. The Mechanism of Rotating Proton Pumping ATPases. *Biochim. Biophys. Acta, Bioenerg.* **2010**, *1797*, 1343−1352.
(55) von Ballmoos, C.; Wiedenmann, A.; Dimroth, P. Essentials for ATP Synthesis by F_1F_0 ATP Synthases. *Annu. Rev. Biochem.* **2009**, *78*, 649−672.
(56) Nyblom, M.; Poulsen, H.; Gourdon, P.; Reinhard, L.; Andersson, M.; Lindahl, E.; Fedosova, N.; Nissen, P. Crystal Structure of Na^+, K^+-ATPase in the Na^+-Bound State. *Science* **2013**, *342*, 123−127.
(57) Nakamoto, R. K.; Scanlon, J. A. B.; Al-Shawi, M. K. The Rotary Mechanism of the ATP Synthase. *Arch. Biochem. Biophys.* **2008**, *476*, 43−50.
(58) Toyoshima, C.; Inesi, G. Structural Basis of Ion Pumping by Ca^{2+}-ATPase of the Sarcoplasmic Reticulum. *Annu. Rev. Biochem.* **2004**, *73*, 269−292.
(59) Kastritis, P. L.; Bonvin, A. M. J. J. On the Binding of Macromolecular Interactions: Daring to Ask Why Proteins Interact. *J. R. Soc., Interface* **2012**, *10*, 20120835.
(60) Maloney, P. C.; Kashket, E. R.; Wilson, T. H. A Protonmotive Force Drives ATP Synthesis in Bacteria. *Proc. Natl. Acad. Sci. U. S. A.* **1974**, *71*, 3896−3900.
(61) Møller, J. V.; Nissen, P.; Sørensen, T. L. M.; Maire, M. l. Transport Mechanism of the Sarcoplasmic Reticulum Ca^{2+}-ATPase Pump. *Curr. Opin. Struct. Biol.* **2005**, *15*, 387−393.
(62) Birge, R. R. Nature of the Primary Photochemical Events in Rhodopsin and Bacteriorhodopsin. *Biochim. Biophys. Acta, Bioenerg.* **1990**, *1016*, 293−327.
(63) Neutze, R.; Pebay-Peyroula, E.; Edman, K.; Royant, A.; Navarro, J.; Landau, E. M. Bacteriorhodopsin: A High-resolution Structural View of Vectorial Proton Transport. *Biochim. Biophys. Acta, Biomembr.* **2002**, *1565*, 144−167.
(64) Lanyi, J. K.; Luecke, H. Bacteriorhodopsin. *Curr. Opin. Struct. Biol.* **2001**, *11*, 415−419.
(65) Shibata, M.; Yamashita, H.; Uchihashi, T.; Kandori, H.; Ando, T. High-speed Atomic Force Microscopy Shows Dynamic Molecular Processes in Photoactivated Bacteriorhodopsin. *Nat. Nanotechnol.* **2010**, *5*, 208−212.
(66) Hirai, T.; Subramaniam, S. Protein Conformational Changes in the Bacteriorhodopsin Photocycle: Comparison of Findings from Electron and X-Ray Crystallographic Analyses. *PLoS One* **2009**, *4*, e5769.
(67) Haupts, U.; Tittor, J.; Oesterhelt, D. Closing in on Bactereorhodopsin: Progress in Understanding the Molecule. *Annu. Rev. Biophys. Biomol. Struct.* **1999**, *28*, 367−399.
(68) Yonath, A. Hibernating Bears, Antibiotics, and the Evolving Ribosome (Nobel Lecture). *Angew. Chem., Int. Ed.* **2010**, *49*, 4340−4354.
(69) Ramakrishnan, V. Unraveling the Structure of the Ribosome (Nobel Lecture). *Angew. Chem., Int. Ed.* **2010**, *49*, 4355−4380.
(70) Steitz, T. A. From the Structure and Function of the Ribosome to New Antibiotics (Nobel Lecture). *Angew. Chem., Int. Ed.* **2010**, *49*, 4381−4398.
(71) Bruck, I.; O'Donnell, M. The Ring-type Polymerase Sliding Clamp Family. *Genome Biol.* **2001**, *2*, reviews3001.1−reviews3001.3.
(72) Astumian, R. D. Comment: Detailed Balance Revisited. *Phys. Chem. Chem. Phys.* **2009**, *11*, 9592−9594.
(73) Astumian, R. D. Adiabatic Operation of a Molecular Machine. *Proc. Natl. Acad. Sci. U. S. A.* **2007**, *104*, 19715−19718.
(74) Mattia, E.; Otto, S. Supramolecular Systems Chemistry. *Nat. Nanotechnol.* **2015**, *10*, 111−119.
(75) Chatterjee, M. N.; Kay, E. R.; Leigh, D. A. Beyond Switches: Ratcheting a Particle Energetically Uphill with a Compartmentalized Molecular Machine. *J. Am. Chem. Soc.* **2006**, *128*, 4058−4073.
(76) Astumian, R. D. Stochastic Conformational Pumping: A Mechanism for Free-energy Transduction by Molecules. *Annu. Rev. Biophys.* **2011**, *40*, 289−313.

DOI: 10.1021/acs.chemrev.5b00146
Chem. Rev. 2015, 115, 10081−10206

(77) Astumian, R. D. Microscopic Reversibility as the Organizing Principle of Molecular Machines. *Nat. Nanotechnol.* **2012**, *7*, 684−688.
(78) Simon, M. S.; Peskin, C. S.; Oster, G. F. What Drives the Translocation of Proteins? *Proc. Natl. Acad. Sci. U. S. A.* **1992**, *89*, 3770−3774.
(79) Astumian, R. D. Thermodynamics and Kinetics of a Brownian Motor. *Science* **1997**, *276*, 917−922.
(80) Bier, M. Brownian Ratchets in Physics and Biology. *Contemp. Phys.* **1997**, *38*, 371−379.
(81) Juelicher, F.; Ajdari, A.; Prost, J. Modeling Molecular Motors. *Rev. Mod. Phys.* **1997**, *69*, 1269−1281.
(82) Astumian, R. D. Making Molecules into Motors. *Sci. Am.* **2001**, *285*, 56−64.
(83) Lipowsky, R.; Jaster, N. Molecular Motor Cycles: From Ratchets to Networks. *J. Stat. Phys.* **2003**, *110*, 1141−1167.
(84) Parrondo, J. M. R.; Dinís, L. Brownian Motion and Gambling: From Ratchets to Paradoxical Games. *Contemp. Phys.* **2004**, *45*, 147−157.
(85) Astumian, R. D. Design Principles for Brownian Molecular Machines: How to Swim in Molasses and Walk in a Hurricane. *Phys. Chem. Chem. Phys.* **2007**, *9*, 5067−5083.
(86) Parrondo, J. M. R.; de Cisneros, B. J. Energetics of Brownian Motors: A Review. *Appl. Phys. A: Mater. Sci. Process.* **2002**, *75*, 179−191.
(87) Reimann, P.; Hänggi, P. Introduction to the Physics of Brownian Motors. *Appl. Phys. A: Mater. Sci. Process.* **2002**, *75*, 169−178.
(88) Landauer, R. Inadequacy of Entropy and Entropy Derivatives in Characterizing the Steady State. *Phys. Rev. A: At., Mol., Opt. Phys.* **1975**, *12*, 636−638.
(89) Büttiker, M. Transport as a Consequence of State-dependent Diffusion. *Z. Phys. B: Condens. Matter* **1987**, *68*, 161−167.
(90) Landauer, R. Motion out of Noisy States. *J. Stat. Phys.* **1988**, *53*, 233−248.
(91) Van Kampen, N. G. Relative Stability in Nonuniform Temperature. *IBM J. Res. Dev.* **1988**, *32*, 107−111.
(92) Sinha, K.; Moss, F. Analog Simulation of a Simple System with State-dependent Diffusion. *J. Stat. Phys.* **1989**, *54*, 1411−1423.
(93) Rousselet, J.; Salome, L.; Ajdari, A.; Prostt, J. Directional Motion of Brownian Particles Induced by a Periodic Asymmetric Potential. *Nature* **1994**, *370*, 446−447.
(94) Faucheux, L. P.; Bourdieu, L. S.; Kaplan, P. D.; Libchaber, A. J. Optical Thermal Ratchet. *Phys. Rev. Lett.* **1995**, *74*, 1504−1507.
(95) Faucheux, L. P.; Libchaber, A. Selection of Brownian Particles. *J. Chem. Soc., Faraday Trans.* **1995**, *91*, 3163−3166.
(96) Faucheux, L. P.; Stolovitzky, G.; Libchaber, A. Periodic Forcing of a Brownian Particle. *Phys. Rev. E: Stat. Phys., Plasmas, Fluids, Relat. Interdiscip. Top.* **1995**, *51*, 5239−5250.
(97) Astumian, R. D.; Bier, M. Mechanochemical Coupling of the Motion of Molecular Motors to ATP Hydrolysis. *Biophys. J.* **1996**, *70*, 637−653.
(98) Gorre, L.; Ioannidis, E.; Silberzan, P. Rectified Motion of a Mercury Drop in an Asymmetric Structure. *Europhys. Lett.* **1996**, *33*, 267−272.
(99) Zhou, H.-X.; Chen, Y.-D. Chemically Driven Motility of Brownian Particles. *Phys. Rev. Lett.* **1996**, *77*, 194−197.
(100) Gorre-Talini, L.; Jeanjean, S.; Silberzan, P. Sorting of Brownian Particles by the Pulsed Application of an Asymmetric Potential. *Phys. Rev. E: Stat. Phys., Plasmas, Fluids, Relat. Interdiscip. Top.* **1997**, *56*, 2025−2034.
(101) Gorre-Talini, L.; Silberzan, P. Force-Free Motion of a Mercury Drop Alternatively Submitted to Shifted Asymmetric Potentials. *J. Phys. I (France)* **1997**, *7*, 1475−1485.
(102) Astumian, R. D.; Derényi, I. Fluctuation Driven Transport and Models of Molecular Motors and Pumps. *Eur. Biophys. J.* **1998**, *27*, 474−489.
(103) Gorre-Talini, L.; Spatz, J. P.; Silberzan, P. Dielectrophoretic Ratchets. *Chaos* **1998**, *8*, 650−656.
(104) Linke, H.; Sheng, W.; Löfgren, A.; Hongqi, X.; Omling, P.; Lindelof, P. E. A Quantum Dot Ratchet: Experiment and Theory. *Europhys. Lett.* **1998**, *44*, 341−347.
(105) Lorke, A.; Wimmer, S.; Jager, B.; Kotthaus, J. P.; Wegscheider, W.; Bichler, M. Far-infrared and Transport Properties of Antidot Arrays with Broken Symmetry. *Phys. B* **1998**, *249*−*251*, 312−316.
(106) Bekele, M.; Rajesh, S.; Ananthakrishna, G.; Kumar, N. Effect of Landauer's Blow Torch on the Equilibration Rate in a Bistable Potential. *Phys. Rev. E: Stat. Phys., Plasmas, Fluids, Relat. Interdiscip. Top.* **1999**, *59*, 143−149.
(107) Derényi, I.; Bier, M.; Astumian, R. D. Generalized Efficiency and its Application to Microscopic Engines. *Phys. Rev. Lett.* **1999**, *83*, 903−906.
(108) Linke, H.; Humphrey, T. E.; Löfgren, A.; Sushkov, A. O.; Newbury, R.; Taylor, R. P.; Omling, P. Experimental Tunneling Ratchets. *Science* **1999**, *286*, 2314−2317.
(109) Mennerat-Robilliard, C.; Lucas, D.; Guibal, S.; Tabosa, J.; Jurczak, C.; Courtois, J. Y.; Grynberg, G. Ratchet for Cold Rubidium Atoms: The Asymmetric Optical Lattice. *Phys. Rev. Lett.* **1999**, *82*, 851−854.
(110) Parmeggiani, A.; Jülicher, F.; Ajdari, A.; Prost, J. Energy Transduction of Isothermal Ratchets: Generic Aspects and Specific Examples Close to and Far from Equilibrium. *Phys. Rev. E: Stat. Phys., Plasmas, Fluids, Relat. Interdiscip. Top.* **1999**, *60*, 2127−2140.
(111) Switkes, M.; Marcus, C. M.; Campman, K.; Gossard, A. C. An Adiabatic Quantum Electron Pump. *Science* **1999**, *283*, 1905−1908.
(112) van Oudenaarden, A.; Boxer, S. G. Brownian Ratchets: Molecular Separations in Lipid Bilayers Supported on Patterned Arrays. *Science* **1999**, *285*, 1046−1048.
(113) Linke, H.; Sheng, W. D.; Svensson, A.; Löfgren, A.; Christensson, L.; Xu, H. Q.; Omling, P.; Lindelof, P. E. Asymmetric Nonlinear Conductance of Quantum Dots with Broken Inversion Symmetry. *Phys. Rev. B: Condens. Matter Mater. Phys.* **2000**, *61*, 15914−15926.
(114) Lipowsky, R. Molecular Motors and Stochastic Models. In *Stochastic Processes in Physics, Chemistry, and Biology*; Freund, J., Pöschel, T., Eds.; Springer: Berlin Heidelberg, 2000; Vol. *557*, pp 21−31.
(115) Mahadevan, L.; Matsudaira, P. Motility Powered by Supramolecular Springs and Ratchets. *Science* **2000**, *288*, 95−99.
(116) Bustamante, C.; Keller, D.; Oster, G. The Physics of Molecular Motors. *Acc. Chem. Res.* **2001**, *34*, 412−420.
(117) Höhberger, E. M.; Lorke, A.; Wegscheider, W.; Bichler, M. Adiabatic Pumping of Two-dimensional Electrons in a Ratchet-type Lateral Superlattice. *Appl. Phys. Lett.* **2001**, *78*, 2905−2907.
(118) Astumian, R. D. Protein Conformational Fluctuations and Free-energy Transduction. *Appl. Phys. A: Mater. Sci. Process.* **2002**, *75*, 193−206.
(119) Linke, H.; Humphrey, T. E.; Lindelof, P. E.; Löfgren, A.; Newbury, R.; Omling, P.; Sushkov, A. O.; Taylor, R. P.; Xu, H. Quantum Ratchets and Quantum Heat Pumps. *Appl. Phys. A: Mater. Sci. Process.* **2002**, *75*, 237−246.
(120) Marquet, C.; Buguin, A.; Talini, L.; Silberzan, P. Rectified Motion of Colloids in Asymmetrically Structured Channels. *Phys. Rev. Lett.* **2002**, *88*, 168301.
(121) Huang, L. R.; Cox, E. C.; Austin, R. H.; Sturm, J. C. Tilted Brownian Ratchet for DNA Analysis. *Anal. Chem.* **2003**, *75*, 6963−6967.
(122) Matthias, S.; Muller, F. Asymmetric Pores in a Silicon Membrane Acting as Massively Parallel Brownian Ratchets. *Nature* **2003**, *424*, 53−57.
(123) Mogilner, A.; Oster, G. Polymer Motors: Pushing out the Front and Pulling up the Back. *Curr. Biol.* **2003**, *13*, R721−R733.
(124) Oster, G.; Wang, H. Rotary Protein Motors. *Trends Cell Biol.* **2003**, *13*, 114−121.
(125) Kurzyński, M.; Chełminiak, P. Stochastic Action of Actomyosin Motor. *Phys. A* **2004**, *336*, 123−132.
(126) de Souza Silva, C. C.; Van de Vondel, J.; Morelle, M.; Moshchalkov, V. V. Controlled Multiple Reversals of a Ratchet Effect. *Nature* **2006**, *440*, 651−654.
(127) Linke, H.; Downton, M. T.; Zuckermann, M. J. Performance Characteristics of Brownian Motors. *Chaos* **2005**, *15*, 26111.
(128) Reimann, P. Brownian Motors: Noisy Transport Far from Equilibrium. *Phys. Rep.* **2002**, *361*, 57−265.

DOI: 10.1021/acs.chemrev.5b00146
Chem. Rev. 2015, 115, 10081−10206

(129) Gabryś, B. J.; Pesz, K.; Bartkiewicz, S. J. Brownian Motion, Molecular Motors and Ratchets. *Phys. A* **2004**, *336*, 112−122.
(130) Mislow, K. Stereochemical Consequences of Correlated Rotation in Molecular Propellers. *Acc. Chem. Res.* **1976**, *9*, 26−33.
(131) Rappoport, Z.; Biali, S. E. Sterically Crowded Stable Simple Enols. *Acc. Chem. Res.* **1988**, *21*, 442−449.
(132) Rappoport, Z.; Biali, S. E. Threshold Rotational Mechanisms and Enantiomerization Barriers of Polyarylvinyl Propellers. *Acc. Chem. Res.* **1997**, *30*, 307−314.
(133) Wolf, C. *Dynamic Stereochemistry of Chiral Compounds*; RSC Publishing: UK, 2008; Chapter 8, pp 399−443.
(134) Gust, D.; Mislow, K. Analysis of Isomerization in Compounds Displaying Restricted Rotation of Aryl Groups. *J. Am. Chem. Soc.* **1973**, *95*, 1535−1547.
(135) Mislow, K.; Gust, D.; Finocchiaro, P.; Boettcher, R. Stereochemical Correspondence Among Molecular Propellers. *Stereochemistry I*; Springer: Berlin, Heidelberg, 1974; Vol. *47*, pp 1−28.
(136) Katoono, R.; Kawai, H.; Fujiwara, K.; Suzuki, T. Dynamic Molecular Propeller: Supramolecular Chirality Sensing by Enhanced Chiroptical Response through the Transmission of Point Chirality to Mobile Helicity. *J. Am. Chem. Soc.* **2009**, *131*, 16896−16904.
(137) Driesschaert, B.; Robiette, R.; Le Duff, C. S.; Collard, L.; Robeyns, K.; Gallez, B.; Marchand-Brynaert, J. Configurationally Stable Tris(tetrathioaryl)methyl Molecular Propellers. *Eur. J. Org. Chem.* **2012**, 6517−6525.
(138) Katoono, R.; Kawai, H.; Ohkita, M.; Fujiwara, K.; Suzuki, T. A C(3)-symmetric Chiroptical Molecular Propeller Based on Hexakis-(phenylethynyl)benzene with a Threefold Terephthalamide: Stereospecific Propeller Generation Through the Cooperative Transmission of Point Chiralities on the Host and Guest upon Complexation. *Chem. Commun.* **2013**, *49*, 10352−10354.
(139) Finocchiaro, P.; Gust, D.; Mislow, K. Structure and Dynamic Stereochemistry of Trimesitylmethane. I. Synthesis and Nuclear Magnetic Resonance Studies. *J. Am. Chem. Soc.* **1974**, *96*, 2165−2167.
(140) Ōki, M. Unusually High Barriers to Rotation Involving the Tetrahedral Carbon Atom. *Angew. Chem., Int. Ed. Engl.* **1976**, *15*, 87−93.
(141) Yamamoto, G.; Ōki, M. Dual Mechanisms of the Aryl Group Rotation in 9-(3,5-dimethylbenzyl) Triptycene Derivatives. *Chem. Lett.* **1979**, 1251−1254.
(142) Yamamoto, G.; Ōki, M. Two Consecutive Gear Motions in Conformational Interconversion in 9-(2-methylbenzyl)triptycene Derivatives. *Chem. Lett.* **1979**, 1255−1258.
(143) Yamaoto, G.; Ōki, M. Restricted Rotation Involving the Tetrahedral Carbon. XXXV. Stereodynamics of 9-(3,5-Dimethylbenzyl)triptycene Derivatives. *Bull. Chem. Soc. Jpn.* **1981**, *54*, 473−480.
(144) Yamamoto, G.; Ōki, M. Restricted Rotation Involving the Tetrahedral Carbon. XXXVI. Stereodynamics of 9-(2-MethylbenzyI)-triptycene Derivatives. *Bull. Chem. Soc. Jpn.* **1981**, *54*, 481−487.
(145) Yamamoto, G.; Ōki, M. Restricted Rotation Involving the Tetrahedral Carbon. Part 46. Correlated Rotation in 9-(2,4,6-trimethylbenzyl)triptycenes. Direct and Roundabout Enantiomerization-diastereomerization Processes. *J. Org. Chem.* **1983**, *48*, 1233−1236.
(146) Yamamoto, G. Molecular Gears with Two-toothed and Three-toothed Wheels. *J. Mol. Struct.* **1985**, *126*, 413−420.
(147) Yamamoto, G.; Ōki, M. Restricted Rotation Involving the Tetrahedral Carbon. LVII. Stereodynamics of 9-(2-Alkylphenoxy)-1,4-dimethyltriptycenes. *Bull. Chem. Soc. Jpn.* **1985**, *58*, 1953−1961.
(148) Yamamoto, G.; Ōki, M. Restricted Rotation Involving the Tetrahedral Carbon. LIX. Stereodynamics of Singly peri-Substituted 9-(3,5-Dimethylphenoxy)triptycene Derivatives. *Bull. Chem. Soc. Jpn.* **1986**, *59*, 3597−3603.
(149) Yamamoto, G. Detailed Dynamic NMR Study of a Molecular Gear, 1-Methoxy-9-(3,5-dimethylbenzyl)triptycene. *Bull. Chem. Soc. Jpn.* **1989**, *62*, 4058−4060.
(150) Hiizu Iwamura, K. M. Stereochemical Consequences of Dynamic Gearing. *Acc. Chem. Res.* **1988**, *21*, 175−182.
(151) Kawada, Y.; Iwamura, H. Unconventional Synthesis and Conformational Flexibility of Bis(1-triptycyl) ether. *J. Org. Chem.* **1980**, *45*, 2548−2550.
(152) Kawada, Y.; Iwamura, H. Bis(4-chloro-1-triptycyl) ether. Separation of a Pair of Phase Isomers of Labeled Bevel Gears. *J. Am. Chem. Soc.* **1981**, *103*, 958−960.
(153) Kawada, Y.; Iwamura, H. Bis(4-chloro-1-triptycyl) ether. Separation of a Pair of Phase Isomers of Labeled Bevel Gears. *Tetrahedron Lett.* **1981**, *22*, 1533−1536.
(154) Kawada, Y.; Iwamura, H. Correlated Rotation in Bis(9-triptycyl)methanes and Bis(9-triptycyl) Ethers. Separation and Interconversion of the Phase Isomers of Labeled Bevel Gears. *J. Am. Chem. Soc.* **1983**, *105*, 1449−1459.
(155) Kawada, Y.; Okamoto, Y.; Iwamura, H. Correlated Internal Rotation in Bis(2,6-dichloro-9-triptycyl)methane. To what Extent can Phase Isomers be Separated and Identified? *Tetrahedron Lett.* **1983**, *24*, 5359−5362.
(156) Iwamura, H.; Ito, T.; Ito, H.; Toriumi, K.; Kawada, Y.; Osawa, E.; Fujiyoshi, T.; Jaime, C. Crystal and Molecular Structure of Bis(9-triptycyl) Ether. *J. Am. Chem. Soc.* **1984**, *106*, 4712−4717.
(157) Iwamura, H. Molecular Design of Correlated Internal Rotation. *J. Mol. Struct.* **1985**, *126*, 401−412.
(158) Koga, N.; Iwamura, H. Barrier to Coupled Internal Rotation in Bis(9-triptycyl) Ether. Kinetics of Intramolecular Exciplex Formation in Racemic 2,3-Benzo-9-triptycyl 2-(N,N-dimethylaminomethyl)-9-triptycyl ether. *J. Am. Chem. Soc.* **1985**, *107*, 1426−1427.
(159) Koga, N.; Iwamura, H. A Kinetic Study of Coupled Internal Rotation in Racemic 2,3-Benzo-9-triptycyl 2-(dimethylaminomethyl)-9-triptycyl ether by Means of Exciplex Fluorescence Dynamics. *Chem. Lett.* **1986**, 247−250.
(160) Kawada, Y.; Yamazaki, H.; Koga, G.; Murata, S.; Iwamura, H. Bis(9-triptycyl)amines, A Missing Link Between the Corresponding Methanes and Ethers. An Unconventional Synthesis and Influence of Nitrogen Configurational Inversion on the Coupled Disrotatory Trajectory. *J. Org. Chem.* **1986**, *51*, 1472−1477.
(161) Kawada, Y.; Ishikawa, J.; Yamazaki, H.; Koga, G.; Murata, S.; Iwamura, H. Bis(9-triptycyl)amines, A Missing Link Between the Corresponding Methanes and Ethers. An Unconventional Synthesis and Influence of Nitrogen Configurational Inversion on the Coupled Disrotatory Trajectory. *Tetrahedron Lett.* **1987**, *28*, 445−448.
(162) Hounshell, W. D.; Johnson, C. A.; Guenzi, A.; Cozzi, F.; Mislow, K. Sterochemical Consequences of Dynamic Gearing in Substituted bis (9-triptycyl) Methanes and Related Molecules. *Proc. Natl. Acad. Sci. U. S. A.* **1980**, *77*, 6961−6964.
(163) Cozzi, F.; Guenzi, A.; Johnson, C. A.; Mislow, K. Stereoisomerism and Correlated Rotation in Molecular Gear Systems. Residual Diastereomers of Bis(2,3-dimethyl-9-triptycyl)methane. *J. Am. Chem. Soc.* **1981**, *103*, 957−958.
(164) Johnson, C. A.; Guenzi, A.; Mislow, K. Restricted Gearing and Residual Stereoisomerism in Bis(1,4-dimethyl-9-triptycyl)methane. *J. Am. Chem. Soc.* **1981**, *103*, 6240−6242.
(165) Johnson, C. A.; Guenzi, A.; Nachbar, R. B., Jr.; Blount, J. F.; Wennerstroem, O.; Mislow, K. Crystal and Molecular Structure of Bis(9-triptycyl) ketone and Bis(9-triptycyl)methane. *J. Am. Chem. Soc.* **1982**, *104*, 5163−5168.
(166) Buergi, H. B.; Hounshell, W. D.; Nachbar, J. R. B.; Mislow, K. Conformational Dynamics of Propane, di-tert-Butylmethane, and Bis(9-triptycyl)methane. An Analysis of the Symmetry of Two Threefold Rotors on a Rigid Frame in Terms of Nonrigid Molecular Structure and Energy Hypersurfaces. *J. Am. Chem. Soc.* **1983**, *105*, 1427−1438.
(167) Guenzi, A.; Johnson, C. A.; Cozzi, F.; Mislow, K. Dynamic Gearing and Residual Stereoisomerism in Labeled Bis(9-triptycyl)-methane and Related Molecules. Synthesis and Stereochemistry of Bis(2,3-dimethyl-9-triptycyl)methane, Bis(2,3-dimethyl-9-triptycyl)-carbinol, and Bis(1,4-dimethyl-9-triptycyl) Methane. *J. Am. Chem. Soc.* **1983**, *105*, 1438−1448.
(168) Koga, N.; Kawada, Y.; Iwamura, H. Recognition of the Phase Relationship between Remote Substituents in 9,10-Bis(3-chloro-9-

DOI: 10.1021/acs.chemrev.5b00146
Chem. Rev. 2015, 115, 10081−10206

triptycycloxy)triptycene Molecules Undergoing Rapid Internal Rotation Cooperatively. *J. Am. Chem. Soc.* **1983**, *105*, 5498−5499.
(169) Yamamoto, G. Molecular Gears with Two-toothed and Three-thoothed Wheels. *J. Mol. Struct.* **1985**, *126*, 413−420.
(170) Yamamoto, G. Dynamic Stereochemistry of Molecular Geras, 9-Benzyltriptycene and 9-Phenoxytriptycene, Studied by ^{13}C Dynamic NMR Spectroscopy and Molecular Mechanics Calculations. *Tetrahedron* **1990**, *46*, 2761−2772.
(171) Chance, J. M.; Geiger, J. H.; Okamoto, Y.; Aburatani, R.; Mislow, K. Stereochemical Consequences of a Parity Restriction on Dynamic Gearing in Tris(9-triptycyl)germanium Chloride and Tris(9-triptycyl)-cyclopropenium Perchlorate. *J. Am. Chem. Soc.* **1990**, *112*, 3540−3547.
(172) Kawada, Y.; Sakai, H.; Oguri, M.; Koga, G. Preparation of an Dynamic Gearing in *cis*-1,2-Bis(9-triptycyl)ethylene. *Tetrahedron Lett.* **1994**, *35*, 139−142.
(173) Nikitin, K.; Müller-Bunz, H.; Ortin, Y.; Risse, W.; McGlinchey, M. J. Twin Triptycyl Spinning Tops: A Simple Case of Molecular Gearing with Dynamic C_2 Symmetry. *Eur. J. Org. Chem.* **2008**, *2008*, 3079−3084.
(174) Frantz, D. K.; Linden, A.; Baldridge, K. K.; Siegel, J. S. Molecular Spur Gears Comprising Triptycene Rotators and Bibenzimidazole-based Stators. *J. Am. Chem. Soc.* **2012**, *134*, 1528−1535.
(175) Stevens, A. M.; Richards, C. J. A Metallocene Molecular Gear. *Tetrahedron Lett.* **1997**, *38*, 7805−7808.
(176) Brydges, S.; Harrington, L. E.; McGlinchey, M. J. Sterically Hindered Organometallics: Multi-n-rotor (n = 5, 6 and 7) Molecular Propellers and the Search for Correlated Rotations. *Coord. Chem. Rev.* **2002**, *233*, 75−105.
(177) Kuttenberger, M.; Frieser, M.; Hofweber, M.; Mannschreck, A. Axially Chiral Thioamides of Acrylic Acid: Correlated and Uncorrelated Internal Rotations. *Tetrahedron: Asymmetry* **1998**, *9*, 3629−3645.
(178) Clayden, J.; Pink, J. H. Concerted Rotation in a Tertiary Aromatic Amide: Towards a Simple Molecular Gear. *Angew. Chem., Int. Ed.* **1998**, *37*, 1937−1939.
(179) Johnston, E. R.; Fortt, R.; Barborak, J. C. Correlated Rotation in a Conformationally Restricted Amide. *Magn. Reson. Chem.* **2000**, *38*, 932−936.
(180) Bragg, R. A.; Clayden, J. Using Symmetry to Monitor Geared Bond Rotation in Aromatic Amides by Dynamic NMR. *Org. Lett.* **2000**, *2*, 3351−3354.
(181) Bragg, R. A.; Clayden, J.; Morris, G. A.; Pink, J. H. Stereodynamics of Bond Rotation in Tertiary Aromatic Amides. *Chem. - Eur. J.* **2002**, *8*, 1279−1289.
(182) Hellwinkel, D.; Melan, M.; Degel, C. R. Die Stereochemie *ortho*-Substituierter Triphenylamin-derivate. *Tetrahedron* **1973**, *29*, 1895−1907.
(183) Hummel, J. P.; Gust, D.; Mislow, K. Mechanism of Stereoisomerization in Triarylboranes. *J. Am. Chem. Soc.* **1974**, *96*, 3679−3681.
(184) Wille, E. E.; Stephenson, D. S.; Capriel, P.; Binsch, G. Iterative Analysis of Exchange-Broadened NMR Band Shapes. The Mechanism of Correlated Rotations in Triaryl Derivatives of Phosphorus and Arsenic. *J. Am. Chem. Soc.* **1982**, *104*, 405−415.
(185) Clegg, W.; Lockhart, J. C.; McDonnell, M. B. Comparison of the Steric Barriers in Three- and Two-bladed Propeller Crowns. *J. Chem. Soc., Perkin Trans. 1* **1985**, 1019−1023.
(186) Berg, U.; Liljefors, T.; Roussel, C.; Sandstroem, J. Steric Interplay Between Alkyl Groups Bonded to Planar Frameworks. *Acc. Chem. Res.* **1985**, *18*, 80−86.
(187) Biali, S. E.; Rappoport, Z. Stable Simple Enols. 8.′ Synthesis and Keto Enol Equilibria of the Elusive 2,2-Dimesitylethanal and 1,2,2-Trimesitylethanone. Conformations of 1,2,2-Trimesitylethanone and 1,2,2-Trimesitylethanol. *J. Am. Chem. Soc.* **1985**, *107*, 1007−1015.
(188) Hansen, P. E.; Spanget-Lansen, J.; Laali, K. K. Conformational Studies of Phenyl and (1-Pyrenyl) Triarylmethylcarbenium Ions: Semiempirical Calculations and NMR Investigations under Stable Ion Conditions. *J. Org. Chem.* **1998**, *63*, 1827−1835.
(189) Yamaguchi, S.; Akiyama, S.; Tamao, K. Synthesis, Structures, Photophysical Properties, and Dynamic Stereochemistry of Tri(9-anthryl)silane Derivatives. *Organometallics* **1998**, *17*, 4347−4352.
(190) Sedo, J.; Ventosa, N.; Molins, M. A.; Pons, M.; Rovira, C.; Veciana, J. Stereoisomerism of Molecular Multipropellers. 2. Dynamic Stereochemistry of Bis- and Tris-Triaryl Systems. *J. Org. Chem.* **2001**, *66*, 1579−1589.
(191) Grilli, S.; Lunazzi, L.; Mazzanti, A. Conformational Studies by Dynamic NMR. 83.1 Correlated Enantiomerization Pathways for the Stereolabile Propeller Antipodes of Dimesityl Substituted Ethanol and Ethers. *J. Org. Chem.* **2001**, *66*, 5853−5858.
(192) Benincori, T.; Celentano, G.; Pilati, T.; Ponti, A.; Rizzo, S.; Sannicolò, F. Configurationally Stable Molecular Propellers: First Resolution of Residual Enantiomers. *Angew. Chem., Int. Ed.* **2006**, *45*, 6193−6196.
(193) Bulo, R. E.; Allaart, F.; Ehlers, A. W.; de Kanter, F. J. J.; Schakel, M.; Lutz, M.; Spek, A. L.; Lammertsma, K. Circumambulatory Rearrangement with Characteristics of a 2:1 Covalent Molecular Bevel Gear. *J. Am. Chem. Soc.* **2006**, *128*, 12169−12173.
(194) Romeo, R.; Carnabuci, S.; Fenech, L.; Plutino, M. R.; Albinati, A. Overcrowded Organometallic Platinum(II) Complexes That Behave as Molecular Gears. *Angew. Chem., Int. Ed.* **2006**, *45*, 4494−4498.
(195) Peck, T.-G.; Lai, Y.-H. Conformational Isomerism in 1,2-Di-*o*-tolylnaphthalenes: Selective Rotation of the 2-Aryl Ring. *Tetrahedron* **2009**, *65*, 3664−3667.
(196) Mati, I. K.; Cockroft, S. L. Molecular Balances for Quantifying Non-covalent Interactions. *Chem. Soc. Rev.* **2010**, *39*, 4195−4205.
(197) Hiraoka, S.; Harano, K.; Tanaka, T.; Shiro, M.; Shionoya, M. Quantitative Formation of Sandwich-shaped Trinuclear Silver(I) Complexes and Dynamic Nature of Their P ≤ > M Flip Motion in Solution. *Angew. Chem., Int. Ed.* **2003**, *42*, 5182−5185.
(198) Hiraoka, S.; Shiro, M.; Shionoya, M. Heterotopic Assemblage of Two Different Disk-Shaped Ligands through Trinuclear Silver (I) Complexation: Ligand Exchange-Driven Molecular Motion. *J. Am. Chem. Soc.* **2004**, *126*, 1214−1218.
(199) Hiraoka, S.; Okuno, E.; Tanaka, T.; Shiro, M.; Shionoya, M. Ranging Correlated Motion (1.5 nm) of Two Coaxially Arranged Rotors Mediated by Helix Inversion of a Supramolecular Transmitter. *J. Am. Chem. Soc.* **2008**, *130*, 9089−9098.
(200) Hiraoka, S.; Hirata, K.; Shionoya, M. A Molecular Ball Bearing Mediated by Multiligand Exchange in Concert. *Angew. Chem., Int. Ed.* **2004**, *43*, 3814−3818.
(201) Okuno, E.; Hiraoka, S.; Shionoya, M. A Synthetic Approach to a Molecular Crank Mechanism: Toward Intramolecular Motion Transformation Between Rotation and Translation. *Dalton Trans.* **2010**, *39*, 4107−4116.
(202) Liu, S.; Kondratuk, D. V.; Rousseaux, S. A.; Gil-Ramirez, G.; O'Sullivan, M. C.; Cremers, J.; Claridge, T. D.; Anderson, H. L. Caterpillar Track Complexes in Template-directed Synthesis and Correlated Molecular Motion. *Angew. Chem., Int. Ed.* **2015**, *54*, 5355−5359.
(203) Kelly, T. R.; Bowyer, M. C.; Bhaskar, K. V.; Bebbington, D.; Garcia, A.; Lang, F.; Kim, M. H.; Jette, M. P. A Molecular Brake. *J. Am. Chem. Soc.* **1994**, *116*, 3657−3658.
(204) Kelly, T. R. Progress Toward a Rationally Designed Molecular Motor. *Acc. Chem. Res.* **2001**, *34*, 514−522.
(205) Sestelo, J. P.; Kelly, T. R. A Prototype of a Rationally Designed Chemically Powered Brownian Motor. *Appl. Phys. A: Mater. Sci. Process.* **2002**, *75*, 337−343.
(206) Jog, P. V.; Brown, R. E.; Bates, D. K. A Redox-Mediated Molecular Brake: Dynamic NMR Study of 2-[2-(Methylthio)phenyl]-isoindolin-1-one and S-Oxidized Counterparts. *J. Org. Chem.* **2003**, *68*, 8240−8243.
(207) Dial, B. E.; Pellechia, P. J.; Smith, M. D.; Shimizu, K. D. Proton Grease: An Acid Accelerated Molecular Rotor. *J. Am. Chem. Soc.* **2012**, *134*, 3675−3678.
(208) Dial, B. E.; Rasberry, R. D.; Bullock, B. N.; Smith, M. D.; Pellechia, P. J.; Profeta, S.; Shimizu, K. D. Guest-Accelerated Molecular Rotor. *Org. Lett.* **2011**, *13*, 244−247.

DOI: 10.1021/acs.chemrev.5b00146
Chem. Rev. 2015, 115, 10081−10206

(209) Kanazawa, H.; Higuchi, M.; Yamamoto, K. An Electric Cyclophane: Cavity Control Based on the Rotation of a Paraphenylene by Redox Switching. *J. Am. Chem. Soc.* **2005**, *127*, 16404−16405.
(210) Tomohiro, Y.; Satake, A.; Kobuke, Y. Synthesis of Bipyridylene-Bridged Bisporphyrin by Nickel-Mediated Coupling Reaction: ON−OFF Control of Cofacial Porphyrin Unit by Reversible Complexation. *J. Org. Chem.* **2001**, *66*, 8442−8446.
(211) Zehm, D.; Fudickar, W.; Linker, T. Molecular Switches Flipped by Oxygen. *Angew. Chem., Int. Ed.* **2007**, *46*, 7689−7692.
(212) Kelly, T. R.; Tellitu, I.; Sestelo, J. P. In Search of Molecular Ratchets. *Angew. Chem., Int. Ed. Engl.* **1997**, *36*, 1866−1868.
(213) Kelly, T. R.; Sestelo, J. P.; Tellitu, I. New Molecular Devices: In Search of a Molecular Ratchet. *J. Org. Chem.* **1998**, *63*, 3655−3665.
(214) Sebastian, K. L. Molecular Ratchets: Verification of the Principle of Detailed Balance and the Second Law of Dynamics. *Phys. Rev. E: Stat. Phys., Plasmas, Fluids, Relat. Interdiscip. Top.* **2000**, *61*, 937−939.
(215) Davis, A. P. Tilting at Windmills? The Second Law Survives. *Angew. Chem., Int. Ed.* **1998**, *37*, 909−910.
(216) Kelly, T. R.; De Silva, H.; Silva, R. A. Unidirectional Rotary Motion in a Molecular System. *Nature* **1999**, *401*, 150−152.
(217) Kelly, T. R.; Silva, R. A.; Silva, H. D.; Jasmin, S.; Zhao, Y. A Rationally Designed Prototype of a Molecular Motor. *J. Am. Chem. Soc.* **2000**, *122*, 6935−6949.
(218) Kelly, T. R.; Cai, X.; Damkaci, F.; Panicker, S. B.; Tu, B.; Bushell, S. M.; Cornella, I.; Piggott, M. J.; Salives, R.; Cavero, M. Progress Toward a Rationally Designed, Chemically Powered Rotary Molecular Motor. *J. Am. Chem. Soc.* **2007**, *129*, 376−386.
(219) Mock, W. L.; Ochwat, K. J. Theory and Example of a Small-molecule Motor. *J. Phys. Org. Chem.* **2003**, *16*, 175−182.
(220) Dahl, B. J.; Branchaud, B. P. Synthesis and Characterization of a Functionalized Chiral Biaryl Capable of Exhibiting Unidirectional Bond Rotation. *Tetrahedron Lett.* **2004**, *45*, 9599−9602.
(221) Lin, Y.; Dahl, B. J.; Branchaud, B. P. Net Directed 180° Aryl−aryl Bond Rotation in a Prototypical Achiral Biaryl Lactone Synthetic Molecular Motor. *Tetrahedron Lett.* **2005**, *46*, 8359−8362.
(222) Fletcher, S. P.; Dumur, F.; Pollard, M. M.; Feringa, B. L. A Reversible, Unidirectional Molecular Rotary Motor Driven by Chemical Energy. *Science* **2005**, *310*, 80−82.
(223) Siegel, J. Chemistry. Inventing the Nanomolecular Wheel. *Science* **2005**, *310*, 63−64.
(224) Tashiro, K.; Konishi, K.; Aida, T. Enantiomeric Resolution of Chiral Metallobis(porphyrin)s: Studies on Rotatbility of Electronically Coupled Porphyrin Ligands. *Angew. Chem., Int. Ed. Engl.* **1997**, *36*, 856−858.
(225) Tashiro, K.; Fujiwara, T.; Konishi, K.; Aida, T. *Chem. Commun.* **1998**, 1121−1122.
(226) Ikeda, M.; Takeuchi, M.; Shinkai, S.; Tani, F.; Naruta, Y. Synthesis of New Diaryl-Substituted Triple-Decker and Tetraaryl-substituted Double-Decker Lanthanum(III) Porphyrins and Their Porphyrin Ring Rotational Speed as Compared with that of Double-Decker Cerium(IV) Porphyrins. *Bull. Chem. Soc. Jpn.* **2001**, *74*, 739−746.
(227) Tashiro, K.; Konishi, K.; Aida, T. Metal Bisporphyrin Double-decker Complexes as Redox-Responsive Rotating Modules. Studies on Ligand Rotation Activities of the Reduced and Oxidized Forms Using Chirality as a Probe. *J. Am. Chem. Soc.* **2000**, *122*, 7921−7926.
(228) Buchler, J. W.; Decian, A.; Fischer, J.; Hammerschmitt, P.; Loffler, J.; Scharbert, B.; Weiss, R. Metal-Complexes with Tetrapyrrole Ligands 0.54. Synthesis, Spectra, Structure, and Redox Properties of Cerium(Iv) Bisporphyrinates with Identical and Different Porphyrin Rings in the Sandwich System. *Chem. Ber.* **1989**, *122*, 2219−2228.
(229) Takeuchi, M.; Imada, I.; Shinkai, S. A Strong Positive Allosteric Effect in the Molecular Recognition of Dicarboxylic Acids by a Cerium(IV)Bis[tetrakis(4-pyridyl)-porphyrinte] Double Decker. *Angew. Chem., Int. Ed.* **1998**, *37*, 2096−2099.
(230) Sugasaki, A.; Ikeda, M.; Takeuchi, M.; Robertson, A.; Shinkai, S. Efficient Chirality Transcription Utilizing a Cerium(IV) Double Decker Porphyrin: A Prototype for Development of a Molecular Memory Systems. *J. Chem. Soc., Perkin Trans. 1* **1999**, 3259−3264.
(231) Yamamoto, M.; Sugasaki, A.; Ikeda, M.; Takeuchi, M.; Frimat, K.; James, T. D.; Shinkai, S. Efficient Anion Binding to Cerium(IV)-Bis(porphyrinate) Double Decker Utilizing Positive Homotropic Allosterim. *Chem. Lett.* **2001**, 520−521.
(232) Robertson, A.; Ikeda, M.; Takeuchi, M.; Shinkai, S. Allosteric Binding of K^+ to Crown Ether Macrocycles Appended to a Lanthanum Double Decker System. *Bull. Chem. Soc. Jpn.* **2001**, *74*, 883−888.
(233) Sugasaki, A.; Ikeda, M.; Takeuchi, M.; Shinkai, S. Novel Oligosaccharide Binding to the Cerium(IV) Bis(porphyrinoate) Double Decker: Effective Amplification of a Binding Signal through Positive Homotropic Allosterism. *Angew. Chem., Int. Ed.* **2000**, *39*, 3839−3842.
(234) Ikeda, M.; Shinkai, S.; Osuka, A. Meso−meso-linked Porphyrin Dimer as a Novel Scaffold for the Selective Binding of Oligosaccharides. *Chem. Commun.* **2000**, 1047−1048.
(235) Sugasaki, A.; Ikeda, M.; Takeuchi, M.; Koumoto, K.; Shinkai, S. The First Example of Positive Allosterism in an Aqueous Saccharide-Binding System Designed on a Ce(IV) Bis(porphyrinate) Double Decker Scaffold. *Tetrahedron* **2000**, *56*, 4717−4723.
(236) Ikeda, M.; Tanida, T.; Takeuchi, M.; Shinkai, S. Allosteric Silver (I) Ion Binding with Peripheral π Clefts of a Ce (IV) Double Decker Porphyrin. *Org. Lett.* **2000**, *2*, 1803−1805.
(237) Ikeda, M.; Takeuchi, M.; Shinkai, S.; Tani, F.; Naruta, Y.; Sakamoto, S.; Yamaguchi, K. Allosteric Binding of a Ag^+ Ion to Cerium (IV) Bis-porphyrinates Enhances the Rotational Activity of Porphyrin Ligands. *Chem. - Eur. J.* **2002**, *8*, 5541−5550.
(238) Kubo, Y.; Ikeda, M.; Sugasaki, A.; Takeuchi, M.; Shinkai, S. A Porphyrin Tetramer for a Positive Homotropic Allosteric Recognition System: Efficient Binding Information Transduction Through Butadiynyl Axis Rotation. *Tetrahedron Lett.* **2001**, *42*, 7435−7438.
(239) Shinkai, S.; Ikeda, M.; Sugasaki, A.; Takeuchi, M. Positive Allosteric Systems Designed on Dynamic Supramolecular Scaffolds: Toward Switching and Amplification of Guest Affinity and Selectivity. *Acc. Chem. Res.* **2001**, *34*, 494−503.
(240) Takeuchi, M.; Ikeda, M.; Sugasaki, A.; Shinkai, S. Molecular Design of Artificial Molecular and Ion Recognition Systems with Allosteric Guest Responses. *Acc. Chem. Res.* **2001**, *34*, 865−873.
(241) Ayabe, M.; Ikeda, A.; Kubo, Y.; Takeuchi, M.; Shinkai, S. A Dendritic Porphyrin Receptor for C_{60} Which Features a Profound Positive Allosteric Effect. *Angew. Chem., Int. Ed.* **2002**, *41*, 2790−2792.
(242) Kubo, Y.; Sugasaki, A.; Ikeda, M.; Sugiyasu, K.; Sonoda, K.; Ikeda, A.; Takeuchi, M.; Shinkai, S. Cooperative C-60 Binding to a Porphyrin Tetramer Arranged Around a *p*-Terphenyl Axis in 1:2 Host-guest Stoichiometry. *Org. Lett.* **2002**, *4*, 925−928.
(243) Ercolani, G. The Origin of Cooperativity in Double-Wheel Receptors. Freezing of Internal Rotation or Ligand-Induced Torsional Strain? *Org. Lett.* **2005**, *7*, 803−805.
(244) Shinkai, S.; Takeuchi, M. Molecular Design of Synthetic Receptors with Dynamic, Imprinting, and Allosteric Functions. *Bull. Chem. Soc. Jpn.* **2005**, *78*, 40−51.
(245) Ikeda, T.; Tsukahara, T.; Iino, R.; Takeuchi, M.; Noji, H. Motion Capture and Manipulation of a Single Synthetic Molecular Rotor by Optical Microscopy. *Angew. Chem., Int. Ed.* **2014**, *53*, 10082−10085.
(246) Tanaka, H.; Ikeda, T.; Takeuchi, M.; Sada, K.; Shinkai, S.; Kawai, T. Molecular Rotation in Self-Assembled Multidecker Porphyrin Complexes. *ACS Nano* **2011**, *5*, 9575−9582.
(247) Ogi, S.; Ikeda, T.; Wakabayashi, R.; Shinkai, S.; Takeuchi, M. A Bevel-gear-shaped Rotor Bearing a Double-decker Porphyrin Complex. *Chem. - Eur. J.* **2010**, *16*, 8285−8290.
(248) Ogi, S.; Ikeda, T.; Wakabayashi, R.; Shinkai, S.; Takeuchi, M. Mechanically Interlocked Porphyrin Gears Propagating Two Different Rotational Frequencies. *Eur. J. Org. Chem.* **2011**, *2011*, 1831−1836.
(249) Ogi, S.; Ikeda, T.; Takeuchi, M. Synthetic Molecular Gear Based on Double-Decker Porphyrin Complexes. *J. Inorg. Organomet. Polym. Mater.* **2013**, *23*, 193−199.
(250) Shibata, M.; Tanaka, S.; Ikeda, T.; Shinkai, S.; Kaneko, K.; Ogi, S.; Takeuchi, M. Stimuli-Responsive Folding and Unfolding of a Polymer Bearing Multiple Cerium(IV) Bis(porphyrinate) Joints: Mechano-imitation of the Action of a Folding Ruler. *Angew. Chem., Int. Ed.* **2013**, *52*, 397−400.

DOI: 10.1021/acs.chemrev.5b00146
Chem. Rev. 2015, 115, 10081−10206

(251) Hiraoka, S.; Hisanaga, Y.; Shiro, M.; Shionoya, M. A Molecular Double Ball Bearing: An Ag^{I}–Pt^{II} Dodecanuclear Quadruple-Decker Complex with Three Rotors. *Angew. Chem., Int. Ed.* **2010**, *49*, 1669–1673.
(252) Bohn, R. K.; Haaland, A. On the Molecular Structure of Ferrocene, $Fe(C_5H_5)_2$. *J. Organomet. Chem.* **1966**, *5*, 470–476.
(253) Wang, X. B.; Dai, B.; Woo, H. K.; Wang, L. S. Intramolecular Rotation Through Proton Transfer: $[Fe(\eta^5\text{-}C_5H_4CO_2\text{-})_2]$ versus $[(\eta^5\text{-}C_5H_4CO_2\text{-})Fe(\eta^5\text{-}C_5H_4CO_2H)]$. *Angew. Chem., Int. Ed.* **2005**, *44*, 6022–6024.
(254) Crowley, J. D.; Steele, I. M.; Bosnich, B. Protonmotive Force: Development of Electrostatic Drivers for Synthetic Molecular Motors. *Chem. - Eur. J.* **2006**, *12*, 8935–8951.
(255) Iordache, A.; Oltean, M.; Milet, A.; Thomas, F.; Baptiste, B.; Saint-Aman, E.; Bucher, C. Redox Control of Rotary Motions in Ferrocene-based Elemental Ball Bearings. *J. Am. Chem. Soc.* **2012**, *134*, 2653–2671.
(256) Fukino, T.; Joo, H.; Hisada, Y.; Obana, M.; Yamagishi, H.; Hikima, T.; Takata, M.; Fujita, N.; Aida, T. Manipulation of Discrete Nanostructures by Selective Modulation of Noncovalent Forces. *Science* **2014**, *344*, 499–504.
(257) Warren, L. F., Jr.; Hawthorne, M. F. The Chemistry of the Bis[π-(3)-1,2-dicarbollyl] Metalates of Nickel and Palladium. *J. Am. Chem. Soc.* **1970**, *92*, 1157–1173.
(258) St. Clair, D.; Zalkin, A.; Templeton, D. H. The Crystal Structure of 3,3′-commo-Bis[undecahydro-1,2-dicarba-3-nickela-closo-dodecaborane], a Nickel(IV) Complex of the Dicarbollide Ion. *J. Am. Chem. Soc.* **1970**, *92*, 1173–1179.
(259) Gold, K.; Churchill, M. R. The Crystal Structure and Molecular Configuration of an Asymmetric 1,2-Dimethyl-1,2-dicarbollide Complex of Nickel, Racemic (3,4′)-$[(CH_8)_2B_9C_2H_9]_2Ni$. *J. Am. Chem. Soc.* **1970**, *92*, 1180–1187.
(260) Hawthorne, M. F.; Dunks, G. B. Metallocarboranes That Exhibit Novel Chemical Features: A Virtually Unlimited Variety of Structural and Dynamic Features are Observed in Metallocarborane Chemistry. *Science* **1972**, *178*, 462–471.
(261) Hawthorne, M. F.; Zink, J. I.; Skelton, J. M.; Bayer, M. J.; Liu, C.; Livshits, E.; Baer, R.; Neuhauser, D. Electrical or Photocontrol of the Rotary Motion of a Metallacarborane. *Science* **2004**, *303*, 1849–1851.
(262) Rebek, J. Binding Forces, Equilibria and Rates: New Models for Enzymic Catalysis. *Acc. Chem. Res.* **1984**, *17*, 258–264.
(263) Rebek, J.; Trend, J. E.; Wattley, R. V.; Chakravorti, S. Allosteric Effects in Organic Chemistry. Site-specific Binding. *J. Am. Chem. Soc.* **1979**, *101*, 4333–4337.
(264) Rebek, J.; Wattley, R. V. Allosteric Effects. Remote Control of Ion Transport Selectivity. *J. Am. Chem. Soc.* **1980**, *102*, 4853–4854.
(265) Rebek, J.; Costello, T.; Marshall, L.; Wattley, R.; Gadwood, R. C.; Onan, K. Allosteric Effects in Organic Chemistry: Binding Cooperativity in a Model for Subunit Interactions. *J. Am. Chem. Soc.* **1985**, *107*, 7481–7487.
(266) van Veggel, F. C. J. M.; Verboom, W.; Reinhoudt, D. N. Metallomacrocycles: Supramolecular Chemistry with Hard and Soft Metal Cations in Action. *Chem. Rev.* **1994**, *94*, 279–299.
(267) Linton, B.; Hamilton, A. D. Formation of Artificial Receptors by Metal-Templated Self-Assembly. *Chem. Rev.* **1997**, *97*, 1669–1680.
(268) Robertson, A.; Shinkai, S. Cooperative Binding in Selective Sensors, Catalysts and Actuators. *Coord. Chem. Rev.* **2000**, *205*, 157–199.
(269) Shinkai, S.; Ikeda, M.; Sugasaki, A.; Takeuchi, M. Positive Allosteric Systems Designed on Dynamic Supramolecular Scaffolds: Toward Switching and Amplification of Guest Affinity and Selectivity. *Acc. Chem. Res.* **2001**, *34*, 494–503.
(270) Kovbasyuk, L.; Krämer, R. Allosteric Supramolecular Receptors and Catalysts. *Chem. Rev.* **2004**, *104*, 3161–3188.
(271) Chong, Y. S.; Smith, M. D.; Shimizu, K. D. A Conformationally Programmable Ligand. *J. Am. Chem. Soc.* **2001**, *123*, 7463–7464.
(272) Degenhardt, C. F.; Lavin, J. M.; Smith, M. D.; Shimizu, K. D. Conformationally Imprinted Receptors: Atropisomers with "Write", "Save", and "Erase" Recognition Properties. *Org. Lett.* **2005**, *7*, 4079–4081.
(273) Leighton, P.; Sanders, J. K. M. A Molecular Switch for Control of Conformation: Strained Intramolecular Co-ordination in 4,4′-Bipyridyl-capped Zinc Porphyrins. *J. Chem. Soc., Chem. Commun.* **1984**, 854–856.
(274) Abraham, R. J.; Leighton, P.; Sanders, J. K. M. = Coordination Chemistry and Geometries of Some 4,4′-Bipyridyl-capped Porphyrins. Proton- and Ligand-induced Switching of Conformations. *J. Am. Chem. Soc.* **1985**, *107*, 3472–3478.
(275) Mendez-Arroyo, J.; Barroso-Flores, J.; Lifschitz, A. M.; Sarjeant, A. A.; Stern, C. L.; Mirkin, C. A. A Multi-state, Allosterically-regulated Molecular Receptor with Switchable Selectivity. *J. Am. Chem. Soc.* **2014**, *136*, 10340–10348.
(276) Kennedy, R. D.; Machan, C. W.; McGuirk, C. M.; Rosen, M. S.; Stern, C. L.; Sarjeant, A. A.; Mirkin, C. A. General Strategy for the Synthesis of Rigid Weak-link Approach Platinum(II) Complexes: Tweezers, Triple-layer Complexes, and Macrocycles. *Inorg. Chem.* **2013**, *52*, 5876–5888.
(277) Kuwabara, J.; Yoon, H. J.; Mirkin, C. A.; DiPasquale, A. G.; Rheingold, A. L. Pseudo-allosteric Regulation of the Anion Binding Affinity of a Macrocyclic Coordination Complex. *Chem. Commun.* **2009**, 4557–4559.
(278) Shinkai, S.; Nakaji, T.; Ogawa, T.; Shigematsu, K.; Manabe, O. Photoresponsive Crown Ethers. 2. Photocontrol of Ion Extraction and Ion Transport by a Bis(crown ether) with a Butterfly-like Motion. *J. Am. Chem. Soc.* **1981**, *103*, 111–115.
(279) Hunter, C. A.; Anderson, H. L. What is Cooperativity? *Angew. Chem., Int. Ed.* **2009**, *48*, 7488–7499.
(280) Klarner, F. G.; Kahlert, B. Molecular Tweezers and Clips as Synthetic Receptors. Molecular Recognition and Dynamics in Receptor-substrate Complexes. *Acc. Chem. Res.* **2003**, *36*, 919–932.
(281) Harmata, M. Chiral Molecular Tweezers. *Acc. Chem. Res.* **2004**, *37*, 862–873.
(282) Poulsen, T.; Nielsen, K. A.; Bond, A. D.; Jeppesen, J. O. Bis(tetrathiafulvalene)-Calix[2]pyrrole[2]- thiophene and Its Complexation with TCNQ. *Org. Lett.* **2007**, *9*, 5485–5488.
(283) Sijbesma, R. P.; Wijmenga, S. S.; Nolte, R. J. M. A Molecular Clip That Binds Aromatic Guests by an Induced-fit Mechanism. *J. Am. Chem. Soc.* **1992**, *114*, 9807–9813.
(284) Rowan, A. E.; Elemans, J. A. A. W.; Nolte, R. J. M. Molecular and Supramolecular Objects from Glycoluril. *Acc. Chem. Res.* **1999**, *32*, 995–1006.
(285) Reek, J. N. H.; Engelkamp, H.; Rowan, A. E.; Elemans, J. A. A. W.; Nolte, R. J. M. Conformational Behavior and Binding Properties of Naphthalene-Walled Clips. *Chem. - Eur. J.* **1998**, *4*, 716–722.
(286) Sijbesma, R. P.; Nolte, R. J. M. A Molecular Clip with Allosteric Binding Properties. *J. Am. Chem. Soc.* **1991**, *113*, 6695–6696.
(287) Klarner, F. G.; Benkhoff, J.; Boese, R.; Burkert, U.; Kamieth, M.; Naatz, U. Molecular Tweezers as Synthetic Receptors in Host-guest Chemistry: Inclusion of Cyclohexane and Self-assembly of Aliphatic Side Chains. *Angew. Chem., Int. Ed. Engl.* **1996**, *35*, 1130–1133.
(288) Petitjean, A.; Khoury, R. G.; Kyritsakas, N.; Lehn, J.-M. Dynamic Devices. Shape Switching and Substrate Binding in Ion-Controlled Nanomechanical Molecular Tweezers. *J. Am. Chem. Soc.* **2004**, *126*, 6637–6647.
(289) Hoffmann, R. W. Flexible Molecules with Defined Shape—Conformational Design. *Angew. Chem., Int. Ed. Engl.* **1992**, *31*, 1124–1134.
(290) Yuasa, H.; Hashimoto, H. Bending Trisaccharides by a Chelation-Induced Ring Flip of a Hinge-Like Monosaccharide Unit. *J. Am. Chem. Soc.* **1999**, *121*, 5089–5090.
(291) Izumi, T.; Hashimoto, H.; Yuasa, H. Switching Extended 1,3-Diequatorial and Bent 1,3-Diaxial States of a Disubstituted Hinge Sugar by Ligand Exchange Reactions on Pt(II). *Chem. Commun.* **2004**, 94–95.
(292) Menger, F. M.; Chicklo, P. A.; Sherrod, M. J. Ion-induced Conformational Changes in Kemp's Triacid. *Tetrahedron Lett.* **1989**, *30*, 6943–6946.

DOI: 10.1021/acs.chemrev.5b00146
Chem. Rev. 2015, 115, 10081–10206

(293) Shirodkar, S. M.; Weisman, G. R. Cyclohexane-based 1,3-Dipodands: Complexation and Conformational Biasing. *J. Chem. Soc., Chem. Commun.* **1989**, 236−238.
(294) Raban, M.; Burch, D. L.; Hortelano, E. R.; Durocher, D.; Kost, D. Complete Conformational Switching in a Calcium Ionophore. *J. Org. Chem.* **1994**, *59*, 1283−1287.
(295) Kemp, D. S.; Petrakis, K. S. Synthesis and Conformational Analysis of *cis,cis*-1,3,5-Trimethylcyclohexane-1,3,5-tricarboxylic acid. *J. Org. Chem.* **1981**, *46*, 5140−5143.
(296) Samoshin, V. V.; Chertkov, V. A.; Vatlina, L. P.; Dobretsova, E. K.; Simonov, N. A.; Kastorsky, L. P.; Gremyachinsky, D. E.; Schneider, H.-J. *trans*-1,2-Cyclohexanedicarboxylic Acid Derivatives as pH-Trigger for Conformationally Controlled Crowns. *Tetrahedron Lett.* **1996**, *37*, 3981−3984.
(297) Gil de Oliveira Santos, A.; Klute, W.; Torode, J.; P. W. Bohm, V.; Cabrita, E.; Runsink, J.; W. Hoffmann, R. Flexible Molecules with Defined Shape. X. Synthesis and Conformational Study of 1,5-Diaza-*cis*-decalin. *New J. Chem.* **1998**, *22*, 993−997.
(298) Collin, J.-P.; Durola, F.; Heitz, V.; Reviriego, F.; Sauvage, J.-P.; Trolez, Y. A Cyclic [4]rotaxane that Behaves as a Switchable Molecular Receptor: Formation of a Rigid Scaffold from a Collapsed Structure by Complexation with Copper(I) Ions. *Angew. Chem., Int. Ed.* **2010**, *49*, 10172−10175.
(299) Haberhauer, G. Control of Planar Chirality: The Construction of a Copper-Ion-Controlled Chiral Molecular Hinge. *Angew. Chem., Int. Ed.* **2008**, *47*, 3635−3638.
(300) Haberhauer, G. A Metal-Ion-Driven Supramolecular Chirality Pendulum. *Angew. Chem., Int. Ed.* **2010**, *49*, 9286−9289.
(301) Haberhauer, G.; Kallweit, C. A Bridged Azobenzene Derivative as a Reversible, Light-Induced Chirality Switch. *Angew. Chem., Int. Ed.* **2010**, *49*, 2418−2421.
(302) Timmerman, P.; Verboom, W.; Reinhoudt, D. N. Resorcinarenes. *Tetrahedron* **1996**, *52*, 2663−2704.
(303) Moran, J. R.; Ericson, J. L.; Dalcanale, E.; Bryant, J. A.; Knobler, C. B.; Cram, D. J. Vases and Kites as Cavitands. *J. Am. Chem. Soc.* **1991**, *113*, 5707−5714.
(304) Moran, J. R.; Karbach, S.; Cram, D. J. Cavitands: Synthetic Molecular Vessels. *J. Am. Chem. Soc.* **1982**, *104*, 5826−5828.
(305) Skinner, P. J.; Cheetham, A. G.; Beeby, A.; Gramlich, V.; Diederich, F. Conformational Switching of Resorcin[4]arene Cavitands by Protonation, Preliminary Communication. *Helv. Chim. Acta* **2001**, *84*, 2146−2153.
(306) Azov, V. A.; Diederich, F.; Lill, Y.; Hecht, B. Synthesis and Conformational Switching of Partially and Differentially Bridged Resorcin[4]arenes Bearing Fluorescent Dye Labels. Preliminary Communication. *Helv. Chim. Acta* **2003**, *86*, 2149−2155.
(307) Azov, V. A.; Jaun, B.; Diederich, F. NMR Investigations into the Vase-Kite Conformational Switching of Resorcin[4]arene Cavitands. *Helv. Chim. Acta* **2004**, *87*, 449−462.
(308) Frei, M.; Marotti, F.; Diederich, F. Zn^{II}-induced Conformational Control of Amphiphilic Cavitands in Langmuir Monolayers. *Chem. Commun.* **2004**, 1362−1363.
(309) Pochorovski, I.; Ebert, M.-O.; Gisselbrecht, J.-P.; Boudon, C.; Schweizer, W. B.; Diederich, F. Redox-Switchable Resorcin[4]arene Cavitands: Molecular Grippers. *J. Am. Chem. Soc.* **2012**, *134*, 14702−14705.
(310) Pochorovski, I.; Milić, J.; Kolarski, D.; Gropp, C.; Schweizer, W. B.; Diederich, F. Evaluation of Hydrogen-Bond Acceptors for Redox-Switchable Resorcin[4]arene Cavitands. *J. Am. Chem. Soc.* **2014**, *136*, 3852−3858.
(311) Rudkevich, D. M.; Hilmersson, G.; Rebek, J. Intramolecular Hydrogen Bonding Controls the Exchange Rates of Guests in a Cavitand. *J. Am. Chem. Soc.* **1997**, *119*, 9911−9912.
(312) Rudkevich, D. M.; Hilmersson, G.; Rebek, J. Self-Folding Cavitands. *J. Am. Chem. Soc.* **1998**, *120*, 12216−12225.
(313) Ma, S.; Rudkevich, D. M.; Rebek, J. J. Supramolecular Isomerism in Caviplexes. *Angew. Chem., Int. Ed.* **1999**, *38*, 2600−2602.
(314) Tucci, F. C.; Rudkevich, D. M.; Rebek, J. J. Velcrands with Snaps and Their Conformational Control. *Chem. - Eur. J.* **2000**, *6*, 1007−1016.
(315) Haino, T.; Rudkevich, D. M.; Shivanyuk, A.; Rissanen, K.; Rebek, J. J. Induced-Fit Molecular Recognition with Water-Soluble Cavitands. *Chem. - Eur. J.* **2000**, *6*, 3797−3805.
(316) Far, A. R.; Shivanyuk, A.; Rebek, J. Water-Stabilized Cavitands. *J. Am. Chem. Soc.* **2002**, *124*, 2854−2855.
(317) Amrhein, P.; Wash, P. L.; Shivanyuk, A.; Rebek, J. Metal Ligation Regulates Conformational Equilibria and Binding Properties of Cavitands. *Org. Lett.* **2002**, *4*, 319−321.
(318) Tucker, J. A.; Knobler, C. B.; Trueblood, K. N.; Cram, D. J. Host-guest Complexation. 49. Cavitands Containing Two Binding Cavities. *J. Am. Chem. Soc.* **1989**, *111*, 3688−3699.
(319) Amrhein, P.; Shivanyuk, A.; Johnson, D. W.; Rebek, J. Metal-Switching and Self-Inclusion of Functional Cavitands. *J. Am. Chem. Soc.* **2002**, *124*, 10349−10358.
(320) Ikeda, A.; Shinkai, S. Novel Cavity Design Using Calix[n]arene Skeletons: Toward Molecular Recognition and Metal Binding. *Chem. Rev.* **1997**, *97*, 1713−1734.
(321) Ashton, P. R.; Ballardini, R.; Balzani, V.; Boyd, S. E.; Credi, A.; Gandolfi, M. T.; Gómez-López, M.; Iqbal, S.; Philp, D.; Preece, J. A. Simple Mechanical Molecular and Supramolecular Machines: Photochemical and Electrochemical Control of Switching Processes. *Chem. - Eur. J.* **1997**, *3*, 152−170.
(322) Ashton, P. R.; Gómez-López, M.; Iqbal, S.; Preece, J. A.; Stoddart, J. F. A Self-Complexing Macrocycle Acting as a Chromophoric Receptor. *Tetrahedron Lett.* **1997**, *38*, 3635−3638.
(323) Brondsted Nielsen, M.; Becher, J. 'Self-complexing' Tetrathiafulvalene Macrocycles; A Tetrathiafulvalene Switch. *Chem. Commun.* **1998**, 475−476.
(324) Brøndsted Nielsen, M.; Hansen, J. G.; Becher, J. Self-Complexing Tetrathiafulvalene-Based Donor−Acceptor Macrocycles. *Eur. J. Org. Chem.* **1999**, *1999*, 2807−2815.
(325) Balzani, V.; Ceroni, P.; Credi, A.; Gomez-Lopez, M.; Hamers, C.; Stoddart, J. F.; Wolf, R. Controlled Dethreading/rethreading of a Scorpion-like Pseudorotaxane and a Related Macrobicyclic Self-complexing System. *New J. Chem.* **2001**, *25*, 25−31.
(326) Liu, Y.; Flood, A. H.; Stoddart, J. F. Thermally and Electrochemically Controllable Self-Complexing Molecular Switches. *J. Am. Chem. Soc.* **2004**, *126*, 9150−9151.
(327) Qu, D.-H.; Feringa, B. L. Controlling Molecular Rotary Motion with a Self-Complexing Lock. *Angew. Chem., Int. Ed.* **2010**, *49*, 1107−1110.
(328) Jones, I. M.; Lingard, H.; Hamilton, A. D. pH-Dependent Conformational Switching in 2,6-Benzamidodiphenylacetylenes. *Angew. Chem., Int. Ed.* **2011**, *50*, 12569−12571.
(329) Pramanik, S.; De, S.; Schmittel, M. Bidirectional Chemical Communication between Nanomechanical Switches. *Angew. Chem., Int. Ed.* **2014**, *53*, 4709−4713.
(330) Dolain, C.; Maurizot, V.; Huc, I. Protonation-Induced Transition between Two Distinct Helical Conformations of a Synthetic Oligomer via a Linear Intermediate. *Angew. Chem., Int. Ed.* **2003**, *42*, 2738−2740.
(331) Piguet, C.; Bernardinelli, G.; Hopfgartner, G. Helicates as Versatile Supramolecular Complexes. *Chem. Rev.* **1997**, *97*, 2005−2062.
(332) Hill, D. J.; Mio, M. J.; Prince, R. B.; Hughes, T. S.; Moore, J. S. A Field Guide to Foldamers. *Chem. Rev.* **2001**, *101*, 3893−4012.
(333) Cheng, R. P.; Gellman, S. H.; DeGrado, W. F. β-Peptides: From Structure to Function. *Chem. Rev.* **2001**, *101*, 3219−3232.
(334) Albrecht, M. Let's Twist Again"Double-Stranded, Triple-Stranded, and Circular Helicates. *Chem. Rev.* **2001**, *101*, 3457−3498.
(335) Williams, A. Helical Complexes and Beyond. *Chem. - Eur. J.* **1997**, *3*, 15−19.
(336) Gellman, S. H. Foldamers: A Manifesto. *Acc. Chem. Res.* **1998**, *31*, 173−180.
(337) Rowan, A. E.; Nolte, R. J. M. Helical Molecular Programming. *Angew. Chem., Int. Ed.* **1998**, *37*, 63−68.
(338) Cubberley, M. S.; Iverson, B. L. Models of Higher-order Structure: Foldamers and Beyond. *Curr. Opin. Chem. Biol.* **2001**, *5*, 650−653.

DOI: 10.1021/acs.chemrev.5b00146
Chem. Rev. 2015, 115, 10081−10206

(339) Schmuck, C. Molecules with Helical Structure: How To Build a Molecular Spiral Staircase. *Angew. Chem., Int. Ed.* **2003**, *42*, 2448−2452.
(340) Albrecht, M. Artificial Molecular Double-Stranded Helices. *Angew. Chem., Int. Ed.* **2005**, *44*, 6448−6451.
(341) Gong, B. Crescent Oligoamides: From Acyclic "Macrocycles" to Folding Nanotubes. *Chem. - Eur. J.* **2001**, *7*, 4336−4342.
(342) Sanford, A. R.; Yamato, K.; Yang, X.; Yuan, L.; Han, Y.; Gong, B. Well-defined Secondary Structures. *Eur. J. Biochem.* **2004**, *271*, 1416−1425.
(343) Huc, I. Aromatic Oligoamide Foldamers. *Eur. J. Org. Chem.* **2004**, *2004*, 17−29.
(344) Constable, E. C. Oligopyridines as Helicating Ligands. *Tetrahedron* **1992**, *48*, 10013−10059.
(345) Seebach, D.; Matthews, J. *β*-Peptides: A Surprise at Every Turn. *Chem. Commun.* **1997**, 2015−2022.
(346) Nielsen, P. E.; Haaima, G. Peptide Nucleic Acid (PNA). A DNA Mimic with a Pseudopeptide Backbone. *Chem. Soc. Rev.* **1997**, *26*, 73−78.
(347) Nowick, J. S. Chemical Models of Protein *β*-Sheets. *Acc. Chem. Res.* **1999**, *32*, 287−296.
(348) Stigers, K. D.; Soth, M. J.; Nowick, J. S. Designed Molecules that Fold to Mimic Protein Secondary Structures. *Curr. Opin. Chem. Biol.* **1999**, *3*, 714−723.
(349) Nielsen, P. E. Peptide Nucleic Acid. A Molecule with Two Identities. *Acc. Chem. Res.* **1999**, *32*, 624−630.
(350) Kirshenbaum, K.; Zuckermann, R. N.; Dill, K. A. Designing Polymers That Mimic Biomolecules. *Curr. Opin. Struct. Biol.* **1999**, *9*, 530−535.
(351) Herdewijn, P. Conformationally Restricted Carbohydrate-modified Nucleic Acids and Antisense Technology. *Biochim. Biophys. Acta, Gene Struct. Expression* **1999**, *1489*, 167−179.
(352) Patch, J. A.; Barron, A. E. Mimicry of Bioactive Peptides via Non-natural, Sequence-specific Peptidomimetic Oligomers. *Curr. Opin. Chem. Biol.* **2002**, *6*, 872−877.
(353) Martinek, T. A.; Fülöp, F. Side-chain Control of *β*-Peptide Secondary Structures. *Eur. J. Biochem.* **2003**, *270*, 3657−3666.
(354) Cheng, R. P. Beyond *de novo* Protein Design — *de novo* Design of Non-natural Folded Oligomers. *Curr. Opin. Struct. Biol.* **2004**, *14*, 512−520.
(355) Licini, G.; Prins, L. J.; Scrimin, P. Oligopeptide Foldamers: From Structure to Function. *Eur. J. Org. Chem.* **2005**, *2005*, 969−977.
(356) Nelson, J. C.; Saven, J. G.; Moore, J. S.; Wolynes, P. G. Solvophobically Driven Folding of Nonbiological Oligomers. *Science* **1997**, *277*, 1793−1796.
(357) Prince, R. B.; Saven, J. G.; Wolynes, P. G.; Moore, J. S. Cooperative Conformational Transitions in Phenylene Ethynylene Oligomers: Chain-Length Dependence. *J. Am. Chem. Soc.* **1999**, *121*, 3114−3121.
(358) Lahiri, S.; Thompson, J. L.; Moore, J. S. Solvophobically Driven *π*-Stacking of Phenylene Ethynylene Macrocycles and Oligomers. *J. Am. Chem. Soc.* **2000**, *122*, 11315−11319.
(359) Hill, D. J.; Moore, J. S. Helicogenicity of Solvents in the Conformational Equilibrium of Oligo(m-phenylene ethynylene)s: Implications for Foldamer Research. *Proc. Natl. Acad. Sci. U. S. A.* **2002**, *99*, 5053−5057.
(360) Hofacker, A. L.; Parquette, J. R. Dendrimer Folding in Aqueous Media: An Example of Solvent-Mediated Chirality Switching. *Angew. Chem., Int. Ed.* **2005**, *44*, 1053−1057.
(361) Berl, V.; Huc, I.; Khoury, R. G.; Krische, M. J.; Lehn, J.-M. Interconversion of Single and Double Helices Formed from Synthetic Molecular Strands. *Nature* **2000**, *407*, 720−723.
(362) Berl, V.; Huc, I.; Khoury, R. G.; Lehn, J.-M. Helical Molecular Programming: Folding of Oligopyridine-dicarboxamides into Molecular Single Helices. *Chem. - Eur. J.* **2001**, *7*, 2798−2809.
(363) Berl, V.; Huc, I.; Khoury, R. G.; Lehn, J.-M. Helical Molecular Programming: Supramolecular Double Helices by Dimerization of Helical Oligopyridine-dicarboxamide Strands. *Chem. - Eur. J.* **2001**, *7*, 2810−2820.
(364) Hanan, G. S.; Lehn, J.-M.; Kyritsakas, N.; Fischer, J. Molecular Helicity: A General Approach for Helicity Induction in a Polyheterocyclic Molecular Strand. *J. Chem. Soc., Chem. Commun.* **1995**, 765−766.
(365) Bassani, D. M.; Lehn, J.-M.; Baum, G.; Fenske, D. Designed Self-Generation of an Extended Helical Structure From an Achiral Polyheterocylic Strand. *Angew. Chem., Int. Ed. Engl.* **1997**, *36*, 1845−1847.
(366) Ohkita, M.; Lehn, J.-M.; Baum, G.; Fenske, D. Helicity Coding: Programmed Molecular Self-Organization of Achiral Nonbiological Strands into Multiturn Helical Superstructures: Synthesis and Characterization of Alternating Pyridine−Pyrimidine Oligomers. *Chem. - Eur. J.* **1999**, *5*, 3471−3481.
(367) Stadler, A.-M.; Kyritsakas, N.; Lehn, J.-M. Reversible Folding/unfolding of Linear Molecular Strands into Helical Channel-like Complexes upon Proton-modulated Binding and Release of Metal Ions. *Chem. Commun.* **2004**, 2024−2025.
(368) Kolomiets, E.; Berl, V.; Odriozola, I.; Stadler, A.-M.; Kyritsakas, N.; Lehn, J.-M. Contraction/extension Molecular Motion by Protonation/deprotonation Induced Structural Switching of Pyridine Derived Oligoamides. *Chem. Commun.* **2003**, 2868−2869.
(369) Barboiu, M.; Lehn, J.-M. Dynamic Chemical Devices: Modulation of Contraction/extension Molecular Motion by Coupled-ion Binding/pH Change-induced Structural Switching. *Proc. Natl. Acad. Sci. U. S. A.* **2002**, *99*, 5201−5206.
(370) Barboiu, M.; Vaughan, G.; Kyritsakas, N.; Lehn, J.-M. Dynamic Chemical Devices: Generation of Reversible Extension/Contraction Molecular Motion by Ion-Triggered Single/Double Helix Interconversion. *Chem. - Eur. J.* **2003**, *9*, 763−769.
(371) Stadler, A.-M.; Lehn, J.-M. P. Coupled Nanomechanical Motions: Metal-Ion-Effected, pH-Modulated, Simultaneous Extension/Contraction Motions of Double-Domain Helical/Linear Molecular Strands. *J. Am. Chem. Soc.* **2014**, *136*, 3400−3409.
(372) Dugave, C.; Demange, L. *cis-trans* Isomerization of Organic Molecules and Biomolecules: Implications and Applications. *Chem. Rev.* **2003**, *103*, 2475−2532.
(373) Waldeck, D. H. Photoisomerization Dynamics of Stilbenes. *Chem. Rev.* **1991**, *91*, 415−436.
(374) Bandara, H. M.; Burdette, S. C. Photoisomerization in Different Classes of Azobenzene. *Chem. Soc. Rev.* **2012**, *41*, 1809−1825.
(375) Cheetham, A. G.; Hutchings, M. G.; Claridge, T. D. W.; Anderson, H. L. Enzymatic Synthesis and Photoswitchable Enzymatic Cleavage of a Peptide-linked Rotaxane. *Angew. Chem., Int. Ed.* **2006**, *45*, 1596−1599.
(376) Haberhauer, G.; Kallweit, C.; Wölper, C.; Bläser, D. An Azobenzene Unit Embedded in a Cyclopeptide as a Type-Specific and Spatially Directed Switch. *Angew. Chem., Int. Ed.* **2013**, *52*, 7879−7882.
(377) Clever, G. H.; Tashiro, S.; Shionoya, M. Light-Triggered Crystallization of a Molecular Host-Guest Complex. *J. Am. Chem. Soc.* **2010**, *132*, 9973−9975.
(378) Irie, M. Diarylethenes for Memories and Switches. *Chem. Rev.* **2000**, *100*, 1685−1716.
(379) Irie, M. Photochromism: Memories and Switches - Introduction. *Chem. Rev.* **2000**, *100*, 1683−1683.
(380) van Herpt, J. T.; Areephong, J.; Stuart, M. C.; Browne, W. R.; Feringa, B. L. Light-controlled Formation of Vesicles and Supramolecular Organogels by a Cholesterol-bearing Amphiphilic Molecular Switch. *Chem. - Eur. J.* **2014**, *20*, 1737−1742.
(381) Hou, L.; Zhang, X.; Pijper, T. C.; Browne, W. R.; Feringa, B. L. Reversible Photochemical Control of Singlet Oxygen Generation Using Diarylethene Photochromic Switches. *J. Am. Chem. Soc.* **2014**, *136*, 910−913.
(382) Kudernac, T.; Kobayashi, T.; Uyama, A.; Uchida, K.; Nakamura, S.; Feringa, B. L. Tuning the Temperature Dependence for Switching in Dithienylethene Photochromic Switches. *J. Phys. Chem. A* **2013**, *117*, 8222−8229.
(383) Yokoyama, Y. Fulgides for Memories and Switches. *Chem. Rev.* **2000**, *100*, 1717−1739.

DOI: 10.1021/acs.chemrev.5b00146
Chem. Rev. 2015, 115, 10081−10206

(384) Santiago, A.; Becker, R. S. Photochromic Fulgides - Spectroscopy and Mechanism of Photoreactions. *J. Am. Chem. Soc.* **1968**, *90*, 3654−3658.
(385) Berkovic, G.; Weiss, V. Spiropyrans and Spirooxazines for Memories and Switches. *Chem. Rev.* **2000**, *100*, 1741−1753.
(386) Feringa, B. L.; Huck, N. P. M.; Schoevaars, A. M. Chiroptical Molecular Switches. *Adv. Mater.* **1996**, *8*, 681−684.
(387) Feringa, B. L.; van Delden, R. A.; Koumura, N.; Geertsema, E. M. Chiroptical Molecular Switches. *Chem. Rev.* **2000**, *100*, 1789−1816.
(388) Browne, B. L. F. a. W. *Molecular Switches*, 2nd ed.; Wiley-VCH: Weinheim, 2011.
(389) Shinkai, S.; Honda, Y.; Kusano, Y.; Manabe, O. A Photoresponsive Cylindrical Ionophore. *J. Chem. Soc., Chem. Commun.* **1982**, 848−850.
(390) Feringa, B. L.; Jager, W. F.; de Lange, B. Organic Materials for Reversible Optical Data Storage. *Tetrahedron* **1993**, *49*, 8267−8310.
(391) Momotake, A.; Arai, T. Synthesis, Excited State Properties, and Dynamic Structural Change of Photoresponsive Dendrimers. *Polymer* **2004**, *45*, 5369−5390.
(392) Momotake, A.; Arai, T. Photochemistry and Photophysics of Stilbene Dendrimers and Related Compounds. *J. Photochem. Photobiol., C* **2004**, *5*, 1−25.
(393) Tie, C.; Gallucci, J. C.; Parquette, J. R. Helical Conformational Dynamics and Photoisomerism of Alternating Pyridinedicarboxamide/*m*-(Phenylazo)azobenzene Oligomers. *J. Am. Chem. Soc.* **2006**, *128*, 1162−1171.
(394) Yager, K. G.; Barrett, C. J. Novel Photo-switching Using Azobenzene Functional Materials. *J. Photochem. Photobiol., A* **2006**, *182*, 250−261.
(395) Russew, M. M.; Hecht, S. Photoswitches: From Molecules to Materials. *Adv. Mater.* **2010**, *22*, 3348−3360.
(396) Fischer, G. Peptidyl-Prolyl *cis/trans* Isomerases and Their Effectors. *Angew. Chem., Int. Ed. Engl.* **1994**, *33*, 1415−1436.
(397) Fischer, G. Chemical Aspects of Peptide Bond Isomerization. *Chem. Soc. Rev.* **2000**, *29*, 119−127.
(398) Beharry, A. A.; Woolley, G. A. Azobenzene Photoswitches for Biomolecules. *Chem. Soc. Rev.* **2011**, *40*, 4422−4437.
(399) Beharry, A. A.; Wong, L.; Tropepe, V.; Woolley, G. A. Fluorescence Imaging of Azobenzene Photoswitching *In Vivo*. *Angew. Chem., Int. Ed.* **2011**, *50*, 1325−1327.
(400) Szymanski, W.; Beierle, J. M.; Kistemaker, H. A.; Velema, W. A.; Feringa, B. L. Reversible Photocontrol of Biological Systems by the Incorporation of Molecular Photoswitches. *Chem. Rev.* **2013**, *113*, 6114−6178.
(401) Kienzler, M. A.; Reiner, A.; Trautman, E.; Yoo, S.; Trauner, D.; Isacoff, E. Y. A Red-Shifted, Fast-Relaxing Azobenzene Photoswitch for Visible Light Control of an Ionotropic Glutamate Receptor. *J. Am. Chem. Soc.* **2013**, *135*, 17683−17686.
(402) Kamiya, Y.; Asanuma, H. Light-Driven DNA Nanomachine with a Photoresponsive Molecular Engine. *Acc. Chem. Res.* **2014**, *47*, 1663−1672.
(403) Velema, W. A.; Szymanski, W.; Feringa, B. L. Photopharmacology: Beyond Proof of Principle. *J. Am. Chem. Soc.* **2014**, *136*, 2178−2191.
(404) Velema, W. A.; van der Berg, J. P.; Hansen, M. J.; Szymanski, W.; Driessen, A. J.; Feringa, B. L. Optical Control of Antibacterial Activity. *Nat. Chem.* **2013**, *5*, 924−928.
(405) Szymanski, W.; Yilmaz, D.; Kocer, A.; Feringa, B. L. Bright Ion Channels and Lipid Bilayers. *Acc. Chem. Res.* **2013**, *46*, 2910−2923.
(406) Kocer, A.; Walko, M.; Meijberg, W.; Feringa, B. L. A Light-actuated Nanovalve Derived from a Channel Protein. *Science* **2005**, *309*, 755−758.
(407) Muraoka, T.; Kinbara, K.; Aida, T. Mechanical Twisting of a Guest by a Photoresponsive Host. *Nature* **2006**, *440*, 512−515.
(408) Muraoka, T.; Kinbara, K.; Aida, T. Reversible Operation of Chiral Molecular Scissors by Redox and UV Light. *Chem. Commun.* **2007**, 1441−1443.
(409) Merino, E.; Ribagorda, M. Control Over Molecular Motion Using the *cis-trans* Photoisomerization of the Azo Group. *Beilstein J. Org. Chem.* **2012**, *8*, 1071−1090.
(410) Marchi, E.; Baroncini, M.; Bergamini, G.; Van Heyst, J.; Vogtle, F.; Ceroni, P. Photoswitchable Metal Coordinating Tweezers Operated by Light-harvesting Dendrimers. *J. Am. Chem. Soc.* **2012**, *134*, 15277−15280.
(411) Raymo, F. M. Intermolecular Coupling of Motion Under Photochemical Control. *Angew. Chem., Int. Ed.* **2006**, *45*, 5249−5251.
(412) Kai, H.; Nara, S.; Kinbara, K.; Aida, T. Toward Long-distance Mechanical Communication: Studies on a Ternary Complex Interconnected by a Bridging Rotary Module. *J. Am. Chem. Soc.* **2008**, *130*, 6725−6727.
(413) Muraoka, T.; Kinbara, K.; Kobayashi, Y.; Aida, T. Light-Driven Open-Close Motion of Chiral Molecular Scissors. *J. Am. Chem. Soc.* **2003**, *125*, 5612−5613.
(414) Norikane, Y.; Tamaoki, N. Light-Driven Molecular Hinge: A New Molecular Machine Showing a Light-Intensity-Dependent Photoresponse that Utilizes the Trans-Cis Isomerization of Azobenzene. *Org. Lett.* **2004**, *6*, 2595−2598.
(415) Muraoka, T.; Kinbara, K. Development of Photoresponsive Supramolecular Machines Inspired by Biological Molecular Systems. *J. Photochem. Photobiol., C* **2012**, *13*, 136−147.
(416) Li, Z.; Liang, J.; Xue, W.; Liu, G.; Liu, S. H.; Yin, J. Switchable Azo-macrocycles: From Molecules to Functionalisation. *Supramol. Chem.* **2014**, *26*, 54−65.
(417) Basheer, M. C.; Oka, Y.; Mathews, M.; Tamaoki, N. A Light-controlled Molecular Brake with Complete ON-OFF Rotation. *Chem. - Eur. J.* **2010**, *16*, 3489−3496.
(418) Hashim, P. K.; Thomas, R.; Tamaoki, N. Induction of Molecular Chirality by Circularly Polarized Light in Cyclic Azobenzene with a Photoswitchable Benzene Rotor. *Chem. - Eur. J.* **2011**, *17*, 7304−7312.
(419) Baroncini, M.; Silvi, S.; Venturi, M.; Credi, A. Reversible Photoswitching of Rotaxane Character and Interplay of Thermodynamic Stability and Kinetic Lability in a Self-assembling Ring-axle Molecular System. *Chem. - Eur. J.* **2010**, *16*, 11580−11587.
(420) Liu, F.; Morokuma, K. Computational Study on the Working Mechanism of a Stilbene Light-Driven Molecular Rotary Motor: Sloped Minimal Energy Path and Unidirectional Nonadiabatic Photoisomerization. *J. Am. Chem. Soc.* **2012**, *134*, 4864−4876.
(421) Pospíšil, L.; Bednárová, L.; Štěpánek, P.; Slavíček, P.; Vávra, J.; Hromadová, M.; Dlouhá, H.; Tarábek, J.; Teplý, F. Intense Chiroptical Switching in a Dicationic Helicene-Like Derivative: Exploration of a Viologen-Type Redox Manifold of a Non-Racemic Helquat. *J. Am. Chem. Soc.* **2014**, *136*, 10826−10829.
(422) Ruangsupapichat, N.; Pollard, M. M.; Harutyunyan, S. R.; Feringa, B. L. Reversing the Direction in a Light-driven Rotary Molecular Motor. *Nat. Chem.* **2011**, *3*, 53−60.
(423) Feringa, B. L. In Control of Motion: From Molecular Switches to Molecular Motors. *Acc. Chem. Res.* **2001**, *34*, 504−513.
(424) Feringa, B. L.; van Delden, R. A.; ter Wiel, M. K. J. In Control of Switching, Motion, and Organization. *Pure Appl. Chem.* **2003**, *75*, 563−575.
(425) Feringa, B. L. The Art of Building Small: From Molecular Switches to Molecular Motors. *J. Org. Chem.* **2007**, *72*, 6635−6652.
(426) Feringa, B. L.; Koumura, N.; van Delden, R. A.; ter Wiel, M. K. J. Light-driven Molecular Switches and Motors. *Appl. Phys. A: Mater. Sci. Process.* **2002**, *75*, 301−308.
(427) Feringa, B. L. Molecular Switches and Motors. *AIP Conf. Proc.* **2013**, *1519*, 73−75.
(428) Cnossen, A.; Browne, W. R.; Feringa, B. L. Unidirectional Light-Driven Molecular Motors Based on Overcrowded Alkenes. *Top. Curr. Chem.* **2014**, *354*, 139−162.
(429) Koumura, N.; Zijlstra, R. W. J.; van Delden, R. A.; Harada, N.; Feringa, B. L. Light-driven Monodirectional Molecualr Rotor. *Nature* **1999**, *401*, 152−155.
(430) Harada, N.; Koumura, N.; Feringa, B. L. Chemistry of Unique Chiral Olefins. 3. synthesis and Absolute Stereochemistry of trans-and

DOI: 10.1021/acs.chemrev.5b00146
Chem. Rev. 2015, 115, 10081−10206

cis-1,1′,2,2′3,3′,4,4′-Octahydro-3,3′-dimethyl-4,4′-biphenanthrylidenes. *J. Am. Chem. Soc.* **1997**, *119*, 7256−7264.
(431) Harada, N.; Saito, A.; Koumura, N.; Uda, H.; deLange, B.; Jager, W. F.; Wynberg, H.; Feringa, B. L. Chemistry of Unique Chiral Olefins 0.1. Synthesis, Enantioresolution, Circular Dichroism, and Theoretical Determination of the Absolute Stereochemistry of *trans*- and *cis*-1,1′,2,2′,3,3′,4,4′-octahydro-4,4′-biphenanthrylidenes. *J. Am. Chem. Soc.* **1997**, *119*, 7241−7248.
(432) Harada, N.; Saito, A.; Koumura, N.; Roe, D. C.; Jager, W. F.; Zijlstra, R. W. J.; deLange, B.; Feringa, B. L. Chemistry of Unique Chiral Olefins 0.2. Unexpected Thermal Racemization of *cis*-1,1′,2,2′,3,3′,4,4′-octahydro-4,4′-biphenanthrylidene. *J. Am. Chem. Soc.* **1997**, *119*, 7249−7255.
(433) Zijlstra, R. W. J.; van Duijnen, P. T.; Feringa, B. L.; Steffen, T.; Duppen, K.; Wiersma, D. A. Excited-State Dynamics of Tetraphenylethylene: Ultrafast Stokes Shift, Isomerization, and Charge Separation. *J. Phys. Chem. A* **1997**, *101*, 9828−9836.
(434) Koumura, N.; Harada, N. Photochemistry and Absolute Stereochemistry of Unique Chiral Olefins, *trans*- and *cis*-1,1′,2,2′,3,3′,4,4′-Octahydro-3,3′-dimethyl-4,4′-biphenanthrylidenes. *Chem. Lett.* **1998**, 1151−1152.
(435) Zijlstra, R. W. J.; Jager, W. F.; de Lange, B.; van Duijnen, P. Th.; Feringa, B. L.; Goto, H.; Saito, A.; Koumura, N.; Harada, N. Chemistry of Unique Chiral Olefins. 4. Theoretical Studies of the Racemization Mechanism of *trans*- and *cis*-1,1′,2,2′,3,3′,4,4′-Octahydro-4,4′-biphenanthrylidenes. *J. Org. Chem.* **1999**, *64*, 1667−1674.
(436) Zijlstra, R. W. J.; Jager, W. F.; de Lange, B.; van Duijnen, P. T.; Feringa, B. L.; Goto, H.; Saito, A.; Koumura, N.; Harada, N. Chemistry of Unique Chiral Olefins. 4. Theoretical Studies of the Racemization Mechanism of *trans*- and *cis*-1,1 ′,2,2 ′,3,3 ′,4,4 ′-octahydro-4,4 ′-biphenanthrylidenes. *J. Org. Chem.* **1999**, *64*, 1667−1674.
(437) ter Wiel, M. K. J.; Koumura, N.; Van Delden, R. A.; Meetsma, A.; Harada, N.; Feringa, B. L. Chiral Overcrowded Alkenes; Asymmetric Synthesis of (3*S*,3′*S*)-(*M*,*M*)-(*E*)-(+)-1,1′,2,2′,3,3′,4,4′-octahydro-3,3′,7,7′-Tetramethyl-4,4′-biphenanthrylidenes. *Chirality* **2000**, *12*, 734−741.
(438) ter Wiel, M. K. J.; van Delden, R. A.; Meetsma, A.; Feringa, B. L. Increased Speed of Rotation for The Smallest Light-Driven Molecular Motor. *J. Am. Chem. Soc.* **2003**, *125*, 15076−15086.
(439) ter Wiel, M. K. J.; van Delden, R. A.; Meetsma, A.; Feringa, B. L. Light-Driven Molecular Motors: Stepwise Thermal Helix Inversion during Unidirectional Rotation of sterically Overcrowded Biphenanthrylidenes. *J. Am. Chem. Soc.* **2005**, *127*, 14208−14222.
(440) Kuwahara, S.; Fujita, T.; Harada, N. A New Model of Light-Powered Chiral Molecular Motor with Higher Speed of Rotation, Part 2 - Dynamics of Motor Rotation. *Eur. J. Org. Chem.* **2005**, *2005*, 4544−4556.
(441) Klok, M.; Walko, M.; Geertsema, E. M.; Ruangsupapichat, N.; Kistemaker, J. C. M.; Meetsma, A.; Feringa, B. L. New Mechanistic Insight in the Thermal Helix Inversion of Second - Second Generation Moelcular Motors. *Chem. - Eur. J.* **2008**, *14*, 11183−11193.
(442) ter Wiel, M. K.; Kwit, M. G.; Meetsma, A.; Feringa, B. L. Synthesis, Stereochemistry, and Photochemical and Thermal Behavior of Bis-*tert*-butyl Substituted Overcrowded Alkenes. *Org. Biomol. Chem.* **2007**, *5*, 87−96.
(443) Pollard, M. M.; Meetsma, A.; Feringa, B. L. A Redesign of Light-driven Rotary Molecular Motors. *Org. Biomol. Chem.* **2008**, *6*, 507−512.
(444) Caroli, G.; Kwit, M. G.; Feringa, B. L. Photochemical and Thermal Behavior of Light-driven Unidirectional Molecular Motor with Long Alkyl Chains. *Tetrahedron* **2008**, *64*, 5956−5962.
(445) Koumura, N.; Geertsma, E. M.; Meetsma, A.; Feringa, B. L. Light-Driven Molecular Rotor: Unidirectional Rotation Controlled by a Single Stereogenic Center. *J. Am. Chem. Soc.* **2000**, *122*, 12005−12006.
(446) Pollard, M. M.; ter Wiel, M. K. J.; van Delden, R. A.; Vicario, J.; Koumura, N.; van den Brom, J. R.; Meetsma, A.; Feringa, B. L. Light-Driven Rotary Molecular Motors on Gold Nanoparticles. *Chem. - Eur. J.* **2008**, *14*, 11610−11622.
(447) van Delden, R. A.; Koumura, N.; Schoevaars, A.; Meetsma, A.; Feringa, B. L. A Donor−acceptor Substituted Molecular Motor: Unidirectional Rotation Driven by Visible Light. *Org. Biomol. Chem.* **2003**, *1*, 33−35.
(448) Geertsema, E. M.; Koumura, N.; ter Wiel, M. K. J.; Meetsma, A.; Feringa, B. L. In Control of the Speed of Rotation in Molecular Motors. Unexpected Retardation of Rotary Motion. *Chem. Commun.* **2002**, 2962−2963.
(449) Koumura, N.; Geertsema, E. M.; van Gelder, M. B.; Meetsma, A.; Feringa, B. L. Second Generation Light-Driven Molecular Motors. Unidirectional Rotation Controlled by a Single Stereogenic Center with Near-Perfect Photoequilibria and Acceleration of the Speed of Rotation by Structural Modification. *J. Am. Chem. Soc.* **2002**, *124*, 5037−5051.
(450) ter Wiel, M. K.; van Delden, R. A.; Meetsma, A.; Feringa, B. L. Increased Speed of Rotation for the Smallest Light-Driven Molecular Motor. *J. Am. Chem. Soc.* **2003**, *125*, 15076−15086.
(451) Pijper, D.; van Delden, R. A.; Meetsma, A.; Feringa, B. L. Acceleration of a Nanomotor: Electronic Control of the Rotary Speed of a Light-Driven Molecular Rotor. *J. Am. Chem. Soc.* **2005**, *127*, 17612−17613.
(452) Vicario, J.; Walko, M.; Meetsma, A.; Feringa, B. L. Fine Tuning of the Rotary Motion by Structural Modification in Light-driven Unidirectional Molecular Motors. *J. Am. Chem. Soc.* **2006**, *128*, 5127−5135.
(453) Conyard, J.; Addison, K.; Heisler, I. A.; Cnossen, A.; Browne, W. R.; Feringa, B. L.; Meech, S. R. Ultrafast Dynamics in the Power Stroke of a Molecular Rotary Motor. *Nat. Chem.* **2012**, *4*, 547−551.
(454) Schoevaars, A. M.; Kruizinga, W.; Zijlstra, R. W. J.; Veldman, N.; Spek, A. L.; Feringa, B. L. Toward a Switchable Molecular Rotor. Unexpected Dynamic Behavior of Functionalized Overcrowded Alkenes. *J. Org. Chem.* **1997**, *62*, 4943−4948.
(455) ter Wiel, M. K.; van Delden, R. A.; Meetsma, A.; Feringa, B. L. Control of Rotor Motion in a Light-driven Molecular Motor: Towards a Molecular Gearbox. *Org. Biomol. Chem.* **2005**, *3*, 4071−4076.
(456) Greb, L.; Lehn, J.-M. Light-Driven Molecular Motors: Imines as Four-Step or Two-Step Unidirectional Rotors. *J. Am. Chem. Soc.* **2014**, *136*, 13114−13117.
(457) Padwa, A. Photochemistry of the Crbon-Nitrogen Double Bond. *Chem. Rev.* **1977**, *77*, 37−68.
(458) Pratt, A. C. The Photochemistry of Imines. *Chem. Soc. Rev.* **1977**, *6*, 63−81.
(459) Pierre Courot, R. P.; le Saint, Jaques Photochromisme par Isomerization Syn-anti de Phenylhydrazones-2 de Tricetones-1,2,3 et de Dicetones-1,2 Substituees. *Tetrahedron Lett.* **1976**, *17*, 1181−1184.
(460) Pichon, R.; le Saint, J.; Courtot, P. Photoisomerization d'Arylhydrazones-2 de Dicetones-1,2 Substituees en 2 Mecanisme d'Isomerization Thermique de la Double Liaison C═N. *Tetrahedron* **1981**, *37*, 1517−1524.
(461) Chaur, M. N.; Collado, D.; Lehn, J.-M. Configurational and Constitutional Information Storage: Multiple Dynamics in Systems Based on Pyridyl and Acyl Hydrazones. *Chem. - Eur. J.* **2011**, *17*, 248−258.
(462) Burdette, S. C. Molecular Switches: Hydrazones Double Down on Zinc. *Nat. Chem.* **2012**, *4*, 695−696.
(463) Tatum, L. A.; Su, X.; Aprahamian, I. Simple Hydrazone Building Blocks for Complicated Functional Materials. *Acc. Chem. Res.* **2014**, *47*, 2141−2149.
(464) Su, X.; Aprahamian, I. Hydrazone-based Switches, Metallo-assemblies and Sensors. *Chem. Soc. Rev.* **2014**, *43*, 1963−1981.
(465) Su, X.; Aprahamian, I. Zinc(II)-Regulation of Hydrazone Switch Isomerization Kinetics. *Org. Lett.* **2013**, *15*, 5952−5955.
(466) Croteau, M. L.; Su, X.; Wilcox, D. E.; Aprahamian, I. Metal Coordination and Isomerization of a Hydrazone Switch. *ChemPlusChem* **2014**, *79*, 1214−1224.
(467) Foy, J. T.; Ray, D.; Aprahamian, I. Regulating Signal Enhancement with Coordination-coupled Deprotonation of a Hydrazone Switch. *Chem. Sci.* **2015**, *6*, 209−213.
(468) Langde, S. M.; Aprahamian, I. A ph Activated Configurational Rotary Switch: Controlling the *E*/*Z* Isomerization in Hydrazones. *J. Am. Chem. Soc.* **2009**, *131*, 18269−18271.

DOI: 10.1021/acs.chemrev.5b00146
Chem. Rev. 2015, 115, 10081−10206

(469) Su, X.; Robbins, T. F.; Aprahamian, I. Switching Through Coordination-coupled Proton Transfer. *Angew. Chem., Int. Ed.* **2011**, *50*, 1841−1844.
(470) Landge, S. M.; Tkatchouk, E.; Benitez, D.; Lanfranchi, D. A.; Elhabiri, M.; Goddard, W. A., III; Aprahamian, I. Isomerization Mechanism in Hydrazone-based Rotary Switches: Lateral Shift, Rotation, or Tautomerization? *J. Am. Chem. Soc.* **2011**, *133*, 9812−9823.
(471) Ray, D.; Foy, J. T.; Hughes, R. P.; Aprahamian, I. A Switching Cascade of Hydrazone-based Rotary Switches Through Coordination-coupled Proton Relays. *Nat. Chem.* **2012**, *4*, 757−762.
(472) Su, X.; Voskian, S.; Hughes, R. P.; Aprahamian, I. Manipulating Liquid-Crystal Properties Using a pH Activated Hydrazone Switch. *Angew. Chem., Int. Ed.* **2013**, *52*, 10734−10739.
(473) Siegel, J. S. Supramolecular Chemistry. Concepts and Perspectives - Lehn, J. -M. *Science* **1996**, *271*, 949−949.
(474) Amendola, V.; Fabbrizzi, L.; Mangano, C.; Pallavicini, P. Molecular Movements and Translocations Controlled by Transition Metals and Signaled by Light Emission. *Struct. Bonding (Berlin)* **2001**, *99*, 79−115.
(475) Miyazawa, A.; Fujiyoshi, Y.; Unwin, N. Structure and Gating Mechanism of the Acetylcholine Receptor Pore. *Nature* **2003**, *423*, 949−955.
(476) Kaempfer, R. Ribosomal Subunit Exchange during Protein Synthesis. *Proc. Natl. Acad. Sci. U. S. A.* **1968**, *61*, 106−113.
(477) Nakahata, M.; Takashima, Y.; Hashidzume, A.; Harada, A. Redox-Generated Mechanical Motion of a Supramolecular Polymeric Actuator Based on Host-Guest Interactions. *Angew. Chem., Int. Ed.* **2013**, *52*, 5731−5735.
(478) De Santis, G.; Fabbrizzi, L.; Iacopino, D.; Pallavicini, P.; Perotti, A.; Poggi, A. Electrochemically Switched Anion Translocation in a Multicomponent Coordination Compound. *Inorg. Chem.* **1997**, *36*, 827−832.
(479) Akutagawa, T.; Koshinaka, H.; Sato, D.; Takeda, S.; Noro, S. I.; Takahashi, H.; Kumai, R.; Tokura, Y.; Nakamura, T. Ferroelectricity and Polarity Control in Solid-state Flip-flop Supramolecular Rotators. *Nat. Mater.* **2009**, *8*, 342−347.
(480) Ikeda, A.; Tsudera, T.; Shinkai, S. Molecular Design of a "Molecular Syringe" Mimic for Metal Cations Using a 1,3-Alternate Calix[4]arene Cavity. *J. Org. Chem.* **1997**, *62*, 3568−3574.
(481) Knipe, P. C.; Thompson, S.; Hamilton, A. D. Ion-mediated Conformational Switches. *Chem. Sci.* **2015**, *6*, 1630−1639.
(482) Su, X.; Robbins, T. F.; Aprahamian, I. Switching Through Coordination-Coupled Proton Transfer. *Angew. Chem., Int. Ed.* **2011**, *50*, 1841−1844.
(483) Su, X.; Voskian, S.; Hughes, R. P.; Aprahamian, I. Manipulating Liquid-Crystal Properties Using a pH Activated Hydrazone Switch. *Angew. Chem., Int. Ed.* **2013**, *52*, 10734−10739.
(484) Su, X.; Lessing, T.; Aprahamian, I. The Importance of the Rotor in Hydrazone-based Molecular Switches. *Beilstein J. Org. Chem.* **2012**, *8*, 872−876.
(485) Su, X.; Aprahamian, I. Switching Around Two Axles: Controlling the Configuration and Conformation of a Hydrazone-Based Switch. *Org. Lett.* **2011**, *13*, 30−33.
(486) del Barrio, J.; Horton, P. N.; Lairez, D.; Lloyd, G. O.; Toprakcioglu, C.; Scherman, O. A. Photocontrol over Cucurbit[8]uril Complexes: Stoichiometry and Supramolecular Polymers. *J. Am. Chem. Soc.* **2013**, *135*, 11760−11763.
(487) Lan, Y.; Wu, Y. C.; Karas, A.; Scherman, O. A. Photoresponsive Hybrid Raspberry-Like Colloids Based on Cucurbit[8]uril Host-Guest Interactions. *Angew. Chem., Int. Ed.* **2014**, *53*, 2166−2169.
(488) Ashton, P. R.; Campbell, P. J.; Chrystal, E. J. T.; Glink, P. T.; Menzer, S.; Philp, D.; Spencer, N.; Stoddart, J. F.; Tasker, P. A.; Williams, D. J. Dialkylammonium Ion Crown-Ether Complexes - the Forerunners of a New Family of Interlocked Molecules. *Angew. Chem., Int. Ed. Engl.* **1995**, *34*, 1865−1869.
(489) Ashton, P. R.; Chrystal, E. J. T.; Glink, P. T.; Menzer, S.; Schiavo, C.; Stoddart, J. F.; Tasker, P. A.; Williams, D. J. Doubly Encircled and Double-Stranded Pseudorotaxanes. *Angew. Chem., Int. Ed. Engl.* **1995**, *34*, 1869−1871.
(490) Ashton, P. R.; Chrystal, E. J. T.; Glink, P. T.; Menzer, S.; Schiavo, C.; Spencer, N.; Stoddart, J. F.; Tasker, P. A.; White, A. J. P.; Williams, D. J. Pseudorotaxanes Formed Between Secondary Dialkylammonium Salts and Crown Ethers. *Chem. - Eur. J.* **1996**, *2*, 709−728.
(491) Ashton, P. R.; Fyfe, M. C. T.; Glink, P. T.; Menzer, S.; Stoddart, J. F.; White, A. J. P.; Williams, D. J. Molecular Meccano, Part 24. Multiply Stranded and Multiply Encircled Pseudorotaxanes. *J. Am. Chem. Soc.* **1997**, *119*, 12514−12524.
(492) Ashton, P. R.; Fyfe, M. C. T.; Martinez-Diaz, M. V.; Menzer, S.; Schiavo, C.; Stoddart, J. F.; White, A. J. P.; Williams, D. J. Molecular Meccano. Part 39 - Doubly Docked Pseudorotaxanes. *Chem. - Eur. J.* **1998**, *4*, 1523−1534.
(493) Loeb, S. J.; Tiburcio, J.; Vella, S. J. [2]Pseudorotaxane Formation with N-benzylanilinium Axles and 24-Crown-8 Ether Wheels. *Org. Lett.* **2005**, *7*, 4923−4926.
(494) Baroncini, M.; Gao, C.; Carboni, V.; Credi, A.; Previtera, E.; Semeraro, M.; Venturi, M.; Silvi, S. Light Control of Stoichiometry and Motion in Pseudorotaxanes Comprising a Cucurbit[7]uril Wheel and an Azobenzene-Bipyridinium Axle. *Chem. - Eur. J.* **2014**, *20*, 10737−10744.
(495) Credi, A.; Dumas, S.; Silvi, S.; Venturi, M.; Arduini, A.; Pochini, A.; Secchi, A. Viologen-calix[6]arene Pseudorotaxanes. Ion-pair Recognition and Threading/dethreading Molecular Motions. *J. Org. Chem.* **2004**, *69*, 5881−5887.
(496) Balzani, V.; Credi, A.; Marchioni, F.; Stoddart, J. F. Artificial Molecular-level Machines. Dethreading-rethreading of a Pseudorotaxane Powered Exclusively by Light Energy. *Chem. Commun.* **2001**, 1860−1861.
(497) Baroncini, M. A Simple Molecular Machine Operated by Photoinduced Proton Transfer. *Springer Theses*; Springer: New York, 2011; Chapter 7, pp 71−76; 10.1007/978-3-642-19285-2_7.
(498) Jeppesen, J. O.; Becher, J.; Stoddart, J. F. Poised on the Brink Between a Bistable Complex and a Compound. *Org. Lett.* **2002**, *4*, 557−560.
(499) Rekharsky, M. V.; Yamamura, H.; Kawai, M.; Osaka, I.; Arakawa, R.; Sato, A.; Ko, Y. H.; Selvapalam, N.; Kim, K.; Inoue, Y. Sequential Formation of a Ternary Complex Among Dihexylammonium, Cucurbit[6]uril, and Cyclodextrin with Positive Cooperativity. *Org. Lett.* **2006**, *8*, 815−818.
(500) Balzani, V.; Credi, A.; Venturi, M. Controlled Disassembling of Self-assembling Systems: Toward Artificial Molecular-level Devices and Machines. *Proc. Natl. Acad. Sci. U. S. A.* **2002**, *99*, 4814−4817.
(501) Huang, F.; Fronczek, F. R.; Gibson, H. W. A Cryptand/bisparaquat [3]Pseudorotaxane by Cooperative Complexation. *J. Am. Chem. Soc.* **2003**, *125*, 9272−9273.
(502) Huang, F.; Gibson, H. W.; Bryant, W. S.; Nagvekar, D. S.; Fronczek, F. R. First Pseudorotaxane-like [3]Complexes based on Cryptands and Paraquat: Self-assembly and Crystal Structures. *J. Am. Chem. Soc.* **2003**, *125*, 9367−9371.
(503) Inoue, Y.; Kanbara, T.; Yamamoto, T. Construction of New [2]Pseudorotaxanes by Hydrogen Bonding Assembly of Macrocyclic Tetrathiolactam with Amides and an Ester. *Tetrahedron Lett.* **2004**, *45*, 4603−4606.
(504) Sambrook, M. R.; Beer, P. D.; Wisner, J. A.; Paul, R. L.; Cowley, A. R.; Szemes, F.; Drew, M. G. Anion-templated Assembly of Pseudorotaxanes: Importance of Anion Template, Strength of Ion-pair Thread Association, and Macrocycle Ring Size. *J. Am. Chem. Soc.* **2005**, *127*, 2292−2302.
(505) Yonemura, H.; Kusano, S.; Matsuo, T.; Yamada, S. Effect of pi-System on Long-range Photoinduced Electron Transfer in Through-ring alpha-Cyclodextrin Complexes of Carbazole-viologen Linked Compounds. *Tetrahedron Lett.* **1998**, *39*, 6915−6918.
(506) Montalti, M.; Ballardini, R.; Prodi, L.; Balzani, V. Electronic Energy Transfer in Adducts of Aromatic Crown Ethers with Protonated 9-Methylaminomethylanthracene. *Chem. Commun.* **1996**, 2011−2012.
(507) Asakawa, M.; Ashton, P. R.; Balzani, V.; Credi, A.; Mattersteig, G.; Matthews, O. A.; Montalti, M.; Spencer, N.; Stoddart, J. F.; Venturi, M. Electrochemically Induced Molecular Motions in Pseudorotaxanes: A Case of Dual-mode (Oxidative and Reductive) Dethreading. *Chem. - Eur. J.* **1997**, *3*, 1992−1996.

DOI: 10.1021/acs.chemrev.5b00146
Chem. Rev. 2015, 115, 10081−10206

(508) Credi, A.; Balzani, V.; Langford, S. J.; Stoddart, J. F. Logic Operations at the Molecular Level. An XOR Gate Based on a Molecular Machine. *J. Am. Chem. Soc.* **1997**, *119*, 2679−2681.
(509) Ashton, P. R.; Ballardini, R.; Balzani, V.; GomezLopez, M.; Lawrence, S. E.; MartinezDiaz, M. V.; Montalti, M.; Piersanti, A.; Prodi, L.; Stoddart, J. F.; et al. Molecular Meccano. 26. Hydrogen-bonded Complexes of Aromatic Crown Ethers with (9-Anthracenyl)-methylammonium Derivatives. Supramolecular Photochemistry and Photophysics. pH-Controllable Supramolecular Switching. *J. Am. Chem. Soc.* **1997**, *119*, 10641−10651.
(510) Devonport, W.; Blower, M. A.; Bryce, M. R.; Goldenberg, L. M. A Redox-active Tetrathiafulvalene [2]Pseudorotaxane: Spectroelectrochemical and Cyclic Voltammetric Studies of the Highly-reversible Complexation/decomplexation Process. *J. Org. Chem.* **1997**, *62*, 885−887.
(511) Montalti, M.; Prodi, L. A Supramolecular Assembly Controlled by Anions: Threading and Unthreading of a Pseudorotaxane. *Chem. Commun.* **1998**, 1461−1462.
(512) Matthews, O. A.; Raymo, F. M.; Stoddart, J. F.; White, A. J. P.; Williams, D. J. Acid/Base-controlled Supramolecular Switch. *New J. Chem.* **1998**, *22*, 1131−1134.
(513) Asakawa, M.; Ashton, P. R.; Balzani, V.; Boyd, S. E.; Credi, A.; Mattersteig, G.; Menzer, S.; Montalti, M.; Raymo, F. M.; Ruffilli, C.; et al. Molecular Meccano, 49 - Pseudorotaxanes and Catenanes Containing a Redox-active Unit Derived from Tetrathiafulvalene. *Eur. J. Org. Chem.* **1999**, *1999*, 985−994.
(514) Balzani, V. V.; Credi, A.; Mattersteig, G.; Matthews, O. A.; Raymo, F. M.; Stoddart, J. F.; Venturi, M.; White, A. J.; Williams, D. J. Switching of Pseudorotaxanes and Catenanes Incorporating a Tetrathiafulvalene Unit by Redox and Chemical Inputs. *J. Org. Chem.* **2000**, *65*, 1924−1936.
(515) Balzani, V. V.; Becher, J.; Credi, A.; Nielsen, M. B.; Raymo, F. M.; Stoddart, J. F.; Talarico, A. M.; Venturi, M. The Electrochemically-driven Decomplexation/recomplexation of Inclusion Adducts of Ferrocene Derivatives with an Electron-accepting Receptor. *J. Org. Chem.* **2000**, *65*, 1947−1956.
(516) Fujimoto, T.; Nakamura, A.; Inoue, Y.; Sakata, Y.; Kaneda, T. Photoswitching of the Association of a Permethylated alpha-Cyclodextrin-azobenzene Dyad Forming a Janus [2]Pseudorotaxane. *Tetrahedron Lett.* **2001**, *42*, 7987−7989.
(517) Kuwabara, J.; Stern, C. L.; Mirkin, C. A. A Coordination Chemistry Approach to a Multieffector Enzyme Mimic. *J. Am. Chem. Soc.* **2007**, *129*, 10074−10075.
(518) Zheng, Y.; Yu, Z. Y.; Parker, R. M.; Wu, Y. C.; Abell, C.; Scherman, O. A. Interfacial Assembly of Dendritic Microcapsules with Host-guest Chemistry. *Nat. Commun.* **2014**, *5*, 5772.
(519) Horie, M.; Suzaki, Y.; Osakada, K. Formation of Pseudorotaxane Induced by Electrochemical Oxidation of Ferrocene-containing Axis Molecule in the Presence of Crown Ether. *J. Am. Chem. Soc.* **2004**, *126*, 3684−3685.
(520) Ballardini, R.; Balzani, V.; Credi, A.; Gandolfi, M. T.; Langford, S. J.; Menzer, S.; Prodi, L.; Stoddart, J. F.; Venturi, M.; Williams, D. J. Simple Molecular Machines: Chemically Driven Unthreading and Rethreading of a [2]Pseudorotaxane. *Angew. Chem., Int. Ed. Engl.* **1996**, *35*, 978−981.
(521) Ballardini, R.; Balzani, V.; Gandolfi, M. T.; Prodi, L.; Venturi, M.; Philp, D.; Ricketts, H. G.; Stoddart, J. F. A Photochemically Driven Molecular Machine. *Angew. Chem., Int. Ed. Engl.* **1993**, *32*, 1301−1303.
(522) Mock, W. L.; Pierpont, J. A Cucurbituril-Based Molecular Switch. *J. Chem. Soc., Chem. Commun.* **1990**, 1509−1511.
(523) Asakawa, M.; Ashton, P. R.; Balzani, V.; Brown, C. L.; Credi, A.; Matthews, O. A.; Newton, S. P.; Raymo, F. M.; Shipway, A. N.; Spencer, N.; et al. Photoactive Azobenzene-containing Supramolecular Complexes and Related Interlocked Molecular Compounds. *Chem. - Eur. J.* **1999**, *5*, 860−875.
(524) Jeppesen, J. O.; Vignon, S. A.; Stoddart, J. F. In the Twilight Zone Between [2]Pseudorotaxanes and [2]Rotaxanes. *Chem. - Eur. J.* **2003**, *9*, 4611−4625.
(525) Jun, S. I.; Lee, J. W.; Sakamoto, S.; Yamaguchi, K.; Kim, K. Rotaxane-based Molecular Switch with Fluorescence Signaling. *Tetrahedron Lett.* **2000**, *41*, 471−475.
(526) Asakawa, M.; Iqbal, S.; Stoddart, J. F.; Tinker, N. D. Prototype of an Optically Responsive Molecular Switch Based on Pseudorotaxane. *Angew. Chem., Int. Ed. Engl.* **1996**, *35*, 976−978.
(527) Ashton, P. R.; Balzani, V.; Kocian, O.; Prodi, L.; Spencer, N.; Stoddart, J. F. A Light-fueled "Piston Cylinder" Molecular-level Machine. *J. Am. Chem. Soc.* **1998**, *120*, 11190−11191.
(528) Ishow, E.; Credi, A.; Balzani, V.; Spadola, F.; Mandolini, L. A Molecular-level Plug/socket System: Electronic Energy Transfer From a Binaphthyl Unit Incorporated into a Crown Ether to an Anthracenyl Unit Linked to an Ammonium Ion. *Chem. - Eur. J.* **1999**, *5*, 984−989.
(529) Ballardini, R.; Balzani, V.; Clemente-Leon, M.; Credi, A.; Gandolfi, M. T.; Ishow, E.; Perkins, J.; Stoddart, J. F.; Tseng, H. R.; Wenger, S. Photoinduced Electron Transfer in a Triad That can be Assembled/disassembled by Two Different External Inputs. Toward Molecular-level Electrical Extension Cables. *J. Am. Chem. Soc.* **2002**, *124*, 12786−12795.
(530) Jeon, W. S.; Ziganshina, A. Y.; Lee, J. W.; Ko, Y. H.; Kang, J. K.; Lee, C.; Kim, K. A [2]Pseudorotaxane-based Molecular Machine: Reversible Formation of a Molecular Loop Driven by Electrochemical and Photochemical Stimuli. *Angew. Chem., Int. Ed.* **2003**, *42*, 4097−4100.
(531) Jeon, W. S.; Kim, E.; Ko, Y. H.; Hwang, I.; Lee, J. W.; Kim, S. Y.; Kim, H. J.; Kim, K. Molecular Loop Lock: A Redox-driven Molecular Machine Based on a Host-stabilized Charge-transfer Complex. *Angew. Chem., Int. Ed.* **2005**, *44*, 87−91.
(532) Credi, A.; Montalti, M.; Balzani, V.; Langford, S. J.; Raymo, F. M.; Stoddart, J. F. Simple Molecular-level Machines. Interchange Between Different Threads in Pseudorotaxanes. *New J. Chem.* **1998**, *22*, 1061−1065.
(533) Ashton, P. R.; Balzani, V.; Becher, J.; Credi, A.; Fyfe, M. C. T.; Mattersteig, G.; Menzer, S.; Nielsen, M. B.; Raymo, F. M.; Stoddart, J. F.; et al. A Three-pole Supramolecular Switch. *J. Am. Chem. Soc.* **1999**, *121*, 3951−3957.
(534) Chang, K. J.; An, Y. J.; Uh, H.; Jeong, K. S. Reversible Control of Assembly and Disassembly of Interlocked Supermolecules. *J. Org. Chem.* **2004**, *69*, 6556−6563.
(535) Kaiser, G.; Jarrosson, T.; Otto, S.; Ng, Y. F.; Bond, A. D.; Sanders, J. K. M. Lithium-templated Synthesis of a Donor-acceptor Pseudorotaxane and Catenane. *Angew. Chem., Int. Ed.* **2004**, *43*, 1959−1962.
(536) Venturi, M.; Dumas, S.; Balzani, V.; Cao, J. G.; Stoddart, J. F. Threading/dethreading Processes in Pseudorotaxanes. A Thermodynamic and Kinetic Study. *New J. Chem.* **2004**, *28*, 1032−1037.
(537) Nygaard, S.; Laursen, B. W.; Flood, A. H.; Hansen, C. N.; Jeppesen, J. O.; Stoddart, J. F. Quantifying the Working Stroke of Tetrathiafulvalene-based Electrochemically-driven Linear Motor-molecules. *Chem. Commun.* **2006**, 144−146.
(538) Mirzoian, A.; Kaifer, A. E. Reactive Pseudorotaxanes: Inclusion Complexation of Reduced Viologens by the Hosts beta-Cyclodextrin and Heptakis(2,6-di-O-methyl)-beta-cyclodextrin. *Chem. - Eur. J.* **1997**, *3*, 1052−1058.
(539) Eliadou, K.; Yannakopoulou, K.; Rontoyianni, A.; Mavridis, I. M. NMR Detection of Simultaneous Formation of [2]- and [3]-Pseudorotaxanes in Aqueous Solution Between alpha-Cyclodextrin and Linear Aliphatic alpha,omega-Amino Acids, an alpha,omega-Diamine and an alpha,omega-Diacid of Similar Length, and Comparison with the Solid-state Structures. *J. Org. Chem.* **1999**, *64*, 6217−6226.
(540) Huh, K. M.; Ooya, T.; Sasaki, S.; Yui, N. Polymer Inclusion Complex Consisting of Poly(epsilon-lysine) and alpha-Cyclodextrin. *Macromolecules* **2001**, *34*, 2402−2404.
(541) Wisner, J. A.; Beer, P. D.; Drew, M. G. B. A Demonstration of Anion Templation and Selectivity in Pseudorotaxane Formation. *Angew. Chem., Int. Ed.* **2001**, *40*, 3606−3609.
(542) Wisner, J. A.; Beer, P. D.; Berry, N. G.; Tomapatanaget, B. Anion Recognition as a Method for Templating Pseudorotaxane Formation. *Proc. Natl. Acad. Sci. U. S. A.* **2002**, *99*, 4983−4986.

DOI: 10.1021/acs.chemrev.5b00146
Chem. Rev. 2015, 115, 10081−10206

(543) Anelli, P. L.; Ashton, P. R.; Spencer, N.; Slawin, A. M. Z.; Stoddart, J. F.; Williams, D. J. Self-Assembling [2]Pseudorotaxanes. *Angew. Chem., Int. Ed. Engl.* **1991**, *30*, 1036−1039.
(544) Kraus, T.; Budesinsky, M.; Cvacka, J. C.; Sauvage, J.-P. Copper(I)-directed Formation of a Cyclic Pseudorotaxane Tetramer and its Trimeric Homologue. *Angew. Chem., Int. Ed.* **2006**, *45*, 258−261.
(545) Ashton, P. R.; Baxter, I.; Fyfe, M. C. T.; Raymo, F. M.; Spencer, N.; Stoddart, J. F.; White, A. J. P.; Williams, D. J. Rotaxane or Pseudorotaxane? That is the Question! *J. Am. Chem. Soc.* **1998**, *120*, 2297−2307.
(546) Collin, J.-P.; Gavina, P.; Sauvage, J.-P. Electrochemically Induced Molecular Motions in a Copper(I) Complex Pseudorotaxane. *Chem. Commun.* **1996**, 2005−2006.
(547) Wezenberg, S. J.; Vlatkovic, M.; Kistemaker, J. C.; Feringa, B. L. Multi-state Regulation of the Dihydrogen Phosphate Binding Affinity to a Light- and Heat-responsive Bis-urea Receptor. *J. Am. Chem. Soc.* **2014**, *136*, 16784−16787.
(548) Terashima, T.; Mes, T.; De Greef, T. F.; Gillissen, M. A.; Besenius, P.; Palmans, A. R.; Meijer, E. W. Single-chain Folding of Polymers for Catalytic Systems in Water. *J. Am. Chem. Soc.* **2011**, *133*, 4742−4745.
(549) Giuseppone, N.; Lutz, J. F. Materials Chemistry: Catalytic Accordions. *Nature* **2011**, *473*, 40−41.
(550) Zayed, J. M.; Nouvel, N.; Rauwald, U.; Scherman, O. A. Chemical Complexity−supramolecular Self-assembly of Synthetic and Biological Building Blocks in Water. *Chem. Soc. Rev.* **2010**, *39*, 2806−2816.
(551) Lee, T. C.; Kalenius, E.; Lazar, A. I.; Assaf, K. I.; Kuhnert, N.; Grun, C. H.; Janis, J.; Scherman, O. A.; Nau, W. M. Chemistry Inside Molecular Containers in the Gas Phase. *Nat. Chem.* **2013**, *5*, 376−382.
(552) Zhang, J.; Coulston, R. J.; Jones, S. T.; Geng, J.; Scherman, O. A.; Abell, C. One-step Fabrication of Supramolecular Microcapsules from Microfluidic Droplets. *Science* **2012**, *335*, 690−694.
(553) Goldup, S. Artificial Molecular Machines: Two Steps Uphill. *Nat. Nanotechnol.* **2015**, *10*, 488−489.
(554) Nakamura, T.; Takashima, Y.; Hashidzume, A.; Yamaguchi, H.; Harada, A. A Metal-ion-responsive Adhesive Material via Switching of Molecular Recognition Properties. *Nat. Commun.* **2014**, *5*, 4622.
(555) Adams, H.; Chekmeneva, E.; Hunter, C. A.; Misuraca, M. C.; Navarro, C.; Turega, S. M. Quantification of the Effect of Conformational Restriction on Supramolecular Effective Molarities. *J. Am. Chem. Soc.* **2013**, *135*, 1853−1863.
(556) Ariga, K.; Ito, H.; Hill, J. P.; Tsukube, H. Molecular Recognition: From Solution Science to Nano/materials Technology. *Chem. Soc. Rev.* **2012**, *41*, 5800−5835.
(557) Rieth, S.; Hermann, K.; Wang, B. Y.; Badjic, J. D. Controlling the Dynamics of Molecular Encapsulation and Gating. *Chem. Soc. Rev.* **2011**, *40*, 1609−1622.
(558) Witlicki, E. H.; Johnsen, C.; Hansen, S. W.; Silverstein, D. W.; Bottomley, V. J.; Jeppesen, J. O.; Wong, E. W.; Jensen, L.; Flood, A. H. Molecular Logic Gates Using Surface-Enhanced Raman-Scattered Light. *J. Am. Chem. Soc.* **2011**, *133*, 7288−7291.
(559) Berryman, O. B.; Sather, A. C.; Rebek, J. A Light Controlled Cavitand Wall Regulates Guest Binding. *Chem. Commun.* **2011**, *47*, 656−658.
(560) Dube, H.; Ajami, D.; Rebek, J. Photochemical Control of Reversible Encapsulation. *Angew. Chem., Int. Ed.* **2010**, *49*, 3192−3195.
(561) Rogez, G.; Ribera, B. F.; Credi, A.; Ballardini, R.; Gandolfi, M. T.; Balzani, V.; Liu, Y.; Northrop, B. H.; Stoddart, J. F. A Molecular Plug-socket Connector. *J. Am. Chem. Soc.* **2007**, *129*, 4633−4642.
(562) Arduini, A.; Bussolati, R.; Credi, A.; Secchi, A.; Silvi, S.; Semeraro, M.; Venturi, M. Toward Directionally Controlled Molecular Motions and Kinetic Intra- and Intermolecular Self-Sorting: Threading Processes of Nonsymmetric Wheel and Axle Components. *J. Am. Chem. Soc.* **2013**, *135*, 9924−9930.
(563) Baroncini, M.; Silvi, S.; Venturi, M.; Credi, A. Photoactivated Directionally Controlled Transit of a Non-Symmetric Molecular Axle Through a Macrocycle. *Angew. Chem., Int. Ed.* **2012**, *51*, 4223−4226.
(564) Cao, D.; Amelia, M.; Klivansky, L. M.; Koshkakaryan, G.; Khan, S. I.; Semeraro, M.; Silvi, S.; Venturi, M.; Credi, A.; Liu, Y. Probing Donor-Acceptor Interactions and Co-Conformational Changes in Redox Active Desymmetrized [2]Catenanes. *J. Am. Chem. Soc.* **2010**, *132*, 1110−1122.
(565) Leblond, J.; Petitjean, A. Molecular Tweezers: Concepts and Applications. *ChemPhysChem* **2011**, *12*, 1043−1051.
(566) Legouin, B.; Gayral, M.; Uriac, P.; Cupif, J. F.; Levoin, N.; Toupet, L.; van de Weghe, P. Molecular Tweezers: Synthesis and Formation of Host-Guest Complexes. *Eur. J. Org. Chem.* **2010**, *2010*, 5503−5508.
(567) Bier, D.; Rose, R.; Bravo-Rodriguez, K.; Bartel, M.; Ramirez-Anguita, J. M.; Dutt, S.; Wilch, C.; Klarner, F. G.; Sanchez-Garcia, E.; Schrader, T.; Ottmann, C. Molecular Tweezers Modulate 14−3-3 Protein-protein Interactions. *Nat. Chem.* **2013**, *5*, 234−239.
(568) Colquhoun, H. M.; Zhu, Z. X. Recognition of Polyimide Sequence Information by a Molecular Tweezer. *Angew. Chem., Int. Ed.* **2004**, *43*, 5040−5045.
(569) Gianneschi, N. C.; Cho, S. H.; Nguyen, S. T.; Mirkin, C. A. Reversibly Addressing an Allosteric Catalyst *in situ*: Catalytic Molecular Tweezers. *Angew. Chem., Int. Ed.* **2004**, *43*, 5503−5507.
(570) Guther, R.; Nieger, M.; Vogtle, F. Molecular Tweezers with a Hydrocarbon Skeleton and Convergent Carboxyl Groups. *Angew. Chem., Int. Ed. Engl.* **1993**, *32*, 601−603.
(571) Hardouin-Lerouge, M.; Hudhomme, P.; Salle, M. Molecular Clips and Tweezers Hosting Neutral Guests. *Chem. Soc. Rev.* **2011**, *40*, 30−43.
(572) Klarner, F. G.; Schrader, T. Aromatic Interactions by Molecular Tweezers and Clips in Chemical and Biological Systems. *Acc. Chem. Res.* **2013**, *46*, 967−978.
(573) Leblond, J.; Gao, H.; Petitjean, A.; Leroux, J. C. pH-Responsive Molecular Tweezers. *J. Am. Chem. Soc.* **2010**, *132*, 8544−8545.
(574) Zimmerman, S. C. Rigid Molecular Tweezers as Hosts for the Complexation of Neutral Guests. *Top. Curr. Chem.* **1993**, *165*, 71−102.
(575) Shinkai, S.; Nakaji, T.; Ogawa, T.; Shigematsu, K.; Manabe, O. Photoresponsive Crown Ethers 0.2. Photocontrol of Ion Extraction and Ion-Transport by a Bis(Crown Ether) with a Butterfly-Like Motion. *J. Am. Chem. Soc.* **1981**, *103*, 111−115.
(576) Shinkai, S.; Ishihara, M.; Ueda, K.; Manabe, O. Photoresponsive Crown Ethers 0.14. Photoregulated Crown Metal Complexation by Competitive Intramolecular Tail(Ammonium)-Biting. *J. Chem. Soc., Perkin Trans. 2* **1985**, 511−518.
(577) Perez, E. M.; Sanchez, L.; Fernandez, G.; Martin, N. exTTF as a Building Block for Fullerene Receptors. Unexpected Solvent-dependent Positive Homotropic Cooperativity. *J. Am. Chem. Soc.* **2006**, *128*, 7172−7173.
(578) Zimmerman, S. C.; Vanzyl, C. M.; Hamilton, G. S. Rigid Molecular Tweezers - Preorganized Hosts for Electron-Donor Acceptor Complexation in Organic-Solvents. *J. Am. Chem. Soc.* **1989**, *111*, 1373−1381.
(579) Molt, O.; Rubeling, D.; Schrader, T. A Selective Biomimetic Tweezer for Noradrenaline. *J. Am. Chem. Soc.* **2003**, *125*, 12086−12087.
(580) Etxebarria, J.; Vidal-Ferran, A.; Ballester, P. The Effect of Complex Stoichiometry in Supramolecular Chirality Transfer to Zinc Bisporphyrin Systems. *Chem. Commun.* **2008**, 5939−5941.
(581) Ulrich, S.; Petitjean, A.; Lehn, J.-M. Metallo-Controlled Dynamic Molecular Tweezers: Design, Synthesis, and Self-Assembly by Metal-Ion Coordination. *Eur. J. Inorg. Chem.* **2010**, *2010*, 1913−1928.
(582) Petitjean, A.; Khoury, R. G.; Kyritsakas, N.; Lehn, J.-M. Dynamic Devices. Shape Switching and Substrate Binding in Ion-controlled Nanomechanical Molecular Tweezers. *J. Am. Chem. Soc.* **2004**, *126*, 6637−6647.
(583) Petitjean, A.; Kyritsakas, N.; Lehn, J.-M. Ion-triggered Multistate Molecular Switching Device Based on Regioselective Coordination-controlled Ion Binding. *Chem. - Eur. J.* **2005**, *11*, 6818−6828.
(584) Linke-Schaetzel, M.; Anson, C. E.; Powell, A. K.; Buth, G.; Palomares, E.; Durrant, J. D.; Balaban, T. S.; Lehn, J.-M. Dynamic Chemical Devices: Photoinduced Electron Transfer and its Ion-

DOI: 10.1021/acs.chemrev.5b00146
Chem. Rev. 2015, 115, 10081−10206

triggered Switching in Nanomechanical Butterfly-type Bis(porphyrin)-terpyridines. *Chem. - Eur. J.* **2006**, *12*, 1931−1940.
(585) Oliveri, C. G.; Ulmann, P. A.; Wiester, M. J.; Mirkin, C. A. Heteroligated Supramolecular Coordination Complexes Formed via the Halide-Induced Ligand Rearrangement Reaction. *Acc. Chem. Res.* **2008**, *41*, 1618−1629.
(586) Oliveri, C. G.; Nguyen, S. T.; Mirkin, C. A. A Highly Modular and Convergent Approach for the Synthesis of Stimulant-responsive Heteroligated Cofacial Porphyrin Tweezer Complexes. *Inorg. Chem.* **2008**, *47*, 2755−2763.
(587) Skibinski, M.; Gomez, R.; Lork, E.; Azov, V. A. Redox Responsive Molecular Tweezers with Tetrathiafulvalene Units: Synthesis, Electrochemistry, and Binding Properties. *Tetrahedron* **2009**, *65*, 10348−10354.
(588) Tian, F.; Jiao, D. Z.; Biedermann, F.; Scherman, O. A. Orthogonal Switching of a Single Supramolecular Complex. *Nat. Commun.* **2012**, *3*, 1207.
(589) Miwa, K.; Furusho, Y.; Yashima, E. Ion-triggered Spring-like Motion of a Double helicate Accompanied by Anisotropic Twisting. *Nat. Chem.* **2010**, *2*, 444−449.
(590) Yamamoto, S.; Iida, H.; Yashima, E. Guest-Induced Unidirectional Dual Rotary and Twisting Motions of a Spiroborate-Based Double-Stranded Helicate Containing a Bisporphyrin Unit. *Angew. Chem., Int. Ed.* **2013**, *52*, 6849−6853.
(591) Ferrand, Y.; Gan, Q.; Kauffmann, B.; Jiang, H.; Huc, I. Template-Induced Screw Motions within an Aromatic Amide Foldamer Double Helix. *Angew. Chem., Int. Ed.* **2011**, *50*, 7572−7575.
(592) Hua, Y.; Liu, Y.; Chen, C. H.; Flood, A. H. Hydrophobic Collapse of Foldamer Capsules Drives Picomolar-level Chloride Binding in Aqueous Acetonitrile Solutions. *J. Am. Chem. Soc.* **2013**, *135*, 14401−14412.
(593) Juwarker, H.; Jeong, K. S. Anion-controlled Foldamers. *Chem. Soc. Rev.* **2010**, *39*, 3664−3674.
(594) Gan, Q.; Ronson, T. K.; Vosburg, D. A.; Thoburn, J. D.; Nitschke, J. R. Cooperative Loading and Release Behavior of a Metal-Organic Receptor. *J. Am. Chem. Soc.* **2015**, *137*, 1770−1773.
(595) Hua, Y. R.; Flood, A. H. Flipping the Switch on Chloride Concentrations with a Light-Active Foldamer. *J. Am. Chem. Soc.* **2010**, *132*, 12838−12840.
(596) Li, Y.; Flood, A. H.; Pure, C.-H. Hydrogen Bonding to Chloride Ions: A Preorganized and Rigid Macrocyclic Receptor. *Angew. Chem., Int. Ed.* **2008**, *47*, 2649−2652.
(597) Li, Y.; Flood, A. H. Strong, Size-selective, and Electronically Tunable C-H···Halide Binding with Steric Control over Aggregation From Synthetically Modular, Shape-persistent [34]Triazolophanes. *J. Am. Chem. Soc.* **2008**, *130*, 12111−12122.
(598) Hua, Y.; Flood, A. H. Click Chemistry Generates Privileged CH Hydrogen-bonding Triazoles: The Latest Addition to Anion Supramolecular Chemistry. *Chem. Soc. Rev.* **2010**, *39*, 1262−1271.
(599) Juwarker, H.; Lenhardt, J. M.; Pham, D. M.; Craig, S. L. 1,2,3-Triazole CH···Cl^- Contacts Guide Anion Binding and Concomitant Folding in 1,4-Diaryl Triazole Oligomers. *Angew. Chem., Int. Ed.* **2008**, *47*, 3740−3743.
(600) Meudtner, R. M.; Hecht, S. Helicity Inversion in Responsive Foldamers Induced by Achiral Halide Ion Guests. *Angew. Chem., Int. Ed.* **2008**, *47*, 4926−4930.
(601) Lee, S.; Hua, Y. R.; Flood, A. H. beta-Sheet-like Hydrogen Bonds Interlock the Helical Turns of a Photoswitchable Foldamer To Enhance the Binding and Release of Chloride. *J. Org. Chem.* **2014**, *79*, 8383−8396.
(602) Lee, S.; Flood, A. H. Photoresponsive Receptors for Binding and Releasing Anions. *J. Phys. Org. Chem.* **2013**, *26*, 79−86.
(603) Suk, J.-m.; Naidu, V. R.; Liu, X.; Lah, M. S.; Jeong, K.-S. A Foldamer-Based Chiroptical Molecular Switch That Displays Complete Inversion of the Helical Sense upon Anion Binding. *J. Am. Chem. Soc.* **2011**, *133*, 13938−13941.
(604) Campbell, V. E.; de Hatten, X.; Delsuc, N.; Kauffmann, B.; Huc, I.; Nitschke, J. R. Cascading Transformations within a Dynamic Self-assembled System. *Nat. Chem.* **2010**, *2*, 684−687.
(605) Lanyi, J. K. Bacteriorhodopsin as a Model for Proton Pumps. *Nature* **1995**, *375*, 461−463.
(606) Amendola, V.; Fabbrizzi, L.; Mangano, C.; Pallavicini, P. Molecular Machines Based on Metal Ion Translocation. *Acc. Chem. Res.* **2001**, *34*, 488−493.
(607) Zhao, J. Z.; Ji, S. M.; Chen, Y. H.; Guo, H. M.; Yang, P. Excited State Intramolecular Proton Transfer (ESIPT): From Principal Photophysics to the Development of New Chromophores and Applications in Fluorescent Molecular Probes and Luminescent Materials. *Phys. Chem. Chem. Phys.* **2012**, *14*, 8803−8817.
(608) Iijima, T.; Momotake, A.; Shinohara, Y.; Sato, T.; Nishimura, Y.; Arai, T. Excited-State Intramolecular Proton Transfer of Naphthalene-Fused 2-(2′-Hydroxyaryl)benzazole Family. *J. Phys. Chem. A* **2010**, *114*, 1603−1609.
(609) Fabbrizzi, L.; Gatti, F.; Pallavicini, P.; Zambarbieri, E. Redox-driven Intramolecular Anion Translocation Between Transition Metal Centers. *Chem. - Eur. J.* **1999**, *5*, 682−690.
(610) Yoo, H. J.; Mirkin, C. A.; DiPasquale, A. G.; Rheingold, A. L.; Stern, C. L. Reversible CO-Induced Chloride Shuttling in Rh-I Tweezer Complexes Containing Urea-Functionalized Hemilabile Ligands. *Inorg. Chem.* **2008**, *47*, 9727−9729.
(611) Zelikovich, L.; Libman, J.; Shanzer, A. Molecular Redox Switches Based on Chemical Triggering of Iron Translocation in Triple-Stranded Helical Complexes. *Nature* **1995**, *374*, 790−792.
(612) Amendola, V.; Fabbrizzi, L.; Mangano, C.; Miller, H.; Pallavicini, P.; Perotti, A.; Taglietti, A. Signal Amplification by a Fluorescent Indicator of a pH-Driven Intramolecular Translocation of a Copper(II) Ion. *Angew. Chem., Int. Ed.* **2002**, *41*, 2553−2356.
(613) Amendola, V.; Fabbrizzi, L.; Mangano, C.; Pallavicini, P.; Perotti, A.; Taglietti, A. pH-Controlled Translocation of Ni^{II} Within a Ditopic Receptor Bearing an Appended Anthracene Fragment: A Mechanical Switch of Fluorescence. *J. Chem. Soc. Dalton* **2000**, 185−189.
(614) Colasson, B.; Le Poul, N.; Le Mest, Y.; Reinaud, O. Electrochemically Triggered Double Translocation of Two Different Metal Ions with a Ditopic Calix[6]arene Ligand. *J. Am. Chem. Soc.* **2010**, *132*, 4393−4398.
(615) Dotz, K. H.; Jahr, H. C. Tunable Haptotropic Metal Migration in Fused Arenes: Towards Organometallic Switches. *Chem. Rec.* **2004**, *4*, 61−71.
(616) Murahashi, T.; Shirato, K.; Fukushima, A.; Takase, K.; Suenobu, T.; Fukuzumi, S.; Ogoshi, S.; Kurosawa, H. Redox-induced Reversible Metal Assembly Through Translocation and Reversible Ligand Coupling in Tetranuclear Metal Sandwich Frameworks. *Nat. Chem.* **2012**, *4*, 52−58.
(617) Wozny, M.; Pawlowska, J.; Osior, A.; Swider, P.; Bilewicz, R.; Korybut-Daszkiewicz, B. An Electrochemically Switchable Foldamer - A Surprising Feature of a Rotaxane with Equivalent Stations. *Chem. Sci.* **2014**, *5*, 2836−2842.
(618) Chao, S.; Romuald, C.; Fournel-Marotte, K.; Clavel, C.; Coutrot, F. A Strategy Utilizing a Recyclable Macrocycle Transporter for the Efficient Synthesis of a Triazolium-Based [2]Rotaxane. *Angew. Chem., Int. Ed.* **2014**, *53*, 6914−6919.
(619) Langton, M. J.; Blackburn, O. A.; Lang, T.; Faulkner, S.; Beer, P. D. Nitrite-Templated Synthesis of Lanthanide-Containing [2]-Rotaxanes for Anion Sensing. *Angew. Chem., Int. Ed.* **2014**, *53*, 11463−11466.
(620) Nygaard, S.; Laursen, B. W.; Hansen, T. S.; Bond, A. D.; Flood, A. H.; Jeppesen, J. O. Preparation of Cyclobis(paraquat-p-phenylene)-Based [2]Rotaxanes Without Flexible Glycol Chains. *Angew. Chem., Int. Ed.* **2007**, *46*, 6093−6097.
(621) Klivansky, L. M.; Koshkakaryan, G.; Cao, D.; Liu, Y. Linear π-Acceptor-Templated Dynamic Clipping to Macrobicycles and [2]-Rotaxanes. *Angew. Chem., Int. Ed.* **2009**, *48*, 4185−4189.
(622) Prikhod'ko, A. I.; Sauvage, J.-P. Passing Two Strings through the Same Ring Using an Octahedral Metal Center as Template: A New Synthesis of [3]Rotaxanes. *J. Am. Chem. Soc.* **2009**, *131*, 6794−6807.
(623) Goldup, S. M.; Leigh, D. A.; Lusby, P. J.; McBurney, R. T.; Slawin, A. M. Z. Active Template Synthesis of Rotaxanes and Molecular

DOI: 10.1021/acs.chemrev.5b00146
Chem. Rev. 2015, 115, 10081−10206

Shuttles with Switchable Dynamics by Four-Component Pd^{II}-Promoted Michael Additions. *Angew. Chem., Int. Ed.* **2008**, *47*, 3381−3384.
(624) Ikeda, T.; Higuchi, M.; Kurth, D. G. From Thiophene [2]Rotaxane to Polythiophene Polyrotaxane. *J. Am. Chem. Soc.* **2009**, *131*, 9158−9159.
(625) Collin, J.-P.; Durola, F.; Frey, J.; Heitz, V.; Reviriego, F.; Sauvage, J.-P.; Trolez, Y.; Rissanen, K. Templated Synthesis of Cyclic [4]Rotaxanes Consisting of Two Stiff Rods Threaded through Two Bis-macrocycles with a Large and Rigid Central Plate as Spacer. *J. Am. Chem. Soc.* **2010**, *132*, 6840−6850.
(626) Xue, Z.; Mayer, M. F. Actuator Prototype: Capture and Release of a Self-Entangled [1]Rotaxane. *J. Am. Chem. Soc.* **2010**, *132*, 3274−3276.
(627) Altieri, A.; Aucagne, V.; Carrillo, R.; Clarkson, G. J.; D'Souza, D. M.; Dunnett, J. A.; Leigh, D. A.; Mullen, K. M. Sulfur-containing Amide-based [2]Rotaxanes and Molecular Shuttles. *Chem. Sci.* **2011**, *2*, 1922−1928.
(628) De Bo, G.; De Winter, J.; Gerbaux, P.; Fustin, C.-A. Rotaxane-Based Mechanically Linked Block Copolymers. *Angew. Chem., Int. Ed.* **2011**, *50*, 9093−9096.
(629) Zhang, Z.-J.; Zhang, H.-Y.; Wang, H.; Liu, Y. A Twin-Axial Hetero[7]rotaxane. *Angew. Chem., Int. Ed.* **2011**, *50*, 10834−10838.
(630) Li, H.; Fahrenbach, A. C.; Coskun, A.; Zhu, Z.; Barin, G.; Zhao, Y.-L.; Botros, Y. Y.; Sauvage, J.-P.; Stoddart, J. F. A Light-Stimulated Molecular Switch Driven by Radical−Radical Interactions in Water. *Angew. Chem., Int. Ed.* **2011**, *50*, 6782−6788.
(631) Nepogodiev, S. A.; Stoddart, J. F. Cyclodextrin-Based Catenanes and Rotaxanes. *Chem. Rev.* **1998**, *98*, 1959−1976.
(632) Dietrich-Buchecker, C. O.; Sauvage, J.-P. Interlocking of Molecular Threads: from the Statistical Approach to the Templated Synthesis of Catenands. *Chem. Rev.* **1987**, *87*, 795−810.
(633) Anderson, S.; Anderson, H. L.; Sanders, J. K. M. Expanding Roles for Templates in Synthesis. *Acc. Chem. Res.* **1993**, *26*, 469−475.
(634) Fuller, A.-M.; Leigh, D. A.; Lusby, P. J.; Oswald, I. D. H.; Parsons, S.; Walker, D. B. A 3D Interlocked Structure from a 2D Template: Structural Requirements for the Assembly of a Square-Planar Metal-Coordinated [2]Rotaxane. *Angew. Chem., Int. Ed.* **2004**, *43*, 3914−3918.
(635) Cantrill, S. J.; Chichak, K. S.; Peters, A. J.; Stoddart, J. F. Nanoscale Borromean Rings. *Acc. Chem. Res.* **2005**, *38*, 1−9.
(636) Chambron, J.-C.; Collin, J.-P.; Heitz, V.; Jouvenot, D.; Kern, J.-M.; Mobian, P.; Pomeranc, D.; Sauvage, J.-P. Rotaxanes and Catenanes Built Around Octahedral Transition Metals. *Eur. J. Org. Chem.* **2004**, *2004*, 1627−1638.
(637) Dietrich-Buchecker, C.; Rapenne, G.; Sauvage, J.-P. Synthesis of Catenanes and Molecular Knots by Copper(I)-directed Formation of the Precursors Followed by Ruthenium(II)-Catalysed Ring-closing Metathesis. *Coord. Chem. Rev.* **1999**, *185*−*186*, 167−176.
(638) Fujita, M. Self-Assembly of [2]Catenanes Containing Metals in Their Backbones. *Acc. Chem. Res.* **1999**, *32*, 53−61.
(639) Fujita, M.; Ogura, K. Transition-metal-directed Assembly of Well-defined Organic Architectures Possessing Large Voids: From Macrocycles to [2] Catenanes. *Coord. Chem. Rev.* **1996**, *148*, 249−264.
(640) Busch, D. H.; Stephenson, N. A. Molecular Organization, Portal to Supramolecular Chemistry: Structural Analysis of the Factors Associated with Molecular Organization in Coordination and Inclusion Chemistry, Including the Coordination Template Effect. *Coord. Chem. Rev.* **1990**, *100*, 119−154.
(641) Sauvage, J.-P. Interlacing Molecular Threads on Transition Metals: Catenands, Catenates, and Knots. *Acc. Chem. Res.* **1990**, *23*, 319−327.
(642) Hubin, T. J.; Busch, D. H. Template Routes to Interlocked Molecular Structures and Orderly Molecular Entanglements. *Coord. Chem. Rev.* **2000**, *200*−*202*, 5−52.
(643) Hoss, R.; Vögtle, F. Template Syntheses. *Angew. Chem., Int. Ed. Engl.* **1994**, *33*, 375−384.
(644) Claessens, C. G.; Stoddart, J. F. $\pi-\pi$ Interactions in Self-Assembly. *J. Phys. Org. Chem.* **1997**, *10*, 254−272.
(645) Gillard, R. E.; Raymo, F. M.; Stoddart, J. F. Controlling Self-Assembly. *Chem. - Eur. J.* **1997**, *3*, 1933−1940.
(646) Philp, D.; Stoddart, J. F. Self-Assembly in Organic Synthesis. *Synlett* **1991**, *1991*, 445−458.
(647) Hogg, L.; Leigh, D. A.; Lusby, P. J.; Morelli, A.; Parsons, S.; Wong, J. K. Y. A Simple General Ligand System for Assembling Octahedral Metal−Rotaxane Complexes. *Angew. Chem., Int. Ed.* **2004**, *43*, 1218−1221.
(648) Hannam, J. S.; Kidd, T. J.; Leigh, D. A.; Wilson, A. J. Magic Rod" Rotaxanes: The Hydrogen Bond-Directed Synthesis of Molecular Shuttles under Thermodynamic Control. *Org. Lett.* **2003**, *5*, 1907−1910.
(649) Leigh, D. A.; Lusby, P. J.; Teat, S. J.; Wilson, A. J.; Wong, J. K. Y. Benzylic Imine Catenates: Readily Accessible Octahedral Analogues of the Sauvage Catenates. *Angew. Chem., Int. Ed.* **2001**, *40*, 1538−1543.
(650) Kidd, T. J.; Leigh, D. A.; Wilson, A. J. Organic "Magic Rings": The Hydrogen Bond-Directed Assembly of Catenanes under Thermodynamic Control. *J. Am. Chem. Soc.* **1999**, *121*, 1599−1600.
(651) Seel, C.; Vögtle, F. Templates, "Wheeled Reagents", and a New Route to Rotaxanes by Anion Complexation: The Trapping Method. *Chem. - Eur. J.* **2000**, *6*, 21−24.
(652) Aucagne, V.; Leigh, D. A.; Lock, J. S.; Thomson, A. R. Rotaxanes of Cyclic Peptides. *J. Am. Chem. Soc.* **2006**, *128*, 1784−1785.
(653) Biscarini, F.; Cavallini, M.; Leigh, D. A.; León, S.; Teat, S. J.; Wong, J. K. Y.; Zerbetto, F. The Effect of Mechanical Interlocking on Crystal Packing: Predictions and Testing. *J. Am. Chem. Soc.* **2002**, *124*, 225−233.
(654) Johnston, A. G.; Leigh, D. A.; Nezhat, L.; Smart, J. P.; Deegan, M. D. Structurally Diverse and Dynamically Versatile Benzylic Amide [2]Catenanes Assembled Directly from Commercially Available Precursors. *Angew. Chem., Int. Ed. Engl.* **1995**, *34*, 1212−1216.
(655) Johnston, A. G.; Leigh, D. A.; Pritchard, R. J.; Deegan, M. D. Facile Synthesis and Solid-State Structure of a Benzylic Amide [2]Catenane. *Angew. Chem., Int. Ed. Engl.* **1995**, *34*, 1209−1212.
(656) Jäger, R.; Vögtle, F. A New Synthetic Strategy towards Molecules with Mechanical Bonds: Nonionic Template Synthesis of Amide-Linked Catenanes and Rotaxanes. *Angew. Chem., Int. Ed. Engl.* **1997**, *36*, 930−944.
(657) Aucagne, V.; Hänni, K. D.; Leigh, D. A.; Lusby, P. J.; Walker, D. B. Catalytic "Click" Rotaxanes: A Substoichiometric Metal-Template Pathway to Mechanically Interlocked Architectures. *J. Am. Chem. Soc.* **2006**, *128*, 2186−2187.
(658) Crowley, J. D.; Hänni, K. D.; Lee, A.-L.; Leigh, D. A. [2]Rotaxanes through Palladium Active-Template Oxidative Heck Cross-Couplings. *J. Am. Chem. Soc.* **2007**, *129*, 12092−12093.
(659) Crowley, J. D.; Hänni, K. D.; Leigh, D. A.; Slawin, A. M. Z. Diels−Alder Active-Template Synthesis of Rotaxanes and Metal-Ion-Switchable Molecular Shuttles. *J. Am. Chem. Soc.* **2010**, *132*, 5309−5314.
(660) Crowley, J. D.; Goldup, S. M.; Gowans, N. D.; Leigh, D. A.; Ronaldson, V. E.; Slawin, A. M. Z. An Unusual Nickel−Copper-Mediated Alkyne Homocoupling Reaction for the Active-Template Synthesis of [2]Rotaxanes. *J. Am. Chem. Soc.* **2010**, *132*, 6243−6248.
(661) De Bo, G.; Kuschel, S.; Leigh, D. A.; Lewandowski, B.; Papmeyer, M.; Ward, J. W. Efficient Assembly of Threaded Molecular Machines for Sequence-Specific Synthesis. *J. Am. Chem. Soc.* **2014**, *136*, 5811−5814.
(662) Goldup, S. M.; Leigh, D. A.; Lusby, P. J.; McBurney, R. T.; Slawin, A. M. Z. Gold(I)-Template Catenane and Rotaxane Synthesis. *Angew. Chem., Int. Ed.* **2008**, *47*, 6999−7003.
(663) Goldup, S. M.; Leigh, D. A.; McBurney, R. T.; McGonigal, P. R.; Plant, A. Ligand-assisted Nickel-catalysed sp^3-sp^3 Homocoupling of Unactivated Alkyl Bromides and its Application to the Active Template Synthesis of Rotaxanes. *Chem. Sci.* **2010**, *1*, 383−386.
(664) Ahmed, R.; Altieri, A.; D'Souza, D. M.; Leigh, D. A.; Mullen, K. M.; Papmeyer, M.; Slawin, A. M. Z.; Wong, J. K. Y.; Woollins, J. D. Phosphorus-Based Functional Groups as Hydrogen Bonding Templates for Rotaxane Formation. *J. Am. Chem. Soc.* **2011**, *133*, 12304−12310.
(665) Cheng, H. M.; Leigh, D. A.; Maffei, F.; McGonigal, P. R.; Slawin, A. M. Z.; Wu, J. En Route to a Molecular Sheaf: Active Metal Template Synthesis of a [3]Rotaxane with Two Axles Threaded through One Ring. *J. Am. Chem. Soc.* **2011**, *133*, 12298−12303.

DOI: 10.1021/acs.chemrev.5b00146
Chem. Rev. 2015, 115, 10081−10206

(666) Lewandowski, B.; De Bo, G.; Ward, J. W.; Papmeyer, M.; Kuschel, S.; Aldegunde, M. J.; Gramlich, P. M. E.; Heckmann, D.; Goldup, S. M.; D'Souza, D. M.; Fernandes, A. E.; Leigh, D. A. Sequence-Specific Peptide Synthesis by an Artificial Small-Molecule Machine. *Science* **2013**, *339*, 189−193.
(667) Leigh, D. A.; Lusby, P. J.; McBurney, R. T.; Morelli, A.; Slawin, A. M. Z.; Thomson, A. R.; Walker, D. B. Getting Harder: Cobalt(III)-Template Synthesis of Catenanes and Rotaxanes. *J. Am. Chem. Soc.* **2009**, *131*, 3762−3771.
(668) Berná, J.; Goldup, S. M.; Lee, A.-L.; Leigh, D. A.; Symes, M. D.; Teobaldi, G.; Zerbetto, F. Cadiot−Chodkiewicz Active Template Synthesis of Rotaxanes and Switchable Molecular Shuttles with Weak Intercomponent Interactions. *Angew. Chem., Int. Ed.* **2008**, *47*, 4392−4396.
(669) Liu, L.; Liu, Y.; Liu, P.; Wu, J.; Guan, Y.; Hu, X.; Lin, C.; Yang, Y.; Sun, X.; Ma, J.; Wang, L. Phosphine Oxide Functional Group Based Three-station Molecular Shuttle. *Chem. Sci.* **2013**, *4*, 1701−1706.
(670) Xue, M.; Yang, Y.; Chi, X.; Yan, X.; Huang, F. Development of Pseudorotaxanes and Rotaxanes: From Synthesis to Stimuli-Responsive Motions to Applications. *Chem. Rev.* **2015**, *115*, 7398.
(671) Franz, M.; Januszewski, J. A.; Wendinger, D.; Neiss, C.; Movsisyan, L. D.; Hampel, F.; Anderson, H. L.; Gorling, A.; Tykwinski, R. R. Cumulene Rotaxanes: Stabilization and Study of [9]Cumulenes. *Angew. Chem., Int. Ed.* **2015**, *54*, 6645−6649.
(672) Langton, M. J.; Matichak, J. D.; Thompson, A. L.; Anderson, H. L. Template-directed Synthesis of π-Conjugated Porphyrin [2]-Rotaxanes and a [4]Catenane Based on a Six-porphyrin Nanoring. *Chem. Sci.* **2011**, *2*, 1897−1901.
(673) Lee, S.; Chen, C. H.; Flood, A. H. A Pentagonal Cyanostar Macrocycle with Cyanostilbene CH Donors Binds Anions and Forms Dialkylphosphate [3]Rotaxanes. *Nat. Chem.* **2013**, *5*, 704−710.
(674) Lahlali, H.; Jobe, K.; Watkinson, M.; Goldup, S. M. Macrocycle Size Matters: "Small" Functionalized Rotaxanes in Excellent Yield Using the CuAAC Active Template Approach. *Angew. Chem., Int. Ed.* **2011**, *50*, 4151−4155.
(675) Winn, J.; Pinczewska, A.; Goldup, S. M. Synthesis of a Rotaxane Cu(I) Triazolide under Aqueous Conditions. *J. Am. Chem. Soc.* **2013**, *135*, 13318−13321.
(676) Bordoli, R. J.; Goldup, S. M. An Efficient Approach to Mechanically Planar Chiral Rotaxanes. *J. Am. Chem. Soc.* **2014**, *136*, 4817−4820.
(677) Hübner, G. M.; Gläser, J.; Seel, C.; Vögtle, F. High-Yielding Rotaxane Synthesis with an Anion Template. *Angew. Chem., Int. Ed.* **1999**, *38*, 383−386.
(678) Hiratani, K.; Suga, J.-i.; Nagawa, Y.; Houjou, H.; Tokuhisa, H.; Numata, M.; Watanabe, K. A new Synthetic Method for Rotaxanes via Tandem Claisen Rearrangement, Diesterification, and Aminolysis. *Tetrahedron Lett.* **2002**, *43*, 5747−5750.
(679) Hannam, J. S.; Lacy, S. M.; Leigh, D. A.; Saiz, C. G.; Slawin, A. M. Z.; Stitchell, S. G. Controlled Submolecular Translational Motion in Synthesis: A Mechanically Interlocking Auxiliary. *Angew. Chem., Int. Ed.* **2004**, *43*, 3260−3264.
(680) Kameta, N.; Hiratani, K.; Nagawa, Y. A Novel Synthesis of Chiral Rotaxanes via Covalent Bond Formation. *Chem. Commun.* **2004**, 466−467.
(681) Reuter, C.; Wienand, W.; Hübner, G. M.; Seel, C.; Vögtle, F. High-Yield Synthesis of Ester, Carbonate, and Acetal Rotaxanes by Anion Template Assistance and their Hydrolytic Dethreading. *Chem. - Eur. J.* **1999**, *5*, 2692−2697.
(682) Schalley, C. A.; Silva, G.; Nising, C. F.; Linnartz, P. Analysis and Improvement of an Anion-Templated Rotaxane Synthesis. *Helv. Chim. Acta* **2002**, *85*, 1578−1596.
(683) Mahoney, J. M.; Shukla, R.; Marshall, R. A.; Beatty, A. M.; Zajicek, J.; Smith, B. D. Templated Conversion of a Crown Ether-Containing Macrobicycle into [2]Rotaxanes. *J. Org. Chem.* **2002**, *67*, 1436−1440.
(684) Li, X.-Y.; Illigen, J.; Nieger, M.; Michel, S.; Schalley, C. A. Tetra- and Octalactam Macrocycles and Catenanes with Exocyclic Metal Coordination Sites: Versatile Building Blocks for Supramolecular Chemistry. *Chem. - Eur. J.* **2003**, *9*, 1332−1347.
(685) Nagawa, Y.; Suga, J.-i.; Hiratani, K.; Koyama, E.; Kanesato, M. [3]Rotaxane Synthesized via Covalent Bond Formation Can Recognize Cations Forming a Sandwich Structure. *Chem. Commun.* **2005**, 749−751.
(686) Schill, G.; Zollenkopf, H.; Rotaxan-Verbindungen, I. *Justus Liebigs Ann. Chem.* **1969**, *721*, 53−74.
(687) Langton, M. J.; Robinson, S. W.; Marques, I.; Felix, V.; Beer, P. D. Halogen Bonding in Water Results in Enhanced Anion Recognition in Acyclic and Rotaxane Hosts. *Nat. Chem.* **2014**, *6*, 1039−1043.
(688) Aucagne, V.; Berna, J.; Crowley, J. D.; Goldup, S. M.; Hanni, K. D.; Leigh, D. A.; Lusby, P. J.; Ronaldson, V. E.; Slawin, A. M.; Viterisi, A.; Walker, D. B. Catalytic "Active-metal" Template Synthesis of [2]Rotaxanes, [3]Rotaxanes, and Molecular Shuttles, and Some Observations on the Mechanism of the Cu(I)-Catalyzed Azide-alkyne 1,3-Cycloaddition. *J. Am. Chem. Soc.* **2007**, *129*, 11950−11963.
(689) Browne, C.; Ronson, T. K.; Nitschke, J. R. Palladium-Templated Subcomponent Self-Assembly of Macrocycles, Catenanes, and Rotaxanes. *Angew. Chem., Int. Ed.* **2014**, *53*, 10701−10705.
(690) Anelli, P. L.; Spencer, N.; Stoddart, J. F. A Molecular Shuttle. *J. Am. Chem. Soc.* **1991**, *113*, 5131−5133.
(691) Ashton, P. R.; Johnston, M. R.; Stoddart, J. F.; Tolley, M. S.; Wheeler, J. W. The Template-directed Synthesis of Porphyrin-stoppered [2]Rotaxanes. *J. Chem. Soc., Chem. Commun.* **1992**, 1128−1131.
(692) Ashton, P. R.; Philp, D.; Spencer, N.; Stoddart, J. F. A New Design Strategy for the Self-assembly of Molecular Shuttles. *J. Chem. Soc., Chem. Commun.* **1992**, 1124−1128.
(693) Lane, A. S.; Leigh, D. A.; Murphy, A. Peptide-Based Molecular Shuttles. *J. Am. Chem. Soc.* **1997**, *119*, 11092−11093.
(694) Leigh, D. A.; Murphy, A.; Smart, J. P.; Slawin, A. M. Z. Glycylglycine Rotaxanes—The Hydrogen Bond Directed Assembly of Synthetic Peptide Rotaxanes. *Angew. Chem., Int. Ed. Engl.* **1997**, *36*, 728−732.
(695) Leigh, D. A.; Murphy, A.; Smart, J. P.; Deleuze, M. S.; Zerbetto, F. Controlling the Frequency of Macrocyclic Ring Rotation in Benzylic Amide [2]Catenanes. *J. Am. Chem. Soc.* **1998**, *120*, 6458−6467.
(696) Leigh, D. A.; Troisi, A.; Zerbetto, F. A Quantum-Mechanical Description of Macrocyclic Ring Rotation in Benzylic Amide [2]-Catenanes. *Chem. - Eur. J.* **2001**, *7*, 1450−1454.
(697) Deleuze, M. S.; Leigh, D. A.; Zerbetto, F. How Do Benzylic Amide [2]Catenane Rings Rotate? *J. Am. Chem. Soc.* **1999**, *121*, 2364−2379.
(698) Panman, M. R.; Bakker, B. H.; den Uyl, D.; Kay, E. R.; Leigh, D. A.; Buma, W. J.; Brouwer, A. M.; Geenevasen, J. A. J.; Woutersen, S. Water Lubricates Hydrogen-bonded Molecular Machines. *Nat. Chem.* **2013**, *5*, 929−934.
(699) Ghosh, P.; Federwisch, G.; Kogej, M.; Schalley, C. A.; Haase, D.; Saak, W.; Lutzen, A.; Gschwind, R. M. Controlling the Rate of Shuttling Motions in [2]Rotaxanes by Electrostatic Interactions: A Cation as Solvent-tunable Brake. *Org. Biomol. Chem.* **2005**, *3*, 2691−2700.
(700) Cao, J.; Fyfe, M. C. T.; Stoddart, J. F.; Cousins, G. R. L.; Glink, P. T. Molecular Shuttles by the Protecting Group Approach†. *J. Org. Chem.* **2000**, *65*, 1937−1946.
(701) Jiang, L.; Okano, J.; Orita, A.; Otera, J. Intermittent Molecular Shuttle as a Binary Switch. *Angew. Chem., Int. Ed.* **2004**, *43*, 2121−2124.
(702) Leigh, D. A.; Lusby, P. J.; Slawin, A. M. Z.; Walker, D. B. Rare and Diverse Binding Modes Introduced through Mechanical Bonding. *Angew. Chem., Int. Ed.* **2005**, *44*, 4557−4564.
(703) Martinez-Cuezva, A.; Berna, J.; Orenes, R.-A.; Pastor, A.; Alajarin, M. Small-Molecule Recognition for Controlling Molecular Motion in Hydrogen-Bond-Assembled Rotaxanes. *Angew. Chem., Int. Ed.* **2014**, *53*, 6762−6767.
(704) Berna, J.; Alajarin, M.; Marin-Rodriguez, C.; Franco-Pujante, C. Redox Divergent Conversion of a [2]Rotaxane into Two Distinct Degenerate Partners with Different Shuttling Dynamics. *Chem. Sci.* **2012**, *3*, 2314−2320.

DOI: 10.1021/acs.chemrev.5b00146
Chem. Rev. 2015, 115, 10081−10206

(705) Hirose, K.; Shiba, Y.; Ishibashi, K.; Doi, Y.; Tobe, Y. A Shuttling Molecular Machine with Reversible Brake Function. *Chem. - Eur. J.* **2008**, *14*, 3427−3433.
(706) Leigh, D. A.; Troisi, A.; Zerbetto, F. Reducing Molecular Shuttling to a Single Dimension. *Angew. Chem., Int. Ed.* **2000**, *39*, 350−353.
(707) Günbaş, D. D.; Brouwer, A. M. Degenerate Molecular Shuttles with Flexible and Rigid Spacers. *J. Org. Chem.* **2012**, *77*, 5724−5735.
(708) Andersen, S. S.; Share, A. I.; Poulsen, B. L. C.; Kørner, M.; Duedal, T.; Benson, C. R.; Hansen, S. W.; Jeppesen, J. O.; Flood, A. H. Mechanistic Evaluation of Motion in Redox-Driven Rotaxanes Reveals Longer Linkers Hasten Forward Escapes and Hinder Backward Translations. *J. Am. Chem. Soc.* **2014**, *136*, 6373−6384.
(709) Young, P. G.; Hirose, K.; Tobe, Y. Axle Length Does Not Affect Switching Dynamics in Degenerate Molecular Shuttles with Rigid Spacers. *J. Am. Chem. Soc.* **2014**, *136*, 7899−7906.
(710) Yoon, I.; Benítez, D.; Zhao, Y.-L.; Miljanić, O. Š.; Kim, S.-Y.; Tkatchouk, E.; Leung, K. C. F.; Khan, S. I.; Goddard, W. A., III; Stoddart, J. F. Functionally Rigid and Degenerate Molecular Shuttles. *Chem. - Eur. J.* **2009**, *15*, 1115−1122.
(711) Benniston, A. C.; Harriman, A. A Light-Induced Molecular Shuttle Based on a [2]Rotaxane-Derived Triad. *Angew. Chem., Int. Ed. Engl.* **1993**, *32*, 1459−1461.
(712) Murakami, H.; Kawabuchi, A.; Kotoo, K.; Kunitake, M.; Nakashima, N. A Light-driven Molecular Shuttle Based on a Rotaxane. *J. Am. Chem. Soc.* **1997**, *119*, 7605−7606.
(713) Murakami, H.; Kawabuchi, A.; Matsumoto, R.; Ido, T.; Nakashima, N. A Multi-mode-driven Molecular Shuttle: Photochemically and Thermally Reactive Azobenzene Rotaxanes. *J. Am. Chem. Soc.* **2005**, *127*, 15891−15899.
(714) Clegg, W.; Gimenez-Saiz, C.; Leigh, D. A.; Murphy, A.; Slawin, A. M. Z.; Teat, S. J. "Smart" Rotaxanes: Shape Memory and Control in Tertiary Amide Peptido[2]rotaxanes. *J. Am. Chem. Soc.* **1999**, *121*, 4124−4129.
(715) Asakawa, M.; Brancato, G.; Fanti, M.; Leigh, D. A.; Shimizu, T.; Slawin, A. M. Z.; Wong, J. K. Y.; Zerbetto, F.; Zhang, S. W. Switching "On" and "Off" the Expression of Chirality in Peptide Rotaxanes. *J. Am. Chem. Soc.* **2002**, *124*, 2939−2950.
(716) Dong, S.; Yuan, J.; Huang, F. A Pillar[5]arene/imidazolium [2]Rotaxane: Solvent- and Thermo-driven Molecular Motions and Supramolecular Gel Formation. *Chem. Sci.* **2014**, *5*, 247−252.
(717) Zhang, Z.; Han, C.; Yu, G.; Huang, F. A Solvent-driven Molecular Spring. *Chem. Sci.* **2012**, *3*, 3026−3031.
(718) Bissell, R. A.; Cordova, E.; Kaifer, A. E.; Stoddart, J. F. A Chemically and Electrochemically Switchable Molecular Shuttle. *Nature* **1994**, *369*, 133−137.
(719) Castro, R.; Berardi, M. J.; Cordova, E.; de Olza, M. O.; Kaifer, A. E.; Evanseck, J. D. Unexpected Roles of Guest Polarizability and Maximum Hardness, and of Host Solvation in Supramolecular Inclusion Complexes: A Dual Theoretical and Experimental Study. *J. Am. Chem. Soc.* **1996**, *118*, 10257−10268.
(720) Castro, R.; Nixon, K. R.; Evanseck, J. D.; Kaifer, A. E. Effects of Side Arm Length and Structure of *para*-Substituted Phenyl Derivatives on Their Binding to the Host Cyclobis(paraquat-p-phenylene). *J. Org. Chem.* **1996**, *61*, 7298−7303.
(721) Kaminski, G. A.; Jorgensen, W. L. Host-guest Chemistry of Rotaxanes and Catenanes: Application of a Polarizable All-atom Force Field to Cyclobis(paraquat-p-phenylene) Complexes with Disubstituted Benzenes and Biphenyls. *J. Chem. Soc., Perkin Trans. 2* **1999**, 2365−2375.
(722) Macias, A. T.; Kumar, K. A.; Marchand, A. P.; Evanseck, J. D. Computational Studies of Inclusion Phenomena and Synthesis of a Novel and Selective Molecular Receptor for 1,4-Disubstituted Benzenes and 4,4′-Disubstituted Biphenyls. *J. Org. Chem.* **2000**, *65*, 2083−2089.
(723) Zhang, K. C.; Liu, L.; Mu, T. W.; Guo, Q. X. *Ab initio* Calculations on the Inclusion Complexation of Cyclobis(paraquat-p-phenylene). *Chem. Phys. Lett.* **2001**, *333*, 195−198.
(724) Grabuleda, X.; Ivanov, P.; Jaime, C. Shuttling Process in [2]Rotaxanes. Modeling by Molecular Dynamics and Free Energy Perturbation Simulations. *J. Phys. Chem. B* **2003**, *107*, 7582−7588.
(725) Grabuleda, X.; Jaime, C. Molecular Shuttles. A Computational Study (MM and MD) on the Translational Isomerism in Some [2]Rotaxanes. *J. Org. Chem.* **1998**, *63*, 9635−9643.
(726) Ercolani, G.; Mencarelli, P. Role of Face-to-face and Edge-to-face Aromatic Interactions in the Inclusion Complexation of Cyclobis-(paraquat-p-phenylene): A Theoretical Study. *J. Org. Chem.* **2003**, *68*, 6470−6473.
(727) Castro, R.; Davidov, P. D.; Kumar, K. A.; Marchand, A. P.; Evanseck, J. D.; Kaifer, A. E. Inclusion Complexation of Cyclobis-(paraquat-p-phenylene) and Related Cyclophane Derivatives with Substituted Aromatics: Cooperative Non-covalent Cavity and External Interactions. *J. Phys. Org. Chem.* **1997**, *10*, 369−382.
(728) Grabuleda, X.; Ivanov, P.; Jaime, C. Computational Studies on Pseudorotaxanes by Molecular Dynamics and Free Energy Perturbation Simulations. *J. Org. Chem.* **2003**, *68*, 1539−1547.
(729) Martinez-Diaz, M. V.; Spencer, N.; Stoddart, J. F. The Self-assembly of a Switchable [2]Rotaxane. *Angew. Chem., Int. Ed. Engl.* **1997**, *36*, 1904−1907.
(730) Badjic, J. D.; Balzani, V.; Credi, A.; Silvi, S.; Stoddart, J. F. A Molecular Elevator. *Science* **2004**, *303*, 1845−1849.
(731) Leigh, D. A.; Thomson, A. R. Switchable Dual Binding Mode Molecular Shuttle. *Org. Lett.* **2006**, *8*, 5377−5379.
(732) Vella, S. J.; Tiburcio, J.; Loeb, S. J. Optically Sensed, Molecular Shuttles Driven by Acid-base Chemistry. *Chem. Commun.* **2007**, 4752−4754.
(733) Zheng, H. Y.; Zhou, W. D.; Lv, J.; Yin, X. D.; Li, Y. J.; Liu, H. B.; Li, Y. L. A Dual-Response [2]Rotaxane Based on a 1,2,3-Triazole Ring as a Novel Recognition Station. *Chem. - Eur. J.* **2009**, *15*, 13253−13262.
(734) Tuncel, D.; Katterle, M. pH-triggered Dethreading-rethreading and Switching of Cucurbit[6]uril on Bistable [3]Pseudorotaxanes and [3]Rotaxanes. *Chem. - Eur. J.* **2008**, *14*, 4110−4116.
(735) Kolchinski, A. G.; Busch, D. H.; Alcock, N. W. Gaining Control over Molecular Threading - Benefits of 2nd Coordination Sites and Aqueous-Organic Interfaces in Rotaxane Synthesis. *J. Chem. Soc., Chem. Commun.* **1995**, 1289−1291.
(736) Glink, P. T.; Schiavo, C.; Stoddart, J. F.; Williams, D. J. The Genesis of a New Range of Interlocked Molecules. *Chem. Commun.* **1996**, 1483−1490.
(737) Cantrill, S. J.; Pease, A. R.; Stoddart, J. F. A Molecular Meccano Kit. *J. Chem. Soc. Dalton* **2000**, 3715−3734.
(738) Ashton, P. R.; Glink, P. T.; Stoddart, J. F.; Tasker, P. A.; White, A. J. P.; Williams, D. J. Self-assembling [2]- and [3]Rotaxanes from Secondary Dialkylammonium Salts and Crown Ethers. *Chem. - Eur. J.* **1996**, *2*, 729−736.
(739) Ashton, P. R.; Ballardini, R.; Balzani, V.; Baxter, I.; Credi, A.; Fyfe, M. C. T.; Gandolfi, M. T.; Gomez-Lopez, M.; Martinez-Diaz, M. V.; Piersanti, A.; et al. Acid-base Controllable Molecular Shuttles. *J. Am. Chem. Soc.* **1998**, *120*, 11932−11942.
(740) Garaudee, S.; Silvi, S.; Venturi, M.; Credi, A.; Flood, A. H.; Stoddart, J. F. Shuttling Dynamics in an Acid-base-switchable [2]Rotaxane. *ChemPhysChem* **2005**, *6*, 2145−2152.
(741) Frankfort, L.; Sohlberg, K. Semi-empirical Study of a pH-switchable [2] Rotaxane. *J. Mol. Struct.: THEOCHEM* **2003**, *621*, 253−260.
(742) Elizarov, A. M.; Chiu, S. H.; Stoddart, J. F. An Acid-base Switchable [2]Rotaxane. *J. Org. Chem.* **2002**, *67*, 9175−9181.
(743) Badjic, J. D.; Ronconi, C. M.; Stoddart, J. F.; Balzani, V.; Silvi, S.; Credi, A. Operating Molecular Elevators. *J. Am. Chem. Soc.* **2006**, *128*, 1489−1499.
(744) Bruns, C. J.; Stoddart, J. F. Molecular Machines Muscle Up. *Nat. Nanotechnol.* **2012**, *8*, 9−10.
(745) Clark, P. G.; Day, M. W.; Grubbs, R. H. Switching and Extension of a [c2]Daisy-Chain Dimer Polymer. *J. Am. Chem. Soc.* **2009**, *131*, 13631−13633.
(746) Du, G. Y.; Moulin, E.; Jouault, N.; Buhler, E.; Giuseppone, N. Muscle-like Supramolecular Polymers: Integrated Motion from

DOI: 10.1021/acs.chemrev.5b00146
Chem. Rev. 2015, 115, 10081−10206

Thousands of Molecular Machines. *Angew. Chem., Int. Ed.* **2012**, *51*, 12504−12508.
(747) Keaveney, C. M.; Leigh, D. A. Shuttling Through Anion Recognition. *Angew. Chem., Int. Ed.* **2004**, *43*, 1222−1224.
(748) Hesseler, B.; Zindler, M.; Herges, R.; Lüning, U. A Shuttle for the Transport of Protons Based on a [2]Rotaxane. *Eur. J. Org. Chem.* **2014**, *2014*, 3885−3901.
(749) Hesseler, B.; Zindler, M.; Herges, R.; Lüning, U. A Shuttle for the Transport of Protons Based on a [2]Rotaxane. *Eur. J. Org. Chem.* **2014**, *2014*, 3885−3901.
(750) Crowley, J. D.; Leigh, D. A.; Lusby, P. J.; McBurney, R. T.; Perret-Aebi, L. E.; Petzold, C.; Slawin, A. M. Z.; Symes, M. D. A Switchable Palladium-complexed Molecular Shuttle and its Metastable Positional Isomers. *J. Am. Chem. Soc.* **2007**, *129*, 15085−15090.
(751) Buyukcakir, O.; Yasar, F. T.; Bozdemir, O. A.; Icli, B.; Akkaya, E. U. Autonomous Shuttling Driven by an Oscillating Reaction: Proof of Principle in a Cucurbit[7]uril-Bodipy Pseudorotaxane. *Org. Lett.* **2013**, *15*, 1012−1015.
(752) Joosten, A.; Trolez, Y.; Collin, J.-P.; Heitz, V.; Sauvage, J.-P. Copper(I)-Assembled [3]Rotaxane Whose Two Rings Act as Flapping Wings. *J. Am. Chem. Soc.* **2012**, *134*, 1802−1809.
(753) Ashton, P. R.; Bissell, R. A.; Spencer, N.; Stoddart, J. F.; Tolley, M. S. Towards Controllable Molecular Shuttles - 1. *Synlett* **1992**, *1992*, 914−918.
(754) Ashton, P. R.; Bissell, R. A.; Gorski, R.; Philp, D.; Spencer, N.; Stoddart, J. F.; Tolley, M. S. Towards Controllable Molecular Shuttles - 2. *Synlett* **1992**, *1992*, 919−922.
(755) Ashton, P. R.; Bissell, R. A.; Spencer, N.; Stoddart, J. F.; Tolley, M. S. Towards Controllable Molecular Shuttles - 3. *Synlett* **1992**, *1992*, 923−926.
(756) Anelli, P. L.; Asakawa, M.; Ashton, P. R.; Bissell, R. A.; Clavier, G.; Gorski, R.; Kaifer, A. E.; Langford, S. J.; Mattersteig, G.; Menzer, S.; et al. Toward Controllable Molecular Shuttles. *Chem. - Eur. J.* **1997**, *3*, 1113−1135.
(757) Brouwer, A. M.; Frochot, C.; Gatti, F. G.; Leigh, D. A.; Mottier, L.; Paolucci, F.; Roffia, S.; Wurpel, G. W. H. Photoinduction of Fast, Reversible Translational Motion in a Hydrogen-bonded Molecular Shuttle. *Science* **2001**, *291*, 2124−2128.
(758) Altieri, A.; Gatti, F. G.; Kay, E. R.; Leigh, D. A.; Martel, D.; Paolucci, F.; Slawin, A. M. Z.; Wong, J. K. Y. Electrochemically Switchable Hydrogen-bonded Molecular Shuttles. *J. Am. Chem. Soc.* **2003**, *125*, 8644−8654.
(759) Zheng, X. G.; Sohlberg, K. Modeling of a Rotaxane-based Molecular Device. *J. Phys. Chem. A* **2003**, *107*, 1207−1215.
(760) Raiteri, P.; Bussi, G.; Cucinotta, C. S.; Credi, A.; Stoddart, J. F.; Parrinello, M. Unravelling the Shuttling Mechanism in a Photo-switchable Multicomponent Bistable Rotaxane. *Angew. Chem., Int. Ed.* **2008**, *47*, 3536−3539.
(761) Tseng, H. R.; Vignon, S. A.; Stoddart, J. F. Toward Chemically Controlled Nanoscale Molecular Machinery. *Angew. Chem., Int. Ed.* **2003**, *42*, 1491−1495.
(762) Fioravanti, G.; Haraszkiewicz, N.; Kay, E. R.; Mendoza, S. M.; Bruno, C.; Marcaccio, M.; Wiering, P. G.; Paolucci, F.; Rudolf, P.; Brouwer, A. M.; et al. Three State Redox-active Molecular Shuttle That Switches in Solution and on a Surface. *J. Am. Chem. Soc.* **2008**, *130*, 2593−2601.
(763) Zhao, Y. L.; Dichtel, W. R.; Trabolsi, A.; Saha, S.; Aprahamian, I.; Stoddart, J. F. A Redox-switchable alpha-Cyclodextrin-based [2]-Rotaxane. *J. Am. Chem. Soc.* **2008**, *130*, 11294−11296.
(764) Saha, S.; Flood, A. H.; Stoddart, J. F.; Impellizzeri, S.; Silvi, S.; Venturi, M.; Credi, A. A Redox-driven Multicomponent Molecular Shuttle. *J. Am. Chem. Soc.* **2007**, *129*, 12159−12171.
(765) Barnes, J. C.; Fahrenbach, A. C.; Dyar, S. M.; Frasconi, M.; Giesener, M. A.; Zhu, Z. X.; Liu, Z. C.; Hartlieb, K. J.; Carmieli, R.; Wasielewski, M. R.; et al. Mechanically Induced Intramolecular Electron Transfer in a Mixed-valence Molecular Shuttle. *Proc. Natl. Acad. Sci. U. S. A.* **2012**, *109*, 11546−11551.
(766) Amabilino, D. B.; Ashton, P. R.; Boyd, S. E.; GomezLopez, M.; Hayes, W.; Stoddart, J. F. Translational Isomerism in Some Two- and Three-station [2]Rotaxanes. *J. Org. Chem.* **1997**, *62*, 3062−3075.
(767) Asakawa, M.; Ashton, P. R.; Balzani, V.; Credi, A.; Hamers, C.; Mattersteig, G.; Montalti, M.; Shipway, A. N.; Spencer, N.; Stoddart, J. F.; et al. A Chemically and Electrochemically Switchable [2]Catenane Incorporating a Tetrathiafulvalene Unit. *Angew. Chem., Int. Ed.* **1998**, *37*, 333−337.
(768) Jeppesen, J. O.; Perkins, J.; Becher, J.; Stoddart, J. F. Slow Shuttling in an Amphiphilic Bistable [2]Rotaxane Incorporating a Tetrathiafulvalene Unit. *Angew. Chem., Int. Ed.* **2001**, *40*, 1216−1221.
(769) Tseng, H. R.; Vignon, S. A.; Celestre, P. C.; Perkins, J.; Jeppesen, J. O.; Di Fabio, A.; Ballardini, R.; Gandolfi, M. T.; Venturi, M.; Balzani, V.; et al. Redox-controllable Amphiphilic [2]Rotaxanes. *Chem. - Eur. J.* **2004**, *10*, 155−172.
(770) Flood, A. H.; Peters, A. J.; Vignon, S. A.; Steuerman, D. W.; Tseng, H. R.; Kang, S.; Heath, J. R.; Stoddart, J. F. The Role of Physical Environment on Molecular Electromechanical Switching. *Chem. - Eur. J.* **2004**, *10*, 6558−6564.
(771) Jeppesen, J. O.; Nygaard, S.; Vignon, S. A.; Stoddart, J. F. Honing up a Genre of Amphiphilic Bistable [2]rotaxanes for Device Settings. *Eur. J. Org. Chem.* **2005**, *2005*, 196−220.
(772) Choi, J. W.; Flood, A. H.; Steuerman, D. W.; Nygaard, S.; Braunschweig, A. B.; Moonen, N. N. P.; Laursen, B. W.; Luo, Y.; DeIonno, E.; Peters, A. J.; et al. Ground-state Equilibrium Thermodynamics and Switching Kinetics of Bistable [2]Rotaxanes Switched in Solution, Polymer Gels, and Molecular Electronic Devices. *Chem. - Eur. J.* **2006**, *12*, 261−279.
(773) Kang, S. S.; Vignon, S. A.; Tseng, H. R.; Stoddart, J. F. Molecular Shuttles Based on Tetrathiafulvalene Units and 1,5-Dioxynaphthalene Ring Systems. *Chem. - Eur. J.* **2004**, *10*, 2555−2564.
(774) Jeppesen, J. O.; Nielsen, K. A.; Perkins, J.; Vignon, S. A.; Di Fabio, A.; Ballardini, R.; Gandolfi, M. T.; Venturi, M.; Balzani, V.; Becher, J.; et al. Amphiphilic Bistable Rotaxanes. *Chem. - Eur. J.* **2003**, *9*, 2982−3007.
(775) Ashton, P. R.; Ballardini, R.; Balzani, V.; Credi, A.; Dress, K. R.; Ishow, E.; Kleverlaan, C. J.; Kocian, O.; Preece, J. A.; Spencer, N.; et al. A Photochemically Driven Molecular-level Abacus. *Chem. - Eur. J.* **2000**, *6*, 3558−3574.
(776) Ballardini, R.; Balzani, V.; Dehaen, W.; Dell'Erba, A. E.; Raymo, F. M.; Stoddart, J. F.; Venturi, M. Molecular Meccano, 56 - Anthracene-containing [2]Rotaxanes: Synthesis, Spectroscopic, and Electrochemical Properties. *Eur. J. Org. Chem.* **2000**, *2000*, 591−602.
(777) Kihara, N.; Hashimoto, M.; Takata, T. Redox Behavior of Ferrocene-containing Rotaxane: Transposition of the Rotaxane Wheel by Redox Reaction of a Ferrocene Moiety Tethered at the End of the Axle. *Org. Lett.* **2004**, *6*, 1693−1696.
(778) Armaroli, N.; Balzani, V.; Collin, J.-P.; Gavina, P.; Sauvage, J.-P.; Ventura, B. Rotaxanes Incorporating Two Different Coordinating Units in Their Thread: Synthesis and Electrochemically and Photochemically Induced Molecular Motions. *J. Am. Chem. Soc.* **1999**, *121*, 4397−4408.
(779) Trabolsi, A.; Khashab, N.; Fahrenbach, A. C.; Friedman, D. C.; Colvin, M. T.; Cotí, K. K.; Benítez, D.; Tkatchouk, E.; Olsen, J.-C.; Belowich, M. E.; et al. Radically Enhanced Molecular Recognition. *Nat. Chem.* **2010**, *2*, 42−49.
(780) Vignon, S. A.; Jarrosson, T.; Iijima, T.; Tseng, H. R.; Sanders, J. K. M.; Stoddart, J. F. Switchable Neutral Bistable Rotaxanes. *J. Am. Chem. Soc.* **2004**, *126*, 9884−9885.
(781) Marlin, D. S.; Cabrera, D. G.; Leigh, D. A.; Slawin, A. M. Z. Complexation-induced Translational Isomerism: Shuttling Through Stepwise Competitive Binding. *Angew. Chem., Int. Ed.* **2006**, *45*, 77−83.
(782) Marlin, D. S.; Cabrera, D. G.; Leigh, D. A.; Slawin, A. M. Z. An Allosterically Regulated Molecular Shuttle. *Angew. Chem., Int. Ed.* **2006**, *45*, 1385−1390.
(783) Barrell, M. J.; Leigh, D. A.; Lusby, P. J.; Slawin, A. M. Z. An Ion-Pair Template for Rotaxane Formation and its Exploitation in an Orthogonal Interaction Anion-Switchahle Molecular Shuttle. *Angew. Chem., Int. Ed.* **2008**, *47*, 8036−8039.

DOI: 10.1021/acs.chemrev.5b00146
Chem. Rev. 2015, 115, 10081−10206

(784) Spence, G. T.; Pitak, M. B.; Beer, P. D. Anion-Induced Shuttling of a Naphthalimide Triazolium Rotaxane. *Chem. - Eur. J.* **2012**, *18*, 7100−7108.
(785) Caballero, A.; Swan, L.; Zapata, F.; Beer, P. D. Iodide-Induced Shuttling of a Halogen- and Hydrogen-Bonding Two-Station Rotaxane. *Angew. Chem., Int. Ed.* **2014**, *53*, 11854−11858.
(786) Collins, C. G.; Peck, E. M.; Kramer, P. J.; Smith, B. D. Squaraine Rotaxane Shuttle as a Ratiometric Deep-red Optical Chloride Sensor. *Chem. Sci.* **2013**, *4*, 2557−2563.
(787) You, Y. C.; Tzeng, M. C.; Lai, C. C.; Chiu, S. H. Using Oppositely Charged Ions To Operate a Three-Station [2]Rotaxane in Two Different Switching Modes. *Org. Lett.* **2012**, *14*, 1046−1049.
(788) Collin, J.-P.; Frey, J.; Heitz, V.; Sauvage, J.-P.; Tock, C.; Allouche, L. Adjustable Receptor Based on a [3]Rotaxane Whose Two Threaded Rings Are Rigidly Attached to Two Porphyrinic Plates: Synthesis and Complexation Studies. *J. Am. Chem. Soc.* **2009**, *131*, 5609−5620.
(789) Leigh, D. A.; Perez, E. M. Shuttling Through Reversible Covalent Chemistry. *Chem. Commun.* **2004**, 2262−2263.
(790) Abraham, W.; Grubert, L.; Grummt, U. W.; Buck, K. A Photoswitchable Rotaxane with a Folded Molecular Thread. *Chem. - Eur. J.* **2004**, *10*, 3562−3568.
(791) Schmidt-Schaffer, S.; Grubert, L.; Grummt, U. W.; Buck, K.; Abraham, W. A Photoswitchable Rotaxane with an Unfolded Molecular Thread. *Eur. J. Org. Chem.* **2006**, *2006*, 378−398.
(792) Umehara, T.; Kawai, H.; Fujiwara, K.; Suzuki, T. Entropy- and Hydrolytic-driven Positional Switching of Macrocycle Between Imine- and Hydrogen-bonding Stations in Rotaxane-based Molecular Shuttles. *J. Am. Chem. Soc.* **2008**, *130*, 13981−13988.
(793) Berna, J.; Alajarin, M.; Orenes, R. A. Azodicarboxamides as Template Binding Motifs for the Building of Hydrogen-Bonded Molecular Shuttles. *J. Am. Chem. Soc.* **2010**, *132*, 10741−10747.
(794) Balzani, V.; Clemente-Leon, M.; Credi, A.; Ferrer, B.; Venturi, M.; Flood, A. H.; Stoddart, J. F. Autonomous Artificial Nanomotor Powered by Sunlight. *Proc. Natl. Acad. Sci. U. S. A.* **2006**, *103*, 1178−1183.
(795) Wurpel, G. W. H.; Brouwer, A. M.; van Stokkum, I. H. M.; Farran, A.; Leigh, D. A. Enhanced Hydrogen Bonding Induced by Optical Excitation: Unexpected Subnanosecond Photoinduced Dynamics in a Peptide-based [2]Rotaxane. *J. Am. Chem. Soc.* **2001**, *123*, 11327−11328.
(796) Wang, Q. C.; Qu, D. H.; Ren, J.; Chen, K. C.; Tian, H. A Lockable Light-driven Molecular Shuttle with a Fluorescent Signal. *Angew. Chem., Int. Ed.* **2004**, *43*, 2661−2665.
(797) Bottari, G.; Dehez, F.; Leigh, D. A.; Nash, P. J.; Perez, E. M.; Wong, J. K. Y.; Zerbetto, F. Entropy-driven Translational Isomerism: A Tristable Molecular Shuttle. *Angew. Chem., Int. Ed.* **2003**, *42*, 5886−5889.
(798) Altieri, A.; Bottari, G.; Dehez, F.; Leigh, D. A.; Wong, J. K. Y.; Zerbetto, F. Remarkable Positional Discrimination in Bistable Light- and Heat-switchable Hydrogen-bonded Molecular Shuttles. *Angew. Chem., Int. Ed.* **2003**, *42*, 2296−2300.
(799) Qu, D. H.; Wang, G. C.; Ren, J.; Tian, H. A Light-driven Rotaxane Molecular Shuttle with Dual Fluorescence Addresses. *Org. Lett.* **2004**, *6*, 2085−2088.
(800) Zhou, W. D.; Li, J. B.; He, X. R.; Li, C. H.; Lv, J.; Li, Y. L.; Wang, S.; Liu, H. B.; Zhu, D. B. A Molecular Shuttle for Driving a Multilevel Fluorescence Switch. *Chem. - Eur. J.* **2008**, *14*, 754−763.
(801) Qu, D. H.; Ji, F. Y.; Wang, Q. C.; Tian, H. A Double INHIBIT Logic Gate Employing Configuration and Fluorescence Changes. *Adv. Mater.* **2006**, *18*, 2035−2038.
(802) Zhou, W. D.; Chen, D. G.; Li, J. B.; Xu, J. L.; Lv, J.; Liu, H. B.; Li, Y. L. Photoisomerization of Spiropyran for Driving a Molecular Shuttle. *Org. Lett.* **2007**, *9*, 3929−3932.
(803) Gunbas, D. D.; Zalewski, L.; Brouwer, A. M. Solvatochromic Rotaxane Molecular Shuttles. *Chem. Commun.* **2011**, *47*, 4977−4979.
(804) Hanke, A.; Metzler, R. Towards the Molecular Workshop: Entropy-driven Designer Molecules, Entropy Activation, and Nanomechanical Devices. *Chem. Phys. Lett.* **2002**, *359*, 22−26.
(805) Gong, C. G.; Gibson, H. W. Controlling Microstructure in Polymeric Molecular Shuttles: Solvent-induced Localization of Macrocycles in Poly(urethane/crown Ether) Rotaxanes. *Angew. Chem., Int. Ed. Engl.* **1997**, *36*, 2331−2333.
(806) Meng, Z.; Xiang, J. F.; Chen, C. F. Tristable [n]Rotaxanes: From Molecular Shuttle to Molecular Cable Car. *Chem. Sci.* **2014**, *5*, 1520−1525.
(807) Busseron, E.; Coutrot, F. N-benzyltriazolium as Both Molecular Station and Barrier in [2]Rotaxane Molecular Machines. *J. Org. Chem.* **2013**, *78*, 4099−106.
(808) Serreli, V.; Lee, C. F.; Kay, E. R.; Leigh, D. A. A Molecular Information Ratchet. *Nature* **2007**, *445*, 523−527.
(809) Alvarez-Perez, M.; Goldup, S. M.; Leigh, D. A.; Slawin, A. M. Z. A Chemically-driven Molecular Information Ratchet. *J. Am. Chem. Soc.* **2008**, *130*, 1836−1838.
(810) Carlone, A.; Goldup, S. M.; Lebrasseur, N.; Leigh, D. A.; Wilson, A. A Three-compartment Chemically-driven Molecular Information Ratchet. *J. Am. Chem. Soc.* **2012**, *134*, 8321−8323.
(811) Li, H.; Cheng, C. Y.; McGonigal, P. R.; Fahrenbach, A. C.; Frasconi, M.; Liu, W. G.; Zhu, Z. X.; Zhao, Y. L.; Ke, C. F.; Lei, J. Y.; et al. Relative Unidirectional Translation in an Artificial Molecular Assembly Fueled by Light. *J. Am. Chem. Soc.* **2013**, *135*, 18609−18620.
(812) Cheng, C.; McGonigal, P. R.; Schneebeli, S. T.; Li, H.; Vermeulen, N. A.; Ke, C.; Stoddart, J. F. An Artificial Molecular Pump. *Nat. Nanotechnol.* **2015**, *10*, 547−553.
(813) Cheng, C.; McGonigal, P. R.; Liu, W.-G.; Li, H.; Vermeulen, N. A.; Ke, C.; Frasconi, M.; Stern, C. L.; Goddard, W. A., III; Stoddart, J. F. Energetically Demanding Transport in a Supramolecular Assembly. *J. Am. Chem. Soc.* **2014**, *136*, 14702−14705.
(814) Baroncini, M.; Silvi, S.; Venturi, M.; Credi, A. Photoactivated Directionally Controlled Transit of a Non-Symmetric Molecular Axle Through a Macrocycle. *Angew. Chem., Int. Ed.* **2012**, *51*, 4223−4226.
(815) Ragazzon, G.; Baroncini, M.; Silvi, S.; Venturi, M.; Credi, A. Light-powered Autonomous and Directional Molecular Motion of a Dissipative Self-assembling System. *Nat. Nanotechnol.* **2014**, *10*, 70−75.
(816) Martinez-Cuezva, A.; Pastor, A.; Cioncoloni, G.; Orenes, R.-A.; Alajarin, M.; Symes, M. D.; Berna, J. Versatile Control of the Submolecular Motion of Di(acylamino)pyridine-based [2]Rotaxanes. *Chem. Sci.* **2015**, *6*, 3087−3094.
(817) Leigh, D. A.; Lusby, P. J.; Slawin, A. M. Z.; Walker, D. B. Half-rotation in a Kinetically Locked [2] Catenane Induced by Transition Metal Ion Substitution. *Chem. Commun.* **2012**, *48*, 5826−5828.
(818) Letinois-Halbes, U.; Hanss, D.; Beierle, J. M.; Collin, J.-P.; Sauvage, J.-P. A Fast-moving [2]Rotaxane Whose Stoppers are Remote from the Copper Complex Core. *Org. Lett.* **2005**, *7*, 5753−5756.
(819) Nakatani, Y.; Furusho, Y.; Yashima, E. Amidinium Carboxylate Salt Bridges as a Recognition Motif for Mechanically Interlocked Molecules: Synthesis of an Optically Active [2]Catenane and Control of Its Structure. *Angew. Chem., Int. Ed.* **2010**, *49*, 5463−5467.
(820) Bermudez, V.; Capron, N.; Gase, T.; Gatti, F. G.; Kajzar, F.; Leigh, D. A.; Zerbetto, F.; Zhang, S. W. Influencing Intramolecular Motion with an Alternating Electric Field. *Nature* **2000**, *406*, 608−611.
(821) Brancato, G.; Coutrot, F.; Leigh, D. A.; Murphy, A.; Wong, J. K. Y.; Zerbetto, F. From Reactants to Products via Simple Hydrogen-bonding Networks: Information Transmission in Chemical Reactions. *Proc. Natl. Acad. Sci. U. S. A.* **2002**, *99*, 4967−4971.
(822) Lukin, O.; Kubota, T.; Okamoto, Y.; Schelhase, F.; Yoneva, A.; Muller, W. M.; Muller, U.; Vogtle, F. Knotaxanes - Rotaxanes with Knots as Stoppers. *Angew. Chem., Int. Ed.* **2003**, *42*, 4542−4545.
(823) Kapitulnik, A.; Casalnuovo, S.; Lim, K. C.; Heeger, A. J. Electric-Field Coupling to Slow Elastic Modes in Gels of Conjugated Polymers. *Phys. Rev. Lett.* **1984**, *53*, 469−472.
(824) Lim, K. C.; Kapitulnik, A.; Zacher, R.; Heeger, A. J. Conformation of Polydiacetylene Macromolecules in Solution - Field-Induced Birefringence and Rotational Diffusion Constant. *J. Chem. Phys.* **1985**, *82*, 516−521.
(825) Gatti, F. G.; Lent, S.; Wong, J. K. Y.; Bottari, G.; Altieri, A.; Morales, M. A. F.; Teat, S. J.; Frochot, C.; Leigh, D. A.; Brouwer, A. M.; et al. Photoisomerization of a Rotaxane Hydrogen Bonding Template:

DOI: 10.1021/acs.chemrev.5b00146
Chem. Rev. 2015, 115, 10081−10206

Light-induced Acceleration of a Large Amplitude Rotational Motion. *Proc. Natl. Acad. Sci. U. S. A.* **2003**, *100*, 10−14.
(826) Leigh, D. A.; Moody, K.; Smart, J. P.; Watson, K. J.; Slawin, A. M. Z. Catenane Chameleons: Environment-sensitive Translational Isomerism in Amphiphilic Benzylic Amide [2]Catenanes. *Angew. Chem., Int. Ed. Engl.* **1996**, *35*, 306−310.
(827) Kemsley, J. Water Lubricates Molecular Machines. *Chem. Eng. News* **2013**, *91*, 43−43.
(828) Rijs, A. M.; Compagnon, I.; Oomens, J.; Hannam, J. S.; Leigh, D. A.; Buma, W. J. Stiff, and Sticky in the Right Places: Binding Interactions in Isolated Mechanically Interlocked Molecules Probed by Mid-Infrared Spectroscopy. *J. Am. Chem. Soc.* **2009**, *131*, 2428−2429.
(829) Rijs, A. M.; Sändig, N.; Blom, M. N.; Oomens, J.; Hannam, J. S.; Leigh, D. A.; Zerbetto, F.; Buma, W. J. Controlled Hydrogen-Bond Breaking in a Rotaxane by Discrete Solvation. *Angew. Chem., Int. Ed.* **2010**, *49*, 3896−3900.
(830) Linke, M.; Chambron, J. C.; Heitz, V.; Sauvage, J.-P.; Semetey, V. Complete Rearrangement of a Multi-porphyrinic Rotaxane by Metallation-demetallation of the Central Coordination Site. *Chem. Commun.* **1998**, 2469−2470.
(831) Raehm, L.; Kern, J. M.; Sauvage, J.-P. A Transition Metal Containing Rotaxane in Motion: Electrochemically Induced Pirouetting of the Ring on the Threaded Dumbbell. *Chem. - Eur. J.* **1999**, *5*, 3310−3317.
(832) Kern, J. M.; Raehm, L.; Sauvage, J.-P.; Divisia-Blohorn, B.; Vidal, P. L. Controlled Molecular Motions in Copper-complexed Rotaxanes: An XAS Study. *Inorg. Chem.* **2000**, *39*, 1555−1560.
(833) Weber, N.; Hamann, C.; Kern, J. M.; Sauvage, J.-P. Synthesis of a Copper [3]Rotaxane Able to Function as an Electrochemically Driven Oscillatory Machine in Solution, and to Form SAMs on a Metal Surface. *Inorg. Chem.* **2003**, *42*, 6780−6792.
(834) Poleschak, I.; Kern, J. M.; Sauvage, J.-P. A Copper-complexed Rotaxane in Motion: Pirouetting of the Ring on the Millisecond Timescale. *Chem. Commun.* **2004**, 474−476.
(835) Ballesteros, B.; Faust, T. B.; Lee, C. F.; Leigh, D. A.; Muryn, C. A.; Pritchard, R. G.; Schultz, D.; Teat, S. J.; Timco, G. A.; Winpenny, R. E. P. Synthesis, Structure, and Dynamic Properties of Hybrid Organic-Inorganic Rotaxanes. *J. Am. Chem. Soc.* **2010**, *132*, 15435−15444.
(836) Lee, C. F.; Leigh, D. A.; Pritchard, R. G.; Schultz, D.; Teat, S. J.; Timco, G. A.; Winpenny, R. E. P. Hybrid Organic-inorganic Rotaxanes and Molecular Shuttles. *Nature* **2009**, *458*, 314−318.
(837) van Quaethem, A.; Lussis, P.; Leigh, D. A.; Duwez, A. S.; Fustin, C. A. Probing the Mobility of Catenane Rings in Single Molecules. *Chem. Sci.* **2014**, *5*, 1449−1452.
(838) Evans, N. H.; Serpell, C. J.; Beer, P. D. A [2]Catenane Displaying Pirouetting Motion Triggered by Debenzylation and Locked by Chloride Anion Recognition. *Chem. - Eur. J.* **2011**, *17*, 7734−7738.
(839) Andrievsky, A.; Ahuis, F.; Sessler, J. L.; Vogtle, F.; Gudat, D.; Moini, M. Bipyrrole-based [2]Catenane: A New Type of Anion Receptor. *J. Am. Chem. Soc.* **1998**, *120*, 9712−9713.
(840) Leontiev, A. V.; Serpell, C. J.; White, N. G.; Beer, P. D. Cation-induced Molecular Motion of Spring-like [2]Catenanes. *Chem. Sci.* **2011**, *2*, 922−927.
(841) Fang, L.; Wang, C.; Fahrenbach, A. C.; Trabolsi, A.; Botros, Y. Y.; Stoddart, J. F. Dual Stimulus Switching of a [2]Catenane in Water. *Angew. Chem., Int. Ed.* **2011**, *50*, 1805−1809.
(842) Amabilino, D. B.; Dietrich-Buchecker, C. O.; Livoreil, A.; PerezGarcia, L.; Sauvage, J.-P.; Stoddart, J. F. A Switchable Hybrid [2]-Catenane Based on Transition Metal Complexation and pi-Electron Donor-acceptor Interactions. *J. Am. Chem. Soc.* **1996**, *118*, 3905−3913.
(843) Balzani, V.; Credi, A.; Langford, S. J.; Raymo, F. M.; Stoddart, J. F.; Venturi, M. Constructing Molecular Machinery: A Chemically-switchable [2]Catenane. *J. Am. Chem. Soc.* **2000**, *122*, 3542−3543.
(844) Grunder, S.; McGrier, P. L.; Whalley, A. C.; Boyle, M. M.; Stern, C.; Stoddart, J. F. A Water-Soluble pH-Triggered Molecular Switch. *J. Am. Chem. Soc.* **2013**, *135*, 17691−17694.
(845) Korybut-Daszkiewicz, B.; Wieckowska, A.; Bilewicz, R.; Domagala, S.; Wozniak, K. An Electrochemically Controlled Molecular Shuttle. *Angew. Chem., Int. Ed.* **2004**, *43*, 1668−1672.
(846) Flamigni, L.; Talarico, A. M.; Serroni, S.; Puntoriero, F.; Gunter, M. J.; Johnston, M. R.; Jeynes, T. P. Photoinduced Electron Transfer Between the Interlocked Components of Porphyrin Catenanes: Effect of the Presence of Nonequivalent Reduction Sites on the Charge Recombination Rate. *Chem. - Eur. J.* **2003**, *9*, 2649−2659.
(847) Zheng, X. G.; Sohlberg, K. Modeling Bistability and Switching in a [2]Catenane. *Phys. Chem. Chem. Phys.* **2004**, *6*, 809−815.
(848) Ceccarelli, M.; Mercuri, F.; Passerone, D.; Parrinello, M. The Microscopic Switching Mechanism of a [2]Catenane. *J. Phys. Chem. B* **2005**, *109*, 17094−17099.
(849) Ashton, P. R.; Baldoni, V.; Balzani, V.; Credi, A.; Hoffmann, H. D. A.; Martinez-Diaz, M. V.; Raymo, F. M.; Stoddart, J. F.; Venturi, M. Dual-mode "Co-conformational" Switching in Catenanes Incorporating Bipyridinium and Dialkylammonium Recognition Sites. *Chem. - Eur. J.* **2001**, *7*, 3482−3493.
(850) Hamilton, D. G.; Montalti, M.; Prodi, L.; Fontani, M.; Zanello, P.; Sanders, J. K. M. Photophysical and Electrochemical Characterization of the Interactions Between Components in Neutral pi-Associated [2]Catenanes. *Chem. - Eur. J.* **2000**, *6*, 608−617.
(851) Ashton, P. R.; Ballardini, R.; Balzani, V.; Credi, A.; Gandolfi, M. T.; Menzer, S.; Perezgarcia, L.; Prodi, L.; Stoddart, J. F.; Venturi, M. Molecular Meccano 0.4. The Self-Assembly of [2]Catenanes Incorporating Photoactive and Electroactive Pi-Extended Systems. *J. Am. Chem. Soc.* **1995**, *117*, 11171−11197.
(852) Ashton, P. R.; Ballardini, R.; Balzani, V.; Gandolfi, M. T.; Marquis, D. J. F.; Perezgarcia, L.; Prodi, L.; Stoddart, J. F.; Venturi, M. The Self-Assembly of Controllable [2]Catenanes. *J. Chem. Soc., Chem. Commun.* **1994**, 177−180.
(853) Livoreil, A.; Dietrich-Buchecker, C. O.; Sauvage, J.-P. Electrochemically Triggered Swinging of a [2]-Catenate. *J. Am. Chem. Soc.* **1994**, *116*, 9399−9400.
(854) Baumann, F.; Livoreil, A.; Kaim, W.; Sauvage, J.-P. Changeover in a Multimodal Copper(II) Catenate as Monitored by EPR Spectroscopy. *Chem. Commun.* **1997**, 35−36.
(855) Livoreil, A.; Sauvage, J.-P.; Armaroli, N.; Balzani, V.; Flamigni, L.; Ventura, B. Electrochemically and Photochemically Driven Ring Motions in a Disymmetrical Copper [2]-Catenate. *J. Am. Chem. Soc.* **1997**, *119*, 12114−12124.
(856) Cardenas, D. J.; Livoreil, A.; Sauvage, J.-P. Redox Control of the Ring-gliding Motion in a Cu-complexed Catenane: A Process Involving Three Distinct Geometries. *J. Am. Chem. Soc.* **1996**, *118*, 11980−11981.
(857) Dietrich-Buchecker, C.; Sauvage, J.-P. Templated Synthesis of Interlocked Macrocyclic Ligands, the Catenands - Preparation and Characterization of the Prototypical Bis-30 Membered Ring-System. *Tetrahedron* **1990**, *46*, 503−512.
(858) Cesario, M.; Dietrich-Buchecker, C. O.; Guilhem, J.; Pascard, C.; Sauvage, J.-P. Molecular-Structure of a Catenand and Its Copper(I) Catenate - Complete Rearrangement of the Interlocked Macrocyclic Ligands by Complexation. *J. Chem. Soc., Chem. Commun.* **1985**, 244−247.
(859) Cesario, M.; Dietrich, C. O.; Edel, A.; Guilhem, J.; Kintzinger, J. P.; Pascard, C.; Sauvage, J.-P. Topological Enhancement of Basicity - Molecular-Structure and Solution Study of a Monoprotonated Catenand. *J. Am. Chem. Soc.* **1986**, *108*, 6250−6254.
(860) Albrechtgary, A. M.; Dietrich-Buchecker, C.; Saad, Z.; Sauvage, J.-P. Topological Kinetic Effects - Complexation of Interlocked Macrocyclic Ligands by Cationic Species. *J. Am. Chem. Soc.* **1988**, *110*, 1467−1472.
(861) Dietrich-Buchecker, C.; Sauvage, J.-P.; Kern, J. M. Synthesis and Electrochemical Studies of Catenates - Stabilization of Low Oxidation-States by Interlocked Macrocyclic Ligands. *J. Am. Chem. Soc.* **1989**, *111*, 7791−7800.
(862) Albrechtgary, A. M.; Dietrich-Buchecker, C.; Saad, Z.; Sauvage, J.-P. Formation of Li+ and Cd2+ Catenates, a Reaction with a Negative Enthalpy of Activation. *J. Chem. Soc., Chem. Commun.* **1992**, 280−282.
(863) Armaroli, N.; Decola, L.; Balzani, V.; Sauvage, J.-P.; Dietrich-Buchecker, C. O.; Kern, J. M.; Bailal, A. Absorption and Emission Properties of a 2-Catenand, Its Protonated Forms, and Its Complexes with Li^+, Cu^+, Ag^+, Co^{2+}, Ni^{2+}, Zn^{2+}, Pd^{2+} and Cd^{2+} - Tuning of the

DOI: 10.1021/acs.chemrev.5b00146
Chem. Rev. 2015, 115, 10081−10206

Luminescence over the Whole Visible Spectral Region. *J. Chem. Soc., Dalton Trans.* **1993**, 3241−3247.
(864) Sauvage, J.-P.; Weiss, J. Synthesis of Dicopper(I) [3]Catenates - Multiring Interlocked Coordinating Systems. *J. Am. Chem. Soc.* **1985**, *107*, 6108−6110.
(865) Dietrich-Buchecker, C. O.; Khemiss, A.; Sauvage, J.-P. High-Yield Synthesis of Multiring Copper(I) Catenates by Acetylenic Oxidative Coupling. *J. Chem. Soc., Chem. Commun.* **1986**, 1376−1378.
(866) Mohr, B.; Weck, M.; Sauvage, J. P.; Grubbs, R. H. High-yield synthesis of [2]catenanes by intramolecular ring-closing metathesis. *Angew. Chem., Int. Ed. Engl.* **1997**, *36*, 1308−1310.
(867) Koizumi, M.; Dietrich-Buchecker, C.; Sauvage, J.-P. A [2]Catenane Containing 1,1′-Binaphthyl Units and 1,10-Phenanthroline Fragments: Synthesis and Intermolecular Energy Transfer Processes. *Eur. J. Org. Chem.* **2004**, *2004*, 770−775.
(868) Fuller, A. M. L.; Leigh, D. A.; Lusby, P. J.; Slawin, A. M. Z.; Walker, D. B. Selecting Topology and Connectivity Through Metal-directed Macrocyclization Reactions: A Square Planar Palladium [2]Catenate and Two Noninterlocked Isomers. *J. Am. Chem. Soc.* **2005**, *127*, 12612−12619.
(869) Leigh, D. A.; Lusby, P. J.; Slawin, A. M. Z.; Walker, D. B. Half-rotation in a [2] Catenane via Interconvertible Pd(II) Coordination Modes. *Chem. Commun.* **2005**, 4919−4921.
(870) Mobian, P.; Kern, J. M.; Sauvage, J.-P. Light-driven Machine Prototypes Based on Dissociative Excited States: Photoinduced Decoordination and Thermal Recoordination of a Ring in a Ruthenium-(II)-containing [2]Catenane. *Angew. Chem., Int. Ed.* **2004**, *43*, 2392−2395.
(871) Baranoff, E.; Collin, J.-P.; Furusho, Y.; Laemmel, A. C.; Sauvage, J.-P. A Photochromic System Based on Photochemical or Thermal Chelate Exchange on $Ru(phen)_2L^{2+}$ (L = Diimine or Dinitrile Ligand). *Chem. Commun.* **2000**, 1935−1936.
(872) Collin, J.-P.; Laemmel, A. C.; Sauvage, J.-P. Photochemical Expulsion of a $Ru(phen)_2$ Unit From a Macrocyclic Receptor and its Thermal Reco-ordination. *New J. Chem.* **2001**, *25*, 22−24.
(873) Laemmel, A. C.; Collin, J.-P.; Sauvage, J.-P.; Accorsi, G.; Armaroli, N. Macrocyclic complexes of $[Ru(N\text{-}N)_2]^{2+}$ Units [N-N = 1,10 Phenanthroline or 4-(*p*-Anisyl)-1,10-Phenanthroline]: Synthesis and Photochemical Expulsion Studies. *Eur. J. Inorg. Chem.* **2003**, *2003*, 467−474.
(874) Bonnet, S.; Collin, J.-P.; Sauvage, J.-P. A Ru(terpy) (phen)-Incorporating Ring and its Light-induced Geometrical Changes. *Chem. Commun.* **2005**, 3195−3197.
(875) Collin, J.-P.; Jouvenot, D.; Koizumi, M.; Sauvage, J.-P. Light-driven Expulsion of the Sterically Hindering Ligand L in Tris-diimine Ruthenium(II) Complexes of the $Ru(phen)_2L^{2+}$ Family: A Pronounced Ring Effect. *Inorg. Chem.* **2005**, *44*, 4693−4698.
(876) Arico, F.; Mobian, P.; Kern, J. M.; Sauvage, J.-P. Synthesis of a [2]Catenane Around a $Ru(diimine)_3^{2+}$ Scaffold by Ring-closing Metathesis of olefins. *Org. Lett.* **2003**, *5*, 1887−1890.
(877) Pomeranc, D.; Jouvenot, D.; Chambron, J. C.; Collin, J.-P.; Heitz, V.; Sauvage, J.-P. Templated Synthesis of a Rotaxane with a $[Ru(diimine)_3]^{2+}$ Core. *Chem. - Eur. J.* **2003**, *9*, 4247−4254.
(878) Laemmel, A. C.; Collin, J.-P.; Sauvage, J.-P. Efficient and Selective Photochemical Labilization of a Given Bidentate Ligand in Mixed Ruthenium(II) Complexes of the $Ru(phen)_2L^{2+}$ and $Ru(bipy)_2L^{2+}$ Family (L = Sterically Hindering Chelate). *Eur. J. Inorg. Chem.* **1999**, *1999*, 383−386.
(879) Vogtle, F.; Muller, W. M.; Muller, U.; Bauer, M.; Rissanen, K. Photoswitchable Catenanes. *Angew. Chem., Int. Ed. Engl.* **1993**, *32*, 1295−1297.
(880) Ashton, P. R.; Blower, M.; Philp, D.; Spencer, N.; Stoddart, J. F.; Tolley, M. S.; Ballardini, R.; Ciano, M.; Balzani, V.; Gandolfi, M. T.; et al. The Control of Translational Isomerism in Catenated Structures. *New J. Chem.* **1993**, *17*, 689−695.
(881) Raymo, F. M.; Houk, K. N.; Stoddart, J. F. Origins of Selectivity in Molecular and Supramolecular Entities: Solvent and Electrostatic Control of the Translational Isomerism in [2]Catenanes. *J. Org. Chem.* **1998**, *63*, 6523−6528.
(882) Ballardini, R.; Balzani, V.; Gandolfi, M. T.; Gillard, R. E.; Stoddart, J. F.; Tabellini, E. The Synthesis and Spectroscopic Properties of Macrocyclic Polyethers Containing Two Different Aromatic Moieties and Their [2]Catenanes Incorporating Cyclobis(paraquat-*p*-phenylene). *Chem. - Eur. J.* **1998**, *4*, 449−459.
(883) Leigh, D. A.; Wong, J. K. Y.; Dehez, F.; Zerbetto, F. Unidirectional Rotation in a Mechanically Interlocked Molecular Rotor. *Nature* **2003**, *424*, 174−179.
(884) Baranoff, E. D.; Voignier, J.; Yasuda, T.; Heitz, V.; Sauvage, J.-P.; Kato, T. A Liquid-Crystalline [2]Catenane and Its Copper(I) Complex. *Angew. Chem., Int. Ed.* **2007**, *46*, 4680−4683.
(885) Hernandez, J. V.; Kay, E. R.; Leigh, D. A. A Reversible Synthetic Rotary Molecular Motor. *Science* **2004**, *306*, 1532−1537.
(886) Karczmarek, J.; Wright, J.; Corkum, P.; Ivanov, M. Optical Centrifuge for Molecules. *Phys. Rev. Lett.* **1999**, *82*, 3420−3423.
(887) Villeneuve, D. M.; Aseyev, S. A.; Dietrich, P.; Spanner, M.; Ivanov, M. Y.; Corkum, P. B. Forced Molecular Rotation in an Optical Centrifuge. *Phys. Rev. Lett.* **2000**, *85*, 542−545.
(888) Charlier, J. C.; Michenaud, J.-P. Energetics of Multilayered Carbon Tubules. *Phys. Rev. Lett.* **1993**, *70*, 1858−1861.
(889) Merkle, R. C. A Proof About Molecular Bearings. *Nanotechnology* **1993**, *4*, 86−90.
(890) Tuzun, R. E.; Noid, D. W.; Sumpter, B. G. The Dynamics of Molecular Bearings. *Nanotechnology* **1995**, *6*, 64−74.
(891) Han, J.; Globus, A.; Jaffe, R.; Deardorff, G. Molecular Dynamics Simulations of Carbon Nanotube-based Gears. *Nanotechnology* **1997**, *8*, 95−102.
(892) Sohlberg, K.; Tuzun, R. E.; Sumpter, B. G.; Noid, D. W. Application of Rigid-body dynamics and Semiclassical Mechanics to Molecular Bearings. *Nanotechnology* **1997**, *8*, 103−111.
(893) Globus, A.; Bauschlicher, C. W., Jr.; Han, J.; Jaffe, R. L.; Levit, C.; Srivastava, D. Machine Phase Fullerene Nanotechnology. *Nanotechnology* **1998**, *9*, 192−199.
(894) Kwon, Y.-K.; Tomanek, D. Electronic and Structural Properties of Multiwall Carbon Nanotubes. *Phys. Rev. B: Condens. Matter Mater. Phys.* **1998**, *58*, R16001, 10.1103/PhysRevB.58.R16001.
(895) Tuzun, R. E.; Sohlberg, K.; Noid, D. W.; Sumpter, B. G. Docking Envelopes for the Assembly of Molecular Bearings. *Nanotechnology* **1998**, *9*, 37−48.
(896) Palser, A. H. R. Interlayer Interactions in Graphite and Carbon Nanotubes. *Phys. Chem. Chem. Phys.* **1999**, *1*, 4459−4464.
(897) Cumings, J. Low-Friction Nanoscale Linear Bearing Realized from Multiwall Carbon Nanotubes. *Science* **2000**, *289*, 602−604.
(898) Kolmogorov, A. N.; Crespi, V. H. The Smoothest Bearings: Interlayer Sliding in Multiwalled Carbon Nanotubes. *Phys. Rev. Lett.* **2000**, *85*, 4727−4730.
(899) Yu, M.-F.; Yakobson, B. I.; Ruoff, R. S. Controlled Sliding and Pullout of Nested Shells in Individual Multiwalled Carbon Nanotubes. *J. Phys. Chem. B* **2000**, *104*, 8764−8767.
(900) Saito, R.; Matsuo, R.; Kimura, T.; Dresselhaus, G.; Dresselhaus, M. S. Anomalous Potential Barrier of Double-wall Carbon Nanotubes. *Chem. Phys. Lett.* **2001**, *348*, 187−193.
(901) Damnjanović, M.; Vuković, T.; Milošević, I. Super-slippery Carbon Nanotubes. *Eur. Phys. J. B* **2002**, *25*, 131−134.
(902) Zheng, Q.; Jiang, Q. Multiwalled Carbon Nanotubes as Gigahertz Oscillators. *Phys. Rev. Lett.* **2002**, *88*, 045503.
(903) Zheng, Q.; Liu, J.; Jiang, Q. Excess van der Waals Interaction Energy of a Multiwalled Carbon Nanotube with an Extruded Core and the Induced Core Oscillation. *Phys. Rev. B: Condens. Matter Mater. Phys.* **2002**, *65*, 245409.1−245409.6.
(904) Damnjanović, M.; Dobardzic, E.; Milosevic, I.; Vukovic, T.; Nikolic, B. Lattice Dynamics and Symmetry of Double Wall Carbon Nanotubes. *New J. Phys.* **2003**, *5*, 148.
(905) Guo, W.; Guo, Y.; Gao, H.; Zheng, Q.; Zhong, W. Energy Dissipation in Gigahertz Oscillators from Multiwalled Carbon Nanotubes. *Phys. Rev. Lett.* **2003**, *91*, 125501.
(906) Legoas, S.; Coluci, V.; Braga, S.; Coura, P.; Dantas, S.; Galvão, D. Molecular-Dynamics Simulations of Carbon Nanotubes as Gigahertz Oscillators. *Phys. Rev. Lett.* **2003**, *90*, 055504.

DOI: 10.1021/acs.chemrev.5b00146
Chem. Rev. 2015, 115, 10081−10206

(907) Lozovik, Y. E.; Minogin, A. V.; Popov, A. M. Nanomachines Based on Carbon Nanotubes. *Phys. Lett. A* **2003**, *313*, 112−121.
(908) Lozovik, Y. E.; Minogin, A. V.; Popov, A. M. Possible Nanomachines: Nanotube Walls as Movable Elements. *JETP Lett.* **2003**, *77*, 631−635.
(909) Servantie, J.; Gaspard, P. Methods of Calculation of a Friction Coefficient: Application to Nanotubes. *Phys. Rev. Lett.* **2003**, *91*, 185503.
(910) Vukovic, T.; Damnjanovic, M.; Milosevic, I. Interaction Between Layers of the Multi-wall Carbon Nanotubes. *Phys. E* **2003**, *16*, 259−268.
(911) Lin, J.-S.; Lin, J.-H.; Chang, C.-C. Molecular Dynamics Simulations of the Rotary Motor F_0 Under External Electric Fields Across the Membrane. *Biophys. J.* **2010**, *98*, 1009−1017.
(912) Williams, P. A.; Papadakis, S. J.; Patel, A. M.; Falvo, M. R.; Washburn, S.; Superfine, R. Fabrication of Nanometer-scale Mechanical Devices Incorporating Individual Multiwalled Carbon Nanotubes as Torsional Springs. *Appl. Phys. Lett.* **2003**, *82*, 805−907.
(913) Zhao, Y.; Ma, C.-C.; Chen, G.; Jiang, Q. Energy Dissipation Mechanisms in Carbon Nanotube Oscillators. *Phys. Rev. Lett.* **2003**, *91*, 175504.
(914) Belikov, A. V.; Lozovik, Y. E.; Nikolaev, A. G.; Popov, A. M. Double-wall Nanotubes: Classification and Barriers to Walls Relative Rotation, Sliding and Screwlike Motion. *Chem. Phys. Lett.* **2004**, *385*, 72−78.
(915) Bourlon, B.; Glattli, D. C.; Miko, C.; Forro, L.; Bachtold, A. Carbon Nanotube Based Bearing for Rotational Motions. *Nano Lett.* **2004**, *4*, 709−712.
(916) Kang, J. W.; Hwang, H. J. Gigahertz Actuator of Multiwall Marbon Nanotube Encapsulating Metallic Ions: Molecular Dynamics Simulations. *J. Appl. Phys.* **2004**, *96*, 3900−3905.
(917) Kang, J. W.; Hwang, H. J. Nanoscale Carbon Nanotube Motor Schematics and Simulations for Micro-electro-mechanical Machines. *Nanotechnology* **2004**, *15*, 1633−1638.
(918) Legoas, S. B.; Coluci, V. R.; Braga, S. F.; Coura, P. Z.; Dantas, S. O.; Galvão, D. S. Gigahertz Nanomechanical Oscillators Based on Carbon Nanotubes. *Nanotechnology* **2004**, *15*, S184−S189.
(919) Papadakis, S.; Hall, A.; Williams, P.; Vicci, L.; Falvo, M.; Superfine, R.; Washburn, S. Resonant Oscillators with Carbon-Nanotube Torsion Springs. *Phys. Rev. Lett.* **2004**, *93*, 146101.
(920) Regan, B. C.; Aloni, S.; Ritchie, R. O.; Dahmen, U.; Zettl, A. Carbon Nanotubes as Nanoscale Mass Conveyors. *Nature* **2004**, *428*, 924−927.
(921) Tangney, P.; Louie, S.; Cohen, M. Dynamic Sliding Friction between Concentric Carbon Nanotubes. *Phys. Rev. Lett.* **2004**, *93*, 065530.
(922) Tu, Z. C.; Ou-Yang, Z. C. A Molecular Motor Constructed from a Double-walled Carbon Nanotube Driven by Temperature Variation. *J. Phys.: Condens. Matter* **2004**, *16*, 1287−1292.
(923) Bichoutskaia, E.; Popov, A.; El-Barbary, A.; Heggie, M.; Lozovik, Y. *Ab initio* Study of Relative Motion of Walls in Carbon Nanotubes. *Phys. Rev. B: Condens. Matter Mater. Phys.* **2005**, *71*, 113403.
(924) Kang, J. W.; Song, K. O.; Kwon, O. K.; Hwang, H. J. Carbon Nanotube Oscillator Operated by Thermal Expansion of Encapsulated Gases. *Nanotechnology* **2005**, *16*, 2670−2676.
(925) Meyer, J. C.; Paillet, M.; Roth, S. Single-molecule Torsional Pendulum. *Science* **2005**, *309*, 1539−1541.
(926) Regan, B. C.; Aloni, S.; Jensen, K.; Ritchie, R. O.; Zettl, A. Nanocrystal-Powered Nanomotor. *Nano Lett.* **2005**, *5*, 1730−1733.
(927) Tu, Z.; Hu, X. Molecular Motor Constructed From a Double-walled Carbon Nanotube Driven by Axially Varying Voltage. *Phys. Rev. B: Condens. Matter Mater. Phys.* **2005**, *72*, 033404.
(928) Tasis, D.; Tagmatarchis, N.; Bianco, A.; Prato, M. Chemistry of Carbon Nanotubes. *Chem. Rev.* **2006**, *106*, 1105−1136.
(929) Yuzvinsky, T. D.; Fennimore, A. M.; Kis, A.; Zettl, A. Controlled Placement of Highly Aligned Carbon Nanotubes for the Manufacture of Arrays of Nanoscale Torsional Actuators. *Nanotechnology* **2006**, *17*, 434−438.
(930) Li, R.; Sun, D.; Zhang, B. Motion and Energy Dissipation of Single-walled Carbon Nanotube on Graphite by Molecular Dynamics Simulation. *Mater. Res. Express* **2014**, *1*, 025046.
(931) Bedard, T. C.; Moore, J. S. Design and Synthesis of Molecular Turnstiles. *J. Am. Chem. Soc.* **1995**, *117*, 10662−10671.
(932) Hsu, L. Y.; Li, E. Y.; Rabitz, H. Single-molecule Electric Revolving Door. *Nano Lett.* **2013**, *13*, 5020−5025.
(933) Troisi, A.; Ratner, M. Molecular Rectification Through Electric Field Induced Conformational Changes. *J. Am. Chem. Soc.* **2002**, *124*, 14528−14529.
(934) Troisi, A.; Ratner, M. A. Conformational Molecular Rectifiers. *Nano Lett.* **2004**, *4*, 591−595.
(935) Goychuk, I.; Haenggi, P. Quantum Rectifiers From Harmonic Mixing. *Europhys. Lett.* **1998**, *43*, 503−509.
(936) Kornilovitch, P.; Bratkovsky, A.; Williams, R. Bistable Molecular Conductors with a Field-switchable Dipole Group. *Phys. Rev. B: Condens. Matter Mater. Phys.* **2002**, *66*, 245413.
(937) Ghosh, A. W.; Rakshit, T.; Datta, S. Gating of a Molecular Transistor: Electrostatic and Conformational. *Nano Lett.* **2004**, *4*, 565−568.
(938) Tuzun, R. E.; Noid, D. W.; Sumpter, B. G. Dynamics of a Laser Driven Molecular Motor. *Nanotechnology* **1995**, *6*, 52−63.
(939) Hoki, K.; Gonzalez, L.; Fujimura, Y. Control of Molecular Handedness Using Pump-dump Laser Pulses. *J. Chem. Phys.* **2002**, *116*, 2433−2438.
(940) Hoki, K.; Yamaki, M.; Fujimura, Y. Chiral Molecular Motors Driven by a Nonhelical Laser Pulse. *Angew. Chem., Int. Ed.* **2003**, *42*, 2976−2978.
(941) Hoki, K.; Yamaki, M.; Koseki, S.; Fujimura, Y. Mechanism of Unidirectional Motions of Chiral Molecular Motors Driven by Linearly Polarized Pulses. *J. Chem. Phys.* **2003**, *119*, 12393−12398.
(942) Hoki, K.; Yamaki, M.; Koseki, S.; Fujimura, Y. Molecular Motors Driven by Laser Pulses: Role of Molecular Chirality and Photon Helicity. *J. Chem. Phys.* **2003**, *118*, 497−504.
(943) Hoki, K.; Sato, M.; Yamaki, M.; Sahnoun, R.; Gonzalez, L.; Koseki, S.; Fujimura, Y. Chiral Molecular Motors Ignited by Femtosecond Pump-dump Laser Pulses. *J. Phys. Chem. B* **2004**, *108*, 4916−4921.
(944) Kono, H.; Sato, Y.; Tanaka, N.; Kato, T.; Nakai, K.; Koseki, S.; Fujimura, Y. Quantum Mechanical Study of Electronic and Nuclear Dynamics of Molecules in Intense Laser Fields. *Chem. Phys.* **2004**, *304*, 203−226.
(945) Hoki, K.; Sato, M.; Yamaki, M.; Sahnoun, R.; Gonzalez, L.; Koseki, S.; Fujimura, Y. Chiral Molecular Motors Ignited by Femtosecond Pump−Dump Laser Pulses. *J. Phys. Chem. B* **2004**, *108*, 4916−4921.
(946) Yamaki, M.; Hoki, K.; Ohtsuki, Y.; Kono, H.; Fujimura, Y. Quantum Control of Unidirectional Rotations of a Chiral Molecular Motor. *Phys. Chem. Chem. Phys.* **2005**, *7*, 900−904.
(947) Yamaki, M.; Hoki, K.; Ohtsuki, Y.; Kono, H.; Fujimura, Y. Quantum Control of a Chiral Molecular Motor Driven by Laser Pulses. *J. Am. Chem. Soc.* **2005**, *127*, 7300−7301.
(948) Yamaki, M.; Hoki, K.; Kono, H.; Fujimura, Y. Quantum Control of a Chiral Molecular Motor Driven by Femtosecond Laser Pulses: Mechanisms of Regular and Reverse Rotations. *Chem. Phys.* **2008**, *347*, 272−274.
(949) Yamaki, M.; Hoki, K.; Teranishi, T.; Chung, W.; Pichierri, F.; Kono, H.; Fujimura, Y. Theoretical Design of an Aromatic Hydrocarbon Rotor Driven by a Circularly Polarized Electric Field. *J. Phys. Chem. A* **2007**, *111*, 9374−9378.
(950) Yamaki, M.; Nakayama, S.; Hoki, K.; Kono, H.; Fujimura, Y. Quantum Dynamics of Light-driven Chiral Molecular Motors. *Phys. Chem. Chem. Phys.* **2009**, *11*, 1662−1678.
(951) Fujimura, Y.; González, L.; Kröner, D.; Manz, J.; Mehdaoui, I.; Schmidt, B. Quantum Ignition of Intramolecular Rotation by Means of IR+UV Laser Pulses. *Chem. Phys. Lett.* **2004**, *386*, 248−253.
(952) Jian, H.; Tour, J. En Route to Surface-bound Electric Field-driven Molecular Motors. *J. Org. Chem.* **2003**, *68*, 5091−5103.
(953) Caskey, D.; Shoemaker, R.; Michl, J. Toward Self-assembled Surface-mounted Prismatic Altitudinal Rotors. A Test Case: Molecular Rectangle. *Org. Lett.* **2004**, *6*, 2093−2096.

DOI: 10.1021/acs.chemrev.5b00146
Chem. Rev. 2015, 115, 10081−10206

(954) Zheng, X.; Mulcahy, M.; Horinek, D.; Galeotti, F.; Magnera, T.; Michl, J. Dipolar and Nonpolar Altitudinal Molecular Rotors Mounted on an Au(111) Surface. *J. Am. Chem. Soc.* **2004**, *126*, 4540−4542.
(955) Magnera, T.; Michl, J.; Kelly, T. Altitudinal Surface-mounted Molecular Rotors. *Molecular Machines* **2005**, *262*, 63−97.
(956) Caskey, D.; Michl, J. Toward Self-assembled Surface-mounted Prismatic Altitudinal Rotors. A Test Case: Trigonal and Tetragonal Prisms. *J. Org. Chem.* **2005**, *70*, 5442−5448.
(957) Kottas, G.; Clarke, L.; Horinek, D.; Michl, J. Artificial Molecular Rotors. *Chem. Rev.* **2005**, *105*, 1281−1376.
(958) Mulcahy, M.; Magnera, T.; Michl, J. Molecular Rotors on Au(111): Rotator Orientation from IR Spectroscopy. *J. Phys. Chem. C* **2009**, *113*, 20698−20704.
(959) Mulcahy, M.; Bastl, Z.; Stensrud, K.; Magnera, T.; Michl, J. Mercury-Mediated Attachment of Metal-Sandwich-Based Altitudinal Molecular Rotors to Gold Surfaces. *J. Phys. Chem. C* **2010**, *114*, 14050−14060.
(960) Kobr, L.; Zhao, K.; Shen, Y.; Comotti, A.; Bracco, S.; Shoemaker, R.; Sozzani, P.; Clark, N.; Price, J.; Rogers, C.; et al. Inclusion Compound Based Approach to Arrays of Artificial Dipolar Molecular Rotors. A Surface Inclusion. *J. Am. Chem. Soc.* **2012**, *134*, 10122−10131.
(961) Casher, D. L.; Kobr, L.; Michl, J. Average Orientation of a Molecular Rotor Embedded in a Langmuir-Blodgett Monolayer. *Langmuir* **2012**, *28*, 1625−1637.
(962) Kobr, L.; Zhao, K.; Shen, Y.; Polivkova, K.; Shoemaker, R.; Clark, N.; Price, J.; Rogers, C.; Michl, J. Inclusion Compound Based Approach to Arrays of Artificial Dipolar Molecular Rotors: Bulk Inclusions. *J. Org. Chem.* **2013**, *78*, 1768−1777.
(963) Clarke, L. I.; Horinek, D.; Kottas, G. S.; Varaksa, N.; Magnera, T. F.; Hinderer, T. P.; Horansky, R. D.; Michl, J.; Price, J. C. The Dielectric Response of Chloromethylsilyl and Dichloromethylsilyl Dipolar Rotors on Fused Silica Surfaces. *Nanotechnology* **2002**, *13*, 533−540.
(964) Michl, J.; Magnera, T. F. Two-dimensional Supramolecular Chemistry with Molecular Tinkertoys. *Proc. Natl. Acad. Sci. U. S. A.* **2002**, *99*, 4788−4792.
(965) Horinek, D.; Michl, J. Molecular Dynamics Simulation of an Electric Field Driven Dipolar Molecular Rotor Attached to a Quartz Glass Surface. *J. Am. Chem. Soc.* **2003**, *125*, 11900−11910.
(966) Horinek, D.; Michl, J. Surface-mounted Altitudinal Molecular Rotors in Alternating Electric Field: Single-molecule Parametric Oscillator Molecular Dynamics. *Proc. Natl. Acad. Sci. U. S. A.* **2005**, *102*, 14175−14180.
(967) Vacek, J.; Michl, J. Molecular Dynamics of a Grid-mounted Molecular Dipolar Rotor in a Rotating Electric Field. *Proc. Natl. Acad. Sci. U. S. A.* **2001**, *98*, 5481−5486.
(968) Vacek, J.; Michl, J. Artificial Surface-mounted Molecular Rotors: Molecular Dynamics Simulations. *Adv. Funct. Mater.* **2007**, *17*, 730−739.
(969) Prokop, A.; Vacek, J.; Michl, J. Friction in Carborane-Based Molecular Rotors Driven by Gas Flow or Electric Field: Classical Molecular Dynamics. *ACS Nano* **2012**, *6*, 1901−1914.
(970) Dunitz, J. D.; Maverick, E. F.; Trueblood, K. N. Atomic Motions in Molecular Crystals from Diffraction Measurements. *Angew. Chem., Int. Ed. Engl.* **1988**, *27*, 880−895.
(971) Akutagawa, T.; Shitagami, K.; Nishihara, S.; Takeda, S.; T, H.; Nakamura, T.; Hosokoshi, Y.; Inoue, K.; Ikeuchi, S.; Miyazaki, Y.; Saito, K. Molecular Rotor of $Cs_2([18]crown\text{-}6)_3$ in the Solid State Coupled with the Magnetism of $[Ni(dmit)_2]$. *J. Am. Chem. Soc.* **2005**, *127*, 4397−4402.
(972) Khuong, T.; Nunez, J.; Godinez, C.; Garcia-Garibay, M. Crystalline Molecular Machines: A Quest Toward Solid-state Dynamics and Function. *Acc. Chem. Res.* **2006**, *39*, 413−422.
(973) Karlen, S.; Reyes, H.; Taylor, R.; Khan, S.; Hawthorne, M.; Garcia-Garibay, M. Symmetry and Dynamics of Molecular Rotors in Amphidynamic Molecular Cystals. *Proc. Natl. Acad. Sci. U. S. A.* **2010**, *107*, 14973−14977.
(974) Lemouchi, C.; Iliopoulos, K.; Zorina, L.; Simonov, S.; Wzietek, P.; Cauchy, T.; Rodríguez-Fortea, A.; Canadell, E.; Kaleta, J.; Michl, J.; et al. Crystalline Arrays of Pairs of Molecular Rotors: Correlated Motion, Rotational Barriers, and Space-Inversion Symmetry Breaking Due to Conformational Mutations. *J. Am. Chem. Soc.* **2013**, *135*, 9366−9376.
(975) Zhang, Q.-C.; Wu, F.-T.; Hao, H.-M.; Xu, H.; Zhao, H.-X.; Long, L.-S.; Huang, R.-B.; Zheng, L.-S. Modulating the Rotation of a Molecular Rotor through Hydrogen-Bonding Interactions between the Rotator and Stator. *Angew. Chem., Int. Ed.* **2013**, *52*, 12602−12605.
(976) Karlen, S. D.; Garcia-Garibay, M. A. *Amphidynamic Crystals: Structural Blueprints for Molecular Machines* **2005**, *262*, 179−227.
(977) Shima, T.; Hampel, F.; Gladysz, J. A. Molecular gyroscopes: $[Fe(CO)_3]$ and $[Fe(CO)_2(NO)]^+$ rotators encased in three-spoke stators; facile assembly by alkene metatheses. *Angew. Chem., Int. Ed.* **2004**, *43*, 5537−5540.
(978) Skopek, K.; Hershberger, M.; Gladysz, J. Gyroscopes and the chemical literature: 1852−2002. *Coord. Chem. Rev.* **2007**, *251*, 1723−1733.
(979) Commins, P.; Nunez, J.; Garcia-Garibay, M. Synthesis of Bridged Molecular Gyroscopes with Closed Topologies: Triple One-Pot Macrocyclization. *J. Org. Chem.* **2011**, *76*, 8355−8363.
(980) Karlen, S. D.; Godinez, C. E.; Garcia-Garibay, M. A. Improved physical properties and rotational dynamics in a molecular gyroscope with an asymmetric stator structure. *Org. Lett.* **2006**, *8*, 3417−3420.
(981) Horansky, R.; Clarke, L.; Winston, E.; Price, J.; Karlen, S.; Jarowski, P.; Santillan, R.; Garcia-Garibay, M. Dipolar rotor-rotor interactions in a difluorobenzene molecular rotor crystal. *Phys. Rev. B: Condens. Matter Mater. Phys.* **2006**, *74*, 054306.
(982) Setaka, W.; Yamaguchi, K. Order-disorder transition of dipolar rotor in a crystalline molecular gyrotop and its optical change. *J. Am. Chem. Soc.* **2013**, *135*, 14560−14563.
(983) Shima, T.; Hampel, F.; Gladysz, J. Molecular gyroscopes: $\{Fe(CO)_3\}$ and $\{Fe(CO)_2(NO)\}^+$ rotators encased in three-spoke stators; facile assembly by alkene metatheses. *Angew. Chem., Int. Ed.* **2004**, *43*, 5537−5540.
(984) Zeits, P.; Rachiero, G.; Harnpel, F.; Reibenspies, J.; Gladysz, J. Gyroscope-Like Platinum and Palladium Complexes with *Trans*-Spanning Bis(pyridine) Ligands. *Organometallics* **2012**, *31*, 2854−2877.
(985) Dominguez, Z.; Dang, H.; Strouse, M. J.; Garcia-Garibay, M. A. Molecular "Compasses" and "Gyroscopes." III. Dynamics of a Phenylene Rotor and Clathrated Benzene in a Slipping-Gear Crystal Lattice. *J. Am. Chem. Soc.* **2002**, *124*, 7719−7727.
(986) Dominguez, Z.; Dang, H.; Strouse, M.; Garcia-Garibay, M. Molecular ″compasses″ and ″gyroscopes″. I. Expedient synthesis and solid state dynamics of an open rotor with a bis(triarylmethyl) frame. *J. Am. Chem. Soc.* **2002**, *124*, 2398−2399.
(987) Marahatta, A. B.; Kanno, M.; Hoki, K.; Setaka, W.; Irle, S., II; Kono, H. Theoretical Investigation of the Structures and Dynamics of Crystalline Molecular Gyroscopes. *J. Phys. Chem. C* **2012**, *116*, 24845−24854.
(988) Dominguez, Z.; Khuong, T.; Dang, H.; Sanrame, C.; Nunez, J.; Garcia-Garibay, M. Molecular compasses and gyroscopes with polar rotors: Synthesis and characterization of crystalline forms. *J. Am. Chem. Soc.* **2003**, *125*, 8827−8837.
(989) Godinez, C.; Zepeda, G.; Mortko, C.; Dang, H.; Garcia-Garibay, M. Molecular crystals with moving parts: Synthesis, characterization, and crystal packing of molecular gyroscopes with methyl-substituted triptycyl frames. *J. Org. Chem.* **2004**, *69*, 1652−1662.
(990) Khuong, T.; Zepeda, G.; Ruiz, R.; Khan, S.; Garcia-Garibay, M. Molecular compasses and gyroscopes: Engineering molecular crystals with fast internal rotation. *Cryst. Growth Des.* **2004**, *4*, 15−18.
(991) Binhi, V. N.; Savin, A. V. Molecular Gyroscopes and Biological Effects of Weak Extremely Low-Frequency Magnetic Fields. *Phys. Rev. E: Stat. Phys., Plasmas, Fluids, Relat. Interdiscip. Top.* **2002**, *65*, 051912.
(992) Karlen, S.; Ortiz, R.; Chapman, O.; Garcia-Garibay, M. Effects of rotational symmetry order on the solid state dynamics of phenylene and diamantane rotators. *J. Am. Chem. Soc.* **2005**, *127*, 6554−6555.
(993) Gardinier, J. R.; Pellechia, P. J.; Smith, M. D. Ionic rotors. preparation, structure, and dynamic solid-state 2D NMR study of the 1,4-diethynylbenzenebis(triphenylborate) dianion. *J. Am. Chem. Soc.* **2005**, *127*, 12448−12449.

DOI: 10.1021/acs.chemrev.5b00146
Chem. Rev. 2015, 115, 10081−10206

(994) Karlen, S. D.; Garcia-Garibay, M. A. Highlighting gyroscopic motion in crystals in 13C CPMAS spectra by specific isotopic substitution and restricted cross polarization. *Chem. Commun.* **2005**, 189−191.
(995) Karlen, S. D.; Khan, S. I.; Garcia-Garibay, M. A. Removal of Conflicting Molecular Symmetries Restores a HexagonalArray of Six-Fold Phenyl Embraces in a bis(Trityl)-Containing Compound. I. Crystals of 1,1,1,6,6,6-Hexaphenyl-2,4-hexadiyne. *Cryst. Growth Des.* **2005**, *5*, 53−55.
(996) Karlen, S.; Khan, S.; Garcia-Garibay, M. Crystalline molecular gyroscopes: The effects of subtle molecular differences on the crystal packing of triphenylmethyl and triphenylsilyl stators. *Mol. Cryst. Liq. Cryst.* **2006**, *456*, 221−230.
(997) Nunez, J.; Khuong, T.; Campos, L.; Farfan, N.; Dang, H.; Karlen, S.; Garcia-Garibay, M. Crystal phases and phase transitions in a highly polymorphogenic solid-state molecular gyroscope with meta-methoxytrityl frames. *Cryst. Growth Des.* **2006**, *6*, 866−873.
(998) Garcia-Garibay, M.; Godinez, C. Engineering Crystal Packing and Internal Dynamics in Molecular Gyroscopes by Refining their Components. Fast Exchange of a Phenylene Rotator by H-2 NMR. *Cryst. Growth Des.* **2009**, *9*, 3124−3128.
(999) Rodriguez-Molina, B.; Ochoa, M.; Farfan, N.; Santillan, R.; Garcia-Garibay, M. Synthesis, Characterization, and Rotational Dynamics of Crystalline Molecular Compasses with N-Heterocyclic Rotators. *J. Org. Chem.* **2009**, *74*, 8554−8565.
(1000) O'Brien, Z.; Natarajan, A.; Khan, S.; Garcia-Garibay, M. Synthesis and Solid-State Rotational Dynamics of Molecular Gyroscopes with a Robust and Low Density Structure Built with a Phenylene Rotator and a Tri(meta-terphenyl)methyl Stator. *Cryst. Growth Des.* **2011**, *11*, 2654−2659.
(1001) O'Brien, Z.; Karlen, S.; Khan, S.; Garcia-Garibay, M. Solid-State Molecular Rotors with Perdeuterated Stators: Mechanistic Insights from Biphenylene Rotational Dynamics in Ordered and Disordered Crystal Forms. *J. Org. Chem.* **2010**, *75*, 2482−2491.
(1002) Escalante-Sanchez, E.; Rodriguez-Molina, B.; Garcia-Garibay, M. Toward Crystalline Molecular Rotors with Linearly Conjugated Diethynyl-Phenylene Rotators and Pentiptycene Stators. *J. Org. Chem.* **2012**, *77*, 7428−7434.
(1003) Horansky, R.; Clarke, L.; Price, J.; Khuong, T.; Jarowski, P.; Garcia-Garibay, M. Dielectric response of a dipolar molecular rotor crystal. *Phys. Rev. B: Condens. Matter Mater. Phys.* **2005**, *72*, 10.1103/PhysRevB.72.014302.
(1004) Ozin, G. A.; Manners, I.; Fournier-Bidoz, S.; Arsenault, A. Dream Nanomachines. *Adv. Mater.* **2005**, *17*, 3011−3018.
(1005) Ebbens, S. J.; Howse, J. R. In pursuit of propulsion at the nanoscale. *Soft Matter* **2010**, *6*, 726−738.
(1006) Young, N. O.; G, J. S.; Block, M. J. The motion of bubbles in a vertical temperature gradient. *J. Fluid Mech.* **1959**, *6*, 350−356.
(1007) Scriven, L. E.; Sternling, C. V. The Marangoni Effects. *Nature* **1960**, *187*, 186−188.
(1008) Cazabat, A. M.; Heslot, F.; Troian, S. M.; Carles, P. Fingering instability of thin spreading films driven by temperature gradients. *Nature* **1990**, *346*, 824−826.
(1009) Barton, K. D.; Shankar Subramanian, R. The migration of liquid drops in a vertical temperature gradient. *J. Colloid Interface Sci.* **1989**, *133*, 211−222.
(1010) Burns, M. A.; Mastrangelo, C. H.; Sammarco, T. S.; Man, F. P.; Webster, J. R.; Johnsons, B. N.; Foerster, B.; Jones, D.; Fields, Y.; Kaiser, A. R.; Burke, D. T. Microfabricated structures for integrated DNA analysis. *Proc. Natl. Acad. Sci. U. S. A.* **1996**, *93*, 5556−5561.
(1011) Kataoka, D. E.; Troian, S. M. Patterning liquid flow on the microscopic scale. *Nature* **1999**, *402*, 794−797.
(1012) Kumar, G.; Prabhu, K. N. Review of non-reactive and reactive wetting of liquids on surfaces. *Adv. Colloid Interface Sci.* **2007**, *133*, 61−89.
(1013) Gennes, P. G. d. Forced wetting by a reactive fluid. *Europhys. Lett.* **1997**, *39*, 407−412.
(1014) de Gennes, P. G. The dynamics of reactive wetting on solid surfaces. *Phys. A* **1998**, *249*, 196−205.
(1015) Bain, C. D.; Burnett-Hall, G. D.; Montgomerie, R. R. Rapid motion of liquid drops. *Nature* **1994**, *372*, 414−415.
(1016) Dos Santos, F. D.; Ondarçuhu, T. Free-Running Droplets. *Phys. Rev. Lett.* **1995**, *75*, 2972−2975.
(1017) Lee, S.-W.; Laibinis, P. E. Directed Movement of Liquids on Patterned Surfaces Using Noncovalent Molecular Adsorption. *J. Am. Chem. Soc.* **2000**, *122*, 5395−5396.
(1018) Mitsumata, T.; Ikeda, K.; Gong, J. P.; Osada, Y. Solvent-driven chemical motor. *Appl. Phys. Lett.* **1998**, *73*, 2366−2368.
(1019) Ismagilov, R. F.; Schwartz, A.; Bowden, N.; Whitesides, G. M. Autonomous Movement and Self-Assembly. *Angew. Chem., Int. Ed.* **2002**, *41*, 652−654.
(1020) Paxton, W. F.; Kistler, K. C.; Olmeda, C. C.; Sen, A.; St. Angelo, S. K.; Cao, Y.; Mallouk, T. E.; Lammert, P. E.; Crespi, V. H. Catalytic Nanomotors: Autonomous Movement of Striped Nanorods. *J. Am. Chem. Soc.* **2004**, *126*, 13424−13431.
(1021) Golestanian, R.; Liverpool, T. B.; Ajdari, A. Propulsion of a Molecular Machine by Asymmetric Distribution of Reaction Products. *Phys. Rev. Lett.* **2005**, *94*, 220801.
(1022) Dhar, P.; Fischer, T. M.; Wang, Y.; Mallouk, T. E.; Paxton, W. F.; Sen, A. Autonomously Moving Nanorods at a Viscous Interface. *Nano Lett.* **2006**, *6*, 66−72.
(1023) Paxton, W. F.; Sen, A.; Mallouk, T. E. Motility of Catalytic Nanoparticles through Self-Generated Forces. *Chem. - Eur. J.* **2005**, *11*, 6462−6470.
(1024) Kline, T. R.; Paxton, W. F.; Wang, Y.; Velegol, D.; Mallouk, T. E.; Sen, A. Catalytic Micropumps: Microscopic Convective Fluid Flow and Pattern Formation. *J. Am. Chem. Soc.* **2005**, *127*, 17150−17151.
(1025) Mano, N.; Heller, A. Bioelectrochemical Propulsion. *J. Am. Chem. Soc.* **2005**, *127*, 11574−11575.
(1026) Catchmark, J. M.; Subramanian, S.; Sen, A. Directed Rotational Motion of Microscale Objects Using Interfacial Tension Gradients Continually Generated via Catalytic Reactions. *Small* **2005**, *1*, 202−206.
(1027) Fournier-Bidoz, S.; Arsenault, A. C.; Manners, I.; Ozin, G. A. Synthetic self-propeled nanorotors. *Chem. Commun.* **2005**, 441−443.
(1028) Valadares, L. F.; Tao, Y.-G.; Zacharia, N. S.; Kitaev, V.; Galembeck, F.; Kapral, R.; Ozin, G. A. Catalytic Nanomotors: Self-Propeled Sphere Dimers. *Small* **2010**, *6*, 565−572.
(1029) Qin, L.; Banholzer, M. J.; Xu, X.; Huang, L.; Mirkin, C. A. Rational Design and Synthesis of Catalytically Driven Nanorotors. *J. Am. Chem. Soc.* **2007**, *129*, 14870−14871.
(1030) Wang, Y.; Fei, S.-t.; Byun, Y.-M.; Lammert, P. E.; Crespi, V. H.; Sen, A.; Mallouk, T. E. Dynamic Interactions between Fast Microscale Rotors. *J. Am. Chem. Soc.* **2009**, *131*, 9926−9927.
(1031) Vicario, J.; Eelkema, R.; Browne, W. R.; Meetsma, A.; La Crois, R. M.; Feringa, B. L. Catalytic molecular motors: fuelling autonomous movement by a surface bound synthetic manganese catalase. *Chem. Commun.* **2005**, 3936−3938.
(1032) Lee, T.-C.; Alarcón-Correa, M.; Miksch, C.; Hahn, K.; Gibbs, J. G.; Fischer, P. Self-Propeling Nanomotors in the Presence of Strong Brownian Forces. *Nano Lett.* **2014**, *14*, 2407−2412.
(1033) Pantarotto, D.; Browne, W. R.; Feringa, B. L. Autonomous propulsion of carbon nanotubes powered by a multienzyme ensemble. *Chem. Commun.* **2008**, 1533−1535.
(1034) Gao, W.; Feng, X.; Pei, A.; Gu, Y.; Li, J.; Wang, J. Seawater-driven magnesium based Janus micromotors for environmental remediation. *Nanoscale* **2013**, *5*, 4696−4700.
(1035) Pavlick, R. A.; Sengupta, S.; McFadden, T.; Zhang, H.; Sen, A. A Polymerization-Powered Motor. *Angew. Chem., Int. Ed.* **2011**, *50*, 9374−9377.
(1036) Taylor, G. Analysis of the Swimming of Microscopic Organisms. *Proc. R. Soc. London, Ser. A* **1951**, *209*, 447−461.
(1037) Shapere, A.; Wilczek, F. Self-Propulsion at Low Reynolds Number. *Phys. Rev. Lett.* **1987**, *58*, 2051−2054.
(1038) Alfred Shapere, F. W. Geometry of self-propulsion at low Reynolds number. *J. Fluid Mech.* **1989**, *198*, 557−585.
(1039) Stone, H. A.; Samuel, A. D. T. Propulsion of Microorganisms by Surface Distortions. *Phys. Rev. Lett.* **1996**, *77*, 4102−4104.

DOI: 10.1021/acs.chemrev.5b00146
Chem. Rev. 2015, 115, 10081−10206

(1040) Ajdari, A.; Stone, H. A. A note on swimming using internally generated traveling waves. *Phys. Fluids* **1999**, *11*, 1275−1277.
(1041) Dreyfus, R.; Baudry, J.; Stone, H. A. Purcell's "rotator": mechanical rotation at low Reynolds number. *Eur. Phys. J. B* **2005**, *47*, 161−164.
(1042) Purcell, E. M. The efficiency of propulsion by a rotating flagellum. *Proc. Natl. Acad. Sci. U. S. A.* **1997**, *94*, 11307−11311.
(1043) Wiggins, C. H.; Goldstein, R. E. Flexive and Propulsive Dynamics of Elastica at Low Reynolds Number. *Phys. Rev. Lett.* **1998**, *80*, 3879−3882.
(1044) Camalet, S.; Jülicher, F.; Prost, J. Self-Organized Beating and Swimming of Internally Driven Filaments. *Phys. Rev. Lett.* **1999**, *82*, 1590−1593.
(1045) Becker, L. E.; Koehler, S. A.; Stone, H. A. On self-propulsion of micro-machines at low Reynolds number: Purcell's three-link swimmer. *J. Fluid Mech.* **2003**, *490*, 15−35.
(1046) Najafi, A.; Golestanian, R. Simple swimmer at low Reynolds number: Three linked spheres. *Phys. Rev. E* **2004**, *69*, 062901.
(1047) Avron, J. E.; Gat, O.; Kenneth, O. Optimal Swimming at Low Reynolds Numbers. *Phys. Rev. Lett.* **2004**, *93*, 186001.
(1048) Avron, J. E.; Kenneth, O.; Oaknin, D. H. Pushmepullyou: an efficient micro-swimmer. *New J. Phys.* **2005**, *7*, 234.
(1049) Porto, M.; Urbakh, M.; Klafter, J. Atomic Scale Engines: Cars and Wheels. *Phys. Rev. Lett.* **2000**, *84*, 6058−6061.
(1050) Wang, Z. Bioinspired laser-operated molecular locomotive. *Phys. Rev. E* **2004**, *70*, 031903.
(1051) Dreyfus, R.; Baudry, J.; Roper, M. L.; Fermigier, M.; Stone, H. A.; Bibette, J. Microscopic artificial swimmers. *Nature* **2005**, *437*, 862−865.
(1052) Baranova, N. B.; Zel'dovich, B. Y. Separation of mirror isomeric molecules by radio-frequency electric field of rotating polarization. *Chem. Phys. Lett.* **1978**, *57*, 435−437.
(1053) Space, B.; Rabitz, H.; Lörincz, A.; Moore, P. Feasibility of using photophoresis to create a concentration gradient of solvated molecules. *J. Chem. Phys.* **1996**, *105*, 9515−9524.
(1054) Arai, Y.; Yasuda, R.; Akashi, K.; Harada, Y.; Miyata, H.; Kinosita, K.; Itoh, H. Tying a molecular knot with optical tweezers. *Nature* **1999**, *399*, 446−448.
(1055) Neuman, K. C.; Block, S. M. Optical trapping. *Rev. Sci. Instrum.* **2004**, *75*, 2787−2809.
(1056) Zhuang, X. W. Unraveling DNA condensation with optical tweezers. *Science* **2004**, *305*, 188−190.
(1057) Allemand, J. F.; Bensimon, D.; Croquette, V. Stretching DNA and RNA to probe their interactions with proteins. *Curr. Opin. Struct. Biol.* **2003**, *13*, 266−274.
(1058) Bustamante, C.; Macosko, J. C.; Wuite, G. J. Grabbing the cat by the tail: manipulating molecules one by one. *Nat. Rev. Mol. Cell Biol.* **2000**, *1*, 130−136.
(1059) Mehta, A. D.; Rief, M.; Spudich, J. A.; Smith, D. A.; Simmons, R. M. Single-molecule biomechanics with optical methods. *Science* **1999**, *283*, 1689−1695.
(1060) Yanagida, T.; Harada, Y.; Ishijima, A. Nano-manipulation of actomyosin molecular motors in vitro: a new working principle. *Trends Biochem. Sci.* **1993**, *18*, 319−324.
(1061) Lensen, D.; Elemans, J. A. A. W. Artificial molecular rotors and motors on surfaces: STM reveals and triggers. *Soft Matter* **2012**, *8*, 9053−9063.
(1062) Binning, G.; Rohrer, H.; Gerber, C.; Weibel, E. Surface Studies by Scanning Tunneling Microscopy. *Phys. Rev. Lett.* **1982**, *49*, 57−61.
(1063) Binnig, G.; Rohrer, H. Scanning Tunneling Microscopy - from Birth to Adolescence. *Usp. Fiz. Nauk* **1988**, *154*, 261−278.
(1064) Binnig, G.; Rohrer, H. Scanning Tunneling Microscopy - from Birth to Adolescence. *Angew. Chem., Int. Ed. Engl.* **1987**, *26*, 606−614.
(1065) Binnig, G.; Rohrer, H. Scanning Tunneling Microscopy - from Birth to Adolescence. *Rev. Mod. Phys.* **1987**, *59*, 615−625.
(1066) Block, S. M. Making light work with optical tweezers. *Nature* **1992**, *360*, 493−495.
(1067) Kuo, S. C.; Sheetz, M. P. Optical tweezers in cell biology. *Trends Cell Biol.* **1992**, *2*, 116−118.
(1068) Iancu, V.; Hla, S.-W. Realization of a four-step molecular switch in scanning tunneling microscope manipulation of single chlorophyll-a molecules. *Proc. Natl. Acad. Sci. U. S. A.* **2006**, *103*, 13718−13721.
(1069) Chiang, S. Introduction: Force and Tunneling Microscopy. *Chem. Rev.* **1997**, *97*, 1015−1016.
(1070) Gimzewski, J. K.; Joachim, C. Nanoscale science of single molecules using local probes. *Science* **1999**, *283*, 1683−1688.
(1071) Stroscio, J. A.; Eigler, D. M. Atomic and molecular manipulation with the scanning tunneling microscope. *Science* **1991**, *254*, 1319−1326.
(1072) Avouris, P. Manipulation of Matter at the Atomic and Molecular-Levels. *Acc. Chem. Res.* **1995**, *28*, 95−102.
(1073) Gimzewski, J. K.; Jung, T. A.; Cuberes, M. T.; Schlittler, R. R. Scanning tunneling microscopy of individual molecules: beyond imaging. *Surf. Sci.* **1997**, *386*, 101−114.
(1074) Rosei, F.; Schunack, M.; Naitoh, Y.; Jiang, P.; Gourdon, A.; Laegsgaard, E.; Stensgaard, I.; Joachim, C.; Besenbacher, F. Properties of large organic molecules on metal surfaces. *Prog. Surf. Sci.* **2003**, *71*, 95−146.
(1075) Takano, H.; Kenseth, J. R.; Wong, S. S.; O'Brien, J. C.; Porter, M. D. Chemical and biochemical analysis using scanning force microscopy. *Chem. Rev.* **1999**, *99*, 2845−2890.
(1076) Guthold, M.; Falvo, M.; Matthews, W. G.; Paulson, S.; Mullin, J.; Lord, S.; Erie, D.; Washburn, S.; Superfine, R.; Brooks, F. P., Jr.; Taylor, R. M., 2nd Investigation and modification of molecular structures with the nanoManipulator. *J. Mol. Graphics Modell.* **1999**, *17*, 187−197.
(1077) Kawakami, M.; Taniguchi, Y. Recent Advances in Single-Molecule Biophysics with the Use of Atomic Force Microscopy. *Adv. Chem. Phys.* **2012**, *146*, 89−132.
(1078) Giessibl, F. J. Advances in atomic force microscopy. *Rev. Mod. Phys.* **2003**, *75*, 949−983.
(1079) Hansma, P. K.; Elings, V. B.; Marti, O.; Bracker, C. E. Scanning tunneling microscopy and atomic force microscopy: application to biology and technology. *Science* **1988**, *242*, 209−216.
(1080) Engel, A.; Gaub, H. E.; Muller, D. J. Atomic force microscopy: a forceful way with single molecules. *Curr. Biol.* **1999**, *9*, R133−R136.
(1081) Clausen-Schaumann, H.; Seitz, M.; Krautbauer, R.; Gaub, H. E. Force spectroscopy with single bio-molecules. *Curr. Opin. Chem. Biol.* **2000**, *4*, 524−530.
(1082) Samori, B. Stretching single molecules along unbinding and unfolding pathways with the scanning force microscope. *Chem. - Eur. J.* **2000**, *6*, 4249−4255.
(1083) Janshoff, A.; Neitzert, M.; Oberdorfer, Y.; Fuchs, H. Force Spectroscopy of Molecular Systems-Single Molecule Spectroscopy of Polymers and Biomolecules. *Angew. Chem., Int. Ed.* **2000**, *39*, 3212−3237.
(1084) Rief, M.; Grubmuller, H. Force spectroscopy of single biomolecules. *ChemPhysChem* **2002**, *3*, 255−261.
(1085) Best, R. B.; Clarke, J. What can atomic force microscopy tell us about protein folding? *Chem. Commun.* **2002**, 183−192.
(1086) Hla, S. W.; Meyer, G.; Rieder, K. H. Inducing single-molecule chemical reactions with a UHV-STM: a new dimension for nano-science and technology. *ChemPhysChem* **2001**, *2*, 361−366.
(1087) Joachim, C.; Gimzewski, J. K. A nanoscale single-molecule amplifier and its consequences. *Proc. IEEE* **1998**, *86*, 184−190.
(1088) Joachim, C.; Gimzewski, J. K.; Aviram, A. Electronics using hybrid-molecular and mono-molecular devices. *Nature* **2000**, *408*, 541−548.
(1089) Moresco, F. Manipulation of large molecules by low-temperature STM: model systems for molecular electronics. *Phys. Rep.* **2004**, *399*, 175−225.
(1090) Bhushan, B.; Israelachvili, J. N.; Landman, U. Nanotribology - Friction, Wear and Lubrication at the Atomic-Scale. *Nature* **1995**, *374*, 607−616.
(1091) Luan, B. Q.; Robbins, M. O. The breakdown of continuum models for mechanical contacts. *Nature* **2005**, *435*, 929−932.
(1092) Buldum, A.; Lu, J. P. Atomic scale sliding and rolling of carbon nanotubes. *Phys. Rev. Lett.* **1999**, *83*, 5050−5053.

DOI: 10.1021/acs.chemrev.5b00146
Chem. Rev. 2015, 115, 10081−10206

(1093) Kang, J. W.; Hwang, H. J. Fullerene nano ball bearings: an atomistic study. *Nanotechnology* **2004**, *15*, 614−621.
(1094) Sasaki, N.; Miura, K. Key issues of nanotribology for successful nanofabrication - From basis to C-60 molecular bearings. *Jpn. J. Appl. Phys. 1* **2004**, *43*, 4486−4491.
(1095) Falvo, M. R.; Taylor, R. M., 2nd; Helser, A.; Chi, V.; Brooks, F. P., Jr.; Washburn, S.; Superfine, R. Nanometre-scale rolling and sliding of carbon nanotubes. *Nature* **1999**, *397*, 236−238.
(1096) Falvo, M. R.; Steele, J.; Taylor, R. M. Superfine, R. Gearlike rolling motion mediated by commensurate contact: Carbon nanotubes on HOPG. *Phys. Rev. B: Condens. Matter Mater. Phys.* **2000**, *62*, 10665−10667.
(1097) Miura, K.; Takagi, T.; Kamiya, S.; Sahashi, T.; Yamauchi, M. Natural rolling of zigzag multiwalled carbon nanotubes on graphite. *Nano Lett.* **2001**, *1*, 161−163.
(1098) Moriarty, P.; Ma, Y. R.; Upward, M. D.; Beton, P. H. Translation, rotation and removal of C-60 on Si(100)-2 × 1 using anisotropic molecular manipulation. *Surf. Sci.* **1998**, *407*, 27−35.
(1099) Miura, K.; Kamiya, S.; Sasaki, N. C-60 molecular bearings. *Phys. Rev. Lett.* **2003**, *90*, 10.1103/PhysRevLett.90.055509.
(1100) Keeling, D. L.; Humphry, M. J.; Fawcett, R. H. J.; Beton, P. H.; Hobbs, C.; Kantorovich, L. Bond breaking coupled with translation in rolling of covalently bound molecules. *Phys. Rev. Lett.* **2005**, *94*, 94.
(1101) Otero, R.; Hummelink, F.; Sato, F.; Legoas, S. B.; Thostrup, P.; Laegsgaard, E.; Stensgaard, I.; Galvao, D. S.; Besenbacher, F. Lock-and-key effect in the surface diffusion of large organic molecules probed by STM. *Nat. Mater.* **2004**, *3*, 779−782.
(1102) Eigler, D. M.; Lutz, C. P.; Rudge, W. E. An Atomic Switch Realized with the Scanning Tunneling Microscope. *Nature* **1991**, *352*, 600−603.
(1103) Stipe, B. C.; Rezaei, M. A.; Ho, W. Inducing and viewing the rotational motion of a single molecule. *Science* **1998**, *279*, 1907−1909.
(1104) Stipe, B. C.; Rezaei, M. A.; Ho, W. Coupling of vibrational excitation to the rotational motion of a single adsorbed molecule. *Phys. Rev. Lett.* **1998**, *81*, 1263−1266.
(1105) Wintjes, N.; Bonifazi, D.; Cheng, F.; Kiebele, A.; Stöhr, M.; Jung, T.; Spillmann, H.; Diederich, F. A Supramolecular Multiposition Rotary Device. *Angew. Chem., Int. Ed.* **2007**, *46*, 4089−4092.
(1106) Jung, T. A.; Schlittler, R. R.; Gimzewski, J. K.; Tang, H.; Joachim, C. Controlled room-temperature positioning of individual molecules: Molecular flexure and motion. *Science* **1996**, *271*, 181−184.
(1107) Jung, T. A.; Schlittler, R. R.; Gimzewski, J. K. Conformational identification of individual adsorbed molecules with the STM. *Nature* **1997**, *386*, 696−698.
(1108) Moresco, F.; Meyer, G.; Rieder, K. H.; Ping, H.; Tang, H.; Joachim, C. TBPP molecules on copper surfaces: a low temperature scanning tunneling microscope investigation. *Surf. Sci.* **2002**, *499*, 94−102.
(1109) Moresco, F.; Meyer, G.; Rieder, K. H.; Tang, H.; Gourdon, A.; Joachim, C. Low temperature manipulation of big molecules in constant height mode. *Appl. Phys. Lett.* **2001**, *78*, 306−308.
(1110) Moresco, F.; Meyer, G.; Rieder, K. H.; Tang, H.; Gourdon, A.; Joachim, C. Conformational changes of single molecules induced by scanning tunneling microscopy manipulation: A route to molecular switching. *Phys. Rev. Lett.* **2001**, *86*, 672−675.
(1111) Moresco, F.; Meyer, G.; Rieder, K. H.; Tang, H.; Gourdon, A.; Joachim, C. Recording intramolecular mechanics during the manipulation of a large molecule. *Phys. Rev. Lett.* **2001**, *87*, 10.1103/PhysRevLett.87.088302.
(1112) Cuberes, M. T.; Schlittler, R. R.; Gimzewski, J. K. Room-temperature repositioning of individual C-60 molecules at Cu steps: Operation of a molecular counting device. *Appl. Phys. Lett.* **1996**, *69*, 3016−3018.
(1113) Gimzewski, J. K.; Joachim, C.; Schlittler, R. R.; Langlais, V.; Tang, H.; Johannsen, I. Rotation of a single molecule within a supramolecular bearing. *Science* **1998**, *281*, 531−533.
(1114) Griessl, S. J. H.; Lackinger, M.; Jamitzky, F.; Markert, T.; Hietschold, M.; Heckl, W. A. Incorporation and manipulation of coronene in an organic template structure. *Langmuir* **2004**, *20*, 9403−9407.
(1115) Joachim, C.; Gimzewski, J. K. Single molecular rotor at the nanoscale. *Struct. Bonding (Berlin)* **2001**, *99*, 1−18.
(1116) Stranick, S. J.; Kamna, M. M.; Weiss, P. S. Atomic-scale dynamics of a two-dimensional gas-solid interface. *Science* **1994**, *266*, 99−102.
(1117) Kwon, K. Y.; Wong, K. L.; Pawin, G.; Bartels, L.; Stolbov, S.; Rahman, T. S. Unidirectional adsorbate motion on a high-symmetry surface: "Walking" molecules can stay the course. *Phys. Rev. Lett.* **2005**, *95*, 10.1103/PhysRevLett.95.166101.
(1118) Das, B.; Sebastian, K. L. Adsorbed hypostrophene: can it roll on a surface by rearrangement of bonds? *Chem. Phys. Lett.* **2000**, *330*, 433−439.
(1119) Das, B.; Sebastian, K. L. Molecular wheels on surfaces. *Chem. Phys. Lett.* **2002**, *357*, 25−31.
(1120) Fujikawa, Y.; Sadowski, J. T.; Kelly, K. F.; Nakayama, K. S.; Mickelson, E. T.; Hauge, R. H.; Margrave, J. L.; Sakurai, T. Adsorption of fluorinated C-60 on the Si(111)-(7 × 7) surface studied by scanning tunneling microscopy and high-resolution electron energy loss spectroscopy. *Jpn. J. Appl. Phys. 1* **2002**, *41*, 245−249.
(1121) Joachim, C.; Tang, H.; Moresco, F.; Rapenne, G.; Meyer, G. The design of a nanoscale molecular barrow. *Nanotechnology* **2002**, *13*, 330−335.
(1122) Jimenez-Bueno, G.; Rapenne, G. Technomimetic molecules: synthesis of a molecular wheelbarrow. *Tetrahedron Lett.* **2003**, *44*, 6261−6263.
(1123) Rapenne, G. Synthesis of technomimetic molecules: towards rotation control in single-molecular machines and motors. *Org. Biomol. Chem.* **2005**, *3*, 1165−1169.
(1124) Grill, L.; Rieder, K. H.; Moresco, F.; Jimenez-Bueno, G.; Wang, C.; Rapenne, G.; Joachim, C. Imaging of a molecular wheelbarrow by scanning tunneling microscopy. *Surf. Sci.* **2005**, *584*, L153−L158.
(1125) Grill, L.; Rieder, K. H.; Moresco, F.; Rapenne, G.; Stojkovic, S.; Bouju, X.; Joachim, C. Rolling a single molecular wheel at the atomic scale. *Nat. Nanotechnol.* **2007**, *2*, 95−98.
(1126) Vaughan, O. P.; Williams, F. J.; Bampos, N.; Lambert, R. M. A chemically switchable molecular pinwheel. *Angew. Chem., Int. Ed.* **2006**, *45*, 3779−3781.
(1127) Wong, K. L.; Pawin, G.; Kwon, K. Y.; Lin, X.; Jiao, T.; Solanki, U.; Fawcett, R. H. J.; Bartels, L.; Stolbov, S.; Rahman, T. S. A molecule carrier. *Science* **2007**, *315*, 1391−1393.
(1128) Chiaravalloti, F.; Gross, L.; Rieder, K. H.; Stojkovic, S. M.; Gourdon, A.; Joachim, C.; Moresco, F. A rack-and-pinion device at the molecular scale. *Nat. Mater.* **2007**, *6*, 30−33.
(1129) Shirai, Y.; Osgood, A. J.; Zhao, Y.; Kelly, K. F.; Tour, J. M. Directional control in Thermally Driven Single-molecule Nanocars. *Nano Lett.* **2005**, *5*, 2330−2334.
(1130) Chu, P. L. E.; Wang, L. Y.; Khatua, S.; Kolomeisky, A. B.; Link, S.; Tour, J. M. Synthesis and Single-Molecule Imaging of Highly Mobile Adamantane-Wheeled Nanocars. *ACS Nano* **2013**, *7*, 35−41.
(1131) Khatua, S.; Guerrero, J. M.; Claytor, K.; Vives, G.; Kolomeisky, A. B.; Tour, J. M.; Link, S. Micrometer-Scale Translation and Monitoring of Individual Nanocars on Glass. *ACS Nano* **2009**, *3*, 351−356.
(1132) Morin, J. F.; Shirai, Y.; Tour, J. M. En route to a motorized nanocar. *Org. Lett.* **2006**, *8*, 1713−1716.
(1133) Tierney, H. L.; Murphy, C. J.; Jewell, A. D.; Baber, A. E.; Iski, E. V.; Khodaverdian, H. Y.; McGuire, A. F.; Klebanov, N.; Sykes, E. C. H. Experimental demonstration of a single-molecule electric motor. *Nat. Nanotechnol.* **2011**, *6*, 625−629.
(1134) Tanaka, H.; Ikeda, T.; Takeuchi, M.; Sada, K.; Shinkai, S.; Kawai, T. Molecular Rotation in Self-Assembled Multidecker Porphyrin Complexes. *ACS Nano* **2011**, *5*, 9575−9582.
(1135) Kudernac, T.; Ruangsupapichat, N.; Parschau, M.; Macia, B.; Katsonis, N.; Harutyunyan, S. R.; Ernst, K. H.; Feringa, B. L. Electrically driven directional motion of a four-wheeled molecule on a metal surface. *Nature* **2011**, *479*, 208−211.

DOI: 10.1021/acs.chemrev.5b00146
Chem. Rev. 2015, 115, 10081−10206

(1136) Hao, X.; Zhu, N.; Gschneidtner, T.; Jonsson, E. O.; Zhang, J. D.; Moth-Poulsen, K.; Wang, H. D.; Thygesen, K. S.; Jacobsen, K. W.; Ulstrup, J.; et al. Direct measurement and modulation of single-molecule coordinative bonding forces in a transition metal complex. *Nat. Commun.* **2013**, *4*, 2121.
(1137) Biscarini, F.; Gebauer, W.; Di Domenico, D.; Zamboni, R.; Pascual, J. I.; Leigh, D. A.; Murphy, A.; Tetard, D. STM investigation of flexible supramolecules: Benzylic amide [2] catenanes. *Synth. Met.* **1999**, *102*, 1466−1467.
(1138) Samori, P.; Jackel, F.; Unsal, O.; Godt, A.; Rabe, J. P. Ordered nanostructures of a [2]catenane through self-assembly at surfaces - An STM study with sub-molecular resolution. *ChemPhysChem* **2001**, *2*, 461−464.
(1139) Shigekawa, H.; Miyake, K.; Sumaoka, J.; Harada, A.; Komiyama, M. The molecular abacus: STM manipulation of cyclodextrin necklace. *J. Am. Chem. Soc.* **2000**, *122*, 5411−5412.
(1140) Feng, M.; Guo, X. F.; Lin, X.; He, X. B.; Ji, W.; Du, S. X.; Zhang, D. Q.; Zhu, D. B.; Gao, H. J. Stable, reproducible nanorecording on rotaxane thin films. *J. Am. Chem. Soc.* **2005**, *127*, 15338−15339.
(1141) Cavallini, M.; Biscarini, F.; Leon, S.; Zerbetto, F.; Bottari, G.; Leigh, D. A. Information storage using supramolecular surface patterns. *Science* **2003**, *299*, 531−531.
(1142) Brough, B.; Northrop, B. H.; Schmidt, J. J.; Tseng, H. R.; Houk, K. N.; Stoddart, J. F.; Ho, C. M. Evaluation of synthetic linear motor-molecule actuation energetics. *Proc. Natl. Acad. Sci. U. S. A.* **2006**, *103*, 8583−8588.
(1143) Lussis, P.; Svaldo-Lanero, T.; Bertocco, A.; Fustin, C. A.; Leigh, D. A.; Duwez, A. S. A single synthetic small molecule that generates force against a load. *Nat. Nanotechnol.* **2011**, *6*, 553−557.
(1144) Luo, Y.; Collier, C. P.; Jeppesen, J. O.; Nielsen, K. A.; DeIonno, E.; Ho, G.; Perkins, J.; Tseng, H. R.; Yamamoto, T.; Stoddart, J. F.; Heath, J. R. Two-dimensional molecular electronics circuits. *ChemPhysChem* **2002**, *3*, 519−525.
(1145) Huang, T. J.; Flood, A.; Chu, C. W.; Kang, S.; Guo, T. F.; Yamamoto, T.; Tseng, H. R.; Yu, B. D.; Yang, Y.; Stoddart, J. F.; Ho, C. M. In situ infrared spectroscopic studies of molecular behavior in nanoelectronic devices. *IEEE-NANO* **2003**, *2*, 698−701.
(1146) Collier, C. P.; Wong, E. W.; Belohradsky, M.; Raymo, F. M.; Stoddart, J. F.; Kuekes, P. J.; Williams, R. S.; Heath, J. R. Electronically configurable molecular-based logic gates. *Science* **1999**, *285*, 391−394.
(1147) Kitagawa, K.; Morita, T.; Kimura, S. A helical molecule that exhibits two lengths in response to an applied potential. *Angew. Chem., Int. Ed.* **2005**, *44*, 6330−6333.
(1148) Carella, A.; Rapenne, G.; Launay, J. P. Design and synthesis of the active part of a potential molecular motor. *New J. Chem.* **2005**, *29*, 288−290.
(1149) Carella, A.; Jaud, J.; Rapenne, G.; Launay, J. P. Technomimetic molecules: synthesis of ruthenium(II) 1,2,3,4,5-penta(*p*-bromophenyl)-cyclopentadienyl hydrotris(indazolyl)borate, an organometallic molecular turnstile. *Chem. Commun.* **2003**, 2434−2435.
(1150) DeIonno, E.; Tseng, H. R.; Harvey, D. D.; Stoddart, J. F.; Heath, J. R. Infrared spectroscopic characterization of [2]rotaxane molecular switch tunnel junction devices. *J. Phys. Chem. B* **2006**, *110*, 7609−7612.
(1151) Flood, A. H.; Wong, E. W.; Stoddart, J. F. Models of charge transport and transfer in molecular switch tunnel junctions of bistable catenanes and rotaxanes. *Chem. Phys.* **2006**, *324*, 280−290.
(1152) Flood, A. H.; Nygaard, S.; Laursen, B. W.; Jeppesen, J. O.; Stoddart, J. F. Locking down the electronic structure of (monopyrrolo)-tetrathiafulvalene in [2]rotaxanes. *Org. Lett.* **2006**, *8*, 2205−2208.
(1153) Loppacher, C.; Guggisberg, M.; Pfeiffer, O.; Meyer, E.; Bammerlin, M.; Luthi, R.; Schlittler, R.; Gimzewski, J. K.; Tang, H.; Joachim, C. Direct determination of the energy required to operate a single molecule switch. *Phys. Rev. Lett.* **2003**, *90*, 10.1103/PhysRevLett.90.066107.
(1154) Viala, C.; Secchi, A.; Gourdon, A. Synthesis of polyaromatic hydrocarbons with a central rotor. *Eur. J. Org. Chem.* **2002**, *2002*, 4185−4189.
(1155) Gourdon, A. Synthesis of "molecular landers". *Eur. J. Org. Chem.* **1998**, *1998*, 2797−2801.
(1156) Langlais, V. J.; Schlittler, R. R.; Tang, H.; Gourdon, A.; Joachim, C.; Gimzewski, J. K. Spatially resolved tunneling along a molecular wire. *Phys. Rev. Lett.* **1999**, *83*, 2809−2812.
(1157) Moresco, F.; Gross, L.; Grill, L.; Alemani, M.; Gourdon, A.; Joachim, C.; Rieder, K. H. Contacting a single molecular wire by STM manipulation. *Appl. Phys. A: Mater. Sci. Process.* **2005**, *80*, 913−920.
(1158) Moresco, F.; Gourdon, A. Scanning tunneling microscopy experiments on single molecular landers. *Proc. Natl. Acad. Sci. U. S. A.* **2005**, *102*, 8809−8814.
(1159) Soukiassian, L.; Mayne, A. J.; Comtet, G.; Hellner, L.; Dujardin, G.; Gourdon, A. Selective internal manipulation of a single molecule by scanning tunneling microscopy. *J. Chem. Phys.* **2005**, *122*, 134704.
(1160) Lastapis, M.; Martin, M.; Riedel, D.; Hellner, L.; Comtet, G.; Dujardin, G. Picometer-scale electronic control of molecular dynamics inside a single molecule. *Science* **2005**, *308*, 1000−1003.
(1161) Metiu, H. Special topic: Single-molecule physics and chemistry - Preface. *J. Chem. Phys.* **2002**, *117*, 10923−10923.
(1162) Barbara, P. F. Single-molecule spectroscopy. *Acc. Chem. Res.* **2005**, *38*, 503−503.
(1163) Chiou, P. Y.; Ohta, A. T.; Wu, M. C. Massively parallel manipulation of single cells and microparticles using optical images. *Nature* **2005**, *436*, 370−372.
(1164) Dholakia, K. Micromanipulation - Optoelectronic tweezers. *Nat. Mater.* **2005**, *4*, 579−580.
(1165) Moerner, W. E.; Basche, T. Optical Spectroscopy of Single Impurity Molecules in Solids. *Angew. Chem., Int. Ed. Engl.* **1993**, *32*, 457−476.
(1166) Moerner, W. E. Examining Nanoenvironments in Solids on the Scale of a Single, Isolated Impurity Molecule. *Science* **1994**, *265*, 46−53.
(1167) Moerner, W. E. High-resolution optical spectroscopy of single molecules in solids. *Acc. Chem. Res.* **1996**, *29*, 563−571.
(1168) Xie, X. S. Single-molecule spectroscopy and dynamics at room temperature. *Acc. Chem. Res.* **1996**, *29*, 598−606.
(1169) Goodwin, P. M.; Ambrose, W. P.; Keller, R. A. Single-molecule detection in liquids by laser-induced fluorescence. *Acc. Chem. Res.* **1996**, *29*, 607−613.
(1170) Nie, S. M.; Zare, R. N. Optical detection of single molecules. *Annu. Rev. Biophys. Biomol. Struct.* **1997**, *26*, 567−596.
(1171) Plakhotnik, T.; Donley, E. A.; Wild, U. P. Single-molecule spectroscopy. *Annu. Rev. Phys. Chem.* **1997**, *48*, 181−212.
(1172) Xie, X. S.; Trautman, J. K. Optical studies of single molecules at room temperature. *Annu. Rev. Phys. Chem.* **1998**, *49*, 441−480.
(1173) Moerner, W. E.; Orrit, M. Illuminating single molecules in condensed matter. *Science* **1999**, *283*, 1670−1676.
(1174) Weiss, S. Fluorescence spectroscopy of single biomolecules. *Science* **1999**, *283*, 1676−1683.
(1175) Ambrose, W. P.; Goodwin, P. M.; Jett, J. H.; Van Orden, A.; Werner, J. H.; Keller, R. A. Single molecule fluorescence spectroscopy at ambient temperature. *Chem. Rev.* **1999**, *99*, 2929−2956.
(1176) Deniz, A. A.; Laurence, T. A.; Dahan, M.; Chemla, D. S.; Schultz, P. G.; Weiss, S. Ratiometric single-molecule studies of freely diffusing biomolecules. *Annu. Rev. Phys. Chem.* **2001**, *52*, 233−253.
(1177) Moerner, W. E. A dozen years of single-molecule spectroscopy in physics, chemistry, and biophysics. *J. Phys. Chem. B* **2002**, *106*, 910−927.
(1178) Keller, R. A.; Ambrose, W. P.; Arias, A. A.; Gai, H.; Emory, S. R.; Goodwin, P. M.; Jett, J. H. Analytical applications of single-molecule detection. *Anal. Chem.* **2002**, *74*, 316a−324a.
(1179) Bohmer, M.; Enderlein, J. Fluorescence spectroscopy of single molecules under ambient conditions: Methodology and technology. *ChemPhysChem* **2003**, *4*, 793−808.
(1180) Moerner, W. E.; Fromm, D. P. Methods of single-molecule fluorescence spectroscopy and microscopy. *Rev. Sci. Instrum.* **2003**, *74*, 3597−3619.
(1181) Tinnefeld, P.; Sauer, M. Branching out of single-molecule fluorescence spectroscopy: Challenges for chemistry and influence on biology. *Angew. Chem., Int. Ed.* **2005**, *44*, 2642−2671.

DOI: 10.1021/acs.chemrev.5b00146
Chem. Rev. 2015, 115, 10081−10206

(1182) Fang, N.; Lee, H.; Sun, C.; Zhang, X. Sub-diffraction-limited optical imaging with a silver superlens. *Science* **2005**, *308*, 534−537.
(1183) Nishimura, D.; Takashima, Y.; Aoki, H.; Takahashi, T.; Yamaguchi, H.; Ito, S.; Harada, A. Single-Molecule Imaging of Rotaxanes Immobilized on Glass Substrates: Observation of Rotary Movement. *Angew. Chem., Int. Ed.* **2008**, *47*, 6077−6079.
(1184) Crooks, R. M.; Ricco, A. J. New organic materials suitable for use in chemical sensor arrays. *Acc. Chem. Res.* **1998**, *31*, 219−227.
(1185) Goldenberg, L. M.; Bryce, M. R.; Petty, M. C. Chemosensor devices: voltammetric molecular recognition at solid interfaces. *J. Mater. Chem.* **1999**, *9*, 1957−1974.
(1186) Flink, S.; van Veggel, F. C. J. M.; Reinhoudt, D. N. Sensor functionalities in self-assembled monolayers. *Adv. Mater.* **2000**, *12*, 1315−1328.
(1187) Shipway, A. N.; Katz, E.; Willner, I. Nanoparticle arrays on surfaces for electronic, optical, and sensor applications. *ChemPhysChem* **2000**, *1*, 18−52.
(1188) Katz, E.; Willner, I. Probing biomolecular interactions at conductive and semiconductive surfaces by impedance spectroscopy: Routes to impedimetric immunosensors, DNA-Sensors, and enzyme biosensors. *Electroanalysis* **2003**, *15*, 913−947.
(1189) Cooke, G. Electrochemical and photochemical control of host-guest complexation at surfaces. *Angew. Chem., Int. Ed.* **2003**, *42*, 4860−4870.
(1190) Astruc, D.; Daniel, M. C.; Ruiz, J. Dendrimers and gold nanoparticles as exo-receptors sensing biologically important anions. *Chem. Commun.* **2004**, 2637−2649.
(1191) Drechsler, U.; Erdogan, B.; Rotello, V. M. Nanoparticles: Scaffolds for molecular recognition. *Chem. - Eur. J.* **2004**, *10*, 5570−5579.
(1192) Mallouk, T. E.; Gavin, J. A. Molecular recognition in lamellar solids and thin films. *Acc. Chem. Res.* **1998**, *31*, 209−217.
(1193) Chia, S. Y.; Cao, J. G.; Stoddart, J. F.; Zink, J. I. Working supramolecular machines trapped in glass and mounted on a film surface. *Angew. Chem., Int. Ed.* **2001**, *40*, 2447−2451.
(1194) Gase, T.; Grando, D.; Chollet, P. A.; Kajzar, F.; Murphy, A.; Leigh, D. A. Linear and unanticipated second-order nonlinear optical properties of benzylic amide [2]Catenane thin films: Evidence of partial rotation of the interlocked molecular rings in the solid state. *Adv. Mater.* **1999**, *11*, 1303−1306.
(1195) Deleuze, M. S. Can benzylic amide [2]catenane rings rotate on graphite? *J. Am. Chem. Soc.* **2000**, *122*, 1130−1143.
(1196) Bidan, G.; Billon, M.; Divisia-Blohorn, B.; Kern, J. M.; Raehm, L.; Sauvage, J.-P. Electrode-deposited films of polyrotaxanes: electrochemically induced gliding motion. *New J. Chem.* **1998**, *22*, 1139−1141.
(1197) Raehm, L.; Kern, J. M.; Sauvage, J.-P.; Hamann, C.; Palacin, S.; Bourgoin, J. P. Disulfide- and thiol-incorporating copper catenanes: Synthesis deposition onto gold, and surface studies. *Chem. - Eur. J.* **2002**, *8*, 2153−2162.
(1198) Tseng, H. R.; Wu, D. M.; Fang, N. X. L.; Zhang, X.; Stoddart, J. F. The metastability of an electrochemically controlled nanoscale machine on gold surfaces. *ChemPhysChem* **2004**, *5*, 111−116.
(1199) Huang, T. J.; Tseng, H. R.; Sha, L.; Lu, W. X.; Brough, B.; Flood, A. H.; Yu, B. D.; Celestre, P. C.; Chang, J. P.; Stoddart, J. F.; Ho, C. M. Mechanical shuttling of linear motor-molecules in condensed phases on solid substrates. *Nano Lett.* **2004**, *4*, 2065−2071.
(1200) Long, B.; Nikitin, K.; Fitzmaurice, D. Assembly of an electronically switchable rotaxane on the surface of a titanium dioxide nanoparticle. *J. Am. Chem. Soc.* **2003**, *125*, 15490−15498.
(1201) Nikitin, K.; Fitzmaurice, D. The oxidation-state dependent structural conformation and supramolecular function of a redox-active [2]rotaxane in solution. *J. Am. Chem. Soc.* **2005**, *127*, 8067−8076.
(1202) van Delden, R. A.; ter Wiel, M. K. J.; Pollard, M. M.; Vicario, J.; Koumura, N.; Feringa, B. L. Unidirectional molecular motor on a gold surface. *Nature* **2005**, *437*, 1337−1340.
(1203) Hou, S. M.; Sagara, T.; Xu, D. C.; Kelly, T. R.; Ganz, E. Investigation of triptycene-based surface-mounted rotors. *Nanotechnology* **2003**, *14*, 566−570.
(1204) Jensen, K.; Girit, Ç.; Mickelson, W.; Zettl, A. Tunable Nanoresonators Constructed from Telescoping Nanotubes. *Phys. Rev. Lett.* **2006**, *96*, 215503.
(1205) Deshpande, V. V.; Chiu, H. Y.; Postma, H. W. C.; Mikó, C.; Forró, L.; Bockrath, M. Carbon Nanotube Linear Bearing Nanoswitches. *Nano Lett.* **2006**, *6*, 1092−1095.
(1206) Ebron, V. H.; Yang, Z.; Seyer, D. J.; Kozlov, M. E.; Oh, J.; Xie, H.; Razal, J.; Hall, L. J.; Ferraris, J. P.; MacDiarmid, A. G.; Baughman, R. H. Fuel-Powered Artificial Muscles. *Science* **2006**, *311*, 1580−1583.
(1207) Huang, T. J.; Flood, A. H.; Brough, B.; Liu, Y.; Bonvallet, P. A.; Kang, S. S.; Chu, C. W.; Guo, T. F.; Lu, W. X.; Yang, Y.; et al. Understanding and harnessing biomimetic molecular machines for NEMS actuation materials. *IEEE Trans. Autom. Sci. Eng.* **2006**, *3*, 254−259.
(1208) Yamaguchi, H.; Kobayashi, Y.; Kobayashi, R.; Takashima, Y.; Hashidzume, A.; Harada, A. Photoswitchable gel assembly based on molecular recognition. *Nat. Commun.* **2012**, *3*, 603.
(1209) Zheng, Y.; Hashidzume, A.; Takashima, Y.; Yamaguchi, H.; Harada, A. Switching of macroscopic molecular recognition selectivity using a mixed solvent system. *Nat. Commun.* **2012**, *3*, 831.
(1210) Abelow, A. E.; Zharov, I. Reversible nanovalves in inorganic materials. *J. Mater. Chem.* **2012**, *22*, 21810−21818.
(1211) Adiga, S. P.; Brenner, D. W. Toward designing smart nanovalves: Modeling of flow control through nanopores via the helix-coil transition of grafted polypeptide chains. *Macromolecules* **2007**, *40*, 1342−1348.
(1212) Angelos, S.; Yang, Y. W.; Patel, K.; Stoddart, J. F.; Zink, J. I. pH-responsive supramolecular nanovalves based on cucurbit[6]uril pseudorotaxanes. *Angew. Chem., Int. Ed.* **2008**, *47*, 2222−2226.
(1213) Chen, T.; Fu, J. J. pH-responsive nanovalves based on hollow mesoporous silica spheres for controlled release of corrosion inhibitor. *Nanotechnology* **2012**, *23*, 235605.
(1214) Croissant, J.; Chaix, A.; Mongin, O.; Wang, M.; Clement, S.; Raehm, L.; Durand, J. O.; Hugues, V.; Blanchard-Desce, M.; Maynadier, M.; et al. Two-Photon-Triggered Drug Delivery *via* Fluorescent Nanovalves. *Small* **2014**, *10*, 1752−1755.
(1215) Hwang, A. A.; Lu, J.; Tamanoi, F.; Zink, J. I. Functional Nanovalves on Protein-Coated Nanoparticles for In vitro and In vivo Controlled Drug Delivery. *Small* **2015**, *11*, 319−328.
(1216) Dong, J. Y.; Xue, M.; Zink, J. I. Functioning of nanovalves on polymer coated mesoporous silica Nanoparticles. *Nanoscale* **2013**, *5*, 10300−10306.
(1217) Lau, Y. A.; Ferris, D. P.; Zink, J. I. Photo-driven nano-impellers and nanovalves for on-command drug release. *Proc. SPIE* **2010**, *7574*, 75740P, 10.1117/12.841175.
(1218) Li, Q. L.; Wang, L.; Qiu, X. L.; Sun, Y. L.; Wang, P. X.; Liu, Y.; Li, F.; Qi, A. D.; Gao, H.; Yang, Y. W. Stimuli-responsive biocompatible nanovalves based on beta-cyclodextrin modified poly(glycidyl methacrylate). *Polym. Chem.* **2014**, *5*, 3389−3395.
(1219) Liu, J. S.; Du, X. Z. pH- and competitor-driven nanovalves of cucurbit[7]uril pseudorotaxanes based on mesoporous silica supports for controlled release. *J. Mater. Chem.* **2010**, *20*, 3642−3649.
(1220) Liu, J. S.; Du, X. Z.; Zhang, X. F. Enzyme-Inspired Controlled Release of Cucurbit[7]uril Nanovalves by Using Magnetic Mesoporous Silica. *Chem. - Eur. J.* **2011**, *17*, 810−815.
(1221) Luo, G. F.; Chen, W. H.; Liu, Y.; Zhang, J.; Cheng, S. X.; Zhuo, R. X.; Zhang, X. Z. Charge-reversal plug gate nanovalves on peptide-functionalized mesoporous silica nanoparticles for targeted drug delivery. *J. Mater. Chem. B* **2013**, *1*, 5723−5732.
(1222) Meng, H. A.; Xue, M.; Xia, T. A.; Zhao, Y. L.; Tamanoi, F.; Stoddart, J. F.; Zink, J. I.; Nel, A. E. Autonomous in Vitro Anticancer Drug Release from Mesoporous Silica Nanoparticles by pH-Sensitive Nanovalves. *J. Am. Chem. Soc.* **2010**, *132*, 12690−12697.
(1223) Saha, S.; Leung, K. C. F.; Nguyen, T. D.; Stoddart, J. F.; Zink, J. I. Nanovalves. *Adv. Funct. Mater.* **2007**, *17*, 685−693.
(1224) Yang, Y. W. Towards biocompatible nanovalves based on mesoporous silica nanoparticles. *MedChemComm* **2011**, *2*, 1033−1049.
(1225) Zhou, Y.; Tan, L. L.; Li, Q. L.; Qiu, X. L.; Qi, A. D.; Tao, Y. C.; Yang, Y. W. Acetylcholine-Triggered Cargo Release from Supra-

DOI: 10.1021/acs.chemrev.5b00146
Chem. Rev. 2015, 115, 10081−10206

molecular Nanovalves Based on Different Macrocyclic Receptors. *Chem. - Eur. J.* **2014**, *20*, 2998−3004.
(1226) Hernandez, R.; Tseng, H. R.; Wong, J. W.; Stoddart, J. F.; Zink, J. I. An operational supramolecular nanovalve. *J. Am. Chem. Soc.* **2004**, *126*, 3370−3371.
(1227) *Unimolecular and Supramolecular Electronics II: Chemistry and Physics Meet at Metal-Molecule Interfaces*; 2012; Vol. *313*, pp 1−272.
(1228) Joachim, C. Molecular wires and logic circuits integration in a single molecule? *Nanotechnology* **2003**, *2*, 80−81.
(1229) Joachim, C. Molecular and intramolecular electronics. *Superlattices Microstruct.* **2000**, *28*, 305−315.
(1230) Joachim, C.; Ratner, M. A. Molecular electronics. *Proc. Natl. Acad. Sci. U. S. A.* **2005**, *102*, 8800−8800.
(1231) Schenning, A. P. H. J.; Jonkheijm, P.; Hoeben, F. J. M.; van Herrikhuyzen, J.; Meskers, S. C. J.; Meijer, E. W.; Herz, L. M.; Daniel, C.; Silva, C.; Phillips, R. T.; et al. Towards supramolecular electronics. *Synth. Met.* **2004**, *147*, 43−48.
(1232) Weiss, J. Supramolecular approaches to nano and molecular electronics. *Coord. Chem. Rev.* **2010**, *254*, 2247−2248.
(1233) Flood, A. H.; Stoddart, J. F.; Steuerman, D. W.; Heath, J. R. Chemistry. Whence molecular electronics? *Science* **2004**, *306*, 2055−2056.
(1234) Blanco, M. J.; Jimenez, M. C.; Chambron, J. C.; Heitz, V.; Linke, M.; Sauvage, J.-P. Rotaxanes as new architectures for photoinduced electron transfer and molecular motions. *Chem. Soc. Rev.* **1999**, *28*, 293−305.
(1235) Huang, T. J. Towards artificial molecular motor-based electroactive/photoactive biomimetic muscles - art. no. 65240H. *P. Soc. Photo. Opt. Ins.* **2007**, *6524*, H5240−H5240.
(1236) Juluri, B. K.; Kumar, A. S.; Liu, Y.; Ye, T.; Yang, Y. W.; Flood, A. H.; Fang, L.; Stoddart, J. F.; Weiss, P. S.; Huang, T. J. A Mechanical Actuator Driven Electrochemically by Artificial Molecular Muscles. *ACS Nano* **2009**, *3*, 291−300.
(1237) Li, D. B.; Paxton, W. F.; Baughman, R. H.; Huang, T. J.; Stoddart, J. F.; Weiss, P. S. Molecular, Supramolecular, and Macromolecular Motors and Artificial Muscles. *MRS Bull.* **2009**, *34*, 671−681.
(1238) Liu, Y.; Flood, A. H.; Bonvallett, P. A.; Vignon, S. A.; Northrop, B. H.; Tseng, H. R.; Jeppesen, J. O.; Huang, T. J.; Brough, B.; Baller, M.; Magonov, S.; Solares, S. D.; Goddard, W. A., III; Ho, C. M.; Stoddart, J. F. Linear artificial molecular muscles. *J. Am. Chem. Soc.* **2005**, *127*, 9745−9759.
(1239) Park, J. K.; Carr, J.; Calhoun, B.; Moore, R. B. Enhanced actuation in artificial muscles through supra-molecular orientation of ionic domains. *Polym. Prepr.* **2006**, *47*, 484−485.
(1240) Otero, T. F.; Grande, H.; Rodriguez, J. Reversible electrochemical reactions in conducting polymers: A molecular approach to artificial muscles. *J. Phys. Org. Chem.* **1996**, *9*, 381−386.
(1241) Valero, L.; Arias-Pardilla, J.; Cauich-Rodriguez, J.; Smit, M. A.; Otero, T. F. Characterization of the movement of polypyrrole-dodecylbenzenesulfonate-perchlorate/tape artificial muscles. Faradaic control of reactive artificial molecular motors and muscles. *Electrochim. Acta* **2011**, *56*, 3721−3726.
(1242) Takashima, Y.; Hatanaka, S.; Otsubo, M.; Nakahata, M.; Kakuta, T.; Hashidzume, A.; Yamaguchi, H.; Harada, A. Expansion-contraction of photoresponsive artificial muscle regulated by host-guest interactions. *Nat. Commun.* **2012**, *3*, 1270.
(1243) Ceroni, P.; Credi, A.; Venturi, M. Light to investigate (read) and operate (write) molecular devices and machines. *Chem. Soc. Rev.* **2014**, *43*, 4068−4083.
(1244) Hutchison, K. A.; Parakka, J. P.; Kesler, B. S.; Schumaker, R. R. Chiropticenes: Molecular chiroptical dipole switches for optical data storage. *Micro-Nano-Photonic Mater. Dev.* **2000**, *3937*, 64−72.
(1245) Berna, J.; Leigh, D. A.; Lubomska, M.; Mendoza, S. M.; Perez, E. M.; Rudolf, P.; Teobaldi, G.; Zerbetto, F. Macroscopic transport by synthetic molecular machines. *Nat. Mater.* **2005**, *4*, 704−710.
(1246) Silvi, S.; Arduini, A.; Pochini, A.; Secchi, A.; Tomasulo, M.; Raymo, F. M.; Baroncini, M.; Credi, A. A simple molecular machine operated by photoinduced proton transfer. *J. Am. Chem. Soc.* **2007**, *129*, 13378−13379.
(1247) Silvi, S.; Constable, E. C.; Housecroft, C. E.; Beves, J. E.; Dunphy, E. L.; Tomasulo, M.; Raymo, F. M.; Credi, A. Photochemical switching of luminescence and singlet oxygen generation by chemical signal communication. *Chem. Commun.* **2009**, 1484−1486.
(1248) Tatum, L. A.; Foy, J. T.; Aprahamian, I. Waste Management of Chemically Activated Switches: Using a Photoacid To Eliminate Accumulation of Side Products. *J. Am. Chem. Soc.* **2014**, *136*, 17438−17441.
(1249) Jousselme, B.; Blanchard, P.; Levillain, E.; Delaunay, J.; Allain, M.; Richomme, P.; Rondeau, D.; Gallego-Planas, N.; Roncali, J. Crown-annelated oligothiophenes as model compounds for molecular actuation. *J. Am. Chem. Soc.* **2003**, *125*, 1363−1370.
(1250) Roncali, J.; Garreau, R.; Delabouglise, D.; Garnier, F.; Lemaire, M. Modification of the Structure and Electrochemical Properties of Poly(Thiophene) by Ether Groups. *J. Chem. Soc., Chem. Commun.* **1989**, 679−681.
(1251) Roncali, J.; Shi, L. H.; Garnier, F. Effects of Environmental-Factors on the Electrooptical Properties of Conjugated Polymers Containing Oligo(Oxyethylene) Substituents. *J. Phys. Chem.* **1991**, *95*, 8983−8989.
(1252) Marsella, M. J.; Swager, T. M. Designing Conducting Polymer-Based Sensors - Selective Ionochromic Response in Crown-Ether Containing Polythiophenes. *J. Am. Chem. Soc.* **1993**, *115*, 12214−12215.
(1253) Wang, B.; Wasielewski, M. R. Design and synthesis of metal ion-recognition-induced conjugated polymers: An approach to metal ion sensory materials. *J. Am. Chem. Soc.* **1997**, *119*, 12−21.
(1254) Marsella, M. J.; Newland, R. J.; Carroll, P. J.; Swager, T. M. Ionoresistivity as a Highly Sensitive Sensory Probe - Investigations of Polythiophenes Functionalized with Calix[4]Arene-Based Ion Receptors. *J. Am. Chem. Soc.* **1995**, *117*, 9842−9848.
(1255) Roncali, J. Electrogenerated functional conjugated polymers as advanced electrode materials. *J. Mater. Chem.* **1999**, *9*, 1875−1893.
(1256) McQuade, D. T.; Pullen, A. E.; Swager, T. M. Conjugated polymer-based chemical sensors. *Chem. Rev.* **2000**, *100*, 2537−2574.
(1257) Barbarella, G.; Melucci, M.; Sotgiu, G. The versatile thiophene: An overview of recent research on thiophene-based materials. *Adv. Mater.* **2005**, *17*, 1581−1593.
(1258) Jousselme, B.; Blanchard, P.; Gallego-Planas, N.; Delaunay, J.; Allain, M.; Richomme, P.; Levillain, E.; Roncali, J. Photomechanical actuation and manipulation of the electronic properties of linear π-conjugated systems. *J. Am. Chem. Soc.* **2003**, *125*, 2888−2889.
(1259) Jousselme, B.; Blanchard, P.; Gallego-Planas, N.; Levillain, E.; Delaunay, J.; Allain, M.; Richomme, P.; Roncali, J. Photomechanical control of the electronic properties of linear π-conjugated systems. *Chem. - Eur. J.* **2003**, *9*, 5297−5306.
(1260) Clayden, J.; Lund, A.; Vallverdu, L. S.; Helliwell, M. Ultra-remote stereocontrol by conformational communication of information along a carbon chain. *Nature* **2004**, *431*, 966−971.
(1261) Barton, D. H. R.; Cookson, R. C. The Principles of Conformational Analysis. *Q. Rev., Chem. Soc.* **1956**, *10*, 44−82.
(1262) Browne, W. R.; Pollard, M. M.; de Lange, B.; Meetsma, A.; Feringa, B. L. Reversible three-state switching of luminescence: a new twist to electro- and photochromic behavior. *J. Am. Chem. Soc.* **2006**, *128*, 12412−12413.
(1263) Nilsson, J. R.; O'Sullivan, M. C.; Li, S.; Anderson, H. L.; Andreasson, J. A photoswitchable supramolecular complex with release-and-report capabilities. *Chem. Commun.* **2015**, *51*, 847−850.
(1264) Zigon, N.; Larpent, P.; Jouaiti, A.; Kyritsakas, N.; Hosseini, M. W. Optical reading of the open and closed states of a molecular turnstile. *Chem. Commun.* **2014**, *50*, 5040−5042.
(1265) Dube, H.; Ams, M. R.; Rebek, J. Supramolecular Control of Fluorescence through Reversible Encapsulation. *J. Am. Chem. Soc.* **2010**, *132*, 9984−9985.
(1266) Tzeli, D.; Theodorakopoulos, G.; Petsalakis, I. D.; Ajami, D.; Rebek, J. Conformations and Fluorescence of Encapsulated Stilbene. *J. Am. Chem. Soc.* **2012**, *134*, 4346−4354.
(1267) Masar, M. S.; Gianneschi, N. C.; Oliveri, C. G.; Stern, C. L.; Nguyen, S. T.; Mirkin, C. A. Allosterically regulated supramolecular

DOI: 10.1021/acs.chemrev.5b00146
Chem. Rev. 2015, 115, 10081−10206

catalysis of acyl transfer reactions for signal amplification and detection of small molecules. *J. Am. Chem. Soc.* **2007**, *129*, 10149−10158.
(1268) Riddle, J. A.; Jiang, X.; Huffman, J.; Lee, D. Signal-amplifying resonance energy transfer: A dynamic multichromophore array for allosteric switching. *Angew. Chem., Int. Ed.* **2007**, *46*, 7019−7022.
(1269) Jiang, X.; Bollinger, J. C.; Lee, D. Two-dimensional electronic conjugation: Cooperative folding and fluorescence switching. *J. Am. Chem. Soc.* **2006**, *128*, 11732−11733.
(1270) Riddle, J. A.; Jiang, X.; Lee, D. W. Conformational dynamics for chemical sensing: simplicity and diversity. *Analyst* **2008**, *133*, 417−422.
(1271) Opsitnick, E.; Lee, D. Two-dimensional electronic conjugation: Statics and dynamics at structural domains beyond molecular wires. *Chem. - Eur. J.* **2007**, *13*, 7041−7049.
(1272) Onagi, H.; Rebek, J. Fluorescence resonance energy transfer across a mechanical bond of a rotaxane. *Chem. Commun.* **2005**, 4604−4606.
(1273) Azov, V. A.; Schlegel, A.; Diederich, F. Geometrically precisely defined multinanometer expansion/contraction motions in a resorcin[4]arene cavitand based molecular switch. *Angew. Chem., Int. Ed.* **2005**, *44*, 4635−4638.
(1274) Li, Y. J.; Li, H.; Li, Y. L.; Liu, H. B.; Wang, S.; He, X. R.; Wang, N.; Zhu, D. B. Energy transfer switching in a bistable molecular machine. *Org. Lett.* **2005**, *7*, 4835−4838.
(1275) Raker, J.; Glass, T. E. Cooperative ratiometric chemosensors: Pinwheel receptors with an integrated fluorescence system. *J. Org. Chem.* **2001**, *66*, 6505−6512.
(1276) Barboiu, M.; Prodi, L.; Montalti, M.; Zaccheroni, N.; Kyritsakas, N.; Lehn, J.-M. Dynamic chemical devices: Modulation of photophysical properties by reversible, ion-triggered, and proton-fueled nanomechanical shape-flipping molecular motions. *Chem. - Eur. J.* **2004**, *10*, 2953−2959.
(1277) Zhong, Z.; Zhao, Y. Cholate-glutamic acid hybrid foldamer and its fluorescent detection of Zn^{2+}. *Org. Lett.* **2007**, *9*, 2891−2894.
(1278) Kim, U. I.; Suk, J. M.; Naidu, V. R.; Jeong, K. S. Folding and anion-binding properties of fluorescent oligoindole foldamers. *Chem. - Eur. J.* **2008**, *14*, 11406−11414.
(1279) Yuasa, H.; Miyagawa, N.; Izumi, T.; Nakatani, M.; Izumi, M.; Hashimoto, H. Hinge sugar as a movable component of an excimer fluorescence sensor. *Org. Lett.* **2004**, *6*, 1489−1492.
(1280) Monahan, C.; Bien, J. T.; Smith, B. D. Fluorescence sensing due to allosteric switching of pyrene functionalized *cis*-cyclohexane-1,3-dicarboxylate. *Chem. Commun.* **1998**, 431−432.
(1281) Krauss, R.; Weinig, H. G.; Seydack, M.; Bendig, J.; Koert, U. Molecular signal transduction through conformational transmission of a perhydroanthracene transducer. *Angew. Chem., Int. Ed.* **2000**, *39*, 1835−1837.
(1282) Koert, U.; Krauss, R.; Weinig, H. G.; Heumann, C.; Ziemer, B.; Mugge, C.; Seydack, M.; Bendig, J. 2,3,6,7-tetrasubstituted decalins: Biconformational transducers for molecular signal transduction. *Eur. J. Org. Chem.* **2001**, *2001*, 575−586.
(1283) Berna, J.; Franco-Pujante, C.; Alajarin, M. Competitive binding for triggering a fluorescence response in a hydrazodicarboxamide-based [2]rotaxane. *Org. Biomol. Chem.* **2014**, *12*, 474−478.
(1284) Zhou, W.; Wu, Y.; Zhai, B. Q.; Wang, Q. C.; Qu, D. H. An anthracene-containing bistable [2]rotaxane featuring color and fluorescence changes. *RSC Adv.* **2014**, *4*, 5148−5151.
(1285) Perez, E. M.; Dryden, D. T. F.; Leigh, D. A.; Teobaldi, G.; Zerbetto, F. A generic basis for some simple light-operated mechanical molecular machines. *J. Am. Chem. Soc.* **2004**, *126*, 12210−12211.
(1286) Buschel, M.; Helldobler, M.; Daub, J. Electronic coupling in 6,6″-donor-substituted terpyridines: tuning of the mixed valence state by proton and metal ion complexation. *Chem. Commun.* **2002**, 1338−1339.
(1287) Glass, T. E. Cooperative chemical sensing with bis-tritylacetylenes: Pinwheel receptors with metal ion recognition properties. *J. Am. Chem. Soc.* **2000**, *122*, 4522−4523.
(1288) Raker, J.; Glass, T. E. Selectivity via cooperative interactions: Detection of dicarboxylates in water by a pinwheel chemosensor. *J. Org. Chem.* **2002**, *67*, 6113−6116.
(1289) Karle, M.; Bockelmann, D.; Schumann, D.; Griesinger, C.; Koert, U. Conformative coupling of two conformational molecular switches. *Angew. Chem., Int. Ed.* **2003**, *42*, 4546−4549.
(1290) Zhao, Y.; Zhong, Z. Detection of Hg^{2+} in aqueous solutions with a foldamer-based fluorescent sensor modulated by surfactant micelles. *Org. Lett.* **2006**, *8*, 4715−4717.
(1291) Qu, D. H.; Wang, Q. C.; Tian, H. A half adder based on a photochemically driven [2]rotaxane. *Angew. Chem., Int. Ed.* **2005**, *44*, 5296−5299.
(1292) Li, H.; Zhang, J. N.; Zhou, W.; Zhang, H.; Zhang, Q.; Qu, D. H.; Tian, H. Dual-Mode Operation of a Bistable [1]Rotaxane with a Fluorescence Signal. *Org. Lett.* **2013**, *15*, 3070−3073.
(1293) Qu, D. H.; Wang, Q. C.; Tian, H. Photodriven and thermal-driven shuttling of alpha-cyclodextrin on the molecular rotaxane containing azobenzene. *Mol. Cryst. Liq. Cryst.* **2005**, *430*, 59−65.
(1294) Qu, D. H.; Wang, Q. C.; Ma, X.; Tian, H. A [3]Rotaxane with three stable states that responds to multiple-inputs and displays dual fluorescence addresses. *Chem. - Eur. J.* **2005**, *11*, 5929−5937.
(1295) Lin, Y. C.; Chen, C. T. Alkaline Earth Metal Ion Induced CoilHelixCoil Transition of LysineCoumarinAzacrown Hybrid Foldamers with OFFOFFON Fluorescence Switching. *Chem. - Eur. J.* **2013**, *19*, 2531−2538.
(1296) Coskun, A.; Friedman, D. C.; Li, H.; Patel, K.; Khatib, H. A.; Stoddart, J. F. A Light-Gated STOP−GO Molecular Shuttle. *J. Am. Chem. Soc.* **2009**, *131*, 2493−2495.
(1297) Cao, J. J.; Ma, X.; Min, M. R.; Cao, T. T.; Wu, S. F.; Tian, H. INHIBIT logic operations based on light-driven beta-cyclodextrin pseudo[1]rotaxane with room temperature phosphorescence addresses. *Chem. Commun.* **2014**, *50*, 3224−3226.
(1298) Brown, R. A.; Diemer, V.; Webb, S. J.; Clayden, J. End-to-end conformational communication through a synthetic purinergic receptor by ligand-induced helicity switching. *Nat. Chem.* **2013**, *5*, 853−860.
(1299) Muraoka, T.; Kinbara, K.; Aida, T. A self-locking molecule operative with a photoresponsive key. *J. Am. Chem. Soc.* **2006**, *128*, 11600−11605.
(1300) Clayden, J.; Vassiliou, N. Stereochemical relays: communication via conformation. *Org. Biomol. Chem.* **2006**, *4*, 2667−2678.
(1301) Jiang, X.; Lim, Y. K.; Zhang, B. J.; Opsitnick, E. A.; Baik, M. H.; Lee, D. Dendritic molecular switch: chiral folding and helicity inversion. *J. Am. Chem. Soc.* **2008**, *130*, 16812−16822.
(1302) Clayden, J.; Castellanos, A.; Sola, J.; Morris, G. A. Quantifying End-to-End Conformational Communication of Chirality through an Achiral Peptide Chain. *Angew. Chem., Int. Ed.* **2009**, *48*, 5962−5965.
(1303) Mathews, M.; Tamaoki, N. Reversibly tunable helicity induction and inversion in liquid crystal self-assembly by a planar chiroptic trigger molecule. *Chem. Commun.* **2009**, 3609−3611.
(1304) Akine, S.; Hotate, S.; Nabeshima, T. A molecular leverage for helicity control and helix inversion. *J. Am. Chem. Soc.* **2011**, *133*, 13868−13871.
(1305) Wei, K.; Ni, J.; Min, Y.; Chen, S.; Liu, Y. Unexpected helicity control and helix inversion: homochiral helical nanotubes consisting of an achiral ligand. *Chem. Commun.* **2013**, *49*, 8220−8222.
(1306) Sargsyan, G.; Schatz, A. A.; Kubelka, J.; Balaz, M. Formation and helicity control of ssDNA templated porphyrin nanoassemblies. *Chem. Commun.* **2013**, *49*, 1020−1022.
(1307) De Poli, M.; Clayden, J. Thionoglycine as a multifunctional spectroscopic reporter of screw-sense preference in helical foldamers. *Org. Biomol. Chem.* **2014**, *12*, 836−843.
(1308) Duan, P.; Cao, H.; Zhang, L.; Liu, M. Gelation induced supramolecular chirality: chirality transfer, amplification and application. *Soft Matter* **2014**, *10*, 5428−5448.
(1309) Nguyen, B. T.; Anslyn, E. V. Indicator-displacement assays. *Coord. Chem. Rev.* **2006**, *250*, 3118−3127.
(1310) Gassensmith, J. J.; Matthys, S.; Lee, J. J.; Wojcik, A.; Kamat, P. V.; Smith, B. D. Squaraine Rotaxane as a Reversible Optical Chloride Sensor. *Chem. - Eur. J.* **2010**, *16*, 2916−2921.
(1311) Langton, M. J.; Beer, P. D. Rotaxane and catenane host structures for sensing charged guest species. *Acc. Chem. Res.* **2014**, *47*, 1935−1949.

DOI: 10.1021/acs.chemrev.5b00146
Chem. Rev. 2015, 115, 10081−10206

(1312) Hsueh, S. Y.; Lai, C. C.; Chiu, S. H. Squaraine-Based [2]Rotaxanes that Function as Visibly Active Molecular Switches. *Chem. - Eur. J.* **2010**, *16*, 2997−3000.
(1313) Klajn, R.; Fang, L.; Coskun, A.; Olson, M. A.; Wesson, P. J.; Stoddart, J. F.; Grzybowski, B. A. Metal Nanoparticles Functionalized with Molecular and Supramolecular Switches. *J. Am. Chem. Soc.* **2009**, *131*, 4233−4235.
(1314) Cheng, H. B.; Zhang, H. Y.; Liu, Y. Dual-Stimulus Luminescent Lanthanide Molecular Switch Based on an Unsymmetrical Diarylperfluorocyclopentene. *J. Am. Chem. Soc.* **2013**, *135*, 10190−10193.
(1315) Allenmark, S. Induced circular dichroism by chiral molecular interaction. *Chirality* **2003**, *15*, 409−422.
(1316) Prins, L. J.; Huskens, J.; de Jong, F.; Timmerman, P.; Reinhoudt, D. N. Complete asymmetric induction of supramolecular chirality in a hydrogen-bonded assembly. *Nature* **1999**, *398*, 498−502.
(1317) Mineo, P.; Villari, V.; Scamporrino, E.; Micali, N. Supramolecular chirality induced by a weak thermal force. *Soft Matter* **2014**, *10*, 44−47.
(1318) Tachibana, Y.; Kihara, N.; Takata, T. Asymmetric benzoin condensation catalyzed by chiral rotaxanes tethering a thiazolium salt moiety via the cooperation of the component: Can rotaxane be an effective reaction field? *J. Am. Chem. Soc.* **2004**, *126*, 13560−13560.
(1319) Havinga, E. Spontaneous Formation of Optically Active Substances. *Biochim. Biophys. Acta* **1954**, *13*, 171−174.
(1320) Suarez, M.; Branda, N.; Lehn, J.-M.; Decian, A.; Fischer, J. Supramolecular chirality: Chiral hydrogen-bonded supermolecules from achiral molecular components. *Helv. Chim. Acta* **1998**, *81*, 1−13.
(1321) Evan-Salem, T.; Baruch, I.; Avram, L.; Cohen, Y.; Palmer, L. C.; Rebek, J. Resorcinarenes are hexameric capsules in solution. *Proc. Natl. Acad. Sci. U. S. A.* **2006**, *103*, 12296−12300.
(1322) Rivera, J. M.; Martin, T.; Rebek, J. Chiral spaces: Dissymmetric capsules through self-assembly. *Science* **1998**, *279*, 1021−1023.
(1323) Woods, C. R.; Benaglia, M.; Cozzi, F.; Siegel, J. S. Enantioselective synthesis of copper(I) bipyridine based helicates by chiral templating of secondary structure: Transmission of stereochemistry on the nanometer scale. *Angew. Chem., Int. Ed. Engl.* **1996**, *35*, 1830−1833.
(1324) Kaminker, R.; de Hatten, X.; Lahav, M.; Lupo, F.; Gulino, A.; Evmenenko, G.; Dutta, P.; Browne, C.; Nitschke, J. R.; van der Boom, M. E. Assembly of Surface-Confined Homochiral Helicates: Chiral Discrimination of DOPA and Unidirectional Charge Transfer. *J. Am. Chem. Soc.* **2013**, *135*, 17052−17059.
(1325) Miyake, H.; Tsukube, H. Coordination chemistry strategies for dynamic helicates: time-programmable chirality switching with labile and inert metal helicates. *Chem. Soc. Rev.* **2012**, *41*, 6977−6991.
(1326) Bottari, G.; Leigh, D. A.; Perez, E. M. Chiroptical switching in a bistable molecular shuttle. *J. Am. Chem. Soc.* **2003**, *125*, 13360−13361.
(1327) Zhou, W. D.; Xu, J. L.; Zheng, H. Y.; Yin, X. D.; Zuo, Z. C.; Liu, H. B.; Li, Y. L. Distinct Nanostructures from a Molecular Shuttle: Effects of Shuttling Movement on Nanostructural Morphologies. *Adv. Funct. Mater.* **2009**, *19*, 141−149.
(1328) Ji, F. Y.; Zhu, L. L.; Zhang, D.; Chen, Z. F.; Tian, H. Coordination-driven self-organization of switchable [2]rotaxane. *Tetrahedron* **2009**, *65*, 9081−9085.
(1329) Hsueh, S. Y.; Kuo, C. T.; Lu, T. W.; Lai, C. C.; Liu, Y. H.; Hsu, H. F.; Peng, S. M.; Chen, C. H.; Chiu, S. H. Acid/Base- and Anion-Controllable Organogels Formed From a Urea-Based Molecular Switch. *Angew. Chem., Int. Ed.* **2010**, *49*, 9170−9173.
(1330) Gong, H.-Y.; Rambo, B. M.; Karnas, E.; Lynch, V. M.; Sessler, J. L. A 'Texas-sized' molecular box that forms an anion-induced supramolecular necklace. *Nat. Chem.* **2010**, *2*, 406−409.
(1331) Fasano, V.; Baroncini, M.; Moffa, M.; Iandolo, D.; Camposeo, A.; Credi, A.; Pisignano, D. Organic Nanofibers Embedding Stimuli-Responsive Threaded Molecular Components. *J. Am. Chem. Soc.* **2014**, *136*, 14245−14254.
(1332) Jimenez, M. C.; Dietrich-Buchecker, C.; Sauvage, J.-P. Towards synthetic molecular muscles: Contraction and stretching of a linear rotaxane dimer. *Angew. Chem., Int. Ed.* **2000**, *39*, 3284−3287.
(1333) Gao, L.; Zhang, Z.; Zheng, B.; Huang, F. Construction of muscle-like metallo-supramolecular polymers from a pillar[5]arene-based [c2]daisy chain. *Polym. Chem.* **2014**, *5*, 5734−5739.
(1334) Yan, X.; Zheng, B.; Huang, F. Integrated motion of molecular machines in supramolecular polymeric scaffolds. *Polym. Chem.* **2013**, *4*, 2395−2399.
(1335) Bruns, C. J.; Frasconi, M.; Iehl, J.; Hartlieb, K. J.; Schneebeli, S. T.; Cheng, C.; Stupp, S. I.; Stoddart, J. F. Redox Switchable Daisy Chain Rotaxanes Driven by Radical−Radical Interactions. *J. Am. Chem. Soc.* **2014**, *136*, 4714−4723.
(1336) Silvi, S.; Venturi, M.; Credi, A. Artificial molecular shuttles: from concepts to devices. *J. Mater. Chem.* **2009**, *19*, 2279−2294.
(1337) Balzani, V.; Credi, A.; Silvi, S.; Venturi, M. Artificial nanomachines based on interlocked molecular species: recent advances. *Chem. Soc. Rev.* **2006**, *35*, 1135−1149.
(1338) Romuald, C.; Arda, A.; Clavel, C.; Jimenez-Barbero, J.; Coutrot, F. Tightening or loosening a pH-sensitive double-lasso molecular machine readily synthesized from an ends-activated [c2]daisy chain. *Chem. Sci.* **2012**, *3*, 1851−1857.
(1339) Fang, L.; Hmadeh, M.; Wu, J.; Olson, M. A.; Spruell, J. M.; Trabolsi, A.; Yang, Y.-W.; Elhabiri, M.; Albrecht-Gary, A.-M.; Stoddart, J. F. Acid−Base Actuation of [c2]Daisy Chains. *J. Am. Chem. Soc.* **2009**, *131*, 7126−7134.
(1340) Dawson, R. E.; Lincoln, S. F.; Easton, C. J. The foundation of a light driven molecular muscle based on stilbene and alpha-cyclodextrin. *Chem. Commun.* **2008**, 3980−3982.
(1341) Huang, T. J.; Brough, B.; Ho, C. M.; Liu, Y.; Flood, A. H.; Bonvallet, P. A.; Tseng, H. R.; Stoddart, J. F.; Baller, M.; Magonov, S. A nanomechanical device based on linear molecular motors. *Appl. Phys. Lett.* **2004**, *85*, 5391−5393.
(1342) Ooya, T.; Yui, N. Synthesis of theophylline−polyrotaxane conjugates and their drug release via supramolecular dissociation. *J. Controlled Release* **1999**, *58*, 251−269.
(1343) Tooru, O.; Atsushi, Y.; Motoichi, K.; Yuko, S.; Atsushi, M.; Nobuhiko, Y. Effects of polyrotaxane structure on polyion complexation with DNA. *Sci. Technol. Adv. Mater.* **2004**, *5*, 363−369.
(1344) Ooya, T.; Choi, H. S.; Yamashita, A.; Yui, N.; Sugaya, Y.; Kano, A.; Maruyama, A.; Akita, H.; Ito, R.; Kogure, K.; Harashima, H. Biocleavable Polyrotaxane−Plasmid DNA Polyplex for Enhanced Gene Delivery. *J. Am. Chem. Soc.* **2006**, *128*, 3852−3853.
(1345) Moon, C.; Kwon, Y. M.; Lee, W. K.; Park, Y. J.; Yang, V. C. In vitro assessment of a novel polyrotaxane-based drug delivery system integrated with a cell-penetrating peptide. *J. Controlled Release* **2007**, *124*, 43−50.
(1346) Zhang, X.; Zhu, X.; Ke, F.; Ye, L.; Chen, E.-q.; Zhang, A.-y.; Feng, Z.-g. Preparation and self-assembly of amphiphilic triblock copolymers with polyrotaxane as a middle block and their application as carrier for the controlled release of Amphotericin B. *Polymer* **2009**, *50*, 4343−4351.
(1347) Harada, A. H. A.; Yamaguchi, H.; Takashima, Y. Polymeric Rotaxanes. *Chem. Rev.* **2009**, *109*, 5974−6023.
(1348) Li, J. J.; Zhao, F.; Li, J. Polyrotaxanes for applications in life science and biotechnology. *Appl. Microbiol. Biotechnol.* **2011**, *90*, 427−443.
(1349) Hashidzume, A.; Yamaguchi, H.; Harada, A. Cyclodextrin-Based Molecular Machines. *Topics Curr. Chem.* **2014**, *354*, 71−110.
(1350) Fernandes, A.; Viterisi, A.; Coutrot, F.; Potok, S.; Leigh, D. A.; Aucagne, V.; Papot, S. Rotaxane-Based Propeptides: Protection and Enzymatic Release of a Bioactive Pentapeptide. *Angew. Chem., Int. Ed.* **2009**, *48*, 6443−6447.
(1351) Fernandes, A.; Viterisi, A.; Aucagne, V.; Leigh, D. A.; Papot, S. Second generation specific-enzyme-activated rotaxane propeptides. *Chem. Commun.* **2012**, *48*, 2083−2085.
(1352) Barat, R.; Legigan, T.; Tranoy-Opalinski, I.; Renoux, B.; Peraudeau, E.; Clarhaut, J.; Poinot, P.; Fernandes, A. E.; Aucagne, V.; Leigh, D. A.; Papot, S. A mechanically interlocked molecular system programmed for the delivery of an anticancer drug. *Chem. Sci.* **2015**, *6*, 2608−2613.

DOI: 10.1021/acs.chemrev.5b00146
Chem. Rev. 2015, 115, 10081−10206

(1353) Singleton, M. R.; Dillingham, M. S.; Wigley, D. B. Structure and mechanism of helicases and nucleic acid translocases. *Annu. Rev. Biochem.* **2007**, *76*, 23−50.
(1354) Virag, L.; Szabo, C. The therapeutic potential of poly(ADP-ribose) polymerase inhibitors. *Pharmacol. Rev.* **2002**, *54*, 375−429.
(1355) Gore, J.; Bryant, Z.; Stone, M. D.; Nollmann, M. N.; Cozzarelli, N. R.; Bustamante, C. Mechanochemical analysis of DNA gyrase using rotor bead tracking. *Nature* **2006**, *439*, 100−104.
(1356) Reece, R. J.; Maxwell, A. DNA Gyrase - Structure and Function. *Crit. Rev. Biochem. Mol. Biol.* **1991**, *26*, 335−375.
(1357) Chen, S. H.; Chan, N. L.; Hsieh, T. S. New Mechanistic and Functional Insights into DNA Topoisomerases. *Annu. Rev. Biochem.* **2013**, *82*, 139−170.
(1358) Wang, J. C. Cellular roles of DNA topoisomerases: A molecular perspective. *Nat. Rev. Mol. Cell Biol.* **2002**, *3*, 430−440.
(1359) von Ballmoos, C.; Cook, G. M.; Dimroth, P. Unique rotary ATP synthase and its biological diversity. *Annu. Rev. Biophys.* **2008**, *37*, 43−64.
(1360) Gadsby, D. C. Ion channels versus ion pumps: the principal difference, in principle. *Nat. Rev. Mol. Cell Biol.* **2009**, *10*, 344−352.
(1361) Yoneda, Y. How proteins are transported from cytoplasm to the nucleus. *J. Biochem.* **1997**, *121*, 811−817.
(1362) Sweeney, H. L.; Houdusse, A. Structural and Functional Insights into the Myosin Motor Mechanism. *Annu. Rev. Biophys.* **2010**, *39*, 539−557.
(1363) Koonce, M. P.; Samso, M. Of rings and levers: the dynein motor comes of age. *Trends Cell Biol.* **2004**, *14*, 612−619.
(1364) Vale, R. D. The molecular motor toolbox for intracellular transport. *Cell* **2003**, *112*, 467−480.
(1365) Schliwa, M.; Woehlke, G. Molecular motors. *Nature* **2003**, *422*, 759−765.
(1366) Ptacin, J. L.; Lee, S. F.; Garner, E. C.; Toro, E.; Eckart, M.; Comolli, L. R.; Moerner, W.; Shapiro, L. A spindle-like apparatus guides bacterial chromosome segregation. *Nat. Cell Biol.* **2010**, *12*, 791−798.
(1367) Saffarian, S.; Collier, I. E.; Marmer, B. L.; Elson, E. L.; Goldberg, G. Interstitial collagenase is a Brownian ratchet driven by proteolysis of collagen. *Science* **2004**, *306*, 108−111.
(1368) Xie, P. Molecular motors that digest their track to rectify Brownian motion: processive movement of exonuclease enzymes. *J. Phys.: Condens. Matter* **2009**, *21*, 375108.
(1369) von Delius, M.; Leigh, D. A. Walking molecules. *Chem. Soc. Rev.* **2011**, *40*, 3656−3676.
(1370) Vale, R. D.; Reese, T. S.; Sheetz, M. P. Identification of a Novel Force-Generating Protein, Kinesin, Involved in Microtubule-Based Motility. *Cell* **1985**, *42*, 39−50.
(1371) Block, S. M. Kinesin motor mechanics: Binding, stepping, tracking, gating, and limping. *Biophys. J.* **2007**, *92*, 2986−2995.
(1372) Asbury, C. L.; Fehr, A. N.; Block, S. M. Kinesin moves by an asymmetric hand-over-hand mechanism. *Science* **2003**, *302*, 2130−2134.
(1373) Yildiz, A.; Tomishige, M.; Vale, R. D.; Selvin, P. R. Kinesin walks hand-over-hand. *Science* **2004**, *303*, 676−678.
(1374) Howard, J.; Hudspeth, A. J.; Vale, R. D. Movement of Microtubules by Single Kinesin Molecules. *Nature* **1989**, *342*, 154−158.
(1375) Block, S. M.; Goldstein, L. S. B.; Schnapp, B. J. Bead Movement by Single Kinesin Molecules Studied with Optical Tweezers. *Nature* **1990**, *348*, 348−352.
(1376) Hackney, D. D. Highly Processive Microtubule-Stimulated ATP Hydrolysis by Dimeric Kinesin Head Domains. *Nature* **1995**, *377*, 448−450.
(1377) Vale, R. D.; Funatsu, T.; Pierce, D. W.; Romberg, L.; Harada, Y.; Yanagida, T. Direct observation of single kinesin molecules moving along microtubules. *Nature* **1996**, *380*, 451−453.
(1378) Hirokawa, N.; Nitta, R.; Okada, Y. The mechanisms of kinesin motor motility: lessons from the monomeric motor KIF1A. *Nat. Rev. Mol. Cell Biol.* **2009**, *10*, 877−884.
(1379) Yin, P.; Yan, H.; Daniell, X. G.; Turberfield, A. J.; Reif, J. H. A unidirectional DNA walker that moves autonomously along a track. *Angew. Chem., Int. Ed.* **2004**, *43*, 4906−4911.
(1380) Tian, Y.; He, Y.; Chen, Y.; Yin, P.; Mao, C. D. Molecular devices - A DNAzyme that walks processively and autonomously along a one-dimensional track. *Angew. Chem., Int. Ed.* **2005**, *44*, 4355−4358.
(1381) Muscat, R. A.; Bath, J.; Turberfield, A. J. Small Molecule Signals that Direct the Route of a Molecular Cargo. *Small* **2012**, *8*, 3593−3597.
(1382) You, M. X.; Chen, Y.; Zhang, X. B.; Liu, H. P.; Wang, R. W.; Wang, K. L.; Williams, K. R.; Tan, W. H. An Autonomous and Controllable Light-Driven DNA Walking Device. *Angew. Chem., Int. Ed.* **2012**, *51*, 2457−2460.
(1383) You, M. X.; Huang, F. J.; Chen, Z.; Wang, R. W.; Tan, W. H. Building a Nanostructure with Reversible Motions Using Photonic Energy. *ACS Nano* **2012**, *6*, 7935−7941.
(1384) Perl, A.; Gomez-Casado, A.; Thompson, D.; Dam, H. H.; Jonkheijm, P.; Reinhoudt, D. N.; Huskens, J. Gradient-driven motion of multivalent ligand molecules along a surface functionalized with multiple receptors. *Nat. Chem.* **2011**, *3*, 317−322.
(1385) Weimann, D. P.; Winkler, H. D. F.; Falenski, J. A.; Koksch, B.; Schalley, C. A. Highly dynamic motion of crown ethers along oligolysine peptide chains. *Nat. Chem.* **2009**, *1*, 668−668.
(1386) Strawser, D.; Karton, A.; Zenkina, E. V.; Iron, M. A.; Shimon, L. J. W.; Martin, J. M. L.; van der Boom, M. E. Platinum stilbazoles: Ring-walking coupled with aryl-halide bond activation. *J. Am. Chem. Soc.* **2005**, *127*, 9322−9323.
(1387) Tkachov, R.; Senkovskyy, V.; Komber, H.; Sommer, J. U.; Kiriy, A. Random Catalyst Walking along Polymerized Poly(3-hexylthlophene) Chains in Kumada Catalyst-Transfer Polycondensation. *J. Am. Chem. Soc.* **2010**, *132*, 7803−7810.
(1388) Claisen, L.; Tietze, E.; Über den Mechanismus. der Umlagerung der Phenol-allyläther. *Ber. Dtsch. Chem. Ges. B* **1925**, *58*, 275−281.
(1389) Claisen, L. The rearrangement of phenol-allyl-ather in C-allyl-phenole. *Ber. Dtsch. Chem. Ges.* **1912**, *45*, 3157−3166.
(1390) Cope, A. C.; Hardy, E. M. The introduction of substituted vinyl groups. VI. The regeneration of substituted vinyl malonic esters from their sodium enolates. *J. Am. Chem. Soc.* **1940**, *62*, 3319−3323.
(1391) Cope, A. C.; Hardy, E. M. The introduction of substituted vinyl groups V A rearrangement involving the migration of an allyl group in a three-carbon system. *J. Am. Chem. Soc.* **1940**, *62*, 441−444.
(1392) Cope, A. C.; Hartung, W. H.; Hancock, E. M.; Crossley, F. S. Substituted vinyl barbituric acids IV Derivatives containing a primary 1-alkenyl group. *J. Am. Chem. Soc.* **1940**, *62*, 1199−1201.
(1393) Cope, A. C.; Hartung, W. H.; Hancock, E. M.; Crossley, F. S. The introduction of substituted vinyl groups IV (Primary 1-alkenyl) alkyl malonic esters. *J. Am. Chem. Soc.* **1940**, *62*, 314−316.
(1394) Mitra, S.; Lawton, R. G. Reagents for the Cross-Linking of Proteins by Equilibrium Transfer Alkylation. *J. Am. Chem. Soc.* **1979**, *101*, 3097−3110.
(1395) Kovaricek, P.; Lehn, J.-M. Merging Constitutional and Motional Covalent Dynamics in Reversible Imine Formation and Exchange Processes. *J. Am. Chem. Soc.* **2012**, *134*, 9446−9455.
(1396) Kovaricek, P.; Lehn, J.-M. Directional Dynamic Covalent Motion of a Carbonyl Walker on a Polyamine Track. *Chem. - Eur. J.* **2015**, *21*, 9380−9384.
(1397) Campana, A. G.; Carlone, A.; Chen, K.; Dryden, D. T. F.; Leigh, D. A.; Lewandowska, U.; Mullen, K. M. A Small Molecule that Walks Non-Directionally Along a Track Without External Intervention. *Angew. Chem., Int. Ed.* **2012**, *51*, 5480−5483.
(1398) Campana, A. G.; Leigh, D. A.; Lewandowska, U. One-Dimensional Random Walk of a Synthetic Small Molecule Toward a Thermodynamic Sink. *J. Am. Chem. Soc.* **2013**, *135*, 8639−8645.
(1399) von Delius, M.; Geertsema, E. M.; Leigh, D. A. A synthetic small molecule that can walk down a track. *Nat. Chem.* **2010**, *2*, 96−101.
(1400) von Delius, M.; Geertsema, E. M.; Leigh, D. A.; Tang, D. T. D. Design, Synthesis, and Operation of Small Molecules That Walk along Tracks. *J. Am. Chem. Soc.* **2010**, *132*, 16134−16145.
(1401) Pulcu, G. S.; Mikhailova, E.; Choi, L. S.; Bayley, H. Continuous observation of the stochastic motion of an individual small-molecule walker. *Nat. Nanotechnol.* **2014**, *10*, 76−83.

DOI: 10.1021/acs.chemrev.5b00146
Chem. Rev. 2015, 115, 10081−10206

(1402) Haq, S.; Wit, B.; Sang, H.; Floris, A.; Wang, Y.; Wang, J.; Pérez-García, L.; Kantorovitch, L.; Amabilino, D. B.; Raval, R. A Small Molecule Walks Along a Surface Between Porphyrin Fences That Are Assembled In Situ. *Angew. Chem., Int. Ed.* **2015**, *54*, 7101−7105.
(1403) Beves, J. E.; Blanco, V.; Blight, B. A.; Carrillo, R.; D'Souza, D. M.; Howgego, D.; Leigh, D. A.; Slawin, A. M. Z.; Symes, M. D. Toward Metal Complexes That Can Directionally Walk Along Tracks: Controlled Stepping of a Molecular Biped with a Palladium(II) Foot. *J. Am. Chem. Soc.* **2014**, *136*, 2094−2100.
(1404) Barrell, M. J.; Campana, A. G.; von Delius, M.; Geertsema, E. M.; Leigh, D. A. Light-Driven Transport of a Molecular Walker in Either Direction along a Molecular Track. *Angew. Chem., Int. Ed.* **2011**, *50*, 285−290.
(1405) Luning, U. Switchable catalysis. *Angew. Chem., Int. Ed.* **2012**, *51*, 8163−8165.
(1406) Kumagai, N.; Shibasaki, M. Catalytic chemical transformations with conformationally dynamic catalytic systems. *Catal. Sci. Technol.* **2013**, *3*, 41−57.
(1407) Neilson, B. M.; Bielawski, C. W. Illuminating Photoswitchable Catalysis. *ACS Catal.* **2013**, *3*, 1874−1885.
(1408) Leigh, D. A.; Marcos, V.; Wilson, M. R. Rotaxane Catalysts. *ACS Catal.* **2014**, *4*, 4490−4497.
(1409) Blanco, V.; Leigh, D. A.; Marcos, V. Artificial switchable catalysts. *Chem. Soc. Rev.* **2015**, *44*, 5341−5370.
(1410) Wiester, M. J.; Ulmann, P. A.; Mirkin, C. A. Enzyme Mimics Based Upon Supramolecular Coordination Chemistry. *Angew. Chem., Int. Ed.* **2011**, *50*, 114−137.
(1411) Yoon, H. J.; Mirkin, C. A. PCR-like cascade reactions in the context of an allosteric enzyme mimic. *J. Am. Chem. Soc.* **2008**, *130*, 11590−11591.
(1412) Yoon, H. J.; Heo, J.; Mirkin, C. A. Allosteric regulation of phosphate diester transesterification based upon a dinuclear zinc catalyst assembled via the weak-link approach. *J. Am. Chem. Soc.* **2007**, *129*, 14182−14183.
(1413) Vlatkovic, M.; Bernardi, L.; Otten, E.; Feringa, B. L. Dual stereocontrol over the Henry reaction using a light- and heat-triggered organocatalyst. *Chem. Commun.* **2014**, *50*, 7773−7775.
(1414) Stoll, R. S.; Hecht, S. Artificial Light-Gated Catalyst Systems. *Angew. Chem., Int. Ed.* **2010**, *49*, 5054−5075.
(1415) Imahori, T.; Kurihara, S. Stimuli-responsive Cooperative Catalysts Based on Dynamic Conformational Changes toward Spatiotemporal Control of Chemical Reactions. *Chem. Lett.* **2014**, *43*, 1524−1531.
(1416) Frank Wuerthner; Julius Rebek, J. Light-Switchable Catalysis in Synthetic Receptors. *Angew. Chem., Int. Ed. Engl.* **1995**, *34*, 446−448.
(1417) Berryman, O. B.; Sather, A. C.; Lledo, A.; Rebek, J., Jr. Switchable catalysis with a light-responsive cavitand. *Angew. Chem., Int. Ed.* **2011**, *50*, 9400−9403.
(1418) Peters, M. V.; Stoll, R. S.; Kuhn, A.; Hecht, S. Photoswitching of basicity. *Angew. Chem., Int. Ed.* **2008**, *47*, 5968−5972.
(1419) Osorio-Planes, L.; Rodriguez-Escrich, C.; Pericas, M. A. Photoswitchable thioureas for the external manipulation of catalytic activity. *Org. Lett.* **2014**, *16*, 1704−1707.
(1420) Viehmann, P.; Hecht, S. Design and synthesis of a photoswitchable guanidine catalyst. *Beilstein J. Org. Chem.* **2012**, *8*, 1825−1830.
(1421) Neilson, B. M.; Bielawski, C. W. Photoswitchable Organocatalysis: Using Light To Modulate the Catalytic Activities of *N*-Heterocyclic Carbenes. *J. Am. Chem. Soc.* **2012**, *134*, 12693−12699.
(1422) Neilson, B. M.; Bielawski, C. W. Photoswitchable Metal-Mediated Catalysis: Remotely Tuned Alkene and Alkyne Hydroborations. *Organometallics* **2013**, *32*, 3121−3128.
(1423) Wilson, D.; Branda, N. R. Turning ″on″ and ″off″ a pyridoxal 5′-phosphate mimic using light. *Angew. Chem., Int. Ed.* **2012**, *51*, 5431−5434.
(1424) Wang, J.; Feringa, B. L. Dynamic control of chiral space in a catalytic asymmetric reaction using a molecular motor. *Science* **2011**, *331*, 1429−1432.
(1425) Zhao, D.; Neubauer, T. M.; Feringa, B. L. Dynamic control of chirality in phosphine ligands for enantioselective catalysis. *Nat. Commun.* **2015**, *6*, 6652.
(1426) Li, Y.; Feng, Y.; He, Y. M.; Chen, F.; Pan, J.; Fan, Q. H. Supramolecular chiral phosphorous ligands based on a [2]-pseudorotaxane complex for asymmetric hydrogenation. *Tetrahedron Lett.* **2008**, *49*, 2878−2881.
(1427) Tachibana, Y.; Kihara, N.; Nakazono, K.; Takata, T. Thiazolium-Tethering Rotaxane-Catalyzed Asymmetric Benzoin Condensation: Unique Asymmetric Field Constructed by the Cooperation of Rotaxane Components. *Phosphorus, Sulfur Silicon Relat. Elem.* **2010**, *185*, 1182−1205.
(1428) Suzaki, Y.; Shimada, K.; Chihara, E.; Saito, T.; Tsuchido, Y.; Osakada, K. [3]Rotaxane-Based Dinuclear Palladium Catalysts for Ring-closure Mizoroki-Heck Reaction. *Org. Lett.* **2011**, *13*, 3774−3777.
(1429) Caputo, C. B.; Zhu, K. L.; Vukotic, V. N.; Loeb, S. J.; Stephan, D. W. Heterolytic Activation of H2 Using a Mechanically Interlocked Molecule as a Frustrated Lewis Base. *Angew. Chem., Int. Ed.* **2013**, *52*, 960−963.
(1430) Miyagawa, N.; Watanabe, M.; Matsuyama, T.; Koyama, Y.; Moriuchi, T.; Hirao, T.; Furusho, Y.; Takata, T. Successive catalytic reactions specific to Pd-based rotaxane complexes as a result of wheel translation along the axle. *Chem. Commun.* **2010**, *46*, 1920−1922.
(1431) Blanco, V.; Carlone, A.; Hanni, K. D.; Leigh, D. A.; Lewandowski, B. A rotaxane-based switchable organocatalyst. *Angew. Chem., Int. Ed.* **2012**, *51*, 5166−5169.
(1432) Blanco, V.; Leigh, D. A.; Lewandowska, U.; Lewandowsld, B.; Marcos, V. Exploring the Activation Modes of a Rotaxane-Based Switchable Organocatalyst. *J. Am. Chem. Soc.* **2014**, *136*, 15775−15780.
(1433) Blanco, V.; Leigh, D. A.; Marcos, V.; Morales-Serna, J. A.; Nussbaumer, A. L. A Switchable [2]Rotaxane Asymmetric Organocatalyst That Utilizes an Acyclic Chiral Secondary Amine. *J. Am. Chem. Soc.* **2014**, *136*, 4905−4908.
(1434) Beswick, J.; Blanco, V.; De Bo, G.; Leigh, D. A.; Lewandowska, U.; Lewandowski, B.; Mishiro, K. Selecting reactions and reactants using a switchable rotaxane organocatalyst with two different active sites. *Chem. Sci.* **2015**, *6*, 140−143.
(1435) Yoon, H. J.; Kuwabara, J.; Kim, J. H.; Mirkin, C. A. Allosteric supramolecular triple-layer catalysts. *Science* **2010**, *330*, 66−69.
(1436) Wiester, M. J.; Braunschweig, A. B.; Yoo, H.; Mirkin, C. A. Solvent and Temperature Induced Switching Between Structural Isomers of Rh-I Phosphinoalkyl Thioether (PS) Complexes. *Inorg. Chem.* **2010**, *49*, 7188−7196.
(1437) McGuirk, C. M.; Mendez-Arroyo, J.; Lifschitz, A. M.; Mirkin, C. A. Allosteric Regulation of Supramolecular Oligomerization and Catalytic Activity via Coordination-Based Control of Competitive Hydrogen-Bonding Events. *J. Am. Chem. Soc.* **2014**, *136*, 16594−16601.
(1438) Lifschitz, A. M.; Young, R. M.; Mendez-Arroyo, J.; Stern, C. L.; McGuirk, C. M.; Wasielewski, M. R.; Mirkin, C. A. An allosteric photoredox catalyst inspired by photosynthetic machinery. *Nat. Commun.* **2015**, *6*, 6541.
(1439) Schmittel, M.; De, S.; Pramanik, S. Reversible ON/OFF nanoswitch for organocatalysis: mimicking the locking and unlocking operation of CaMKII. *Angew. Chem., Int. Ed.* **2012**, *51*, 3832−3836.
(1440) Schmittel, M.; Pramanik, S.; De, S. A reversible nanoswitch as an ON-OFF photocatalyst. *Chem. Commun.* **2012**, *48*, 11730−11732.
(1441) Samanta, S. K.; Schmittel, M. Four-component supramolecular nanorotors. *J. Am. Chem. Soc.* **2013**, *135*, 18794−18797.
(1442) Zahn, S. Electron-Induced Inversion of Helical Chirality in Copper Complexes of *N*,*N*-Dialkylmethionines. *Science* **2000**, *288*, 1404−1407.
(1443) Canary, J. W.; Mortezaei, S.; Liang, J. Redox-reconfigurable tripodal coordination complexes: stereodynamic molecular switches. *Chem. Commun.* **2010**, *46*, 5850−5860.
(1444) Berova, N.; Nakanishi, K. o.; Woody, R. *Circular Dichroism: Principles and Applications*, 2nd ed.; Wiley-VCH: New York, 2000.
(1445) Mortezaei, S.; Catarineu, N. R.; Canary, J. W. A redox-reconfigurable, ambidextrous asymmetric catalyst. *J. Am. Chem. Soc.* **2012**, *134*, 8054−8057.

DOI: 10.1021/acs.chemrev.5b00146
Chem. Rev. 2015, 115, 10081−10206

(1446) Gartner, Z. J.; Kanan, M. W.; Liu, D. R. Multistep Small-Molecule Synthesis Programmed by DNA Templates. *J. Am. Chem. Soc.* **2002**, *124*, 10304−10306.
(1447) He, Y.; Liu, D. R. Autonomous multistep organic synthesis in a single isothermal solution mediated by a DNA walker. *Nat. Nanotechnol.* **2010**, *5*, 778−782.
(1448) He, Y.; Liu, D. R. A Sequential Strand-Displacement Strategy Enables Efficient Six-Step DNA-Templated Synthesis. *J. Am. Chem. Soc.* **2011**, *133*, 9972−9975.
(1449) McKee, M. L.; Milnes, P. J.; Bath, J.; Stulz, E.; O'Reilly, R. K.; Turberfield, A. J. Programmable One-Pot Multistep Organic Synthesis Using DNA Junctions. *J. Am. Chem. Soc.* **2012**, *134*, 1446−1449.
(1450) McKee, M. L.; Milnes, P. J.; Bath, J.; Stulz, E.; Turberfield, A. J.; O'Reilly, R. K. Multistep DNA-Templated Reactions for the Synthesis of Functional Sequence Controlled Oligomers. *Angew. Chem., Int. Ed.* **2010**, *49*, 7948−7951.
(1451) Gartner, Z. J.; Kanan, M. W.; Liu, D. R. Expanding the Reaction Scope of DNA-Templated Synthesis. *Angew. Chem., Int. Ed.* **2002**, *41*, 1796−1800.
(1452) Gartner, Z. J.; Liu, D. R. The Generality of DNA-Templated Synthesis as a Basis for Evolving Non-Natural Small Molecules. *J. Am. Chem. Soc.* **2001**, *123*, 6961−6963.
(1453) Li, X.; Gartner, Z. J.; Tse, B. N.; Liu, D. R. Translation of DNA into Synthetic N-Acyloxazolidines. *J. Am. Chem. Soc.* **2004**, *126*, 5090−5092.
(1454) Gartner, Z. J.; Grubina, R.; Calderone, C. T.; Liu, D. R. Two Enabling Architectures for DNA-Templated Organic Synthesis. *Angew. Chem., Int. Ed.* **2003**, *42*, 1370−1375.
(1455) Gu, H.; Chao, J.; Xiao, S. J.; Seeman, N. C. A proximity-based programmable DNA nanoscale assembly line. *Nature* **2010**, *465*, 202−205.
(1456) Thordarson, P.; Bijsterveld, E. J. A.; Rowan, A. E.; Nolte, R. J. M. Epoxidation of polybutadiene by a topologically linked catalyst. *Nature* **2003**, *424*, 915−918.
(1457) Elemans, J. A. A. W.; Bijsterveld, E. J. A.; Rowan, A. E.; Nolte, R. J. M. A host-guest epoxidation catalyst with enhanced activity and stability. *Chem. Commun.* **2000**, 2443−2444.
(1458) Monnereau, C.; Ramos, P. H.; Deutman, A. B. C.; Elemans, J. A. A. W.; Nolte, R. J. M.; Rowan, A. E. Porphyrin Macrocyclic Catalysts for the Processive Oxidation of Polymer Substrates. *J. Am. Chem. Soc.* **2010**, *132*, 1529−1531.
(1459) Deutman, A. B. C.; Monnereau, C.; Elemans, J. A. A. W.; Ercolani, G.; Nolte, R. J. M.; Rowan, A. E. Mechanism of Threading a Polymer Through a Macrocyclic Ring. *Science* **2008**, *322*, 1668−1671.
(1460) Takashima, Y.; Osaki, M.; Ishimaru, Y.; Yamaguchi, H.; Harada, A. Artificial Molecular Clamp: A Novel Device for Synthetic Polymerases. *Angew. Chem., Int. Ed.* **2011**, *50*, 7524−7528.
(1461) Dawson, P.; Muir, T.; Clark-Lewis, I.; Kent, S. Synthesis of proteins by native chemical ligation. *Science* **1994**, *266*, 776−779.
(1462) Hughs, M.; Jimenez, M.; Khan, S.; Garcia-Garibay, M. A. Synthesis, rotational dynamics, and photophysical characterization of a crystalline linearly conjugated phenyleneethynylene molecular dirotor. *J. Org. Chem.* **2013**, *78*, 5293−5302.
(1463) Garcia-Garibay, M. A. Crystalline molecular machines: encoding supramolecular dynamics into molecular structure. *Proc. Natl. Acad. Sci. U. S. A.* **2005**, *102*, 10771−10776.
(1464) Rodriguez-Molina, B.; Pozos, A.; Cruz, R.; Romero, M.; Flores, B.; Farfan, N.; Santillan, R.; Garcia-Garibay, M. A. Synthesis and solid state characterization of molecular rotors with steroidal stators: ethisterone and norethisterone. *Org. Biomol. Chem.* **2010**, *8*, 2993−3000.
(1465) Vogelsberg, C. S.; Garcia-Garibay, M. A. Crystalline molecular machines: function, phase order, dimensionality, and composition. *Chem. Soc. Rev.* **2012**, *41*, 1892−1910.
(1466) Rodriguez-Molina, B.; Perez-Estrada, S.; Garcia-Garibay, M. A. Amphidynamic crystals of a steroidal bicyclo[2.2.2]octane rotor: a high symmetry group that rotates faster than smaller methyl and methoxy groups. *J. Am. Chem. Soc.* **2013**, *135*, 10388−10395.
(1467) Staehle, I. O.; Rodríguez-Molina, B.; Khan, S. I.; Garcia-Garibay, M. A. Engineered Photochromism in Crystalline Salicylidene Anilines by Facilitating Rotation to Reach the Colored *trans*-Keto Form. *Cryst. Growth Des.* **2014**, *14*, 3667−3673.
(1468) Jiang, X.; Rodriguez-Molina, B.; Nazarian, N.; Garcia-Garibay, M. A. Rotation of a bulky triptycene in the solid state: toward engineered nanoscale artificial molecular machines. *J. Am. Chem. Soc.* **2014**, *136*, 8871−8874.
(1469) Commins, P.; Garcia-Garibay, M. A. Photochromic molecular gyroscope with solid state rotational states determined by an azobenzene bridge. *J. Org. Chem.* **2014**, *79*, 1611−1619.
(1470) Karlen, S. D.; Ortiz, R.; Chapman, O. L.; Garcia-Garibay, M. A. Effects of Rotational Symmetry Order on the Solid State Dynamics Phenylene and Diamantane Rotators. *J. Am. Chem. Soc.* **2005**, *127*, 6554−6555.
(1471) Comotti, A.; Bracco, S.; Valsesia, P.; Beretta, M.; Sozzani, P. Fast molecular rotor dynamics modulated by guest inclusion in a highly organized nanoporous organosilica. *Angew. Chem., Int. Ed.* **2010**, *49*, 1760−1764.
(1472) Vogelsberg, C. S.; Bracco, S.; Beretta, M.; Comotti, A.; Sozzani, P.; Garcia-Garibay, M. A. Dynamics of molecular rotors confined in two dimensions: transition from a 2D rotational glass to a 2D rotational fluid in a periodic mesoporous organosilica. *J. Phys. Chem. B* **2012**, *116*, 1623−1632.
(1473) Comotti, A.; Bracco, S.; Yamamoto, A.; Beretta, M.; Hirukawa, T.; Tohnai, N.; Miyata, M.; Sozzani, P. Engineering switchable rotors in molecular crystals with open porosity. *J. Am. Chem. Soc.* **2014**, *136*, 618−621.
(1474) Comotti, A.; Bracco, S.; Ben, T.; Qiu, S.; Sozzani, P. Molecular rotors in porous organic frameworks. *Angew. Chem., Int. Ed.* **2014**, *53*, 1043−1047.
(1475) Vukotic, V. N.; Kelong Zhu, K. J. H.; Schurko, R. W.; Loeb, S. J. Metal−organic frameworks with dynamic interlocked components. *Nat. Chem.* **2012**, *4*, 456−460.
(1476) Zhu, K.; O'Keefe, C. A.; Vukotic, V. N.; Schurko, R. W.; Loeb, S. J. A molecular shuttle that operates inside a metal-organic framework. *Nat. Chem.* **2015**, *7*, 514−519.
(1477) Ahuja, R. C.; Caruso, P. L.; Mobius, D.; Wildburg, G.; Ringsdorf, H.; Philp, D.; Preece, J. A.; Stoddart, J. F. Molecular-Organization Via Ionic Interactions at Interfaces 0.1. Monolayers and Lb Films of Cyclic Bisbipyridinium Tetracations and Dimyristoylphosphatidic Acid. *Langmuir* **1993**, *9*, 1534−1544.
(1478) Collier, C. P.; Mattersteig, G.; Wong, E. W.; Luo, Y.; Beverly, K.; Sampaio, J.; Raymo, F. M.; Stoddart, J. F.; Heath, J. R. A [2]catenane-based solid state electronically reconfigurable switch. *Science* **2000**, *289*, 1172−1175.
(1479) Pease, A. R.; Jeppesen, J. O.; Stoddart, J. F.; Luo, Y.; Collier, C. P.; Heath, J. R. Switching devices based on interlocked molecules. *Acc. Chem. Res.* **2001**, *34*, 433−444.
(1480) Heath, J. R.; Ratner, M. A. Molecular electronics. *Phys. Today* **2003**, *56*, 43−49.
(1481) Heath, J. R.; Stoddart, J. F.; Williams, R. S. More on molecular electronics. *Science* **2004**, *303*, 1136−1137.
(1482) Flood, A. H.; Ramirez, R.; Deng, W.; Muller, R.; Goddard, W. A., III; Stoddart, J. F. Meccano on the nanoscale - A blueprint for making some of the world's tiniest machines. *Aust. J. Chem.* **2004**, *57*, 301−322.
(1483) Mendes, P.; Flood, A. H.; Stoddart, J. F. Nanoelectronic devices from self-organized molecular switches. *Appl. Phys. A: Mater. Sci. Process.* **2005**, *80*, 1197−1209.
(1484) Beckman, R.; Beverly, K.; Boukai, A.; Bunimovich, Y.; Choi, J. W.; DeIonno, E.; Green, J.; Johnston-Halperin, E.; Luo, Y.; Sheriff, B.; Stoddart, J. F.; Heath, J. R. Spiers Memorial Lecture Molecular mechanics and molecular electronics. *Faraday Discuss.* **2006**, *131*, 9−22.
(1485) Coskun, A.; Spruell, J. M.; Barin, G.; Dichtel, W. R.; Flood, A. H.; Botros, Y. Y.; Stoddart, J. F. High hopes: can molecular electronics realise its potential? *Chem. Soc. Rev.* **2012**, *41*, 4827−4859.
(1486) Steuerman, D. W.; Tseng, H. R.; Peters, A. J.; Flood, A. H.; Jeppesen, J. O.; Nielsen, K. A.; Stoddart, J. F.; Heath, J. R. Molecular-

DOI: 10.1021/acs.chemrev.5b00146
Chem. Rev. 2015, 115, 10081−10206

mechanical switch-based solid-state electrochromic devices. *Angew. Chem., Int. Ed.* **2004**, *43*, 6486−6491.
(1487) Deng, W. Q.; Muller, R. P.; Goddard, W. A., III Mechanism of the Stoddart-Heath bistable rotaxane molecular switch. *J. Am. Chem. Soc.* **2004**, *126*, 13562−13563.
(1488) Norgaard, K.; Laursen, B.; Nygaard, S.; Kjaer, K.; Tseng, H.; Flood, A. H.; Stoddart, J. F.; Bjornholm, T. Structural evidence of mechanical shuttling in condensed monolayers of bistable rotaxane molecules. *Angew. Chem., Int. Ed.* **2005**, *44*, 7035−7039.
(1489) Dichtel, W.; Heath, J. R.; Stoddart, J. F. Designing bistable [2] rotaxanes for molecular electronic devices. *Philos. Trans. R. Soc., A* **2007**, *365*, 1607−1625.
(1490) Nygaard, S.; Leung, K. C. F.; Aprahamian, I.; Ikeda, T.; Saha, S.; Laursen, B. W.; Kim, S. Y.; Hansen, S. W.; Stein, P. C.; Flood, A. H.; Stoddart, J. F.; Jeppesen, J. O. Functionally rigid bistable [2]rotaxanes. *J. Am. Chem. Soc.* **2007**, *129*, 960−970.
(1491) Coskun, A.; Saha, S.; Aprahamian, I.; Stoddart, J. F. A reverse donor-acceptor bistable [2]Catenane. *Org. Lett.* **2008**, *10*, 3187−3190.
(1492) Dey, S. K.; Coskun, A.; Fahrenbach, A. C.; Barin, G.; Basuray, A. N.; Trabolsi, A.; Botros, Y. Y.; Stoddart, J. F. A redox-active reverse donor-acceptor bistable [2]rotaxane. *Chem. Sci.* **2011**, *2*, 1046−1053.
(1493) Wang, C.; Cao, D.; Fahrenbach, A. C.; Grunder, S.; Dey, S. K.; Sarjeant, A. A.; Stoddart, J. F. The effects of conformation on the noncovalent bonding interactions in a bistable donor-acceptor [3]-catenane. *Chem. Commun.* **2012**, *48*, 9245−9247.
(1494) Fahrenbach, A. C.; Bruns, C. J.; Li, H.; Trabolsi, A.; Coskun, A.; Stoddart, J. F. Ground-State Kinetics of Bistable Redox-Active Donor-Acceptor Mechanically Interlocked Molecules. *Acc. Chem. Res.* **2014**, *47*, 482−493.
(1495) Olson, M. A.; Braunschweig, A. B.; Fang, L.; Ikeda, T.; Klajn, R.; Trabolsi, A.; Wesson, P. J.; Benitez, D.; Mirkin, C. A.; Grzybowski, B. A.; et al. A Bistable Poly[2]catenane Forms Nanosuperstructures. *Angew. Chem., Int. Ed.* **2009**, *48*, 1792−1797.
(1496) Asakawa, M.; Higuchi, M.; Mattersteig, G.; Nakamura, T.; Pease, A. R.; Raymo, F. M.; Shimizu, T.; Stoddart, J. F. Current/Voltage Characteristics of Monolayers of Redox-Switchable [2]Catenanes on Gold. *Adv. Mater.* **2000**, *12*, 1099−1102.
(1497) Deng, W.-Q.; Flood, A. H.; Stoddart, J. F.; Goddard, W. A., III An Electrochemical Color-Switchable RGB Dye: Tristable [2]Catenane. *J. Am. Chem. Soc.* **2005**, *127*, 15994−15995.
(1498) Kim, Y.-H.; Jang, S.; Jang, Y.; Goddard, W. A., III First-Principles Study of the Switching Mechanism of [2]Catenane Molecular Electronic Devices. *Phys. Rev. Lett.* **2005**, *94*, 156801.
(1499) Ahuja, R. C.; Caruso, P.-L.; Moebius, D.; Philp, D.; Preece, J. A.; Ringsdorf, H.; Stoddart, J. F.; Wildburg, G. *Thin Solid Films* **1996**, *285*, 671−677.
(1500) Brown, C. L.; Jonas, U.; Preece, J. A.; Ringsdorf, H.; Seitz, M.; Stoddart, J. F. Introduction of [2]Catenanes into Langmuir Films and Langmuir−Blodgett Multilayers. A Possible Strategy for Molecular Information Storage Materials. *Langmuir* **2000**, *16*, 1924−1930.
(1501) Norgaard, K.; Jeppesen, J. O.; Laursen, B. W.; Simonsen, J. B.; Weygand, M. J.; Kjaer, K.; Stoddart, J. F.; Bjornholm, T. *J. Phys. Chem. B* **2005**, *109*, 1063−1066.
(1502) Heinrich, T.; Traulsen, C. H. H.; Holzweber, M.; Richter, S.; Kunz, V.; Kastner, S. K.; Krabbenborg, S. O.; Huskens, J.; Unger, W. E. S.; Schalley, C. A. Coupled Molecular Switching Processes in Ordered Mono- and Multilayers of Stimulus-Responsive Rotaxanes on Gold Surfaces. *J. Am. Chem. Soc.* **2015**, *137*, 4382−4390.
(1503) Pace, G.; Petitjean, A.; Lalloz-Vogel, M.-N.; Harrowfield, J.; Lehn, J.-M.; Samorì, P. Subnanometer-Resolved Patterning of Bicomponent Self-Assembled Monolayers on Au(111). *Angew. Chem., Int. Ed.* **2008**, *47*, 2484−2488.
(1504) Jang, S. S.; Jang, Y. H.; Kim, Y.-H.; Goddard, W. A., III; Flood, A. H.; Laursen, B. W.; Tseng, H.-R.; Stoddart, J. F.; Jeppesen, J. O.; Choik, J. W.; et al. Structures and Properties of Self-Assembled Monolayers of Bistable [2]Rotaxanes on Au (111) Surfaces from Molecular Dynamics Simulations Validated with Experiment. *J. Am. Chem. Soc.* **2005**, *127*, 1563−1575.
(1505) Jang, Y. H.; Jang, S. S.; Goddard, W. A., III Molecular Dynamics Simulation Study on a Monolayer of Half [2]Rotaxane Self-Assembled on Au(111). *J. Am. Chem. Soc.* **2005**, *127*, 4959−4964.
(1506) Richter, S.; Poppenberg, J.; Traulsen, C. H. H.; Darlatt, E.; Sokolowski, A.; Sattler, D.; Unger, W. E. S.; Schalley, C. A. Deposition of Ordered Layers of Tetralactam Macrocycles and Ether Rotaxanes on Pyridine-Terminated Self-Assembled Monolayers on Gold. *J. Am. Chem. Soc.* **2012**, *134*, 16289−16297.
(1507) Wong, E. W.; Collier, C. P.; Behloradsky, M.; Raymo, F. M.; Stoddart, J. F.; Heath, J. R. Fabrication and transport properties of single-molecule-thick electrochemical junctions. *J. Am. Chem. Soc.* **2000**, *122*, 5831−5840.
(1508) Collier, C. P.; Jeppesen, J. O.; Luo, Y.; Perkins, J.; Wong, E. W.; Heath, J. R.; Stoddart, J. F. Molecular-based electronically switchable tunnel junction devices. *J. Am. Chem. Soc.* **2001**, *123*, 12632−12641.
(1509) Lee, I. C.; Frank, C. W.; Yamamoto, T.; Tseng, H. R.; Flood, A. H.; Stoddart, J. F.; Jeppesen, J. O. Langmuir and Langmuir-Blodgett films of amphiphilic bistable rotaxanes. *Langmuir* **2004**, *20*, 5809−5828.
(1510) Jang, S. S.; Jang, Y. H.; Kim, Y. H.; Goddard, W. A., III; Choi, J. W.; Heath, J. R.; Laursen, B. W.; Flood, A. H.; Stoddart, J. F.; Norgaard, K.; et al. Molecular dynamics simulation of amphiphilic bistable [2]rotaxane Langmuir monolayers at the air/water interface. *J. Am. Chem. Soc.* **2005**, *127*, 14804−14816.
(1511) Mendes, P. M.; Lu, W.; Tseng, H. R.; Shinder, S.; Iijima, T.; Miyaji, M.; Knobler, C. M.; Stoddart, J. F. A soliton phenomenon in langmuir monolayers of amphiphilic bistable rotaxanes. *J. Phys. Chem. B* **2006**, *110*, 3845−3848.
(1512) Ferri, V.; Elbing, M.; Pace, G.; Dickey, M. D.; Zharnikov, M.; Samori, P.; Mayor, M.; Rampi, M. A. Light-powered electrical switch based on cargo-lifting azobenzene monolayers. *Angew. Chem., Int. Ed.* **2008**, *47*, 3407−3409.
(1513) Green, J. E.; Choi, J. W.; Boukai, A.; Bunimovich, Y.; Johnston-Halperin, E.; DeIonno, E.; Luo, Y.; Sheriff, B. A.; Xu, K.; Shin, Y. S.; Tseng, H. R.; Stoddart, J. F.; Heath, J. R. A 160-kilobit molecular electronic memory patterned at 10(11) bits per square centimetre. *Nature* **2007**, *445*, 414−417.
(1514) Yu, H.; Luo, Y.; Beverly, K.; Stoddart, J. F.; Tseng, H. R.; Heath, J. R. The molecule-electrode interface in single-molecule transistors. *Angew. Chem., Int. Ed.* **2003**, *42*, 5706−5711.
(1515) Lau, C. N.; Stewart, D. R.; Williams, R. S.; Bockrath, M. Direct Observation of Nanoscale Switching Centers in Metal/Molecule/Metal Structures. *Nano Lett.* **2004**, *4*, 569−572.
(1516) Avellini, T.; Li, H.; Coskun, A.; Barin, G.; Trabolsi, A.; Basuray, A. N.; Dey, S. K.; Credi, A.; Silvi, S.; Stoddart, J. F.; Venturi, M. Photoinduced Memory Effect in a Redox Controllable Bistable Mechanical Molecular Switch. *Angew. Chem., Int. Ed.* **2012**, *51*, 1611−1615.
(1517) Ichimura, K. Photoalignment of Liquid-Crystal Systems. *Chem. Rev.* **2000**, *100*, 1847−1873.
(1518) Hoogboom, J.; Rasing, T.; Rowan, A. E.; Nolte, R. J. M. LCD alignment layers. Controlling nematic domain properties. *J. Mater. Chem.* **2006**, *16*, 1305−1314.
(1519) Yu, Y.; Ikeda, T. Soft Actuators Based on Liquid-Crystalline Elastomers. *Angew. Chem., Int. Ed.* **2006**, *45*, 5416−5418.
(1520) Geelhaar, T.; Griesar, K.; Reckmann, B. 125Years of Liquid CrystalsA Scientific Revolution in the Home. *Angew. Chem., Int. Ed.* **2013**, *52*, 8798−8809.
(1521) Feringa, B. L.; Huck, N. P. M.; van Doren, H. A. Chiroptical Switching between Liquid Crystalline Phases. *J. Am. Chem. Soc.* **1995**, *117*, 9929−9930.
(1522) Huck, N. P. M.; Jager, W. F.; de Lange, B.; Feringa, B. L. Dynamic Control and Amplification of Molecular Chirality by Circular Polarized Light. *Science* **1996**, *273*, 1686−1688.
(1523) Sagisaka, T.; Yokoyama, Y. Reversible Control of the Pitch of Cholesteric Liquid Crystals by Photochromism of Chiral Fulgide Derivatives. *Bull. Chem. Soc. Jpn.* **2000**, *73*, 191−196.
(1524) Palffy-Muhoray, P.; Kosa, T.; Weinan, E. Dynamics of a Light Driven Molecular Motor. *Mol. Cryst. Liq. Cryst.* **2002**, *375*, 577−591.

DOI: 10.1021/acs.chemrev.5b00146
Chem. Rev. 2015, 115, 10081−10206

(1525) van Delden, R. A.; Mecca, T.; Rosini, C.; Feringa, B. L. A chiroptical molecular switch with distinct chiral and photochromic entities and its application in optical switching of a cholesteric liquid crystal. *Chem. - Eur. J.* **2004**, *10*, 61−70.
(1526) Kosa, T.; Palffy-Muhoray, P. Brownian motors in the photoalignment of liquid crystals. *Int. J. Eng. Sci.* **2000**, *38*, 1077−1084.
(1527) Palffy-Muhoray, P.; Kosa, T.; E, W. Brownian motors in the photoalignment of liquid crystals. *Appl. Phys. A: Mater. Sci. Process.* **2002**, *75*, 293−300.
(1528) van Delden, R. A.; Koumura, N.; Harada, N.; Feringa, B. L. Unidirectional rotary motion in a liquid crystalline environment: color tuning by a molecular motor. *Proc. Natl. Acad. Sci. U. S. A.* **2002**, *99*, 4945−4949.
(1529) van Delden, R. A.; van Gelder, M. B.; Huck, N. P. M.; Feringa, B. L. Controlling the Color of Cholesteric Liquid-Crystalline Films by Photoirradiation of a Chiroptical Molecular Switch Used as Dopant. *Adv. Funct. Mater.* **2003**, *13*, 319−324.
(1530) Setaka, W.; Yamaguchi, K. Thermal modulation of birefringence observed in a crystalline molecular gyrotop. *Proc. Natl. Acad. Sci. U. S. A.* **2012**, *109*, 9271−9275.
(1531) Setaka, W.; Yamaguchi, K. A Molecular Balloon: Expansion of a Molecular Gyrotop Cage Due to Rotation of the Phenylene Rotor. *J. Am. Chem. Soc.* **2012**, *134*, 12458−12461.
(1532) Setaka, W.; Higa, S.; Yamaguchi, K. Ring-closing metathesis for the synthesis of a molecular gyrotop. *Org. Biomol. Chem.* **2014**, *12*, 3354−3357.
(1533) Suzaki, Y.; Taira, T.; Osakada, K.; Horie, M. Rotaxanes and pseudorotaxanes with Fe-, Pd- and Pt-containing axles. Molecular motion in the solid state and aggregation in solution. *Dalton Trans.* **2008**, 4823−4833.
(1534) Horie, M.; Suzaki, Y.; Hashizume, D.; Abe, T.; Wu, T.; Sassa, T.; Hosokai, T.; Osakada, K. Thermally-induced phase transition of pseudorotaxane crystals: changes in conformation and interaction of the molecules and optical properties of the crystals. *J. Am. Chem. Soc.* **2012**, *134*, 17932−17944.
(1535) Horie, M.; Sassa, T.; Hashizume, D.; Suzaki, Y.; Osakada, K.; Wada, T. A Crystalline Supramolecular Switch: Controlling the Optical Anisotropy through the Collective Dynamic Motion of Molecules. *Angew. Chem., Int. Ed.* **2007**, *46*, 4983−4986.
(1536) Leigh, D. A.; Morales, M. A.; Perez, E. M.; Wong, J. K.; Saiz, C. G.; Slawin, A. M.; Carmichael, A. J.; Haddleton, D. M.; Brouwer, A. M.; Buma, W. J.; Wurpel, G. W.; Leon, S.; Zerbetto, F. Patterning through controlled submolecular motion: rotaxane-based switches and logic gates that function in solution and polymer films. *Angew. Chem., Int. Ed.* **2005**, *44*, 3062−3067.
(1537) Yasushi Okumura, K. I. The Polyrotaxane Gel: A Topological Gel by Figure-of-Eight Cross-links. *Adv. Mater.* **2001**, *13*, 485−487.
(1538) Ito, K. Novel Cross-Linking Concept of Polymer Network: Synthesis, Structure, and Properties of Slide-Ring Gels with Freely Movable Junctions. *Polym. J.* **2007**, *39*, 489−499.
(1539) Ma, X.; Wang, Q.; Qu, D.; Xu, Y.; Ji, F.; Tian, H. A light-driven pseudo[4]rotaxane encoded by induced circular dichroism in a hydrogel. *Adv. Funct. Mater.* **2007**, *17*, 829−837.
(1540) Taira, T.; Suzaki, Y.; Osakada, K. Thermosensitive hydrogels composed of cyclodextrin pseudorotaxanes. Role of [3]pseudorotaxane in the gel formation. *Chem. Commun.* **2009**, 7027−7029.
(1541) Suzaki, Y.; Taira, T.; Osakada, K. Physical gels based on supramolecular gelators, including host-guest complexes and pseudorotaxanes. *J. Mater. Chem.* **2011**, *21*, 930−938.
(1542) Zhu, L.; Ma, X.; Ji, F.; Wang, Q.; Tian, H. Effective enhancement of fluorescence signals in rotaxane-doped reversible hydrosol-gel systems. *Chem. - Eur. J.* **2007**, *13*, 9216−9222.
(1543) Madden, J. D. W.; Vandesteeg, N. A.; Anquetil, P. A.; Madden, P. G. A.; Takshi, A.; Pytel, R. Z.; Lafontaine, S. R.; Wieringa, P. A.; Hunter, I. W. Artificial muscle technology: physical principles and naval prospects. *IEEE J. Oceanic Eng.* **2004**, *29*, 706−728.
(1544) Baughman, R. H. Playing Nature's Game with Artificial Muscles. *Science* **2005**, *308*, 63−65.
(1545) Frank, S.; Lauterbur, P. C. Voltage-sensitive magnetic gels as magnetic resonance monitoring agents. *Nature* **1993**, *363*, 334−336.
(1546) Osada, Y.; Gong, J. Stimuli-responsive polymer gels and their application to chemomechanical systems. *Prog. Polym. Sci.* **1993**, *18*, 187−226.
(1547) Osada, Y.; Gong, J.-P. Soft and Wet Materials: Polymer Gels. *Adv. Mater.* **1998**, *10*, 827−837.
(1548) Berndt, I.; Popescu, C.; Wortmann, F.-J.; Richtering, W. Mechanics versus Thermodynamics: Swelling in Multiple-Temperature-Sensitive Core−Shell Microgels. *Angew. Chem., Int. Ed.* **2006**, *45*, 1081−1085.
(1549) Juodkazis, S.; Mukai, N.; Wakaki, R.; Yamaguchi, A.; Matsuo, S.; Misawa, H. Reversible phase transitions in polymer gels induced by radiation forces. *Nature* **2000**, *408*, 178−181.
(1550) Yoshida, R.; Takahashi, T.; Yamaguchi, T.; Ichijo, H. Self-Oscillating Gel. *J. Am. Chem. Soc.* **1996**, *118*, 5134−5135.
(1551) Berndt, I.; Pedersen, J. S.; Richtering, W. Temperature-Sensitive Core−Shell Microgel Particles with Dense Shell. *Angew. Chem., Int. Ed.* **2006**, *45*, 1737−1741.
(1552) Kiyonaka, S.; Sugiyasu, K.; Shinkai, S.; Hamachi, I. First Thermally Responsive Supramolecular Polymer Based on Glycosylated Amino Acid. *J. Am. Chem. Soc.* **2002**, *124*, 10954−10955.
(1553) You, J.-O.; Almeda, D.; Ye, G.; Auguste, D. Bioresponsive matrices in drug delivery. *J. Biol. Eng.* **2010**, *4*, 15.
(1554) Chaterji, S.; Kwon, I. K.; Park, K. Smart polymeric gels: Redefining the limits of biomedical devices. *Prog. Polym. Sci.* **2007**, *32*, 1083−1122.
(1555) Schild, H. G. Poly(*N*-isopropylacrylamide): experiment, theory and application. *Prog. Polym. Sci.* **1992**, *17*, 163−249.
(1556) Shahinpoor, M.; Bar-Cohen, Y.; Simpson, J. O.; Smith, J. Ionic polymer-metal composites (IPMCs) as biomimetic sensors, actuators and artificial muscles - a review. *Smart Mater. Struct.* **1998**, *7*, R15−R30.
(1557) Urry, D. W. Physical Chemistry of Biological Free Energy Transduction As Demonstrated by Elastic Protein-Based Polymers. *J. Phys. Chem. B* **1997**, *101*, 11007−11028.
(1558) Urry, D. W. Five axioms for the functional design of peptide-based polymers as molecular machines and materials: Principle for macromolecular assemblies. *Biopolymers* **1998**, *47*, 167−178.
(1559) Steinberg, I. Z.; Oplatka, A.; Katchalsky, A. Mechanochemical Engines. *Nature* **1966**, *210*, 568−571.
(1560) Sussman, M. V.; Katchalsky, A. Mechanochemical Turbine: A New Power Cycle. *Science* **1970**, *167*, 45−47.
(1561) Yoshida, R.; Kokufuta, E.; Yamaguchi, T. Beating polymer gels coupled with a nonlinear chemical reaction. *Chaos* **1999**, *9*, 260−266.
(1562) Yoshida, R.; Otoshi, G.; Yamaguchi, T.; Kokufuta, E. Traveling Chemical Waves for Measuring Solute Diffusivity in Thermosensitive Poly(N-isopropylacrylamide) Gel. *J. Phys. Chem. A* **2001**, *105*, 3667−3672.
(1563) Yoshida, R.; Takei, K.; Yamaguchi, T. Self-Beating Motion of Gels and Modulation of Oscillation Rhythm Synchronized with Organic Acid. *Macromolecules* **2003**, *36*, 1759−1761.
(1564) Crook, C. J.; Smith, A.; Jones, R. A. L.; Ryan, A. J. Chemically induced oscillations in a pH-responsive hydrogel. *Phys. Chem. Chem. Phys.* **2002**, *4*, 1367−1369.
(1565) Howse, J. R.; Topham, P.; Crook, C. J.; Gleeson, A. J.; Bras, W.; Jones, R. A. L.; Ryan, A. J. Reciprocating Power Generation in a Chemically Driven Synthetic Muscle. *Nano Lett.* **2006**, *6*, 73−77.
(1566) Jones, C. D.; Lyon, L. A. Synthesis and Characterization of Multiresponsive Core−Shell Microgels. *Macromolecules* **2000**, *33*, 8301−8306.
(1567) Berndt, I.; Richtering, W. Doubly Temperature Sensitive Core−Shell Microgels. *Macromolecules* **2003**, *36*, 8780−8785.
(1568) Beebe, D. J.; Moore, J. S.; Bauer, J. M.; Yu, Q.; Liu, R. H.; Devadoss, C.; Jo, B.-H. Functional hydrogel structures for autonomous flow control inside microfluidic channels. *Nature* **2000**, *404*, 588−590.
(1569) Yu, Q.; Bauer, J. M.; Moore, J. S.; Beebe, D. J. Responsive biomimetic hydrogel valve for microfluidics. *Appl. Phys. Lett.* **2001**, *78*, 2589−2591.

DOI: 10.1021/acs.chemrev.5b00146
Chem. Rev. 2015, 115, 10081−10206

(1570) Liu, R. H.; Yu, Q.; Beebe, D. J. Fabrication and characterization of hydrogel-based microvalves. *J. Microelectromech. Syst.* **2002**, *11*, 45−53.
(1571) Osada, Y.; Okuzaki, H.; Hori, H. A polymer gel with electrically driven motility. *Nature* **1992**, *355*, 242−244.
(1572) Galaev, I. Y.; Mattiasson, B. 'Smart' polymers and what they could do in biotechnology and medicine. *Trends Biotechnol.* **1999**, *17*, 335−340.
(1573) Peppas, N. A.; Huang, Y.; Torres-Lugo, M.; Ward, J. H.; Zhang, J. Physicochemical Foundations and Structural Design of Hydrogels in Medicine and Biology. *Annu. Rev. Biomed. Eng.* **2000**, *2*, 9−29.
(1574) Qiu, Y.; Park, K. Environment-sensitive hydrogels for drug delivery. *Adv. Drug Delivery Rev.* **2001**, *53*, 321−339.
(1575) Jeong, B.; Gutowska, A. Lessons from nature: stimuli-responsive polymers and their biomedical applications. *Trends Biotechnol.* **2002**, *20*, 305−311.
(1576) Kopecek, J. Polymer chemistry: Swell gels. *Nature* **2002**, *417*, 388−391.
(1577) Langer, R.; Tirrell, D. A. Designing materials for biology and medicine. *Nature* **2004**, *428*, 487−492.
(1578) Lin, K.-J.; Fu, S.-J.; Cheng, C.-Y.; Chen, W.-H.; Kao, H.-M. Towards Electrochemical Artificial Muscles: A Supramolecular Machine Based on a One-Dimensional Copper-Containing Organophosphonate System. *Angew. Chem., Int. Ed.* **2004**, *43*, 4186−4189.
(1579) Li, C.; Madsen, J.; Armes, S. P.; Lewis, A. L. A New Class of Biochemically Degradable, Stimulus-Responsive Triblock Copolymer Gelators. *Angew. Chem., Int. Ed.* **2006**, *45*, 3510−3513.
(1580) Samoei, G. K.; Wang, W.; Escobedo, J. O.; Xu, X.; Schneider, H.-J.; Cook, R. L.; Strongin, R. M. A Chemomechanical Polymer that Functions in Blood Plasma with High Glucose Selectivity. *Angew. Chem., Int. Ed.* **2006**, *45*, 5319−5322.
(1581) Dong, L.; Agarwal, A. K.; Beebe, D. J.; Jiang, H. Adaptive liquid microlenses activated by stimuli-responsive hydrogels. *Nature* **2006**, *442*, 551−554.
(1582) Oya, T.; Enoki, T.; Grosberg, A. Y.; Masamune, S.; Sakiyama, T.; Takeoka, Y.; Tanaka, K.; Wang, G.; Yilmaz, Y.; Feld, M. S.; Dasari, R.; Tanaka, T. Reversible Molecular Adsorption Based on Multiple-Point Interaction by Shrinkable Gels. *Science* **1999**, *286*, 1543−1545.
(1583) Pennadam, S. S.; Lavigne, M. D.; Dutta, C. F.; Firman, K.; Mernagh, D.; Górecki, D. C.; Alexander, C. Control of A Multisubunit DNA Motor by a Thermoresponsive Polymer Switch. *J. Am. Chem. Soc.* **2004**, *126*, 13208−13209.
(1584) Kokufata, E.; Zhang, Y.-Q.; Tanaka, T. Saccharide-sensitive phase transition of a lectin-loaded gel. *Nature* **1991**, *351*, 302−304.
(1585) Irie, M.; Misumi, Y.; Tanaka, T. Stimuli-responsive polymers: chemical induced reversible phase separation of an aqueous solution of poly(N-isopropylacrylamide) with pendent crown ether groups. *Polymer* **1993**, *34*, 4531−4535.
(1586) Lee, K.; Asher, S. A. Photonic Crystal Chemical Sensors: pH and Ionic Strength. *J. Am. Chem. Soc.* **2000**, *122*, 9534−9537.
(1587) Miyata, T.; Asami, N.; Uragami, T. A reversibly antigen-responsive hydrogel. *Nature* **1999**, *399*, 766−769.
(1588) Schneider, H.-J.; Tianjun, L.; Lomadze, N. Molecular Recognition in a Supramolecular Polymer System Translated into Mechanical Motion. *Angew. Chem., Int. Ed.* **2003**, *42*, 3544−3546.
(1589) Sharma, A. C.; Jana, T.; Kesavamoorthy, R.; Shi, L.; Virji, M. A.; Finegold, D. N.; Asher, S. A. A General Photonic Crystal Sensing Motif: Creatinine in Bodily Fluids. *J. Am. Chem. Soc.* **2004**, *126*, 2971−2977.
(1590) Goponenko, A. V.; Asher, S. A. Modeling of Stimulated Hydrogel Volume Changes in Photonic Crystal Pb^{2+} Sensing Materials. *J. Am. Chem. Soc.* **2005**, *127*, 10753−10759.
(1591) Holtz, J. H.; Asher, S. A. Polymerized colloidal crystal hydrogel films as intelligent chemical sensing materials. *Nature* **1997**, *389*, 829−832.
(1592) Holtz, J. H.; Holtz, J. S. W.; Munro, C. H.; Asher, S. A. Intelligent Polymerized Crystalline Colloidal Arrays: Novel Chemical Sensor Materials. *Anal. Chem.* **1998**, *70*, 780−791.
(1593) Asher, S. A.; Alexeev, V. L.; Goponenko, A. V.; Sharma, A. C.; Lednev, I. K.; Wilcox, C. S.; Finegold, D. N. Photonic Crystal Carbohydrate Sensors: Low Ionic Strength Sugar Sensing. *J. Am. Chem. Soc.* **2003**, *125*, 3322−3329.
(1594) Alexeev, V. L.; Sharma, A. C.; Goponenko, A. V.; Das, S.; Lednev, I. K.; Wilcox, C. S.; Finegold, D. N.; Asher, S. A. High Ionic Strength Glucose-Sensing Photonic Crystal. *Anal. Chem.* **2003**, *75*, 2316−2323.
(1595) Asher, S. A.; Sharma, A. C.; Goponenko, A. V.; Ward, M. M. Photonic Crystal Aqueous Metal Cation Sensing Materials. *Anal. Chem.* **2003**, *75*, 1676−1683.
(1596) Schneider, H.-J.; Liu, T. Large macroscopic size changes in chemomechanical polymers with binding sites for metal ions. *Chem. Commun.* **2004**, 100−101.
(1597) Schneider, H.-J.; Tianjun, L.; Lomadze, N. Sensitivity increase in molecular recognition by decrease of the sensing particle size and by increase of the receptor binding site - a case with chemomechanical polymers. *Chem. Commun.* **2004**, 2436−2437.
(1598) Schneider, H. J.; Tianjun, L.; Lomadze, N.; Palm, B. Cooperativity in a Chemomechanical Polymer: A Chemically Induced Macroscopic Logic Gate. *Adv. Mater.* **2004**, *16*, 613−615.
(1599) Wei, Z. G.; Sandstroröm, R.; Miyazaki, S. Shape-memory materials and hybrid composites for smart systems: Part I Shape-memory materials. *J. Mater. Sci.* **1998**, *33*, 3743−3762.
(1600) Lendlein, A.; Kelch, S. Shape-Memory Polymers. *Angew. Chem., Int. Ed.* **2002**, *41*, 2034−2057.
(1601) Scott, T. F.; Schneider, A. D.; Cook, W. D.; Bowman, C. N. Photoinduced Plasticity in Cross-Linked Polymers. *Science* **2005**, *308*, 1615−1617.
(1602) Lendlein, A.; Jiang, H.; Junger, O.; Langer, R. Light-induced shape-memory polymers. *Nature* **2005**, *434*, 879−882.
(1603) Baughman, R. H.; Cui, C.; Zakhidov, A. A.; Iqbal, Z.; Barisci, J. N.; Spinks, G. M.; Wallace, G. G.; Mazzoldi, A.; De Rossi, D.; Rinzler, A. G.; Jaschinski, O.; Roth, S.; Kertesz, M. Carbon Nanotube Actuators. *Science* **1999**, *284*, 1340−1344.
(1604) Raguse, B.; Müller, K. H.; Wieczorek, L. Nanoparticle Actuators. *Adv. Mater.* **2003**, *15*, 922−926.
(1605) Herrmann, L. O.; Valev, V. K.; Tserkezis, C.; Barnard, J. S.; Kasera, S.; Scherman, O. A.; Aizpurua, J.; Baumberg, J. J. Threading plasmonic nanoparticle strings with light. *Nat. Commun.* **2014**, *5*, 4568.
(1606) Jager, E. W. H.; Smela, E.; Inganäs, O. Microfabricating Conjugated Polymer Actuators. *Science* **2000**, *290*, 1540−1545.
(1607) Smela, E. Conjugated Polymer Actuators for Biomedical Applications. *Adv. Mater.* **2003**, *15*, 481−494.
(1608) Baughman, R. H. Conducting polymer artificial muscles. *Synth. Met.* **1996**, *78*, 339−353.
(1609) Otero, T. F.; Sansieña, J. M. Soft and Wet Conducting Polymers for Artificial Muscles. *Adv. Mater.* **1998**, *10*, 491−494.
(1610) Sansinena, J.; Olazabal, V.; Otero, T.; Sansinena, J.; Polo da Fonseca, C.; De Paoli, M.-A. A solid state artificial muscle based on polypyrrole and a solid polymeric electrolyte working in air. *Chem. Commun.* **1997**, 2217−2218.
(1611) Madden, J. D.; Cush, R. A.; Kanigan, T. S.; Brenan, C. J.; Hunter, I. W. Encapsulated polypyrrole actuators. *Synth. Met.* **1999**, *105*, 61−64.
(1612) Lu, W.; Fadeev, A. G.; Qi, B.; Smela, E.; Mattes, B. R.; Ding, J.; Spinks, G. M.; Mazurkiewicz, J.; Zhou, D.; Wallace, G. G.; MacFarlane, D. R.; Forsyth, S. A.; Forsyth, M. Use of Ionic Liquids for π-Conjugated Polymer Electrochemical Devices. *Science* **2002**, *297*, 983−987.
(1613) Yu, H.-h.; Xu, B.; Swager, T. M. A Proton-Doped Calix[4]-arene-Based Conducting Polymer. *J. Am. Chem. Soc.* **2003**, *125*, 1142−1143.
(1614) Scherlis, D. A.; Marzari, N. π-Stacking in Thiophene Oligomers as the Driving Force for Electroactive Materials and Devices. *J. Am. Chem. Soc.* **2005**, *127*, 3207−3212.
(1615) Hugel, T.; Holland, N. B.; Cattani, A.; Moroder, L.; Seitz, M.; Gaub, H. E. Single-Molecule Optomechanical Cycle. *Science* **2002**, *296*, 1103−1106.
(1616) Kumar, G. S.; Neckers, D. C. Photochemistry of azobenzene-containing polymers. *Chem. Rev.* **1989**, *89*, 1915−1925.

DOI: 10.1021/acs.chemrev.5b00146
Chem. Rev. 2015, 115, 10081−10206

(1617) Natansohn, A.; Rochon, P. Photoinduced Motions in Azo-Containing Polymers. *Chem. Rev.* **2002**, *102*, 4139−4176.
(1618) Maxein, G.; Zentel, R. Photochemical Inversion of the Helical Twist Sense in Chiral Polyisocyanates. *Macromolecules* **1995**, *28*, 8438−8440.
(1619) Okamoto, Y.; Nakano, T. Asymmetric Polymerization. *Chem. Rev.* **1994**, *94*, 349−372.
(1620) Nakano, T.; Okamoto, Y. Synthetic Helical Polymers: Conformation and Function. *Chem. Rev.* **2001**, *101*, 4013−4038.
(1621) Dumont, M.; El Osman, A. On spontaneous and photoinduced orientational mobility of dye molecules in polymers. *Chem. Phys.* **1999**, *245*, 437−462.
(1622) Delaire, J. A.; Nakatani, K. Linear and Nonlinear Optical Properties of Photochromic Molecules and Materials. *Chem. Rev.* **2000**, *100*, 1817−1846.
(1623) Kim, D. Y.; Tripathy, S. K.; Li, L.; Kumar, J. Laser-induced holographic surface relief gratings on nonlinear optical polymer films. *Appl. Phys. Lett.* **1995**, *66*, 1166−1168.
(1624) Viswanathan, N.; Yu Kim, D.; Bian, S.; Williams, J.; Liu, W.; Li, L.; Samuelson, L.; Kumar, J.; K. Tripathy, S. Surface relief structures on azo polymer films. *J. Mater. Chem.* **1999**, *9*, 1941−1955.
(1625) Yager, K. G.; Barrett, C. J. All-optical patterning of azo polymer films. *Curr. Opin. Solid State Mater. Sci.* **2001**, *5*, 487−494.
(1626) Tanchak, O. M.; Barrett, C. J. Light-Induced Reversible Volume Changes in Thin Films of Azo Polymers: The Photomechanical Effect. *Macromolecules* **2005**, *38*, 10566−10570.
(1627) Labarthet, F. L.; Bruneel, J.-L.; Buffeteau, T.; Sourisseau, C.; Huber, M. R.; Zilker, S. J.; Bieringer, T. Photoinduced orientations of azobenzene chromophores in two distinct holographic diffraction gratings as studied by polarized Raman confocal microspectrometry. *Phys. Chem. Chem. Phys.* **2000**, *2*, 5154−5167.
(1628) Schulz, B. M.; Huber, M. R.; Bieringer, T.; Krausch, G.; Zilker, S. J. Length-scale dependence of surface relief gratings in azobenzene side-chain polymers. *Synth. Met.* **2001**, *124*, 155−157.
(1629) Xie, P.; Zhang, R. Liquid crystal elastomers, networks and gels: advanced smart materials. *J. Mater. Chem.* **2005**, *15*, 2529−2550.
(1630) Li, M. H.; Keller, P.; Li, B.; Wang, X.; Brunet, M. Light-Driven Side-On Nematic Elastomer Actuators. *Adv. Mater.* **2003**, *15*, 569−572.
(1631) Buguin, A.; Li, M.-H.; Silberzan, P.; Ladoux, B.; Keller, P. Micro-Actuators: When Artificial Muscles Made of Nematic Liquid Crystal Elastomers Meet Soft Lithography. *J. Am. Chem. Soc.* **2006**, *128*, 1088−1089.
(1632) Finkelmann, H.; Nishikawa, E.; Pereira, G. G.; Warner, M. A New Opto-Mechanical Effect in Solids. *Phys. Rev. Lett.* **2001**, *87*, 015501.
(1633) Hogan, P. M.; Tajbakhsh, A. R.; Terentjev, E. M. UV manipulation of order and macroscopic shape in nematic elastomers. *Phys. Rev. E: Stat. Phys., Plasmas, Fluids, Relat. Interdiscip. Top.* **2002**, *65*, 041720.
(1634) Ikeda, T.; Nakano, M.; Yu, Y.; Tsutsumi, O.; Kanazawa, A. Anisotropic Bending and Unbending Behavior of Azobenzene Liquid-Crystalline Gels by Light Exposure. *Adv. Mater.* **2003**, *15*, 201−205.
(1635) Camacho-Lopez, M.; Finkelmann, H.; Palffy-Muhoray, P.; Shelley, M. Fast liquid-crystal elastomer swims into the dark. *Nat. Mater.* **2004**, *3*, 307−310.
(1636) Iamsaard, S.; Aßhoff, S. J.; Matt, B.; Kudernac, T.; Cornelissen Jeroen, J. L. M.; Fletcher, S. P.; Katsonis, N. Conversion of light into macroscopic helical motion. *Nat. Chem.* **2014**, *6*, 229−235.
(1637) Eelkema, R.; Pollard, M. M.; Vicario, J.; Katsonis, N.; Ramon, B. S.; Bastiaansen, C. W. M.; Broer, D. J.; Feringa, B. L. Molecular machines: Nanomotor rotates microscale objects. *Nature* **2006**, *440*, 163−163.
(1638) Chen, J.; Kistemaker, J. C.; Robertus, J.; Feringa, B. L. Molecular stirrers in action. *J. Am. Chem. Soc.* **2014**, *136*, 14924−14932.
(1639) Fritz, J.; Baller, M. K.; Lang, H. P.; Rothuizen, H.; Vettiger, P.; Meyer, E.-J.; Güntherodt, H.; Gerber, C.; Gimzewski, J. K. Translating Biomolecular Recognition into Nanomechanics. *Science* **2000**, *288*, 316−318.
(1640) Wu, G.; Ji, H.; Hansen, K.; Thundat, T.; Datar, R.; Cote, R.; Hagan, M. F.; Chakraborty, A. K.; Majumdar, A. Origin of nano-mechanical cantilever motion generated from biomolecular interactions. *Proc. Natl. Acad. Sci. U. S. A.* **2001**, *98*, 1560−1564.
(1641) Dhayal, B.; Henne, W. A.; Doorneweerd, D. D.; Reifenberger, R. G.; Low, P. S. Detection of Bacillus subtilis Spores Using Peptide-Functionalized Cantilever Arrays. *J. Am. Chem. Soc.* **2006**, *128*, 3716−3721.
(1642) Wu, G.; Datar, R. H.; Hansen, K. M.; Thundat, T.; Cote, R. J.; Majumdar, A. Bioassay of prostate-specific antigen (PSA) using microcantilevers. *Nat. Biotechnol.* **2001**, *19*, 856−860.
(1643) McKendry, R.; Zhang, J.; Arntz, Y.; Strunz, T.; Hegner, M.; Lang, H. P.; Baller, M. K.; Certa, U.; Meyer, E.; Güntherodt, H.-J.; et al. Multiple label-free biodetection and quantitative DNA-binding assays on a nanomechanical cantilever array. *Proc. Natl. Acad. Sci. U. S. A.* **2002**, *99*, 9783−9788.
(1644) Shu, W.; Liu, D.; Watari, M.; Riener, C. K.; Strunz, T.; Welland, M. E.; Balasubramanian, S.; McKendry, R. A. DNA Molecular Motor Driven Micromechanical Cantilever Arrays. *J. Am. Chem. Soc.* **2005**, *127*, 17054−17060.
(1645) Su, M.; Dravid, V. P. Surface Combustion Microengines Based on Photocatalytic Oxidations of Hydrocarbons at Room Temperature. *Nano Lett.* **2005**, *5*, 2023−2028.
(1646) Ji, H.-F.; Feng, Y.; Xu, X.; Purushotham, V.; Thundat, T.; Brown, G. M. Photon-driven nanomechanical cyclic motion. *Chem. Commun.* **2004**, 2532−2533.
(1647) Li, Q.; Fuks, G.; Moulin, E.; Maaloum, M.; Rawiso, M.; Kulic, I.; Foy, J. T.; Giuseppone, N. Macroscopic contraction of a gel induced by the integrated motion of light-driven molecular motors. *Nat. Nanotechnol.* **2015**, *10*, 161−165.
(1648) Coleman, A. C.; Beierle, J. M.; Stuart, M. C.; Macia, B.; Caroli, G.; Mika, J. T.; van Dijken, D. J.; Chen, J.; Browne, W. R.; Feringa, B. L. Light-induced disassembly of self-assembled vesicle-capped nanotubes observed in real time. *Nat. Nanotechnol.* **2011**, *6*, 547−552.
(1649) Milner, S. T. Polymer Brushes. *Science* **1991**, *251*, 905−914.
(1650) Tsukruk, V. V. Assembly of supramolecular polymers in ultrathin films. *Prog. Polym. Sci.* **1997**, *22*, 247−311.
(1651) Nath, N.; Chilkoti, A. Creating "Smart" Surfaces Using Stimuli Responsive Polymers. *Adv. Mater.* **2002**, *14*, 1243−1247.
(1652) Cole, M. A.; Voelcker, N. H.; Thissen, H.; Griesser, H. J. Stimuli-responsive interfaces and systems for the control of protein−surface and cell−surface interactions. *Biomaterials* **2009**, *30*, 1827−1850.
(1653) Xia, F.; Zhu, Y.; Feng, L.; Jiang, L. Smart responsive surfaces switching reversibly between super-hydrophobicity and super-hydrophilicity. *Soft Matter* **2009**, *5*, 275−281.
(1654) Luzinov, I.; Minko, S.; Tsukruk, V. V. Adaptive and responsive surfaces through controlled reorganization of interfacial polymer layers. *Prog. Polym. Sci.* **2004**, *29*, 635−698.
(1655) Huber, D. L.; Manginell, R. P.; Samara, M. A.; Kim, B.-I.; Bunker, B. C. Programmed Adsorption and Release of Proteins in a Microfluidic Device. *Science* **2003**, *301*, 352−354.
(1656) Rama Rao, G. V.; López, G. P. Encapsulation of Poly(N-Isopropyl Acrylamide) in Silica: A Stimuli-Responsive Porous Hybrid Material That Incorporates Molecular Nano-Valves. *Adv. Mater.* **2000**, *12*, 1692−1695.
(1657) Rao, G. V. R.; Balamurugan, S.; Meyer, D. E.; Chilkoti, A.; López, G. P. Hybrid Bioinorganic Smart Membranes That Incorporate Protein-Based Molecular Switches. *Langmuir* **2002**, *18*, 1819−1824.
(1658) Rama Rao, G. V.; Krug, M. E.; Balamurugan, S.; Xu, H.; Xu, Q.; López, G. P. Synthesis and Characterization of Silica−Poly(N-isopropylacrylamide) Hybrid Membranes: Switchable Molecular Filters. *Chem. Mater.* **2002**, *14*, 5075−5080.
(1659) Liu; Dunphy, D. R.; Atanassov, P.; Bunge, S. D.; Chen, Z.; López, G. P.; Boyle, T. J.; Brinker, C. J. Photoregulation of Mass Transport through a Photoresponsive Azobenzene-Modified Nanoporous Membrane. *Nano Lett.* **2004**, *4*, 551−554.
(1660) Casasús, R.; Marcos, M. D.; Martínez-Máñez, R.; Ros-Lis, J. V.; Soto, J.; Villaescusa, L. A.; Amorós, P.; Beltrán, D.; Guillem, C.; Latorre, J. Toward the Development of Ionically Controlled Nanoscopic Molecular Gates. *J. Am. Chem. Soc.* **2004**, *126*, 8612−8613.

DOI: 10.1021/acs.chemrev.5b00146
Chem. Rev. 2015, 115, 10081−10206

(1661) Pardo-Yissar, V.; Gabai, R.; Shipway, A. N.; Bourenko, T.; Willner, I. Gold Nanoparticle/Hydrogel Composites with Solvent-Switchable Electronic Properties. *Adv. Mater.* **2001**, *13*, 1320−1323.
(1662) Huang, F. H.; Scherman, O. A. Supramolecular polymers. *Chem. Soc. Rev.* **2012**, *41*, 5879−5880.
(1663) Appel, E. A.; del Barrio, J.; Loh, X. J.; Scherman, O. A. Supramolecular polymeric hydrogels. *Chem. Soc. Rev.* **2012**, *41*, 6195−6214.
(1664) Nguyen, T. D.; Tseng, H.-R.; Celestre, P. C.; Flood, A. H.; Liu, Y.; Stoddart, J. F.; Zink, J. I. A reversible molecular valve. *Proc. Natl. Acad. Sci. U. S. A.* **2005**, *102*, 10029−10034.
(1665) Klajn, R.; Olson, M. A.; Wesson, P. J.; Fang, L.; Coskun, A.; Trabolsi, A.; Soh, S.; Stoddart, J. F.; Grzybowski, B. A. Dynamic hook-and-eye nanoparticle sponges. *Nat. Chem.* **2009**, *1*, 733−738.
(1666) Shipway, A. N.; Willner, I. Electronically Transduced Molecular Mechanical and Information Functions on Surfaces. *Acc. Chem. Res.* **2001**, *34*, 421−432.
(1667) Pardo-Yissar, V.; Katz, E.; Willner, I.; Kotlyar, A. B.; Sanders, C.; Lill, H. Biomaterial engineered electrodes for bioelectronics. *Faraday Discuss.* **2000**, *116*, 119−134.
(1668) Willner, I.; Willner, B. Layered molecular optoelectronic assemblies. *J. Mater. Chem.* **1998**, *8*, 2543−2556.
(1669) Willner, I.; Pardo-Yissar, V.; Katz, E.; Ranjit, K. T. A photoactivated 'molecular train' for optoelectronic applications: light-stimulated translocation of a β-cyclodextrin receptor within a stoppered azobenzene-alkyl chain supramolecular monolayer assembly on a Au-electrode. *J. ElectroAnal. Chem.* **2001**, *497*, 172−177.
(1670) Katz, E.; Sheeney-Haj-Ichia, L.; Willner, I. Electrical Contacting of Glucose Oxidase in a Redox-Active Rotaxane Configuration. *Angew. Chem., Int. Ed.* **2004**, *43*, 3292−3300.
(1671) Sheeney-Haj-Ichia, L.; Willner, I. Enhanced Photoelectrochemistry in Supramolecular CdS-Nanoparticle-Stoppered Pseudorotaxane Monolayers Assembled on Electrodes. *J. Phys. Chem. B* **2002**, *106*, 13094−13097.
(1672) Katz, E.; Lioubashevsky, O.; Willner, I. Electromechanics of a Redox-Active Rotaxane in a Monolayer Assembly on an Electrode. *J. Am. Chem. Soc.* **2004**, *126*, 15520−15532.
(1673) Blossey, R. Self-cleaning surfaces - virtual realities. *Nat. Mater.* **2003**, *2*, 301−306.
(1674) Xin, B.; Hao, J. Reversibly switchable wettability. *Chem. Soc. Rev.* **2010**, *39*, 769−782.
(1675) Hua, Z.; Yang, J.; Wang, T.; Liu, G.; Zhang, G. Transparent Surface with Reversibly Switchable Wettability between Superhydrophobicity and Superhydrophilicity. *Langmuir* **2013**, *29*, 10307−10312.
(1676) Brochard, F. Motions of droplets on solid surfaces induced by chemical or thermal gradients. *Langmuir* **1989**, *5*, 432−438.
(1677) Chaudhury, M. K.; Whitesides, G. M. How to Make Water Run Uphill. *Science* **1992**, *256*, 1539−1541.
(1678) Daniel, S.; Chaudhury, M. K.; Chen, J. C. Fast Drop Movements Resulting from the Phase Change on a Gradient Surface. *Science* **2001**, *291*, 633−636.
(1679) Daniel, S.; Sircar, S.; Gliem, J.; Chaudhury, M. K. Ratcheting Motion of Liquid Drops on Gradient Surfaces†. *Langmuir* **2004**, *20*, 4085−4092.
(1680) Liu, Y.; Mu, L.; Liu, B.; Kong, J. Controlled Switchable Surface. *Chem. - Eur. J.* **2005**, *11*, 2622−2631.
(1681) Lahann, J.; Mitragotri, S.; Tran, T.-N.; Kaido, H.; Sundaram, J.; Choi, I. S.; Hoffer, S.; Somorjai, G. A.; Langer, R. A Reversibly Switching Surface. *Science* **2003**, *299*, 371−374.
(1682) Wang, X.; Kharitonov, A. B.; Katz, E.; Willner, I. Potential-controlled molecular machinery of bipyridinium monolayer-functionalized surfaces: an electrochemical and contact angle analysis. *Chem. Commun.* **2003**, 1542−1543.
(1683) Wan, P.; Jiang, Y.; Wang, Y.; Wang, Z.; Zhang, X. Tuning surface wettability through photocontrolled reversible molecular shuttle. *Chem. Commun.* **2008**, 5710−5712.
(1684) Zhang, X.; Zhao, H.; Tian, D.; Deng, H.; Li, H. A Photoresponsive Wettability Switch Based on a Dimethylamino Calix[4]arene. *Chem. - Eur. J.* **2014**, *20*, 9367−9371.
(1685) Chen, K.-Y.; Ivashenko, O.; Carroll, G. T.; Robertus, J.; Kistemaker, J. C. M.; London, G.; Browne, W. R.; Rudolf, P.; Feringa, B. L. Control of Surface Wettability Using Tripodal Light-Activated Molecular Motors. *J. Am. Chem. Soc.* **2014**, *136*, 3219−3224.
(1686) Gau, H.; Herminghaus, S.; Lenz, P.; Lipowsky, R. Liquid Morphologies on Structured Surfaces: From Microchannels to Microchips. *Science* **1999**, *283*, 46−49.
(1687) Gallardo, B. S.; Gupta, V. K.; Eagerton, F. D.; Jong, L. I.; Craig, V. S.; Shah, R. R.; Abbott, N. L. Electrochemical Principles for Active Control of Liquids on Submillimeter Scales. *Science* **1999**, *283*, 57−60.
(1688) Daniel, S.; Chaudhury, M. K. Rectified Motion of Liquid Drops on Gradient Surfaces Induced by Vibration. *Langmuir* **2002**, *18*, 3404−3407.
(1689) Suda, H.; Yamada, S. Force Measurements for the Movement of a Water Drop on a Surface with a Surface Tension Gradient. *Langmuir* **2003**, *19*, 529−531.
(1690) Choi, S.-H.; Zhang Newby, B.-m. Micrometer-Scaled Gradient Surfaces Generated Using Contact Printing of Octadecyltrichlorosilane. *Langmuir* **2003**, *19*, 7427−7435.
(1691) Grunze, M. Driven Liquids. *Science* **1999**, *283*, 41−42.
(1692) Reyes, D. R.; Iossifidis, D.; Auroux, P.-A.; Manz, A. Micro Total Analysis Systems. 1. Introduction, Theory, and Technology. *Anal. Chem.* **2002**, *74*, 2623−2636.
(1693) Ichimura, K.; Oh, S.-K.; Nakagawa, M. Light-Driven Motion of Liquids on a Photoresponsive Surface. *Science* **2000**, *288*, 1624−1626.
(1694) Minko, S.; Müller, M.; Motornov, M.; Nitschke, M.; Grundke, K.; Stamm, M. Two-Level Structured Self-Adaptive Surfaces with Reversibly Tunable Properties. *J. Am. Chem. Soc.* **2003**, *125*, 3896−3900.
(1695) Sun, T.; Wang, G.; Feng, L.; Liu, B.; Ma, Y.; Jiang, L.; Zhu, D. Reversible Switching between Superhydrophilicity and Superhydrophobicity. *Angew. Chem., Int. Ed.* **2004**, *43*, 357−360.
(1696) Fu, Q.; Rama Rao, G. V.; Basame, S. B.; Keller, D. J.; Artyushkova, K.; Fulghum, J. E.; López, G. P. Reversible Control of Free Energy and Topography of Nanostructured Surfaces. *J. Am. Chem. Soc.* **2004**, *126*, 8904−8905.
(1697) Rosario, R.; Gust, D.; Garcia, A. A.; Hayes, M.; Taraci, J. L.; Clement, T.; Dailey, J. W.; Picraux, S. T. Lotus Effect Amplifies Light-Induced Contact Angle Switching. *J. Phys. Chem. B* **2004**, *108*, 12640−12642.
(1698) Ariga, K.; Ji, Q.; Mori, T.; Naito, M.; Yamauchi, Y.; Abe, H.; Hill, J. P. Enzyme nanoarchitectonics: organization and device application. *Chem. Soc. Rev.* **2013**, *42*, 6322−6345.
(1699) Teller, C.; Willner, I. Functional nucleic acid nanostructures and DNA machines. *Curr. Opin. Biotechnol.* **2010**, *21*, 376−391.
(1700) Hirokawa, N.; Noda, Y.; Tanaka, Y.; Niwa, S. Kinesin superfamily motor proteins and intracellular transport. *Nat. Rev. Mol. Cell Biol.* **2009**, *10*, 682−696.
(1701) Montemagno, C.; Bachand, G. Constructing nanomechanical devices powered by biomolecular motors. *Nanotechnology* **1999**, *10*, 225−231.
(1702) Hess, H.; Vogel, V. Molecular shuttles based on motor proteins: active transport in synthetic environments. *Rev. Mol. Biotechnol.* **2001**, *82*, 67−85.
(1703) Adachi, K.; Yasuda, R.; Noji, H.; Itoh, H.; Harada, Y.; Yoshida, M.; Kinosita, K. Stepping rotation of F-1-ATPase visualized through angle-resolved single-fluorophore imaging. *Proc. Natl. Acad. Sci. U. S. A.* **2000**, *97*, 7243−7247.
(1704) Yasuda, R.; Noji, H.; Yoshida, M.; Kinosita, K.; Itoh, H. Resolution of distinct rotational substeps by submillisecond kinetic analysis of F-1-ATPase. *Nature* **2001**, *410*, 898−904.
(1705) Hirono-Hara, Y.; Noji, H.; Nishiura, M.; Muneyuki, E.; Hara, K. Y.; Yasuda, R.; Kinosita, K., Jr.; Yoshida, M. Pause and rotation of F(1)-ATPase during catalysis. *Proc. Natl. Acad. Sci. U. S. A.* **2001**, *98*, 13649−13654.
(1706) Noji, H.; Yasuda, R.; Yoshida, M.; Kinosita, K., Jr. Direct observation of the rotation of F_1-ATPase. *Nature* **1997**, *386*, 299−302.

DOI: 10.1021/acs.chemrev.5b00146
Chem. Rev. 2015, 115, 10081−10206

(1707) Yasuda, R.; Noji, H.; Kinosita, K.; Yoshida, M. F_1-ATPase is a highly efficient molecular motor that rotates with discrete 120 degree steps. *Cell* **1998**, *93*, 1117−1124.
(1708) Diez, M.; Zimmermann, B.; Borsch, M.; Konig, M.; Schweinberger, E.; Steigmiller, S.; Reuter, R.; Felekyan, S.; Kudryavtsev, V.; Seidel, C. A. M.; Graber, P. Proton-powered subunit rotation in single membrane-bound F_0F_1-ATP synthase. *Nat. Struct. Mol. Biol.* **2004**, *11*, 135−141.
(1709) Itoh, H.; Takahashi, A.; Adachi, K.; Noji, H.; Yasuda, R.; Yoshida, M.; Kinosita, K. Mechanically driven ATP synthesis by F_1-ATPase. *Nature* **2004**, *427*, 465−468.
(1710) Soong, R. K.; Bachand, G. D.; Neves, H. P.; Olkhovets, A. G.; Craighead, H. G.; Montemagno, C. D. Powering an inorganic nanodevice with a biomolecular motor. *Science* **2000**, *290*, 1555−1558.
(1711) Duan, L.; He, Q.; Wang, K. W.; Yan, X. H.; Cui, Y.; Moewald, H.; Li, J. B. Adenosine triphosphate biosynthesis catalyzed by F0F1 ATP synthase assembled in polymer microcapsules. *Angew. Chem., Int. Ed.* **2007**, *46*, 6996−7000.
(1712) Oiwa, K.; Chaen, S.; Kamitsubo, E.; Shimmen, T.; Sugi, H. Steady-state force-velocity relation in the ATP-dependent sliding movement of myosin-coated beads on actin cables in vitro studied with a centrifuge microscope. *Proc. Natl. Acad. Sci. U. S. A.* **1990**, *87*, 7893−7897.
(1713) Reuther, C.; Hajdo, L.; Tucker, R.; Kasprzak, A. A.; Diez, S. Biotemplated nanopatterning of planar surfaces with molecular motors. *Nano Lett.* **2006**, *6*, 2177−2183.
(1714) Ramachandran, S.; Ernst, K. H.; Bachand, G. D.; Vogel, V.; Hess, H. Selective loading of kinesin-powered molecular shuttles with protein cargo and its application to biosensing. *Small* **2006**, *2*, 330−334.
(1715) Diez, S.; Reuther, C.; Dinu, C.; Seidel, R.; Mertig, M.; Pompe, W.; Howard, J. Stretching and transporting DNA molecules using motor proteins. *Nano Lett.* **2003**, *3*, 1251−1254.
(1716) Dumont, E. L. P.; Do, C.; Hess, H. Molecular wear of microtubules propeled by surface-adhered kinesins. *Nat. Nanotechnol.* **2015**, *10*, 166−169.
(1717) Yu, T. Y.; Wang, Q.; Johnson, D. S.; Wang, M. D.; Ober, C. K. Functional hydrogel surfaces: Binding kinesin-based molecular motor proteins to selected patterned sites. *Adv. Funct. Mater.* **2005**, *15*, 1303−1309.
(1718) Yildiz, A.; Selvin, P. R. Kinesin: walking, crawling or sliding along? *Trends Cell Biol.* **2005**, *15*, 112−120.
(1719) Beeg, J.; Klumpp, S.; Dimova, R.; Gracia, R. S.; Unger, E.; Lipowsky, R. Transport of beads by several kinesin motors. *Biophys. J.* **2008**, *94*, 532−541.
(1720) Yamasaki, H.; Nakayama, H. Fluctuation analysis of myosin-coated bead movement along actin bundles of Nitella. *Biochem. Biophys. Res. Commun.* **1996**, *221*, 831−836.
(1721) Spudich, J. A.; Kron, S. J.; Sheetz, M. P. Movement of Myosin-Coated Beads on Oriented Filaments Reconstituted from Purified Actin. *Nature* **1985**, *315*, 584−586.
(1722) Sheetz, M. P.; Spudich, J. A. Movement of myosin-coated fluorescent beads on actin cables in vitro. *Nature* **1983**, *303*, 31−35.
(1723) Yokokawa, R.; Takeuchi, S.; Kon, T.; Nishiura, M.; Sutoh, K.; Fujita, H. Unidirectional transport of kinesin-coated beads on microtubules oriented in a microfluidic device. *Nano Lett.* **2004**, *4*, 2265−2270.
(1724) Bormuth, V.; Varga, V.; Howard, J.; Schaffer, E. Protein Friction Limits Diffusive and Directed Movements of Kinesin Motors on Microtubules. *Science* **2009**, *325*, 870−873.
(1725) Agarwal, A.; Katira, P.; Hess, H. Millisecond Curing Time of a Molecular Adhesive Causes Velocity-Dependent Cargo-Loading of Molecular Shuttles. *Nano Lett.* **2009**, *9*, 1170−1175.
(1726) Bohm, K. J.; Stracke, R.; Muhlig, P.; Unger, E. Motor protein-driven unidirectional transport of micrometer-sized cargoes across isopolar microtubule arrays. *Nanotechnology* **2001**, *12*, 238−244.
(1727) Bottier, C.; Fattaccioli, J.; Tarhan, M. C.; Yokokawa, R.; Morin, F. O.; Kim, B.; Collard, D.; Fujita, H. Active transport of oil droplets along oriented microtubules by kinesin molecular motors. *Lab Chip* **2009**, *9*, 1694−1700.
(1728) Nitta, T.; Tanahashi, A.; Obara, Y.; Hirano, M.; Razumova, M.; Regnier, M.; Hess, H. Comparing guiding track requirements for myosin- and kinesin-powered molecular shuttles. *Nano Lett.* **2008**, *8*, 2305−2309.
(1729) Vikhorev, P. G.; Vikhoreva, N. N.; Mansson, A. Bending flexibility of actin filaments during motor-induced sliding. *Biophys. J.* **2008**, *95*, 5809−5819.
(1730) Vikhorev, P. G.; Vikhoreva, N. N.; Sundberg, M.; Balaz, M.; Albet-Torres, N.; Bunk, R.; Kvennefors, A.; Liljesson, K.; Nicholls, I. A.; Nilsson, L.; Omling, P.; Tagerud, S.; Montelius, L.; Mansson, A. Diffusion dynamics of motor-driven transport: gradient production and self-organization of surfaces. *Langmuir* **2008**, *24*, 13509−13517.
(1731) Campbell, J.; Paul, D.; Kurabayashi, K.; Meyhofer, E. A Kinesin Driven Enzyme Linked Immunosorbant Assay (ELISA) for Ultra Low Protein Detection Applications. *Biophys. J.* **2014**, *106*, 622a−622a.
(1732) Kakugo, A.; Sugimoto, S.; Gong, J. P.; Osada, Y. Gel machines constructed from chemically cross-linked actins and myosins. *Adv. Mater.* **2002**, *14*, 1124−1126.
(1733) Sanchez, T.; Chen, D. T. N.; DeCamp, S. J.; Heymann, M.; Dogic, Z. Spontaneous motion in hierarchically assembled active matter. *Nature* **2012**, *491*, 431−434.
(1734) Marchetti, M. C. Active Matter Spontaneous flows and self-propeled drops. *Nature* **2012**, *491*, 340−341.
(1735) Kinosita, K.; Yasuda, R.; Noji, H.; Adachi, K. A rotary molecular motor that can work at near 100% efficiency. *Philos. Trans. R. Soc., B* **2000**, *355*, 473−489.
(1736) Boyer, P. D. The ATP synthase - A splendid molecular machine. *Annu. Rev. Biochem.* **1997**, *66*, 717−749.
(1737) Yoshida, M.; Muneyuki, E.; Hisabori, T. ATP synthase - A marvellous rotary engine of the cell. *Nat. Rev. Mol. Cell Biol.* **2001**, *2*, 669−677.
(1738) Howard, J. The movement of kinesin along microtubules. *Annu. Rev. Physiol.* **1996**, *58*, 703−729.
(1739) Oesterhelt, D.; Brauchle, C.; Hampp, N. Bacteriorhodopsin - a Biological-Material for Information-Processing. *Q. Rev. Biophys.* **1991**, *24*, 425−478.
(1740) Schick, G. A.; Lawrence, A. F.; Birge, R. R. Biotechnology and Molecular Computing. *Trends Biotechnol.* **1988**, *6*, 159−163.
(1741) Birge, R. R. Photophysics and Molecular Electronic Applications of the Rhodopsins. *Annu. Rev. Phys. Chem.* **1990**, *41*, 683−733.
(1742) Chen, Z. P.; Birge, R. R. Protein-Based Artificial Retinas. *Trends Biotechnol.* **1993**, *11*, 292−300.
(1743) Hampp, N.; Silber, A. Functional dyes from nature: Potentials for technical applications. *Pure Appl. Chem.* **1996**, *68*, 1361−1366.
(1744) Birge, R. R.; Gillespie, N. B.; Izaguirre, E. W.; Kusnetzow, A.; Lawrence, A. F.; Singh, D.; Song, Q. W.; Schmidt, E.; Stuart, J. A.; Seetharaman, S.; Wise, K. J. Biomolecular electronics: Protein-based associative processors and volumetric memories. *J. Phys. Chem. B* **1999**, *103*, 10746−10766.
(1745) Hampp, N. Bacteriorhodopsin as a photochromic retinal protein for optical memories. *Chem. Rev.* **2000**, *100*, 1755−1776.
(1746) Masthay, M. B.; Sammeth, D. M.; Helvenston, M. C.; Buckman, C. B.; Li, W. Y.; Cde-Baca, M. J.; Kofron, J. T. The laser-induced blue state of bacteriorhodopsin: Mechanistic and color regulatory roles of protein-protein interactions, protein-lipid interactions, and metal ions. *J. Am. Chem. Soc.* **2002**, *124*, 3418−3430.
(1747) Einati, H.; Mishra, D.; Friedman, N.; Sheves, M.; Naaman, R. Light-Controlled Spin Filtering in Bacteriorhodopsin. *Nano Lett.* **2015**, *15*, 1052−1056.
(1748) Rakovich, A.; Nabiev, I.; Sukhanova, A.; Lesnyak, V.; Gaponik, N.; Rakovich, Y. P.; Donegan, J. F. Large Enhancement of Nonlinear Optical Response in a Hybrid Nanobiomaterial Consisting of Bacteriorhodopsin and Cadmium Telluride Quantum Dots. *ACS Nano* **2013**, *7*, 2154−2160.
(1749) Jin, Y. D.; Friedman, N.; Sheves, M.; Cahen, D. Bacteriorhodopsin-monolayer-based planar metal-insulator-metal junctions via biomimetic vesicle fusion: Preparation, characterization, and

DOI: 10.1021/acs.chemrev.5b00146
Chem. Rev. 2015, 115, 10081−10206

bio-optoelectronic characteristics. *Adv. Funct. Mater.* **2007**, *17*, 1417−1428.
(1750) Szacilowski, K. Digital information processing in molecular systems. *Chem. Rev.* **2008**, *108*, 3481−3548.
(1751) Matile, S.; Som, A.; Sorde, N. Recent synthetic ion channels and pores. *Tetrahedron* **2004**, *60*, 6405−6435.
(1752) Gokel, G. W.; Negin, S. Synthetic Ion Channels: From Pores to Biological Applications. *Acc. Chem. Res.* **2013**, *46*, 2824−2833.
(1753) Sakai, N.; Matile, S. Synthetic Ion Channels. *Langmuir* **2013**, *29*, 9031−9040.
(1754) Fyles, T. M. Synthetic ion channels in bilayer membranes. *Chem. Soc. Rev.* **2007**, *36*, 335−347.
(1755) Carr, R.; Weinstock, I. A.; Sivaprasadarao, A.; Muller, A.; Aksimentiev, A. Synthetic Ion Channels via Self-Assembly: A Route for Embedding Porous Polyoxometalate Nanocapsules in Lipid Bilayer Membranes. *Nano Lett.* **2008**, *8*, 3916−3921.
(1756) Branton, D.; Deamer, D. W.; Marziali, A.; Bayley, H.; Benner, S. A.; Butler, T.; Di Ventra, M.; Garaj, S.; Hibbs, A.; Huang, X.; Jovanovich, S. B.; Krstic, P. S.; Lindsay, S.; Ling, X. S.; Mastrangelo, C. H.; Meller, A.; Oliver, J. S.; Pershin, Y. V.; Ramsey, J. M.; Riehn, R.; Soni, G. V.; Tabard-Cossa, V.; Wanunu, M.; Wiggin, M.; Schloss, J. A. The potential and challenges of nanopore sequencing. *Nat. Biotechnol.* **2008**, *26*, 1146−1153.
(1757) Kang, X.-f.; Gu, L.-Q.; Cheley, S.; Bayley, H. Single Protein Pores Containing Molecular Adapters at High Temperatures. *Angew. Chem., Int. Ed.* **2005**, *44*, 1495−1499.
(1758) Meller, A.; Nivon, L.; Branton, D. Voltage-Driven DNA Translocations through a Nanopore. *Phys. Rev. Lett.* **2001**, *86*, 3435−3438.
(1759) Gershow, M.; Golovchenko, J. A. Recapturing and trapping single molecules with a solid-state nanopore. *Nat. Nanotechnol.* **2007**, *2*, 775−779.
(1760) Lubensky, D. K.; Nelson, D. R. Driven Polymer Translocation Through a Narrow Pore. *Biophys. J.* **1999**, *77*, 1824−1838.
(1761) Holden, M. A.; Bayley, H. Direct Introduction of Single Protein Channels and Pores into Lipid Bilayers. *J. Am. Chem. Soc.* **2005**, *127*, 6502−6503.
(1762) González, J. E.; Oades, K.; Leychkis, Y.; Harootunian, A.; Negulescu, P. A. Cell-based assays and instrumentation for screening ion-channel targets. *Drug Discovery Today* **1999**, *4*, 431−439.
(1763) Jentsch, T. J.; Hubner, C. A.; Fuhrmann, J. C. Ion channels: Function unravelled by dysfunction. *Nat. Cell Biol.* **2004**, *6*, 1039−1047.
(1764) Majd, S.; Yusko, E. C.; Billeh, Y. N.; Macrae, M. X.; Yang, J.; Mayer, M. Applications of biological pores in nanomedicine, sensing, and nanoelectronics. *Curr. Opin. Biotechnol.* **2010**, *21*, 439−476.
(1765) Koçer, A.; Walko, M.; Bulten, E.; Halza, E.; Feringa, B. L.; Meijberg, W. Rationally Designed Chemical Modulators Convert a Bacterial Channel Protein into a pH-Sensory Valve. *Angew. Chem., Int. Ed.* **2006**, *45*, 3126−3130.
(1766) Kiwada, T.; Sonomura, K.; Sugiura, Y.; Asami, K.; Futaki, S. Transmission of Extramembrane Conformational Change into Current: Construction of Metal-Gated Ion Channel. *J. Am. Chem. Soc.* **2006**, *128*, 6010−6011.
(1767) Sukharev, S.; Anishkin, A. Mechanosensitive channels: what can we learn from 'simple' model systems? *Trends Neurosci.* **2004**, *27*, 345−351.
(1768) Louhivuori, M.; Risselada, H. J.; van der Giessen, E.; Marrink, S. J. Release of content through mechano-sensitive gates in pressurized liposomes. *Proc. Natl. Acad. Sci. U. S. A.* **2010**, *107*, 19856−19860.
(1769) Steinberg-Yfrach, G.; Rigaud, J.-L.; Durantini, E. N.; Moore, A. L.; Gust, D.; Moore, T. A. Light-driven production of ATP catalysed by F0F1-ATP synthase in an artificial photosynthetic membrane. *Nature* **1998**, *392*, 479−482.
(1770) Banghart, M.; Borges, K.; Isacoff, E.; Trauner, D.; Kramer, R. H. Light-activated ion channels for remote control of neuronal firing. *Nat. Neurosci.* **2004**, *7*, 1381−1386.
(1771) Volgraf, M.; Gorostiza, P.; Numano, R.; Kramer, R. H.; Isacoff, E. Y.; Trauner, D. Allosteric control of an ionotropic glutamate receptor with an optical switch. *Nat. Chem. Biol.* **2006**, *2*, 47−52.
(1772) Stein, M.; Breit, A.; Fehrentz, T.; Gudermann, T.; Trauner, D. Optical Control of TRPV1 Channels. *Angew. Chem., Int. Ed.* **2013**, *52*, 9845−9848.
(1773) Schoenberger, M.; Damijonaitis, A.; Zhang, Z. N.; Nagel, D.; Trauner, D. Development of a New Photochromic Ion Channel Blocker via Azologization of Fomocaine. *ACS Chem. Neurosci.* **2014**, *5*, 514−518.
(1774) Schonberger, M.; Althaus, M.; Fronius, M.; Clauss, W.; Trauner, D. Controlling epithelial sodium channels with light using photoswitchable amilorides. *Nat. Chem.* **2014**, *6*, 712−719.
(1775) Kramer, R. H.; Chambers, J. J.; Trauner, D. Photochemical tools for remote control of ion channels in excitable cells. *Nat. Chem. Biol.* **2005**, *1*, 360−365.
(1776) Banghart, M. R.; Mourot, A.; Fortin, D. L.; Yao, J. Z.; Kramer, R. H.; Trauner, D. Photochromic Blockers of Voltage-Gated Potassium Channels. *Angew. Chem., Int. Ed.* **2009**, *48*, 9097−9101.
(1777) Mourot, A.; Fehrentz, T.; Le Feuvre, Y.; Smith, C. M.; Herold, C.; Dalkara, D.; Nagy, F.; Trauner, D.; Kramer, R. H. Rapid optical control of nociception with an ion-channel photoswitch. *Nat. Methods* **2012**, *9*, 396−402.
(1778) Lougheed, T.; Borisenko, V.; Hennig, T.; Ruck-Braun, K.; Woolley, G. A. Photomodulation of ionic current through hemithioindigo-modified gramicidin channels. *Org. Biomol. Chem.* **2004**, *2*, 2798−2801.
(1779) Banghart, M. R.; Volgraf, M.; Trauner, D. Engineering light-gated ion channels. *Biochemistry* **2006**, *45*, 15129−15141.
(1780) Brieke, C.; Rohrbach, F.; Gottschalk, A.; Mayer, G.; Heckel, A. Light-Controlled Tools. *Angew. Chem., Int. Ed.* **2012**, *51*, 8446−8476.
(1781) Shinbo, T.; Kurihara, K.; Kobatake, Y.; Kamo, N. Active transport of picrate anion through organic liquid membrane. *Nature* **1977**, *270*, 277−278.
(1782) Grimaldi, J. J.; Boileau, S.; Lehn, J.-M. Light-driven, carrier-mediated electron transfer across artificial membranes. *Nature* **1977**, *265*, 229−230.
(1783) Grimaldi, J. J.; Lehn, J.-M. Transport processes in organic chemistry. 5. Multicarrier transport: coupled transport of electrons and metal cations mediated by an electron carrier and a selective cation carrier. *J. Am. Chem. Soc.* **1979**, *101*, 1333−1334.
(1784) Anderson, S. S.; Lyle, I. G.; Paterson, R. Electron transfer across membranes using vitamin K1 and coenzyme Q10 as carrier molecules. *Nature* **1976**, *259*, 147−148.
(1785) Steinberg-Yfrach, G.; Liddell, P. A.; Hung, S.-C.; Moore, A. L.; Gust, D.; Moore, T. A. Conversion of light energy to proton potential in liposomes by artificial photosynthetic reaction centers. *Nature* **1997**, *385*, 239−241.
(1786) Bennett, I. M.; Farfano, H. M. V.; Bogani, F.; Primak, A.; Liddell, P. A.; Otero, L.; Sereno, L.; Silber, J. J.; Moore, A. L.; Moore, T. A.; Gust, D. Active transport of Ca^{2+} by an artificial photosynthetic membrane. *Nature* **2002**, *420*, 398−401.
(1787) Meyer, T. J. Chemical approaches to artificial photosynthesis. *Acc. Chem. Res.* **1989**, *22*, 163−170.
(1788) Wasielewski, M. R. Photoinduced electron transfer in supramolecular systems for artificial photosynthesis. *Chem. Rev.* **1992**, *92*, 435−461.
(1789) Gust, D.; Moore, T. A.; Moore, A. L. Molecular mimicry of photosynthetic energy and electron transfer. *Acc. Chem. Res.* **1993**, *26*, 198−205.
(1790) Kurreck, H.; Huber, M. Model Reactions for Photosynthesis—Photoinduced Charge and Energy Transfer between Covalently Linked Porphyrin and Quinone Units. *Angew. Chem., Int. Ed. Engl.* **1995**, *34*, 849−866.
(1791) Balzani, V.; Credi, A.; Venturi, M. Photoprocesses. *Curr. Opin. Chem. Biol.* **1997**, *1*, 506−513.
(1792) Gust, D.; Moore, T. A.; Moore, A. L. Mimicking Photosynthetic Solar Energy Transduction. *Acc. Chem. Res.* **2001**, *34*, 40−48.
(1793) Dürr, H.; Bossmann, S. Ruthenium Polypyridine Complexes. On the Route to Biomimetic Assemblies as Models for the Photosynthetic Reaction Center. *Acc. Chem. Res.* **2001**, *34*, 905−917.

DOI: 10.1021/acs.chemrev.5b00146
Chem. Rev. 2015, 115, 10081−10206

(1794) Sun, L.; Hammarstrom, L.; Akermark, B.; Styring, S. Towards artificial photosynthesis: ruthenium-manganese chemistry for energy production. *Chem. Soc. Rev.* **2001**, *30*, 36−49.
(1795) Holten, D.; Bocian, D. F.; Lindsey, J. S. Probing Electronic Communication in Covalently Linked Multiporphyrin Arrays. A Guide to the Rational Design of Molecular Photonic Devices. *Acc. Chem. Res.* **2002**, *35*, 57−69.
(1796) Imahori, H.; Mori, Y.; Matano, Y. Nanostructured artificial photosynthesis. *J. Photochem. Photobiol., C* **2003**, *4*, 51−83.
(1797) Guldi, D. M. Fullerene-porphyrin architectures; photosynthetic antenna and reaction center models. *Chem. Soc. Rev.* **2002**, *31*, 22−36.
(1798) Imahori, H. Porphyrin-fullerene linked systems as artificial photosynthetic mimics. *Org. Biomol. Chem.* **2004**, *2*, 1425−1433.
(1799) Alstrum-Acevedo, J. H.; Brennaman, M. K.; Meyer, T. J. Chemical Approaches to Artificial Photosynthesis. 2. *Inorg. Chem.* **2005**, *44*, 6802−6827.
(1800) Paddon-Row, M. N. Investigating long-range electron-transfer processes with rigid, covalently linked donor-(norbornylogous bridge)-acceptor systems. *Acc. Chem. Res.* **1994**, *27*, 18−25.
(1801) Nicoletta, F. P.; Cupelli, D.; Formoso, P.; De Filpo, G.; Colella, V.; Gugliuzza, A. Light Responsive Polymer Membranes: A Review. *Membranes* **2012**, *2*, 134−197.
(1802) Limburg, B.; Laisné, G.; Bouwman, E.; Bonnet, S. Enhanced Photoinduced Electron Transfer at the Surface of Charged Lipid Bilayers. *Chem. - Eur. J.* **2014**, *20*, 8965−8972.
(1803) Banerji, N.; Fürstenberg, A.; Bhosale, S.; Sisson, A. L.; Sakai, N.; Matile, S.; Vauthey, E. Ultrafast Photoinduced Charge Separation in Naphthalene Diimide Based Multichromophoric Systems in Liquid Solutions and in a Lipid Membrane. *J. Phys. Chem. B* **2008**, *112*, 8912−8922.
(1804) Numata, T.; Murakami, T.; Kawashima, F.; Morone, N.; Heuser, J. E.; Takano, Y.; Ohkubo, K.; Fukuzumi, S.; Mori, Y.; Imahori, H. Utilization of Photoinduced Charge-Separated State of Donor−Acceptor-Linked Molecules for Regulation of Cell Membrane Potential and Ion Transport. *J. Am. Chem. Soc.* **2012**, *134*, 6092−6095.
(1805) Garg, V.; Kodis, G.; Chachisvilis, M.; Hambourger, M.; Moore, A. L.; Moore, T. A.; Gust, D. Conformationally Constrained Macrocyclic Diporphyrin−Fullerene Artificial Photosynthetic Reaction Center. *J. Am. Chem. Soc.* **2011**, *133*, 2944−2954.
(1806) Rutherford, A. W.; Moore, T. A. Mimicking photosynthesis, but just the best bits. *Nature* **2008**, *453*, 449−449.
(1807) Bhosale, S.; Sisson, A. L.; Talukdar, P.; Fürstenberg, A.; Banerji, N.; Vauthey, E.; Bollot, G.; Mareda, J.; Röger, C.; Würthner, F.; Sakai, N.; Matile, S. Photoproduction of Proton Gradients with π-Stacked Fluorophore Scaffolds in Lipid Bilayers. *Science* **2006**, *313*, 84−86.
(1808) Tan, S. C.; Crouch, L. I.; Jones, M. R.; Welland, M. Generation of Alternating Current in Response to Discontinuous Illumination by Photoelectrochemical Cells Based on Photosynthetic Proteins. *Angew. Chem., Int. Ed.* **2012**, *51*, 6667−6671.
(1809) Xie, X.; Crespo, G. A.; Mistlberger, G.; Bakker, E. Photocurrent generation based on a light-driven proton pump in an artificial liquid membrane. *Nat. Chem.* **2014**, *6*, 202−207.
(1810) Simmel, F. C.; Yurke, B. Using DNA to construct and power a nanoactuator. *Phys. Rev. E: Stat. Phys., Plasmas, Fluids, Relat. Interdiscip. Top.* **2001**, *63*, 041913.
(1811) Li, J. W. J.; Tan, W. H. A single DNA molecule nanomotor. *Nano Lett.* **2002**, *2*, 315−318.
(1812) Niemeyer, C. M.; Adler, M. Nanomechanical devices based on DNA. *Angew. Chem., Int. Ed.* **2002**, *41*, 3779−3783.
(1813) Simmel, F. C.; Yurke, B. A DNA-based molecular device switchable between three distinct mechanical states. *Appl. Phys. Lett.* **2002**, *80*, 883−885.
(1814) Yan, H.; Zhang, X. P.; Shen, Z. Y.; Seeman, N. C. A robust DNA mechanical device controlled by hybridization topology. *Nature* **2002**, *415*, 62−65.
(1815) Seeman, N. C. Biochemistry and structural DNA nanotechnology: An evolving symbiotic relationship. *Biochemistry* **2003**, *42*, 7259−7269.
(1816) Feng, L. P.; Park, S. H.; Reif, J. H.; Yan, H. A two-state DNA lattice switched by DNA nanoactuator. *Angew. Chem., Int. Ed.* **2003**, *42*, 4342−4346.
(1817) Liu, D. S.; Balasubramanian, S. A proton-fueled DNA nanomachine. *Angew. Chem., Int. Ed.* **2003**, *42*, 5734−5736.
(1818) Chen, Y.; Lee, S. H.; Mao, C. A DNA nanomachine based on a duplex-triplex transition. *Angew. Chem., Int. Ed.* **2004**, *43*, 5335−5338.
(1819) Chen, Y.; Wang, M. S.; Mao, C. D. An autonomous DNA nanomotor powered by a DNA enzyme. *Angew. Chem., Int. Ed.* **2004**, *43*, 3554−3557.
(1820) Chen, Y.; Mao, C. D. Putting a brake on an autonomous DNA nanomotor. *J. Am. Chem. Soc.* **2004**, *126*, 8626−8627.
(1821) Seeman, N. C. From genes to machines: DNA nanomechanical devices. *Trends Biochem. Sci.* **2005**, *30*, 119−125.
(1822) Simmel, F. C.; Dittmer, W. U. DNA nanodevices. *Small* **2005**, *1*, 284−299.
(1823) Beissenhirtz, M. K.; Willner, I. DNA-based machines. *Org. Biomol. Chem.* **2006**, *4*, 3392−3401.
(1824) Bath, J.; Turberfield, A. J. DNA nanomachines. *Nat. Nanotechnol.* **2007**, *2*, 275−284.
(1825) Krishnan, Y.; Simmel, F. C. Nucleic Acid Based Molecular Devices. *Angew. Chem., Int. Ed.* **2011**, *50*, 3124−3156.
(1826) Liu, X. Q.; Lu, C. H.; Willner, I. Switchable Reconfiguration of Nucleic Acid Nanostructures by Stimuli-Responsive DNA Machines. *Acc. Chem. Res.* **2014**, *47*, 1673−1680.
(1827) Wang, F.; Willner, B.; Willner, I. DNA-based machines. *Top. Curr. Chem.* **2014**, *354*, 279−338.
(1828) Tang, Y.; Ge, B.; Sen, D.; Yu, H. Z. Functional DNA switches: rational design and electrochemical signaling. *Chem. Soc. Rev.* **2014**, *43*, 518−529.
(1829) Venkataraman, S.; Dirks, R. M.; Rothemund, P. W.; Winfree, E.; Pierce, N. A. An autonomous polymerization motor powered by DNA hybridization. *Nat. Nanotechnol.* **2007**, *2*, 490−494.
(1830) Tomov, T. E.; Tsukanov, R.; Liber, M.; Masoud, R.; Plavner, N.; Nir, E. Rational design of DNA motors: fuel optimization through single-molecule fluorescence. *J. Am. Chem. Soc.* **2013**, *135*, 11935−11941.
(1831) Dittmer, W. U.; Simmel, F. C. Transcriptional control of DNA-based nanomachines. *Nano Lett.* **2004**, *4*, 689−691.
(1832) Dittmer, W. U.; Kempter, S.; Radler, J. O.; Simmel, F. C. Using gene regulation to program DNA-based molecular devices. *Small* **2005**, *1*, 709−712.
(1833) Shin, J. S.; Pierce, N. A. A synthetic DNA walker for molecular transport. *J. Am. Chem. Soc.* **2004**, *126*, 10834−10835.
(1834) Sherman, W. B.; Seeman, N. C. A precisely controlled DNA biped walking device. (vol 4, pg 1801, 2004). *Nano Lett.* **2004**, *4*, 1801−1801.
(1835) Kelly, T. R. Molecular motors: synthetic DNA-based walkers inspired by kinesin. *Angew. Chem., Int. Ed.* **2005**, *44*, 4124−4127.
(1836) Omabegho, T.; Sha, R.; Seeman, N. C. A bipedal DNA Brownian motor with coordinated legs. *Science* **2009**, *324*, 67−71.
(1837) Reif, J. H. The design of autonomous DNA nanomechanical devices: Walking and rolling DNA. *DNA Comp.* **2003**, *2568*, 22−37.
(1838) Yin, P.; Turberfield, A. J.; Reif, J. H. Designs of autonomous unidirectional walking DNA devices. *DNA Comp.* **2005**, *3384*, 410−425.
(1839) Yurke, B.; Turberfield, A. J.; Mills, A. P.; Simmel, F. C.; Neumann, J. L. A DNA-fueled molecular machine made of DNA. *Nature* **2000**, *406*, 605−608.
(1840) Tian, Y.; Mao, C. D. Molecular gears: A pair of DNA circles continuously rolls against each other. *J. Am. Chem. Soc.* **2004**, *126*, 11410−11411.
(1841) Wang, C.; Huang, Z.; Lin, Y.; Ren, J.; Qu, X. Artificial DNA nano-spring powered by protons. *Adv. Mater.* **2010**, *22*, 2792−2798.
(1842) Lund, K.; Manzo, A. J.; Dabby, N.; Michelotti, N.; Johnson-Buck, A.; Nangreave, J.; Taylor, S.; Pei, R.; Stojanovic, M. N.; Walter, N. G.; Winfree, E.; Yan, H. Molecular robots guided by prescriptive landscapes. *Nature* **2010**, *465*, 206−210.
(1843) Muscat, R. A.; Bath, J.; Turberfield, A. J. A programmable molecular robot. *Nano Lett.* **2011**, *11*, 982−987.

DOI: 10.1021/acs.chemrev.5b00146
Chem. Rev. 2015, 115, 10081−10206

(1844) Shelley, F. J.; Wickham, M. E.; Katsuda, Y.; Hidaka, K.; Bath, J.; Sugiyama, H.; Turberfield, A. J. *Nat. Nanotechnol.* **2011**, *6*, 166−169.
(1845) Ackermann, D.; Jester, S.-S.; Famulok, M. Design Strategy for DNA Rotaxanes with a Mechanically Reinforced PX100 Axle. *Angew. Chem., Int. Ed.* **2012**, *51*, 6771−6775.
(1846) Ackermann, Damian; S, T. L.; Hannam, Jeffrey S.; Purohit, Chandra S.; Heckel, Alexander; Famulok, Michael A Double-Stranded DNA Rotaxane. *Nat. Nanotechnol.* **2010**, *5*, 436−442.
(1847) Schmidt, T. L.; Heckel, A. Construction of a structurally defined double-stranded DNA catenane. *Nano Lett.* **2011**, *11*, 1739−1742.
(1848) Lohmann, F.; Ackermann, D.; Famulok, M. Reversible light switch for macrocycle mobility in a DNA rotaxane. *J. Am. Chem. Soc.* **2012**, *134*, 11884−11887.
(1849) Elbaz, J.; Wang, Z. G.; Wang, F.; Willner, I. Programmed dynamic topologies in DNA catenanes. *Angew. Chem., Int. Ed.* **2012**, *51*, 2349−2353.
(1850) Onizuka, K.; Nagatsugi, F.; Ito, Y.; Abe, H. Automatic pseudorotaxane formation targeting on nucleic acids using a pair of reactive oligodeoxynucleotides. *J. Am. Chem. Soc.* **2014**, *136*, 7201−7204.
(1851) Niemeyer, C. M. DNA as a material for Nanotechnology. *Angew. Chem., Int. Ed. Engl.* **1997**, *36*, 585−587.
(1852) Seeman, N. C. Nucleic Acid Nanostructures and Topology. *Angew. Chem., Int. Ed.* **1998**, *37*, 3220−3238.
(1853) Seeman, N. C. DNA nanotechnology: novel DNA constructions. *Annu. Rev. Biophys. Biomol. Struct.* **1998**, *27*, 225−248.
(1854) Seeman, N. C.; Wang, H.; Yang, X.; Liu, F.; Mao, C.; Sun, W.; Wenzler, L.; Shen, Z.; Sha, R.; Yan, H.; et al. New Motifs in DNA Nanotechnology. *Nanotechnology* **1998**, *9*, 257−273.
(1855) Yang, X.; Vologodskii, A. V.; Liu, B.; Kemper, B.; Seeman, N. C. Torsional control of double-stranded DNA branch migration. *Biopolymers* **1998**, *45*, 69−83.
(1856) Mao, C.; Sun, W.; Shen, Z.; Seeman, N. C. A nanomechanical device based on the B−Z transition of DNA. *Nature* **1999**, *397*, 144−146.
(1857) Niemeyer, C. M. Progress in "engineering up" nanotechnology devices utilizing DNA asa construction material. *Appl. Phys. A: Mater. Sci. Process.* **1999**, *68*, 119−124.
(1858) Seeman, N. C. DNA engineering and its application to nanotechnology. *Trends Biotechnol.* **1999**, *17*, 437−443.
(1859) Niemeyer, C. M. Self-assembled nanostructures based on DNA: towards the development of nanobiotechnology. *Curr. Opin. Chem. Biol.* **2000**, *4*, 609−618.
(1860) Seeman, N. C.; Belcher, A. M. Emulating biology: building nanostructures from the bottom up. *Proc. Natl. Acad. Sci. U. S. A.* **2002**, *99*, 6451−6455.
(1861) Seeman, N. C. At the Crossroads of Chemistry, Biology, and Materials. *Chem. Biol.* **2003**, *10*, 1151−1159.
(1862) Seeman, N. C. DNA in a Material World. *Nature* **2003**, *421*, 427−431.
(1863) Seeman, N. C. Molecular Engineering: Nanotechnology and the Double Helix. *Sci. Am.* **2004**, *290*, 34−43.
(1864) Yan, H. Materials science. Nucleic acid nanotechnology. *Science* **2004**, *306*, 2048−2049.
(1865) Brucale, M.; Zuccheri, G.; Samori, B. The dynamic properties of an intramolecular transition from DNA duplex to cytosine-thymine motif triplex. *Org. Biomol. Chem.* **2005**, *3*, 575−577.
(1866) Aldaye, F. A.; Palmer, A. L.; Sleiman, H. F. Assembling materials with DNA as the guide. *Science* **2008**, *321*, 1795−1799.
(1867) Gothelf, K. V. Materials science. LEGO-like DNA structures. *Science* **2012**, *338*, 1159−1160.
(1868) Marras, A. E.; Zhou, L. F.; Su, H. J.; Castro, C. E. Programmable motion of DNA origami mechanisms. *Proc. Natl. Acad. Sci. U. S. A.* **2015**, *112*, 713−718.
(1869) Zhang, D. Y.; Seelig, G. Dynamic DNA nanotechnology using strand-displacement reactions. *Nat. Chem.* **2011**, *3*, 103−113.
(1870) Hamada, S.; Murata, S. Substrate-Assisted Assembly of Interconnected Single-Duplex DNA Nanostructures. *Angew. Chem., Int. Ed.* **2009**, *48*, 6820−6823.
(1871) Kalle Gehring, J.-L. L. a. M. G. A tetrameric DNA structure with protonated cytosine. *Nature* **1993**, *363*, 561−565.
(1872) Chen, L.; C, L.; Zhang, X.; Rich, A. Crystal structure of a four-stranded intercalated DNA: d(C4). *Biochemistry* **1994**, *33*, 13540−13546.
(1873) Alberti, P.; Mergny, J. L. DNA duplex-quadruplex exchange as the basis for a nanomolecular machine. *Proc. Natl. Acad. Sci. U. S. A.* **2003**, *100*, 1569−1573.
(1874) Dittmer, W. U.; Reuter, A.; Simmel, F. C. A DNA-based machine that can cyclically bind and release thrombin. *Angew. Chem., Int. Ed.* **2004**, *43*, 3550−3553.
(1875) Davis, J. T.; Spada, G. P. Supramolecular architectures generated by self-assembly of guanosine derivatives. *Chem. Soc. Rev.* **2007**, *36*, 296−313.
(1876) Collie, G. W.; Parkinson, G. N. The application of DNA and RNA G-quadruplexes to therapeutic medicines. *Chem. Soc. Rev.* **2011**, *40*, 5867−5892.
(1877) Miyake, Y.; Togashi, H.; Tashiro, M.; Yamaguchi, M.; Oda, S.; Kudo, M.; Tanaka, Y.; Kondo, Y.; Sawa, R.; Fujimoto, T.; et al. Mercury^{II}-Mediated Formation of Thymine−Hg^{II}−Thymine Base Pairs in DNA Duplexes. *J. Am. Chem. Soc.* **2006**, *128*, 2172−2173.
(1878) Tanaka, Y.; Oda, S.; Yamaguchi, H.; Kondo, Y.; Kojima, C.; Ono, A. 15N−15N *J*-Coupling Across Hg^{II}: Direct Observation of Hg^{II}-Mediated T−T Base Pairs in a DNA Duplex. *J. Am. Chem. Soc.* **2007**, *129*, 244−245.
(1879) Yurke, B.; Tuberfield, A. J.; Mills, A. P., Jr.; Simmel, F. C.; Neumann, J. L. A DNA-fuelled molecular machine made of DNA. *Nature* **2000**, *406*, 605−608.
(1880) Turberfield, A.; Mitchell, J.; Yurke, B.; Mills, A.; Blakey, M.; Simmel, F. DNA Fuel for Free-Running Nanomachines. *Phys. Rev. Lett.* **2003**, *90*, 118102.
(1881) Liu, D.; Bruckbauer, A.; Abell, C.; Balasubramanian, S.; Kang, D.-J.; Klenerman, D.; Zhou, D. A Reversible pH-Driven DNA Nanoswitch Array. *J. Am. Chem. Soc.* **2006**, *128*, 2067−2071.
(1882) Liang, X.; Nishioka, H.; Takenaka, N.; Asanuma, H. A DNA nanomachine powered by light irradiation. *ChemBioChem* **2008**, *9*, 702−705.
(1883) Li, D.; Wieckowska, A.; Willner, I. Optical Analysis of Hg^{2+} Ions by Oligonucleotide−Gold-Nanoparticle Hybrids and DNA-Based Machines. *Angew. Chem.* **2008**, *120*, 3991−3995.
(1884) Song, G.; Chen, M.; Chen, C.; Wang, C.; Hu, D.; Ren, J.; Qu, X. Design of proton-fueled tweezers for controlled, multi-function DNA-based molecular device. *Biochimie* **2010**, *92*, 121−127.
(1885) Saghatelian, A.; Volcker, N. H.; Guckian, K. M.; Lin, V. S. Y.; Ghadin, M. R. DNA-Based Photonic Logic Gates: AND, NAND, and INHIBIT. *J. Am. Chem. Soc.* **2003**, *125*, 346−347.
(1886) Okamoto, A.; Tanaka, K.; Saito, I. DNA Logic Gates. *J. Am. Chem. Soc.* **2004**, *126*, 9458−9463.
(1887) Lee, J. F.; Stovall, G. M.; Ellington, A. D. Aptamer therapeutics advance. *Curr. Opin. Chem. Biol.* **2006**, *10*, 282−289.
(1888) Shlyahovsky, B.; Li, Y.; Lioubashevski, O.; Elbaz, J.; Willner, I. Logic Gates and Antisense DNA Devices Operating on a Translator Nucleic Acid Scaffold. *ACS Nano* **2009**, *3*, 1831−1843.
(1889) Wilner, O. I.; Shimron, S.; Weizmann, Y.; Wang, Z.-G.; Willner, I. Self-Assembly of Enzymes on DNA Scaffolds: En Route to Biocatalytic Cascades and the Synthesis of Metallic Nanowires. *Nano Lett.* **2009**, *9*, 2040−2043.
(1890) Wilner, O. I.; Weizmann, Y.; Gill, R.; Lioubashevski, O.; Freeman, R.; Willner, I. Enzyme cascades activated on topologically programmed DNA scaffolds. *Nat. Nanotechnol.* **2009**, *4*, 249−254.
(1891) Teller, C.; Willner, I. Organizing protein-DNA hybrids as nanostructures with programmed functionalities. *Trends Biotechnol.* **2010**, *28*, 619−628.
(1892) Qian, L.; Winfree, E.; Bruck, J. Neural network computation with DNA strand displacement cascades. *Nature* **2011**, *475*, 368−372.

DOI: 10.1021/acs.chemrev.5b00146
Chem. Rev. 2015, 115, 10081−10206

(1893) Winfree, L. Q. a. E. Scaling Up Digital Circuit Computation with DNA Strand Displacement Cascades. *Science* **2011**, *332*, 1196−1201.
(1894) Pei, H.; Liang, L.; Yao, G.; Li, J.; Huang, Q.; Fan, C. Reconfigurable Three-Dimensional DNA Nanostructures for the Construction of Intracellular Logic Sensors. *Angew. Chem., Int. Ed.* **2012**, *51*, 9020−9024.
(1895) Fu, Y.; Zeng, D.; Chao, J.; Jin, Y.; Zhang, Z.; Liu, H.; Li, D.; Ma, H.; Huang, Q.; Gothelf, K. V.; Fan, C. Single-step rapid assembly of DNA origami nanostructures for addressable nanoscale bioreactors. *J. Am. Chem. Soc.* **2013**, *135*, 696−702.
(1896) Miyamoto, T.; Razavi, S.; DeRose, R.; Inoue, T. Synthesizing biomolecule-based Boolean logic gates. *ACS Synth. Biol.* **2013**, *2*, 72−82.
(1897) Gibbons, A.; Amos, M.; Hodgson, D. DNA computing. *Curr. Opin. Biotechnol.* **1997**, *8*, 103−106.
(1898) Cox, J. C.; Cohen, D. S.; Ellington, A. D. The complexities of DNA computation. *Trends Biotechnol.* **1999**, *17*, 151−154.
(1899) Ruben, A. J.; Landweber, L. F. The past, present and future of molecular computing. *Nat. Rev. Mol. Cell Biol.* **2000**, *1*, 69−72.
(1900) Gillmor, S. D.; Rugheimer, P. P.; Lagally, M. G. Computation with DNA on surfaces. *Surf. Sci.* **2002**, *500*, 699−721.
(1901) Reif, J. H. Computing: Successes and challenges. *Science* **2002**, *296*, 478−479.
(1902) Livstone, M. S.; van Noort, D.; Landweber, L. F. Molecular computing revisited: a Moore's law? *Trends Biotechnol.* **2003**, *21*, 98−101.
(1903) Condon, A. Automata make antisense. *Nature* **2004**, *429*, 351−352.
(1904) Hasty, J.; McMillen, D.; Collins, J. J. Engineered gene circuits. *Nature* **2002**, *420*, 224−230.
(1905) Kim, J.; Lee, J.; Hamada, S.; Murata, S.; Ha Park, S. Self-replication of DNA rings. *Nat. Nanotechnol.* **2015**, *10*, 528−533.
(1906) Park, S. Y.; Lytton-Jean, A. K.; Lee, B.; Weigand, S.; Schatz, G. C.; Mirkin, C. A. DNA-programmable nanoparticle crystallization. *Nature* **2008**, *451*, 553−556.
(1907) Nykypanchuk, D.; Maye, M. M.; van der Lelie, D.; Gang, O. DNA-guided crystallization of colloidal nanoparticles. *Nature* **2008**, *451*, 549−552.
(1908) Wang, T.; Sha, R. J.; Dreyfus, R.; Leunissen, M. E.; Maass, C.; Pine, D. J.; Chaikin, P. M.; Seeman, N. C. Self-replication of information-bearing nanoscale patterns. *Nature* **2011**, *478*, 225−228.
(1909) Stojanovic, M. N.; Stefanovic, D. A deoxyribozyme-based molecular automaton. *Nat. Biotechnol.* **2003**, *21*, 1069−1074.
(1910) Tabor, J. J.; Ellington, A. D. Playing to win at DNA computation. *Nat. Biotechnol.* **2003**, *21*, 1013−1015.
(1911) Macdonald, J.; Li, Y.; Sutovic, M.; Lederman, H.; Pendri, K.; Lu, W. H.; Andrews, B. L.; Stefanovic, D.; Stojanovic, M. N. Medium scale integration of molecular logic gates in an automaton. *Nano Lett.* **2006**, *6*, 2598−2603.
(1912) Liu, M.; Fu, J.; Hejesen, C.; Yang, Y.; Woodbury, N. W.; Gothelf, K.; Liu, Y.; Yan, H. A DNA tweezer-actuated enzyme nanoreactor. *Nat. Commun.* **2013**, *4*, 2127.
(1913) Elbaz, J.; Wang, Z.-G.; Orbach, R.; Willner, I. pH-stimulated concurrent mechanical activation of two DNA "tweezers". A "SET-RESET" logic gate system. *Nano Lett.* **2009**, *9*, 4510−4514.
(1914) Wang, Z.-G.; Elbaz, J.; Remacle, F.; Levine, R. D.; Willner, I. All-DNA finite-state automata with finite memory. *Proc. Natl. Acad. Sci. U. S. A.* **2010**, *107*, 21996−22001.
(1915) Xin, L.; Zhou, C.; Yang, Z.; Liu, D. Regulation of an enzyme cascade reaction by a DNA machine. *Small* **2013**, *9*, 3088−3091.
(1916) Elbaz, J.; Cecconello, A.; Fan, Z.; Govorov, A. O.; Willner, I. Powering the programmed nanostructure and function of gold nanoparticles with catenated DNA machines. *Nat. Commun.* **2013**, *4*, 2000.
(1917) Lange, H.; Juarez, B. H.; Carl, A.; Richter, M.; Bastus, N. G.; Weller, H.; Thomsen, C.; von Klitzing, R.; Knorr, A. Tunable plasmon coupling in distance-controlled gold nanoparticles. *Langmuir* **2012**, *28*, 8862−8866.
(1918) Kuzyk, A.; Schreiber, R.; Fan, Z.; Pardatscher, G.; Roller, E. M.; Hogele, A.; Simmel, F. C.; Govorov, A. O.; Liedl, T. DNA-based self-assembly of chiral plasmonic nanostructures with tailored optical response. *Nature* **2012**, *483*, 311−314.
(1919) Liu, Y.; Kuzuya, A.; Sha, R.; Guillaume, J.; Wang, R.; Canary, J. W.; Seeman, N. C. Coupling Across a DNA Helical Turn Yields a Hybrid DNA/Organic Catenane Doubly Tailed with Functional Termini. *J. Am. Chem. Soc.* **2008**, *130*, 10882−10883.
(1920) Han, D.; Pal, S.; Liu, Y.; Yan, H. Folding and cutting DNA into reconfigurable topological nanostructures. *Nat. Nanotechnol.* **2010**, *5*, 712−717.
(1921) Lu, C. H.; Cecconello, A.; Elbaz, J.; Credi, A.; Willner, I. A three-station DNA catenane rotary motor with controlled directionality. *Nano Lett.* **2013**, *13*, 2303−2308.
(1922) Samori, B.; Zuccheri, G. DNA codes for nanoscience. *Angew. Chem., Int. Ed.* **2005**, *44*, 1166−1181.
(1923) Chen, Y.; Mao, C. Reprogramming DNA-directed reactions on the basis of a DNA conformational change. *J. Am. Chem. Soc.* **2004**, *126*, 13240−13241.
(1924) Storhoff, J. J.; Mirkin, C. A. Programmed materials synthesis with DNA. *Chem. Rev.* **1999**, *99*, 1849−1862.
(1925) Braun, E.; Keren, K. From DNA to transistors. *Adv. Phys.* **2004**, *53*, 441−496.
(1926) Wengel, J. Nucleic acid nanotechnology - towards Angstrom-scale engineering. *Org. Biomol. Chem.* **2004**, *2*, 277−280.
(1927) Feldkamp, U.; Niemeyer, C. M. Rational design of DNA nanoarchitectures. *Angew. Chem., Int. Ed.* **2006**, *45*, 1856−1876.
(1928) Broude, N. E. Stem-loop oligonucleotides: a robust tool for molecular biology and biotechnology. *Trends Biotechnol.* **2002**, *20*, 249−256.
(1929) Tan, W. H.; Wang, K. M.; Drake, T. J. Molecular beacons. *Curr. Opin. Chem. Biol.* **2004**, *8*, 547−553.
(1930) Shen, W. Q.; Bruist, M. F.; Goodman, S. D.; Seeman, N. C. A protein-driven DNA device that measures the excess binding energy of proteins that distort DNA. *Angew. Chem., Int. Ed.* **2004**, *43*, 4750−4752.
(1931) Nutiu, R.; Li, Y. F. A DNA-protein nanoengine for "On-Demand" release and precise delivery of molecules. *Angew. Chem., Int. Ed.* **2005**, *44*, 5464−5467.
(1932) Loh, I. Y.; Cheng, J.; Tee, S. R.; Efremov, A.; Wang, Z. S. From Bistate Molecular Switches to Self-Directed Track-Walking Nanomotors. *ACS Nano* **2014**, *8*, 10293−10304.
(1933) Leigh, D. A.; Lewandowska, U.; Lewandowski, B.; Wilson, M. R. Synthetic Molecular Walkers. *Top. Curr. Chem.* **2014**, *354*, 111−138.
(1934) Wang, C. Y.; Ren, J. S.; Qu, X. G. A stimuli responsive DNA walking device. *Chem. Commun.* **2011**, *47*, 1428−1430.
(1935) Liedl, T.; Olapinski, M.; Simmel, F. C. A Surface-Bound DNA Switch Driven by a Chemical Oscillator. *Angew. Chem., Int. Ed.* **2006**, *45*, 5007−5010.
(1936) Bromley, E. H.; Kuwada, N. J.; Zuckermann, M. J.; Donadini, R.; Samii, L.; Blab, G. A.; Gemmen, G. J.; Lopez, B. J.; Curmi, P. M.; Forde, N. R.; Woolfson, D. N.; Linke, H. The Tumbleweed: towards a synthetic proteinmotor. *HFSP J.* **2009**, *3*, 204−212.
(1937) Rothemund, P. W. Folding DNA to create nanoscale shapes and patterns. *Nature* **2006**, *440*, 297−302.
(1938) Smith, L. M. Nanotechnology: Molecular robots on the move. *Nature* **2010**, *465*, 167−168.
(1939) Wickham, S. F.; Endo, M.; Katsuda, Y.; Hidaka, K.; Bath, J.; Sugiyama, H.; Turberfield, A. J. Direct observation of stepwise movement of a synthetic molecular transporter. *Nat. Nanotechnol.* **2011**, *6*, 166−169.
(1940) Bath, J.; Green, S. J.; Turberfield, A. J. A free-running DNA motor powered by a nicking enzyme. *Angew. Chem., Int. Ed.* **2005**, *44*, 4358−4361.
(1941) Mai, J.; Sokolov, I. M.; Blumen, A. Directed particle diffusion under "burnt bridges" conditions. *Phys. Rev. E: Stat. Phys., Plasmas, Fluids, Relat. Interdiscip. Top.* **2001**, *64*, 011102.
(1942) Antal, T.; Krapivsky, P. L. "Burnt-bridge" mechanism of molecular motor motion. *Phys. Rev. E* **2005**, *72*, 10.1103/PhysRevE.72.046104.

DOI: 10.1021/acs.chemrev.5b00146
Chem. Rev. 2015, 115, 10081−10206

(1943) Yin, P.; Choi, H. M.; Calvert, C. R.; Pierce, N. A. Programming biomolecular self-assembly pathways. *Nature* **2008**, *451*, 318−322.
(1944) Green, S. J.; Bath, J.; Turberfield, A. J. Coordinated chemomechanical cycles: a mechanism for autonomous molecular motion. *Phys. Rev. Lett.* **2008**, *101*, 238101.
(1945) Bath, J.; Green, S. J.; Allen, K. E.; Turberfield, A. J. Mechanism for a directional, processive, and reversible DNA motor. *Small* **2009**, *5*, 1513−1516.
(1946) Pei, R.; Taylor, S. K.; Stefanovic, D.; Rudchenko, S.; Mitchell, T. E.; Stojanovic, M. N. Behavior of polycatalytic assemblies in a substrate-displaying matrix. *J. Am. Chem. Soc.* **2006**, *128*, 12693−12699.
(1947) You, M.; Chen, Y.; Zhang, X.; Liu, H.; Wang, R.; Wang, K.; Williams, K. R.; Tan, W. An autonomous and controllable light-driven DNA walking device. *Angew. Chem., Int. Ed.* **2012**, *51*, 2457−2460.
(1948) Kay, E. R.; Leigh, D. A. Rise of the Molecular Machines. *Angew. Chem., Int. Ed.* **2015**, *54*, 10080−10088.
(1949) Turing, A. M. *Proc. London Math. Soc.* **1937**, *42*, 230−265.

DOI: 10.1021/acs.chemrev.5b00146
Chem. Rev. 2015, 115, 10081−10206